Annals of the
International Society of
Dynamic Games

David M. Ramsey
Jérôme Renault
Editors

Advances in Dynamic Games

Games of Conflict, Evolutionary Games, Economic Games, and Games Involving Common Interest

Birkhäuser

Annals of the International Society of Dynamic Games

Volume 17

David M. Ramsey · Jérôme Renault
Editors

Advances in Dynamic Games

Games of Conflict, Evolutionary Games, Economic Games, and Games Involving Common Interest

Birkhäuser

Editors
David M. Ramsey
Faculty of Computer Science
and Management
Wrocław University of Science
and Technology
Wrocław, Poland

Jérôme Renault
Toulouse School of Economics
University Toulouse Capitole and ANITI
Toulouse, France

ISSN 2474-0179 ISSN 2474-0187 (electronic)
Annals of the International Society of Dynamic Games
ISBN 978-3-030-56533-6 ISBN 978-3-030-56534-3 (eBook)
https://doi.org/10.1007/978-3-030-56534-3

Mathematics Subject Classification: 91A25, 91A22, 91A23, 91A24, 91A26, 91A80

This book is published under the imprint Birkhäuser, www.birkhauser-science.com by the registered company Springer Nature Switzerland AG
The registered company address is: Gewerbestrasse 11, 6330 Cham, Switzerland

Preface

Game theory can be used to model the interaction between decision-makers in a wide range of scenarios spanning from pure conflict to situations in which the participants have clear common interests. This is illustrated by the variety of chapters in this volume, many of which are based on papers presented at the International Symposium on Dynamic Games and Applications, which took place in Grenoble, France in July 2018. The chapters are grouped into four sections, namely: Games of Conflict, Evolutionary Games, Economic Games and Games Involving Common Interest.

The first section, which includes five papers, presents games that model situations in which there is a clear conflict between the interests of the participants. These games can be interpreted, sometimes loosely and sometimes strictly, as pursuit-evasion games. In the chapter "Quick Construction of Dangerous Disturbances in Conflict Control Problems", Martynov et al. consider a model of a differential game with linear controls. One player, the controller, aims to reach a point in the target set at the termination time, whilst the aim of the other player, the disturber, aims to stop the controller from arriving at such a point at the appointed time. The authors present an example illustrating how this approach can be applied to flight simulators.

In the chapter "Isaacs' Two-on-One Pursuit-Evasion Game", Pachter considers differential games in which there are two pursuers and one evader. Isaacs' results on such games are adapted in order to classify these games into two situations: cases where only one pursuer is required and those where co-ordination between the two pursuers is required. Models of this type can illustrate both conflict and cooperation. Whilst there exists pure conflict between the pursuers and the evader, when the pursuers can be interpreted as individual decision-makers, then they often need to co-ordinate their actions in order to achieve a joint goal.

In the chapter "A Normal Form Game Model of Search and Pursuit", Alpern and Lee consider a searcher-evader game in which the evader can choose from a finite set of hiding places. The amount of time a searcher requires to investigate a hiding place, as well as the probability of finding the evader given that it is located there, depends on the place. The goal of the searcher is to find the evader in a fixed

amount of time. The authors consider both models where the probabilities of finding the evader in a given location are known and those where these probabilities can take one of two values and the searcher uses Bayesian inference.

In the chapter "Computation of Robust Capture Zones Using Interval-Based Viability Techniques in Presence of State Uncertainties", Turetsky and Le Ménec consider a differential pursuit-evasion game, where there is one pursuer and one evader. They derive robust capture zones, sets of locations of the pursuer relative to the evader which guarantee that the pursuer can capture the evader within a fixed time regardless of the strategy of the evader.

To conclude this section, in the chapter "Convergence of Numerical Method for Time-Optimal Differential Games with Lifeline", Munts and Kumkov consider a similar game to the one presented in the opening chapter. However, whilst the goal of one player is to guide the system to a state in the target set, the other player can win not just by avoiding such a situation, but by attaining a state in the so-called lifeline set.

The second section contains three chapters devoted to the field of evolutionary games. In the chapter "A Partnership Formation Game with Common Preferences and Scramble Competition", Ramsey considers a mate choice game in which a large set of players all search for a partner at the start of the breeding season. This game models scramble competition, i.e. as players form pairs and thus leave the mating pool, the distribution of the attractiveness of prospective partners changes and it generally becomes harder to find a partner.

In the chapter "The Replicator Dynamics for Games in Metric Spaces: Finite Approximations", Mendoza-Palacios and Hernández-Lerma consider the evolutionary dynamics of games in which the strategy sets are metric spaces. This is illustrated by a game in which the players choose their level of aggression from the interval $[0, 1]$. They derive conditions stating when the evolution of such a system can be approximated by a sequence of dynamical systems defined on finite spaces.

At the end of this section, in the chapter "Eco-evolutionary Spatial Dynamics of Nonlinear Social Dilemmas", Gokhale and Park consider the relation between spatial dynamics and the evolution of behaviour in generalised public goods games. In public goods games, the higher the level of cooperation between members of a group, the greater the benefits obtained by the group as a whole. However, individuals who cooperate the least obtain the greatest payoff. As a result, such games are clear illustrations of the role of conflict and cooperation in games (or in evolutionarily terms, the role of selection at the level of individuals and selection at the level of groups).

The third section contains three chapters presenting models that can be applied in the field of economics. In the chapter "Heuristic Optimization for Multi-Depot Vehicle Routing Problem in ATM Network Model", Platonova et al. consider an optimisation model that considers the location of branches of a bank and cash machines in order to provide the best service to customers whilst minimise costs. Although this model is not strictly game-theoretic, descriptions of how it can be adapted to game-theoretic scenarios are presented.

In the chapter "Load Balancing Congestion Games and Their Asymptotic Behavior", Altman et al. consider a game which has applications to communication networks. The players are atomic, i.e. the actions of an individual can affect the level of congestion along a given link. The authors show that in such games multiple equilibria can exist.

To conclude this section, in the chapter "Non-deceptive Counterfeiting and Consumer Welfare: A Differential Game Approach", Crettez et al. present a differential game that models the effect of the counterfeiting of goods produced by a prestigious brand. The originality of this model lies in the fact that it considers the welfare of consumers. This allows new insight to policy-makers on how such situations are legislated.

The final section contains two chapters presenting models of games in which there are common interests. Both papers consider the consumption of a commonly held resource. In the chapter "Equilibrium Coalition Structures of Differential Games in Partition Function Form", Hoof presents a model of the consumption of a non-renewable resource as a cooperative game. The extraction rates are chosen by the players, such that the overall rate at which a resource is extracted is proportional to the amount of the resource available (the constant of proportionality is equal to sum of the rates chosen). By cooperating, coalitions of players maximise the discounted payoff of the coalition as a whole, rather than individually maximising the payoff of each player, given the behaviour of others.

In the final chapter, Kordonis considers a different approach to achieving cooperation based on the concept of Kant's Categorial Imperative. This concept states that members of a population should use the rule that would maximise the overall payoff to the population when this rule is adopted by the population as a whole. The general model is illustrated by an example based on a fishing game, i.e. a model of the consumption of a renewable resource.

The chapters were evaluated by independent reviewers. We thank the authors for their contributions and the reviewers for their benevolent work and expert comments. Overall, this volume of Advance in Dynamic Games presents the full range between pure competition and cooperation, as well as applications of these ideas to various scientific disciplines. We wish the reader a pleasant journey.

Wrocław, Poland — David M. Ramsey
Toulouse, France — Jérôme Renault

Nikolai Botkin Memorial

On September 14, 2019, Nikolai Dmitrievich Botkin, who made a great contribution to the theory of differential games and numerical methods, passed away.

Nikolai Botkin was born on March 22, 1956, and raised in the city of Sysert, Sverdlovsk region, Russia. His father was a mathematics teacher and his mother, a physics teacher. Nikolai was fond of natural subjects since childhood and in 1973, he entered the Faculty of Mathematics and Mechanics of the Ural State University in Sverdlovsk (now Yekaterinburg). During his studies, Nikolai became interested in Bellman's dynamic programming principle. After graduation, he was accepted into the department of Dynamical Systems headed by A. I. Subbotin, which is part of the Institute of Mathematics and Mechanics of the Ural Branch of the Russian Academy of Sciences.

His works, performed in the early 80s under the guidance of V. S. Patsko, were connected with the theory of differential games and its numerical methods that had just begun to develop. Nikolai Botkin created the first algorithms for solving linear differential games; he obtained a posteriori estimates of the accuracy of numerical solutions and developed algorithms for optimal positional control in such problems. In 1983, Nikolai Botkin defended his Ph.D. thesis on "Numerical solution of linear

differential games." The methods developed by him were successfully applied in 1982–1992 to aviation problems of optimal control of an aircraft in the presence of wind disturbances in frames of joint research with the Academy of Civil Aviation in Leningrad. Based on an analysis of the asymptotic behaviour of solutions to nonlinear differential games in 1992, he proposed an algorithm for computing the discriminating kernel of differential inclusion.

After receiving a grant from the Humboldt Foundation in 1992, Nikolai Botkin lived and worked in Germany (1992–1993 University of Würzburg, 1993–1999 and 2006–2019 Technical University of Munich, 1999–2006 Research Center caesar, Bonn). His research interests covered many areas of applied mathematics. As a leading researcher, he participated in numerous scientific projects in the field of elasticity theory, hydrodynamics, thermodynamics, homogenization theory, phase-field models, optimization and optimal control of ordinary differential equations and distributed systems. Whilst working at the center of advanced European studies and research (caesar) in close contact with physicists, biologists and engineers, he was actively engaged in the creation of innovative devices and instruments in the field of composite materials, sensors, cryopreservation of living cells and tissues. This motivated him to develop new mathematical models, theoretical methods and computational algorithms. Returning in 2006 to the chair of Mathematical Modelling at the Technical University of Munich headed at that time by K.-H. Hoffmann, and continuing to work on the cryopreservation project, and then participating in a joint project with King Abdullah University of Science and Technology on CO_2 sequestration, Nikolai resumed work on numerical methods for solving differential games. One of his brilliant achievements at this time was the development of a grid method (implemented in the form of an algorithm and corresponding programs) for solving a wide class of multidimensional nonlinear differential games with state constraints. Using these algorithms, Nikolai Botkin, with his students, formulated and investigated a number of aircraft control problems in the presence of wind disturbances. He also applied methods and algorithms for solving differential games to study biomedical problems, which is extremely unique.

N. Botkin spent considerable time reviewing articles for various mathematical journals.

As an enthusiastic and versatile mathematician, Nikolai Botkin had a rare quality of solving complex applied problems, starting with the development of the model, its theoretical investigation, and ending with the development of algorithms for computing solutions up to their implementation in real systems and devices. Colleagues and students appreciated his deep knowledge, determination and perseverance. Other students, not only from the mathematics faculty, came to him for help with completing a diploma or other work, knowing that Nikolai could solve a variety of problems.

Nikolai was a friendly and cheerful person; he loved to joke and tell funny stories, was a keen table tennis player, and fond of reading books on physics and science fiction.

A sudden, premature death prevented the implementation of many of his scientific ideas and plans but his scientific results remain in 243 published works, of which about 100 are devoted to differential games.

Contents

Games of Conflict

Quick Construction of Dangerous Disturbances in Conflict Control Problems

Kirill Martynov, Nikolai D. Botkin, Varvara L. Turova, and Johannes Diepolder

Abstract The paper is devoted to the construction of dangerous disturbances in linear conflict control problems. Using the technique of sequential linearization, dangerous disturbances can also be constructed for nonlinear systems such as aircraft dynamics equations, including filters, servomechanisms, etc. The procedure proposed is based on a dynamic programming method and consists in the backward integration of ordinary matrix differential equations defining centers, sizes, and orientations of time-dependent parallelotopes forming a repulsive tube in the time-space domain. A feedback disturbance strategy can keep the state vector of the conflict control system outside the repulsive tube for all admissible inputs of the control.

The original version of this chapter was revised: This chapter has been changed to open access under a CC BY 4.0 license. The correction to this chapter is available at https://doi.org/10.1007/978-3-030-56534-3_14

K. Martynov (✉)
Department of Informatics, Technical University of Munich, Boltzmannstr. 3, 85748 Garching near Munich, Germany
e-mail: kirill.martynov@tum.de

N. D. Botkin · V. L. Turova
Mathematical Faculty, Technical University of Munich, Boltzmannstr. 3, 85748 Garching near Munich, Germany
e-mail: botkin@ma.tum.de

V. L. Turova
e-mail: turova@ma.tum.de

J. Diepolder
Institute of Flight System Dynamics, Technical University of Munich, Boltzmannstr. 15, 85748 Garching near Munich, Germany
e-mail: johannes.diepolder@tum.de

D. M. Ramsey and J. Renault (eds.), *Advances in Dynamic Games*,
Annals of the International Society of Dynamic Games 17,
https://doi.org/10.1007/978-3-030-56534-3_1

1 Introduction

One of the important problems in control engineering is generation of extremal disturbances for various types of dynamical systems. This is of interest in many application areas because such disturbances can be used to evaluate the robustness of models and quality of controllers.

This paper concerns with generation of feedback disturbances for linear conflict control systems where the aim of the disturbance is to deflect the state vector from a target set at a fixed termination time for all admissible controls. It is assumed that the target set and the constraints imposed on the control and disturbance variables are represented by parallelotopes. Starting with the parallelotope representing the target set and integrating backward in time a system of ordinary vector-matrix differential equations yield parallelotopes forming a repulsive tube in the time-space domain. It is proven that a certain feedback disturbance can keep all trajectories outside the repulsive tube, and therefore outside the target set at the termination time.

It should be noted that the minimal repulsive tube can be computed using general grid methods for solving differential games [3, 4, 8]. Nevertheless, such methods require large computation resources on multiprocessor computer platforms. More appropriate for linear conflict control problems are methods proposed in [5, 12] where repulsive tubes are approximated by polyhedrons, which however involves solving a lot of linear programming problems. Therefore, such methods also require significant computer resources. In contrast, the scheme suggested in the current paper is computationally cheap so that it can run in real time on a common computer. Moreover, high-dimensional models can be effectively treated with this method. Finally, disturbances for nonlinear models can be constructed by applying techniques of sequential linearization. Thus, the approach presented in this paper is rather general and can be used in various areas. As a demonstration of the method, generation of dangerous disturbances for aircraft control problems is considered.

The paper is structured as follows: In Sect. 2, a formal statement of the problem and some definitions are given. Section 3 contains a detailed description of the method for constructing repulsive feedback disturbances and provides a proof of their correctness. In Sect. 4, some numerical aspects of the method are addressed. It is shown that the method can be implemented in the discrete-time scheme. In Sect. 5, the method is applied to a three-dimensional linear differential game. This simple example allows us to visualize and clearly demonstrate in which extent the constructed repulsive tube is minimal. Section 6 considers the problem of aircraft take-off under windshear conditions. This example demonstrates a technique of generating dangerous disturbances for nonlinear models. Section 7 describes the construction of disturbances for a linearized aircraft closed-loop system for the lateral dynamics.

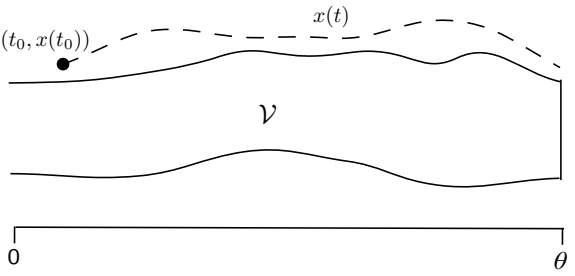

Fig. 1 Repulsive tube $\mathcal{V}$ with a sample trajectory $x(t)$

2 Problem Formulation

First, introduce the following notation. For a set $\mathcal{V} \subset [0, \theta] \times \mathbb{R}^d$ and $t \in [0, \theta]$, the set $\mathcal{V}(t) := \{x \in \mathbb{R}^d : (t, x) \in \mathcal{V}\}$ is called cross section of $\mathcal{V}$ at t. For a vector $x \in \mathbb{R}^d$, the norm $\|x\|_\infty$ is defined as $\max\{|x_i|, i = 1, ..., d\}$. Let the superscript T denotes the transposition operation.

Consider a linear conflict control problem

$$\dot{x} = A\,x + u + v, \quad x \in \mathbb{R}^d, \ \ t \in [0, \theta], \ \ x(\theta) \in \mathcal{M} \subset \mathbb{R}^d. \tag{1}$$

Here, u and v, respectively, denote the control and disturbance variables constrained as follows: $u(t) \in \mathcal{R} \subset \mathbb{R}^d$, $v(t) \in \mathcal{Q} \subset \mathbb{R}^d$. The problem is considered on a time interval $[0, \theta]$. The aim of the control is to meet the target set $\mathcal{M}$ at the termination time θ, whereas the aim of the disturbance is opposite. The objective of this paper is to propose a method of constructing a feedback disturbance $v(t, x)$ which deflects all trajectories from the target set at the termination time. More precisely, the problem is formulated as follows:

Problem 1 Find a tube $\mathcal{V} \subset [0, \theta] \times \mathbb{R}^d$, $\mathcal{V}(\theta) = \mathcal{M}$ such that there exists a feedback disturbance $v(t, x)$ fulfilling the following condition: If $(t_0, x(t_0)) \notin int(\mathcal{V})$, then $(t, x(t)) \notin int(\mathcal{V})$, $t \in [t_0, \theta]$, for all possible controls.

Remark 1 In what follows, $\mathcal{V}$ and $v(t, x)$ from the formulation of Problem 1 are called *repulsive tube* and *repulsive disturbance*, respectively. It will be shown below that the knowledge of a repulsive tube allows us to find explicitly a repulsive disturbance appearing in the formulation of Problem 1.

The main property of repulsive tubes is illustrated in Fig. 1.

3 Construction of Repulsive Tubes

This section describes the computation of time-dependent parallelotopes that form a repulsive tube in $[0, \theta] \times \mathbb{R}^d$ and define a repulsive feedback disturbance. This

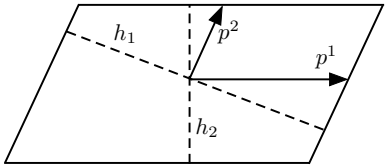

Fig. 2 Two-dimensional parallelotope $\mathcal{V}_\mathcal{P}$ with the axes $p^1,\ p^2$ and the corresponding distance $h_1,\ h_2$

approach raises from the idea by E. K. Kostousova to use parallelotopes for constructing feedback controls, see a detailed description in [7].

A *parallelotope* is defined as

$$\mathcal{V}_\mathcal{P}[p,\, P] := \{x \in \mathbb{R}^d | x = p + P\,\varepsilon,\ \|\varepsilon\|_\infty \le 1\}, \tag{2}$$

where $p \in \mathbb{R}^d$ and $P \in \mathbb{R}^{d\times\hat{d}},\ \hat{d} \le d$, are its center and shape matrix, respectively. Note that $\hat{d} = d$ in our consideration. The columns of the matrix P are called *axes* of the parallelotope $\mathcal{V}_\mathcal{P}$ and denoted as $p^1, ..., p^{\hat{d}} \in \mathbb{R}^d$. Furthermore, let $h_i(\mathcal{V}_\mathcal{P})$ be the euclidean distance between two opposite faces of $\mathcal{V}_\mathcal{P}$ along the axis p^i, and $h_{min}(\mathcal{V}_\mathcal{P}) = \min\{h_i(\mathcal{V}_\mathcal{P}) \mid 1 \le i \le \hat{d}\}$. Figure 2 shows p^i and h_i for a two-dimensional parallelotope.

Further, it is assumed that the following problem data are represented by parallelotopes:

$$\begin{aligned} &\mathcal{M} = \mathcal{V}_\mathcal{P}[p_f, P_f],\ p_f \in \mathbb{R}^d,\ P_f \in \mathbb{R}^{d\times d},\ det\ P_f \ne 0, \\ &\mathcal{R} = \mathcal{V}_\mathcal{P}[r, R],\ R \in \mathbb{R}^{d\times d_1}, \quad \mathcal{Q} = \mathcal{V}_\mathcal{P}[q, Q],\ Q \in \mathbb{R}^{d\times d_2}. \end{aligned} \tag{3}$$

Remark 2 The system matrix A as well as the constraints on the control and disturbance inputs may depend on time. Thus, in general, $A = A(t)$, $\mathcal{R} = \mathcal{V}_\mathcal{P}[r(t), R(t)]$, and $\mathcal{Q} = \mathcal{V}_\mathcal{P}[q(t), Q(t)]$. In the following, this time-dependence is not shown explicitly in order to simplify the notation.

Remark 3 Parallelotope-shaped representation of the control and disturbance constraints is fairly generic and allows to capture different common types of constraints. For example, consider a control $u \in \mathbb{R}^2$ subject to

$$\begin{aligned} -\hat{u}_1(t) \le u_1(t) \le \hat{u}_1(t) \\ -\hat{u}_2(t) \le u_2(t) \le \hat{u}_2(t). \end{aligned}$$

Such constraints can be easily represented with the parallelotope notation discussed above by choosing:

$$\mathcal{R} = \mathcal{V}_\mathcal{P}\left[\begin{pmatrix}0\\0\end{pmatrix}, \begin{pmatrix}\hat{u}_1(t) & 0\\ 0 & \hat{u}_2(t)\end{pmatrix}\right].$$

With the assumptions introduced in (3), the following system of ODEs defines a repulsive tube $\mathcal{V}_{\mathcal{P}}(t) = \mathcal{V}_{\mathcal{P}}[p(t),\, P(t)],\, t \in [0, \theta]$:

$$\frac{dp}{dt} = A\, p + r + q, \quad p(\theta) = p_f, \tag{4}$$

$$\frac{dP}{dt} = A\, P + P\, \mathrm{diag}\, \beta(t, P) + Q\, \Gamma(t), \quad P(\theta) = P_f, \tag{5}$$

$$\beta = -\mathrm{Abs}(P^{-1}\, R)\, e, \text{ where } (\mathrm{Abs}(P))_{ij} = |P_{ij}|,\ e = (1, 1, ..., 1)^T \in \mathbb{R}^{d_1}, \tag{6}$$

$$\Gamma(t) \in \mathbb{R}^{d_2 \times d}, \ \max_{1 \le i \le d_2} \sum_{j=1}^{d} |\Gamma_{ij}(t)| \le 1. \tag{7}$$

In (6) and (7), the matrices diag β and Γ, respectively, represent the influence of the control and disturbance capacities on the repulsive tube. Note that the time evolution of the matrix Γ, satisfying the condition (7), should be chosen in such a way that the repulsive tube maximally decreases backward in time. Below, this principle will be discussed more exactly.

A repulsive feedback disturbance appearing in the statement of Problem 1 may be defined as follows:

$$v(t, x) = q(t) + Q(t)\, \Gamma(t)\, \frac{P(t)^{-1}\, (x - p(t))}{\max(\| P(t)^{-1}\, (x - p(t))\|_{\infty}, 1)}. \tag{8}$$

Theorem 1 *Let Eqs. (4)–(5), with relations (6)–(7), be solvable on* $[0, \theta]$, *and* $\det\big(P(t)\big) \neq 0,\ t \in [0, \theta]$, *then the tube* $\mathcal{V}_{\mathcal{P}}(\cdot)$ *and the disturbance strategy (8) provide a solution to Problem 1.*

Proof Observe that the condition $\det\big(P(t)\big) \neq 0,\ t \in [0, \theta]$, define the vector function

$$\xi(t, x) := P(t)^{-1}(x - p(t))$$

and note that the vector $\xi(t, x) \in \mathbb{R}^d$ defines relative coordinates of any point x in the parallelotope $\mathcal{V}_{\mathcal{P}}(t)$. It is easily seen that a point x lies outside the interior of the parallelotope $\mathcal{V}_{\mathcal{P}}(t)$ whenever $\|\xi(t, x)\|_{\infty} \ge 1$.

Let $x(\cdot)$ be a trajectory of (1) corresponding to the disturbance (8) and starting from a position (t_0, x_0) such that $\|\xi(t_0, x_0)\|_{\infty} \ge 1$. Denote $K(t) := \mathrm{cl}\left(\mathbb{R}^d \setminus \mathcal{V}_{\mathcal{P}}(t)\right)$ and prove that $x(t) \in K(t),\ t \in [t_0, \theta]$. Bearing in mind that $\|\xi(t, x)\|_{\infty} = \max\limits_{j \in \overline{1,d}} |\xi_j(t, x)|$ introduce the functions

$$g_j(t, x) = \begin{cases} \xi_j(t, x), & j \in \overline{1, d} \\ -\xi_j(t, x), & j \in \overline{d+1, 2d} \end{cases}. \tag{9}$$

Obviously, the graph K of the mapping $K(\cdot)$ on $[t_0, \theta]$ is given as follows:

$$K = \bigcup_{j=1}^{2d} K_j, \quad \text{where} \quad K_j = \{(t,x) : g_j(t,x) \geq 1,\ t_0 \leq t \leq \theta, x \in \mathbb{R}^d\}. \quad (10)$$

According to [2, Table 4.1], the contingent cone to K at any point $(t,x) \in K$ is given by the formula

$$T_K(t,x) = \bigcup_{j \in J(t,x)} T_{K_j}(t,x),$$

where $J(t,x) = \{j \in \overline{1,2d} : (t,x) \in K_j\}$, and $T_{K_j}(t,x)$ is the contingent cone to K_j at (t,x).

Following to [2, Chap. 4.1.1], it holds for $(t,x) \in K_j$, $t \in [t_0, \theta)$:

$$T_{K_j}(t,x) = \begin{cases} \mathbb{R} \times \mathbb{R}^d, & \text{if } t > t_0,\ g_j(t,x) > 1, \\ \mathbb{R}^+ \times \mathbb{R}^d, & \text{if } t = t_0,\ g_j(t,x) > 1, \\ \{(\tau \in \mathbb{R}, \eta \in \mathbb{R}^d) :\ \tau \frac{\partial g_j}{\partial t}(t,x) + \eta^T \nabla_x g_j(t,x) \geq 0\}, & \text{if } t > t_0,\ g_j(t,x) = 1, \\ \{(\tau \in \mathbb{R}^+, \eta \in \mathbb{R}^d) : \tau \frac{\partial g_j}{\partial t}(t,x) + \eta^T \nabla_x g_j(t,x) \geq 0\}, & \text{if } t = t_0,\ g_j(t,x) = 1. \end{cases} \quad (11)$$

According to [1, Theorem 11.1.3], the condition $(1, \dot{x}(t)) \in T_K\big(t, x(t)\big)$, $t \in [t_0, \theta)$, guarantees the inclusion $x(t) \in K(t)$, $t \in [t_0, \theta]$. Let us prove the validity of that condition.

If $\|\xi(t, x(t))\|_\infty > 1$, one of the first two relations of (11) holds for some index $j \in J\big(t, x(t)\big)$, which provides the desired result due to (10).

The "boundary" case, $\|\xi(t, x(t))\|_\infty = 1$, is being treated as follows: Obviously, there exists an index $j_0 \in J(t, x(t))$ such that the third relation of (11) holds. Assume that $j_0 \in \overline{1,d}$ (the case $j_0 \in \overline{d+1, 2d}$ is considered analogously). The full time derivative of the vector function $\xi\big(t, x(t)\big)$ reads

$$\frac{d\xi}{dt} = -P^{-1}\frac{dP}{dt}P^{-1}(x-p) + P^{-1}\frac{d}{dt}(x-p) =$$
$$= -P^{-1}(AP + Q\Gamma + P\operatorname{diag}\beta)\xi + P^{-1}(A(x-p) + (v-q) + (u-r))$$

if formulas (1), (4), (5), and the definition of ξ are used. Note that every admissible control u satisfies the relation $u - r = R\alpha$ at time t, where α is a vector such that $\|\alpha\|_\infty \leq 1$. Additionally, using (8) yields

$$\frac{d\xi}{dt} = -P^{-1}Q\Gamma\Big(\xi - \frac{\xi}{\max(\|\xi\|_\infty), 1)}\Big) - (\operatorname{diag}\beta)\xi + P^{-1}R\alpha.$$

The equalities $\|\xi(t, x(t))\|_\infty = 1$ and $\xi_{j_0}(t, x(t)) = 1$ yield the relations

$$\frac{d\xi_{j_0}}{dt} = -(\beta_{j_0}\xi_{i_0}) + (P^{-1}R\alpha)_{j_0} \geq -\beta_{j_0} - (Abs(P^{-1}R), e)_{j_0} = 0, \tag{12}$$

and therefore,

$$\frac{d\xi_{j_0}}{dt} = \frac{\partial g_{j_0}}{\partial t}(t, x(t)) + \dot{x}(t)^T \nabla_x g_{j_0}(t, x(t)) \geq 0, \tag{13}$$

which implies that $(1, \dot{x}(t)) \in T_K(t, x(t))$ according to (10) and (11). Thus, in all cases, $(1, \dot{x}(t)) \in T_K(t, x(t))$, $t \in [t_0, \theta)$, and therefore, $x(t) \in K(t)$, $t \in [t_0, \theta]$, because of the continuity of $x(t)$ and $K(t)$. Finally, since $K(t) \cap int\big(\mathcal{V}_{\mathcal{P}}(t)\big) = \emptyset$, the condition $x(t) \notin int\big(\mathcal{V}_{\mathcal{P}}(t)\big)$, $t \in [t_0, \theta]$, holds.

Remark 4 Note that the repulsive tube $\mathcal{V}_{\mathcal{P}}$ can degenerate so that $\det\big(P(\hat{t})\big) = 0$ for some $\hat{t} \in [0, \theta)$, and $P(\hat{t})$ is no longer invertible. In this case, the tube $\mathcal{V}_{\mathcal{P}}$ is constructed only on $[\hat{t}, \theta]$, and the disturbance may be set as $v(t) \equiv q$, $t \leq \hat{t}$. Obviously, $x(\hat{t}) \notin \mathcal{V}_{\mathcal{P}}(\hat{t})$, and the rule (8) can be used for $t > \hat{t}$.

As it was mentioned after formula (7), the choice of Γ is crucial for obtaining a possibly smaller repulsive tube, which allows for the application of (8) to a possibly larger set of initial conditions. The following choice is used in the numerical simulations in Sects. 5–7: The whole time interval $[0, \theta]$ is divided into subintervals $(\tau_i, \tau_{i+1}]$, $i = 0, ..., N$, with $\tau_0 = 0$ and $\tau_N = \theta$. The system (4)–(5) is then integrated backward in time from θ to 0, and a constant matrix Γ_k satisfying (7) is chosen for each subinterval $(\tau_{k-1}, \tau_k]$ to minimize the minimum distance between the opposite faces of $\mathcal{V}_{\mathcal{P}}(\tau_{k-1})$. Intuitively, such a choice of Γ yields the strongest contraction of the parallelotope tube along the direction of its shortest axis.

Note that the resulting Γ may be discontinuous at time instants τ_i. However, the number of discontinuities is finite, and solutions of (4)–(5) remain continuous and unique.

4 Numerical Implementation of Repulsive Feedback Disturbances

The proof of appropriateness of the repulsive disturbance (8) is done in Sect. 3 under the assumption of continuous-time scheme. In a discrete-time scheme, the feedback repulsive disturbance (8) may not properly work because the condition (12) holds only on the boundary of $\mathcal{V}_{\mathcal{P}}$. In this section, an extended discrete-time control scheme is presented, and a bound on the time step length of this procedure is evaluated.

Assume for simplicity that the discrete-time scheme involves equidistant time instants t_i corresponding to the step length Δt. As it was declared in the introduction, the disturbance is basically associated with wind, and the maximum expected wind speed can hardly be exactly predicted. Therefore, the extension of disturbance bounds along all parallelotope axes by the factor $1 + \delta$, where $\delta > 0$ is a small parameter, is

not prohibited. Thus, it is now assumed that $v \in \mathcal{V}_{\mathcal{P}}[q, (1+\delta)\,Q]$, and the repulsive disturbance $v(t,x)$ is computed by the formula

$$v(t,x) = q(t) + Q(t)\,\Gamma(t)\,\frac{P^{-1}(t)\,(x - p(t))}{\max(\|P^{-1}(t)\,(x-p(t))\|_\infty/(1+\delta),\,1)}. \tag{14}$$

Note that the function v in (14) is Lipschitzian on each time interval $[t_i, t_{i+1})$ in the following sense:

$$|v(t,y) - v(t_i,x)| \le L\,(|t - t_i| + \|x - y\|),\ t \in [t_i, t_{i+1}) \tag{15}$$

if the matrix Γ is constant on each interval $[t_i, t_{i+1})$. Let $x(\cdot)$ be a trajectory started from a position (t_0, x_0) such that $\|\xi(t_0,x_0)\|_\infty \ge 1+\delta$ and computed in the continuous-time scheme using the disturbance (14). The same argumentation as in the proof of Theorem 1 implies that $\|\xi(t,x(t))\|_\infty \ge 1+\delta,\ t \in [t_0,\theta]$.

Let $x_\Delta(\cdot)$ be the corresponding trajectory (the same control $u(\cdot)$ and the same initial position (t_0,x_0)) computed in the discrete-time scheme using the disturbance (14). In virtue of condition (15), it is possible to prove that

$$\|x(t) - x_\Delta(t)\| \le G\Delta t, \quad G = \exp(H\,\theta), \quad H = \max_{t\in[0,\theta]} \|A(t)\| + L,$$

and therefore, $\|\xi(t,x_\Delta(t))\|_\infty \ge 1 + \delta - MG\Delta t,\ t \in [t_0,\theta]$, where M is the Lipschitz constant of the function $\|\xi(t,x)\|_\infty$ in x. It remains to set $\Delta t \le \delta/(MG)$.

Remark 5 The theoretical bound on the step size Δt may be too small. However, for simulations presented in the following sections, it is possible to maintain the property $\|\xi(t,x_\Delta(t))\|_\infty \ge 1,\ t \in [t_0,\theta]$, for much larger time steps.

Finally, note that for any given problem dimension d (i.e., the state $x \in \mathbb{R}^d$), the computational complexity of the proposed scheme is $O(d^3)$ per time step Δt as it involves matrix equations of dimension d, which can be solved with, e.g., LU-decomposition. Even for fairly low-dimensional problems, this dependency is far superior to complexity of other common methods for construction of disturbances, such as

- grid methods, e.g., [3], that scale as $O(N^d)$ per time step, where N is the grid resolution per dimension,
- methods that represent repulsive tubes with arbitrary convex polygons, e.g., [5], that scale as $O(d!m)$ per time step, where m is the number of inequalities describing the polygon.

Clearly, the difference in complexity between these methods and the presented approach quickly grows with the increasing problem dimension. Thus, the presented method allows us to consider problems that would not be accessible with many other techniques.

5 Application: Simple Example

In this section, the techniques developed in Sects. 3 and 4 are applied to compute a repulsive disturbance in a linear three-dimensional differential game. This example is appropriate to visualize repulsive tubes and demonstrate the proper work of repulsive disturbances.

Consider the following differential game:

$$\begin{aligned}
\dot{x_1} &= x_1 + x_2 + u_1 + v_1,\\
\dot{x_2} &= x_3 + v_2,\\
\dot{x_3} &= x_1 + u_2,\\
\mathcal{M} &= \{x \in \mathbb{R}^3 : \|x\|_\infty \le 1\}.
\end{aligned}$$

The system is considered on the time interval $[0, 1]$. The control and disturbance variables are constrained as follows:

$$|u_i| < 0.5,\ |v_i| < 0.55,\quad i = 1, 2.$$

The repulsive sets $\mathcal{V}_{\mathcal{P}}[p(t_i), P(t_i)]$ are constructed on the uniform time grid $\{t_i = i\,\Delta t\}$ with $\Delta t = 10^{-3}$. The same time sampling is used in the forward integration of the system including the repulsive disturbance (14).

It follows from the general theory of differential games (see [8]) that, in particular, for linear problems there exists a minimal repulsive set $\mathcal{V}_0 \subset [0, \theta] \times \mathbb{R}^d$. This set is also the maximal solvability set and, therefore, it has the following property. If $(t_0, x(t_0)) \notin \mathcal{V}_0$ then there exists a feedback disturbance $v(t, x)$ that prevents any trajectory $x(\cdot)$ from the penetration into $\mathcal{V}_0$. In the opposite case, there exists a feedback control $u(t, x)$ ensuring the condition $(t, x(t)) \in \mathcal{V}_0,\ t \in [t_0, \theta]$, for all trajectories. This alternative is sketched in Fig. 3.

For low-dimensional problems, $\mathcal{V}_0$ can be approximated using grid methods (see, for example, [3] and [4]). In the following simulation, such a grid scheme is used to approximate the cross sections $\mathcal{V}_0(t_i)$ for all time instants $t_i = i\,\Delta t$. For each current state $x(t_i) \in \mathcal{V}_0(t_i)$ it is possible to compute a control $u(t_i, x(t_i))$ which pushes the state vector into the next cross section $\mathcal{V}_0(t_{i+1})$ so that the feedback control $u(t_i, x(t_i))$ can approximately keep (in the discrete-time scheme) all trajectory inside $\mathcal{V}_0$ if the

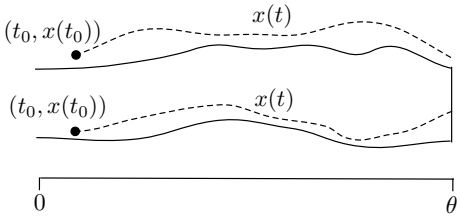

Fig. 3 Property of minimal repulsive tubes

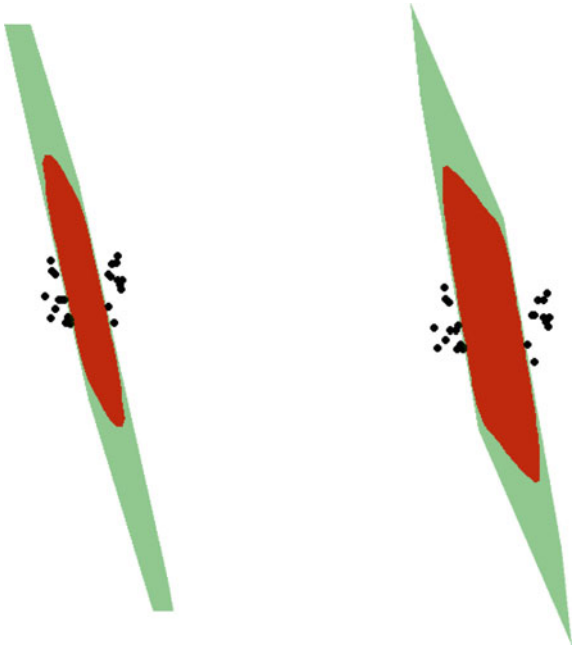

Fig. 4 The sets $\mathcal{V}_{\mathcal{P}}(t)$ (green) and $\mathcal{V}_0(t)$ (red) as well as the current state vectors (for various initial conditions) at $t = 0.0$ (left) and $t = 0.2$ (right)

initial state lies there. This control is used to implement the strategy of the first player in the simulation.

To test the constructed repulsive disturbance, twenty-five initial conditions were generated in the proximity of origin but outside of $\mathcal{V}_{\mathcal{P}}[p(0), P(0)]$. Resulting trajectories as well as cross sections of the repulsive tubes $\mathcal{V}_{\mathcal{P}}$ and $\mathcal{V}_0$ are shown in Figs. 4–6. The results are consistent with the theory: $\mathcal{V}_0(t_i) \subset \mathcal{V}_{\mathcal{P}}(t_i)$ for all t_i, and none of the trajectories penetrates into the tube $\mathcal{V}_{\mathcal{P}}$. Furthermore, one can see that the parallelotope tube $\mathcal{V}_{\mathcal{P}}$ provides a rather good upper estimate of the minimal repulsive tube $\mathcal{V}_0$ along the shortest axis of the parallelotope. This is in agreement with the previously discussed choice of the matrix Γ involved in the construction of $\mathcal{V}_{\mathcal{P}}$.

Remark 6 Note that the view direction in Figs. 4, 5, and 6 is always chosen orthogonal to the minimum width face of $\mathcal{V}_{\mathcal{P}}(t_i)$. Therefore, the view direction is rotating together with the tube $\mathcal{V}_{\mathcal{P}}$. In this way, it is possible to visually demonstrate that all trajectories remain outside of $\mathcal{V}_{\mathcal{P}}$ throughout the whole simulation.

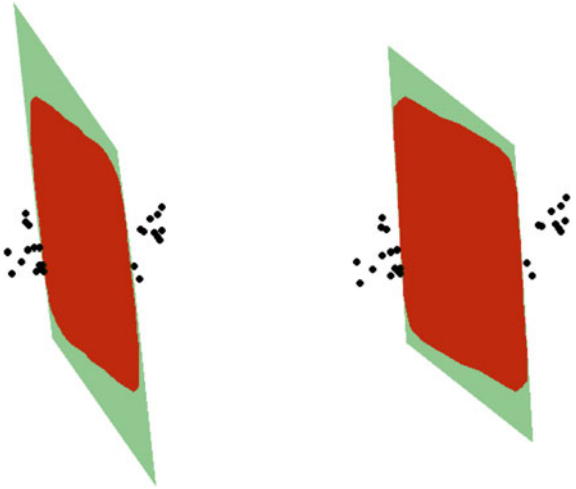

Fig. 5 The sets $\mathcal{V}_{\mathcal{P}}(t)$ (green) and $\mathcal{V}_0(t)$ (red) as well as the current state vectors (for various initial conditions) at $t = 0.4$ (left) and $t = 0.6$ (right)

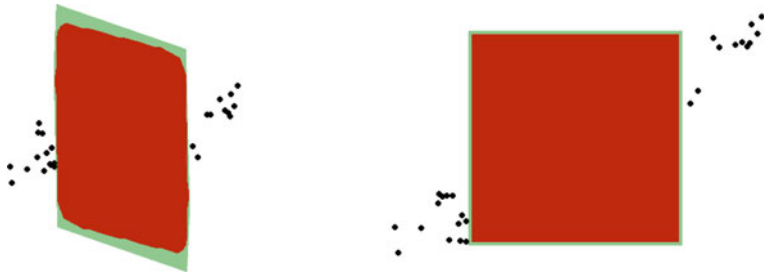

Fig. 6 The sets $\mathcal{V}_{\mathcal{P}}(t)$ (green) and $\mathcal{V}_0(t)$ (red) as well as the current state vectors (for various initial conditions) at $t = 0.8$ (left) and $t = 1.0$ (right)

6 Application: Nonlinear Model of Take-Off

In the following sections, the construction of a repulsive disturbance in a nonlinear model of aircraft take-off is presented. The model has already been considered in several papers devoted to aircraft control (cf. [10, 11]). In contrast to the mentioned works, the problem of finding a dangerous wind disturbance is now considered. More precisely, it is necessary to find a wind disturbance that maximizes the deviation of aerodynamic velocity and kinematic path inclination angle from their reference values.

6.1 Model Equations

A simplified aircraft model is under consideration.

First, the motion in a vertical plane is assumed. Second, the rigid body rotations are neglected to obtain a point-mass model. Third, the thrust force of the engine is kept constant.

The following notation is used:
$V \stackrel{\text{def}}{=}$ aerodynamic velocity of the aircraft, [m/s];
$\gamma \stackrel{\text{def}}{=}$ kinematic path inclination angle, [°];
$x \stackrel{\text{def}}{=}$ horizontal distance, [m];
$h \stackrel{\text{def}}{=}$ altitude, [m];
$\alpha \stackrel{\text{def}}{=}$ aerodynamic angle of attack, [°];
$\sigma \stackrel{\text{def}}{=}$ thrust inclination angle, [°];
$m \stackrel{\text{def}}{=}$ mass of the aircraft, [kg];
$g \stackrel{\text{def}}{=}$ gravitational constant, [m/s^2];
$P \stackrel{\text{def}}{=}$ thrust force, [N];
$D \stackrel{\text{def}}{=}$ drag force, [N];
$L \stackrel{\text{def}}{=}$ lift force, [N];
$\rho \stackrel{\text{def}}{=}$ density of air, [kg/m^3];
$S \stackrel{\text{def}}{=}$ wing area of the aircraft, [m^2];
$W_x \stackrel{\text{def}}{=}$ horizontal wind velocity at the location of the aircraft, [m/s];
$W_h \stackrel{\text{def}}{=}$ vertical wind velocity at the location of the aircraft, [m/s].

The following equations describe the simplified aircraft dynamics:

$$m\dot{V} = P\cos(\alpha+\sigma) - D - mg\,\sin\gamma - m\dot{W}_x\cos\gamma - m\dot{W}_h\sin\gamma, \tag{16}$$

$$mV\dot{\gamma} = P\sin(\alpha+\sigma) + L - mg\,\cos\gamma + m\dot{W}_x\sin\gamma - m\dot{W}_h\cos\gamma, \tag{17}$$

$$\dot{x} = V\cos\gamma + W_x, \tag{18}$$

$$\dot{h} = V\sin\gamma + W_h. \tag{19}$$

The thrust, drag, and lift forces in (16), (17) are approximated by polynomials:

$$P = A_0 + A_1 V + A_2 V^2,$$

$$D = \frac{1}{2}C_D\rho S V^2 \text{ with } C_D = B_0 + B_1\alpha + B_2\alpha^2,$$

$$L = \frac{1}{2}C_L\rho S V^2 \text{ with } C_L = \begin{cases} C_0 + C_1\alpha, & \alpha \le \alpha_{**} \\ C_0 + C_1\alpha + C_2(\alpha-\alpha_{**})^2, & \alpha > \alpha_{**}. \end{cases}$$

Here, the angle of attack, α, is the single control input governed by the pilot. The coefficients A_i, $i = 0, 1, 2$, depend on the altitude and air temperature, whereas

B_i and C_i, $i = 0, 1, 2$, are influenced by the position of flaps and chassis. Finally, m, S, ρ, δ, α_{**}, A_i, B_i, and C_i are constant parameters corresponding to Boeing-727 on take-off. The exact values of them can be found in [10].

The dynamics (16)–(19) is considered on the time interval $[0, \theta]$ with $\theta = 14\,\mathrm{s}$, and appropriate initial conditions are chosen.

The target set $\mathcal{M}$ is defined by maximum permissible deviation of V and γ from their reference values V_0 and γ_0 at $t = \theta$. That is,

$$|V(\theta) - V_0| \le \Delta V, \tag{20}$$

$$|\gamma(\theta) - \gamma_0| \le \Delta\gamma. \tag{21}$$

The reference values V_0 and γ_0 will be discussed below in more detail.

6.2 Relaxed Nonlinear Model

It can be observed that the right-hand sides of Eqs. (16), (17) do not depend on x and h. Therefore, these state variables and the corresponding Eqs. (18), (19) will be excluded from the consideration, keeping in mind that $x(t)$ and $h(t)$ can be reconstructed from $V(t)$ and $\gamma(t)$.

Moreover, jumps in the wind velocity components will be smoothed using first-order filters defined by PT1 transfer functions, which assumes the introduction of artificial disturbances v_1 and v_2, the inputs of these filters.

Thus, similar to [11], we arrive at the following nonlinear model:

$$m\dot{V} = Pcos(\alpha + \sigma) - D - mg\,\sin\gamma - m\dot{W}_x\cos\gamma - m\dot{W}_h\sin\gamma, \tag{22}$$

$$mV\dot{\gamma} = P\sin(\alpha + \sigma) + L - mg\,\cos\gamma + m\dot{W}_x\sin\gamma - m\dot{W}_h\cos\gamma, \tag{23}$$

$$\dot{W}_x = -k(W_x - v_1), \tag{24}$$

$$\dot{W}_h = -k(W_h - v_2). \tag{25}$$

Here, the coefficient $k = 0.5\,\mathrm{s}^{-1}$ defines the smoothing rate of the wind velocity components. The time derivatives $\dot{W}_x$ and $\dot{W}_h$ in (22), (23) are assumed to be replaced by the right-hand sides of (24), (25). The constraints on the artificial disturbances, v_1 and v_2, are chosen as follows:

$$|v_1| \le 13.7\,\mathrm{m/s},\ |v_2| \le 5.5\,\mathrm{m/s}. \tag{26}$$

Similar as in [10], the control parameter is constrained by the inequalities

$$0 \le \alpha \le 16^\circ. \tag{27}$$

Remark 7 Note that any wind disturbance designed for the relaxed system (22)–(25) produces, using (24) and (25), the same performance of V and γ in the original system (16)–(19). Therefore, repulsive disturbances will be designed for the relaxed system.

6.3 Linearization of the Relaxed Model

The relaxed system (22)–(25) is linearized around the reference values (cf. [11]) $V = V_0 = 84.1\,\text{m/s}$, $\gamma = \gamma_0 = 6.989°$, $\alpha = \alpha_0 = 10.367°$, $W_x = W_{x0} = 0$, $W_h = W_{h0} = 0$, $v_1 = 0$, and $v_2 = 0$. Here, the values of V_0, γ_0, and α_0 are chosen such that the right-hand sides of (22) and (23) are equal to zero. Note that the above reference values define a straight ascending trajectory. Such a line would be a perfect take-off path in the absence of wind disturbances. Denote $x_{ref} := (V_0,\ \gamma_0,\ W_{x0},\ W_{h0})^T$ and $u_{ref} := \alpha_0$.

6.4 Linear Conflict Control Problem

Having chosen the reference values, the linearization of the relaxed model yields the following linear conflict control problem (cf. [11]):

$$\dot{x} = A(x - x_{ref}) + B(u - u_{ref}) + Cv, \quad \text{for } t \in [0, \theta], \tag{28}$$

$$x(0) = x_{ref}. \tag{29}$$

Here, x, u, v, A, B, and C are defined as

$$x := \begin{pmatrix} V \\ \gamma \\ W_x \\ W_h \end{pmatrix}, \quad A := \begin{pmatrix} \frac{\partial \dot{V}}{\partial V} & \frac{\partial \dot{V}}{\partial \gamma} & \frac{\partial \dot{V}}{\partial W_x} & \frac{\partial \dot{V}}{\partial W_h} \\ \frac{\partial \dot{\gamma}}{\partial V} & \frac{\partial \dot{\gamma}}{\partial \gamma} & \frac{\partial \dot{\gamma}}{\partial W_x} & \frac{\partial \dot{\gamma}}{\partial W_h} \\ 0 & 0 & -k & 0 \\ 0 & 0 & 0 & -k \end{pmatrix},$$

$$B := \begin{pmatrix} \frac{\partial \dot{V}}{\partial \alpha} \\ \frac{\partial \dot{\gamma}}{\partial \alpha} \\ 0 \\ 0 \end{pmatrix}, \quad u := \alpha, \quad C := \begin{pmatrix} \frac{\partial \dot{V}}{\partial v_1} & \frac{\partial \dot{V}}{\partial v_2} \\ \frac{\partial \dot{\gamma}}{\partial v_1} & \frac{\partial \dot{\gamma}}{\partial v_2} \\ k & 0 \\ 0 & k \end{pmatrix}, \quad v := \begin{pmatrix} v_1 \\ v_2 \end{pmatrix}. \tag{30}$$

All partial derivatives are computed at x_{ref}, u_{ref}, and $v = (0, 0)^T$. Note that the state vector, control parameter, and disturbance inputs are the same as in the nonlinear relaxed model (22)–(25). Therefore, the target set $\mathcal{M}$ and the constraints on the control and disturbance inputs remain the same as in the nonlinear relaxed model.

Remark 8 The system (28)–(30) can be reduced to the form (1) by setting $\overline{x} := x - x_{ref}$, $\overline{u} := B(u - u_{ref})$ and $\overline{v} := Cv$. Obviously, the new target set $\overline{\mathcal{M}}$ and the constraints on the new control $\overline{u}$ and disturbance vector $\overline{v}$ are of the parallelotope type so that the new system satisfies the requirements of Sect. 3.

6.5 Generation of Disturbances

To construct a repulsive disturbance for the relaxed nonlinear model (22)–(25), a parallelotope tube $\mathcal{V}_{\mathcal{P}}$ is constructed for the linearized problem (28)–(30). More precisely, the cross sections $\mathcal{V}_{\mathcal{P}}(t_i) = \mathcal{V}_{\mathcal{P}}[p(t_i), P(t_i)]$ are computed for a time sampling. The disturbance in the relaxed nonlinear model at each time instant t_i is being chosen according to (8) based on the cross section $\mathcal{V}_{\mathcal{P}}(t_i)$.

It should be noted that the condition $x(0) \notin \mathcal{V}_{\mathcal{P}}[p(0), P(0)]$ is required for the application of the feedback rule (8). To satisfy this condition, a scheme with multiple target sets $\overline{\mathcal{M}}^{\mu}$ can be used. Here, $\mu \in \mathbb{R}^+$ is a scaling factor applied to the original target set $\overline{\mathcal{M}} = \mathcal{V}_{\mathcal{P}}[p_f, P_f]$. Therefore,

$$\overline{\mathcal{M}}^{\mu} = \mathcal{V}_{\mathcal{P}}[p_f, \mu\, P_f]. \tag{31}$$

Further, a set of scaling factors $\mu_1 < \mu_2 < \ldots < \mu_M$ is chosen, and multiple target sets $\overline{\mathcal{M}}^{\mu_1}, \ldots, \overline{\mathcal{M}}^{\mu_M}$ are defined according to formula (31). For each $\overline{\mathcal{M}}^{\mu_s}$, $s \in \overline{1, M}$, the corresponding parallelotope repulsive tube $\mathcal{V}_{\mathcal{P}}{}^{\mu_s}$ is constructed. At the current position $(t_i, x(t_i))$ an index $s \in \overline{1, M}$ is chosen in such a way that $x(t_i) \notin \mathcal{V}_{\mathcal{P}}{}^{\mu_s}(t_i)$ and $x(t_i) \in \mathcal{V}_{\mathcal{P}}{}^{\mu_{s+1}}(t_i)$. The repulsive disturbance is computed according to formula (8), based on $\mathcal{V}_{\mathcal{P}}{}^{\mu_s}(t_i) = [p(t_i),\ P^{\mu_s}(t_i)]$.

Remark 9 It is clear that $\mathcal{V}_{\mathcal{P}}{}^{\mu_k}(t_i) \subset \mathcal{V}_{\mathcal{P}}{}^{\mu_s}(t_i)$ whenever $\mu_k < \mu_s$. Therefore, for the linearized system (28)–(30), the repulsive property guarantees that the trajectory does not penetrate into the sets $\mathcal{V}_{\mathcal{P}}{}^{\mu_k}$ with $\mu_k \le \mu_s$ in future time steps. On the other hand, if the control (pilot) plays nonoptimally, the disturbance can achieve that $x(t_r) \notin \mathcal{V}_{\mathcal{P}}{}^{\mu_j}(t_r)$ with $\mu_j > \mu_s$ at some $t_r > t_i$. In such a case, the repulsive cross section $\mathcal{V}_{\mathcal{P}}{}^{\mu_j}(t_r)$ should be used at t_r to increase the deviation of the trajectory from the reference path.

The simulation results for the nonlinear relaxed model (22)–(25) with constraints on the disturbance and control given by (26) and (27) are shown in Figs. 7, 8, 9. Multiple target sets $\overline{\mathcal{M}}^{\mu_s}$, $s \in \overline{1, 25}$, with μ_s uniformly distributed in the interval [0.04; 1], are used. The right-hand sides of inequalities (20) and (21) are chosen

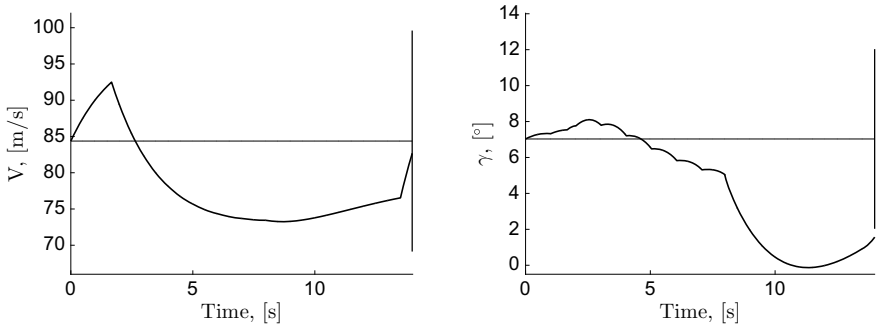

Fig. 7 Left: Aerodynamic velocity V of the aircraft and the reference value V_0 (thin horizontal line). Right: Kinematic path inclination angle γ and the reference value γ_0 (thin horizontal line). The vertical lines at $t = 14\,\mathrm{s}$ show the corresponding projections of the target set

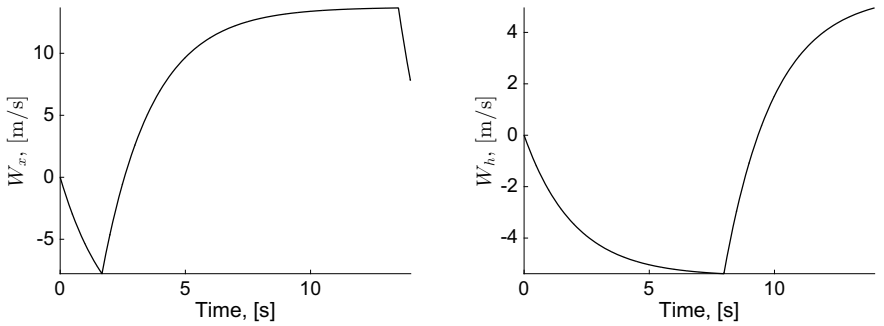

Fig. 8 Left: Horizontal wind velocity W_x along the trajectory (yielded by the disturbance command v_1). Right: Vertical wind velocity W_h along the trajectory (yielded by the disturbance command v_2)

as $\Delta V = 15.2\,\mathrm{m/s}$ and $\Delta\gamma = 5^\circ$, respectively. The repulsive tubes are constructed with the uniform time sampling $t_{i+1} - t_i = 10^{-3}\mathrm{s}$. To play against the repulsive disturbance, a quasi-optimal feedback control strategy $u(t, x)$ based on parallelotope approximations of solvability tubes (see [7]) is used. Such a strategy has already been successfully applied to problems of aircraft control (see [9]).

Simulation results show that the repulsive disturbance provides evasion from the target set, whereas constant disturbances whose values coincide with the vertices of the rectangle given by (26) cannot solve this problem. Figure 10 shows the comparison between the repulsive disturbance and the strongest constant disturbance, $v_1 \equiv -13.7\,\mathrm{m/s}$ and $v_2 \equiv 5.5\,\mathrm{m/s}$, providing the largest deviation among all constant disturbances.

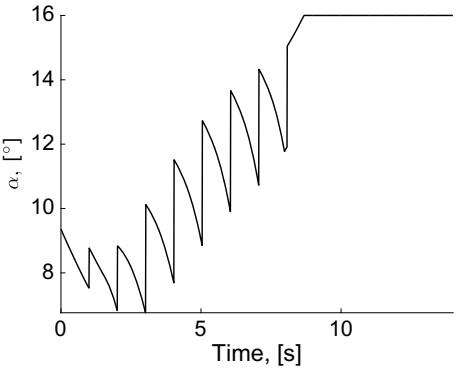

Fig. 9 Angle of attack α (pilot's control)

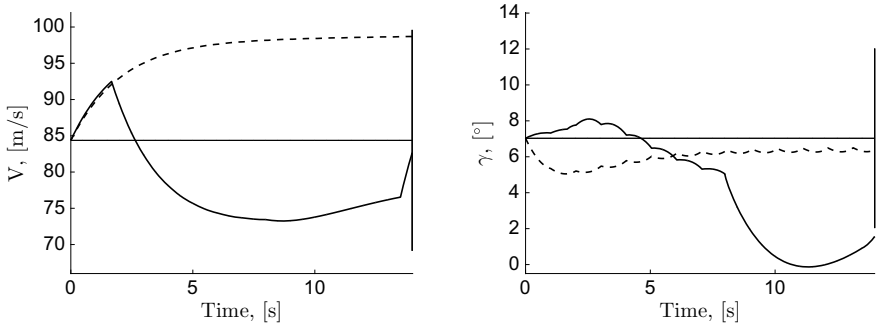

Fig. 10 Left: Aerodynamic velocity V for the repulsive (solid) and optimal constant (dashed) disturbances. Right: Kinematic path inclination angle γ for the repulsive (solid) and optimal constant (dashed) disturbances. The vertical lines at $t = 14$ s show the corresponding projections of the target set. The thin horizontal lines depict the reference values V_0 and γ_0

7 Application: Linear Model of Aircraft Lateral Dynamics

In this section, a repulsive disturbance for a linearized aircraft closed-loop dynamics of lateral motion (see [6]) is constructed. Such a model is derived under the assumption of horizontal balanced flight, which results in decoupling the longitudinal and lateral motions after the linearization.

7.1 Model Equations

The rigid body states for the linearized model of lateral motion are the yaw rate r, roll rate p, side-slip angle β, and roll angle Φ. Furthermore, second-order transfer functions of the form

$$\mathcal{G}(s) = \frac{\omega_0^2}{s^2 + 2d\omega_0 s + \omega_0^2} \tag{32}$$

with natural frequency ω_0 and damping constant d are employed to model the actuator dynamics of the primary control surfaces in the lateral plane. This results in additional states for the aileron position ξ_{pos} and angular rate ξ_{vel}, as well as the rudder position ζ_{pos} and angular rate ζ_{vel}. Moreover, a wind disturbance $V_{W,cmd}$ is introduced by using the following first-order lag filter

$$\dot{V}_W = \tau_W^{-1} \cdot (V_{W,cmd} - V_W) \tag{33}$$

with $\tau_W = 2$, which produces smooth wind profiles for the wind state V_W. Besides this wind disturbance, we additionally consider worst case pilot commands as disturbance inputs, which are the side load factor command δ_{n_y} and the roll angle command δ_Φ. As the control structure under investigation features a proportional and integral part for both the roll angle command and the side load force command, we also include the corresponding states of the integral parts denoted by e_Φ and e_{n_y} as states. Summarizing, the state vector for the linear system

$$\dot{x} = Ax + Cv, \quad \text{with } x(0) = 0 \tag{34}$$

comprises nine states, $x = \left[e_\Phi, e_{n_y}, r, \beta, p, \Phi, \xi_{pos}, \xi_{vel}, \zeta_{pos}, \zeta_{vel}\right]^T$, and the disturbance vector includes three components, $v = \left[\delta_{n_y}, \delta_\Phi, V_{W,cmd}\right]^T$, for the pilot and wind disturbance commands. These components are constrained as follows:

$$|\delta_{n_y}| \leq 0.1\,\text{rad}, \quad |\delta_\Phi| \leq 0.9, \quad |V_{W,cmd}| \leq 10\,\text{m/s}. \tag{35}$$

7.2 Construction of the Disturbance

In (34), the first two components of the state vector x stands for the integrated errors. Therefore, the aim of the disturbance is to maximize the functional $|x_1(\theta)| + |x_2(\theta)|$. This objective is associated with two-dimensional parallelotope target sets

$$\mathcal{M}^c := \mathcal{V}_\mathcal{P}\left[\begin{pmatrix}0\\0\end{pmatrix}, \begin{pmatrix}\frac{c}{\sqrt{2}} & \frac{c}{\sqrt{2}}\\ -\frac{c}{\sqrt{2}} & \frac{c}{\sqrt{2}}\end{pmatrix}\right] = \{x_1, x_2 : |x_1| + |x_2| \leq c\} \tag{36}$$

defined for different positive values of the parameter c.

Note that the approach of Sect. 3 requires the full dimensionality of the target set, i.e., it should involve *all* components of the state vector of system (34). In order to remain in two dimensions, equations (34) will be transformed using the following substitution:

$$y(t) = X(t, \theta)x(t). \tag{37}$$

Here, $X(t,\theta)$ is the fundamental matrix of the homogeneous system $\dot{x} = Ax$. More precisely, $X(t,\theta)$ satisfies the equations

$$\frac{\partial}{\partial t}X(t,\theta) = -X(t,\theta)A, \quad X(\theta,\theta) = Id, \tag{38}$$

with the corresponding identity matrix Id. Since the matrix A in (34) is constant, $X(t,\theta)$ can be computed as

$$X(t,\theta) = e^{A(\theta-t)}. \tag{39}$$

Combining (34), (37), and (38) yields the following system:

$$\dot{y} = X(t,\theta)Cv, \quad \text{with} \quad y(0) = 0. \tag{40}$$

The properties of X imply that $y(\theta) = x(\theta)$, and therefore, only the two first equations of (40) and the two-dimensional target sets $\mathcal{M}^c$ defined by (36) should be used. Similar to Sect. 6.5, a repulsive disturbance will be constructed using the technique of multiple target sets obtained by varying the parameter c in (36).

7.3 Validation Using Optimal Control Theory

It is interesting to compare the result obtained using the repulsive disturbance with that gained from solving an appropriate optimal control problem. In this comparison, the criterion to be maximized is the Mayer cost function $J_M = x_1(\theta) + x_2(\theta)$ which is evaluated at the fixed time instant $\theta = 4\,\text{s}$. In order to solve this optimal control problem numerically, the following trapezoidal collocation scheme, which assumes the uniformly spaced time grid with the discretization step length $t_{i+1} - t_i = \Delta t = 0.004\,\text{s}$, is used:

$$x_{i+1} = x_i + \Delta t \cdot \frac{f(x_i, v_i) + f(x_{i+1}, v_{i+1})}{2}. \tag{41}$$

Here $f(x,v) = Ax + Cv$ according to the notation (34), and the low indices correspond to the time sampling instants, e.g., $x_i = x(t_i)$ and $v_i = v(t_i)$. The initial state $x(t_0) = 0$ is enforced as equality constraint at the beginning of the time interval and the final state is free. The parameter optimization problem resulting from the discretization of the continuous-time optimal control problem is solved using an interior point solver with a feasibility and optimality tolerance of 10^{-7}. See [6] for more details.

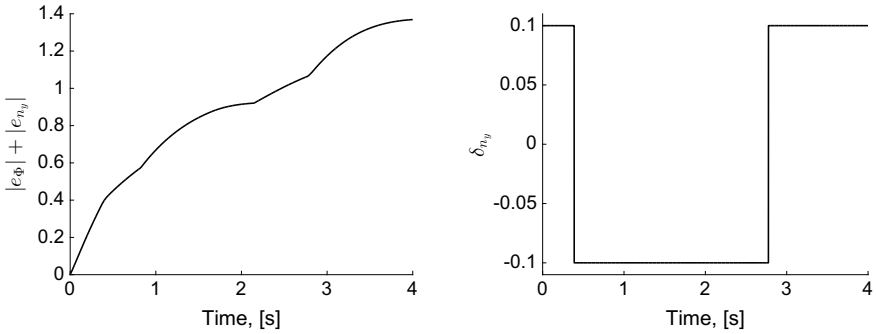

Fig. 11 Left: The absolute values sum of the error components e_Φ and e_{n_y} obtained with the repulsive disturbance. Right: Disturbance δ_{n_y}

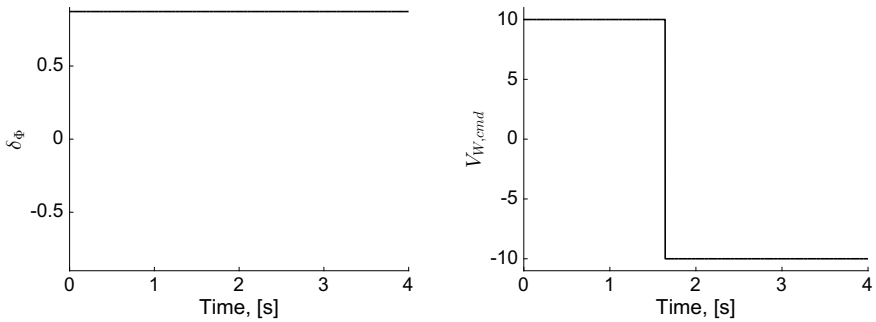

Fig. 12 Left: Disturbance δ_Φ. Right: Disturbance $V_{W,cmd}$

7.4 Simulation Results

Simulation results for the time interval $[0, \theta]$, $\theta = 4$ s, are shown in Figs. 11 and 12. As discussed in Sect. 6.5, the repulsive disturbance can be compared with extreme constant disturbances. In virtue of (35), there are eight extreme points of the disturbance constraint. However, only four of them should be considered due to the symmetry of the system equations. Figure 13 presents the comparison of the extreme and repulsive disturbances. Note that the extreme disturbances perform well, but the repulsive disturbance yields a better result.

Finally, the parallelotope-based repulsive disturbance is compared with that obtained from optimal control theory (see Sect. 7.3). Theoretically, the parallelotope-based repulsive disturbance cannot outperform the optimal one. Nevertheless, the results produced by the both disturbances are very close to each other as it is shown in Fig. 14. Furthermore, Figs. 14 and 15 demonstrate that the parallelotope-based repulsive disturbance and the optimal one produce very similar input signals.

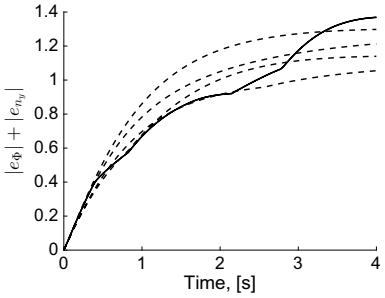

Fig. 13 The absolute values sum of the error components e_Φ and e_{n_y} obtained with the repulsive disturbance (solid line) and all possible constant extreme disturbances (dashed lines)

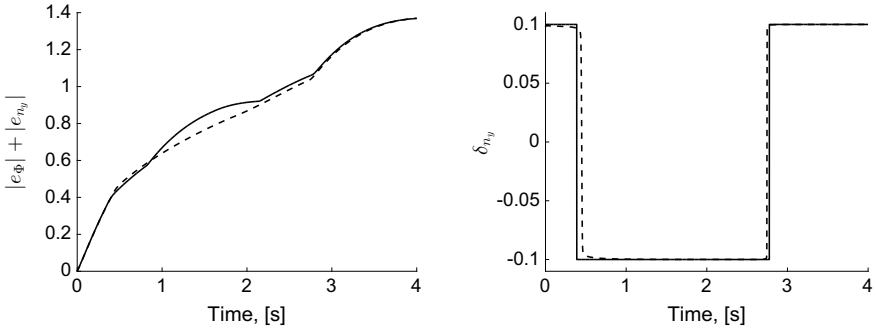

Fig. 14 Left: The absolute values sum of the error components e_Φ and e_{n_y} obtained with the repulsive disturbance (solid line) and the optimal control-based one (dashed line). Right: Disturbance δ_{n_y}, comparison of the repulsive disturbance (solid line) and the optimal control-based one (dashed line)

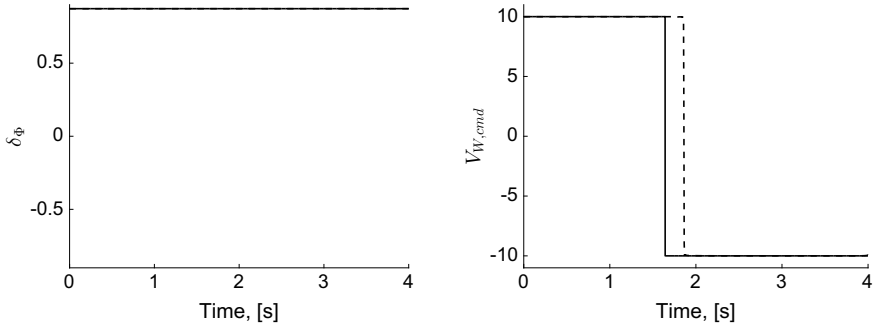

Fig. 15 Left: Disturbance δ_Φ, comparison of the repulsive disturbance (solid line) and the optimal control-based one (dashed line). The lines coincide. Right: Disturbance $V_{W,cmd}$, comparison of the repulsive disturbance (solid line) and the optimal control-based one (dashed line)

8 Conclusion

The results of Sects. 5–7 demonstrate that the method presented can be successfully applied to various types of control systems. In particular, promising results are obtained for a nonlinear model considered in Sect. 6 and a complex linear system treated in Sect. 7. As it is shown, the parallelotope-based repulsive disturbance is expected to provide a near-optimal result. In any case, it significantly outperforms constant extreme disturbances.

The main advantage of the method proposed is its applicability to high-dimensional conflict control problems. The computational efforts are relatively low so that the method may run in real time. Therefore, advanced aircraft models comprising numerous state variables, controllers, filters, etc. can be tested with this approach. One of the main future objectives is the implementation of the method on a real flight simulator.

Acknowledgments This work is supported by the DFG grant TU427/2-1 and HO4190/8-1 as well as TU427/2-2 and HO4190/8-2. Computer resources for this project have been provided by the Gauss Centre for Supercomputing/Leibniz Supercomputing Centre under grant: pr74lu.

References

1. Aubin, J.-P.: Viability Theory. Birkhäuser, Basel (2009)
2. Aubin, J.-P., Frankowska, H.: Set-Valued Analysis. Birkhäuser, Basel (2009)
3. Botkin, N. D., Hoffmann, K.-H., Turova, V. L.: Stable numerical schemes for solving Hamilton–Jacobi–Bellman–Isaacs equations. SIAM J. Sci. Comput. **33**(2), 992–1007 (2011)
4. Botkin, N. D., Hoffmann, K.-H., Mayer, N., Turova, V. L.: Approximation schemes for solving disturbed control problems with non-terminal time and state constraints. Analysis **31**, 355–379 (2011)
5. Botkin, N., Martynov, K., Turova, V., Diepolder, J.: Generation of dangerous disturbances for flight systems. Dynamic Games and Applications **9**(3), 628–651 (2019)
6. Diepolder, J., Gabrys, A., Schatz, S., Bittner, M., Grüter, B., Holzapfel, F., Ben-Asher, J. Z.: Flight control law clearance using worst-case inputs. In: ICAS 30th International Congress of the International Council of the Aeronautical Sciences. ICAS (2016)
7. Kostousova, E. K.: On target control synthesis under set-membership uncertainties using polyhedral techniques. In: Pötzsche, C. et al. (eds.) System Modeling and Optimization, vol. 443, pp. 170–180. Springer-Verlag, Berlin, Heidelberg (2014)
8. Krasovskii, N. N., Subbotin, A. I.: Game-Theoretical Control Problems. Springer, New York (1988)
9. Martynov, K., Botkin, N. D., Turova, V. L., Diepolder, J.: Real-time control of aircraft take-off in windshear. Part I: Aircraft model and control schemes. In: 2017 25th Mediterranean Conference on Control and Automation (MED), pp. 277–284. IEEE (2017)
10. Miele, A., Wang, T., Melvin, W. W.: Optimal take-off trajectories in the presence of windshear. J. Optimiz. Theory App. **49**(1), 1–45 (1986)

11. Turova, V. L.: Application of numerical methods of the theory of differential games to the problems of take-off and abort landing. Trudy Inst. Math. Mech UrO RAN **2**, 188–201 (1992) [in Russian]
12. Zarkh, M. A., Patsko, V. S.: The second player's strategy in a linear differential game. J. Appl. Math. Mech-USS **51**(2), 150–155 (1987)

Isaacs' Two-on-One Pursuit-Evasion Game

Meir Pachter

1 Introduction

In this paper, Isaacs' "Two Cutters and a Fugitive Ship" differential game is revisited. We consider the pursuit-evasion differential game in the Euclidean plane where two pursuers P_1 and P_2, say cutters, chase a fugitive ship, the evader E. All move with simple motion à la Isaacs, the speeds of the cutters each being greater than that of the fugitive ship. Coincidence of E with either one, or both, P_1 and/or P_2, is capture, and time of capture is the payoff of E and the cost of the P_1 & P_2 team. Interestingly, the Two Cutters and Fugitive Ship pursuit game was posed by Hugo Steinhaus back in 1925—his original paper was reprinted in 1960 in [2].[1] The solution of the differential game, sans its justification, is presented in Isaacs' ground breaking book [1, Example 6.8.3, pp. 148–149]. In [1] the players' optimal strategies were derived using a geometric method. In [3] a preliminary attempt at justifying the geometric method was undertaken. In this paper, we provide a proof of the correctness of the geometrically derived optimal pursuit and evasion strategies

[1] Hugo Steinhaus, was a contemporary of Borel and Von Neumann who are credited with laying the foundations of game theory. Borel and Von Neumann mainly considered static games, a.k.a. games in normal form, while referring to dynamic games as games in extensive form, believing that dynamic games can be easily transformed to static games. The requirement of time consistency/subgame perfectness in dynamic games came to the attention of game theorists only in the seventies. From the outset, Steinhaus was certainly attuned to thinking about dynamic games, a.k.a., differential games.

The views expressed in this article are those of the author and do not reflect the official policy or position of the United States Air Force, Department of Defense, or the US Government.

M. Pachter (✉)
Air Force Institute of Technology, Dayton, OH, USA
e-mail: meir.pachter@afit.edu

D. M. Ramsey and J. Renault (eds.), *Advances in Dynamic Games*,
Annals of the International Society of Dynamic Games 17,
https://doi.org/10.1007/978-3-030-56534-3_2

using Isaacs' method for the systematic solution of differential games. The three players' state feedback optimal strategies are synthesized and the Value of the game is derived. The geometric method for solving the Two Cutters and Fugitive Ship differential game is fully justified. Some geometric features, perhaps overlooked by Isaacs, but with a bearing on extensions, are addressed: The state space regions where pursuit devolves into Pure Pursuit (PP) by either P_1 or P_2, or into a pincer movement pursuit by the P_1 & P_2 team who cooperatively chase the evader, are characterized. Thus, a complete solution of the Game of Kind is provided. The analysis undertaken herein provides a vehicle for discussing some salient features of general pursuit-evasion differential games, and opens the door to employing the geometric method to consider operationally relevant group pursuit/swarm attack tactics.

The paper is organized as follows. The geometric method employed by Isaacs to solve the Two Cutters and Fugitive Ship differential game is expounded on in Sect. 2. In Sect. 3 a three-states reduced state space reformulation of the Two Cutters and Fugitive Ship differential game is introduced and the geometric method is employed to yield the players' optimal state feedback strategies and the game's Value function in closed form. Furthermore, the state space regions where either one of the pursuers captures the evader and the state space region where both pursuers cooperatively and isochronously capture the evader are characterized, thus solving the Game of Kind. The reduced state space formulation is required in order to apply Isaacs' method for the systematic solution of differential games to the Two Cutters and Fugitive Ship differential game and prove the correctness of the geometric method. Due to symmetry, it is sufficient to present the solution of the differential game in the positive orthant of the reduced state space. The solution process is presented in Sect. 4: The protagonists' strategies previously obtained using the geometric method are recovered, thus validating the geometric method and providing the solution of the Game of Degree. As it so often happens in differential games, the doctrinaire employment of Isaacs' method towards the solution of even this "simple" differential game is not devoid of complexity. However, the intuition provided by the heuristic geometric approach is instrumental in facilitating the solution process. The Two Cutters and Fugitive Ship is a differential game whose Value function is C^1 in the positive orthant of the reduced state space. The reduced state space of the Two Cutters and Fugitive Ship differential game comprises the first and third quadrants of R^3. The half plane $\{(x, y, z) \mid x \geq 0, y = 0\}$ is a surface of symmetry and the half plane $\{(x, y, z) \mid x \geq 0, z = 0\}$ is a surface of symmetry and also a dispersal surface, where the Value function of the differential game is not differentiable. While dispersal surfaces in differential games are prone to spawning singular surfaces of equivocal or focal type, this is *not* the case in the Two Cutters and Fugitive Ship differential game. The optimal flow field consists of regular trajectories only, and there are no singular surfaces, except the above mentioned "benign" dispersal surface. Conclusions are presented in Sect. 5, where possible extensions are also discussed. In this paper, the solution of the Game of Kind is provided and the geometric method for obtaining the solution of the Game of Degree and thus solving the Two Cutters and Fugitive Ship differential game, is fully justified.

Interestingly, it has been suggested by one of the referees that Isaacs' Two Cutters and Fugitive Ship differential game could also have been addressed building on the method expounded in Ref. [4].

2 The Geometric Method

Without much loss of generality, we assume that the fast pursuers P_1 and P_2 have equal speed, which we normalize to 1. The problem parameter is the speed of the evader E which is $0 \leq \mu < 1$.

There are three players in the Euclidean plane so the realistic state space is obviously R^6;, however, the state space could be reduced to R^4 by collocating the origin of a non- rotating (x, y) Cartesian frame at E's instantaneous position. Since the players are holonomic, the dynamics A matrix is 0—there are no dynamics. This, and the fact that the performance functional is the time-to-capture, yields a Hamiltonian s.t. the costates are all constant. This suggests that the optimal flow field might consist of straight line trajectories. Hence geometry might come into play. Thus, Isaacs directly used a geometric method for the solution of pursuit-evasion games with simple motion, well aware that this might not always be possible, as he amply demonstrated with the Obstacle Tag Chase differential game where the presence of a state constraint brings about the violation of the requirement in dynamic games of time consistency/subgame perfectness. To obtain, albeit without proof, the Two Cutters and Fugitive Ship differential game's solution, Isaacs successfully employed the geometric concept of an Apollonius circle—see Sect. 2.1 below—to delineate the Safe Region (SR) and the Boundary of a Safe Region (BSR) for the Evader. The Apollonius circle concept is conducive to the geometric solution of the Two Cutters and Fugitive Ship differential game, as will be demonstrated in the sequel.

2.1 Apollonius Circle

For the sake of completeness, we provide the geometry of Apollonius circles which will prominently feature in the geometric solution of this differential game with two pursuers and one evader and also in extensions where multiple pursuers are employed. An Apollonius circle is the locus of all points in the plane s.t. the ratio of the distances to two fixed points in the plane, also referred to as foci, is constant; in our case the ratio in question is the Pursuer/Evader speed ratio parameter $\mu < 1$ and the foci are the instantaneous positions of E and P. The Apollonius circle is illustrated in Fig. 1.

The three points P, E and the center O of the Apollonius circle are collinear and E is located between P and O. Let the E-P distance be d. The radius of the Apllonius circle is then

Fig. 1 Apollonius circle

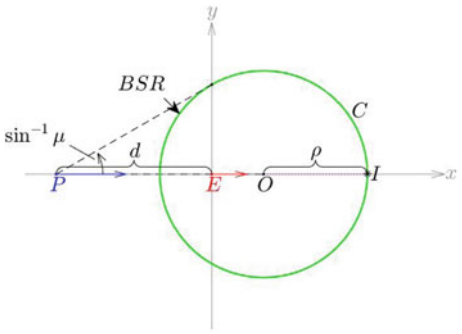

$$\rho = \frac{\mu}{1-\mu^2} d \tag{1}$$

and in Fig. 1 the coordinates of the center of the Apollonius circle are

$$x_O = \frac{\mu^2}{1-\mu^2} d, \quad y_O = 0. \tag{2}$$

2.2 *Isaacs' Geometric Solution*

We first present the solution of the Two Cutters and Fugitive Ship differential game in the realistic plane using the geometric method. Two Apollonius circles, $\mathscr{C}_1$, whose foci are at E and P_1 and the Apollonius circle $\mathscr{C}_2$, whose foci are at E and P_2, feature in this game. E is in the interior of both Apollonius disks but the two Apollonius circles might or might not intersect. Concerning the calculation of the points of intersection, if any, of the Apollonius circles $\mathscr{C}_1$ and $\mathscr{C}_2$: Subtracting the equation of circle $\mathscr{C}_1$ from the equation of circle $\mathscr{C}_2$ yields a linear equation in two unknowns, say, X and Y. One can thus back out Y as a function of X and insert this expression into one of the circle equations, thus obtaining a quadratic equation in X: The calculation of the two points of intersection of the Apollonius circles $\mathscr{C}_1$ and $\mathscr{C}_2$ boils down to the solution of a quadratic equation. The Apollonius circles intersect iff the quadratic equation has real solutions, in other words, the discriminant of the quadratic equation is positive. When the discriminant of the quadratic equation is negative we are automatically notified that the Apollonius circles don't intersect, and because E is in the interior of both Apollonius disks, we conclude that one of the Apollonius disks is contained in the interior of the second Apollonius disk. If $\rho_2 > \rho_1$, which is the case iff E is closer to P_1 than to P_2—see Eq. (1)—the circle $\mathscr{C}_2$ is discarded, and vice versa. The geometry is illustrated in Fig. 2. When the Apollonius circles don't intersect, the pursuer associated with the outer Apollonius circle is irrelevant to the chase. This is so because the configuration is s.t. should P_1 employs PP and E run for his life, player P_2 cannot reach E before the latter is captured by P_1 because he is too far away

Fig. 2 One cutter action

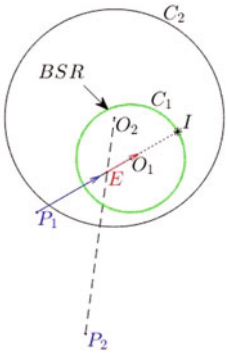

from the P_1/E engagement, or is too slow to close in and join the fight. This renders player P_2 irrelevant. As far as the geometric method is concerned, the Apollonius disk associated with player P_1 is then contained in the interior of the bigger Apollonius disk associated with player P_2, as illustrated in Fig. 2. In this case, the pursuer P_1 on which the inner Apollonius circle is based will singlehandedly capture the evader: He will optimally employ PP while the Evader runs for his life and will be captured at I; the game with two pursuers devolved to the simple pursuit-evasion game with one pursuer and one evader where P_1 employs PP and E runs away from P_1. Similarly, if the Apollonius disk associated with P_2 is contained in the interior of the bigger Apollonius disk associated with player P_1, player P_2 will employ PP while E runs for his life; P_1 is then redundant.

The case considered in [1] where the discriminant of the quadratic equation is positive and the Apollonius circles intersect is illustrated in Fig. 3. Since there are two pursuers, similar to Fig. 6.8.5 in [1], a lens-shaped BSR is formed by the intersection of the two Apollonius circles. To calculate the aim point I which is one of the two points where the Apollonius circles $\mathscr{C}_1$ and $\mathscr{C}_2$ intersect requires solving a quadratic equation; the quadratic equation has two real solutions and among the two points of intersection of the Apollonius circles, the aim point I is the point farthest from E. Thus, E heads toward the most distant point I on the BSR, and so do P_1 and P_2. Thus, it would seem that both pursuers P_1 and P_2 will be active and cooperatively and isochronously capture the evader at point I, as shown in Fig. 3. It is noteworthy that during optimal play the Apollonius circles shrink but the players' aim point I remains fixed. Thus, in contrast to the Obstacle Tag Chase game, time consistency/subgame perfectness is not violated. This bodes well for the correctness of the geometric approach.

When the discriminant of the quadratic equation is zero the quadratic equation has a repeated real root. Geometrically this means that one of the Apollonius circles is tangent from the inside to the second Apollonius circle. The following holds.

Proposition 1 *Assume the Apollonius circles $\mathscr{C}_1$ and $\mathscr{C}_2$ are tangent, that is, the discriminant of the quadratic equation vanishes. The aim point of the three players*

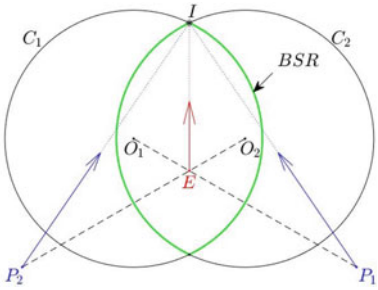

Fig. 3 Solution of two cutters and fugitive ship game

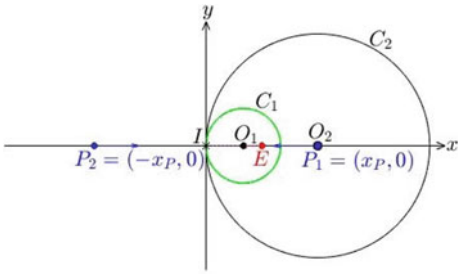

Fig. 4 PP by P_1 *and* P_2

is then the circles' point of tangency, say T, that is, I=T, iff the three players E, P_1 *and* P_2 *are collinear and E is sandwiched between* P_1 *and* P_2.

Thus, when the Apollonius circles $\mathscr{C}_1$ and $\mathscr{C}_2$ are tangent and their point of tangency T is s.t. T = I, the points P_2, T, O_1, E, O_2 and P_1 are collinear and both pursuers employ PP to isochronously capture the evader. This is illustrated in Fig. 4. Note however that when, as above, P_1, P_2 and E are collinear and E is sandwiched between P_1 and P_2, but the Apollonius circles intersect, E will break out—see Fig. 5. If the Apollonius circles $\mathscr{C}_1$ and $\mathscr{C}_2$ are tangent, however E is not on the segment $\overline{P_1 P_2}$, the players' aim point I is not the circles' point of tangency T: If the tangent Apollonius circles are s.t. the Apollonius circle $\mathscr{C}_1$ is contained in the Apollonius disk formed by the Apollonius circle $\mathscr{C}_2$, optimal play then consists of the active player being P_1 and employing PP while E runs away from P_1 and player P_2 is redundant; and if the Apollonius circle $\mathscr{C}_2$ is contained in the Apollonius disk formed by the Apollonius circle $\mathscr{C}_1$, optimal play then consists of the active player being P_2 and employing PP while E runs away from P_2, and now player P_1 is redundant; the circles' point of tangency T plays no role here. This should alert us to the fact that even though the Apollonius circles intersect at their point of tangency, that is, $\mathscr{C}_1 \cap \mathscr{C}_2 \neq \emptyset$ and $T \in \mathscr{C}_1 \cap \mathscr{C}_2$, the players' aim point $I \notin \mathscr{C}_1 \cap \mathscr{C}_2$. The fact that the two Apollonius circles intersect does not automatically imply that during optimal play *both* pursuers will cooperatively and isochronously capture the evader. As we shall see, there are instances where although the Apollonius circles intersect, during optimal play just one of the pursuers singlehandedly captures the evader.

Fig. 5 Breakout of E

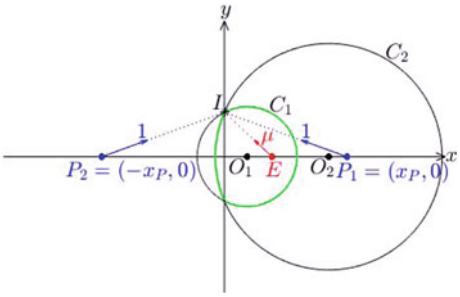

Fig. 6 Solution of the game of kind in the realistic plane

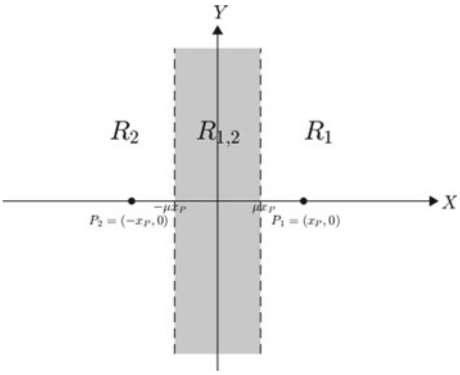

In summary, the solution in the realistic plane of the Game of Kind is illustrated in Fig. 6. Given the position of the pursuers, during optimal play, when the evader is initially in the region R_1 to the right of the right broken line, he will be singlehandedly captured by P_1 in Pure Pursuit (PP), when he is initially in the region R_2 to the left of the left broken line, he will be singlehandedly captured by P_2 in PP, and when the evader is initially in the shaded region $R_{1,2}$ between the right and left broken lines he will isochronously be captured by both pursuers P_1 and P_2. When the evader is initially on the right broken line he will isochronously be captured by both pursuers P_1 and P_2, with P_1 in PP and when the evader is initially on the left broken line he will isochronously be captured by both pursuers P_1 and P_2, with P_2 in PP.

3 Geometric Solution in Reduced State Space

The dimension of the Two Cutters and Fugitive Ship game's state space can be reduced to three using a non-inertial, rotating reference frame, by pegging the x-axis to P_1 and P_2's instantaneous positions. The y-axis is the orthogonal bisector of the $\overline{P_1 P_2}$ segment. In this rotating (x, y) reference frame the states are E's x- and y-coordinates (x_E, y_E) and the x-position x_P of P_1. In this reduced state space the

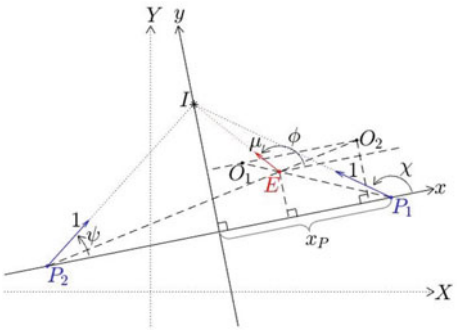

Fig. 7 Rotating reference frame

y-coordinate of P_1 will always be 0 and the position of P_2 will be $(-x_P, 0)$. Due to symmetry, without loss of generality we assume $x_E \geq 0$ and $y_E \geq 0$. The rotating reference frame (x, y) is shown overlaid on the realistic plane (X, Y) in Fig. 7 where the P_1, E and P_2 players' headings χ, ϕ and ψ are also indicated. Without loss of generality, the rotating reference frame (x, y) is initially aligned with the inertial frame (X, Y). Using the rotating reference frame (x, y), the state space of the Two Cutters and Fugitive Ship differential game is reduced to the first and third quadrant of R^3, that is, the set $R^3_1 \cup R^3_3$, where

$$R^3_1 \equiv \{(x_P, x_E, y_E) \mid x_P \geq 0, y_E \geq 0\}, \quad R^3_3 \equiv \{(x_P, x_E, y_E) \mid x_P \geq 0, y_E \leq 0\}.$$

There are two half planes of symmetry, $\{(x_P, x_E, y_E) \mid x_P \geq 0, x_E = 0\}$ and $\{(x_P, x_E, y_E) \mid x_P \geq 0, y_E = 0\}$, the latter also being a dispersal surface. Symmetry allows us to confine our attention to the case where $x_E \geq 0$, $y_E \geq 0$, that is, the state will evolve in the positive orthant of R^3, that is, in

$$R^3_+ = \{(x_P, x_E, y_E) \mid x_P \geq 0, x_E \geq 0, y_E \geq 0\},$$

where the three-state nonlinear dynamics of the Two Cutters and Fugitive Ship differential game are

$$\dot{x}_P = \frac{1}{2}(\cos\chi - \cos\psi), \ x_P(0) = x_{P_0} \tag{3}$$

$$\dot{x}_E = \mu\cos\phi - \frac{1}{2}(\cos\chi + \cos\psi) + \frac{1}{2}\frac{y_E}{x_P}(\sin\chi - \sin\psi), \ x_E(0) = x_{E_0} \tag{4}$$

$$\dot{y}_E = \mu\sin\phi - \frac{1}{2}(\sin\chi + \sin\psi) - \frac{1}{2}\frac{x_E}{x_P}(\sin\chi - \sin\psi), \ y_E(0) = y_{E_0}. \tag{5}$$

3.1 Game of Kind in Reduced State Space

The solution of the Game of Kind in the reduced state space (x_P, x_E, y_E) using the geometric method proceeds as follows.

We have two Apollonius circles: $\mathscr{C}_1$ is based on the instantaneous positions of E and P_1, and $\mathscr{C}_2$ is based on the instantaneous positions of E and P_2. In the (x,y) frame, see Fig. 6 and Eq. (2), the center O_1 of the Apollonius circle $\mathscr{C}_1$ is at

$$x_{O_1} = \frac{1}{1-\mu^2}(x_E - \mu^2 x_P),\ y_{O_1} = \frac{1}{1-\mu^2} y_E$$

Similarly, the center O_2 of the Apollonius circle $\mathscr{C}_2$ is at

$$x_{O_2} = \frac{1}{1-\mu^2}(x_E + \mu^2 x_P),\ y_{O_2} = \frac{1}{1-\mu^2} y_E$$

Thus, using Eq. (1), the equation of the Apollonius circle $\mathscr{C}_1$ is

$$[x - \frac{1}{1-\mu^2}(x_E - \mu^2 x_P)]^2 + (y - \frac{1}{1-\mu^2} y_E)^2 = \frac{\mu^2}{(1-\mu^2)^2}[(x_E - x_P)^2 + y_E^2] \tag{6}$$

and the equation of the Apollonius circle $\mathscr{C}_2$ is

$$[x - \frac{1}{1-\mu^2}(x_E + \mu^2 x_P)]^2 + (y - \frac{1}{1-\mu^2} y_E)^2 = \frac{\mu^2}{(1-\mu^2)^2}[(x_E + x_P)^2 + y_E^2] \tag{7}$$

In the (x, y) reference frame the y-coordinate of the $\mathscr{C}_1$ and $\mathscr{C}_2$ Apollonius circles' centers is the same and therefore the distance d between the circles' centers is

$$d = x_{O_2} - x_{O_1} = \frac{2\mu^2}{1-\mu^2} x_P$$

Hence, because the radii of the Apollonius circles are s.t. $\rho_1 < \rho_2\ iff\ x_E > 0$, the Apollonius circles $\mathscr{C}_1$ and $\mathscr{C}_2$ intersect $iff\ d + \rho_1 > \rho_2$, that is,

$$2\mu x_P + d_1 > d_2$$

In other words, the inequality holds

$$2\mu x_P > \sqrt{(x_P + x_E)^2 + y_E^2} - \sqrt{(x_P - x_E)^2 + y_E^2}$$

which yields the algebraic condition: The Apollonius circles $\mathscr{C}_1$ and $\mathscr{C}_2$ intersect iff

$$\mu^2 y_E^2 + (1-\mu^2)(\mu^2 x_P^2 - x_E^2) \geq 0. \tag{8}$$

In light of this, the upper part R_1^3 of the reduced state space is partitioned as follows:

$$R_1^3 = R_1 \cup R_2 \cup R_{1,2}.$$

During optimal play in R_1, E is captured solely by P_1 while P_2 is redundant, in R_2, E is captured solely by P_2 while P_1 is redundant, while in $R_{1,2}$ E is isochronously captured by P_1 and P_2. At this point it appears that things stand as follows. If condition (8) does not hold and $x_E > 0$ the state is in R_1, where E is captured solo by P_1. If condition (8) does not hold and $x_E < 0$ the state is in R_2, where E is captured solo by P_2: From a kinematic point of view, the state is in R_1 if Collision Course (CC) guidance won't allow P_2 to capture E who is running away from P_1, before P_1, using Pure Pursuit (PP), captures E. Similarly, the state is in R_2 if CC guidance won't allow P_1 to capture E who is running away from P_2, before P_2, using PP, captures E. As far as geometry is concerned, let D_i denote the disk which corresponds to the Apollonius circle $\mathscr{C}_i$, $i = 1, 2$. In view of the discussion from above, it would appear that the set R_1 is characterized by $D_1 \subset D_2$—see Fig. 2; similarly, the set R_2 is characterized by $D_2 \subset D_1$, and if condition (8) holds—see Fig. 3 where the Apollonius circles $\mathscr{C}_1$ and $\mathscr{C}_2$ intersect—one might then be inclined to think that the state is in $R_{1,2}$, so that during optimal play E is isochronously captured by P_1 and P_2. And as far as the characterization of the sets R_1 and R_2 is concerned, since $x_E \geq 0$ implies $\rho_1 \leq \rho_2$, the disk D_2 cannot be contained in the disk D_1, so either $D_1 \subset D_2$ or the Apollonius circles $\mathscr{C}_1$ and $\mathscr{C}_2$ intersect. The geometric condition

$$D_1 \subset D_2 \;\Rightarrow\; d + \rho_1 < \rho_2$$

lets us recover the algebraic condition (8):

$$\mathscr{C}_1 \cap \mathscr{C}_2 \neq \emptyset \;\Leftrightarrow\; d + \rho_1 > \rho_2 \;\Leftrightarrow\; \mu^2 y_E^2 + (1-\mu^2)(\mu^2 x_P^2 - x_E^2) > 0,$$

as expected. The algebraic condition (8) delineates the set in R_+^3,

$$\mathscr{K}_1 = \{(x_P, x_E, y_E) \mid x_P \geq 0, x_E \geq 0, \mu^2 y_E^2 + (1-\mu^2)(\mu^2 x_P^2 - x_E^2) < 0\}.$$

This is a cone whose x_E cross sections are arcs of ellipses—see Fig. 10. When the state is in the interior of the elliptical cone $\mathscr{K}_1$ or in its projection onto the plane $y_E = 0$, $D_1 \subset D_2$ and so E is captured by P_1 only. Thus, one is inclined to set $R_1 \equiv \mathscr{K}_1$. Similarly, when the state is in the interior of the elliptical cone

$$\mathscr{K}_2 = \{(x_P, x_E, y_E) \mid x_P \geq 0, x_E \leq 0, \mu^2 y_E^2 + (1-\mu^2)(\mu^2 x_P^2 - x_E^2) < 0\}$$

or in its projection onto the plane $y_E = 0$, $D_2 \subset D_1$ and so E is captured by P_2 only; the set $\mathscr{K}_2$ is the mirror image of the cone $\mathscr{K}_1$ about the plane $x_E = 0$ and one is inclined to set $R_2 \equiv \mathscr{K}_2$. The boundary of the elliptical cone $\mathscr{K}_1$ is the set of states s.t. the Apollonius circle $\mathscr{C}_1$ is contained in the Apollonius disk formed by the bigger circle $\mathscr{C}_2$ and is tangent to the Apollonius circle $\mathscr{C}_2$; similarly, the boundary of the elliptical cone $\mathscr{K}_2$ is the set of states s.t. the Apollonius circle $\mathscr{C}_2$ is contained in the Apollonius disk formed by the bigger circle $\mathscr{C}_1$ and is tangent to the Apollonius circle $\mathscr{C}_1$. When the state is on the boundary of the elliptical cones $\mathscr{K}_1$ or $\mathscr{K}_2$ the Apollonius circles $\mathscr{C}_1$ and $\mathscr{C}_2$ are tangent, say, at point T. According to Proposition 1, the players' aim point I is the point of tangency T of the Apollonius circles iff $y_E = 0$ and the tangent to the Apollonius circles at $T = I$ is the orthogonal bisector of the segment $\overline{P_1 P_2}$; and from Eq. (8) we deduce $x_E = \mu x_P$; E is then isochronously captured by P_1 and P_2 who employ PP—as illustrated in Fig. 4. Note that if $x_E = 0$, condition (8) holds, so the quarter plane $\{(x_P, x_E, y_E) \mid x_P \geq 0, x_E = 0, y_E \geq 0\} \subset R_{1,2}$ and E is isochronously captured by P_1 and P_2. Obviously E is also isochronously captured by P_1 and P_2 when $x_P = 0$. And so far, it would appear that during "optimal" play, when the state is outside the elliptical cones $\mathscr{K}_1$ and $\mathscr{K}_2$ where the inequality (8) holds, that is, the state is in what appears to be $R_{1,2}$, E will be isochronously captured by the P_1 &P_2 team. Thus, at first blush it would appear that Eq. (8) characterizes the set $R_{1,2}$. However, as will become apparent in the sequel, although in the set $R_{1,2}$ the inequality (8) holds, it also holds in subsets of R_1 and R_2: Eq. (8) does *not* characterize the set $R_{1,2}$.

We must properly characterize the state space regions R_1, R_2 and $R_{1,2}$ in R_1^3. The inequality (8) does not provides the answer and it will be replaced by an alternative condition. In this respect, consider the following. In Fig. 2 let the points E and P_2 be fixed while point P_1 is moved in a clockwise direction, keeping the $P_1 - E$ distance d_1 constant so that the Apollonius circles $\mathscr{C}_1$ and $\mathscr{C}_2$ will eventually intersect, whereupon the inequality (8) will hold. The radius ρ_1 of the Apollonius circle $\mathscr{C}_1$ is kept constant while it is approaching the Apollonius circle $\mathscr{C}_2$ from the inside. The Apollonius circle $\mathscr{C}_1$ first meets the Apollonius circle $\mathscr{C}_2$ tangentially and if the segment $\overline{P_1 E}$ rotates some more clockwise, the circles start intersecting. When this initially happens, the point I in Fig. 2 is still in the interior of the disk formed by the Apollonius circle $\mathscr{C}_2$. Thus, although the Apollonius circles intersect and condition (8) holds, E nevertheless flees toward point I with P_1 in hot pursuit, as if the configuration would have been as illustrated in Fig. 2 where the Apollonius circle $\mathscr{C}_1$ is in the interior of the Apollonius disk formed by the Apollonius circle $\mathscr{C}_2$; it is only when point I on the extension of the segment $\overline{E O}_1$ meets the Apollonius circle $\mathscr{C}_2$ and then exists the disk formed by the Apollonius circle $\mathscr{C}_2$, that both pursuers, P_1 *and* P_2 cooperatively and isochronously capture E in a pincer maneuver. Thus, although the Apollonius circles do intersect, it nevertheless might be the case that neither one of their two points of intersection is the players' aim point I, and as before, only one of the pursuers is active while the Evader runs for his life from the active pursuer. The BSR then has the shape of a thick lens and the Evader's and the active pursuer's aim point I is the point on the thick lens—shaped BSR which is farthest away from E—it is on the circumference of the smaller Apollonius circle,

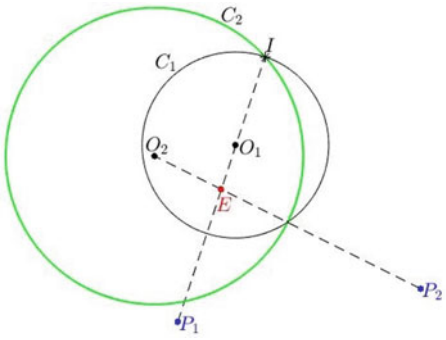

Fig. 8 Critical configuration

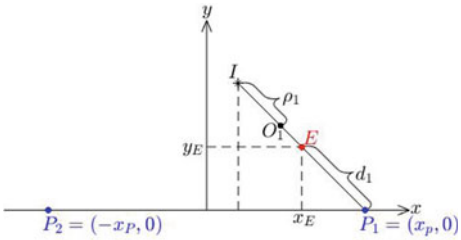

Fig. 9 Interception point I

on its diameter that runs through E, while at the same time it is in the *interior* of the Apollonius disk formed by the bigger Apollonius circle. The critical configuration where point $I \in \mathscr{C}_2$ is illustrated in Fig. 7. Since, without loss of generality, we have assumed $x_E \geq 0$ and $y_E \geq 0$, our universe of discourse will be confined to the positive orthant of R^3, R^3_+. To obtain a correct algebraic characterization of the sets R_1, R_2 and $R_{1,2}$ which will supersede condition (8), proceed as follows.

Calculate the (x, y) coordinates of the critical point I on the circumference of the Apollonius circle $\mathscr{C}_1$ which is antipodal to E, as shown in Fig. 8—see also Fig. 9:

We have

$$\frac{x_P - x_I}{x_P - x_E} = \frac{\rho_1 + \overline{EO}_1 + d_1}{d_1}, \quad \frac{y_I}{y_E} = \frac{\rho_1 + \overline{EO}_1 + d_1}{d_1},$$

where

$$\overline{EO}_1 = \frac{\mu^2}{1-\mu^2} d_1, \quad \rho_1 = \frac{\mu}{1-\mu^2} d_1.$$

Hence

$$x_I = \frac{1}{1-\mu}(x_E - \mu x_P), \quad y_I = \frac{1}{1-\mu} y_E. \tag{9}$$

By construction, $I \in \mathscr{C}_1$ and I is the critical aim point if in addition $I \in \mathscr{C}_2$. To find the points of intersection (x_I, y_I) of the circles $\mathscr{C}_1$ and $\mathscr{C}_2$ boils down to the solution of a quadratic equation:

$$x_I = 0, \quad y_I = \frac{y_E + \sqrt{\mu^2 y_E^2 + (1-\mu^2)(\mu^2 x_P^2 - -x_E^2)}}{1-\mu^2}. \tag{10}$$

Combining Eqs. (9) and (10) we obtain the result

$$x_E = \mu x_P,$$

and the solution of the Game of Kind is as follows.

Theorem 2 *During optimal play the Evader is singlehandedly captured in PP by P_1 if the state is in the set R_1; the set R_1 is the wedge formed by the quarter planes $\{(x_P, x_E, y_E) \mid x_P = 0, x_E \geq 0, y_E \geq 0\}$ and $\{(x_P, x_E, y_E) \mid x_E = \mu x_P, x_P \geq 0, y_E \geq 0\}$. The Evader is singlehandedly captured in PP by P_2 if the state is in the set R_2; the set R_2 is the mirror image of R_1 about the plane $x_E = 0$. The Evader is cooperatively and isochronously captured by P_1 and P_2 if the state is in the set*

$$R_{1,2} = \{(x_P, x_E, y_E) \mid -\mu x_P \leq x_E \leq \mu x_P,\ x_P \geq 0, y_E \geq 0\}$$

The cones $\mathscr{K}_1$ and $\mathscr{K}_2$ and/or condition (8) have no role to play here. The Apollonius circles $\mathscr{C}_1$ and $\mathscr{C}_2$ intersect if $-\mu x_P \leq x_E \leq \mu x_P$.

Remark 2 Proposition 1 is a corollary of Theorem 5.

In summary, the reduced state space of the Two Cutters and Fugitive Ship differential game is the first quadrant of R^3, that is, $R_1^3 = \{(x_P, x_E, y_E) \mid x_P \geq 0, y_E \geq 0\}$. The state space R_1^3 is symmetric about the plane $x_E = 0$; the positive orthant R_+^3 half of the state space where R_1 (and $\mathscr{K}_1$) reside is illustrated in Fig. 9. Since point capture is desired, the terminal set in the R_1 subset of the R_+^3 state space illustrated in Fig. 10 is the straight line $\{(x_P, x_E, y_E) \mid x_E = x_P, x_P \geq 0, y_E = 0\}$ and the terminal set in the $R_{1,2}$ subset of the state space is the origin. However, when the pursuers are endowed with a circular capture set of radius l the set R_1 is no longer a wedge—the surface separating the R_1 and $R_{1,2}$ subsets of the state space is no longer planar. The terminal set in the R_1 subset of the state space is now half a cylinder of radius l raised above the plane $y_E = 0$ and it is centered on the straight line $\{(x_P, x_E, y_E) \mid x_P = x_E, y_E = 0\}$. The terminal set in the $R_{1,2}$ subset of the state space is a quarter circle in the plane $x_E = 0$ of radius l, centered at the origin. The positive orthant R_+^3 of the state space when $l > 0$ is notionally illustrated in Fig. 10 where the region $\mathscr{K}_1$ in the state space where the Cartesian ovals[2] intersect is also shown. The reduced state space also comprises the third quadrant R_3^3 of the reduced state space (x_P, x_E, y_E) but due to

[2]When P is endowed with a capture circle the Apollonius circle locus is replaced with a Cartesian oval.

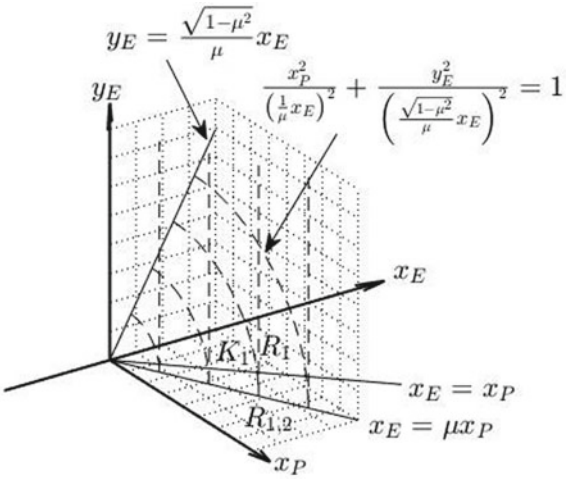

Fig. 10 The positive orthant

symmetry we confine our attention to the first ortant of the reduced state space. The reader is referred to Ref. [5] where the Two-on-One pursuit-evasion differential game with a non-zero capture range is analyzed.

3.2 Game of Degree in Reduced State Space

3.2.1 Game in R_1 and R_2

In R_1 the active pursuer P_1 employs PP while the evader runs for his life. The actions of pursuer P_2 do not affect the outcome of the game and so, for exclusively illustrative purposes, we stipulate that P_2 mirrors the control of P_1. This ensures that the (x, y) frame won't rotate—it would just slide upward along the Y- axis of the realistic plane, which then coincides with the y-axis. The optimal trajectories in R_1 are the family of straight lines

$$x_P(t) = x_{P_0} + \frac{x_{E_0} - x_{P_0}}{\sqrt{(x_{P_0} - x_{E_0})^2 + y_{E_0}^2}}\, t$$

$$x_E(t) = x_{E_0} + \mu \frac{x_{E_0} - x_{P_0}}{\sqrt{(x_{P_0} - x_{E_0})^2 + y_{E_0}^2}}\, t$$

$$y_E(t) = y_{E_0} - (1-\mu) \frac{y_{E_0}}{\sqrt{(x_{P_0} - x_{E_0})^2 + y_{E_0}^2}}\, t.$$

The state $y_E(t)$ is monotonically decreasing and when parameterized by y_E, the optimal trajectories in R_1 are the family of straight lines

$$x_P = \frac{1}{1-\mu}\left(\frac{x_{P_0} - x_{E_0}}{y_{E_0}}\, y_E + x_{E_0} - \mu x_{P_0}\right)$$
$$x_E = \frac{1}{1-\mu}\left(\mu\frac{x_{P_0} - x_{E_0}}{y_{E_0}}\, y_E + x_{E_0} - \mu x_{P_0}\right).$$

In the case of point capture ($l = 0$) these trajectories terminate in the plane $y_E = 0$, on the straight line $x_P = x_E$. The optimal flow field in R_1 consists of the family of straight line trajectories from above, which terminate on the straight line $\{(x_P, x_E, y_E) \mid x_E = x_P, y_E = 0\}$. Similar considerations apply to R_2 where the active pursuer is P_2. The optimal flow field in R_2 is a mirror image of the optimal flow field in R_1.

When $x_p = 0$, P_1 and P_2 are collocated. The half plane $\{(x_P, x_E, y_E) \mid x_P = 0, y_E \geq 0\} \subset R_1 \cup R_2$.

3.2.2 Game in $R_{1,2}$

If the state is in $R_{1,2} = \{(x_P, x_E, y_E) \mid -\mu x_P \leq x_E \leq \mu x_P, x_P \geq 0, y_E \geq 0\}$ E will be isochronously captured by the P_1 & P_2 team. Since $\triangle P_1 P_2 I$ in Fig. 3 is isosceles, the aim point $I = (0, y)$ is obtained upon setting $x = 0$ in Eqs. (6) or (7), which yields a quadratic equation in y. The discriminant of the quadratic equation is positive iff the Apollonius circles $\mathscr{C}_1$ and $\mathscr{C}_2$ intersect, which is the case iff condition (8) holds and is certainly the case if $-\mu x_P \leq x_E \leq \mu x_P$, whereupon

$$y = \frac{1}{1-\mu^2}[y_E + sign(y_E)\sqrt{\mu^2 y_E^2 + (1-\mu^2)(\mu^2 x_P^2 - x_E^2)}],$$

where the function

$$sign(x) \equiv \begin{cases} 1 & if\ x > 0 \\ 0 & if\ x = 0 \\ -1 & if\ x < 0 \end{cases}$$

so

$$y_I = \frac{1}{1-\mu^2}[y_E + sign(y_E)\sqrt{\mu^2 y_E^2 + (1-\mu^2)(\mu^2 x_P^2 - x_E^2)}]. \tag{11}$$

Using the geometric method, the players' optimal state feedback strategies in $R_{1,2}$ are explicitly given by

$$\sin\psi^* = \frac{y_I}{\sqrt{x_P^2 + y_I^2}}, \quad \cos\psi^* = \frac{x_P}{\sqrt{x_P^2 + y_I^2}} \tag{12}$$

$$\sin\chi^* = \frac{y_I}{\sqrt{x_P^2 + y_I^2}}, \quad \cos\chi^* = -\frac{x_P}{\sqrt{x_P^2 + y_I^2}} \tag{13}$$

$$\sin\phi^* = \frac{y_I - y_E}{\sqrt{(y_I - y_E)^2 + x_E^2}}, \quad \cos\phi^* = -\frac{x_E}{\sqrt{(y_I - y_E)^2 + x_E^2}} \tag{14}$$

and the time-to-capture/Value function is

$$V(x_P, x_E, y_E) = \sqrt{x_P^2 + y_I^2}, \tag{15}$$

where the function $y_I(x_P, x_E, y_E)$ is given by Eq. (11).

When the initial state $(x_{P_0}, x_{E_0}, y_{E_0}) \in R_{1,2}$ and P_1, P_2 and E play optimally, the closed- loop dynamics are

$$\dot{x}_P = -\frac{(1-\mu^2)x_P}{\sqrt{(1-\mu^2)(x_P^2 - x_E^2) + (1+\mu^2)y_E^2 + 2y_E\sqrt{\mu^2 y_E^2 + (1-\mu^2)(\mu^2 x_P^2 - x_E^2)}}},$$
$$x_P(0) = x_{P_0}$$

$$\dot{x}_E = -\frac{(1-\mu^2)x_E}{\sqrt{(1-\mu^2)(x_P^2 - x_E^2) + (1+\mu^2)y_E^2 + 2y_E\sqrt{\mu^2 y_E^2 + (1-\mu^2)(\mu^2 x_P^2 - x_E^2)}}},$$
$$x_E(0) = x_{E_0} \tag{16}$$

$$\dot{y}_E = -\frac{(1-\mu^2)y_E}{\sqrt{(1-\mu^2)(x_P^2 - x_E^2) + (1+\mu^2)y_E^2 + 2y_E\sqrt{\mu^2 y_E^2 + (1-\mu^2)(\mu^2 x_P^2 - x_E^2)}}},$$
$$y_E(0) = y_{E_0}, \ 0 \le t.$$

The solution of the system (16) of strongly nonlinear differential equations is simply

$$\begin{aligned} x_P(t) &= (1 - \frac{t}{t_f})x_{P_0} \\ x_E(t) &= (1 - \frac{t}{t_f})x_{E_0} \\ y_E(t) &= (1 - \frac{t}{t_f})y_{E_0}, \ 0 \le t \le t_f, \end{aligned} \tag{17}$$

where

$$t_f = \frac{1}{1-\mu^2}\sqrt{(1-\mu^2)(x_{P_0}^2 - x_{E_0}^2) + (1+\mu^2)y_{E_0}^2 + 2y_E\sqrt{\mu^2 y_{E_0}^2 + (1-\mu^2)(\mu^2 x_{P_0}^2 - x_{E_0}^2)}}. \tag{18}$$

Inserting Eqs. (17) into Eqs. (12)–(14) we obtain the players' constant headings in both the (x, y) and (X, Y) frames

$$\begin{aligned}
\sin\psi^* &= \frac{y_{E_0} + \sqrt{\mu^2 y_{E_0}^2 + (1-\mu^2)(\mu^2 x_{P_0}^2 - x_{E_0}^2)}}{\sqrt{(1-\mu^2)(x_{P_0}^2 - x_{E_0}^2) + (1+\mu^2)y_{E_0}^2 + 2y_{E_0}\sqrt{\mu^2 y_{E_0}^2 + (1-\mu^2)(\mu^2 x_{P_0}^2 - x_{E_0}^2)}}} \\
\cos\psi^* &= \frac{(1-\mu^2)x_{P_0}}{\sqrt{(1-\mu^2)(x_{P_0}^2 - x_{E_0}^2) + (1+\mu^2)y_{E_0}^2 + 2y_{E_0}\sqrt{\mu^2 y_{E_0}^2 + (1-\mu^2)(\mu^2 x_{P_0}^2 - x_{E_0}^2)}}} \\
\chi^* &= \pi - \psi^* \\
\sin\phi^* &= \frac{1}{\mu}\frac{\mu^2 y_{E_0} + \sqrt{\mu^2 y_{E_0}^2 + (1-\mu^2)(\mu^2 x_{P_0}^2 - x_{E_0}^2)}}{\sqrt{(1-\mu^2)(x_{P_0}^2 - x_{E_0}^2) + (1+\mu^2)y_{E_0}^2 + 2y_{E_0}\sqrt{\mu^2 y_{E_0}^2 + (1-\mu^2)(\mu^2 x_{P_0}^2 - x_{E_0}^2)}}} \\
\cos\phi^* &= -\frac{1}{\mu}\frac{(1-\mu^2)x_{E_0}}{\sqrt{(1-\mu^2)(x_{P_0}^2 - x_{E_0}^2) + (1+\mu^2)y_{E_0}^2 + 2y_{E_0}\sqrt{\mu^2 y_{E_0}^2 + (1-\mu^2)(\mu^2 x_{P_0}^2 - x_{E_0}^2)}}}.
\end{aligned} \tag{19}$$

The initial state $(x_{P_0}, x_{E_0}, y_{E_0})$ can momentarily be viewed as the current state and as such, Eq. (19) are explicit state feedback "optimal" strategies, as provided by the geometric method; the attendant Value function is given in Eq. (18).

When the geometric method is applied and P_1 and P_2 play "optimally", from Eq. (19) we deduce that in the (x, y) frame the headings of P_1 and P_2 are mirror images of each other: $\chi^* = \pi - \psi^*$. Therefore, the (x, y) frame does not rotate and the players' headings are constant also in the (inertial) (X, Y) frame of the realistic plane. Hence, in the realistic plane, the "optimal" trajectories are straight lines. Since initially the rotating (x, y) frame is aligned with the (X, Y) frame of the realistic plane, the y-axis stays aligned with the Y-axis while the x-axis stays parallel to the X-axis moving in the upward direction at a constant speed. Therefore the "optimal" trajectories are also straight lines in the (x, y) frame. Thus, when the state feedback strategies (19) synthesized using the geometric method are applied, the closed- loop system's "optimal" flow field in the $R_{1,2}$ region of the reduced state space consists of the family of straight line trajectories (17) which converge at the origin. Moreover, this flow field, which was produced by the geometric method, *covers* the $R_{1,2}$ region of the reduced state space—this, by construction.

At this juncture it is important to recognize that in truth, the herein discussed geometric method only yielded the solution of a related open- loop max- min *optimal control* [6] problem, not the solution of the differential game we are after: The optimal control problem solved so far for initial states $(x_{P_0}, x_{E_0}, y_{E_0}) \in R_{1,2}$ is one where a discriminated evader/ship is obliged to preannounce his control time history, knowing that the pursuers/cutters will then chose a course of action s.t. his time—

to—capture will be minimized; whereupon the evader will set his course so that the time-to-capture is maximized; at best, a lower bound of the Value of the game has been obtained; the optimality of the geometrically derived state feedback strategies (19) has yet to be proved.

4 Isaacs' Method

We now embark on applying Isaacs' method for the systematic solution of differential games to the Two Cutters and Fugitive Ship differential game. Following in Isaacs' footsteps, we solve the Two Cutters and Fugitive Ship differential game in the three-dimensional reduced state space $R_1^3 = \{(x_P, x_E, y_E) \mid x_P \geq 0, y_E \geq 0\}$. In the R_1 and R_2 regions of the reduced state space only one pursuer is active and the game is trivial: Optimal play entails classical PP and pure evasion; the optimal flow field in the R_1 and R_2 regions of the reduced state space is provided in Sect. 3.2.1. The more interesting game takes place in the $R_{1,2}$ region of the reduced state space where under optimal play both pursuers cooperatively and isochronously capture the evader. The objective is to rigorously justify the geometric method in the $R_{1,2}$ region of the state space, that is, validate the tentatively optimal state feedback strategies (19) of the pursuers and the evader and the differential game's Value function (18) presented in Sect. 3.2.2. Due to symmetry, we confine our attention to the part of $R_{1,2}$ which is in the positive orthant R_+^3. Isaacs' method entails Dynamic Programming. We dutifully start from the "end".

The Two Cutters and Fugitive Ship differential game is played in R_1^3, the first quadrant of the three-dimensional state space (x_P, x_E, y_E). In a three- dimensional state space a proper terminal manifold must be a two-dimensional manifold—one cannot really talk about point capture. Hence, we momentarily endow the pursuers with circular capture sets of radius l and in due course we'll let $l \to 0$. Thus, the terminal manifold in the reduced R_1^3 state space is

$$\begin{aligned}\mathscr{T} = &\{(x_P, x_E, y_E) \mid (x_P - x_E)^2 + y_E^2 = l^2, x_P \geq 0, x_E \geq 0, y_E \geq 0\} \\ &\cup\{(x_P, x_E, y_E) \mid (x_P + x_E)^2 + y_E^2 = l^2, x_P \geq 0, x_E \leq 0, y_E \geq 0\}\end{aligned}$$

The two- dimensional terminal manifold $\mathscr{T}$ is not smooth—it is not differentiable in the quarter plane $\{(x_P, x_E, y_E) \mid x_P \geq 0, x_E = 0, y_E \geq 0\} \subset R_{1,2}$. In general, at points where a manifold is not smooth a normal to the surface might not exist, or, a normal to the surface is not unique. When a normal to the surface is not unique, this implies that multiple optimal trajectories will terminate at this point and in doing so, cover a swath of the state space. The locus where the terminal manifold is not differentiable is in the region of interest — it is in the $R_{1,2}$ subset of the R_1^3 state space. In $R_{1,2}$—see Fig. 10—the terminal manifold is

$$\mathscr{T} = \{(x_P, x_E, y_E) \mid x_P^2 + y_E^2 = l^2, x_P \geq 0, x_E = 0, y_E \geq 0\}.$$

It is a quarter circle in the plane $x_E = 0$. Although we have eschewed point capture and have taken the physically sound step of allowing for finite capture sets, the terminal manifold $\mathscr{T}$ in the $R_{1,2}$ region of the state space is of dimension one and not of dimension two, as "required"—this being a manifestation of the fact that the two-dimensional terminal manifold in the R_1^3 state space of the Two Cutters and Fugitive Ship differential game is not smooth. The terminal manifold in the $R_{1,2}$ region of the state space is "rank deficient" and it resides on the boundary of $R_{1,2}$. In the $R_{1,2}$ region of the state space the optimal flow field is s.t. multiple optimal trajectories will terminate at the same point on the quarter circle terminal manifold illustrated in Fig. 10.

When solving the differential game, we are exclusively interested in the inward pointing normals $\mathbf{n}$ to the terminal "surface" $\mathscr{T}$ because they set the terminal conditions of the costate vector. But although the problem formulation is physically sound, our terminal "surface" in $R_{1,2}$, $\mathscr{T}$, is "rank deficient": It is a circular arc in the plane $x_E = 0$ which we now parameterize as follows.

$$\mathscr{T} = \{(x_P, x_E, y_E) \mid x_P = l\cos\xi,\ x_E = 0,\ y_E = l\sin\xi,\ 0 \le \xi \le \frac{\pi}{2}\}. \quad (20)$$

Because the terminal manifold is rank deficient, the normals to the terminal "surface" at a point of the "surface" are not unique. From Eq. (20) we extract the information pertinent to the terminal costates in the part of $R_{1,2}$ which is in the positive orthant R_+^3 of the state space where $x_E > 0$:

$$\boldsymbol{\lambda}(t_f) = -a\begin{pmatrix}\cos\xi\\ b\\ \sin\xi,\end{pmatrix}$$

where $0 \le \xi \le \frac{\pi}{2}$ and the scalars $a > 0, b < 0$; in the half of $R_{1,2}$ which is not in the positive orthant, $b > 0$ and in the plane $x_E = 0, b = 0$. As far as the terminal costate is concerned, the stipulated size l of the pursuers' capture set plays no role here. This is good because down the road we'll be exclusively interested in point capture, that is, $l \to 0$.

The Hamiltonian

$$\begin{aligned} H &= -1 + \frac{1}{2}\lambda_{x_P}(\cos\chi - \cos\psi) + \lambda_{x_E}[\mu\cos\phi - \frac{1}{2}(\cos\chi + \cos\psi) + \frac{1}{2}\frac{y_E}{x_P}(\sin\chi - \sin\psi)] \\ &+\lambda_{y_E}[\mu\sin\phi - \frac{1}{2}(\sin\chi + \sin\psi) - \frac{1}{2}\frac{x_E}{x_P}(\sin\chi - \sin\psi)] \\ &= -1 - \frac{1}{2}[(\lambda_{y_E} + \frac{y_E\lambda_{x_E} - x_E\lambda_{y_E}}{x_P})\sin\psi + (\lambda_{x_E} + \lambda_{x_P})\cos\psi \\ &+(\lambda_{y_E} - \frac{y_E\lambda_{x_E} - x_E\lambda_{y_E}}{x_P})\sin\chi + (\lambda_{x_E} - \lambda_{x_P})\cos\chi] + \mu(\lambda_{y_E}\sin\phi + \lambda_{x_E}\cos\phi). \end{aligned} \quad (21)$$

The costate vector λ is related to the partial derivatives of the Value function $V(x_P, x_E, y_E)$: $\lambda_{x_P} = -V_{x_P}$, $\lambda_{x_E} = -V_{x_E}$ and $\lambda_{y_E} = -V_{y_E}$. Maximizing the Hamil-

tonian in χ and ψ and minimizing the Hamiltonian in ϕ yields the following characterization of the optimal controls.

$$\sin\chi^* = \frac{\frac{y_E\lambda_{x_E} - x_E\lambda_{y_E}}{x_P} - \lambda_{y_E}}{\sqrt{(\lambda_{x_E} - \lambda_{x_P})^2 + (\lambda_{y_E} - \frac{y_E\lambda_{x_E} - x_E\lambda_{y_E}}{x_P})^2}}, \quad \cos\chi^* = \frac{\lambda_{x_P} - \lambda_{x_E}}{\sqrt{(\lambda_{x_E} - \lambda_{x_P})^2 + (\lambda_{y_E} - \frac{y_E\lambda_{x_E} - x_E\lambda_{y_E}}{x_P})^2}} \tag{22}$$

$$\sin\psi^* = \frac{\frac{x_E\lambda_{y_E} - y_E\lambda_{x_E}}{x_P} - \lambda_{y_E}}{\sqrt{(\lambda_{x_E} + \lambda_{x_P})^2 + (\lambda_{y_E} + \frac{y_E\lambda_{x_E} - x_E\lambda_{y_E}}{x_P})^2}}, \quad \cos\psi^* = \frac{-(\lambda_{x_E} + \lambda_{x_P})}{\sqrt{(\lambda_{x_E} + \lambda_{x_P})^2 + (\lambda_{y_E} + \frac{y_E\lambda_{x_E} - x_E\lambda_{y_E}}{x_P})^2}} \tag{23}$$

$$\sin\phi^* = -\frac{\lambda_{y_E}}{\sqrt{\lambda_{x_E}^2 + \lambda_{y_E}^2}}, \quad \cos\phi^* = -\frac{\lambda_{x_E}}{\sqrt{\lambda_{x_E}^2 + \lambda_{y_E}^2}}. \tag{24}$$

In the part of $R_{1,2}$ which is in the positive orthant R_+^3 where $x_E > 0$, the attendant costate equations are

$$\begin{aligned}
\dot\lambda_{x_P} &= \frac{1}{2}\frac{y_E\lambda_{x_E} - x_E\lambda_{y_E}}{x_P^2}(\sin\chi^* - \sin\psi^*), \quad \lambda_{x_P}(t_f) = -a\cos\xi \\
\dot\lambda_{x_E} &= \frac{1}{2}\frac{\lambda_{y_E}}{x_P}(\sin\chi^* - \sin\psi^*), \quad \lambda_{x_E}(t_f) = -ab \\
\dot\lambda_{y_E} &= -\frac{1}{2}\frac{\lambda_{x_E}}{x_P}(\sin\chi^* - \sin\psi^*), \quad \lambda_{y_E}(t_f) = -a\sin\xi,
\end{aligned} \tag{25}$$

where $0 \le \xi \le \frac{\pi}{2}$; the scalars $a > 0, b < 0$.

Insert the controls (22)–(24) into the dynamics equations (3)–(5) and into the costate equations (25) and obtain the Euler-Lagrange/characteristics' equations, a set of six nonlinear differential equations in the variables $x_P, x_E, y_E, \lambda_{x_P}, \lambda_{x_E}, \lambda_{y_E}$.

$$\begin{aligned}
\dot x_P = \frac{1}{2}[&\frac{\lambda_{x_P} - \lambda_{x_E}}{\sqrt{(\lambda_{x_E} - \lambda_{x_P})^2 + (\lambda_{y_E} - \frac{y_E\lambda_{x_E} - x_E\lambda_{y_E}}{x_P})^2}} \\
&+ \frac{(\lambda_{x_E} + \lambda_{x_P})}{\sqrt{(\lambda_{x_E} + \lambda_{x_P})^2 + (\lambda_{y_E} + \frac{y_E\lambda_{x_E} - x_E\lambda_{y_E}}{x_P})^2}}], \quad x_P(0) = x_{P_0}
\end{aligned}$$

$$\begin{aligned}
\dot x_E = -\mu\frac{\lambda_{x_E}}{\sqrt{\lambda_{x_E}^2 + \lambda_{y_E}^2}} - \frac{1}{2}[&\frac{\lambda_{x_P} - \lambda_{x_E}}{\sqrt{(\lambda_{x_E} - \lambda_{x_P})^2 + (\lambda_{y_E} - \frac{y_E\lambda_{x_E} - x_E\lambda_{y_E}}{x_P})^2}} \\
&- \frac{(\lambda_{x_E} + \lambda_{x_P})}{\sqrt{(\lambda_{x_E} + \lambda_{x_P})^2 + (\lambda_{y_E} + \frac{y_E\lambda_{x_E} - x_E\lambda_{y_E}}{x_P})^2}}]
\end{aligned}$$

$$+\frac{1}{2}\frac{y_E}{x_P}\Big[\frac{\frac{y_E\lambda_{x_E}-x_E\lambda_{y_E}}{x_P}-\lambda_{y_E}}{\sqrt{(\lambda_{x_E}-\lambda_{x_P})^2+(\lambda_{y_E}-\frac{y_E\lambda_{x_E}-x_E\lambda_{y_E}}{x_P})^2}}$$
$$-\frac{\frac{x_E\lambda_{y_E}-y_E\lambda_{x_E}}{x_P}-\lambda_{y_E}}{\sqrt{(\lambda_{x_E}+\lambda_{x_P})^2+(\lambda_{y_E}+\frac{y_E\lambda_{x_E}-x_E\lambda_{y_E}}{x_P})^2}}\Big],\quad x_E(0)=x_{E_0}$$

$$\dot{y}_E=-\mu\frac{\lambda_{y_E}}{\sqrt{\lambda_{x_E}^2+\lambda_{y_E}^2}}-\frac{1}{2}\Big[\frac{\frac{y_E\lambda_{x_E}-x_E\lambda_{y_E}}{x_P}-\lambda_{y_E}}{\sqrt{(\lambda_{x_E}-\lambda_{x_P})^2+(\lambda_{y_E}-\frac{y_E\lambda_{x_E}-x_E\lambda_{y_E}}{x_P})^2}}$$
$$+\frac{\frac{x_E\lambda_{y_E}-y_E\lambda_{x_E}}{x_P}-\lambda_{y_E}}{\sqrt{(\lambda_{x_E}+\lambda_{x_P})^2+(\lambda_{y_E}+\frac{y_E\lambda_{x_E}-x_E\lambda_{y_E}}{x_P})^2}}\Big]$$
$$-\frac{1}{2}\frac{x_E}{x_P}\Big[\frac{\frac{y_E\lambda_{x_E}-x_E\lambda_{y_E}}{x_P}-\lambda_{y_E}}{\sqrt{(\lambda_{x_E}-\lambda_{x_P})^2+(\lambda_{y_E}-\frac{y_E\lambda_{x_E}-x_E\lambda_{y_E}}{x_P})^2}}$$
$$-\frac{\frac{x_E\lambda_{y_E}-y_E\lambda_{x_E}}{x_P}-\lambda_{y_E}}{\sqrt{(\lambda_{x_E}+\lambda_{x_P})^2+(\lambda_{y_E}+\frac{y_E\lambda_{x_E}-x_E\lambda_{y_E}}{x_P})^2}}\Big],\quad y_E(0)=y_{E_0}$$

$$\dot{\lambda}_{x_P}=\frac{1}{2}\frac{y_E\lambda_{x_E}-x_E\lambda_{y_E}}{x_P^2}\Big[\frac{\frac{y_E\lambda_{x_E}-x_E\lambda_{y_E}}{x_P}-\lambda_{y_E}}{\sqrt{(\lambda_{x_E}-\lambda_{x_P})^2+(\lambda_{y_E}-\frac{y_E\lambda_{x_E}-x_E\lambda_{y_E}}{x_P})^2}}$$
$$-\frac{\frac{x_E\lambda_{y_E}-y_E\lambda_{x_E}}{x_P}-\lambda_{y_E}}{\sqrt{(\lambda_{x_E}+\lambda_{x_P})^2+(\lambda_{y_E}+\frac{y_E\lambda_{x_E}-x_E\lambda_{y_E}}{x_P})^2}}\Big],\ \lambda_{x_P}(t_f)=-a\cos\xi$$

$$\dot{\lambda}_{x_E}=\frac{1}{2}\frac{\lambda_{y_E}}{x_P}\Big[\frac{\frac{y_E\lambda_{x_E}-x_E\lambda_{y_E}}{x_P}-\lambda_{y_E}}{\sqrt{(\lambda_{x_E}-\lambda_{x_P})^2+(\lambda_{y_E}-\frac{y_E\lambda_{x_E}-x_E\lambda_{y_E}}{x_P})^2}}$$
$$-\frac{\frac{x_E\lambda_{y_E}-y_E\lambda_{x_E}}{x_P}-\lambda_{y_E}}{\sqrt{(\lambda_{x_E}+\lambda_{x_P})^2+(\lambda_{y_E}+\frac{y_E\lambda_{x_E}-x_E\lambda_{y_E}}{x_P})^2}}\Big],\quad \lambda_{x_E}(t_f)=-ab$$

$$\dot{\lambda}_{y_E} = \frac{1}{2}\frac{\lambda_{x_E}}{x_P}\Big[\frac{\frac{x_E\lambda_{y_E}-y_E\lambda_{x_E}}{x_P} - \lambda_{y_E}}{\sqrt{(\lambda_{x_E}+\lambda_{x_P})^2 + (\lambda_{y_E} + \frac{y_E\lambda_{x_E}-x_E\lambda_{y_E}}{x_P})^2}}$$
$$- \frac{\frac{y_E\lambda_{x_E}-x_E\lambda_{y_E}}{x_P} - \lambda_{y_E}}{\sqrt{(\lambda_{x_E}-\lambda_{x_P})^2 + (\lambda_{y_E} - \frac{y_E\lambda_{x_E}-x_E\lambda_{y_E}}{x_P})^2}}\Big], \quad \lambda_{x_E}(t_f) = -a\sin\xi$$

Evidently, the parameters $0 \le \xi \le \frac{\pi}{2}$, $a > 0$ and b will feature in the solution of the Euler-Lagrange equations. The above equations yield a family of optimal trajectories/characteristics parameterized by the two independent parameters b and ξ, and as such, can fill our three- dimensional state space region $R_{1,2}$.

In addition, inserting Eqs. (22)–(24) into the Hamiltonian (21) yields the *optimal* smooth Hamiltonian

$$H = -1 + \frac{1}{2}\Big[\sqrt{(\lambda_{x_E}-\lambda_{x_P})^2 + (\lambda_{y_E} - \frac{y_E\lambda_{x_E}-x_E\lambda_{y_E}}{x_P})^2}$$
$$+ \sqrt{(\lambda_{x_E}+\lambda_{x_P})^2 + (\lambda_{y_E} + \frac{y_E\lambda_{x_E}-x_E\lambda_{y_E}}{x_P})^2}\Big] - \mu\sqrt{\lambda_{x_E}^2+\lambda_{y_E}^2}.$$

The Hamiltonian vanishes and evaluating the *optimal* Hamiltonian at $t = t_f$ allows us to express the parameter a as a function of the parameters b and ξ:

$$1 = \frac{1}{2}\Big[\sqrt{a^2(b-\cos\xi)^2 + (-a\sin\xi - \frac{-abl\sin\xi}{l\cos\xi})^2} + \sqrt{a^2(b+\cos\xi)^2 + (-a\sin\xi + \frac{-abl\sin\xi}{l\cos\xi})^2}\Big]$$
$$- \mu\sqrt{a^2(b+\sin\xi)^2}$$
$$= \frac{1}{2}a\frac{1}{\cos\xi}\Big[\sqrt{(b-\cos\xi)^2\cos^2\xi + (b-\cos\xi)^2\sin^2\xi} + \sqrt{(b+\cos\xi)^2\cos^2\xi + (b+\cos\xi)^2\sin^2\xi}\Big]$$
$$- \mu a \mid b+\sin\xi \mid .$$

Hence

$$a = \frac{\cos\xi}{\frac{1}{2}(\mid b-\cos\xi \mid + \mid b+\cos\xi \mid) - \mu \mid b+\sin\xi \mid \cos\xi}. \tag{26}$$

In view of the relationship (26), the Euler-Lagrange equations are ultimately parameterized by $0 \le \xi \le \frac{\pi}{2}$ and b; the parameter a won't feature in what follows.

Note that in the half plane of symmetry $\{(x_P, x_E, y_E) \mid x_P \ge 0, x_E = 0\}$, $b = 0$, so the smoothness of the Value function is retained under passage from the side of $R_{1,2}$ where $x_E > 0$ and $b < 0$ to the side of $R_{1,2}$ where $x_E < 0$ and $b > 0$.

Isaacs' method mandates that the Euler-Lagrange equations be integrated in retrograde fashion "starting" out from the "initial" condition $x_P = 0$, $x_E = 0$, $y_E = 0$, $\lambda_{x_P} = -a\cos\xi$, $\lambda_{x_E} = -ab$, $\lambda_{y_E} = -a\sin\xi$. One will obtain a family of optimal trajectories $(x_P(\cdot), x_E(\cdot), y_E(\cdot)) \in R_{1,2} \subset R_1^3$ parameterized by $0 \le \xi \le \frac{\pi}{2}$ and b, which potentially covers the state space region $R_{1,2}$. At this point it would seem that

numerical integration is required. However, with the benefit of hindsight, the solution of the Euler-Lagrange equations is embodied in the family of "optimal" trajectories specified by Eq. (17) which, by construction, covers the state space region $R_{1,2}$: We shall show that the trajectories (17) provided by the geometric method are in fact the solution of the Euler-Lagrange equations. This will allow us to finally dispose of the quotation marks when referring to the optimality of the state feedback strategies (19) and the attendant Value function (18).

The proof proceeds as follows. We make the Ansatz that the family of trajectories (17) which cover the state space region $R_{1,2}$ and were generated by the geometric method are the optimal trajectories, and we will show that:

$\forall\ (x_{P_0}, x_{E_0}, y_{E_0}) \in R_{1,2},\ \ \exists$ "initial" costates $0 \leq \xi \leq \frac{\pi}{2}$ and b s.t. the Euler-Lagrange equations are satisfied. Furthermore, the argument is reversible.

First, note that the following holds.

Proposition 3 *If the state's time history is given by Eq. (17), the players' headings are constant and moreover, the headings of the pursuers P_1 and P_2 satisfy*

$$\chi = \pi - \psi$$

Proof See Eq. (19).

We now turn our attention to Eqs. (3)–(5) and (22)–(25).

1. Applying Proposition 4 to the costate equations (25) yields

$$\begin{aligned}
\dot{\lambda}_{x_P} &= 0, \quad \lambda_{x_P}(t_f) = -a\cos\xi \\
\dot{\lambda}_{x_E} &= 0, \quad \lambda_{x_E}(t_f) = -ab \\
\dot{\lambda}_{y_E} &= 0, \quad \lambda_{y_E}(t_f) = -a\sin\xi
\end{aligned}$$

wherefrom we immediately deduce that the costate vector $\boldsymbol{\lambda}$ is constant:

$$\boldsymbol{\lambda}(t) = -a\begin{pmatrix}\cos\xi \\ b \\ \sin\xi\end{pmatrix}, \quad \forall\, 0 \leq t \leq t_f$$

According to the Ansatz, during optimal play the state's time history is given by Eq. (17), and consequently, the costate's constant components are

$$\lambda_{x_P} = -a\cos\xi, \quad \lambda_{x_E} = -ab, \quad \lambda_{y_E} = -a\sin\xi.,$$

We now turn to the optimal control equations. From Eq. (24) we deduce that given the parameters b and ξ, the optimal control ϕ^* of the Evader is constant and

$$\sin\phi^* = \frac{\sin\xi}{\sqrt{b^2 + \sin^2\xi}}, \quad \cos\phi^* = \frac{b}{\sqrt{b^2 + \sin^2\xi}}.$$

And because in view of Proposition 4 the (x, y) frame is not rotating, the optimal course of the Evader is constant, so in the realistic plane (X, Y) the path of the Evader is a straight line. During optimal play E holds course, which is tantamount to E deciding on his course at the initial time $t = 0$. Hence, it stands to reason that without incurring a loss in optimality, also P_1 and P_2 can chose their course at time $t = 0$. That this is indeed so follows from the following argument.

From Eq. (23) we deduce that given the parameters b and ξ, the optimal control $\psi^*(t)$ of P_2 is specified as follows.

$$\sin\psi^* = \frac{(1-\frac{x_E}{x_P})\sin\xi + b\frac{y_E}{x_P}}{\sqrt{(b+\cos\xi)^2 + [(1-\frac{x_E}{x_P})\sin\xi + b\frac{y_E}{x_P}]^2}},\ \cos\psi^* = \frac{b+\cos\xi}{\sqrt{(b+\cos\xi)^2 + [(1-\frac{x_E}{x_P})\sin\xi + b\frac{y_E}{x_P}]^2}}. \tag{27}$$

Now, since $l = 0$, if the family of optimal trajectories is indeed specified by Eq. (17), the state component ratios featuring in Eq. (27) are constant:

$$\frac{x_E(t)}{x_P(t)} = \frac{x_{E_0}}{x_{P_0}},\quad \frac{y_E(t)}{x_P(t)} = \frac{y_{E_0}}{x_{P_0}}.$$

In view of Eq. (27) we conclude that the optimal control ψ^* of P_2 is constant. This, being the case, we evaluate the optimal control of P_2 at time t_f where $(x_P, x_E, y_E)\ |_{t_f} = (l\cos\xi, 0, l\sin\xi)$. The state component ratios at $t = t_f$ are

$$\frac{x_E}{x_P}\ |_{t_f} = 0,\quad \frac{y_E}{x_P}\ |_{t_f} = \tan\xi,\quad \forall\, l \geq 0 \tag{28}$$

Inserting Eq. (28) into Eq. (27) we calculate

$$\sin(\psi^*(t_f)) = \sin\xi,\quad \cos(\psi^*(t_f)) = \cos\xi,$$

that is,

$$\psi^*(t_f) = \xi.$$

Hence, given the parameters b and ξ, if indeed, according to the Ansatz, the family of optimal trajectories is given by Eq. (17), the constant headings of the pursuers P_1 and P_2 are

$$\chi^* \equiv \pi - \xi,\quad \psi^* \equiv \xi.$$

2. Applying Proposition 4 to the dynamics Eqs. (3)–(5) yields

$$\begin{aligned}\dot{x}_P &= -\cos\psi^*\\ \dot{x}_E &= \mu\cos\phi^*\\ \dot{y}_E &= \mu\sin\phi^* - \sin\psi^*\end{aligned}$$

and inserting therein the parameterized by b and ξ optimal controls χ^*, ψ^* and ϕ^*, we obtain

$$\begin{aligned}
\dot{x}_P &= -\cos\xi, \quad x_P(0) = x_{P_0} \\
\dot{x}_E &= \mu \frac{b}{\sqrt{b^2 + \sin^2\xi}}, \quad x_E(0) = x_{E_0} \\
\dot{y}_E &= \mu \frac{\sin\xi}{\sqrt{b^2 + \sin^2\xi}} - \sin\xi, \quad y_E(0) = y_{E_0}.
\end{aligned}$$

Integrating the above differential equations in retrograde fashion and recalling that the trajectories terminate at the origin, we calculate

$$x_{P_0} = \cos\xi \cdot t_f \tag{29}$$

$$x_{E_0} = -\mu \frac{b}{\sqrt{b^2 + \sin^2\xi}} \cdot t_f \tag{30}$$

$$y_{E_0} = (1 - \mu \frac{1}{\sqrt{b^2 + \sin^2\xi}}) \sin\xi \cdot t_f \tag{31}$$

Note Because $y_{E_0} \geq 0$, the parameters b and ξ we are after must satisfy $b^2 + \sin^2\xi \geq \mu^2$. That this is so will become apparent in the sequel.

To complete the proof it behooves on us to show that

$\forall\, (x_{P_0}, x_{E_0}, y_{E_0}) \in R_{1,2}$, $\exists\, b, 0 < \xi < \frac{\pi}{2}$ and $t_f > 0$ s.t. Eqs. (29)–(31) hold—we must be able to solve the three Eqs. (29)–(31) in the three unknowns b, ξ and t_f.

We first remove t_f from further consideration and, provided $b \neq 0$, obtain two equations in the two unknowns b and ξ:

$$\frac{x_{P_0}}{x_{E_0}} = -\frac{\sqrt{b^2 + \sin^2\xi}}{\mu b} \cos\xi \tag{32}$$

$$\frac{y_{E_0}}{x_{P_0}} = (1 - \frac{\mu}{\sqrt{b^2 + \sin^2\xi}}) \tan\xi. \tag{33}$$

We use Eq. (32) to express b as a function of ξ,

$$b = -\frac{\sin\xi\cos\xi}{\sqrt{\mu^2(\frac{x_{P_0}}{x_{E_0}})^2 - \cos^2\xi}}\, sign(x_{E_0}).$$

Note: In the $R_{1,2}$ region of the state space $| x_{E_0} | \leq \mu x_{P_0}$, so the expression under the square root is positive. Also, in the positive orthant, where $x_{E_0} > 0$,

$$b = -\frac{\sin\xi\cos\xi}{\sqrt{\mu^2(\frac{x_{P_0}}{x_{E_0}})^2 - \cos^2\xi}}. \tag{34}$$

We also calculate

$$\sqrt{b^2+\sin^2\xi}=\frac{\mu(\frac{x_{P_0}}{x_{E_0}})\sin\xi}{\sqrt{\mu^2(\frac{x_{P_0}}{x_{E_0}})^2-\cos^2\xi}}. \tag{35}$$

We insert the expression (35) into Eq. (33) and obtain the equation in ξ

$$\frac{y_{E_0}}{x_{P_0}}=[1-\frac{\sqrt{\mu^2(\frac{x_{P_0}}{x_{E_0}})^2-\cos^2\xi}}{(\frac{x_{P_0}}{x_{E_0}})\sin\xi}]\tan\xi$$

which yields

$$y_{E_0}\cos\xi=x_{P_0}\sin\xi-\sqrt{\mu^2x_{P_0}^2-x_{E_0}^2\cos^2\xi}. \tag{36}$$

Note that in the $R_{1,2}$ region of the state space the expression under the square root is positive.

Concerning the existence of a solution of Eq. (36), considers the function

$$f(\xi)\equiv y_{E_0}\cos\xi-x_{P_0}\sin\xi+\sqrt{\mu^2x_{P_0}^2-x_{E_0}^2\cos^2\xi},\quad 0\le\xi\le\frac{\pi}{2}.$$

We calculate

$$f(0)=y_{E_0}+\sqrt{\mu^2x_{P_0}^2-x_{E_0}^2}>0,\qquad f(\frac{\pi}{2})=-(1-\mu)x_{P_0}<0.$$

Hence, $\exists\ 0<\bar{\xi}<\frac{\pi}{2}$ s.t. $f(\bar{\xi})=0$. Solving Eq. (36) analytically boils down to the solution of a quadratic equation. Let

$$x\equiv\cos^2\xi.$$

We obtain the quadratic equation in x

$$(x_{P_0}^4+x_{E_0}^4+y_{E_0}^4+2x_{E_0}^2y_{E_0}^2+2x_{P_0}^2y_{E_0}^2-2x_{P_0}^2x_{E_0}^2)x^2-2x_{P_0}^2[(1-\mu^2)(x_{P_0}^2-x_{E_0}^2)$$
$$.+(1+\mu^2)y_{E_0}^2]x+(1-\mu^2)^2x_{P_0}^4=0.$$

The discriminant of the quadratic equation

$$\Delta=4x_{P_0}^4y_{E_0}^2[\mu^2x_{P_0}^2-x_{E_0}^2+\mu^2(x_{E_0}^2+y_{E_0}^2)].$$

In the state space region $R_{1,2}$, $\mid x_{E_0}\mid<\mu x_{P_0}$, and therefore the discriminant $\Delta>0$. Thus, the quadratic equation has two real roots. Furthermore, consider the quadratic

polynomial

$$g(x) \equiv (x_{P_0}^4 + x_{E_0}^4 + y_{E_0}^4 + 2x_{E_0}^2 y_{E_0}^2 + 2x_{P_0}^2 y_{E_0}^2 - 2x_{P_0}^2 x_{E_0}^2)x^2$$
$$-2x_{P_0}^2[(1-\mu^2)(x_{P_0}^2 - x_{E_0}^2) + (1+\mu^2)y_{E_0}^2]x + (1-\mu^2)^2 x_{P_0}^4.$$

We calculate $g(0) = (1-\mu^2)^2 x_{P_0}^4 > 0$ and $g(1) = (\mu^2 x_{P_0}^2 - x_{E_0}^2 - y_{E_0}^2)^2 > 0$, wherefrom we conclude that the roots of the quadratic equation satisfy $0 < x < 1$, as required. The solution of the quadratic equation is

$$x = x_{P_0}^2 \frac{(1-\mu^2)(x_{P_0}^2 - x_{E_0}^2) + (1+\mu^2)y_{E_0}^2 + 2y_{E_0}\sqrt{\mu^2(x_{P_0}^2 + y_{E_0}^2) - (1-\mu^2)x_{E_0}^2}}{x_{P_0}^4 + x_{E_0}^4 + y_{E_0}^4 + 2x_{E_0}^2 y_{E_0}^2 + 2x_{P_0}^2 y_{E_0}^2 - 2x_{P_0}^2 x_{E_0}^2}$$

and

$$\xi = Arccos(\sqrt{x}).$$

Finally, from Eq. (34),

$$b = -\sqrt{\frac{(1-x)x}{\mu^2(\frac{x_{P_0}}{x_{E_0}})^2 - x}}\, sign(x_E).$$

Next, consider the case where the parameter $b = 0$. The parameter $b = 0$ generates the optimal flow field in the plane of symmetry, that is, the plane $x_E = 0$. Now $b = 0$ and Eqs. (29) and (31) yield

$$x_{P_0} = \cos\xi \cdot t_f$$
$$y_{E_0} = (\sin\xi - \mu) \cdot t_f.$$

We have two equations in the two unknowns ξ and t_f.

Proposition 4 $\forall\, x_P > 0$ *and* $x_E > 0$, $\exists\, \xi > Arcsin(\mu)$ *and* $t_f > 0$ *which satisfy the two equations from above.*

Proof We first eliminate t_f and calculate ξ as follows.

$$\frac{y_{E_0}}{x_{P_0}} = \frac{\sin\xi - \mu}{\cos\xi}$$

and we obtain the quadratic equation in $\cos\xi$,

$$(x_{P_0}^2 + y_{E_0}^2)\cos^2\xi + 2\mu x_{P_0} y_{E_0}\cos\xi - (1-\mu^2)x_{P_0}^2 = 0$$

whereupon

$$\sin\xi = \frac{\mu + \frac{y_{E_0}}{x_{P_0}}\sqrt{1-\mu^2+(\frac{y_{E_0}}{x_{P_0}})^2}}{1+(\frac{y_{E_0}}{x_{P_0}})^2},\quad \cos\xi = \frac{\sqrt{1-\mu^2+(\frac{y_{E_0}}{x_{P_0}})^2}-\mu\frac{y_{E_0}}{x_{P_0}}}{1+(\frac{y_{E_0}}{x_{P_0}})^2}$$

and $\sin\xi > \mu$ because

$$\mu + \frac{y_{E_0}}{x_{P_0}}\sqrt{1-\mu^2+(\frac{y_{E_0}}{x_{P_0}})^2} > \mu + \mu(\frac{y_{E_0}}{x_{P_0}})^2$$

because

$$\sqrt{1-\mu^2+(\frac{y_{E_0}}{x_{P_0}})^2} > \mu\ \frac{y_{E_0}}{x_{P_0}}$$

because

$$1-\mu^2 > (\mu^2-1)(\frac{y_{E_0}}{x_{P_0}})^2$$

because

$$1 > -(\frac{y_{E_0}}{x_{P_0}})^2.$$

Thus, the following holds.

Theorem 5 *The Two Cutters and Fugitive Ship differential game's solution is presented in the three-dimensional reduced state space* $\{(x_P, x_E, y_E) \mid x_P \geq 0\}$ *where there are two half planes of symmetry,* $\{(x_P, x_E, y_E) \mid x_P \geq 0, y_E = 0\}$ *and* $\{(x_P, x_E, y_E) \mid x_P \geq 0, x_E = 0\}$. *Hence, it is sufficient to confine one's attention to the positive orthant of the reduced state space. In the state space region* $R_{1,2}$ *where both Pursuers* P_1 *and* P_2 *actively engage the Evader and which is in the positive orthant, the players' optimal state feedback strategies are derived from Eqs. (19), that is,*

$$\sin\psi^* = \frac{y_E + \sqrt{\mu^2 y_E^2 + (1-\mu^2)(\mu^2 x_P^2 - x_E^2)}}{\sqrt{(1-\mu^2)(x_P^2-x_E^2)+(1+\mu^2)y_E^2+2y_E\sqrt{\mu^2 y_E^2+(1-\mu^2)(\mu^2x_P^2-x_E^2)}}}$$

$$\cos\psi^* = \frac{(1-\mu^2)x_P}{\sqrt{(1-\mu^2)(x_P^2-x_E^2)+(1+\mu^2)y_E^2+2y_E\sqrt{\mu^2 y_E^2+(1-\mu^2)(\mu^2x_P^2-x_E^2)}}}$$

$$\chi^* = \pi - \psi^*$$

$$\sin\phi^* = \frac{1}{\mu}\frac{\mu^2 y_E + \sqrt{\mu^2 y_E^2 + (1-\mu^2)(\mu^2 x_P^2 - x_E^2)}}{\sqrt{(1-\mu^2)(x_P^2-x_E^2)+(1+\mu^2)y_E^2+2y_E\sqrt{\mu^2 y_E^2+(1-\mu^2)(\mu^2x_P^2-x_E^2)}}}$$

$$\cos\phi^* = -\frac{1}{\mu}\frac{(1-\mu^2)x_E}{\sqrt{(1-\mu^2)(x_P^2-x_E^2)+(1+\mu^2)y_E^2+2y_E\sqrt{\mu^2y_E^2+(1-\mu^2)(\mu^2x_P^2-x_E^2)}}}$$

and the Value function, derived from Eq. (18), is

$$V(x_P,x_E,y_E)=\frac{1}{1-\mu^2}\sqrt{(1-\mu^2)(x_P^2-x_E^2)+(1+\mu^2)y_E^2+2y_E\sqrt{\mu^2y_E^2+(1-\mu^2)(\mu^2x_P^2-x_E^2)}}$$

The field of primary optimal trajectories covers the entire state space and the Value function is C^1*, except on the half plane of symmetry* $\{(x_P, x_E, y_E) \mid x_P \geq 0, y_E = 0\}$ *which is a dispersal surface; no additional singular surfaces are present. The field of optimal trajectories is symmetric about the half planes* $\{(x_P, x_E, y_E) \mid x_P \geq 0, y_E = 0\}$ *and* $\{(x_P, x_E, y_E) \mid x_P \geq 0, x_E = 0\}$ *and the optimal trajectories in the half plane* $\{(x_P, x_E, y_E) \mid x_P \geq 0, x_E = 0\}$ *stay there all along. The geometric method yields the correct solution of the differential game.*

Similar to the quadratic cost Ansatz used in the solution of the Linear-Quadratic Differential Game, the Ansatz artifice used herein concerning the trajectories (17) is a self fulfilling prophesy. The geometric method yields the correct solution and one has avoided the need to numerically integrate the Euler-Lagrange system of nonlinear differential equations arising when Isaacs' method is dogmatically applied to the Two Cutters and Fugitive Ship differential game.

In summary, only when we have a complete set of optimal trajectories $filling$ a capture region separated from the escape region by a closed barrier, or possibly, the region of capturability is the whole state space—this, as specified by the solution of the Game of Kind—has a differential game been solved. There are only a few 3-D pursuit-evasion differential games solved, none in a higher dimension. Games in 3-D with no singular surfaces, at least, for a range of parameters and still an acceptable model of conflict situations of interest so that their relevance is preserved, are instances where interesting pursuit-evasion differential games in 3-D have been solved. We refer to the Two Cutters and Fugitive Ship Differential Game, the Differential Game of Guarding a Target [7], and the Active Target Defense Differential Game [8]. The secret sauce is provided by the following.

Theorem 6 *The solution of zero-sum differential games by solving the* $max\ min$ *open-loop optimal control problem using the two sided Pontryagin Maximum Principle and synthesizing the players' state feedback optimal strategies in receding horizon optimal control fashion is valid if and only if the application of Isaacs' method results in primary optimal trajectories only, a.k.a., regular characteristics, which cover the capture zone. The optimal flow field must cover the entire capture zone which was provided by the solution of the Game of Kind, so there is no need for singular surfaces, except a dispersal surface.*

When this is the case *and* the players have simple motion the geometric method applies. This is the reason why in the Two Cutters and Fugitive Ship differential game the geometric method is applicable and therefore the correctness of Isaacs' solution

has been proved. In this paper, we have proven that the application of Isaacs' method yields an optimal flow field which covers the reduced 3-D state space. Having the geometric solution facilitated the proof.

5 Conclusion and Extensions

In this paper Isaacs' Two Cutters and Fugitive Ship differential game has been revisited. The solution of the Game of Kind is provided, that is, the state space regions where under optimal play just one of the pursuers captures the evader, and also the state space region where both pursuers cooperatively capture the target, have been characterized. The solution of the Game of Degree has been obtained using Isaacs' method. Thus, the elegant geometric solution provided by Isaacs is now fully justified. As it so often happens in differential games, the doctrinaire employment of Isaacs' method towards the solution of even the "simple" Two Cutters and Fugitive Ship differential game was not devoid of complexity. However, the intuition provided by the heuristic geometric approach, and also visualizing the game in the realistic plane, are instrumental in facilitating the solution process. The Two Cutters and Fugitive Ship is an interesting differential game where the optimal flow field consists of regular trajectories only. The Value function is C^1, except on a half plane which is a dispersal surface, and there are no additional singular surfaces.

Concerning extensions, the cutters' speed need not be equal, provided that it is higher than the speed of the fugitive ship. Furthermore, it is interesting to also consider the case where the speed of just one of the two cutters, say P_1, is higher than the speed of the fugitive ship while the speed of P_2 is equal to the speed of the fugitive ship. In this case, upon employing the now validated geometric method, the Apollonius circle which is based on E and P_2 devolves into the orthogonal bisector of the segment $\overline{EP}_2$. It makes sense to also stipulate that the cutters P_1 and P_2 are endowed with circular capture sets with radii $l_1 > 0$ and $l_2 > 0$ respectively. In this case, the elegant Apollonius circles will be replaced by Cartesian ovals and the boundary separating the R_1, R_2, and $R_{1,2}$ regions of the state space won't be planar and will be replaced by a more complex surface as illustrated in Fig. 11.

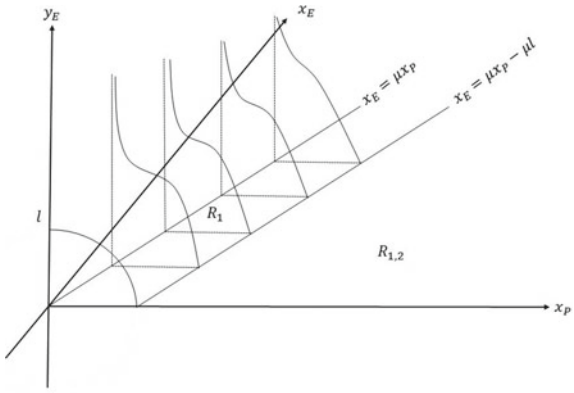

Fig. 11 Positive orthant, $l > 0$

References

1. R. Isaacs: "Differential Games: A Mathematical Theory with Applications Warfare and Pursuit, Control and Optimization", Wiley 1965, pp. 148-149.
2. Hugo Steinhaus: "Definitions for a Theory of Games of Pursuit", Naval Research Logistics Quarterly, Vol. 7, No 2, pp. 105-108, 1960.
3. E. Garcia, Z. Fuchs, D. Milutinovic, D. Casbeer, and M. Pachter: "A Geometric Approach for the Cooperative Two-Pursuers One-Evader Differential Game", Proceedings of the 20th World Congress of IFAC, Toulouse, France, pp. 15774-15779, July 9-14, 2017.
4. S. I. Tarlinskii: "On a Linear Game of Convergence of Several Controlled Objects", Soviet Math. Dokl., Vol. 17, No. 5, 1976, pp. 1354-1358.
5. P. Wasz, M. Pachter and K. Pham: "Two-On-One Pursuit with a Non-Zero Capture Radius", Proceedings of the Mediterranean Control Conference, Akko, Israel, July 1-4, 2019.
6. L. S. Pontryagin, V. G. Boltyanskii, R. V. Gamkrelidze, E.F. Mishchenko: "The Mathematical Theory of Optimal Processes", Interscience, 1962, New York, Chapter 4, Sect. 28.
7. M. Pachter, E. Garcia and D. Casbeer: "The Differential Game of Guarding a Target", AIAA Journal of Guidance, Control and Dynamics, Vol. 40, No. 11, November 2017, pp. 2986-2993.
8. M. Pachter, E. Garcia and D. Casbeer: "Toward a Solution of the Active Target Defense Differential Game", Dynamic Games And Applications, Appeared electronically on march 19, 2018. Vol. 9, No. 1, pp. 165-216, February 2019.

A Normal Form Game Model of Search and Pursuit

Steve Alpern and Viciano Lee

1 Introduction

Traditionally, search games and pursuit games have been studied by different people, using different techniques. Pursuit games are usually of perfect information and are solved in pure strategies using techniques involving differential equations. Search games, on the other hand, typically require mixed strategies. Both Pursuit and Search games were initially modelled and solved by Rufus Isaacs in his book [8]. The first attempt to combine these games was the elegant paper of Gal and Casas [6]. In their model, a hider (a prey animal in their biological setting) begins the game by choosing among a finite set of locations in which to hide. The searcher (a predator) then searches (or inspects) k of these locations, where k is a parameter representing the time or energy available to the searcher. If the hiding location is not among those inspected, the hider wins the game. If the searcher does inspect the location containing the hider, then a pursuit game ensues. Each location has its own capture probability, known to both players, which represents how difficult the pursuit game is for the searcher. If the search-predator successfully pursues and captures the hider-prey, the searcher is said to win the game. This is a simple but useful model that encompasses both the search and the pursuit portions of the predator-prey interaction.

This paper has two parts. In the first part, we relax the assumption of Gal and Casas that all locations are equally easy to search. We give each location its own search time and we give the searcher a total search time. Thus he can inspect any set of locations whose individual search times sum to less than or equal to the searcher's total search time, a measure of his resources or energy (or perhaps the length of

S. Alpern (✉) · V. Lee
University of Warwick, Coventry, UK
e-mail: Steve.Alpern@wbs.ac.uk

V. Lee
e-mail: V.Lee.6@warwick.ac.uk

D. M. Ramsey and J. Renault (eds.), *Advances in Dynamic Games*,
Annals of the International Society of Dynamic Games 17,
https://doi.org/10.1007/978-3-030-56534-3_3

daylight hours, if he is a day predator). We consider two scenarios. The first scenario concerns n hiding locations, in which the search time at each location is inversely proportionate with the capture probability at that location. In the second, we consider that there are many hiding locations, but they come in only two types, identifiable to the players. Locations within a type have the same search time and the same capture probability. There may be any number of locations of each type.

The second part of the paper relaxes the assumption that the players know the capture probability of every location precisely. Rather, we assume that a distribution of capture probabilities is known. The players can learn these probabilities more precisely by repeated play of the game. We analyse a simple model with only two locations and two periods, where one location may be searched in each period. While simple, this model shows how the knowledge that the capture probabilities will be updated in the second period (lowered at a location where there was a successful escape) affects the optimal play of the game.

2 Literature Review

An important contribution of the paper of Gal and Casas discussed in the Introduction is the analysis involves finding a threshold of locations beyond which the searcher can inspect. If this is sufficiently high, for example, if he can inspect all locations, then the hider adopts the pure strategy of choosing the location for which the probability of successful pursuit is the smallest. On the other hand, if k is below this threshold (say $k = 1$), the hider mixes his location so that the probability of being at a location multiplied by its capture probability (the desirability of inspecting such a location) is constant over all locations.

The paper of Gal and Casas [6] requires that the searcher knows his resource level (total search time) k. In a related but not identical model of Lin and Singham [10] it is shown that sometimes the optimal searcher strategy does not depend on k. This paper is not directly related to our findings but reader may find it useful to know the distinction between this paper and ours.

Alpern et al. [2] extended the Gal-Casas model by allowing repeated play in the case where the searcher chose the right location but the pursuit at this hiding location is not successful. They found that the hider should choose his location more randomly when the pursuing searcher is more persistent.

More recently, Hellerstein et al. [7] introduced an algorithm similar to that of the *fictitious* play where the searcher recursively updates his optimal strategy after knowing the response of the opponent's. They apply this technique to games similar to those we consider here. Their algorithm is likely to prove a powerful technique for solving otherwise intractable search games.

More generally, search games are discussed in Alpern and Gal [1] and search and pursuit problems related to robotics are categorized and discussed in Chung et al. [5].

3 Single Period Game with General Search Times

Consider a game where the searcher wishes to find the hider at one of n locations and then attempt to pursue and capture it, within a limited amount of resources denoted by k. Each location i has two associated parameters: a *search time* t_i required to search the location and a *capture probability* $p_i > 0$ that if found at location i the searcher's pursuit will be successful. Both t_i and p_i are known to the searcher and the hider.

The game $G(n, t, p, k)$, where $t = (t_1, \ldots, t_n)$ and $p = (p_1, \ldots, p_n)$ represent the time and capture vectors, is played as follows. The hider picks a location $i \in N \equiv \{1, 2, ..., n\}$ in which to hide. The searcher can then inspect search locations in any order, as long as their total search time does not exceed k. The searcher wins (payoff = 1) if he finds and then captures the hider; otherwise the hider wins (payoff = 0). We can say that this game is a constant sum game where the value $V = V(k)$ is the probability that the predator wins with given total search time k.

A mixed strategy for the hider is a distribution vector $h \in H$, where

$$H = \left\{ h = (h_1, h_2, \ldots, h_n) : h_i \geq 0, \sum_{1}^{n} h_i = 1 \right\}.$$

A pure strategy for the searcher is a set of locations $A \subset N$ which can be searched in total time k. His pure strategy set is denoted by $a(k)$, where

$$a(k) = \{A \subset N : T(A) \equiv \sum_{i \in A} t_i \leq k\}.$$

The statement above simply states that a searcher can inspect any set of locations for which the total search time does not exceed his maximum search time k. A mixed search strategy is a probabilistic choice of these sets.

The payoff P from the perspective of the maximizing searcher is given by

$$P(A, i) = \begin{cases} p_i & \text{if } \ i \in A, \text{ and} \\ 0 & \text{if } \ i \notin A. \end{cases}$$

As part of the analysis of the game, we may wish to consider the best response problem faced by a searcher who knows the distribution h of the hider. The "benefit" of searching each location i is given by $b_i = h_i \ p_i$, the probability that he finds and then captures the hider (prey). Thus when h is known, the problem for the searcher essentially is to choose the set of locations $A \in \alpha(k)$ which maximizes $b(A) = \sum_{i \in A} b_i$. This is a classic Knapsack problem from the Operations Research literature (A seminal book of the Knapsack problem is by Kellerer et al. [9]). The *objects* to be put into the *knapsack* are the locations i. Each has a "weight" t_i and a benefit b_i. He wants to fill the knapsack with as much total benefit subject to a total weight restriction of k.

The knapsack approach illustrates a simple domination argument: the searcher should never leave enough room (time) in his knapsack to put in another object. However to better understand this observation, we show the definition of *Weakly dominant* below

Definition 1 Strategy X weakly dominates strategy Y iff (i) X never provides a lower payoff than Y against all combinations of opposing strategies and (ii) there exists at least one combination of strategies for which the payoffs for X and Y are equal.

Having stated this, we write this simple observation as follows.

Lemma 1 *Fix k. The set $A \in \alpha(k)$ is weakly dominated by the set $A' \in \alpha(k)$ if $A \subset A'$ and there is a location $j \in A' - A$.*

Proof If i is in both A or i is not in A', then $P(A, i) = P\left(A', i\right)$. If $i \in A' - A$ then $P\left(A', i\right) = p_i > 0 = P(A, i)$.

3.1 An Example

To illustrate the general game we consider an example with $n = 4$ locations. The search times are given by $t = (5, 3, 4, 7)$ and the respective capture probabilities are given by $p = (.1, .2, .15, .4)$. In this example it is easiest to name the locations by their search time, so for example the capture probability at location 7 is 0.4. The searcher has total search time given by $k = 7$, so he can search any single location or the pair $\{3, 4\}$. The singleton sets $\{3\}$ and $\{4\}$ are both dominated by $\{3, 4\}$. We put the associated capture time next to the name of each location. Thus the associated reduced matrix game is simply

A\location	5 (.1)	3 (.2)	4 (.15)	7 (.4)
{5}	.1	0	0	0
{7}	0	0	0	.4
{3, 4}	0	.2	.15	0

Solving the matrix game using online solver [4] shows that the prey hides in the four locations with probabilities $(12/23, 0, 8/23, 3/23)$ while the searcher inspects $\{5\}$ with probability $12/23$, $\{7\}$ with probability $3/23$, and $\{3, 4\}$ with probability $8/23$. The value of the game, that is, the probability that the predator-searcher finds and captures the prey-hider, is $6/115$. Our approach in this paper is not to solve games in the numerical fashion, but rather to give general solutions for certain classes of games, as Gal and Casas did for the games with $t_i = 1$.

3.2 The Game with t_i Constant

Choosing all the search times t_i the same, say 1, we may restrict k to integers. This is the original game introduced and solved by Gal and Casas [6]. Since the t_i are the same, we may order the locations by their capture probabilities, either increasing or decreasing. Here we use the increasing order of the original paper. Clearly if $k = 1$ the hider will make sure that all the locations are equally good for the searcher ($p_i h_i$ =constant) and if $k = n$ the hider knows he will be found so he will choose the location with the smallest capture probability (here location 1). The nice result says that there is a threshold value for k which divides the optimal hiding strategies into two extreme types.

Proposition 1 (Gal and Casas [6]) *Consider the game* $G(n, t, p, k)$ *where* $t_i = 1$ *for all* i *and the locations are ordered so that* $p_1 \leq p_2 \leq \cdots \leq p_n$. *Define* $\lambda = \sum_{i=1}^{n} 1/p_i$. *The value of this game is given by* $\min(k\lambda, p_1)$. *If* $k < p_1/\lambda$ *then the unique optimal hiding distribution is* $h_i = \lambda/p_i$, $i = 1, \ldots, n$. *If* $k \geq p_1/\lambda$ *then the unique optimal hiding strategy is to hide at location* 1.

3.3 The Game with $t_i = i$, p_i Decreasing, $k = n$ Odd

We now consider games with $t_i = i$ and p_i decreasing. In some sense locations with higher indices i are better for the hider in that they take up more search time and have a lower capture probability. Indeed if the searcher has enough resource k to search all the locations ($k = \sum_{i=1}^{n} t_i = n(n+1)/2$) then of course the hider should simply hide at location n and keep the value down to p_n. Note that if $k < n$, the hider can win simply by hiding at location n, which takes time $t_n = n$ to search. We give a complete solution for the smallest nontrivial amount of resources (total search time) of $k = n$. Let us first define the following two variables which will be widely used in our main result.

$$S(p) = \sum_{j=m+1}^{2m+1} 1/p_j; \quad \bar{h}_j = 1/\left(p_j S(p)\right).$$

Proposition 2 *Consider the game* $G(n, t, p, k)$, *where* $t_i = i$, p_i *is decreasing in* i *and* $k = n = 2m + 1$. *Then*

1. *An optimal strategy for the searcher is to choose the set* $\{j, n - j\}$ *with probability* $1/\left(p_j\ S(p)\right)$ *for* $j = m + 1, \ldots, n$.
2. *An optimal strategy for the hider is to choose location* j *with probability* $\bar{h}_j$ *for* $j \geq m + 1$ *and not to choose locations* $j \leq m$ *at all.*
3. *The value of the game is* $V = \frac{1}{S(p)}$.

Proof Suppose the searcher adopts the strategy suggested above. Any location i that the hider chooses belongs to one of the sets of the form $\{j, n-j\}$ for $j = m+1, \ldots, n$, where the set $\{n, 0\}$ denotes the set $\{n\}$. Since for $j \geq m+1$ we have $j > n-j$ and the p_i are decreasing, the hider is better off choosing location j. In this case he is found with probability $1/\left(p_j\ S\left(p\right)\right)$ and hence he is captured with probability at least $p_j\ \left(1/\left(p_j\ S\left(p\right)\right)\right) = 1/S\left(p\right)$.

Suppose the hider adopts the hiding distribution suggested above. Note that no pure search strategy can inspect more than one of the locations $j \geq m+1$. Suppose that location j is inspected, then the probability that the searcher finds and captures the hider is given by $\bar{h}_j p_j = 1/\left(p_j S\left(p\right)\right)\ p_j = 1/S\left(p\right)$. It follows that $S\left(p\right)$ is the value of the game.

It is natural to also analyse if Proposition 2 still holds true for $k = n =$ even number. For the simplicity of our notation and better readability of Proposition 2, we decided to write this separate section for even number. In the case where $k = n =$ even, the solution is exactly the same as their odd counterpart. More specifically $k = n = 2m$ has the same value and optimal strategies as $k = n = 2m+1$. However, it is important to note that in the even case, both the searcher's and hider's optimal strategy is unique. For instance, $k = n = 4$ has the same value and optimal strategies as $k = n = 5$. The same can be said for 6 and 7, 8 and 9, etc.

Corollary 1 *Assuming the p_i are strictly decreasing in i, the hider strategy $\bar{h}$ given above is uniquely optimal, but the searcher strategy is not.*

Proof Let $h^* \neq \bar{h}$ be a hiding distribution. We must have $h^*_j + h^*_{n-j} > \bar{h}_j + \bar{h}_{n-j} = 1/\left(p_j S\left(p\right)\right)$ for some $j \geq m+1$; otherwise the total probability given by h^* would be less than 1. Against such a distribution h^*, suppose that the searcher inspects the two locations j and $n-j$. Then the probability that the searcher wins is given by $p_j h^*_j + p_{n-j} h^*_{n-j} \geq p_j \left(h^*_j + h^*_{n-j}\right)$ because $p_j < p_{n-j}$. But by our previous estimate $h^*_j + h^*_{n-j} > 1/\left(p_j S\left(p\right)\right)$ this means the searcher wins with probability at least $p_j \left(1/\left(p_j S\left(p\right)\right)\right) = 1/S\left(p\right)$ and hence h^* is not optimal.

Next, consider the searcher strategy which gives the same probability as above for all the sets $\{j, n-j\}$ for $j \geq m+2$ but gives some of the probability assigned to $\{m+1, m\}$ to the set $\{m+1, m-1\}$. Let's say the probability of $\{m+1, m-1\}$ is a small positive number ε. The total probability of inspecting location $m+1$ (and all larger locations) has not changed. The probability of inspecting location m has gone down by ε. So the only way the new searcher strategy could fail to be optimal is potentially when the hider chooses location m. In this case the probability that the searcher wins is given by

$$\left(\left(1/\left(p_{m+1}\ S\left(p\right)\right)\right) - \varepsilon\right)\ p_m.$$

Comparing this to the value of the game, we consider the difference

$$((1/(p_{m+1}\ S(p))) - \varepsilon)\ \ p_m - \frac{1}{S(p)} = \frac{p_m - p_{m-1}}{p_m\ S(p)} - \varepsilon p_m.$$

Since the first term on the right is positive because $p_m > p_{m-1}$, the difference will be positive for sufficiently small positive ε.

We will now consider an example to show how the solution changes as k goes up from the solved case of $k = n$. We conjecture that there exist a threshold with respect to k in which above that threshold, the hider 's optimal strategy is to hide at location n. To determine that threshold we use the following idea.

Proposition 3 *The game* $G(n, p, t, k)$ *has value* $v = p_n$ *if and only if the value* v' *of the game* $G(n-1, (p_1, \ldots, p_{n-1}), (1, 2, \ldots, n-1), k-n)$ *(with the last location removed and resources reduced by n) is at least* p_n.

Proof Suppose $v = p_n$. Every search set with positive probability must include location n, otherwise simply hiding there implies $v < p_n$. So the remaining part of every search set has $k' = k - n$. With this amount of resources, the searcher must find the hider in the first n locations with probability at least p_n, which is stated in the Proposition. Otherwise, the searcher will either have to not search location n certainly (which gives $v < p_n$) or not search the remaining locations with enough resources to ensure $v \geq p_n$.

3.4 An Example with $k = 10, n = 5$

Consider the example where $p = (.5, .4, .3, .2, .1)$ with $k = 10, n = 5$. Here $p_n = .1$. The game with $p' = (.5, .4, .3, .2)$ and $k' = k - n = 5$ has value at least .1 because of the equiprobable search strategy of $\{1, 4\}$ and $\{2, 3\}$. Here each location in the new game is inspected with the same probability 1/2 and consequently the best the hider can do is to hide in the best location 4, and then the searcher wins with probability $(1/2)(.2) = .1$. It follows from Proposition 3 that the original game has the minimum possible value of $v = p_n = p_5 = .1$.

3.5 Illustrative Examples

In this section, we will use an example to further illustrate Proposition 2 and Corollary 1.

First, we consider the game where $k = n = 5$, $t_i = i$, and $p = (.5, .4, .3, .2, .1)$. The game matrix, excluding dominated search strategies, is given by

A\location	1	2	3	4	5
{5}	0	0	0	0	.1
{1, 4}	.5	0	0	.2	0
{2, 3}	0	.4	.3	0	0
{1, 3}	.5	0	.3	0	0
{1, 2}	.5	.4	0	0	0

The unique solution for the optimal hiding distribution is $(0, 0, 2/11, 3/11, 6/11)$ and the value is $6/110 = 1/(1/.3 + 1/.2 + 1/.1) \simeq .055$. The optimal search strategy mentioned in Proposition 2 is to play {5} , {1, 4} and {2, 3} with respective probabilities $6/11$, $3/11$ and $2/11$. Another strategy is to play {5} and {1, 4} the same but to play {2, 3} and {1, 3} with probabilities $3/22$ and $1/22$. It is of interest to see how the solution of the game changes when k increases from $k = n = 5$ to higher values. We know that we need go no higher than $k = 10$ from Proposition 3 because in the game on locations 1 to 4 with $k' = 10 - 5 = 5$, the searcher can inspect {4, 1} with probability $2/3$ and {3, 2} with probability $1/3$ to ensure winning with probability at least $1/10 = p_5$ (Table 1).

So we know the solution of the game for $k = 5$ and $k \geq 10$. The following table gives the value of the game and the unique optimal hiding distribution for these and intermediate values. (The optimal search strategies are varied and we don't list them, though they are easily calculated).

We know that the value must be nondecreasing in k, but we see that it is not strictly increasing. Roughly speaking (but not precisely), the hider restricts towards fewer and better locations as k increases, staying always at the best location 5 for $k \geq 10$. However there is the anomalous distribution for $k = 9$ which includes sometime hiding at location 2.

Table 1 Optimal hiding distribution and values, $k \geq 5$

$k\backslash i$	1	2	3	4	5	Value
5	0	0	2/11	3/11	6/11	$3/55 \simeq 0.0545$
6	0	0	2/11	3/11	6/11	$3/55 \simeq 0.0545$
6	0	0	0	1/3	2/3	$1/15 \simeq 0.0667$
8	0	0	0	1/3	2/3	$1/15 \simeq 0.0667$
9	0	3/37	4/37	6/37	24/37	$18/185 \simeq 0.0943$
≥ 10	0	0	0	0	1	$1/10 = 0.1$

3.6 Game with Two Types of Locations

In this section we analyse a more specific scenario where all available hiding locations are of two types. This model might be vaguely applied to military practices. Suppose a team of law enforcement is to capture a hiding fugitive in an apartment complex, then all possible hiding locations can be reduced to a number of types, e.g. smaller rooms have similar shorter search times and higher capture probability than a parking lot. Here we solve the resulting search-pursuit game.

Suppose there are two types of locations (hiding places). Type 1 takes time $t_1 = 1$ (this is a normalization) to search, while type 2 takes time $t_2 = \tau$ to search, with τ being an integer. Now let type 1 locations have capture probability p while type 2 locations have capture probability q. Moreover, suppose there are a locations of type 1 and b locations of type 2. The searcher has total search time k. To simplify our results we assume that k is small enough such that $a \geq k$ (the searcher can restrict all his searches to type 1) and $b\tau \geq k$ (he can also restrict all his searches to type 2 locations).

Let $m = \lfloor k/\tau \rfloor$ be the maximum number of type 2 locations that can be searched. The searcher's strategies are to search $j = 0, 1, \ldots, m$ type 2 locations (and hence $k - \tau j$ locations of type 1). Since all locations of a given type are essentially the same, the decision for the hider is simply the probability y to hide at a randomly chosen location of type 1 (and hence hide at a randomly chosen location of type 2 with probability $1 - y$).

Then the probability $P(j, y)$ that the searcher wins the game is given by

$$\begin{aligned} & yp\left(\frac{k - \tau j}{a}\right) - (1 - y)q\left(\frac{j}{b}\right) \\ & = \frac{k}{a}py + \left(\frac{q}{b}(1 - y) - \frac{1}{a}py\tau\right)j. \end{aligned}$$

This will be independent of the searcher's strategy j if

$$\frac{q}{b}(1 - y) - \frac{1}{a}py\tau = 0, \text{ or}$$

$$y = \bar{y} \equiv \frac{aq}{aq + bp\tau}.$$

For $y = \bar{y}$, the capture probability is given by

$$P(j, \bar{y}) = \frac{pqk}{aq + bp\tau}.$$

By playing $y = \bar{y}$, the hider ensures that the capture probability (payoff) does not exceed $P(j, \bar{y})$.

We now consider how to optimize the searcher's strategy. Suppose the searcher searches j locations of type 2 with probability x_j, $j = 0, 1, \ldots, m$. If the hider is at a type 2 location then he is captured with probability

$$\sum_{j=0}^{m} x_j \frac{qj}{b} = \frac{q}{b} \sum_{j=0}^{m} j x_j = \frac{q}{b} \hat{j}, \text{ where}$$
$$\hat{j} = \sum_{j=0}^{m} j x_j$$

is the mean number of searches at type 2 locations. Similarly, if the hider is at a type 1 location, the hider is captured with probability

$$\sum_{j=0}^{m} x_j \frac{p(k - \tau j)}{a} = \frac{pk}{a} - \frac{p\tau}{a} \sum_{j=0}^{m} j x_j$$
$$= \frac{pk}{a} - \frac{p\tau}{a} \hat{j}.$$

It follows that the capture probability will be the same for hiding at either location if we have

$$\frac{q}{b} \hat{j} = \frac{pk}{a} - \frac{p\tau}{a} \hat{j}, \text{ or,}$$
$$\hat{j} = \frac{pbk}{bp\tau + aq}.$$

So for any probability distribution over the pure strategies $j \in \{0, 1, \ldots, m\}$ with mean $\hat{j}$, the probability of capturing a hider located either at a type 1 or a type 2 location is given by

$$\frac{q}{b} \hat{j} = \frac{pk}{a} - \frac{p\tau}{a} \hat{j} = \frac{pqk}{aq + bp\tau}.$$

To summarize, we have shown the following.

Proposition 4 *Suppose all the hiding locations are of two types: a locations of type 1 with search time 1 and capture probability p; b locations of type 2 with search time τ and capture probability q. Suppose a and b are large enough so the searcher can do all his searching at a single location type, that is, $k \leq max(a, \tau b)$. Then the unique optimal strategy for the hider is to hide in a random type 1 location with probability $\bar{y} = \frac{aq}{aq+bp\tau}$ and in a random type 2 location with probability $1 - \bar{y}$. Note that this is independent of k. A strategy for the searcher which inspects j locations*

of type 2 (and thus, $k - j\tau$ for type 1) with probability x_j is optimal if and only if the mean number $\hat{j} = \sum_{j=0}^{m} j x_j$, $m = \lfloor k/\tau \rfloor$ of type 2 locations inspected is given by $\hat{j} = \frac{pbk}{bp\tau + aq}$. If this number is an integer, then the searcher has an optimal pure strategy. The value of the game is given by $\frac{pqk}{aq+bp\tau}$.

4 Game Where Capture Probabilities Are Unknown But Learned

In this section we determine how the players can *learn* the values of the capture probabilities over time, starting with some a priori values and increasing these at locations from which there have been successful escapes. This of course requires that the game is repeated. Here we consider the simplest model, just two rounds. So after a successful escape in the second round, we consider that the hider-prey has won the game (Payoff 0). More rounds of repeated play are considered in Gal et al. [2], but learning is not considered there.

We begin our analysis with two hiding locations, one of which may be searched in each of the two rounds. If the hider is found at location i, he is captured with a probability $1 - q_i$ (escapes with complementary probability q_i). There are two rounds. If the hider is not found (searcher looks in the wrong location) in either round, he wins and the payoff is 0: If the hider is found and captured in either round, the searcher wins and the payoff is 1: If the Hider is found but escapes in the first round, the game is played one more time and both players remember which location the hider escaped from. If the hider escapes in the second (final) round, he wins and the payoff is 0.

The novel feature here is that the capture probabilities must be learned over time. At each location, the capture probability is chosen by Nature before the start of the game, independently with probability 1/2 of being h (high) and probability 1/2 of being l (the low probability), with $h > l$. In the biological scenario, this may be the general distribution of locations in a larger region in which it is easy or hard to escape from. A more general distribution is possible within our model, but this two point distribution is very easy to understand. If there is escape from location i in the first round, then in the second round the probability that the capture probability at i is h goes down (to some value less than $1/2$). This is a type of Bayesian learning, which only takes place after an escape, and only at the location of the escape.

Our model contributes to the realistic interaction between searching-predator and hiding-prey acting in a possibly changing environment. Most often in nature, the searcher has no or incomplete information during the search and pursuit interaction. Particularly in Mech et al. [11], a pack of wolves has to learn over time the difficulty of pursuing their prey in specific terrain. Moreover, hiding-prey such as elk seems to prefer areas with lots toppled dead trees, creating an entanglement of logs difficult to travel through. We focus here on asking questions if learning the capture probabilities will affect the searching and hiding behaviour. More specifically, suppose an elk

manages to escape through the deep forest, should it stay there where he believes the capture probability is low enough, or hide at a different location?

4.1 Normal Form of the Two-Period Learning Game

We use the *normal form* approach, rather than a repeated game approach. A strategy for either player says where he will search/hide in the two periods (assuming the game goes to the second period). Due to the symmetry of the two locations, both players cannot but choose their first period search or hide locations randomly. Thus the players have two strategies: rs (random, same) and rd (random, different). If there is a successful escape from that location, they can either locate in the same location (strategy rs) or the other location (strategy rd). This gives a simple two by two matrix game. In this subsection we calculate its normal form; in the next subsection we present the game solution.

First we compute the payoff for the strategy pair (rs, rs): Half the time both players (searcher and hider) go to different locations in first period, in which case the hider wins and the payoff is 0. So we ignore this, put in a factor of (1/2), and assume they go to the same location in the first period. There is only one location to consider, suppose it has escape probability x. Then, as they both go back to this location in the second period if the hider escapes in the first period, the expected payoff is given by

$$P_x(rs, rs) = (1/2)\ \ ((1-x)1 + x(1-x)). \tag{1}$$

Since x takes values l and h equiprobably we have

$$\begin{aligned} P(rs, rs) &= \frac{P_h(rs, rs) + P_l(rs, rs)}{2} \\ &= \frac{2 - h^2 - l^2}{4}. \end{aligned} \tag{2}$$

It is worth noting two special cases: If both escape probabilities are 1 (escape is certain), then the hider always wins and the payoff is 0. If both escape probabilities are 0 then the searcher wins if and only if they both choose the same location, which has probability $1/2$.

Next we consider the strategy pair (rd, rd). Here we can assume they both go to location 1 in the first period (hence we add the factor of 1/2) and location 2 in the second period. The escape probabilities at these ordered locations 1 and 2 can be any of the following: hh, ll, hl, lh. The first two are straightforward as it is the same as going to the same location twice (already calculated in (2)). We list the calculation of the four ordered hiding locations below, where P_x is given in (1).

$$
\begin{aligned}
P_{hh}(rd, rd) &= P_h(rs, rs) \\
P_{ll}(rd, rd) &= P_l(rs, rs) \\
P_{lh}(rd, rd) &= (1/2)((1-l)1 + l(1-h)) \\
P_{hl}(rd, rd) &= (1/2)((1-h)1 + h(1-l)).
\end{aligned}
$$

Taking the average of these four values gives

$$
P(rd, rd) = \frac{4 - h^2 - l^2 - 2hl}{8} = \frac{4 - (h+l)^2}{8}. \tag{3}
$$

Now consider the strategy pair (rs, rd). If they go to different locations in the first period, the game ends with payoff 0. So again, we put in factor of 1/2 and assume they go to same location in first period. This means that if an escape happens in the first period, the hider wins (payoff 0) in the second period. So the probability the searcher wins is

$$
\begin{aligned}
P(rs, rd) = P(rd, rs) &= (1/2)\Big(1/2((1-h) + (1-l))\Big) \\
&= \frac{2 - (h+l)}{4}.
\end{aligned} \tag{4}
$$

Thus, we have completed the necessary calculations and the game matrix for the strategy pairs rs and rd, with searcher as the maximizer.

To solve this game, we begin with the game matrix as follows:

$$
\begin{aligned}
A = A(l, h) &= \begin{bmatrix} P\,(rs, rs) & P\,(rs, rd) \\ P\,(rd, rs) & P\,(rd, rd) \end{bmatrix} \\
&= \begin{bmatrix} \frac{2-(h^2+l^2)}{4} & \frac{2-(h+l)}{4} \\ \frac{2-(h+l)}{4} & \frac{4-(h+l)^2}{8} \end{bmatrix}
\end{aligned}
$$

Then we take out the fraction 1/8 to the left-hand side of the equation, and we have

$$
8A = \begin{bmatrix} -2h^2 - 2l^2 + 4 & 4 - 2h - 2l \\ 4 - 2h - 2l & 4 - (h+l)^2 \end{bmatrix}
$$

At this point we try to make the right-hand side of the equation to be a diagonal matrix so we can easily compute it. Therefore we can write the equation as follows:

$$
8A - (4 - 2h - 2l)\begin{bmatrix} 1 & 1 \\ 1 & 1 \end{bmatrix} = Y = \begin{bmatrix} -2h^2 + 2h - 2l^2 + 2l & 0 \\ 0 & 2h + 2l - (h+l)^2 \end{bmatrix}.
$$

Note that $V(A)$ is the value of the matrix A. From the equation above, it shows that the right-hand side of the equation is a diagonal matrix, and a simple formula for the value of diagonal matrix games is as follows:

$$V\left(\begin{bmatrix} a & 0 \\ 0 & b \end{bmatrix}\right) = 1/\left(1/a + 1/b\right).$$

Using the above formula, we have

$$V\left(8A - (4 - 2h - 2l)\begin{bmatrix} 1 & 1 \\ 1 & 1 \end{bmatrix}\right) = V(Y) = \frac{1}{\frac{1}{-2h^2+2h-2l^2+2l} + \frac{1}{2h+2l-(h+l)^2}}.$$

Computing this for the value of game matrix A, we have the following equation for $V(A)$,

$$V(A) = \frac{1}{2} - \frac{1}{4}l - \frac{1}{4}h - \frac{1}{8\left(\frac{1}{2h^2-2h+2l^2-2l} - \frac{1}{2h+2l-(h+l)^2}\right)}. \tag{5}$$

It is also important to note that in a diagonal game, players adopt each strategy with a probability inversely proportional to its diagonal element. To obtain this we first calculate the value of $V(Y)$ given above. Then, both the searcher and hider should choose rs and rd with probabilities $V(Y)/a$ and $V(Y)/b$, respectively.

We can now see that, as expected, a successful escape from a location makes that location more attractive to the hider as a future hiding place. This is confirmed in the following.

Proposition 5 *In the learning game when $l < h$, after a successful escape both players should go back to the same location with probability greater than 1/2.*

Proof Let a and b denote, as above, the diagonal elements of Y. We have

$$\begin{aligned} a - b &= \left(-2h^2 + 2h - 2l^2 + 2l\right) - \left(2h + 2l - (h + l)^2\right) \\ &= -(h - l)^2 < 0. \end{aligned}$$

This means that $b > a$ and $V/a > V/b$. Hence by observation (5) the strategy rs should be played with a higher probability (V/a) than rd (probability V/b), in particular with probability more than $1/2$.

4.2 An Example with $l = 1/3$ and $h = 2/3$

A simple example is when the low escape probability is $l = 1/3$ and the high escape probability is $h = 2/3$. This gives the matrix A as

$$A(l,h) = \begin{bmatrix} \frac{13}{36} & \frac{1}{4} \\ \frac{1}{4} & \frac{5}{8} \end{bmatrix}$$

with value $V = V(1/3, 2/3) = 21/68$, and where each of the player optimally plays rs with probability $9/17$ and rd with probability $8/17$.

Suppose there is an escape in the first period at say location 1, then in the second period the hider goes to location 1 with probability 9/17. Since the subjective probability of capture at location 2, from the point of view of either player, remains unchanged at $(1/3 + 2/3)\ /2 = 1/2$; this corresponds to a certain probability x at location 1, that is, a matrix

$$\begin{bmatrix} x & 0 \\ 0 & 1/2 \end{bmatrix}$$

We then have that

$$(9/17)x = (8/17)(1/2) \text{ or,}$$
$$x = 4/9.$$

This corresponds to the probability of escape probability $l = 1/3$ of q, where

$$q1/3 + (1-q)2/3 = 4/9 \text{ or,}$$
$$q = 2/3.$$

Thus, based on the escape at location 1 in the first period, the probability that the escape probability there is 1/3 has gone up from the initial value of 1/2 to the higher value of 2/3.

5 Summary

The breakthrough paper of Gal and Casas [6] gave us a model in which both the search and pursuit elements of predator-prey interactions could be modelled together in a single game. In that paper the capture probabilities depended on the hiding location but the time required to search a location was assumed to be constant. In the first part of this paper, we drop that simplifying assumption. We first consider a particular scenario where we order the locations such that the search times increase while the capture probabilities decrease. We solve this game for the case of a particular total search time of the searcher. We then consider a scenario where there are many hiding locations but they come in only two types. Locations of each type are identical in

that they have the same search times and the same capture probabilities. We solve the resulting search-pursuit game.

In the second part of the paper we deal with the question of how the players (searcher-predator and hider-prey) learn the capture probabilities of the different locations over time. We adopt a simple Bayesian approach. After a successful escape from a given location, both players update their subjective probabilities that it is a location with low or high capture probability; the probability that it is low obviously increases. In the game formulation, the players incorporate into their plan the knowledge that if there is an escape, then that location becomes more favourable to the hider in the next period.

The search-hide and pursuit-evasion game is quite difficult and finding a solution for the most general case is quite challenging. Most probably, it is a good idea for the next step to solve for a more specific question in the problem.

We consider a possible extension to Proposition 4 by analysing larger k . Consider the example $a = b = 1; t_1 = 1; t_2 = 3; k = 4$; and say $p < q$ ($p_1 < p_2$ as in Gal and Casas [6]). The Searcher inspects both cells (one of each type), so he certainly finds the Hider. He captures him with probability p if the hider is at location 1, and q if at location type 2. So the Hider should hide at location of type 2 as it has lower capture probability. The main question will be: How big does k have to be for this to occur? And are there only two solution types as in Gal and Casas [6]? We conjecture that, as in Gal-Casas, there is a critical value of $k = \hat{k}$ such that for $k < \hat{k}$, Proposition 4 applies, and for $k \geq \hat{k}$ the Hider locates in a cell of the type with the lower capture probability.

The game with learning model has also been analysed using dynamic form [3]. This allows more effective analysis for more than two locations and two rounds. Moreover, we believe the next avenue of research is to consider the non-zero-sum game. Indeed, one may argue that a game between a predator and a prey may not necessarily be a (or in our case, constant-sum game), as the predator is hunting it's dinner while the prey is running for survival. This is important if challenging aspect to deal with for future studies.

References

1. Alpern, S., Gal, S.: The Theory of Search Games and Rendezvous. Kluwer Academic Publishers, Dordrecht (2006)
2. Alpern, S., Gal, S., Casas, J.: Prey should hide more randomly when a predator attacks more persistently. Journal of the Royal Society Interface **12**, 20150861 (2015)
3. Alpern, S., Gal, S., Lee, V., Casas, J.: A stochastic game model of searching predators and hiding prey. Journal of the Royal Society Interface, **16**(153), 20190087 (2019)
4. Avis, D., Rosenberg, G., Savani, R., Stengel, B. von: Enumeration of Nash Equilibria for Two-Player Games. Economic Theory **42**, 9-37 (2010). Online solver available at http://banach.lse.ac.uk.
5. Chung, T., Hollinger, G., Isler, V.: Search and pursuit-evasion in mobile robotics. Autonomous Robots, **31**(4):299–316 (2011)

6. Gal, S., Casas, J.: Succession of hide–seek and pursuit–evasion at heterogeneous locations. Journal of the Royal Society Interface **11**, 20140062 (2014).
7. Hellerstein, L., Lidbetter, T., Pirutinsky, D.: Solving Zero-sum Games using Best Response Oracles with Applications to Search Games, Operations Research, **67**(3):731–743 (2019)
8. Isaacs, R.: Differential Games. Wiley, New York (1965)
9. Kellerer, H., Pferschy, U., Pisinger, D.: Knapsack problems. Berlin: Springer (2004)
10. Lin, K. Y., Singham, D.: Finding a hider by an unknown deadline. Operations Research Letters **44**, 25–32 (2016)
11. Mech, L. D., Smith, D. W., MacNulty, D. R.: Wolves on the hunt: the behavior of wolves hunting wild prey. University of Chicago Press (2015)

Computation of Robust Capture Zones Using Interval-Based Viability Techniques in Presence of State Uncertainties

Stéphane Le Ménec and Vladimir Turetsky

1 Introduction

The problem of intercepting a maneuverable target admits different mathematical formulations. It can be formulated as a differential game (quantitative or qualitative) where the interceptor and target play the role of the pursuer and evader, respectively. The optimal pursuer strategies in these games are of a bang-bang type [11]. The other formulation, adopted in this paper, is a robust control problem in a prescribed class of feedback strategies, namely in the classes of linear and saturated linear strategies.

If the pursuer strategy is assigned, the first question is: does this strategy guarantee the capture robustly against any evader's bounded control? If a strategy has such a property, it is called a *robust capturing strategy*. Note that in this definition, no differential game formulation is assumed. The notion of a robust capturing strategy refers to a given strategy and does not mean an optimal strategy in some differential game. However, if it is, for example, a linear strategy, the capture can be achieved by using an excessively large gain thus violating technical and physical control constrains. This implies the next question: from what set of initial conditions this strategy robustly guarantees the capture in such a way that the control constraints are satisfied along any trajectory. Such a set is called *robust capture zone* of an assigned strategy. The problem of constructing a robust capture zone has close connections with invariant set theory [4], stable bridges construction [5, 9], viability theory [3] and other fields of control theory and applications.

S. Le Ménec (✉)
Airbus / MBDA, 1, Avenue Réaumur, 92358 Le Plessis-Robinson Cedex , France
e-mail: stephane.le-menec@mbda-systems.com

V. Turetsky
Department of Applied Mathematics, Ort Braude College of Engineering, 51 Snunit Str, 2161002 Karmiel, Israel
e-mail: turetsky1@braude.ac.il

D. M. Ramsey and J. Renault (eds.), *Advances in Dynamic Games*,
Annals of the International Society of Dynamic Games 17,
https://doi.org/10.1007/978-3-030-56534-3_4

It is crucially important to have an accurate description or a good approximation of the robust capture zone before making a decision in favor of implementing this or another capturing strategy. Choosing a linear (a saturated linear) strategy in practical implementations is caused both by their simple structure and by a non-chattering performance (see, e.g., [13, 14]). Verifying that a linear or saturated linear strategy is robust capturing, and constructing their robust capture zones are based on the robust controllability theory developed by [7].

We apply viability theory tools to reformulate the concept of robust capture zones in terms of capture basin. An interval implementation of capture basin computation is used to numerically approximate robust capture zones. For comparison purpose, we first provide results dealing with linear kinematics that are already obtained in an analytical manner. Then, new results are performed using the same interval analysis based algorithms, the same kinematics, but considering noisy measurements that analytical methods are not able to deal with.

2 Problem Statement and Preliminaries

2.1 Engagement Model

A planar engagement between two moving object—an interceptor (*pursuer*) and a target (*evader*)—is considered. The schematic view of this engagement is shown in Fig. 1. The X-axis of the coordinate system is aligned with the initial line of sight. The origin is collocated with the initial pursuer position. The points (x_p, y_p), (x_e, y_e) are the current coordinates; V_p and V_e are the velocities and a_p, a_e are the lateral accelerations of the pursuer and the evader, respectively; φ_p, φ_e are the respective angles between the velocity vectors and the reference line of sight; and $y = y_e - y_p$ is the relative separation normal to the initial line of sight.

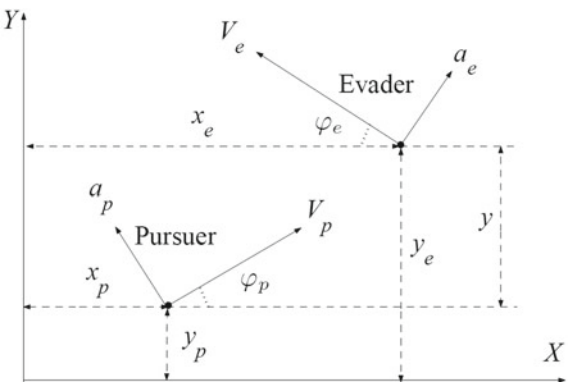

Fig. 1 Interception geometry

It is assumed that the dynamics of each object is expressed by a first-order transfer function with the time constants τ_p and τ_e, respectively. The velocities and the bounds of the lateral acceleration commands of both objects are constant. The dynamics of the pursuer and the evader are described by nonlinear systems of differential equations:

$$\begin{array}{ll} \dot{x}_p = V_p \cos\varphi_p, & x_p(t_0) = 0, \\ \dot{y}_p = V_p \sin\varphi_p, & y_p(t_0) = 0, \\ \dot{\varphi}_p = a_p / V_p, & \varphi_p(t_0) = \varphi_{p0}, \\ \dot{a}_p = (u_p^{\max} u_p - a_p)/\tau_p, & a_p(t_0) = 0, \end{array} \tag{1}$$

$$\begin{array}{ll} \dot{x}_e = -V_e \cos\varphi_e, & x_e(t_0) = r_0, \\ \dot{y}_e = V_e \sin\varphi_e, & y_e(t_0) = 0, \\ \dot{\varphi}_e = a_e / V_e, & \varphi_e(t_0) = \varphi_{p0}, \\ \dot{a}_e = (u_e^{\max} u_e - a_e)/\tau_e, & a_e(t_0) = 0, \end{array} \tag{2}$$

where $t_0 \geq 0$ is the initial time instant, r_0 is the initial distance between the missiles, u_p and u_e are the normalized lateral acceleration commands of the pursuer and the evader, respectively. Below, the strategies of the first player are chosen as functions measurable on time and Lipschitzian on the state variable. So, the trajectory of the system generated by some feedback strategy of the first player and some measurable realization of the second player's control can be considered as a solution of the corresponding Cauchy problem obtained by substituting these control functions into the system dynamics. The functions $u_p(t)$ and $u_e(t)$ should satisfy the constraints

$$|u_p(t)| \leq 1, \quad |u_e(t)| \leq 1, \tag{3}$$

$a_p^{\max}$ and $a_e^{\max}$ are the maximal lateral accelerations. The final time instant of the engagement is

$$t_f = t_f(u_p(\cdot), u_e(\cdot), t_0, \varphi_{p0}, \varphi_{e0}, r_0) =$$

$$\max\{t > 0 : \ \dot{r}(t) \leq 0\}, \tag{4}$$

where

$$r(t) = \sqrt{(x_e(t) - x_p(t))^2 + (y_e(t) - y_p(t))^2}, \tag{5}$$

is the current distance between the missiles. The practical definition (4) means that the engagement is considered in the time interval where the distance between the missiles decreases. Note that in this paper, we do not formulate and solve any nonlinear pursuit-evasion differential game.

2.2 Robust ε-Capture Zone

The objective of the pursuer is to nullify, or at least to make small, the final distance

$$J = J(u_p(\cdot), u_e(\cdot), t_0, \varphi_{p0}, \varphi_{e0}, r_0, a_p^{\max}, a_e^{\max}) = r(t_f). \tag{6}$$

Consider the class $\mathscr{U}$ of feedback strategies $u(t, X_p, X_e)$, where $X_i = (x_i, y_i, \varphi_i, a_i)^T$, $i = p, e$. Note that it is not assumed that $|u(t, X_p, X_e)| \le 1$ for all (t, X_p, X_e). For a given initial distance r_0, for a given pursuer's strategy $u_p(\cdot) \in \mathscr{U}$ and for a given number $\varepsilon > 0$, the set $\Phi = \Phi(u_p(\cdot))$ of initial positions $(t_0, \varphi_{p0}, \varphi_{e0}) \in \mathbb{R}^3$ is called the *robust ε-capture zone* if for all $(t_0, \varphi_{p0}, \varphi_{e0}) \in \Phi$,

1. the final distance (6) satisfies
$$J \le \varepsilon, \tag{7}$$
2. the pursuer's control time realization
$u_p(t) = u_p(t, X_p(t), X_e(t))$ satisfies the constraint (3)

for any evader's control $u_e(t)$ satisfying (3).

The problem of constructing the robust ε-capture zone can be formulated for two information patterns: (i) both state vectors $X_p(t)$ and $X_e(t)$ are known to the pursuer (complete information), (ii) the evader's state vector $X_e(t)$ is estimated assuming a bounded estimation error.

2.3 Linearized Model

Let the relative separation between the missiles be denoted by $y = y_e - y_p$. The corresponding relative velocity is $\dot{y}$. If the aspect angles φ_p and φ_e are small during the engagement then the system (1)–(2) can be linearized [11]:

$$\dot{x} = Ax + bu_p + cu_e, \quad x(0) = x_0, \tag{8}$$

where the state vector is $x = (x_1, x_2, x_3, x_4)^T = (y, \dot{y}, a_e, a_p)^T$, the superscript T denotes the transposition,

$$A = \begin{bmatrix} 0 & 1 & 0 & 0 \\ 0 & 0 & 1 & -1 \\ 0 & 0 & -1/\tau_e & 0 \\ 0 & 0 & 0 & -1/\tau_p \end{bmatrix}, \tag{9}$$

$$b = (0, 0, 0, a_p^{\max}/\tau_p)^T, \quad c = (0, 0, a_e^{\max}/\tau_e, 0)^T, \tag{10}$$

$$x_0 = (0, x_{20}, 0, 0)^T, \quad x_{20} = V_e\varphi_{e0} - V_p\varphi_{p0}. \tag{11}$$

In the linearized system, the final time moment is

$$t_f = r_0/(V_p + V_e). \tag{12}$$

The cost functional (6) becomes

$$J_x = |x_1(t_f)|. \tag{13}$$

The robust capture zone (for $\varepsilon = 0$) of a feedback strategy $u_p(t, x)$ is the set

$$\Phi_x = \Phi_x(u_p(\cdot)) = \Big\{(t_0, \varphi_{p0}, \varphi_{e0}) :$$

$$J_x = 0, |u_p(t, x(t))| \le 1, \ \forall\, u_e(\cdot) : \ |u_e(t)| \le 1\Big\}. \tag{14}$$

2.4 Problem Scalarization

Let introduce the function

$$z(t) = d^T X(t_f, t)x(t), \tag{15}$$

where $x(t)$ is the state vector of (8), $X(t_f, t)$ is the transition matrix of the homogeneous system $\dot{x} = Ax$, $d^T = (1, 0, 0, 0)$. The value of the function $z(t)$ has the following physical interpretation. If $u \equiv 0$ and $v \equiv 0$ on the interval $[t, t_f]$, then the miss distance $|x_1(t_f)|$ equals $|z(t)|$. Therefore, this function is called the *zero-effort miss distance* (ZEM). It is given explicitly by

$$z(t) = x_1(t) + (t_f - t)x_2(t) +$$

$$\tau_e^2 \psi\left((t_f - t)/\tau_e\right) x_3(t) - \tau_p^2 \psi\left((t_f - t)/\tau_p\right) x_4(t), \tag{16}$$

where

$$\psi(\xi) \triangleq \exp(-\xi) + \xi - 1 > 0, \quad \xi > 0. \tag{17}$$

By direct differentiation, $z(t)$ satisfies the differential equation

$$\dot{z} = h_p(t)u_p + h_e(t)u_e, \quad z(0) = z_0 \triangleq t_f x_{20}. \tag{18}$$

where

$$h_p(t) = -\tau_p a_p^{\max} \psi((t_f - t)/\tau_p), \quad h_e(t) = \tau_e a_e^{\max} \psi((t_f - t)/\tau_e). \tag{19}$$

Since $z(t_f) = x_1(t_f)$, the performance index (13) can be rewritten as $J_z = |z(t_f)|$.

For the scalar system (18), the robust capture zone (RCS) of a feedback strategy $u(t, z)$ becomes

$$\Phi_z = \Phi_z(u_p(\cdot)) = \Big\{(t_0, z_0) :$$

$$J_z = 0, |u_p(t, z(t))| \le 1, \ \forall\, u_e(\cdot) : \ |u_e(t)| \le 1\Big\}. \tag{20}$$

2.5 Robust Capture Zone for Linear System

General theoretical results on the properties and the structure of the RCS of linear and saturated linear strategies are outlined in Appendix. In this paper, we deal with linear feedback strategies of the following form:

$$u_p(t, z) = \frac{K(t)z}{(t_f - t)^\alpha}, \tag{21}$$

where $K(t)$ is a positive continuously differentiable function for $t \in [0, t_f]$, $\alpha > 0$. Note that for the coefficient functions $h_p(t)$, $h_e(t)$ given by (19), and for linear strategies (21), the numbers N_p, C_p, N_e, C_e, N_K and C, defined by (53) and (57), are

$$N_p = N_e = 2, \ \ C_p = -\frac{1}{2\tau_p}, \ C_e = \frac{1}{2\tau_e}, N_K = \alpha + 1, \ \ C = \alpha K(t_f). \tag{22}$$

Note that the conditions (I)–(IV) and (VI) of Theorem 1 are satisfied. The condition (V) is formulated as

(IV-α) either

$$\alpha > 3, \tag{23}$$

or

$$\alpha = 3 \ \text{ and } \ K(t_f) > 6\tau_p. \tag{24}$$

Thus, due to Theorem 1, the strategy (21) is robust capturing, if the condition (IV-α) holds.

In what follows, we consider the class of linear robust capturing strategies

$$\mathscr{U} = \Big\{u_p(t, z) = \frac{K(t)z}{(t_f - t)^\alpha} :$$

$$(\alpha > 3) \ \vee \big((\alpha = 3) \ \&(K(t_f) > 6\tau_p a_p^{\max})\big) \Big\} \tag{25}$$

where $K(t) > 0$ is continuously differentiable. Due to [7] (see Theorems 2–6), the robust capture zone of $u_p(\cdot) \in \mathscr{U}$ has a form

$$\Phi_z(u_p(\cdot)) = \Phi_z(K(\cdot), \alpha) = \Big\{(t_0, z_0) : \\ t_0 \in (t_{in}, t_f), \ \ |z_0| \le Z_0(t_0)\Big\}, \tag{26}$$

where $t_{in} \in [0, t_f)$, $Z_0(t) \ge 0$ is a continuous function satisfying

$$Z_0(t) \le \frac{(t_f - t)^\alpha}{K(t)}. \tag{27}$$

This condition means that the robust capture zone is a subset of the domain where the constraint $|u(t, z(t))| \le 1$ is satisfied. The boundary function $Z_0(t)$ and the moment t_{in} are obtained constructively (see for the details in Appendix section "Robust Capture Zone of Linear RCS").

Similar results were established by [7] (see Appendix section "Robust Capture Zone of Saturated Linear RCS") for the class of *saturated* linear robust capturing strategies

$$\mathscr{U}^s = \Big\{u_p^s = \mathrm{sat}(u_p(t, z)), u_p(\cdot) \in \mathscr{U}\Big\}, \tag{28}$$

with $\mathrm{sat}(\cdot)$ function defined as follows:

$$\mathrm{sat}(x) = \max\left(\min\left(x, 1\right), -1\right). \tag{29}$$

For $u_p^s(\cdot) \in \mathscr{U}^s$,

$$\Phi_z(u_p^s(\cdot)) = \Big\{(t_0, z_0) : t_0 \in (t_{in}^s, t_f), \ \ |z_0| \le Z_0^s(t_0)\Big\}, \tag{30}$$

where the boundary function $Z_0^s(t)$ and the moment $t_{in}^s \in [0, t_f)$ are obtained constructively (see for the details in Appendix section "Robust Capture Zone of Saturated Linear RCS").

Due to (15) and (18), for the strategies $u_p(t, x) = u_p(t, d^T X(t_f, t)x)$ and $u_p^s(t, x) = u_p^s(t, d^T X(t_f, t)x)$, the original robust capture zones Φ_x are

$$\Phi_x(u_p(\cdot)) = \Big\{(t_0, \varphi_{p0}, \varphi_{e0}) : \\ t_0 \in (t_{in}, t_f), \ \ |V_e\varphi_{e0} - V_p\varphi_{e0}| \le Z_0(t_0)/t_f\Big\}, \tag{31}$$

and

$$\Phi_x(u_p^s(\cdot)) = \Big\{(t_0, \varphi_{p0}, \varphi_{e0}) :$$

$$t_0 \in (t_{in}^s, t_f), \quad |V_e\varphi_{e0} - V_p\varphi_{e0}| \leq Z_0^s(t_0)/t_f \Big\}, \tag{32}$$

respectively.

2.6 Connections Between Optimal Capture Zones and Robust Capture Zones

Before to provide interval-based results in the case of perfect information and in the case of noisy measurements, we summarize classical results about DGL1 kinematic models (differential game approaches). DGL1 stands for pursuit-evasion linear differential game with terminal criterion (terminal miss distance) and bounded controls. Several versions of DGL like games considering different kinematics have been studied in an extensive manner by researchers as J. Shinar and co-authors [12]. DGL1 describes the player dynamics using first-order transfer functions (between their controls and the achieved accelerations). We summarized the analytical results obtained when applying robust control techniques as well (strategies of the pursuer restricted to linear state feedbacks). In addition, we underline the wording we use to describe capture zones in each case.

The theory of differential games that defines what is an equilibrium (saddle point, Nash equilibrium in the case of the aforementioned pursuit-evasion games) aims to compute optimal strategies for both players and as a consequence *Optimal Capture Zones* (OCZ). In the case of DGL1, the optimal strategies are bang-bang controls (according to the sign of the Zero-Effort-Miss). According to the kinematic parameters ($\mu = \frac{a_p^{max}}{a_E^{max}}$ and $\varepsilon = \frac{\tau_E}{\tau_p}$), the shape of the DGL1 optimal capture zones differs: it is "open" (case 1, $\mu > 1$, top drawing of Fig. 4) or "closed" (case 2, $\mu < 1$ and $\mu\,\varepsilon \geq 1$, top drawing of Fig. 5). Other cases (other numerical parameter settings) may occur; however, case 1 and 2 are the most common, i.e, the most interesting situations.

Robust controllability aims to compute *Robust Capture Zones* (RCZ) in the presence of uncertainties (the evader controls; bang-gang controls in the present situation) assuming that the pursuer applies a state feedback law in place of its optimal strategy. It is of first importance to compare the bang-bang capture zones that are the maximum capture zones respect to the robust capture zones that are smaller but that consider more realistic pursuit strategies. The feedback laws we consider for the pursuer (as described in Sect. 2.5 for $K(t) \equiv K$) are of the following type:

$$u_p(t,\, z) = \frac{K\, z}{(t_f - t)^\alpha} \tag{33}$$

K being a positive real number, α being a positive integer and $u_p(z, t)$ being saturated: $u_p^s = \text{sign}(u_p)$, when $|u_p| > 1$.

Several cases may happen when applying a robust controllability approach:

- We may chose K and α in a way to have $u_p(t, z)$ not reaching the controller limits (saturations). One advantage is then that the $u_p(t, z)$ strategy is a continuous function all along the trajectories.
- We may also apply larger gain values in the Pursuer's feedback guidance law (33). Then, the feedback guidance law has to be saturated. Two situations may occur:
  - If the feedback guidance law reaches saturation all along the boundaries of the optimal (differential game) capture zones, then we obtain robust (controllability) capture zones that are similar to the ones we obtain considering the bang-bang differential game optimal pursuit strategies (top drawings of Figs. 4 and 5).
  - For some K and α values, the feedback guidance law is not reaching maximum values as the differential game strategy does at the optimal capture zone limits and as a consequence the robust capture zone is smaller (bottom drawings of Figs. 4 and 5).

3 Interval Algorithm Approximation

3.1 Viability Kernel and Capture Basin

Viability theory [3] provides a set of concepts and techniques to study continuous dynamical systems. According to viability wording and definitions, a dynamical system is represented by a state variable $x(t) \in \mathbf{K} \subset X = \mathbb{R}^n$, $\mathbf{K}$ compact, regulated by one or more controls ($u_p(.)$ and $u_e(.)$ in the present situation), which evolution is ruled by a continuous dynamic law,

$$\begin{aligned} \dot{x}(t) &= f(x(t), u_p(t, x(t)), u_e(t, x(t))) \in X, \\ u_p(.) &\in \mathscr{U}, \\ u_e(.) &\in \mathscr{V}. \end{aligned}$$

Viability theory systematically studies the properties of viability of the evolutions in some environment (set $\mathbf{K}$ corresponding to the subset of the state space X satisfying a list of constraints, an example would be $|u_p(\cdot)| \leq 1$) at any time or until a finite prescribed time where the evolution reaches a given target ($r(t_f) \leq \varepsilon$ in the present case). Final time is defined by $\tau = t_f - t = 0$ with t regular time, i.e, forward time and τ backward time.

For that purpose it introduces, respectively, the notions of viability kernels and capture basins. The viability kernel of the environment is the subset (possibly empty) of the states in the environment from which starts at least one viable evolution (remaining all the time, i.e., infinite time, in $\mathbf{K}$). The capture basin of the target viable in $\mathbf{K}$ is the subset of the states in $\mathbf{K}$ from which starts at least one viable evolution (i.e., remaining in $\mathbf{K}$) until it reaches the target in finite time (capture zones of differential games). There exists one valid $u_p(t, x(t))$ strategy (retro-actions) for all admissible $u_e(t, x(t))$ strategies that forces the system to end in the target set. Capture basins design retro-actions (feedbacks) which allow to pilot the evolutions so as to maintain viability until, if any, capturing a target.

3.2 Capture Basin Enclosure

First, we start by describing viability algorithms in a general manner before to explain how we use these algorithms in the specific case of the paper. Then, in following sections, we explain how these algorithms are implemented using interval analysis. In a nutshell, once a differential inclusion $\dot{x}(t) \in F(x(t))$ has been discretized in time by $x_{m+1} \in \Upsilon(x_m)$, and "restricted" to grids of the finite-dimensional vector space, then the viable capture basin $\mathrm{Capt}_\Upsilon(\mathbf{K}, C)$ of elements of $\mathbf{K}$ from which an evolution (x_m) viable in $\mathbf{K}$ reaches the target C in finite discrete time can be obtained by two algorithms [10]:

1. The *capture basin algorithm*. It is based on the formula :

$$\mathrm{Capt}_\Upsilon(\mathbf{K}, C) = \bigcup_{m \geq 0} C_m \tag{34}$$

where the *increasing* sequence of subsets $C_m \subset \mathrm{Capt}_\Upsilon(\mathbf{K}, C)$ is iteratively defined by

$$\begin{cases} C_0 = C \\ \forall\, m \geq 1, \quad C_{m+1} := \mathbf{K} \cap (C_m \cup \Upsilon^{-1}(C_m)) \end{cases} \tag{35}$$

2. The *viability kernel algorithm*. Whenever $\mathbf{K} \backslash C$ is *repeller* (for all $x \in \mathbf{K} \setminus C$, all evolutions $x(\cdot)$ leave $\mathbf{K} \setminus C$ in finite time), there is another class of general algorithms allowing to compute viable capture basins (in this context, at convergence, $Viab_\Upsilon(\mathbf{K}, C)$ is $Capt_\Upsilon(\mathbf{K}, C)$):

$$\mathrm{Viab}_\Upsilon(\mathbf{K}, C) = \bigcap_{m \geq 0} K_m \tag{36}$$

where the *decreasing* sequence of subsets $K_m \supset \mathrm{Viab}_\Upsilon(\mathbf{K}, C)$ is iteratively defined by:

$$\begin{cases} K_0 = \mathbf{K} \\ \forall\, m \geq 1, \quad K_{m+1} := C \cup (K_m \cap \Upsilon^{-1}(K_m)) \end{cases} \tag{37}$$

Naturally, both subsets C_m and K_m are computed at each iteration on a grid of the state space. The convergence of the C_m and K_m subsets follows from convergence theorems presented in Chap. 19, p. 769, of *Viability Theory. New Directions*, [1] (see for instance Theorem 19.3, p. 774).

The way we rebuild a robust capture zone is by solving several capture basin and viability kernel problems over time interval slices. The number of capture basin and viability kernel problems we consider is related to the Euler discrete time step we assume (see the interval implementation described in 3.5 for complementary explanations). The viability problems we solve are attainability between set C at t and set

C at $t+1$ considering a small time step, $C(t)$ being the target set. After convergence of the enclosure process, $C(t+1)$ is the target set for the next viability problem to solve. The robust capture zone is then the collection of the capture basins we compute. Convergence of the overall process (robust capture zone shape), i.e., the fact we do not contract the time dimension (and that we mainly take care of the geometric space only) is related to the fact we use at each time step a capture basin algorithm (over-approximation), and a viability kernel algorithm (under-approximation). In a rough manner, in the application we consider, we may say the capture basin algorithm solves the problem "reach the target set $C(t)$ in Δt time by increasing an empty set (at first iteration) up to $C(t+1)$." The viability kernel algorithm with target set $C(t)$ solves the problem "stay viable," i.e., in $\mathbf{K}$ during a Δt period of time by decreasing an initial guess equal to $\mathbf{K}$ at first iteration up to $C(t+1)$. In this context (viability kernel with target set), "stay viable" means reach the target set $C(t)$ after a Δt time period. Convergence of both algorithms to the capture basin (Δt robust capture zone, Δt slice) is strongly related to the repeller assumption stated above.

3.3 Interval Arithmetics

Interval computation [8] is about guaranteed numerical methods for approximating sets, and their application to engineering. Guaranteed means here that outer (and inner if needed depending on the application) approximations of the sets of interest are obtained, which can, at least in principle, be made as precise as desired. It thus becomes possible to achieve tasks such as computing (over and under-approximating) capture basins or capture zones of differential games.

The main tool to be used, so-called interval analysis, is based upon the very simple idea of enclosing real numbers in intervals and real vectors in boxes, i.e, sub-pavings. Interval computation is a special case of computation on sets. The operations on sets fall into two categories. The first one such as union or intersection consists of operations that have a meaning only in a set-theoretic context. The union of two disconnected intervals can be over-approximated by an interval even if it is not an interval in the set-theoretic sense. The second one (thanks to natural arithmetics) consists of the extension of operations that are already defined for numbers (or vectors): addition, multiplication, etc.

Intervals are boxes of dimension one. Inner and outer approximations of sets are sub-pavings. Sub-pavings belong to $\mathbb{IR}^n$ (boxes of finite dimension representing bounded continuous values). For compactness reasons, boxes are written $[x]$, x being a state vector with state variables in $\mathbb{R}$. In a way similar to the definition of elementary operations as addition, multiplication, all the functions in $\mathbb{R}^n$ can be extended to intervals. Composition of elementary functions allows to define inclusion functions:

$$\begin{gathered}[f]:\mathbb{IR}^n \to \mathbb{IR}^m \text{ is an inclusion function of } f \text{ if} \\ \forall [x] \in \mathbb{IR}^n,\ f([x]) \subset [f]([x]).\end{gathered} \tag{38}$$

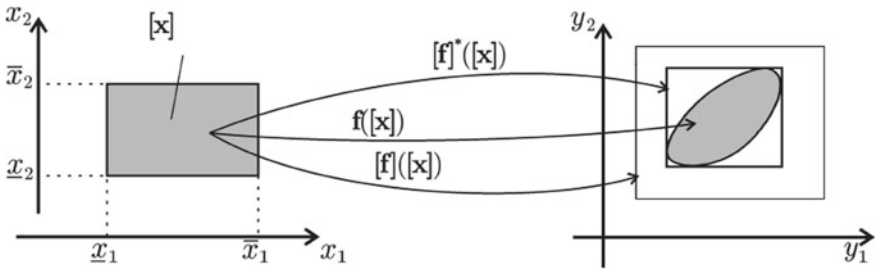

Fig. 2 Inclusion function (drawing with courtesy of Prof. Luc Jaulin, UBO, Brest, France); [] denotes in an usual way intervals and inclusion functions (box over-approximations of function images); in addition, symbol * denotes the minimal inclusion function, which is considered as optimal (reason to use the $*$ symbol).

Inclusion functions provide guaranteed over-approximations (wrapping effect) in $\mathbb{IR}^m$ (see Fig. 2 for illustration purpose).

Thanks to these properties and fast interval-based algorithms (guaranteed integration of sub-pavings, contractor programming [6]) it is possible to implement the viability kernel and capture basin algorithms in a way to solve problems such as those described in [5, 9]. Set invariance [4] has also an interval-based implementation.

3.4 Contractor Programming

Set membership techniques are tools to compute sets $\mathbb{X} \subset \mathbb{R}^n$, $\mathbb{X}$ being a general set (not necessary a box) described by constraints (states that are solutions of constraints). Constraints are geometric conditions on state variables (equalities, inequalities) but also constraints defined by Ordinary Differential Equations (ODE as those governing the player evolutions in differential games). The operator $C_{\mathbb{X}} : \mathbb{IR}^n \to \mathbb{IR}^n$ is a contractor for $\mathbb{X} \subset \mathbb{R}^n$ if

$$\forall [.] \in \mathbb{IR}^n, \begin{cases} C_{\mathbb{X}}([.]) \subset [.] & (contractance), \\ C_{\mathbb{X}}([.]) \cap \mathbb{X} = [.] \cap \mathbb{X} & (completness) \end{cases} \tag{39}$$

After contraction by a $C_{\mathbb{X}}$ operator, all solutions in box [.] that satisfy the $\mathbb{X}$ constraint remain in $C_{\mathbb{X}}([.])$ (completness property). However, $C_{\mathbb{X}}$ operator is not necessarily minimal. After contraction, $C_{\mathbb{X}}([.])$ may still contain values that do not satisfy the $\mathbb{X}$ constraint. Contractor programming has been used to re implement (in a sightly different way) the viability kernel and capture basin algorithms described in Sect. 3.2.

3.5 Interval-Based Backward Reachable Set Computation

1. *ODE constraints*
   Capture zones have been built in an iterative manner (iterative algorithm) following a backward reachable set approach. A backward reachable set is the set of states from which trajectories start that reach some given target set. The backward reachable sets we compute are on fixed limited time horizons with quantifiers (∀, ∃) on controls (differential game context). The target set we consider at time τ to compute reachability in backward time over a time period dt is the backward reachable set computed at time $\tau - dt$ where τ is backward time, i.e, $\tau = t_f - t$, dt is a (small) positive time step. A backward reachable set is represented by an interval $[z] = [z_{min}, z_{max}]$. At time $\tau = dt$ (first step of the algorithm), the target set we consider is $[z_f] = [-\varepsilon, \varepsilon]$ (ε-Capture Zone). A capture zone consists in the sum of the so computed backward reachable sets. At each iteration of the algorithm, each backward reachable set is over- and under-approximated using contractor programming. The over-approximation is a viability kernel with target and the under-approximation is a capture basin as described in Sect. 3.2. The boxes we considered when implementing contractors are $[z(\tau - dt), z(\tau)]$ which are boxes of dimension twice with respect to the problem dimension. In the present case, the boxes are of size 2. ODE contractors are state evolution contractors, i.e., operators that integrate ODE, i.e., that compute state trajectories. ODE are then (time) state constraints. $[z(.)]$ in previous equation are both intervals (of dimension 1). We defined the two following ODE numerical constraints (and the associated contractors):

$$\exists u_p, \forall u_e \mid [z(\tau - dt)] = [\Upsilon]([z(\tau)], [u_p], [u_e]) \tag{40}$$

$$\exists u_e, \forall u_p \mid [z(\tau - dt)] = [\Upsilon]([z(\tau)], [u_p], [u_e]) \tag{41}$$

with $[\Upsilon]$ an inclusion function of the backward time game kinematics integrated over a time period dt. In the present situation, we implement a simple Euler integration scheme:

$$[\Upsilon]([z(\tau - dt)], [u_p], [u_e]) = [z(\tau)] - dt\,.\,[\dot{z}(\tau, [u_p], [u_e])] \tag{42}$$

More complex numerical schemes as Runge Kutta can be considered for ODE integration and full implementation of ODE contractors. Nevertheless, guaranteed integration techniques have to be applied for computing inclusion functions $[\Upsilon]$. More sophisticated approaches as Taylor developments and Picard theorem can be used to compute guaranteed margins [2]. Be aware that inclusion function $[\Upsilon]$ can be a quite large box due to uncertain evader's controls, due to the dt time period and due to margins we have to take into account for guaranteed integration.

2. *Contractor programming based viability kernel with target algorithm*
We apply the contractor corresponding to Eq. (40) to box $[z^+(\tau - dt), [z_{min}, z_{max}]]$ to compute backward reachable set over-approximations (viability kernels). Here, $[z^+(\tau - dt)]$ and $[z_{min}, z_{max}]$ are both one-dimensional intervals; $[z^+(\tau - dt)]$ is the target set for current computation: $[z^+(\tau - dt)]$ is an over-approximation of the reachable set computed at previous iteration, i.e, the viability kernel computed at previous iteration; $[z_{min}, z_{max}]$ is the z domain. In the present case, z_{max} is positive, $z_{min} = -z_{max}$, and z_{max} is large enough to have z_{max} outside the capture zone. Then, we only use the contraction of box $[z_{min}, z_{max}]$ which is the contractor programming based viability kernel.

3. *Contractor programming based capture basin algorithm*
We apply the contractor corresponding to Eq. (41) to compute backward reachable set under-approximations (capture basins). We first define the $Comp\,(a, b)$ interval operator to compute the complement of $[a]$ in $[b]$. For the sake of simplicity, we omit to write brackets around the $[a]$ and $[b]$ intervals when written into the $Comp\,(.)$ operator. In addition, be aware that the result of operator $Comp\,(a, b)$ is a list of potentially non-connected intervals. In the present case, the backward reachable sets being defined by an interval only (box of dimension one), the result of $Comp\,(.)$ is two boxes. The "non-capturing state contractor" (constraint (41)) is applied to the box:

$$[Comp\,(z^-(\tau - dt), [z_{min}, z_{max}]), [z_{min}, z_{max}]]. \tag{43}$$

When computing the capture basin at time τ, the "contractor programming target set" we consider is the complementary set (in $[z_{min}, z_{max}]$) of the under-approximation of the backward reachable set computed at time $\tau - dt$. The under-approximation of the backward reachable set computed at time $\tau - dt$ which is the capture basin at time $\tau - dt$ is denoted $z^-(\tau - dt)$ in the above Eq. (43). As previously (in the case of the viability kernel), we only use the $[z_{min}, z_{max}]$ contraction which is the second component of the box we contract, the component that corresponds to time τ. This interval is the complementary of the capture basin, i.e, we perform a complementary operation respect to the $[z_{min}, z_{max}]$ domain.
In addition, interval refinement process has been also implemented (bisection algorithms) to refine the backward reachable set computation precision. We iterate the viability kernel and capture basin computation process that encloses the differential game barrier until we obtain the precision required. The contractor programming based implementation of the viability kernel and capture basin algorithms is new. This approach differs from the grid based approaches and also differs from the interval computing based implementations that only exploit bisection techniques. These viability kernel and capture basin algorithms take benefits from the computation performance of contractor programming.

When computing robust capture zones (in place of optimal capture zones), we update the constraints (Eqs. (40) and (41)) in a way to not consider anymore quantifiers on u_p.

4. *Contractor programming based viability algorithms*
Define :

- $C_\Upsilon([.])$ a dynamic system evolution contractor,
- $\Upsilon_{capture}$ the capture constraint described by Eq. (40),
- Υ_{evade} the evade constraint described by Eq. (41),
- $C_{\mathbb{X}}([.])[i]$ the i component of the box contracted by operator $C_{\mathbb{X}}([.])$,
- $\mathbb{Z}(\tau)$ the z domain at time τ, which is constant and equal to $[z_{min},\ z_{max}]$ in the present situation.

Then, we may rewrite in a formal manner, the viability kernel with target algorithm:

$$\text{Viab}_\Upsilon\ (\mathbf{K},\ \mathbf{z}^+(\tau\ -\ \mathbf{dt})) = \mathbf{C}_{\text{,capture}}(\mathbf{z}^+(\tau\ -\ \mathbf{dt}),\ \mathbb{Z}(\tau))\ [\mathbf{2}] \tag{44}$$

The same can be done for the capture basin algorithm:

$$\begin{array}{l}\text{Capt}_\Upsilon(\mathbf{K}, \mathbf{z}^-(\tau\ -\ \mathbf{dt})) = ... \\ \quad Comp\ (C_{\Upsilon_{evade}}(Comp\ (z^-(\tau\ -\ dt),\ \mathbb{Z}(\tau - dt))\ , \mathbb{Z}(\tau))\ [2]),\ \mathbb{Z}(\tau))\end{array} \tag{45}$$

By the way, $z^+(\tau\ -\ dt)$ and $z^-(\tau\ -\ dt)$, as described before, are, respectively, the over- and under-approximation of the capture basin at $\tau - dt$. Therefore, from the algorithmic point of view,

$$z^+(\tau\ -\ dt) \approx \text{Viab}_\Upsilon\ (\mathbf{K},\ \mathbf{z}^+(\tau\ -\ \mathbf{2\,dt})) \tag{46}$$

and

$$z^-(\tau\ -\ dt) \approx \text{Capt}_\Upsilon\ (\mathbf{K},\ \mathbf{z}^+(\tau\ -\ \mathbf{2\,dt})) \tag{47}$$

with the following initial conditions:

$$z^+(\tau = 0) = z^-(\tau = 0) = [-\varepsilon,\ \varepsilon] \tag{48}$$

The next section shows results we obtained in the specific context of the pursuit-evasion game described in Sect. 2.

3.6 Numerical Results

- Objectives
  The purpose of the interval-based viability analysis (remaining part of the article) is first to compute in an easy manner robust controllability domains, but also to redo the same computations assuming bounded errors on $z(\tau)$ (that regular construction techniques are not able to do).
  Figure 3 describes how viability kernel with target and capture basin algorithms based on interval contractor programming are used to compute Robust Capture Zone (RCZ). The numerical settings of Fig. 3 are data corresponding to an open DGL1 (bang-bang) Optimal Capture Zone (OCZ), however, because the Pursuer feedback strategy reaches the saturation limits when Time to Go is small only, RZC is smaller and closed.
- Capture zones without noise
  Figure 4 shows Robust Capture Zones in the case of perfect information. The μ and ε numerical parameters are parameters leading to an open Optimal Capture Zone when differential game bang-bang strategies are applied. Kinematics is DGL1 one. The robust control approach has been applied in both cases with P playing the $u_p(t,\ z) = \frac{K(t)\,z}{(t_f - t)^\alpha}$ feedback control law. The top figure corresponds to Pursuer controls saturating all along the RCZ boundaries ($K(t) = k = 10,\ \alpha = 1$), the RCZ is then equal to the OCZ (Differential Game approach). The bottom figure corresponds to Pursuer controls that do not saturate anymore all along the RCZ boundaries ($k = 0.01,\ \alpha = 5$). Both figures are computed following a RCZ approach even if the attainability domain on the top figure is equal to the OCZ one.
  Figure 5 is still a case with perfect information; however, the numerical parameters are DGL1 μ and ε data corresponding to the case of a close Optimal Capture

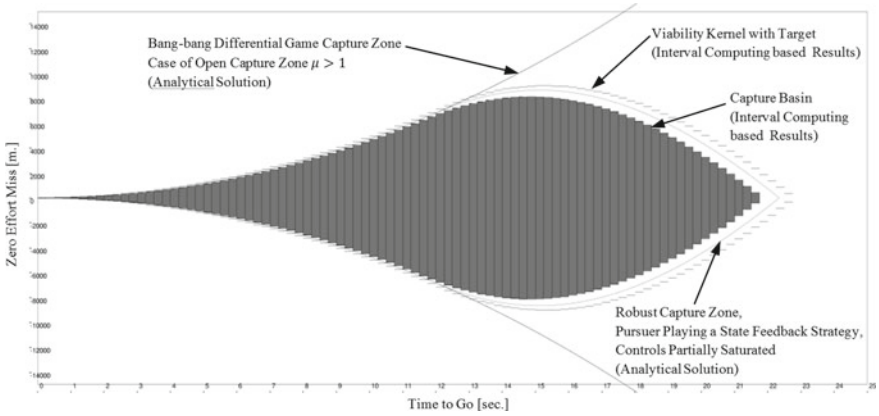

Fig. 3 Viability kernel with target and capture basin algorithms based on interval contractor programming

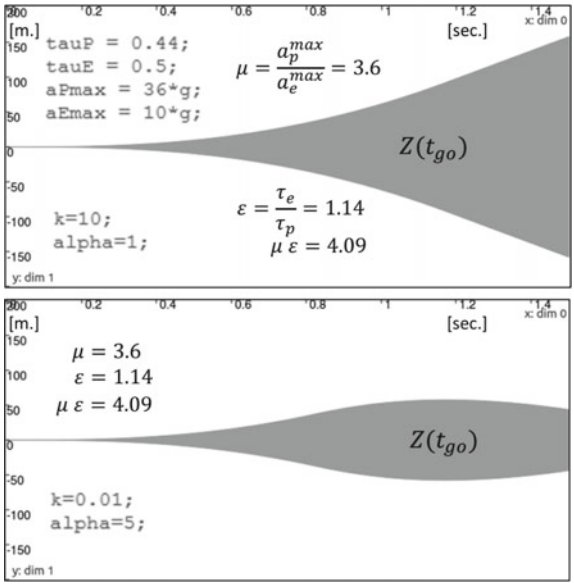

Fig. 4 RCZ in the case of perfect information with open OCZ parameters

Zone. The robust control approach has been applied in both cases with P playing the $u_p\,(t,\,z) = \frac{K(t)\,z}{(t_f - t)^{\alpha}}$ feedback control law. The top figure corresponds to Pursuer controls saturating all along the RCZ boundaries ($k = 10,\ \alpha = 1$). The RCZ is then equal to the OCZ (Differential Game approach). The bottom figure corresponds to Pursuer controls that do not saturate anymore all along the RCZ boundaries ($k = 1,\ \alpha = 5$).

- Capture zones with noise
  Figure 6 are DGL1 μ and ε parameters corresponding to the case of an open OCZ (top figure) and to a close OCZ (bottom figure). RCZ approach has been applied in both cases with P playing the $u_p\,(t,\,z) = \frac{K(t)\,z}{(t_f - t)^{\alpha}}$ feedback control law. All the drawings correspond to Pursuer controls that do not saturate all along the RCZ boundaries. The top figure corresponds to the case of time to go errors: $\hat{t}_{go} =$ "noise_on_Tgo" $. t_{go}$. The bottom figure corresponds to the case of errors on the z state vector: $\hat{z}(t_{go}) =$ "noise_on_Z" $. z(t_{go})$. The dotted lines show the results we obtained without considering t_{go} and z biases (bottom figures in Fig. 4 and Fig. 5).
  The results show that over-estimation of t_{go} or under-estimation of z imply lower P controls than expected respect to OCZ. Therefore, RCZ are smaller than OCZ (in the case of non-saturated feedback guidance laws). Under-estimation of t_{go} or

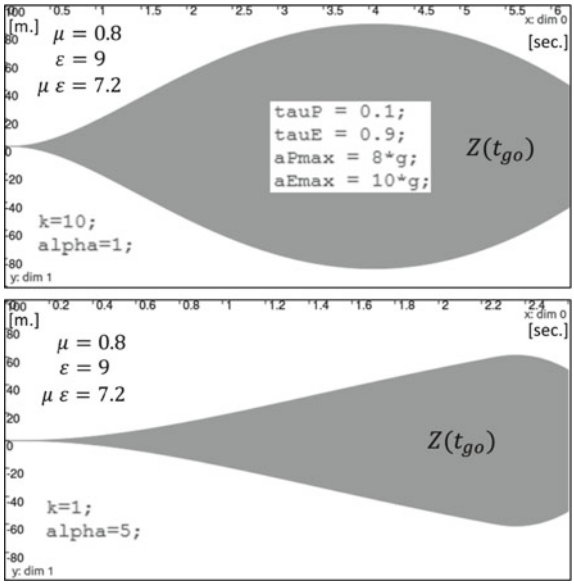

Fig. 5 RCZ in the case of perfect information with close OCZ parameters

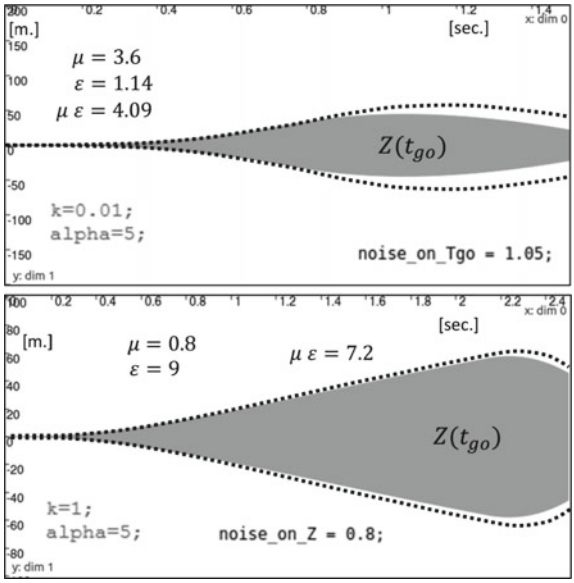

Fig. 6 DGL1 RCZ with noisy measurements, the top figure is RCZ with time to go errors. The bottom figure is RCZ errors on the z state vector. The dotted lines are results without considering t_{go} and z biases

over-estimation of z saturate the P controls and increase the corresponding non-noisy RCZ. Few noise on t_{go} ($+5\%$) may have a lot of impact on the shape of RCZ (see Fig. 6).

4 Conclusions

Interval viability algorithms are powerful techniques to compute capture basins of complex dynamic systems as differential game capture zones, reachable sets, and robust controllability domains. Algorithms to compute robust capture zones in the case of saturated and non-saturated guidance laws have been used for scalar linear systems. Results have been obtained in the case of noisy states as well (robust capture domains also robust to noisy measurements). To consider a more realistic case of refined noisy measurements that are outputs of Kalman filtering and not only rough noise on the Zero-Effort-Miss. The interval viability approach that is not restricted to linear systems and that can be applied to systems of larger dimensions with nonlinearities including saturations and hybrid behaviors will be applied to compute nonlinear noisy robust capture zones. The problem of computing robust capture zones that corresponds to non-saturated guidance laws (non-saturated feedback forms) can be also turned into a problem of viability. The problem of finding feedback guidance law parameters to avoid pursuer control saturations can be also tackled following the proposed approach.

Appendix

Robust Capture Zones: Main Results

In this section, the main results of [7] are briefly outlined. Consider a scalar system

$$\dot{z} = h_p(t)u_p + h_e(t)u_e, \quad z(t_0) = z_0, \quad t_0 \le t \le t_f, \tag{49}$$

where the measurable controls $u_p(t)$ and $u_e(t)$ satisfy the constraints

$$|u_p| \le u_p^{\max}, \tag{50}$$

$$|u_e| \le u_e^{\max}. \tag{51}$$

The feedback strategy $u_p = u_p(t, z)$, given by a function, Lipschitz w.r.t. z, is called *robust capturing strategy* (RCS) if it guarantees

$$z(t_f) = 0, \tag{52}$$

for any measurable bounded $u_e(t)$, i.e., *robustly* w.r.t. to u_e.

In what follows, the functions $h_p(t)$ and $h_e(t)$ satisfy the following assumption: for some N_p, $N_e \ge 0$ there exist finite limits C_p, C_e

$$\lim_{t \to t_f - 0} \frac{h_i(t)}{(t_f - t)^{N_i}} = C_i \ne 0, \quad i = p, e. \tag{53}$$

Linear Robust Capturing Strategies

Consider a linear strategy

$$u_p(t,z) = K(t)z. \tag{54}$$

Theorem 1 *Let the following conditions hold.*

(I) $K(t) \neq 0$ *for* $t \in [0, t_f)$*;*
(II) $K(t)$ *is continuously differentiable for* $t \in [0, t_f)$*;*
(III) one of two limit conditions is satisfied:

$$\lim_{t \to t_f - 0} K(t) = \infty, \tag{55}$$

or

$$\lim_{t \to t_f - 0} K(t) = -\infty; \tag{56}$$

(IV) there exists $N_K > 1$ *such that*

$$\lim_{t \to t_f - 0} \dot{K}(t)(t_f - t)^{N_K} = C \neq 0; \tag{57}$$

(V) either

$$N_K > N_p + 2, \quad \text{and} \quad CC_p < 0, \tag{58}$$

or

$$N_K = N_p + 2, \quad \text{and} \quad CC_p < -(N_K - 1)^2; \tag{59}$$

VI

$$N_e \geq N_p. \tag{60}$$

Then the strategy (54) is robust capturing.

Robust Capture Zone of Linear RCS

General Structure

Define the function

$$F(t,t_0) = \frac{u_p^{\max} - u_e^{\max}|K(t)| \int_{t_0}^{t} G(t,\xi)|h_e(\xi)|d\xi}{|K(t)|G(t,t_0)}, \quad t_0 \in [0,t_f), \tag{61}$$

where

$$G(t,\tau) = \exp\left(\int_{\tau}^{t} K(\eta)h_p(\eta)d\eta\right). \tag{62}$$

The robust capture zone $\Phi_z(u_p(\cdot)) = \Phi_z(K(\cdot))$ of a linear robust transferring strategy (54) is non-empty if and only if there exists $t_0 \in [0, t_f)$ such that

$$\inf_{t\in[t_0,t_f)} F(t,t_0) \geq 0. \tag{63}$$

It is a closed set in the plane (t_0, z_0), symmetric with respect to the axis $z_0 = 0$. It is represented in a form

$$\Phi_z(u_p(\cdot)) = \left\{(t_0,z_0) \in D:\ t_0 \in [t_{in}, t_f),\ \ |z_0| \leq Z_0(t_0)\right\}, \tag{64}$$

where $D = \{(t,z):\ t \in [0,t_f], z \in \mathbb{R}\}$,

$$Z_0(t_0) = \inf_{t\in[t_0,t_f)} F(t,t_0), \tag{65}$$

$$t_{in} = \min\{t_0 \in [0,t_f):\ Z_0(t_0) \geq 0\}, \tag{66}$$

Boundary

Define the function

$$P(t) = \frac{d}{dt}\left(\frac{u_p^{\max}}{|K(t)|}\right) - u_p^{\max}(\mathrm{sign}K(t))h_p(t) - u_e^{\max}|h_e(t)|. \tag{67}$$

It is assumed that $P(t)$ has a finite number of zeros (maybe none) on $(0, t_f)$. Define also the curve

$$z_0 = \frac{u_p^{\max}}{|K(t_0)|},\ \ t \in [0,t_f), \tag{68}$$

and the limiting function

$$\chi(t_0) = \lim_{t\to t_f-0} F(t,t_0). \tag{69}$$

Case 1. Non-empty set of zeros of $P(t)$ on $(0, t_f)$.
Consider the subset

$$\mathcal{T} = \{t_1 < t_2 < ... < t_p:\ P(t_j) = 0,\ P(t_j-0) < 0,\ P(t_j+0) > 0,\ j = 1, ..., p\}. \tag{70}$$

1.1. $\mathscr{T} \neq \emptyset$.

Let for each $j = 1, ..., p$, $Z_j(t_0)$ be the solution of the boundary value problem

$$\frac{dZ_j}{dt_0} = K(t_0)h_p(t_0)Z_j(t_0) + u_e^{\max}|h_e(t_0)|, \quad Z_j(t_j) = \frac{u_p^{\max}}{|K(t_j)|}, \quad t_0 \in [0, t_j]. \quad (71)$$

1.1.1. $P(t) > 0$ for $t \in (t_p, t_f)$.

Theorem 2 *In this case, the upper boundary of $\Phi_z(K(\cdot)$ is a lower envelope of $p + 1$ curves: the curve (68) and the curves $z_0 = Z_j(t_0)$, $j = 1, ..., p$, where $Z_j(t_0)$ are given by (71).*

1.1.2. There exists $\hat{t} \in (t_p, t_f)$ such that $P(t) < 0$ for $t \in (\hat{t}, t_f)$.

In this case, the limiting function (69) exists on some interval $(\tilde{t}_0, t_f)$ and satisfies the differential equation

$$\frac{d\chi(t_0)}{dt_0} = K(t_0)h_p(t_0)\chi(t_0) + u_e^{\max}|h_e(t_0)|, \quad t_0 \in (\tilde{t}_0, t_f), \quad (72)$$

and

$$\lim_{t_0 \to t_f - 0} \chi(t_0) = 0. \quad (73)$$

Theorem 3 *In this case, the upper boundary of $\Phi_z(K(\cdot)$ is a lower envelope of $p + 2$ curves: the curve (68), the curves $z_0 = Z_j(t_0)$, $j = 1, ..., p$, where $Z_j(t_0)$ are given by (71), and the limiting curve (69), $t_0 \in (\tilde{t}_0, t_f)$.*

1.2. $\mathscr{T} = \emptyset$.

Theorem 4 *In this case, the upper boundary of $\Phi_z(K(\cdot)$ is a lower envelope of 2 curves: the curve (68) and the limiting curve (69) for $t_0 \in [t_{in}, t_f)$.*

Case 2. Empty set of zeros of $P(t)$ on $(0, t_f)$.

2.1. $P(t) > 0$ for $t \in (0, t_f)$.

Theorem 5 *In this case,*

$$t_{in} = 0, \quad Z_0(t_0) = \frac{u_p^{\max}}{|K(t_0)|}. \quad (74)$$

2.2. $P(t) < 0$ for $t \in (0, t_f)$.

Theorem 6 *In this case,*

$$t_{in} = t_{in}^{\chi} = \inf\{t_0 \in (\tilde{t}_0, t_f) : \chi(t_0) \geq 0\}, \quad Z_0(t_0) = \chi(t_0). \quad (75)$$

Robust Capture Zone of Saturated Linear RCS

Remark 1 Based on a linear strategy (54), construct its saturated version

$$u_p^{\text{sat}}(t,z) = \begin{cases} u_p^{\max}, & K(t)z > u_p^{\max}, \\ K(t)z, & |K(t)z| \le u_p^{\max} \\ -u_p^{\max}, & K(t)z < -u_p^{\max} \end{cases} \tag{76}$$

If (54) is robust capturing, then (76) is also robust capturing.

Denote $\Phi_z^{\text{sat}}(K(\cdot))$ the robust capture zone of (76).

Robust Capture Zone Structure

Let $z(t; t_0, z_0)$ denote the solution of the differential equation

$$\dot{z} = h_p(t)u_{\text{sat}}(t,z) + u_e^{\max}|h_e(t)|, \tag{77}$$

satisfying $z(t_0) = z_0$. The robust capture zone $\Phi_z^{\text{sat}}(K(\cdot))$ is closed set in the plane (t_0, z_0) symmetric w.r.t. to the axis $z_0 = 0$. It is given by

$$\Phi_z^{\text{sat}}(K(\cdot)) = \{(t_0, z_0) : \ t_0 \in [t_{in}^s, t_f), \ |z_0| \le Z_0^s(t_0)\}, \tag{78}$$

where

$$t_{in}^s = \min\{t_0 \in [0, t_f) : \ \exists z_0 \ge 0 : z(t_f; t_0, z_0) = 0\}, \tag{79}$$

$$Z_0^s(t_0) = z(t_0; t_{in}^s, z_0^s), \tag{80}$$

$$z_0^s = \max\{z_0 \ge 0 : \ z(t_f; t_{in}^s, z_0) = 0\}. \tag{81}$$

Boundary

Define the function

$$Z_m(t) = \int_t^{t_f} \left(u_p^{\max}|h_p(\xi)| - u_e^{\max}|h_e(\xi)|\right) d\xi. \tag{82}$$

It is assumed that

$Z_m 1$ $Z_m(t)$ has no more than a finite number of roots on $[0, t_f]$;

$Z_m 2$ there exists $\delta \in (0, t_f)$ such that $Z_m(t) > 0$ for $t \in (t_f - \delta, t_f)$.

Define the moment

$$t_{in}^m = \sup\{t \in [0, t_f) : Z_m(t) < 0\}, \tag{83}$$

and the set

$$\Phi_z^m = \{(t_0, z_0) : \ t_0 \in [t_{in}^m, t_f), \ |z_0| \le Z_m(t_0)\}. \tag{84}$$

Then,

$$\Phi_z(K(\cdot)) \subseteq \Phi_z^{\text{sat}}(K(\cdot)) \subseteq \Phi_z^m. \tag{85}$$

Define the function

$$P_s(t) = Z_m(t) - \frac{u_p^{\max}}{|K(t)|} = \int_t^{t_f} P(\xi) d\xi. \tag{86}$$

Case 1. $P_s(t) \neq 0, t \in (0, t_f)$.

Theorem 7 *Let $t_{in}^m = 0$ and $Z_m(0) > 0$. Then*

$$\Phi_z^{\text{sat}}(K(\cdot)) = \Phi_z^m, \tag{87}$$

if and only if

$$P_s(t) > 0, \quad t \in [0, t_f). \tag{88}$$

Theorem 8 *Let the function $Z_m(t)$ have no non-zero-crossing roots. Then*

$$\Phi_z^{\text{sat}}(K(\cdot) = \Phi_z(K(\cdot)), \tag{89}$$

if

$$P_s(t) < 0, \quad t \in (0, t_f). \tag{90}$$

In this case,

$$Z_0^s(t_0) = Z_0(t_0) = \chi(t_0). \tag{91}$$

Case 2. There exists $\tilde{t} \in (0, t_f)$ such that $P_s(\tilde{t}) = 0$ and $P_s(t) \neq 0, t \in (\tilde{t}, t_f)$.
Case 2.1. $P_s(t) > 0, t \in (\tilde{t}, t_f)$. In this case,

$$Z_0^s(t_0) = \begin{cases} Z_m(t_0), \ t_0 \in (\tilde{t}, t_f), \\ \\ \tilde{Z}(t_0), \ \ t \in [t_{in}^s, \tilde{t}], \end{cases} \tag{92}$$

where $\tilde{Z}(t)$ is the solution of the differential equation

$$\dot{\tilde{Z}} = h_p(t)u_{\text{sat}}(t, \tilde{Z}) + u_e^{\max}|h_e(t)|, \quad \tilde{Z}(\tilde{t}) = Z_m(\tilde{t}) = \frac{u_p^{\max}}{|K(\tilde{t})|}. \tag{93}$$

If $\tilde{Z}(t) > 0$ for $t \in (0, t_f)$, then $t_{in}^s = 0$, otherwise, t_{in}^s is the first zero of $\tilde{Z}(t)$ from the right.

Case 2.2. $P_s(t) < 0, t \in (\tilde{t}, t_f)$. Let $\Phi_z(K(\cdot))$ is non-trivial, i.e., there exists $t_{in}^{\chi} \in [0, t_f)$. Denote $\bar{t} = \max\{\tilde{t}, t_{in}^{\chi}\}$. Then

$$Z_0^s(t_0) = \begin{cases} \chi(t_0), \ t_0 \in (\bar{t}, t_f), \\ \\ \bar{Z}(t_0), \ t \in [t_{in}^s, \tilde{t}], \end{cases} \tag{94}$$

where $\bar{Z}(t)$ is the solution of the differential equation

$$\dot{\bar{Z}} = h_p(t)u_{\text{sat}}(t, \bar{Z}) + u_e^{\max}|h_e(t)|, \quad \bar{Z}(\bar{t}) = \chi(\bar{t}). \tag{95}$$

If $\bar{Z}(t) > 0$ for $t \in (0, t_f)$, then $t_{in}^s = 0$, otherwise, t_{in}^s is the first zero of $\bar{Z}(t)$ from the right.

References

1. J.-P. Aubin, A. Bayen, and P. Saint-Pierre. *Viability Theory New Directions, Second Edition*. Number ISBN 978-3-642-16683-9. Springer-Verlag, Berlin Heidelberg, 2011.
2. Julien Alexandre Dit Sandretto and Alexandre Chapoutot. Validated explicit and implicit runge-kutta methods. *Reliable Computing, Special issue devoted to material presented at SWIM 2015*, 22:078–103, 2016.
3. Jean-Pierre Aubin. *Viability Theory*. Birkhauser Boston Inc., Cambridge, MA, USA, 1991.
4. F. Blanchini. Set invariance in control. *Automatica*, 35(11):1747 – 1767, 1999.
5. N. D. Botkin, M. A. Zarkh, and V. S. Patsko. Numerical solution of linear differential games. *Lecture Notes in Control and Information Sciences*, 156:226 – 234, 1991.
6. Gilles Chabert and Luc Jaulin. Contractor programming. *Artificial Intelligence, Elsevier*, 173:1079–1100, 2009.
7. V. Y. Glizer and V. Turetsky. *Robust Controllability of Linear Systems*. Nova Science Publishers Inc., New York, NY, 2012.
8. L. Jaulin and E. Walter. Set inversion via interval analysis for nonlinear bounded-error estimation. *Automatica*, 29(4):1053 – 1064, 1993.
9. N.N. Krasovskii and A.I. Subbotin. *Game-Theoretical Control Problems*. Springer Verlag, New York, NY, 1988.
10. Stéphane Le Ménec. Interval computing of the viability kernel with application to robotic collision avoidance. In *Advances in Dynamic and Mean Field Games*, pages 279–299. Birkhäuser Boston, 2017.
11. J. Shinar. Solution techniques for realistic pursuit-evasion games. In C.T. Leondes, editor, *Advances in Control and Dynamic Systems*, volume 17, pages 63 – 124. Academic Press, New York, NY, 1981.

12. J. Shinar and T. Shima. Nonorthodox guidance law development approach for intercepting maneuvering targets. *Journal of Guidance, Control, and Dynamics*, 25(4):658 – 666, August 2002.
13. V. Turetsky and V.Y. Glizer. Continuous feedback control strategy with maximal capture zone in a class of pursuit games. *International Game Theory Review*, 7, 2005.
14. V. Turetsky and J. Shinar. Missile guidance laws based on pursuit-evasion game formulations. *Automatica*, 39(4):607 – 618, 2003.

Convergence of Numerical Method for Time-Optimal Differential Games with Lifeline

Nataly V. Munts and Sergey S. Kumkov

1 Introduction

This paper discusses time-optimal differential games with lifeline and numerical scheme constructing the value function for such games. In games of this type, the first player tends to lead the system to a prescribed closed target set while keeping the trajectory inside some open set where the game takes place. The second player hinders this, because it wins as soon as either the trajectory of the system leaves this open set not touching the target one, or it succeeds in keeping the system infinitely inside this open set.

Apparently, the first, who formulated a problem with lifeline, was R. Isaacs in his book [20]. In his definitions, the *lifeline* is a set, after the reaching of which the second player wins unconditionally. Significant contribution into research of games with lifeline was made by L.A. Petrosyan (see e.g., [28]). However, the authors do not know works, which would consider exhaustively games of this sort: L.A. Petrosyan researched mostly problems with simple motion dynamics, that is, the problems where the players' controls are the velocities of the objects. In books [21, 22] of N.N. Krasovskii and A.I. Subbotin, games with lifeline are analyzed as problems with state constraints: the first player is not supposed to lead the system outside a prescribed set. Also, problems with state constraints have been studied by many authors (see, for example, [3, 10, 11, 19, 29]).

Problems very close to games with lifeline have been studied by French authors P. Cardaliaguet, M. Quincampoix, P. Saint-Pierre [12–15]. For controlled systems on

N. V. Munts (✉) · S. S. Kumkov
Krasovskii Institute of Mathematics and Mechanics, UrB RAS,
S. Kovalevskaya str., 16, 620990 Yekaterinburg, Russia
e-mail: natalymunts@gmail.com

S. S. Kumkov
e-mail: sskumk@gmail.com

D. M. Ramsey and J. Renault (eds.), *Advances in Dynamic Games*,
Annals of the International Society of Dynamic Games 17,
https://doi.org/10.1007/978-3-030-56534-3_5

the basis of the set-valued analysis, the theory of differential inclusions, and the theory of viability, they analyze the sets where the controller is able to keep the system infinitely (viability kernels). Passing to games, the authors consider a situation with two target sets for the first and second players, respectively, to which the players try to guide the system avoiding the target of the opposite player. Another variant considered in these works is games with state constraints for the first player. In these situations, the main objectives are to study victory domains of the players, that is, the sets wherefrom the corresponding player can reach its target without hitting the target of the opposite player (or state constraints). Also, in the terms of viability, the upper value function of such games (the guaranteed result of the first player) is characterized as a function, which epigraph is a viability set of the first player. Grid-geometric algorithms are suggested for approximation of viability kernels and, therefore, for approximation of the upper value. However, we have not found papers of these authors where existence of the value function is proved for games of this type and/or its coincidence with generalized solution of the corresponding boundary value problem of a HJE is justified (although such a connection is mentioned).

The main boost that stimulated the authors to study time-optimal games with lifeline is the investigation of questions connected with numerical methods for solving classic time-optimal games. In particular, in works [1, 2], Italian mathematicians M. Bardi and M. Falcone together with their colleagues suggested a theoretic numerical method for constructing the value function of a time-optimal game (without lifeline) as a generalized (viscosity) solution of the corresponding boundary value problem for HJE. The suggested procedure is of a grid type, and its proof is made in assumption that the grid is infinite and covers the entire game space. But practical computer realization, apparently, deals with a finite grid, which covers only a bounded part of the game space. So, the problem arises what boundary condition to set on the outer boundary of the domain covered by the grid. M. Bardi and M. Falcone suggest to set these conditions to plus infinity, that is, actually declaring that the second player wins when reaching the outer boundary of this domain. Therefore, the practical realization of the procedure solves a game with lifeline. That is why the authors decided to fill this gap connected to the problems with lifeline in a very general formulation.

Also, there is one more grid method for solving time-optimal problems suggested by authors from Germany. In works by N. Botkin, K.-H. Hoffmann, V. Turova, and their colleagues, a numerical procedure is suggested, which is based on a so-called *upwind operator* involving approximations for left and right partial derivatives of the value function in a node (see, for example, [7–9]). This algorithm is applicable to problems with state constraints for the first player, which can be treated as problems with lifeline.

This paper provides a numerical method for constructing the value function of a time-optimal game with lifeline as a viscosity solution of the corresponding boundary value problem for HJE. A pointwise convergence of the numerical method to the value function is proved. The method is just the one suggested by the Italian mathematicians, but its convergence should be proved anew in the framework of the new formulation. Also, theorems on coincidence of the value functions of time-optimal

problems with and without lifeline are proved under a very important assumption that the value function is continuous in the domain where the game takes place. The coincidence of the limit of discrete numerical solutions with the value function needs such a continuity. The continuity can be derived, in particular, from the assumptions of the local dynamic advantage of one player over another near their sets: if the system position is close to the target set, then the first player can guide the system to this set; vice versa, if the system is close to the lifeline, then the second player can push it to the lifeline. These assumptions have been taken for the proof of existence of the generalized solution justified in other papers [24–26] by the authors.

The structure of this paper is as follows. In Sect. 2, the formulation of the problem is given. Section 3 deals with the formulation of the numerical scheme and the convergence of computations performed according to it. In Sect. 4, a proof of convergence of the functions obtained as a result of the computations to the viscosity solution of the corresponding boundary value problem for the HJE coincides with the value function of the original game. Section 5 contains discussion on coincidence of the value function of time-optimal differential games with and without lifeline. In Sect. 6, one can see results of numerical computations performed by the realization of the numerical procedure. The paper is finalized by a conclusion.

2 Problem Formulation

Let us consider a conflict controlled system

$$\dot{x} = f(x, a, b), \qquad t \geq 0,\ a \in A,\ b \in B, \tag{1}$$

where $x \in \mathbb{R}^n$ is the phase vector of the system; a and b are the controls of the first and second players constrained by the compact sets A and B in their Euclidean spaces. We are given a compact set $\mathscr{T}$ and an open set $\mathscr{W} \subset \mathbb{R}^n$ such that $\mathscr{T} \subset \mathscr{W}$ and the boundary $\partial\mathscr{W}$ is bounded. Denote $\mathscr{G} := \mathscr{W} \setminus \mathscr{T}$ and $\mathscr{F} := \mathbb{R}^n \setminus \mathscr{W}$ (see Fig. 1). The game takes place in the set $\mathscr{G}$; the objective of the first player is to guide the system to the set $\mathscr{T}$ as soon as possible keeping the trajectory outside the set $\mathscr{F}$; the objective of the second player is to guide the system to the set $\mathscr{F}$, or if it is impossible, to keep the trajectory inside the set $\mathscr{G}$ forever, or if the latter is impossible too, to postpone reaching the set $\mathscr{T}$ as long as he can.

Such a game can be called a *game with lifeline*; the boundary $\partial\mathscr{F}$ of the set $\mathscr{F}$ is the lifeline where the second player wins unconditionally.

We assume that the following conditions are fulfilled:

C.1 The function $f : \mathbb{R}^n \times A \times B \to \mathbb{R}^n$ is continuous in all variables and Lipschitz continuous in the variable x: for all $x^{(1)}, x^{(2)} \in \mathbb{R}^n$, $a \in A$, $b \in B$

$$\left\| f(x^{(1)}, a, b) - f(x^{(2)}, a, b) \right\| \leq L \|x^{(1)} - x^{(2)}\|; \tag{2}$$

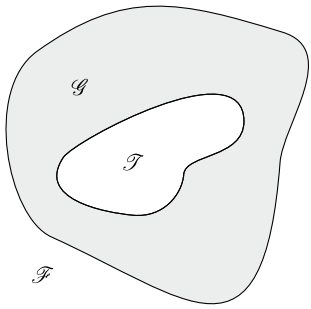

Fig. 1 Sets $\mathscr{T}$, $\mathscr{F}$, and $\mathscr{G}$

moreover, it satisfies Isaacs' condition:

$$\min_{a\in A}\max_{b\in B}\langle p,\, f(x,a,b)\rangle = \max_{b\in B}\min_{a\in A}\langle p,\, f(x,a,b)\rangle \quad \forall p\in\mathbb{R}^n. \tag{3}$$

Here and below, the symbol $\langle\cdot,\cdot\rangle$ stands for the scalar product.

C.2 The boundary $\partial\mathscr{G}$ of the set $\mathscr{G}$ (that is the boundaries $\partial\mathscr{T}$ and $\partial\mathscr{F}$) is compact, smooth, and has a bounded curvature.
Remark. In our previous paper [26], we do not demand the boundedness of the curvature of $\mathscr{G}$. When that paper was written, we thought that a sufficient smoothness of the boundary provides the boundedness of its curvature. It is necessary to prove existence of a generalized solution of the corresponding boundary problem of a Hamilton–Jacobi equation. However, after consultations with specialists in topology, it turned out that even infinitely smooth bounded curve in the plane can have an unbounded curvature. So, this demand should be formulated explicitly.

C.3 One can find a constant $c > 0$ and a bounded uniformly continuous function $\eta : \mathrm{cl}\,\mathscr{G} \cap O(\partial\mathscr{G}, c) \to \mathbb{R}^n$ such that the embedding $O\big(x + t\eta(x), ct\big) \subseteq \mathscr{G}$ is true for all $x \in \mathrm{cl}\,\mathscr{G} \cap O(\partial\mathscr{G}, c)$ and $0 < t \le c$. Here and below, $O(y, r)$ is an open ball of the radius r with the center at the point y, $O(X, r) := \big\{x : \mathrm{dist}(x, X) < r\big\}$ and $O(\varnothing, R) = \varnothing$.
Remark. It seems to us that the latter condition C.3 follows from the previous one C.2, but now we have no proof of this implication. So, we explicitly demand existence of the function η, which is called the generalized normal.

The players' aims of the mentioned kind can be formalized in the following way. Let the function $x(\cdot; x_0)$ be a trajectory of the system emanated from the initial point $x(0) = x_0$. We consider two instants

$$t_* = t_*\big(x(\cdot, x_0)\big) = \min\big\{t \ge 0 : x(t; x_0) \in \mathscr{T}\big\},$$
$$t^* = t^*\big(x(\cdot, x_0)\big) = \min\big\{t \ge 0 : x(t; x_0) \in \mathscr{F}\big\},$$

which are the instants when the trajectory $x(\cdot; x_0)$ hits for the first time the sets $\mathscr{T}$ and $\mathscr{F}$, respectively. If the trajectory doesn't arrive at the set $\mathscr{T}$ ($\mathscr{F}$), then the value t_* (t^*) is equal to $+\infty$.

To say what is a system trajectory, one can use either the formalization with nonanticipating strategies, or the positional formalization of N.N. Krasovskii and A.I. Subbotin [21, 22]. In the latter case, the feedback strategies of the first and the second player are functions $a(\cdot) : \mathbb{R}^n \to A$ and $b(\cdot) : \mathbb{R}^n \to B$, respectively.

We define the result of the game on the trajectory $x(\cdot; x_0)$ as

$$\tau\big(x(\cdot; x_0)\big) = \begin{cases} +\infty, & \text{if } t_* = +\infty \text{ or } t^* < t_*, \\ t_*, & \text{otherwise.} \end{cases} \tag{4}$$

In [23], the authors prove that a time-optimal problem with lifeline has the value function $T(x)$.

The unboundedness of the value function and cost functional can cause some uneasiness of a numerical research of game (1), (4). For this reason, one often substitutes the unbounded cost functional with a bounded one by means of the *Kruzhkov's transform*:

$$J\big(x(\cdot, x_0)\big) = \begin{cases} 1 - \exp\big(-\tau\big(x(\cdot; x_0)\big)\big), & \text{if } \tau\big(x(\cdot; x_0)\big) < +\infty, \\ 1, & \text{otherwise.} \end{cases} \tag{5}$$

In such a case, the value function $v(x)$ also becomes bounded and its magnitude belongs to the range from zero to one:

$$v(x) = \begin{cases} 1 - \exp\big(-T(x)\big), & \text{if } T(x) < +\infty, \\ 1, & \text{otherwise.} \end{cases} \tag{6}$$

3 Numerical Scheme

In general, the numerical scheme construction and justification of its convergence are analogous to the ones in paper [2] where the numerical scheme for the classic time-optimal problem is constructed and its convergence is proved. Herewith, the value function is characterized as the unique generalized (viscosity) solution of the corresponding boundary value problem for HJE.

3.1 Discrete Scheme

Let us replace the continuous dynamics with a discrete one by the time step $h > 0$:

$$x_n = x_{n-1} + hf(x_{n-1}, a_{n-1}, b_{n-1}),\ n = 1, \ldots, N, \quad x_0 \text{ is given,}$$

where $a_n \in A$ and $b_n \in B$.

By the discrete Dynamic Programming Principle, one can get the following characterization for the value function $w_h(\cdot)$ of the discrete time problem:

$$w_h(x) = \begin{cases} \gamma \max\limits_{b\in B} \min\limits_{a\in A} w_h\big(z(x,a,b)\big) + 1 - \gamma, & \text{if } x \in \mathscr{G}, \\ 0, & \text{if } x \in \mathscr{T}, \\ 1, & \text{if } x \in \mathscr{F}. \end{cases}$$

Here, $\gamma = e^{-h}$, $z(x,a,b) = x + hf(x,a,b)$.

Further, let us describe the space discretization. Let us consider a grid $\mathscr{L}$ with the step k, which covers the entire space $\mathbb{R}^n$ and consists of nodes $q_{i_1,\ldots,i_n} = (x_{i_1}, \ldots, x_{i_n})$, $i_1, \ldots, i_n \in \mathbb{Z}$, $x_{i_j} = ki_j$. (Generally speaking, steps along different axes can differ, but this fact doesn't change the main idea of the numerical scheme construction.) Here and below, mostly, a linear indexation q_ν, $\nu \in \mathbb{Z}$, for the nodes of the grid $\mathscr{L}$ is used. The symbol $\mathscr{L}_\mathscr{T}$ stands for the set of those nodes of the grid $\mathscr{L}$, which belong to the set $\mathscr{T}$; the symbol $\mathscr{L}_\mathscr{G}$ denotes the collection of nodes falling into the set $\mathscr{G}$; and the symbol $\mathscr{L}_\mathscr{F}$ stands for the set of nodes from the set $\mathscr{F}$. In theoretical constructions, the grid is assumed infinite.

For every point $x \in \mathbb{R}^n$, one can find a simplex $S(x)$ with vertices $\{q_l(x)\}$ from $\mathscr{L}$ such that the point x belongs to the simplex $S(x)$ and $S(x)$ does not contain other nodes of the grid. It is assumed that with choosing the grid $\mathscr{L}$, we also choose a separation of the game space to simplices with their vertices at nodes of the grid. On the basis of $S(x)$, one can obtain the *barycentric (local) coordinates* $\lambda_l(x)$ of the point x with respect to the vertices $q_l(x)$ of the simplex $S(x)$:

$$x = \sum_{l=1}^{n+1} \lambda_l(x) q_l(x), \qquad \lambda_l(x) \geq 0, \ \sum_{l=1}^{n+1} \lambda_l(x) = 1.$$

Sometimes, the arguments of the coefficients λ and vertices q will be omitted if they are clear from the context.

Let us substitute the function $w_h(\cdot)$ with a new one $w(\cdot)$, which magnitudes $w(q_\nu)$ at the nodes q_ν of the grid $\mathscr{L}$ form an infinite vector $W = \big(w(q_\nu)\big)_{\nu\in\mathbb{Z}}$. The magnitude $w(x)$ at some point x, which is not a node of the grid, can be reconstructed by means of the following piecewise-linear approximation based on the local coordinates of the point x:

$$w_{loc}(x, W) = \sum_{l=1}^{n+1} \lambda_l(x)\, w\big(q_l(x)\big). \tag{7}$$

Hereby, the characterization of the value function of a fully discrete problem is obtained:

$$w(q_\nu) = \begin{cases} \gamma \max\limits_{b\in B} \min\limits_{a\in A} w_{loc}\big(z(q_\nu, a, b), W\big) + 1 - \gamma, & \text{if } q_\nu \in \mathscr{L}_{\mathscr{G}}, \\ 0, & \text{if } q_\nu \in \mathscr{L}_{\mathscr{T}}, \\ 1, & \text{if } q_\nu \in \mathscr{L}_{\mathscr{F}}. \end{cases}$$

This characterization is of a recursive kind, because the magnitude $w(q_\nu)$ at some node q_ν depends on the magnitude of the local reconstruction w_{loc}. Note that the latter in its turn depends on the magnitudes of the function $w(\cdot)$ at nodes of the grid, which may include the node q_ν. Such kind of relations obtained is typical for the dynamic programming principle. In the following, on the basis of this formula, an iterative numerical method for construction of the vector W and function w is proposed. Moreover, from the definition of $w(\cdot)$, one can see that in a practical realization of the numerical method, it is necessary to remember values of this function only at the nodes from $\mathscr{L}_{\mathscr{G}}$. If the set $\mathscr{G}$ is bounded, then $\mathscr{L}_{\mathscr{G}}$ contains only finite number of nodes and can be represented in a computer.

For the chosen grid $\mathscr{L} = \{q_\nu\}_{\nu\in\mathbb{Z}}$, we denote by $\mathscr{M}$ the set of infinite vectors with the elements $W = \big(w(q_\nu)\big)_{\nu\in\mathbb{Z}}$. We denote by $\mathscr{M}_1$ those vectors in the set $\mathscr{M}$, which elements $w(q_\nu)$ satisfy the inequality $0 \le w(q_\nu) \le 1$. For every $s \in \mathbb{Z}$, we define an operator $F_s : \mathscr{M} \to \mathbb{R}$ using a vector $W = \big(w(q_\nu)\big)_{\nu\in\mathbb{Z}}$ in the following way:

$$F_s(W) = \begin{cases} \gamma \max\limits_{b\in B} \min\limits_{a\in A} w_{loc}\big(z(q_s, a, b), W\big) + 1 - \gamma, & \text{if } q_s \in \mathscr{L}_{\mathscr{G}}, \\ 0, & \text{if } q_s \in \mathscr{L}_{\mathscr{T}}, \\ 1, & \text{if } q_s \in \mathscr{L}_{\mathscr{F}}. \end{cases}$$

Here, $w_{loc} : \mathbb{R}^n \times \mathscr{M} \to \mathbb{R}$ is the local reconstruction (7) of the function $w(\cdot)$ corresponding to the vector W. The manifold of values of the operators F_s over all indices s (that is, over all nodes q_s) defines an operator $F : \mathscr{M} \to \mathscr{M}$.

A partial order can be defined in the set $\mathscr{M}$ using the elementwise comparison: $W_1 \le W_2 \Leftrightarrow \forall \nu \in \mathbb{Z}\ w_1(q_\nu) \le w_2(q_\nu)$. Also, in $\mathscr{M}_1$, one can reasonably introduce the norm $\|W\|_\infty = \sup\big\{w(q_\nu) : \nu \in \mathbb{Z}\big\}$.

Let us prove the following lemma on properties of the operator F analogous to the one from paper [2, pp. 124–125, Proposition 2.1].

Lemma 1 *The operator $F : \mathscr{M} \to \mathscr{M}$ has the following properties:*

1. *$F(\mathscr{M}_1) \subseteq \mathscr{M}_1$;*
2. *F is monotone with respect to the partial order in $\mathscr{M}$;*
3. *F is a contraction map in $\mathscr{M}_1$ with respect to the norm $\|\cdot\|_\infty$.*

Proof Basically, the proof repeats the analogous one in [2, pp. 124–125].

1. Let $W \in \mathscr{M}_1$ and $q_s \in \mathscr{L}_{\mathscr{G}}$. Then

$$F_s(W) = \gamma \max_{b\in B} \min_{a\in A} \sum_{m=1}^{n+1} \lambda_m\big(z(q_s, a, b)\big) W_m\big(z(q_s, a, b)\big) + 1 - \gamma.$$

Here, $W_m(z)$ is the element of the vector W corresponding to the node, which is the mth vertex of the simplex $S\big(z(q_s, a, b)\big)$.
Since, $\lambda_m\big(z(q_s, a, b)\big) \geq 0$, $\sum \lambda_m\big(z(q_s, a, b)\big) = 1$, and $0 \leq W_m \leq 1$, we have

$$0 \leq F_s(W) \leq \gamma \max_{b\in B} \min_{a\in A} \sum_{m=1}^{n+1} \lambda_m\big(z(q_s, a, b)\big) + 1 - \gamma = \gamma + 1 - \gamma = 1.$$

If $q_s \notin \mathscr{L}_{\mathscr{G}}$, then $F_s(W) = 0$ or $F_s(W) = 1$. Hence, it appears that $F : \mathscr{M}_1 \to \mathscr{M}_1$.

2. Let $U,\ V \in \mathscr{M}$ and $U \geq V$. If $q_s \in \mathscr{L}_{\mathscr{G}}$, then

$$F_s(V) - F_s(U) = \gamma \max_{b\in B} \min_{a\in A} \sum_{m=1}^{n+1} \lambda_m\big(z(q_s, a, b)\big) V_m\big(z(q_s, a, b)\big) - \gamma \max_{b\in B} \min_{a\in A} \sum_{m=1}^{n+1} \lambda_m\big(z(q_s, a, b)\big) U_m\big(z(q_s, a, b)\big).$$

Let us choose the control $\overline{a}(b)$ of the first player attaining the minimum in $F_s(U)$ for a fixed b. Then the minuend in the inequality increases, because $\overline{a}(b)$ not necessarily attains the minimum in $F_s(V)$, while the subtrahend keeps its value. We get

$$\begin{aligned}
&\gamma \max_{b\in B} \min_{a\in A} \sum_{m=1}^{n+1} \lambda_m\big(z(q_s, a, b)\big) V_m\big(z(q_s, a, b)\big) \\
&\qquad - \gamma \max_{b\in B} \min_{a\in A} \sum_{m=1}^{n+1} \lambda_m\big(z(q_s, a, b)\big) U_m\big(z(q_s, a, b)\big) \\
&\leq \gamma \max_{b\in B} \sum_{m=1}^{n+1} \lambda_m\big(z\big(q_s, \overline{a}(b), b\big)\big) V_m\big(z\big(q_s, \overline{a}(b), b\big)\big) \\
&\qquad - \gamma \max_{b\in B} \sum_{m=1}^{n+1} \lambda_m\big(z\big(q_s, \overline{a}(b), b\big)\big) U_m\big(z\big(q_s, \overline{a}(b), b\big)\big).
\end{aligned}$$

Now, let us consider the control $\overline{b}$ of the second player attaining the maximum in the expression for the minuend, that is,

$$\overline{b} \in \operatorname{Arg}\max_{b\in B} \left[\gamma \sum_{m=1}^{n+1} \lambda_m\big(z\big(q_s, \overline{a}(b), b\big)\big) V_m\big(z\big(q_s, \overline{a}(b), b\big)\big)\right].$$

It follows that

$$\begin{aligned}\gamma \max_{b\in B} \sum_{m=1}^{n+1} \lambda_m\big(z\big(q_s, \overline{a}(b), b\big)\big) V_m\big(z\big(q_s, \overline{a}(b), b\big)\big) \\ - \gamma \max_{b\in B} \sum_{m=1}^{n+1} \lambda_m\big(z\big(q_s, \overline{a}(b), b\big)\big) U_m\big(z\big(q_s, \overline{a}(b), b\big)\big) \\ \le \gamma \sum_{m=1}^{n+1} \lambda_m\big(z\big(q_s, \overline{a}(\overline{b}), \overline{b}\big)\big)\Big(V_m\big(z\big(q_s, \overline{a}(\overline{b}), \overline{b}\big)\big) \\ - U_m\big(z\big(q_s, \overline{a}(\overline{b}), \overline{b}\big)\big)\Big) \le 0.\end{aligned}$$

If $q_s \in \mathscr{L}_{\mathscr{T}}$ or $q_s \in \mathscr{L}_{\mathscr{F}}$, then $F_s(V) - F_s(U) = 0$. Hence, F is the monotone operator.

3. Let $U,\ V \in \mathscr{M}_1$. If $q_s \in \mathscr{L}_{\mathscr{G}}$, then

$$\begin{aligned}\big|F_s(V) - F_s(U)\big| &\le \gamma \sum_{m=1}^{n+1} \lambda_m\big(z\big(q_s, \overline{a}(\overline{b}), \overline{b}\big)\big) \\ &\quad \times \big|V_m\big(z\big(q_s, \overline{a}(\overline{b}), \overline{b}\big)\big) - U_m\big(z\big(q_s, \overline{a}(\overline{b}), \overline{b}\big)\big)\big| \\ &\le \gamma \max_m \big|V_m\big(z\big(q_s, \overline{a}(\overline{b}), \overline{b}\big)\big) - U_m\big(z\big(q_s, \overline{a}(\overline{b}), \overline{b}\big)\big)\big| \\ &\quad \times \sum_{m=1}^{n+1} \lambda_m\big(z\big(q_s, \overline{a}(\overline{b}), \overline{b}\big)\big) \le \gamma \|V - U\|_\infty.\end{aligned}$$

It holds for every $s \in \mathbb{Z}$.

If $q_s \in \mathscr{L}_{\mathscr{T}}$ or $q_s \in \mathscr{L}_{\mathscr{F}}$, then $F_s(V) - F_s(U) = 0$. So, it immediately follows that the function F is a contraction map, since $\gamma = e^{-h} < 1$.

As a consequence from this lemma, one can obtain that there exists a unique fixed point $\mathbf{W} \in \mathscr{M}_1$ of the operator F, which determines a function $\mathbf{w}(\cdot)$ in $\mathbb{R}^n$, $\mathbf{w}(x) \in [0, 1]$. This function depends on the time h and space k discretization steps of the original problem:

$$\mathbf{w}(x) = \begin{cases} \sum\limits_m \lambda_m \mathbf{w}(q_m), & \text{if } x \notin \mathscr{L} \text{ and } x = \sum\limits_m \lambda_m q_m, \\ \gamma \max\limits_{b\in B} \min\limits_{a\in A} \mathbf{w}_{loc}\big(z(q_s, a, b), \mathbf{W}\big) + 1 - \gamma, & \text{if } q_s \in \mathscr{L}_{\mathscr{G}}, \\ 0, & \text{if } q_s \in \mathscr{L}_{\mathscr{T}}, \\ 1, & \text{if } q_s \in \mathscr{L}_{\mathscr{F}}. \end{cases} \tag{8}$$

3.2 Viscosity Solution of Boundary Problem for HJE

Let us consider the following boundary value problem for HJE:

$$\begin{aligned} &z + H(x, Dz) = 0, x \in \mathscr{G}, \\ &z(x) = 0 \text{ if } x \in \partial\mathscr{T}, \\ &z(x) = 1 \text{ if } x \in \partial\mathscr{F}. \end{aligned} \tag{9}$$

Here and below, the symbol Dz denoted the gradient of the function z. The function H is called the *Hamiltonian* and in the case of dynamics (1) is defined as follows:

$$H(x, p) = \max_{a\in A} \min_{b\in B} \langle p, -f(x, a, b)\rangle - 1, \quad x, p \in \mathbb{R}^n. \tag{10}$$

Equations of this type can have no classical solution. That is why we use the notion of the *generalized viscosity solution* introduced in [17] to deal with this problem. In book [30], an alternative method of obtaining a generalized solution of HJE was introduced. It is called the *generalized minimax solution*. Also in book [30], it is proved that viscosity and minimax solutions coincide at the points of continuity.

In [24, 25], the authors prove that the value function of game (1), (5) is a viscosity solution of problem (9). The proof demands smoothness of boundaries $\partial\mathscr{T}$ and $\partial\mathscr{F}$, the boundedness of these boundaries curvature. It was performed under the assumption of the dynamical advantage of each player on the boundaries of the corresponding sets:

$$\begin{aligned} &\forall x \in \partial\mathscr{T} \ \min_{a\in A} \max_{b\in B} \langle n_{\mathscr{T}}(x), f(x, a, b)\rangle < 0, \\ &\forall x \in \partial\mathscr{F} \ \max_{b\in B} \min_{a\in A} \langle n_{\mathscr{F}}(x), f(x, a, b)\rangle < 0. \end{aligned} \tag{11}$$

Here, $n_{\mathscr{T}}(x)$ $\left(n_{\mathscr{F}}(x)\right)$ is a normal vector to the boundary $\partial\mathscr{T}$ $(\partial\mathscr{F})$ of the set $\mathscr{T}$ $(\mathscr{F})$ at the point x directed outward the corresponding set or (what is the same) inward the set $\mathscr{G}$. The sense of these relations is that if the system is at the boundary of the set $\mathscr{T}$ $(\mathscr{F})$, then the first (second) player can guarantee leading the trajectory of the system inside the corresponding set despite the action of the opponent. Combination of these assumptions results in the continuity of the value function inside the set $\mathscr{G}$. Indeed, from the results of paper [26], it follows that under these assumptions an upper generalized solution exists, which is continuous in $\operatorname{cl}\mathscr{G}$. Then, the statements in [30, Sect. 18.6, pp. 224–225] imply that a generalized solution exists, which is continuous in $\mathscr{G}$. Moreover, since the value function coincides with the generalized solution, it is continuous too (the coincidence is proved in [26]).

Definition 1 ([2], *p. 112, Definition 1.3*) For some domain Ω, an upper semicontinuous function $u(\cdot)$ is called a *viscosity subsolution* of Eq. (9) in the domain Ω if for all $\varphi \in C^1(\Omega)$ and for any local maximum point $y \in \Omega$ for $u - \varphi$, the inequality $u(x) + H\left(x, D\varphi(x)\right) \leqslant 0$ holds.

Definition 2 ([2], *p. 112, Definition 1.3*) For some domain Ω, a lower semicontinuous function $u(\cdot)$ is called a *viscosity supersolution* of Eq. (9) in the domain Ω if for all $\varphi \in C^1(\Omega)$ and for any local minimum point $y \in \Omega$ for $u - \varphi$, the inequality $u(x) + H\big(x, D\varphi(x)\big) \geqslant 0$ holds.

Definition 3 Let us consider two sequences of real numbers $h_n > 0$ and $k_n > 0$ (which are time and space discretization steps). We will refer to them as *admissible sequences* if $h_n \to 0$ and $k_n / h_n \to 0$ as $n \to \infty$.

Let us consider admissible sequences of real numbers $h_n > 0$, $k_n > 0$, and a sequence of the solutions $\mathbf{w}_n$ of problem (8) corresponding to these admissible sequences.

The proof of the facts given in the next section is based on the notion of the *weak limit in the viscosity sense* introduced in [1, 6]. An upper and a lower limit of the functional sequence $\mathbf{w}_n$ in the viscosity sense are defined as follows:

$$\begin{aligned} \limsup_{(y,n)\to(x,\infty)} \mathbf{w}_n(y) &:= \lim_{\delta\to 0+} \sup\big\{\mathbf{w}_n(y) : |x-y| \leq \delta, n \geq 1/\delta\big\}, \\ \liminf_{(y,n)\to(x,\infty)} \mathbf{w}_n(y) &:= \lim_{\delta\to 0+} \inf\big\{\mathbf{w}_n(y) : |x-y| \leq \delta, n \geq 1/\delta\big\}. \end{aligned} \tag{12}$$

Note that these limits exist if the functional sequence $\mathbf{w}_n$ is locally uniformly bounded [1, p. 288, Definition 1.4].

Definition 4 For some domain Ω, an upper semicontinuous function $u : \operatorname{cl}\Omega \to \mathbb{R}$ satisfies the boundary condition $u + H(x, Du) \leq 0$ at the boundary $\partial\Omega$ *in the viscosity sense* if for all $\varphi \in C^1(\operatorname{cl}\Omega)$ and a point $x \in \partial\Omega$ such that the function $u - \varphi$ has a local maximum at x, the inequality $u(x) + H(x, D\varphi(x)) \leq 0$ holds.

Definition 5 For some domain Ω, a lower semicontinuous function $u : \operatorname{cl}\Omega \to \mathbb{R}$ satisfies the boundary condition $u + H(x, Du) \geq 0$ at the boundary $\partial\Omega$ *in the viscosity sense* if for all $\varphi \in C^1(\operatorname{cl}\Omega)$ and a point $x \in \partial\Omega$ such that the function $u - \varphi$ has a local minimum at x, the inequality $u(x) + H(x, D\varphi(x)) \geq 0$ holds.

4 Numerical Scheme Convergence

Let us formulate and prove a lemma for a time-optimal game with lifeline analogous to [2, p. 127, Lemma 2.2]. Some derivations in the original lemma were omitted. For example, the proof for an upper solution was absent, proof of the inequalities analogous to (19) and (20) from this paper was not completely performed, and some essential remarks were missed (e.g., in the original lemma the function φ is defined on the closure of the set of the game but is used in a such a way that it is defined on the whole $\mathbb{R}^n$).

Lemma 2 *Let us consider admissible sequences of real numbers $h_n > 0$ and $k_n > 0$, and let $\mathbf{w}_n$ be the corresponding sequence of solutions* (8)*. Denote*

$$\overline{v}(x) := \limsup_{(y,n)\to(x,\infty)} \mathbf{w}_n(y), \quad \underline{v}(x) := \liminf_{(y,n)\to(x,\infty)} \mathbf{w}_n(y). \tag{13}$$

Then the functions $\overline{v}$ and $\underline{v}$ are, respectively, a viscosity subsolution and supersolution of the boundary value problem (9) with the boundary conditions

$$\underline{v} \geq 0 \text{ on } \partial\mathscr{T}, \tag{14}$$

$$\overline{v} \leq 0 \text{ or } \overline{v} + H\big(x, D\overline{v}(x)\big) \leq 0 \text{ on } \partial\mathscr{T}, \tag{15}$$

$$\underline{v} \geq 1 \text{ or } \underline{v} + H\big(x, D\underline{v}(x)\big) \geq 0 \text{ on } \partial\mathscr{F}, \tag{16}$$

$$\overline{v} \leq 1 \text{ on } \partial\mathscr{F}. \tag{17}$$

The second inequalities in (15) and (16) are understood in the viscosity sense.

Proof Proofs of the facts that the boundary conditions (14), (15) are fulfilled and that $\overline{v}$ is a viscosity subsolution are similar to those from [2, pp.127–129]. The fulfilment of the last boundary condition (17) is obvious from the construction of the function $\overline{v}$. Therefore, it is necessary to show only that the function $\underline{v}$ is a viscosity supersolution and that the boundary condition (16) holds. Let us prove these facts simultaneously (in (16), we prove the second inequality).

Choose a function $\varphi \in C^1(\mathbb{R}^n)$ and a point $y \in \operatorname{cl}\mathscr{G}$ such that the function $\underline{v} - \varphi$ attains the local strict minimum at the point y. Although, the function φ in the definition of the viscosity solution is considered only at the set $\operatorname{cl}\mathscr{G}$, we define it in the whole space $\mathbb{R}^n$, because we shall need it henceforth; restriction of the function φ to the set $\operatorname{cl}\mathscr{G}$ is smooth. As far as the property of the point y doesn't change under adding a constant to the function φ, we consider that $\varphi(y) = \underline{v}(y)$. The point y can belong to the set $\mathscr{G}$ or to the boundary $\partial\mathscr{F}$. The case when the point y belongs to the boundary $\partial\mathscr{T}$ does not require consideration, because it is taken into account in condition (14). If $y \in \partial\mathscr{F}$ and $\underline{v}(y) \geq 1$, then inequality (16) holds. Thus hereafter, we shall assume that $\underline{v}(y) < 1$ if $y \in \partial\mathscr{F}$ and $\underline{v}(y) \leq 1$ if $y \in \mathscr{G}$.

It has to be shown that $\underline{v}(y) + H\big(y, D\varphi(y)\big) \geq 0$. Let us choose a sequence of points x_n such that

$$\min_{\operatorname{cl}\left(\mathscr{G}\cap B(y,1)\right)} (\mathbf{w}_n - \varphi) = (\mathbf{w}_n - \varphi)(x_n).$$

The basic property of weak limits in the viscosity sense [1, 5, 18] is the existence of a subsequence (we suppose that it is the sequence x_n itself) such that $x_n \to y$ and $\mathbf{w}_n(x_n) \to \underline{v}(y)$ as $n \to \infty$. It means that one can choose such a number $\varepsilon > 0$ that $B(y,\varepsilon) \subset \mathscr{G}$ if $y \in \mathscr{G}$ or $\varphi(y') < 1 - \varepsilon$ for every $y' \in B(y,\varepsilon)$ if $y \in \partial\mathscr{F}$. It can always be achieved by means of decreasing ε, because if $y \in \partial\mathscr{F}$, then $\varphi(y) = \underline{v}(y) < 1$. Moreover, one can choose such a sufficiently big number n that the following inequalities hold

(a) $x_n \in B(y, \varepsilon/3)$ holds, because x_n converges to the point y as $n \to \infty$;
(b) $\left|h_n f(x_n, a, b)\right| \leq \varepsilon/3$ holds, because h_n tends to 0;

(c) $k_n \cdot \max\left\{2+\sigma, \sqrt{d}\right\} \le \varepsilon/3$ holds, because the sequence k_n tends to 0; here, $\sigma = \max\left\{\left|D\varphi(z)\right| : z \in B(y,1)\right\}$;

(d) $\varphi(x_n) - \mathbf{w}_n(x_n) > -\varepsilon$ holds, because we assume that $\varphi(y) = \underline{v}(y)$; hence, $\varphi(x_n) < \mathbf{w}_n(x_n)$ (as $\varphi(y') < \underline{v}(y')$ and $\underline{v}(y') \le \mathbf{w}_n(y')$ for all y' in some sufficiently small neighborhood of the point y; the points x_n belong to this neighborhood for indices n starting from some sufficiently large index).

The following calculations are made for n fixed, so we temporarily omit the subscript in $h_n, k_n, \mathbf{w}_n, x_n, \gamma_n = e^{-h_n}$.

1. Let $y \in \mathscr{G}$. Let us write the local coordinates of the point x via the vertices q_s of the corresponding simplex: $x = \sum_s \lambda_s q_s$. Note that $q_s \in B(y,\varepsilon)$, because $x \in B(y,\varepsilon/3)$ and $q_s \in B(x,\varepsilon/3)$ (the latter is true due to $k\sqrt{d} \le \varepsilon/3$). So, $q_s \in \mathscr{G}$, whence it follows that for $\mathbf{w}(q_s)$ the following representation holds

$$\mathbf{w}(q_s) = \gamma \max_{b\in B} \min_{a\in A} \mathbf{w}_{loc}\big(z(q_s,a,b), \mathbf{W}\big) + 1 - \gamma.$$

2. Let $y \in \partial\mathscr{F}$. Then $-\varepsilon < \varphi(x) - \mathbf{w}(x) < 1 - \varepsilon - \mathbf{w}(x) \Rightarrow \mathbf{w}(x) < 1$. So, if $x = \sum_s \lambda_s q_s$, then there exists a node q_s such that $\lambda_s \ne 0$ and $\mathbf{w}(q_s) < 1$. Then again for $\mathbf{w}(q_s)$, the following representation holds

$$\mathbf{w}(q_s) = \gamma \max_{b\in B} \min_{a\in A} \mathbf{w}_{loc}\big(z(q_s,a,b), \mathbf{W}\big) + 1 - \gamma.$$

Let us note that

$$\mathbf{w}(q_s) = \gamma \max_{b\in B} \min_{a\in A} \mathbf{w}_{loc}\big(z(q_s,a,b), \mathbf{W}\big) + 1 - \gamma \ge \gamma \min_{a\in A} \mathbf{w}_{loc}\big(z(q_s,a,b), \mathbf{W}\big) + 1 - \gamma$$

for every $b \in B$. Moreover, for every $\rho > 0$, there exists a value $a_s(\rho)$ (for example, the one attaining the minimum) such that the following inequality holds

$$\gamma \min_{a\in A} \mathbf{w}_{loc}\big(z(q_s,a,b), \mathbf{W}\big) + 1 - \gamma > \gamma \mathbf{w}_{loc}\big(z\big(q_s, a_s(\rho), b\big), \mathbf{W}\big) + 1 - \gamma - \rho h.$$

We denote by $z_s(\rho,b) = z\big(q_s, a_s(\rho), b\big) = q_s + hf\big(q_s, a_s(\rho), b\big)$. Whence it follows that for every $\rho > 0$ the relation holds

$$\mathbf{w}(q_s) - \gamma \mathbf{w}_{loc}\big(z_s(\rho,b), \mathbf{W}\big) - (1-\gamma) > -\rho h \quad \forall b \in B. \tag{18}$$

Let $z_s = \sum_p \mu_p q_p$ and b is arbitrary. Now, let us prove that

$$\mathbf{w}(x) - \varphi(x) \le \mathbf{w}_{loc}\big(z_s(\rho,b), \mathbf{W}\big) - \varphi\big(z_s(\rho,b)\big) + \sigma k\sqrt{d} + o_1, \tag{19}$$

where $o_1 = o(|z_s(\rho, b) - q_{p^\star}|)$ and $q_{p^\star}$ is such a vertex of the simplex $S(z_s(\rho, b))$ that $\varphi(q_{p^\star})$ is the minimum magnitude of φ over the vertices of this simplex. Here and below, all o-variables are considered as $n \to \infty$.

If $z_s(\rho, b) \in \operatorname{cl}\mathscr{G}$, then, in virtue of condition (c), we obtain $z_s(\rho, b) \in B(q_s, \varepsilon/3)$. Since $q_s \in B(x, \varepsilon/3)$, one has $z_s(\rho, b) \in B(x, 2\varepsilon/3) \subset B(x, \varepsilon)$. In this case, inequality (19) holds, because x is the point of a local minimum of the function $\mathbf{w} - \varphi$.

Now, let $z_s(\rho, b) \notin \operatorname{cl}\mathscr{G}$. Two cases are possible

1. There is a term in the representation of z_s such that $\mu_p \neq 0$ and $q_p \in \operatorname{cl}\mathscr{G}$. Then, similarly, we get $q_p \in B(z_s(\rho, b), \varepsilon/3)$, $z_s(\rho, b) \in B(q_s, \varepsilon/3)$, and $q_s \in B(x, \varepsilon/3)$. Hence, $q_p \in B(x, \varepsilon)$. From this, it follows that $\mathbf{w}(x) - \varphi(x) \leq \mathbf{w}(q_p) - \varphi(q_p)$, because x is the point of a local minimum of the function $\mathbf{w} - \varphi$.
2. For all p such that $\mu_p \neq 0$, one has that $q_p \notin \operatorname{cl}\mathscr{G}$. Recall that the function φ is defined on the whole space $\mathbb{R}^n$ and that for every $y' \in B(y, \varepsilon)$ the condition $\varphi(y') < 1 - \varepsilon$ holds. Then, in virtue of condition (d), we get

$$\mathbf{w}(x) - \varphi(x) < \varepsilon < 1 - \varphi(q_p) = \mathbf{w}(q_p) - \varphi(q_p),$$

because the function $\mathbf{w}(q_p) = 1$ at the node $q_p \in \mathscr{F}$.

Then

$$\begin{aligned}\mathbf{w}(x) - \varphi(x) &\leq \sum_p \mu_p\big(\mathbf{w}(q_p) - \varphi(q_p)\big) = \sum_p \mu_p \mathbf{w}(q_p) - \sum_p \mu_p \varphi(q_p) \\ &\leq \mathbf{w}_{loc}\big(z_s(\rho, b), \mathbf{W}\big) - \sum_p \mu_p \varphi(q_{p^\star}) = \mathbf{w}_{loc}\big(z_s(\rho, b), \mathbf{W}\big) - \varphi(q_{p^\star}),\end{aligned}$$

where the index $p^\star$ is as defined above.

Note that

$$\begin{aligned}\big|\varphi\big(z_s(\rho, b)\big) - \varphi(q_{p^\star})\big| &\leq \sigma\big|z_s(\rho, b) - q_{p^\star}\big| + o(|z_s(\rho, b) - q_{p^\star}|) \\ &< \sigma k\sqrt{d} + o(|z_s(\rho, b) - q_{p^\star}|).\end{aligned}$$

Then $-\varphi(q_{p^\star}) \leq -\varphi\big(z_s(\rho, b)\big) + \sigma k\sqrt{d} + o_1$. Hence, we obtain inequality (19).

Now, let us show that $\big|\mathbf{w}(x) - \mathbf{w}(q_s)\big| \leq \sigma k\sqrt{d}$.

Since x, q_s belong to one simplex S, then $\mathbf{w}$ is affine in the segment $X = [x, q_s]$. As function $(\mathbf{w} - \varphi)\big|_X$ attains minimum at the point x, we get

$$\frac{|\mathbf{w}(x) - \mathbf{w}(q_s)|}{k\sqrt{d}} \leq \frac{|\mathbf{w}(x) - \mathbf{w}(q_s)|}{|x - q_s|} = |D_X \mathbf{w}| = |D_X \varphi| \leqslant \sigma.$$

We denote by $D_X g$ a derivative of the restriction of a function g to the set X as a derivative of a function of one variable.

Also, let us note that

$$\begin{aligned}\big|\varphi\big(z_s(\rho,b)\big)-\varphi\big(x+hf(x,a_s(\rho),b)\big)\big| &\le \sigma\big|z_s(\rho,b)-x-hf(x,a_s(\rho),b)\big|\\ &= \sigma\big|q_s+hf(q_s,a_s(\rho),b)-x-hf(x,a_s(\rho),b)\big|\\ &\le \sigma\big(|q_s-x|+h\big|f(q_s,a_s(\rho),b)-f(x,a_s(\rho),b)\big|\big)\le\sigma(k\sqrt{d}+hLk).\end{aligned} \tag{20}$$

Now, let us apply the educed inequalities to (18) for any $b\in B$:

$$\begin{aligned}&-\rho h<\mathbf{w}(q_s)-\gamma\mathbf{w}_{loc}\big(z_s(\rho,b),\mathbf{W}\big)-(1-\gamma)\\ &\le \mathbf{w}(x)-\gamma\mathbf{w}_{loc}\big(z_s(\rho,b),\mathbf{W}\big)-(1-\gamma)+\sigma k\sqrt{d}\\ &=(1-\gamma)\mathbf{w}(x)+\gamma\Big(\mathbf{w}(x)-\mathbf{w}_{loc}\big(z_s(\rho,b),\mathbf{W}\big)\Big)-(1-\gamma)+\sigma k\sqrt{d}\\ &\le(1-\gamma)\mathbf{w}(x)+\gamma\Big(\varphi(x)-\varphi\big(z_s(\rho,b)\big)\Big)-(1-\gamma)+(1+\gamma)\sigma k\sqrt{d}+\gamma o_1\\ &\le(1-\gamma)\mathbf{w}(x)+\gamma\Big(\varphi(x)-\varphi\big(x+hf(x,a_s,b)\big)\Big)\\ &\quad-(1-\gamma)+(1+2\gamma+\gamma hL)\sigma k\sqrt{d}+\gamma o_1,\end{aligned}$$

where L is the Lipschitz constant for the function f from condition (2).

Since ρ is arbitrary, it holds

$$\begin{aligned}0\le\frac{1-\gamma_n}{h_n}\mathbf{w}_n(x^n)&\\ +\min_{b\in B}\max_{a\in A}&\left\{\gamma_n\frac{\varphi(x^n)-\varphi\big(x^n+h_nf\big(x^n,a,b\big)\big)}{h_n}-\frac{1-\gamma_n}{h_n}\right\}\\ &+\sigma\frac{k_n}{h_n}\sqrt{d}(1+2\gamma_n+\gamma_nh_nL)+\gamma o_1.\end{aligned}$$

Passing to the limit in n to the infinity, we obtain $0\le\underline{v}(y)+H\big(y,D\varphi(y)\big)$. That establishes relation (16) as far as the fact that $\overline{v}$ and $\underline{v}$ are viscosity subsolution and supersolution of problem (9) with the boundary conditions (14)–(17) in the viscosity sense.

Now, we can prove a theorem on the convergence of the proposed numerical scheme analogous to [2, pp. 125–129, Theorem 2.3]. Firstly, it should be noted that the proof of the auxiliary theorem for a time-optimal problem with lifeline corresponding to [2, pp. 117–118, Theorem 1.10] can be conducted in an analogous way with the set Ω substituted by the set $\mathscr{G}$ and is not given here.

Theorem 1 *Assume that Conditions C.1, C.2, and C.3 hold. Also, suppose that the value function v (6) of game (1), (5) is continuous on the set $\operatorname{cl}\mathscr{G}$. Then the sequence $\{\mathbf{w}_n\}$ converges to the function $v=\overline{v}=\underline{v}$ as $n\to\infty$ uniformly on every compact set $\mathscr{K}\subset\operatorname{cl}\mathscr{G}$.*

Note that conditions (11) are crucial for all constructions and argument carried out by the authors, in particular, in the framework of this paper. Theorem 1 is proved under continuity of the function v, which follows from these assumptions (as it was said in Sect. 3.2).

Proof By Lemma 2, function $\overline{v}$ (13) is a viscosity subsolution of the boundary value problem (9) and the function v is a viscosity supersolution by virtue of [2, pp. 115–116, Theorem 1.6], which is common for the boundary value problems for the HJE. Applying Theorem 1.1 from [4, pp. 23–27], we get that for function $\overline{v}$ (13), the inequality $\overline{v} \le v$ holds on $\operatorname{cl}\mathscr{G}$. In the same manner, it is proved that $v \le \underline{v}$. So, $\overline{v} \le \underline{v}$ in $\operatorname{cl}\mathscr{G}$. By definition of $\underline{v}$ and $\overline{v}$ (as lim inf and lim sup of $\mathbf{w}_n$), one has $\underline{v} \le \overline{v}$. From these two inequalities, we obtain $\underline{v} = \overline{v} = v$.

Let us show that the sequence $\{\mathbf{w}_n\}$ converges to the function v uniformly on compact sets. Suppose by contradiction that there exist $\varepsilon > 0$, $n_m \to \infty$, and $x_m \in \mathscr{K}$ such that $x_m \to x$ and $\left|\mathbf{w}_{n_m}(x_m) - v(x_m)\right| > \varepsilon$. This implies that the sequences can be chosen in such a way that either $\mathbf{w}_{n_m}(x_m) > v(x_m) + \varepsilon$, or $\mathbf{w}_{n_m}(x_m) < v(x_m) - \varepsilon$. Passing to the limit over m and using the definition of $\overline{v}$ and $\underline{v}$ and the continuity of v, we obtain either $\overline{v}(x) \ge v(x) + \varepsilon$, or $\underline{v}(x) \le v(x) - \varepsilon$ what contradicts to coincidence of either v and $\overline{v}$, or v and $\underline{v}$.

5 Connection Between Value Functions of Problems with and Without Lifeline

In this section, we consider the problem of coincidence of the value functions (not processed by Kruzhkov's transform, that is, representing the time of the optimal motion) for the problems with and without lifeline. Let us consider a classic time-optimal problem with dynamics (1), the constraints A and B for the players' controls, and the terminal set $\mathscr{T}$. The result of such a game on a trajectory $x(\cdot; x_0)$ emanated form the initial point x_0 is determined by the payoff functional

$$\widetilde{\tau}\big(x(\cdot; x_0)\big) = \begin{cases} \min\{t : x(t; x_0) \in \mathscr{T}\}, \\ +\infty, \qquad\qquad \text{if } \forall t\ x(t; x_0) \notin \mathscr{T}. \end{cases}$$

Here and below, notations with a tilde stand for the classic time-optimal game (without lifeline).

Let us introduce the guaranteed results of the players and the value function as it is described in books [21, 22]. We define a functional

$$\widetilde{\tau}_\varepsilon\big(x(\cdot)\big) := \min\big\{t \in \mathbb{R}^+ : x(t) \in \mathscr{T}_\varepsilon\big\},$$

where $\mathscr{T}_\varepsilon$ is the ε-neighborhood of the terminal set $\mathscr{T}$: $\mathscr{T}_\varepsilon := \mathscr{T} + B(\mathbf{0}, \varepsilon)$, the symbol $\mathbf{0}$ denotes the origin in the corresponding space. The sign $+$ here stands for the Minkowski sum.

Let $\bar{x} \in B(x_0, \varepsilon)$. Denote by $\mathbb{X}(\bar{x}, \mathscr{A}, \Delta)$ the set of stepwise motions of the first player emanated under its strategy $\mathscr{A}$ from the point $\bar{x}$ in the discrete control scheme [21, 22] with the time step Δ. Also, denote by $\mathbb{X}(x_0, \mathscr{A})$ the set of constructive motions emanated from the point x_0 [21, 22] under the strategy $\mathscr{A}$. The guaranteed result $\widetilde{T}_1^0(x_0)$ of the first player at the point x_0 is defined as follows:

$$\widetilde{T}_1^{\varepsilon}(x_0, \mathscr{A}) := \sup\left\{\widetilde{\tau}_{\varepsilon}\big(x(\cdot)\big) : x(\cdot) \in \mathbb{X}(x_0, \mathscr{A})\right\},$$
$$\widetilde{T}_1^{\varepsilon}(x_0) := \inf_{\mathscr{A} \in \mathbb{A}} \widetilde{T}_1^{\varepsilon}(x_0, \mathscr{A}), \quad \widetilde{T}_1^{0}(x_0) := \lim_{\varepsilon \downarrow 0} \widetilde{T}_1^{\varepsilon}(x_0).$$

The guaranteed result $\widetilde{T}_2^0(x_0)$ of the second player at the point x_0 is defined in a similar way:

$$\widetilde{T}_2^{\varepsilon}(x_0, \mathscr{B}) := \inf\left\{\widetilde{\tau}_{\varepsilon}\big(x(\cdot)\big) : x(\cdot) \in \mathbb{X}(x_0, \mathscr{B})\right\},$$
$$\widetilde{T}_2^{\varepsilon}(x_0) := \sup_{\mathscr{B} \in \mathbb{B}} T_2^{\varepsilon}(x_0, \mathscr{B}), \quad \widetilde{T}_2^{0}(x_0) := \lim_{\varepsilon \downarrow 0} \widetilde{T}_2^{\varepsilon}(x_0),$$

where $\mathbb{X}(x_0, \mathscr{B})$ is the set of constructive motions of the second player emanated from the point x_0 under its strategy $\mathscr{B}$.

It is known that under the assumptions made above, the value function $\widetilde{T}$ of a classic time-optimal problem exists. So, the following equality holds [22]:

$$\widetilde{T}(x_0) := \widetilde{T}_1^0(x_0) = \widetilde{T}_2^0(x_0).$$

Now, let us consider a classic time-optimal problem and a time-optimal problem with lifeline with the same dynamics and sets A, B, and $\mathscr{T}$. We choose a point $x_0 \in \mathbb{R}^n \setminus \mathscr{T}$. Let the magnitude of the value function of classic time-optimal problem be $\widetilde{T}(x_0) = \theta$.

By Condition C.1, the function f is continuous and satisfies the condition of the sublinear growth, that is, there exists a number $\alpha > 0$ such that for every $x \in \mathbb{R}^n$, $a \in A$, and $b \in B$ the following inequality holds

$$\big\|f(x, a, b)\big\| \leq \alpha\big(1 + \|x\|\big).$$

It follows from the global Lipschitz condition. Let us consider a function

$$M\big(x\big) := \max_{a \in A,\ b \in B} \big\|f(x, a, b)\big\|,$$

which provides an upper estimate for the magnitude of possible velocities of the system at the point x. This function also is continuous and satisfies the condition of the sublinear growth with the same constant α; the maximum is attained, because the sets A and B are compact. Let us choose measurable realizations $a(\cdot)$ and $b(\cdot)$ of controls of the first and second players defined for $t \geqslant 0$. They generate a trajectory $x(\cdot) =$

$x(\cdot; x_0)$ of the system emerged from the point x_0. Using the standard reasoning involving the Grönwall's lemma, one can obtain the following estimate: for any trajectory $x(\cdot)$ emanated from a point x_0 under some admissible controls $a(\cdot)$ and $b(\cdot)$ of the players, it is true that $M\big(x\big(t; x_0, a(\cdot), b(\cdot)\big)\big) \le \alpha\big(1 + \|x_0\|\big)e^{\alpha\theta}$ for any $t \in [0, \theta]$.

Let us choose the constant $\widetilde{M}$ such that $\widetilde{M} \ge \alpha\big(1 + \|x_0\|\big)e^{\alpha\theta}$.

Firstly, we consider a classic time-optimal problem. Let us denote an optimal strategy of the first player as $\mathscr{A}^*$. We choose a point $\bar{x} \in B(x_0, \varepsilon)$ and a time partition Δ with the diameter less than ε. Since the strategy $\mathscr{A}^*$ is optimal, for every stepwise motion $x(\cdot) \in \mathbb{X}(\bar{x}, \mathscr{A}^*, \Delta)$ of the system, the inequality $\widetilde{\tau}\big(x(\cdot)\big) \le \theta + \varepsilon$ holds. Hence, $\big\{x(t) : t \in [0, \theta + \varepsilon)\big\} \subset B(x_0, \theta\widetilde{M})$. Passing to the limit $\varepsilon \to 0$, we obtain that for every constructive motion $x(\cdot) \in \mathbb{X}(x_0, \mathscr{A}^*)$, the embedding $\big\{x(t) : t \in [0, \theta]\big\} \subset B(x_0, \theta\widetilde{M})$ holds.

Now, let us consider a time-optimal game with lifeline; the guaranteed results of the first and the second players at the point x_0 are $T_1(x_0)$ and $T_2(x_0)$. As the game set $\mathscr{G}$, we take a set such that $B(x_0, \theta\widetilde{M}) \subset \mathscr{G} \cup \mathscr{T} = \mathscr{W}$. In the game with lifeline, the same strategy $\mathscr{A}^*$ guarantees the same result for the first player. In other words, under the strategy $\mathscr{A}^*$ for every stepwise motion $x(\cdot) \in \mathbb{X}(\bar{x}, \mathscr{A}^*, \Delta)$, the inequality $\tau\big(x(\cdot)\big) \le \theta$ holds. It is true, because all the trajectories are embedded into the set $\mathscr{W}$; as a result, the second player does not get any advantage connected to the existence of the lifeline. Hence, $T_1(x_0) \le \theta$.

Let us conduct similar considerations from the point of view of the second player. Let us take an optimal strategy $\mathscr{B}^*$ of the second player in the classic time-optimal problem and construct a set of stepwise motions $\mathbb{X}(\bar{x}, \mathscr{B}^*, \Delta)$. For every stepwise motion $x(\cdot) \in \mathbb{X}(\bar{x}, \mathscr{B}^*, \Delta)$, the inequality $\widetilde{\tau}\big(x(\cdot)\big) \ge \theta + \varepsilon$ holds. Hence, $\big\{x(t) : t \in [0, \theta + \varepsilon)\big\} \subset B(x_0, \theta\widetilde{M})$. Passing to the limit $\varepsilon \to 0$, we get that the set $\mathscr{G}$ is such that all constructive motions $x(\cdot)$ from the set $\mathbb{X}(x_0, \mathscr{B}^*)$ are embedded into $\mathscr{W}$. Thus, the inequality $\tau\big(x(\cdot)\big) \ge \theta$ holds also in the time-optimal problem with lifeline, and $T_2(x_0) \ge \theta$. So, $T_2(x_0) \ge \theta \ge T_1(x_0)$. For the time-optimal problem with lifeline, the classic inequality $T_2(x_0) \le \theta \le T_1(x_0)$ also holds. Hence, $T_2(x_0) = \theta = T_1(x_0)$.

Then, we get that if we choose the set $\mathscr{G}$ such that $B(x_0, \theta\widetilde{M}) \subset \mathscr{W}$, then the value function of the classic time-optimal problem coincides with the value function of the corresponding time-optimal problem with lifeline at the point x_0.

So, we have proved the following

Theorem 2 *Assume that Condition C.1 holds. Let the value function of a classic time-optimal problem $\widetilde{T}(x_0)$ at a point x_0 be equal to θ. Then there exists such a constant $\widetilde{M} \ge \alpha\big(1 + \|x_0\|\big)e^{\alpha\theta}$ that if a closed ball $B(x_0, \widetilde{M}\theta) \subset \mathscr{W}$, then the magnitude of the value function of the corresponding time-optimal problem with lifeline $T(x_0)$ at the point x_0 is also equal to θ.*

Moreover, an opposite theorem also holds (since the value function of a time-optimal problem with lifeline is always not less than the value function of the corresponding classic time-optimal problem):

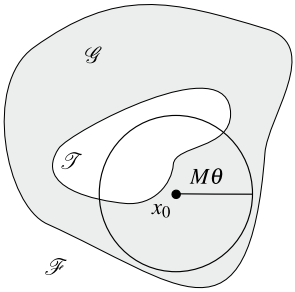

Fig. 2 Illustration to Theorem 3

Theorem 3 *Assume that Condition C.1 holds. Let the function $T(x_0)$ of a time-optimal problem with lifeline at the point x_0 is equal to θ. Then there exists such a constant $M \geq \alpha\big(1 + \|x_0\|\big)e^{\alpha\theta}$ that if a closed ball $B(x_0, M\theta) \subset \mathscr{W}$ (see Fig. 2), then the magnitude of the value function of the classic time-optimal problem $\widetilde{T}(x_0)$ at the point x_0 is equal to θ.*

6 Numerical Examples

The numerical procedure described in Sects. 3 and 4 is constructive except the fact that the set $\mathscr{G}$ is not restricted to be bounded. If the set $\mathscr{G}$ is unbounded, then the grid $\mathscr{L}_{\mathscr{G}}$ covering it is infinite and cannot be represented in computer. However, in the opposite case, if the set $\mathscr{G}$ is bounded, then the straightforward computer realization of the proposed procedure is possible.

For the given time step h and space step k, the computer procedure starts with the initial vector W_0, which consists only of 0 and 1: if a node belongs to the set $\mathscr{G}$, then the magnitude at this node is equal to 1, and if the node belongs to the set $\mathscr{T}$, then the magnitude is equal to 0. The computer procedure iteratively recomputes magnitudes at the nodes of the grid $\mathscr{L}_{\mathscr{G}}$ by the consequent application of the operator F to the initial vector. The procedure stops if the desired number of iterations is achieved.

We have an own cross-platform realization of this numerical method written using the environment .NetCore 3.0 and language C# of version 6.0 or later. A single - threaded program was written and then, by means of the capabilities of C#, it was made multi-threaded in order to compute faster on multi-core processors.

The best probation for the program would be comparison of some results computed by it with some value functions obtained theoretically. However, time-optimal games are extremely hard to solve analytically, so, nowadays, there is no non-trivial problems solved completely. The collection of problems that could be solved analytically includes problems with the simple motion dynamics and problems with one-type objects, which can be reduced to control problems. Problems of these types were used to debug the program and optimize its performance. But for other prob-

lems, we can compare our results only with the numerical ones obtained by other authors. Below, in several subsections, such examples are shown.

6.1 Homicidal Chauffeur Game

In the homicidal chauffeur game [20], a pursuing object, which represents a car with a bounded turn radius, tries to catch up an evading one with dynamics of simple motions, which is treated as a pedestrian.

The original dynamics describing separately both the car and the pedestrian are

$$\begin{aligned} \dot{x}_p &= w_1 \cos\psi, \\ \dot{y}_p &= w_1 \sin\psi, \\ \dot{\psi} &= \frac{w_1}{R} a, \end{aligned} \qquad \begin{aligned} \dot{x}_e &= b_1, \\ \dot{y}_e &= b_2. \end{aligned}$$

Here, (x_p, y_p) and (x_e, y_e) are the geometric positions of the pursuer and the evader in the plane; ψ is the course angle of the car's velocity; w_1 is the magnitude of the linear velocity of the car; the value R/w_1 describes the minimal turn radius of the car. The control $a \in [-1, +1]$ of the pursuer shows how sharply the car turns: the value $a = -1$ corresponds to the maximally sharp right turn, the value $a = +1$ corresponds to the maximally sharp left turn, and $a = 0$ corresponds to the instantaneous rectilinear motion. The control (b_1, b_2) of the pedestrian obeys the constraint $\|(b_1, b_2)\| \le w_2$. The terminal set can be chosen in different ways reflecting one or another model.

A strong disadvantage of this representation of the dynamics is that it has a quite high dimension, namely, 5. However, it permits a reduction of the dimension of the phase vector in the following way. Superpose the origin and the position of the pursuer. Direct the ordinate axis along the current vector of the pursuer's velocity. So, the new state position (x, y) of the system is two-dimensional and its dynamics are the following:

$$\begin{aligned} \dot{x} &= -\frac{w_1}{R} y a + w_2 \sin b, \\ \dot{y} &= \frac{w_1}{R} x a - w_1 + w_2 \cos b. \end{aligned}$$

Here, $b \in [-\pi, \pi]$ is a newly introduced control of the evader.

Two following examples have been taken from work [27]. It is necessary to note that the value function is discontinuous in these examples, so, formally the algorithm is not meant to solve problems of this type. However, as one can see, there is good coincidence of results obtained by us and the other authors. Of course, the coincidence is considered in the areas where the lifeline does not affect the behavior of the players.

The computations have been performed on a computer with the CPU Intel i7 of the 8th generation, which has 6 kernels with HyperThreading. The volume of RAM is 16 GB (however, it is not critical, since in the examples shown below, the program

takes less than 1 Gb for keeping the grid information). The three-dimensional graphs of the value function have been reconstructed from the grid data by means of an algorithm suggested by the authors. Visualization of these graphs was made by a free system MeshLab.

6.1.1 Homicidal Chauffeur Game, Example 1

For the first example, the following parameters have been taken: $w_1 = 3$, $w_2 = 1$, $R = 3$. The terminal set $\mathscr{T}$ is a circle with the center at the origin and the radius equal to 1.0. The set $\mathscr{W} = [-20, 20] \times [-10, 20]$. The time step $h = 0.1$, the spatial step $k = 0.1$. The number of iterations equals 150. The total time of computation was about 2.5 h.

A three-dimensional view of the value function graph is given in Fig. 3. It is restricted to a disk with the center at the point (0, 5) and the radius equal to 15. The magenta-purple area corresponds to the terminal set and small magnitudes of the value function, the yellow color marks places with large times to reach the terminal set. In Fig. 4, one can see contour lines of the value function from 0 to 15 with the step 0.2. The black thick "lines" correspond to the barriers where the value function is discontinuous. This figure and other figures with contour lines have been prepared by means of the system GNU Plot, whose algorithms are oriented to continuous functions, so, near the discontinuities, the picture of contours can be inaccurately restored.

Figure 5 again shows level sets of the value function, not by contours, but by a color gradient filling, which corresponds to the colors in Fig. 3. The red areas stand for the infinite magnitude of the value function, which have been cut off in Fig. 3. These areas appear just due to presence of the lifeline: trajectories leading the system to the terminal set from these areas leave the set $\mathscr{W}$. Also, near the terminal set, one

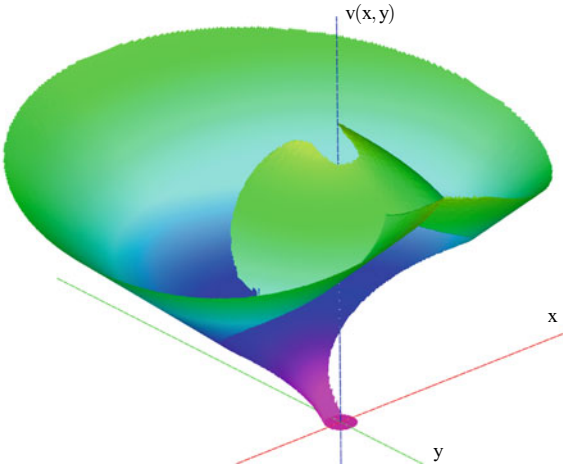

Fig. 3 Homicidal chauffeur, Example 1, a three-dimensional view of the value function graph

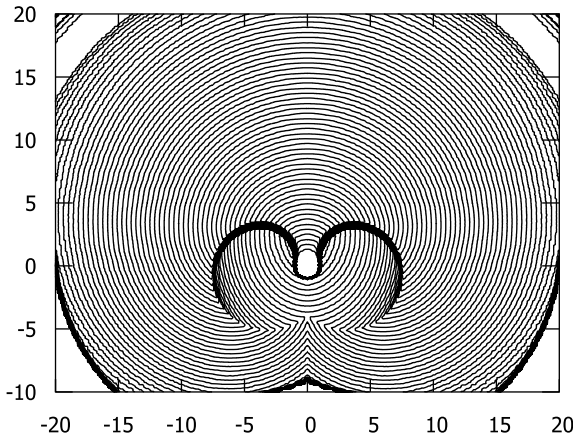

Fig. 4 Homicidal chauffeur, Example 1, contour lines of the value function

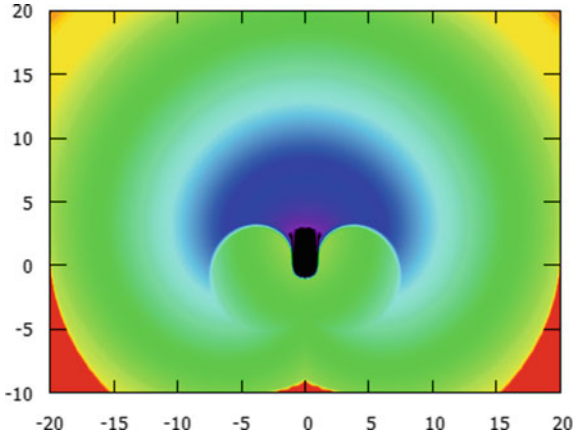

Fig. 5 Homicidal chauffeur, Example 1, the area of the guaranteed coincidence

can see a black spot, which marks the area where the value function of the Homicidal chauffeur game with lifeline coincides with the classic one by Theorem 3. The area is not too large, because the theorem considers all motions of the system including "silly" ones, which go not to the terminal set, but to the lifeline.

6.1.2 Homicidal Chauffeur Game, Example 2

This example uses the same dynamics with the parameters $w_1 = 2$, $w_2 = 0.6$, $R = 0.2$. The terminal set $\mathscr{T}$ is a circle with the center at the point $(0.2, 0.3)$ and the radius is equal to 0.015. The set $\mathscr{W} = [-1.5, 1.5] \times [-1, 1.5]$. The time step $h = 0.001$, the spatial step $k = 0.005$. The number of iterations equals 200. The total time of computation was 7 h and 51 min. A three-dimensional view of the value function graph is given in Fig. 6. It is restricted to a disk with the center at the point $(0, 0.25)$

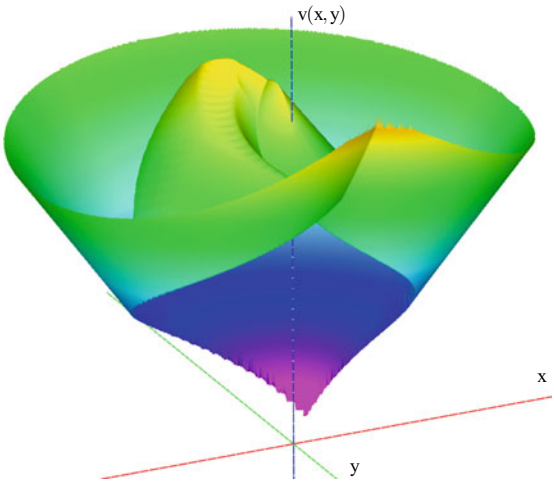

Fig. 6 Homicidal chauffeur, Example 2, a three-dimensional view of the value function graph

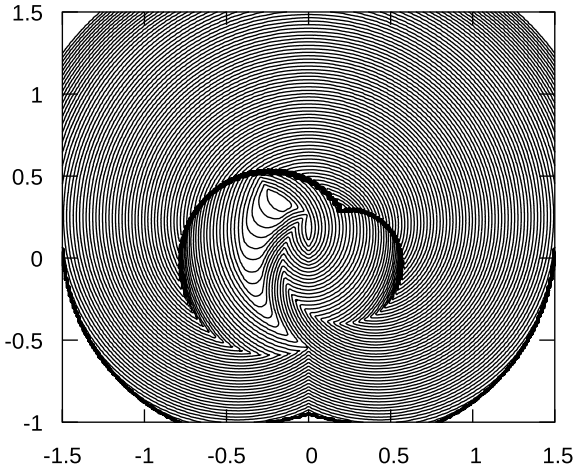

Fig. 7 Homicidal chauffeur, Example 2, contour lines of the value function

and the radius equal to 1.25. The magenta-purple area corresponds to the terminal set and small magnitudes of the value function, the yellow color marks places with large times to reach the terminal set. In Fig. 7, one can see contour lines of the value function from 0 to 1.25 with the step 0.015. The black thick "lines" corresponds to the barriers where the value function is discontinuous. In Fig. 8, a black spot marks the area where the value function of the Homicidal chauffeur game with lifeline certainly coincides with the classic one.

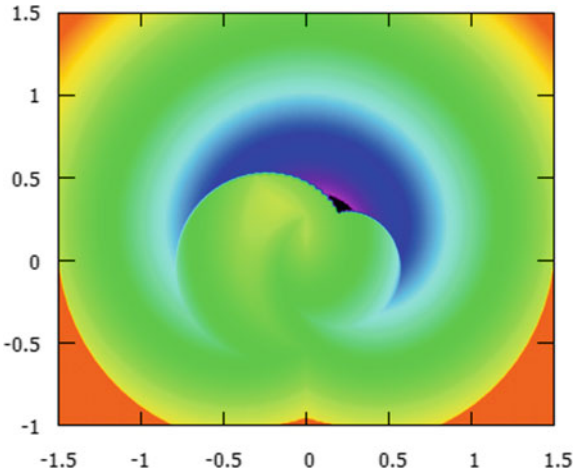

Fig. 8 Homicidal chauffeur, Example 2, the area of the guaranteed coincidence

6.2 Dubins' Car

The (reduced) two-dimensional dynamics of this classic model system are the following:

$$\dot{x} = -ya, \quad \dot{y} = xa - 1.$$

Here, $a \in [-1, 1]$. The time step $h = 0.05$, the spatial discretization step $k = 0.01$. The target set $\mathscr{T} = \left\{(x, y) \in \mathbb{R}^2 : \max\{|x|, |y|\} \leq 0.1\right\}$. The set $\mathscr{W}$ is a square with the center at the origin and sides of length 6. The number of iterations is 150. Actually, the Dubins' car is an optimal control problem, however, we consider this problem as a differential game with the fictitious second player, which does not affect the dynamics and has its control constrained by a one-pointed set coinciding with the origin. The total time of computation was 13 min.

A three-dimensional view of the value function graph is given in Fig. 9. The magenta-purple area corresponds to the terminal set and small magnitudes of the value function, the yellow and orange colors mark places with large times to reach the terminal set. In Fig. 10, one can see contour lines of the value function from 0 to 7 with the step 0.01. The black thick "lines" corresponds to the barriers where the value function is discontinuous. In Fig. 11, a black spot marks the area where the value function of Dubins' car problem with lifeline certainly coincides with the classic one.

Comparison of these results was made with the ones in paper [16] where an analytical study of reachable sets for this problem is set forth. That work studies reachable sets *at instant*, or in other words a problem with a fixed termination instant is considered. Nevertheless, for control problems, situations *at instant* and *upto instant* are connected very tightly (in contrast to differential games). Thus, we compare

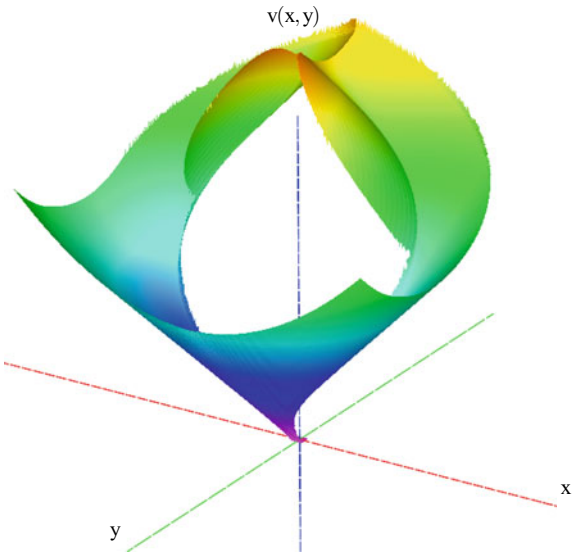

Fig. 9 Dubins' car, a three-dimensional view of the value function graph

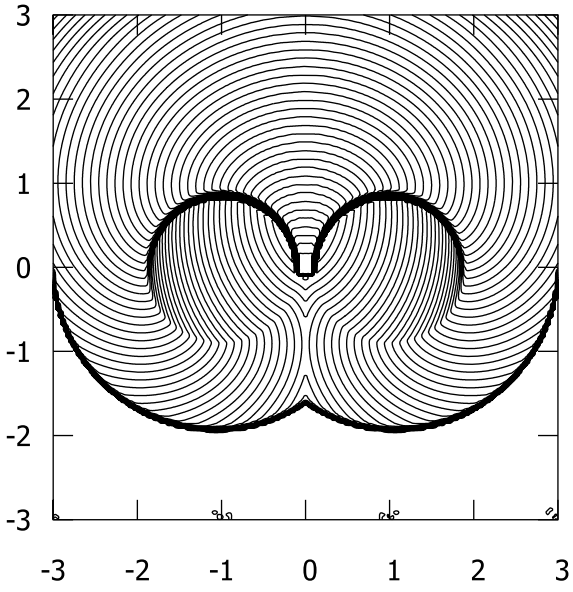

Fig. 10 Dubins' car, contour lines of the value function

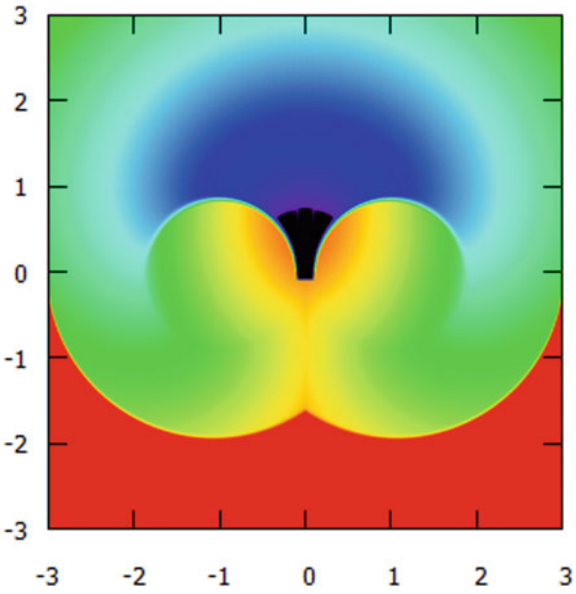

Fig. 11 Dubins' car, the area of the guaranteed coincidence

boundaries of the level sets of the value function for a time-optimal problem and the front parts of the boundaries of the reachable sets *at instant*. The coincidence seems to be good enough.

6.3 Material Point with Shifted Target

Dynamics of the system are the following:

$$\dot{x} = y, \quad \dot{y} = a,$$

where $a \in [-1, 1]$. The target set $\mathscr{T}$ is a square with the center at (0, 1) and sides with length of 0.4. The set $\mathscr{W}$ is a square, the length of sides is equal to 8. The number of iterations is 150. The time step $h = 0.05$, the spatial step $k = 0.01$. A three-dimensional view of the value function graph is given in Fig. 12. The magenta-purple area corresponds to the terminal set and small magnitudes of the value function, the yellow and orange colors mark places with large times to reach the terminal set. In Fig. 13, one can see contour lines of the value function from 0 to 9 with the step 0.01. The black thick "lines" corresponds to the barriers where the value function is discontinuous. In Fig. 14, a black spot marks the area where the value function of the material point problem with lifeline certainly coincides with the classic one.

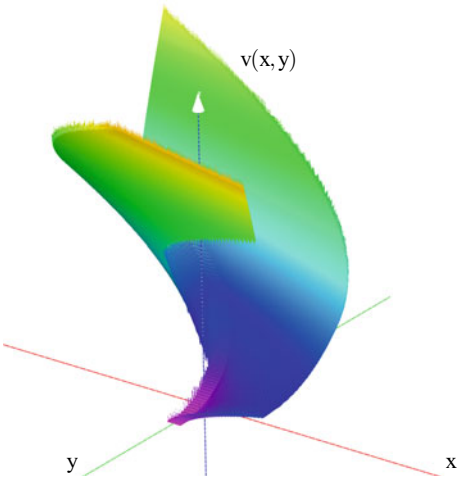

Fig. 12 Material point with shifted target, a three-dimensional view of the value function graph

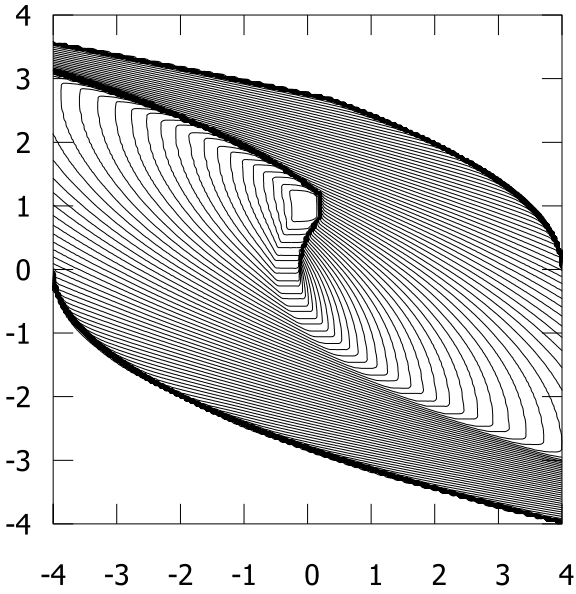

Fig. 13 Material point with shifted target, contour lines of the value function

This control problem is classic and well studied. The boundary of the value function level sets can be obtained by direct integration of trajectories of the system, which can be easily performed due to linearity of the dynamics. There is a good coincidence of theoretical and numerical results.

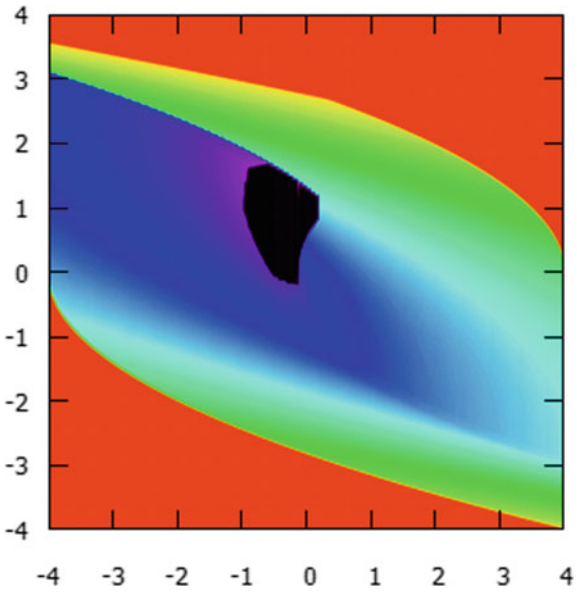

Fig. 14 Material point with shifted target, the area of the guaranteed coincidence

7 Conclusion

The paper discusses proposed numerical method, which constructs the value function of a time-optimal differential game with lifeline as a generalized (viscosity) solution of the corresponding boundary value problem for HJE. Convergence of this method is proved. Previously, authors have proved existence of the generalized solution and its coincidence with the value function of the corresponding time-optimal problem with lifeline under strong conditions (11) of dynamical advantage of each player on the boundary of the corresponding set. It is known that simultaneous accomplishment of these two inequalities results in continuity of the value function. The convergence of the numerical method is proved under the same assumptions. Further, it is planned to prove existence of the generalized solution and its coincidence with the value function under some weaker assumptions. Also, it would be useful to prove convergence of the numerical method to the discontinuous value function of time-optimal problem with lifeline.

References

1. Bardi, M., Capuzzo-Dolcetta, I.: Optimal Control and Viscosity Solutions of Hamilton-Jacobi-Bellman Equations. Birkhäuser, Boston (1997)
2. Bardi, M., Falcone, M., Soravia, P.: Numerical methods for pursuit-evasion games via viscosity solutions. In: M. Bardi, T. Parthasarathy, T.E.S. Raghavan (eds.) Annals of the Interna-

tional Society of Dynamic Games, Vol. 6: Stochastic and Differential Games, pp. 105–175. Birkhäuser, Boston (1999)
3. Bardi, M., Koike, S., Soravia, P.: Pursuit-evasion games with state constraints: dynamic programming and discrete-time approximations. Discrete Cont. Dyn. S. **6**(2), 361–380 (2000)
4. Bardi, M., Soravia, P.: A comparison result for Hamilton-Jacobi equations and applications to some differential games lacking controllability. Funkc. Ekvacioj (37), 19–43 (1994)
5. Barles, G.: Solutions de viscosité des équations de Hamilton-Jacobi. Mathématiques et Applications **17** (1994)
6. Barles, G., Perthame, B.: Discontinuous solutions of deterministic optimal stopping time problems. RAIRO — Modélisation mathématique et analyse numérique **21**(4), 557–579 (1987)
7. Botkin, N.D., Hoffmann, K.H., Mayer, N., Turova, V.L.: Approximation schemes for solving disturbed control problems with non-terminal time and state constraints. Analysis **31**(4), 355–379 (2011)
8. Botkin, N.D., Hoffmann, K.H., Mayer, N., Turova, V.L.: Computation of value functions in nonlinear differential games with state constraints. In: D. Hömberg, F. Tröltzsch (eds.) System Modeling and Optimization. CSMO 2011. IFIP Advances in Information and Communication Technology, vol. 391, pp. 235–244. Springer, Berlin, Heidelberg (2013)
9. Botkin, N.D., Hoffmann, K.H., Turova, V.L.: Stable solutions of Hamilton-Jacobi equations. application to control of freezing processes. Priority programm 1253 "Optimization with Partial Differential Equations", Preprint-Number: SPP1253-080 (2009). https://www-m6.ma.tum.de/~botkin/m6pdf/Preprint-spp1253-080.pdf
10. Breitner, M., Pesch, H., Grimm, W.: Complex differential games of pursuit-evasion type with state constraints, part 1: Necessary conditions for optimal open-loop strategies. JOTA **78**(3), 419–441 (1993)
11. Breitner, M., Pesch, H., Grimm, W.: Complex differential games of pursuit-evasion type with state constraints, part 2: Numerical computation of optimal open-loop strategies. JOTA **78**(3), 443–463 (1993)
12. Cardaliaguet, P., Quincampoix, M., Saint-Pierre, P.: Some algorithms for differential games with two players and one target. RAIRO — Modélisation mathématique et analyse numérique **28**(4), 441–461 (1994)
13. Cardaliaguet, P., Quincampoix, M., Saint-Pierre, P.: Set-valued numerical analysis for optimal control and differential games. In: M. Bardi, T.E.S. Raghavan, T. Parthasarathy (eds.) Annals of the International Society of Dynamic Games, Vol. 4: Stochastic and Differential Games, pp. 177–247. Birkhäuser, Boston (1999)
14. Cardaliaguet, P., Quincampoix, M., Saint-Pierre, P.: Pursuit differential games with state constraints. SIAM J. Control Optim. **39**(5) (2001)
15. Cardaliaguet, P., Quincampoix, M., Saint-Pierre, P.: Differential games through viability theory: Old and recent results. In: S. Jorgensen, M. Quincampoix, T.L. Vincent (eds.) Annals of the International Society of Dynamic Games, Vol. 9: Advances in Dynamic Game Theory, vol. 9, pp. 3–35. Birkhäuser, Boston (2007)
16. Cockayne, E.J., Hall, G.W.C.: Plane motion of a particle subject to curvature constraints. SIAM J. Control Optim. **13**(1), 197–220 (1975)
17. Crandall, M.G., Evans, L.C., Lions, P.L.: Some properties of viscosity solutions of Hamilton-Jacobi equations. T. Am. Math. Soc. **282**(2), 487–502 (1984)
18. Crandall, M.G., Evans, L.C., Lions, P.L.: User's guide to viscosity solutions of second order partial differential equations. B. Am. Math. Soc. (27), 1–67 (1992)
19. Fisac, J., Sastry, S.: The pursuit-evasion-defense differential game in dynamic constrained environments. In: 2015 IEEE 54th Annual Conference on Decision and Control (CDC), December 15–18, 2015. Osaka, Japan, pp. 4549–4556 (2015)
20. Isaacs, R.: Differential Games. John Wiley and Sons, New York (1965)
21. Krasovskii, N.N., Subbotin, A.I.: Positional Differential Games. Nauka, Moscow (1974). (in Russian)
22. Krasovskii, N.N., Subbotin, A.I.: Game-Theoretical Control Problems. Springer-Verlag, New York (1988)

23. Munts, N.V., Kumkov, S.S.: Existence of value function in time-optimal game with life line. In: Proceedings of the 47th International Youth School-conference "Modern Problems in Mathematics and its Applications". Yekaterinburg, Russia, January 31 – February 6, pp. 94–99 (2016). (in Russian)
24. Munts, N.V., Kumkov, S.S.: On coincidence of minimax solution and value function of time-optimal problem with lifeline. Trudy Instituta Matematiki i Mekhaniki UrO RAN (Proceedings of Institute of Mathematics and Mechanics UrB RAS) **24**(2), 200–214 (2018). (in Russian; transl. as [25])
25. Munts, N.V., Kumkov, S.S.: On coincidence of minimax solution and value function of time-optimal problem with lifeline. P. Steklov. Inst. Math. **305**(1), S125–S139 (2019). (transl. of [24])
26. Munts, N.V., Kumkov, S.S.: On time-optimal problems with lifeline. Dyn. Games Appl. **9**(3), 751–770 (2019)
27. Patsko, V.S., Turova, V.L.: Level sets of the value function in differential games with the homicidal chauffeur dynamics. Int. Game Th. Rev. **3**(1), 67–112 (2001)
28. Petrosjan, L.A.: A family of differential survival games in the space R^n. Soviet Math. Dokl. (6), 377–380 (1965)
29. Rakhmanov, A., Ibragimov, G., Ferrara, M.: Linear pursuit differential game under phase constraint on the state of evader. Discrete Dyn. Nat. Soc. (2), 1–6 (2016)
30. Subbotin, A.I.: Generalized Solutions of First Order PDEs: the Dynamical Optimization Perspective. Birkhäuser, Boston (1995)

Nataly V. Munts, Krasovskii Institute of Mathematics and Mechanics, Ural Branch of the Russian Academy of Sciences, S.Kovalevskaya str., 16, Yekaterinburg, 620990 Russia, (natalymunts@gmail.com).

Sergey S. Kumkov, Cand. Sci. (Phys.-Math.), Krasovskii Institute of Mathematics and Mechanics, Ural Branch of the Russian Academy of Sciences, S.Kovalevskaya str., 16, Yekaterinburg, 620990 Russia, (sskumk@gmail.com).

Evolutionary Games

A Partnership Formation Game with Common Preferences and Scramble Competition

David M. Ramsey

1 Introduction

In the economics literature, such games are often termed job search games and have developed from the classical problem of one-sided choice (see Stigler [26]). It is assumed that a job searcher observes a sequence of offers with values from a known distribution (employers are not choosy). The cost of observing a job offer is assumed to be constant. Janetos [11] was the first to consider such a model in the context of mate choice (it was assumed that only females are choosy). These ideas were later developed by Real [23].

In many species, both sexes are choosy. Parker [16] was the first to consider a model of two-sided mate choice. McNamara and Collins [14] presented a model under which searchers explicitly observe a sequence of prospective partners, unlike in Parker's model. However, their conclusions are very similar (players are split into a finite number of types, such that type i males only mate with type i females). These two models assume that mate choice is based on the attractiveness of a prospective partner, individuals prefer partners of high attractiveness and all individuals of a given sex agree upon the attractiveness of a member of the opposite sex. Such preferences are called common. When search costs are sufficiently small, individuals form pairs with those of a similar level of attractiveness. This phenomenon is known as associative pairing (i.e. the individuals forming pairs are similar to each other). Such associative pairing can also result from homotypic preferences (i.e. individuals prefer to mate with prospective partners who are similar to them). Alpern and Reyniers [2] consider a model of mate choice when preferences are homotypic. Ramsey [22] presents a similar game to the one presented here in which preferences are homotypic and there are two types of each sex (e.g. these types can be considered to

D. M. Ramsey (✉)
Department of Operations Research, Wroclaw University of Science and Technology, Wroclaw, Poland
e-mail: david.ramsey@pwr.edu.pl

D. M. Ramsey and J. Renault (eds.), *Advances in Dynamic Games*,
Annals of the International Society of Dynamic Games 17,
https://doi.org/10.1007/978-3-030-56534-3_6

be two sub-species). Real [24] looked in more detail at the associative pairing that results from common preferences. Ramsey [20] considers a model in which mate choice is based on both common and homotypic preferences.

If mating is non-seasonal, then the distribution of attractiveness among those in the mating pool tends to a steady-state distribution, which depends on the strategies used within the population (see Burdett and Coles [5], Smith [25]). However, if mating is seasonal, this distribution changes over time, since individuals leave the mating pool after finding a partner, but are not replaced by new searchers. Such a phenomenon is referred to as scramble competition. Collins and McNamara [7], as well as Ramsey [19], consider such models of one-sided choice. Dechaume-Moncharmont et al. [9] present numerical results based on simulation for a finite-population model of mate choice where only females are choosy, but both sexes mate only once in a season.

Johnstone [12] gives numerical results for a model of two-sided choice with discrete time. Searchers generally become less choosy as time passes, but searchers of low quality may become more choosy just before the end of the season in the hope of obtaining an attractive mate in the last period, when no searcher is choosy. Alpern and Reyniers [3], as well as Alpern and Katrantzi [1], apply a more analytic approach to such problems, while Mazalov and Falko [13] prove some general results. According to these three models, time is discrete and the values of prospective partners have a continuous distribution.

Etienne et al. [10] and Courtiol et al. [8] present models which are similar to the one presented here. The first paper presents a model where only females are choosy. Both sexes have a latent period after pairing, when they cannot mate. This leads to frequency-dependent selection, since the availability of males depends on the strategies used by females. The second paper extends this model to two-sided choice. These models differ from the one presented here, since they assume that time is discrete and mating is non-seasonal, i.e. given the mate choice strategies adopted in the population, the availability of prospective partners (and hence the distribution of the values of available partners) tends to a steady-state distribution. Priklopil [18] present a model of seasonal mating with continuous time in which only females are choosy. Females mate only once in a season and the value of a male comes from a discrete distribution. The optimal strategy of a female is a threshold rule such that a female accepts a male at time t if and only if his value is above a threshold, which may depend on t. As the season progresses, females become less choosy.

When mate choice is mutual and seasonal, then as time passes the distribution of the types of searchers changes and the rate at which prospective partners are found may depend on the proportion of individuals still looking for a partner. At one end of this spectrum, encounters with members of the other sex are not in any way concentrated on individuals still searching for a partner. In this case, the rate of encountering prospective partners is proportional to the fraction of individuals still searching for a mate. This is called the mixing population model. At the other end of this spectrum, encounters with members of the other sex are completely concentrated on individuals still searching for a partner, hence the rate of encountering prospective partners is constant. This is called the singles bar model. McNamara et al. [15] present

a model in which the rate at which prospective partners are found is proportional to the square root of the fraction of individuals still searching for a partner, i.e. the degree of concentration of search on individuals still looking for a partner is intermediate.

In the model presented here, time is continuous and mating is seasonal. The results extend the approach used by Ramsey [21], who derived equilibria for games in which there are only two types of prospective partner. It was shown that multiple equilibria are possible, even when the concept of Nash equilibrium is appropriately refined.

This article gives some general results for equilibria under the mixing population model. A characterization of the possible equilibria is given for the case when there are three levels of attractiveness. In addition, the possible mating patterns are fully described. Finally, some consideration is given to solving problems where there are a larger number of types of prospective partners. The fact that the types of searchers are discrete may be problematic. However, due to limitations on perception, this could be a realistic assumption.

Most models of two-sided mate choice involve discrete time, where multiple pairs of prospective partners meet in parallel. This is appropriate in the context of speed dating, but may be unnatural when applied to species 'in the wild'. Such models indicate that individuals of low quality might become more choosy shortly before the end of the mating season, since there is a chance of being paired with an attractive partner (and being mutually accepted) in the final round. One interesting question is whether this is a general phenomenon or results from the discrete dynamics.

The general model and its specific form under the assumption of a mixing population are described in Sect. 2. Section 3 first recalls some general results on the form of an equilibrium from Ramsey [21] and then gives a new result for the mixing population model. Section 4 extends the approach adopted in [21] to games of this form where there are three levels of attractiveness and gives a characterization of the possible forms of equilibria in such games. Section 5 presents some numerical results for two examples which illustrate the range of equilibria possible and the existence of multiple equilibria. A brief conclusion and directions for future research are given in Sect. 6.

2 The Model

Consider a large population in which there are two equally frequent classes of player. Each player aims to form a partnership with a player from the other class. For simplicity, these classes will be referred to as males and females, although they could also be interpreted as, e.g. employers (job positions) and job seekers. Partnership formation is seasonal. Each player starts searching for a partner at time zero and the amount of time available for searching is μ, where μ is finite. Partnerships are only formed by mutual consent.

As well as being a member of a given class (i.e. male or female), each player has a given level of attractiveness (type). All players of a given class agree about the attractiveness of a prospective partner and each player wishes to pair with an individual of high attractiveness, i.e. preferences are common.

Suppose there are n types of prospective partner. Let the reward obtained by a searcher from pairing with an individual of type i at time t be $v_i e^{-\gamma t}, i \in \{1, 2, \ldots, n\}$, where $v_1 > v_2 > \ldots > v_n > 0$ and γ is the discount factor reflecting the advantage from finding a partner quickly. If a searcher does not find a partner, then his/her payoff is defined to be 0. Based on this, only the relative values of prospective partners are important. Hence, without loss of generality, we assume that $v_n = 1$. Note that it is assumed that the value of a given type is independent of the sex of the searcher. The proportion of players who are of type i is denoted by p_i (again assumed to be independent of sex). Such a problem will be called symmetric with respect to sex. It should be noted that such problems can also be formulated in terms of searching for a partner in which sex (class) is unimportant (e.g. looking for a bridge partner).

Each player searches until he/she finds a mutually acceptable partner. At this time, both of them leave the mating pool. Hence, in the mating pool, the ratio of the number of males to the number of females always equals one. The proportion of individuals still searching and the distribution of types vary over time depending on the set of strategies used by the players (the strategy profile).

We derive equilibria at which all players of the same type use the same strategy for accepting prospective partners, regardless of sex. Such a strategy profile, denoted by π, is defined by a vector of n strategies. Let $\pi = (\pi_1, \pi_2, \ldots, \pi_n)$, where π_i denotes the strategy used by a type i player. A player's strategy can be defined by stating the set of types of acceptable partners at time t for all $t \in [0, \mu]$. Let $S_i(t)$ denote the set of types of prospective partners acceptable to a type i player at time t. We will be particularly interested in strategies based on a continuous threshold, $h(t)$. Under such a rule, a searcher will accept a prospective partner if and only if the value of the prospective partner is $\geq h(t)$.

Since the set of values of prospective partners is discrete, different threshold functions can lead to identical behaviour, regardless of the realization of the search process. Suppose an individual of type i uses a strategy based on a continuous threshold. This strategy can be described by (a) the times at which the set of acceptable partners changes, $t_{1,i}, t_{2,i}, t_{k,i}$, where $0 < t_{1,i} < t_{2,i} < \ldots < t_{k,i} < \mu$ and k is the number of switch times (for convenience define $t_{0,i} = 0$ and $t_{k+1,i} = \mu$) and (b) the set of types of prospective partners that are acceptable to a searcher of type i in the time interval $[t_{j-1,i}, t_{j,i})$, which is denoted S_i^j, for $j = 1, 2, \ldots, k+1$. Note that when $t \in [t_{j-1,i}, t_{j,i})$, then $S_i(t) = S_i^j$. Also, $S_i^1 = \{1, 2, \ldots, m_i\}$ is the set of types of prospective partners that are initially acceptable to a searcher of type i. Note that S_i^{j+1} is obtained from S_i^j either by adding the most attractive type of partner that is not in S_i^j or deleting the least attractive partner that is in S_i^j, as appropriate. For example, suppose there are three types of prospective partner and type 1 searchers only accept partners of type 1 when $t < 2$, accept partners of type 1 or 2 when $2 \leq t < 4$ and for $t \geq 4$ accept any type of prospective partner. Then this strategy can be defined as

$$S_1(t) = \begin{cases} \{1\}, & t < 2 \\ \{1, 2\}, & 2 \leq t < 4 \\ \{1, 2, 3\}, & t \geq 4 \end{cases}.$$

Note that the underlying threshold function, $h(t)$, satisfies $h(t) > v_2$ for $t < 2$, $h(2) = v_2, v_3 < h(t) \leq v_2$ for $2 < t < 4, h(4) = v_3$ and $h(t) < v_3$ for $t > 4$, i.e. this threshold function is not uniquely defined. Strategies that are based on two different threshold functions, but have the same description in the form outlined immediately above, will be treated as being identical.

Denote the expected reward of a type i player still searching at time t and using the strategy θ_i when the rest of the population is following the appropriate strategy from the profile π by $r_i(t; \theta_i, \pi)$. The mathematical description of such a reward requires the derivation of the dynamics of the search process, which are considered at the end of this section. It should be noted that the dynamics of the search process are independent of an individual player, since we are considering a continuum of players. Also, the notation $r_i(t; \theta_i, \pi)$ is used rather than $r_i(t; \theta_i, \pi_{-i})$, which is used in n-player games, since the considered individual of type i is playing against the whole population, which includes a continuum of players of type i.

Let $\pi^* = (\pi_1^*, \pi_2^*, \ldots, \pi_n^*)$ denote a Nash equilibrium. By definition π^* satisfies the following conditions for all i, $1 \leq i \leq n$, θ_i and $t \in [0, \mu]$: $r_i(t; \theta_i, \pi^*) \leq r_i(t; \pi_i^*, \pi^*)$. Hence, it does not pay any player to ever deviate from the appropriate strategy from an equilibrium profile when the rest of the population conform to that equilibrium profile. Without loss of generality, previous discounts can be ignored in the definition of these payoff functions. To simplify the notation, define $r_i(t; \pi_i, \pi) \equiv r_i(t; \pi)$. This is the expected future payoff of a type i player following the appropriate strategy from the profile π.

Non-intuitive Nash equilibria may exist, e.g. when there are two types of player, the following strategy profile is always a Nash equilibrium: (a) players of type 1 (the most attractive) only accept prospective partners of type 2 (the least attractive) and always accepts such partnerships, (b) players of type 2 only accept prospective partners of type 1 (and always accepts such partnerships). However, natural selection favours players who always accept the most attractive prospective partners (e.g. given that future decisions remain the same, a type 1 female obtains a greater expected reward from accepting a type 1 male at time t when there is a positive probability of being accepted than by rejecting such a male). We thus adopt a refinement of the concept of Nash equilibrium based on the optimality criterion of McNamara and Collins [14]: each player accepts a prospective partner if and only if the value that the player would obtain from the pairing (regardless of whether acceptance is mutual) is at least as great as the player's expected reward from future search (ignoring previous discounts). Hence, players always accept a prospective partner of type 1, as the reward that would result from such a partnership is clearly greater than any possible reward from future search. Hence, given the strategy profile used, a type 1 player faces a one-sided search problem where members of the opposite sex are not choosy.

If an individual's strategy satisfies this criterion, then it is optimal given the strategies used by the other players (see Chow [6]). This leads to the following result

Result 1 *A strategy profile where each strategy used satisfies the McNamara-Collins optimality criterion is a Nash equilibrium. At such an equilibrium a type i individual*

accepts a prospective partner of type j if and only if $r_i(t;\pi^*) \le v_j$. Such strategies are by definition threshold strategies (it will be argued later that the threshold functions $\{r_i(t;\pi^*)\}_{i=1}^n$ are continuous).

We now consider the dynamics of the search problem under a given strategy profile. Assume that the players adopt strategy profile π. The distribution of the types of players remaining in the mating pool is independent of sex. Denote by $p_i(t;\pi)$ the proportion of all players who are both still searching at time t and of type i. Thus, $\forall\pi,\ p_i(0;\pi) \equiv p_i$. The proportion of players still searching at time t is denoted by $p(t;\pi)$, i.e. $p(t;\pi) = \sum_{i=1}^n p_i(t;\pi)$. The probability that a player is of type i given that he/she is searching at time t is denoted by $q_i(t;\pi)$, i.e. $q_i(t;\pi) = \frac{p_i(t;\pi)}{p(t;\pi)}$, $i \in 1, 2, \ldots, n$.

Players find prospective partners according to a Poisson process at a rate given by λ, a function of the proportion of players that are still searching. It is assumed that λ is non-decreasing in $p(t;\pi)$, i.e. is non-increasing in time. From the point of view of an individual player, the process of finding prospective partners is stochastic. However, since we are considering a continuum of players, the equations defining the proportions of each type of player who are still searching are deterministic. Dechaume-Moncharmont et al. [9] simulate the evolution of strategies of mate choice based on a similar model where the population is finite.

Prospective partners are chosen at random from the mating pool, i.e. a prospective partner encountered at time t is of type i with probability $q_i(t;\pi)$. By assumption $p(t;\pi) \le \lambda[p(t;\pi)] \equiv \lambda(p) \le 1$ and time is scaled so that $\lambda(1) = 1$. In order to simplify the notation, $p(t;\pi)$ will be abbreviated to p. These assumptions are reasonably natural, as finding prospective partners generally becomes harder as the number of searchers decreases. Ramsey [21] considered the following two extreme cases: (i) $\lambda(p) = 1, \forall p \in [0, 1]$, (ii) $\lambda(p) = p, \forall p \in [0, 1]$. Case i) corresponds to the 'singles bar model', where players concentrate search on members of the opposite sex who have not yet found a partner. Case (ii) corresponds to a 'mixing population', where players meet members of the opposite sex at a constant rate, but the individual encountered is chosen at random from all the players of the opposite sex (i.e. such a player is available with probability p). Hence, the expected number of members of the opposite sex that a player meets during the search period (under the single bars model, the expected number of prospective partners that a player meets) is equal to μ.

Denote by $A_i(t;\pi)$ the set of mutually acceptable types of prospective partners of a type i player at time t. Note that $j \in A_i(t;\pi)$ if and only if $j \in S_i(t)$ and $i \in S_j(t)$. It follows that $j \in A_i(t;\pi) \Leftrightarrow i \in A_j(t;\pi)$. The set $\{A_i(t;\pi)\}_{i=1}^n$ for a given t is called the mating pattern at time t.

Define $\overline{v}_i(t;\pi)$ to be the expected reward obtained by a type i individual following the appropriate strategy from the profile π from pairing with a mutually acceptable prospective partner at time t. Hence,

$$\overline{v}_i(t;\pi) = \frac{\sum_{j \in A_i(t;\pi)} v_j p_j(t;\pi)}{\sum_{j \in A_i(t;\pi)} p_j(t;\pi)}. \tag{1}$$

Now we derive the dynamics of the game under a given strategy profile. Consider a player of type i who is still searching at time t. For small δ, the probability that such a player finds a partner in the time interval $[t, t+\delta]$ is approximately $\delta\lambda(p)\sum_{j\in A_i(t;\pi)} q_j(t;\pi)$. Hence,

$$p_i(t+\delta;\pi) = p_i(t;\pi)[1-\delta\lambda(p)\sum_{j\in A_i(t;\pi)} q_j(t;\pi)] + O(\delta^2)$$

$$\frac{p_i(t+\delta;\pi)-p_i(t;\pi)}{\delta} = -p_i(t;\pi)\lambda(p)\sum_{j\in A_i(t;\pi)} q_j(t;\pi) + O(\delta).$$

Letting $\delta \to 0$, we obtain the differential equation

$$\frac{dp_i(t;\pi)}{dt} = -p_i(t;\pi)\lambda(p)\sum_{j\in A_i(t;\pi)} q_j(t;\pi). \tag{2}$$

Remark 1 Suppose that there is a set of types B, and an interval of time I such that a player of any type in B will pair with a player of any type in B, but not with prospective partners of types not in B when $t \in I$. From Eq. (2), if $i, j \in B$, then the ratio $p_i(t;\pi)/p_j(t;\pi)$ is constant on the interval I.

Under the mixing population model, $\lambda(p) = p$. Hence, Eq. (2) leads to

$$\frac{dp_i(t;\pi)}{dt} = -p_i(t;\pi)\sum_{j\in A_i(t;\pi)} p_j(t;\pi). \tag{3}$$

Let $T_i(\pi)$ be the time at which a type i player following the appropriate strategy from the profile π finds a mutually acceptable partner and $f_i(t;\pi)$ denote the density function of this random variable. When such a player does not find a partner, we define $T_i(\pi) = \mu$. Setting $\alpha_i(t;\pi)$ to be the rate at which such individuals find acceptable partners, it follows that $\alpha_i(t;\pi) = \lambda(p)\sum_{j\in A_i(t;\pi)} q_j(t;\pi)$. Hence, for $0 < t < \mu$,

$$f_i(t;\pi) = \alpha_i(t;\pi)\exp\left[-\int_0^t \alpha_i(s;\pi)ds\right].$$

The future expected reward of such a type i searcher at time t is given by

$$r_i(t;\pi) = \int_t^\mu \bar{v}_i(s;\pi)\alpha_i(s;\pi)\exp\left[-\int_t^s \gamma + \alpha_i(\tau;\pi)d\tau\right]ds. \tag{4}$$

Note that $r_i(t;\pi)$ is a continuous function of t for all i. Under the mixing population model, using Eqs. (1) and (4), since $\lambda(p) = p(t;\pi)$, we obtain

Table 1 Description of the parameters and functions used in the definition of the model

Parameter	Description
μ	Length of mating season (time available for searching for a mate)
n	Number of types of prospective partner
v_i	Value of a partner of type i
γ	Discount rate
p_i	Proportion of individuals that are of type i
$\pi = (\pi_1, \pi_2, \ldots, \pi_n)$	Strategy profile
π_i	Strategy used by individuals of type i
$S_i(t)$	Set of types of prospective partners that are acceptable to a searcher of type i at time t
$A_i(t)$	Set of types of prospective partners that are mutually acceptable to a searcher of type i at time t
$\{A_i(t)\}_{i=1}^n$	Mating pattern at time t.
θ_i	Strategy of an individual of type i who does not use the appropriate strategy from π
$p_i(t;\pi)$	Proportion of all players who are both still searching at time t and of type i $[p_i(0;\pi) \equiv p_i]$
$p(t;\pi) \equiv p$	Proportion of all players who are still searching at time t
$q_i(t;\pi)$	Conditional probability that an individual still searching at time t is of type i
$\lambda(p) \equiv \lambda[p(t;\pi)]$	Rate at which searchers find prospective partners
$\bar{v}_i(t;\pi)$	Mean value of a prospective partner who is mutually acceptable to a searcher of type i at time t
$\alpha_i(t;\pi)$	Rate at which a searcher of type i finds a mutually acceptable partner

$$r_i(t;\pi) = \int_t^{\mu} \left[\sum_{j \in A_i(s;\pi)} v_j p_j(s;\pi) \right] \exp\left[-\int_t^s \gamma + \sum_{j \in A_i(\tau;\pi)} p_j(\tau;\pi) d\tau \right] ds. \tag{5}$$

Table 1 gives a description of the parameters and functions used in the definition of the model.

3 Some General Results

First, we recall some results from Ramsey [21]. The proofs are omitted.

Theorem 1 *If each player uses a threshold strategy and $i < j$, then $r_i(t;\pi) \geq r_j(t;\pi)$.*

Theorem 2 *At an equilibrium, there exists some $t_0 < \mu$, such that all players accept any prospective partner when $t \geq t_0$. When $t \geq t_0$, then $r_i(t;\pi)$ is strictly decreasing in t.*

Theorem 3 *At equilibrium, type i individuals always find prospective partners of type i acceptable.*

The following result regarding the mixing population model is new.

Theorem 4 *Under the mixing population model, if an individual of type 1 finds a prospective partner of type j acceptable at time t_0, then he/she finds a prospective partner of type j acceptable at any time $t \geq t_0$.*

Proof A type 1 player faces a problem of one-sided choice. Let $t_0 < t_1$. A type 1 searcher still searching at time t_0 can ensure the same reward as a type 1 searcher still searching at time t_1 by following the following strategy: Define $p_i(t;\pi) = 0$ for all i and $t > \mu$. Ignore a prospective partner of type i found at time $t_0 + t$ with probability $1 - \frac{p_i(t_1+t;\pi)}{p_i(t_0+t;\pi)}$, otherwise make the same decision that an optimally behaving individual of type 1 would make at time $t_1 + t$. Hence $r_1(t_0;\pi) \geq r_1(t_1;\pi)$ and the theorem follows from the optimality criterion.

Other future reward functions are not necessarily non-increasing in t. Denote the time when type 1 players start accepting prospective partners of type i at an equilibrium by $t^*_{1,i}$. From Theorems 1 and 4, when $t \geq t^*_{1,i}$, players of types $\{1, 2, \ldots, i\}$ face a one-sided search problem and $r_j(t;\pi^*) = r_1(t;\pi^*)$ for $j \in \{1, 2, \ldots, i\}$. Hence, the function r_i is non-increasing on the interval $(t^*_{1,i}, \mu)$. On the other hand, if $t^*_{1,i} > 0$, then $r_1(t^*_{1,i};\pi^*) = r_i(t^*_{1,i};\pi^*) = v_i$ and $\exists \delta > 0$ such that on an interval $(t^*_{1,i} - \delta, t^*_{1,i})$ a searcher of type i is not accepted by any prospective partner of value $> v_i$. Thus, for t in this interval and $\gamma > 0$, $r_i(t;\pi^*) < v_i$. Hence, $r_i(t;\pi^*)$ is increasing on some sub-interval of $(0, t^*_{1,i})$.

It follows that if $A_1(t) = \{1, 2, \ldots, i\}$ at an equilibrium, then $A_j(t) = \{1, 2, \ldots, i\}$ for $j \in \{1, 2, \ldots, i\}$. Hence, $A_1(t)$ defines a subpopulation of searchers that a) are mutually acceptable as partners at time t and b) do not accept any prospective partners who are not from this subpopulation.

However, it is not always true that at a particular equilibrium the population is partitioned at any point in time into subpopulations where prospective partners from the same subpopulation are mutually acceptable and prospective partners from different subpopulations are not mutually acceptable. For example, suppose that at equilibrium $A_1(t) = \{1, 2, \ldots, i\}$ and $A_{i+1}(t) = \{i + 1, i + 2, \ldots i + j\}$. Since type 1 individuals will start accepting type $i + 1$ individuals as partners before they start accepting type $i + j$ individuals, it follows that $r_{i+1}(t;\pi^*) > r_{i+j}(t;\pi^*)$. For this reason, it is possible that type $i + j$ individuals find type $i + j + 1$ individuals acceptable at time t.

Based on these arguments, the number of possible partitions of the set $\{1, 2, \ldots, n\}$ into subsets of consecutive integers gives a lower bound on the number of possible mating patterns at time t at equilibrium. Such a partition can be defined by a binary

string of length $n-1$ such that types i and $i+1$ belong to separate subsets if and only if the i-th element of this binary string equals one. Hence, there are at least 2^{n-1} possible mating patterns, each corresponding to a different system of n differential equations describing the current dynamics of the game. Thus, it seems clear that the complexity of the solutions of such games is at least exponential in the number of types of prospective partner.

4 Games with Three Types of Player

In this section, we consider the form of equilibria when there are three types of player and give a general classification of such equilibria. First, we consider the set of possible mating patterns based on the results given in the previous section. When type 1 players only accept prospective partners of type 1 at time t, then type 2 searchers may either (a) reject prospective partners of type 3 or (b) accept them. In the first case, the mating pattern at time t is given by $A_1(t;\pi^*)=\{1\}$, $A_2(t;\pi^*)=\{2\}$, $A_3(t;\pi^*)=\{3\}$. In the second case, the mating pattern at time t is given by $A_1(t;\pi^*)=\{1\}$, $A_i(t;\pi^*)=\{2,3\}$, $i\in\{2,3\}$. Suppose type 1 players accept prospective partners of types 1 and 2 at time t. From Theorem 3, $A_i(t;\pi^*)=\{1,2\}$, $i\in\{1,2\}$ and $A_3(t;\pi^*)=\{3\}$. The only other possible mating pattern occurs when type 1 players accept any prospective partner at time t. In this case, $A_i(t;\pi^*)=\{1,2,3\}$, $i\in\{1,2,3\}$. Hence, when $n=3$ the number of possible mating patterns is equal to the lower bound described above, i.e. $2^2=4$. These mating patterns will thus be indexed by the binary strings that they correspond to, i.e.

Pattern 00: All players accept any prospective partner (random mating).
Pattern 01: Searchers of types 1 and 2 are mutually acceptable and type 3 searchers only pair with prospective partners of type 3.
Pattern 10: Searchers of type 1 only pair with others of type 1 and searchers of types 2 and 3 are mutually acceptable.
Pattern 11: Searchers only pair with prospective partners of the same type.

Let $M(t;\pi^*)$ denote the mating pattern (given by the appropriate binary string) at time t under an equilibrium profile. To derive the possible forms of equilibria, it is necessary to consider how these mating patterns can change as time passes. From Theorem 2, the equilibrium mating pattern switches to 00 at some time t_0, where $t_0<\mu$, and once this pattern has switched to 00 then it cannot change. Hence, the pattern 00 can be thought of as an absorbing state of the process of how the mating pattern evolves over time at an equilibrium.

Suppose that $M(t;\pi^*)=01$. From Theorem 4, type 1 searchers cannot become more choosy. Hence, this mating pattern can only switch to the pattern 00 and from Theorem 2 must eventually switch to this pattern.

Suppose that $M(t;\pi^*)=10$. Hence, $r_1(t;\pi^*)>v_2$. Eventually, type 1 searchers start accepting prospective partners of type 2, say at time $t^*_{1,2}$. However, since

$r_1(t^*_{1,2};\pi^*)=r_2(t^*_{1,2};\pi^*)=v_2$, from the continuity of the future reward functions, type 2 individuals must stop accepting type 3 individuals at some time $t^{s,*}_{2,3}$, where $t^{s,*}_{2,3}<t^*_{1,2}$. Hence, the mating pattern switches to 11 at time $t^{s,*}_{2,3}$.

Suppose that $M(t;\pi^*)=11$. There are two possible ways in which the mating pattern can change. Firstly, type 1 searchers can start accepting prospective partners of type 2, at time $t^*_{1,2}$. The second possibility is that type 2 searchers start accepting prospective partners of type 3, at time $t^*_{2,3}$. Note that $t^*_{1,2}\neq t^*_{2,3}$. This follows from the facts that $r_2(t^*_{1,2};\pi^*)=v_2$ and $r_2(t^*_{2,3};\pi^*)=v_3<v_2$. In the first case, the mating pattern first switches to 01 and then must switch to 00 (random mating). In the second case, the mating pattern first switches to 10.

The function r is said to 'upcross' the value v at time t_0 when $r(t_0)=v$ and $\exists\delta>0$ such that $r(t)<v$ for t in the interval $(t_0-\delta,t_0)$ and $r(t)>v$ in the interval $(t_0,t_0+\delta)$. The function r is said to 'downcross' the value v at time t_0 when $r(t_0)=v$ and $\exists\delta>0$ such that $r(t)>v$ in the interval $(t_0-\delta,t_0)$ and $r(t)<v$ in the interval $(t_0,t_0+\delta)$. It follows that when r upcrosses v at time t_0, then for values of t slightly smaller than $t_0, r(t)<v$ and for values of t slightly greater than $t_0, r(t)>v$. Similarly, when r downcrosses v at time t_0, then for values of t slightly smaller than $t_0, r(t)>v$ and for values of t slightly greater than $t_0, r(t)<v$. Intuitively, when r_2 downcrosses v_3, then type 2 searchers should switch from rejecting prospective partners of type 3 to accepting them. Analogously, when r_2 upcrosses v_3, then type 2 searchers should switch from accepting prospective partners of type 3 to rejecting them.

The following theorem, when used in conjunction with the arguments presented above, leads to the main theorem of the paper, Theorem 6, which classifies the possible forms of equilibrium profiles in games with three types of prospective partner.

Theorem 5 *At any equilibrium profile, the function r_2 has at most one upcrossing of the value v_3.*

Proof Suppose that the function r_2 upcrosses the value v_3 at times $t_{u,1}$ and $t_{u,2}$, where $t_{u,1}<t_{u,2}$. From the form of an equilibrium $t_{u,2}<t^*_{1,2}$. From the continuity of the function r_2, there must be a downcrossing of the value v_3 at some time t_d, where $t_d\in(t_{u,1},t_{u,2})$. By definition $r_2(t_{u,1};\pi^*)=r_2(t_{u,2};\pi^*)=r_2(t_d;\pi^*)=v_3$. At such an equilibrium, type 2 players reject prospective partners of type 3 when $t\in(t_{u,1},t_d)$ and accept them when $t\in(t_d,t_{u,2})$. Conditioning on whether a type 2 player finds a partner in the time interval $(t_d,t_{u,2})$,

$$r_2(t_d;\pi^*)=v_3=\bar{v}\int_{t_d}^{t_{u,2}}[p_2(t;\pi^*)+p_3(t;\pi^*)]\exp\left[-\int_{t_d}^{t}\gamma+p_2(s;\pi^*)+p_3(s;\pi^*)ds\right]dt+$$
$$+v_3\exp[-\gamma(t_{u,2}-t_d)]\frac{p_2(t_{u,2};\pi^*)}{p_2(t_d;\pi^*)},\qquad(6)$$

where $\bar{v}=\frac{v_2p_2(t_d;\pi^*)+v_3p_3(t_d;\pi^*)}{p_2(t_d;\pi^*)+p_3(t_d;\pi^*)}$.

Assume that $t_d-t_{u,1}\geq t_{u,2}-t_d$. Suppose an individual type 2 player accepts a prospective partner of type i, $i=2,3$ at time $t_{u,1}+t$, where $t\in I=(0,t_{u,2}-t_d)$ with probability $\frac{p_i(t_d+t;\pi^*)}{p_i(t_{u,1}+t;\pi^*)}$ and for $t\notin I$ uses the strategy appropriate to the equilibrium profile. When $t\in I$, such a player finds mutually acceptable partners of a given type at

the same rate as an optimally behaving type 2 player at time $t_d + t$. Conditioning on whether such a player finds a mutually acceptable partner in the interval $(t_{u,1}, t_{u,1}+t_{u,2}-t_d)$, his/her expected future reward at time $t_{u,1}$ is $r_{2,m}(t_{u,1}; \pi^*)$, where

$$r_{2,m}(t_{u,1}; \pi^*) = \overline{v}\int_{t_d}^{t_{u,2}} [p_2(t; \pi^*)+p_3(t; \pi^*)]\exp\left[-\int_{t_d}^{t}\gamma+p_2(s; \pi^*)+p_3(s; \pi^*)ds\right]dt+$$
$$+r_2(t_{u,1}+t_{u,2}-t_d; \pi^*)\exp[-\gamma(t_{u,2}-t_d)]\frac{p_2(t_{u,2}; \pi^*)}{p_2(t_d; \pi^*)}.$$

Note that $r_2(t_{u,1}+t_{u,2}-t_d; \pi^*) \geq v_3$, since $t_{u,1}+t_{u,2}-t_d \in (t_{u,1}, t_d]$. It follows from Eq. (6) that $r_{2,m}(t_{u,1}; \pi^*) \geq v_3$. Note that such a player acts strictly suboptimally, since he/she rejects prospective partners of type 2 with a positive probability. This gives a contradiction, since by assumption $r_2(t_{u,1}; \pi^*) = v_3$.

Now assume that $t_d - t_{u,1} < t_{u,2} - t_d$. Conditioning on whether an optimally behaving type 2 player finds a prospective partner in the interval $(t_d, 2t_d - t_{u,1})$, we obtain

$$r_2(t_d; \pi^*) = \overline{v}\int_{t_d}^{2t_d-t_{u,1}} [p_2(t; \pi^*)+p_3(t; \pi^*)]\exp\left[-\int_{t_d}^{t}\gamma+p_2(s; \pi^*)+p_3(s; \pi^*)ds\right]dt+$$
$$+r_2(2t_d - t_{u,1}; \pi^*)\exp[-\gamma(t_d - t_{u,1})]\frac{p_2(2t_d - t_{u,1}; \pi^*)}{p_2(t_d; \pi^*)}.$$

This equation can be written in the form $r_2(t_d; \pi^*) = R_1 P(A) + R_2[1 - P(A)]$, where $P(A)$ is the probability of such a searcher (call him/her searcher i) finding a partner in the interval $(t_d, 2t_d - t_{u,1})$, R_1 is the expected reward of such a searcher in this case and $R_2 = r_2(2t_d - t_{u,1}; \pi^*)\exp[-\gamma(t_d - t_{u,1})]$ is the expected reward of such a searcher given that a partnership is not formed in this interval.

From the differential equations describing the game's dynamics, $\frac{p_2(t;\pi^*)}{p_3(t;\pi^*)}$ is either non-increasing or increasing on the interval $(t_{u,1}, t_d)$. In the first case, the mean value of a prospective partner is non-increasing in t. Consider a type 2 player (call him/her searcher ii) who accepts any prospective partner on the interval $(t_{u,1}, t_d)$ [of the same length as the interval $(t_d, 2t_d - t_{u,1})$] and thereafter acts optimally. Arguing as above, $r_2(t_{u,1}; \pi^*) \geq R_3 P(B) + R_4[1 - P(B)]$, where $P(B)$ is the probability of such a player finding a partner in the interval $(t_{u,1}, t_d)$, R_3 is the expected reward of such a player in this case and $R_4 = v_3 \exp[-\gamma(t_d - t_{u,1})]$ is the expected reward of this player given that a partnership is not formed in this interval. Since $r_i(t_{u,1}+t; \pi^*) > r_i(t_d+t; \pi^*)$, it follows that $P(B) > P(A)$. Also, the expected value of a prospective partner found at time $t_{u,1}+t$ by searcher ii is at least as great as the expected value of a prospective partner found at time t_d+t by searcher i. Hence, $R_3 \geq R_1$. Also, $R_3 \geq R_4 > R_2$ (the first inequality results from the fact that the reward is the product of the value of the partner found and the discount, which is by definition more severe when a partner is found later) and $R_4 \leq v_3$. Hence,

$$r_2(t_{u,1}; \pi^*) \geq R_3 P(A) + R_4[1 - P(A)] > R_1 P(A) + R_2[1 - P(A)] = r_2(t_d; \pi^*).$$

This contradicts the initial assumption that $r_2(t_{u,1};\pi^*) = r_2(t_d;\pi^*) = v_3$.

Now suppose that $\frac{p_2(t;\pi^*)}{p_3(t;\pi^*)}$ is increasing on the interval $(t_{u,1}, t_d)$. Consider a type 2 player who on the interval $t \in (t_{u,1}, t_d)$ accepts prospective partners of type 2 and 3 at time t with probability 1 and $\beta(t)$, respectively, where $\beta(t) = \frac{p_2(t;\pi^*)p_3(t_d;\pi^*)}{p_3(t;\pi^*)p_2(t_d;\pi^*)}$. Under such a strategy, the ratio between the rate of accepting prospective partners of type 2 and the rate of accepting prospective partners of type 3 when $t \in (t_{u,1}, t_d)$ is $\frac{p_2(t_d;\pi^*)}{p_3(t_d;\pi^*)}$. Assume that for $t \geq t_d$, such a player (call him/her searcher *iii*) follows the optimal strategy. The expected value of a prospective partner accepted by searcher *iii* when $t \in (t_{u,1}, t_d)$ is equal to the expected value of a prospective partner accepted by an optimally behaving type 2 player in the interval $(t_d, 2t_d - t_{u,1})$. Arguing as in the case of searcher *ii*, we obtain $r_2(t_{u,1};\pi) \geq R_5 P(C) + R_4[1 - P(C)]$, where R_5 is the expected reward of searcher *iii* given that he/she forms a partnership in the interval $(t_{u,1}, t_d)$, $P(C)$ is the probability that such a partnership is formed. Since for $t \in (t_{u,1}, t_d)$, $p_2(t;\pi^*) > p_2(t_d;\pi^*)$, it follows that $P(C) > P(A)$ and $R_5 \geq R_1$. The rest of the proof is analogous to the case of searcher *ii* and is hence omitted.

Theorem 6 *When there are three types of prospective partner, any equilibrium can be described by at most four switching times* $t^*_{2,3}$, $t^{s,*}_{2,3}$, $t^*_{1,2}$ *and* $t^*_{1,3}$, *where* $t^*_{2,3} \leq t^{s,*}_{2,3} \leq t^*_{1,2} \leq t^*_{1,3}$. *When* $t^*_{2,3} > 0$, *it denotes the time at which type 2 players start accepting prospective partners of type 3, as long as type 1 players are not yet accepting prospective partners of type 2. When* $t^{s,*}_{2,3} > 0$, *it denotes the time at which type 2 players stop accepting prospective partners of type 3. When* $t^*_{1,2} > 0$, *it denotes the time at which type 1 players start accepting prospective partners of type 2. When* $t^*_{1,3} > 0$, *it denotes the time at which both type 1 and type 2 players start accepting prospective partners of type 3. The possible forms of equilibria are described below:*

0 switching times: Random mating. Each player accepts the first prospective partner ($t^*_{2,3} = t^{s,*}_{2,3} = t^*_{1,2} = t^*_{1,3} = 0$). A necessary and sufficient condition for such an equilibrium is $r_1(0;\pi^*) \leq 1$.

1 switching time: Initially, type 1 and 2 players pair, but type 3 searchers are only acceptable to prospective partners of type 3. Such an equilibrium is characterized by one positive switching time $t^*_{1,3}$, where $r_1(t^*_{1,3};\pi^*) = 1$. The other necessary condition for such an equilibrium is $r_1(0;\pi^*) \leq v_2$.

2 switching times: Initially players only pair with those of the same type. The equilibrium is defined by two positive switching times: $t^*_{1,2}$ and $t^*_{1,3}$, where $t^*_{1,2} < t^*_{1,3}$, $r_1(t^*_{1,2};\pi^*) = v_2$ and $r_1(t^*_{1,3};\pi^*) = 1$. A necessary condition for such an equilibrium is that $r_2(t;\pi^*) > 1$ for $t < t^*_{1,3}$.

3 switching times: Initially, type 2 and 3 players pair, but type 1 searchers only pair with prospective partners of type 1. Such an equilibrium is characterized by three positive switching times: $t^{s,*}_{2,3}$, $t^*_{1,2}$ and $t^*_{1,3}$, where $t^{s,*}_{2,3} < t^*_{1,2} < t^*_{1,3}$, $r_2(t^{s,*}_{2,3};\pi^*) = 1$, $r_1(t^*_{1,2};\pi^*) = v_2$ and $r_1(t^*_{1,3};\pi^*) = 1$. The following is also a necessary condition: $r_2(0;\pi^*) \leq 1$.

4 switching times: Initially players only pair with those of the same type. The equilibrium is defined by four positive switching times: $t^*_{2,3}$, $t^{s,*}_{2,3}$, $t^*_{1,2}$ and $t^*_{1,3}$, where $t^*_{2,3} < t^{s,*}_{2,3} < t^*_{1,2} < t^*_{1,3}$, $r_2(t^*_{2,3}; \pi^*) = r_2(t^{s,*}_{2,3}; \pi^*) = 1$, $r_1(t^*_{1,2}; \pi^*) = v_2$ and $r_1(t^*_{1,3}; \pi^*) = 1$.

These results follow from previous arguments. Note that the equilibrium strategy of type 1 players is given by the switching times $t^*_{1,2}$ and $t^*_{1,3}$. The equilibrium strategy of type 2 players is given by $t^*_{2,3}$, $t^{s,*}_{2,3}$ and $t^*_{1,3}$. Type 3 players accept any prospective partner. These equilibria are considered in more detail in the following section.

5 Examples

Ramsey [21] found that, when there are two types of player, multiple equilibria can occur when highly attractive partners are relatively rare. Example 1 is based on a similar set of problems. Example 2 is based on a set of problems where type 2 and type 3 players are of similar attractiveness. This example illustrates equilibria at which type 2 players can switch from accepting prospective partners of type 3 to rejecting them for some period of time. In both examples, the length of the mating season, as well as the values and initial frequencies of the various types are fixed, but the discount rate γ is varied to illustrate the full range of possible equilibria and the existence of multiple equilibria.

In the first example, it is assumed that $\mu = 100$, $v_1 = 36$, $v_2 = 6$, $v_3 = 1$, $p_1 = 0.01$, $p_2 = 0.09$ and $p_3 = 0.9$. In the second example, it is assumed that $\mu = 100$, $v_1 = 6$, $v_2 = 1.1$, $v_3 = 1$ and $p_1 = p_2 = p_3 = 1/3$. Each of the five following subsections illustrate how to derive (or estimate) an equilibrium with a given number of positive switching times. In each case, the strategy profile is assumed to be of the form considered in that subsection.

Note that the constants of integration appropriate to the systems of differential equations defining the dynamics of the game depend on the strategy profile used. To keep the notation simple, these dependencies are not made explicit. The constant k_i denotes the ratio between the rates at which prospective partners of type i and prospective partners of type 1, respectively, are found when $t \geq t_{1,i}$. The constant $k_{3,2}$ describes the ratio between the rates at which prospective partners of type 3 and prospective partners of type 2, respectively, are found when a type 2 player is mutually acceptable to a type 3 player, but type 1 players only pair with prospective partners of type 1. Any other constant of integration is denoted by c_i and these values are specific to the subsection, i.e. c_1 in Sect. 5.3 is not equivalent to c_1 in Sect. 5.4.

5.1 Random Mating—No Switching Times

First, we consider the conditions required for random mating to be an equilibrium. Intuitively, such an equilibrium exists only for relatively large values of γ. From Eq. (3), the set of differential equations describing the rate at which prospective partners are found under such an equilibrium is given by

$$\frac{dp_i(t;\pi)}{dt} = -p_i(t;\pi)[p_1(t;\pi) + p_2(t;\pi) + p_3(t;\pi)], \quad i \in \{1, 2, 3\}. \tag{7}$$

It follows from these equations and the boundary conditions at $t = 0$ that $p_j(t;\pi) = k_j p_1(t;\pi)$, $j \in \{2, 3\}$, where $k_j = \frac{p_j}{p_1}$. Substituting these relationships into Eq. (7) with $i = 1$, we obtain

$$p_i(t;\pi) = \frac{p_i}{t+1}, \quad i \in \{1, 2, 3\}. \tag{8}$$

A necessary and sufficient condition for random mating to be a Nash equilibrium is given by $r_1(0;\pi) \leq v_3 = 1$. From Eq. (5),

$$\begin{aligned} r_1(0;\pi) &= \int_0^{100} \frac{p_1v_1 + p_2v_2 + p_3}{t+1} \exp\left[-\int_0^t \left\{\gamma + \frac{1}{s+1}\right\} ds\right] dt. \\ &= \int_0^{100} \frac{p_1v_1 + p_2v_2 + p_3}{(t+1)^2} \exp(-\gamma t) dt \leq 1. \end{aligned}$$

This integral was approximated using the inbuilt integration function used in the R package (see Piessens [17]). Solving this inequality numerically with respect to γ, using the method of bisection, it follows that random mating is a Nash equilibrium for Example 1 if and only if $\gamma \geq \gamma_{1,1}$, where $\gamma_{1,1} \approx 0.4575$ and is a Nash equilibrium for Example 2 if and only if $\gamma \geq \gamma_{1,2}$, where $\gamma_{1,2} \approx 1.1905$.

5.2 One Switching Time

At such an equilibrium, type 1 and type 2 players always pair with each other, but only pair with prospective partners of type 3 when $t \geq t^*_{1,3}$. In this section, the strategy profile π denotes any strategy profile of this form such that the switching time, $t_{1,3}$, takes a value in $(0, \mu)$. The strategy profile π^* denotes an equilibrium strategy profile of this form. Note that if such an equilibrium exists, then its derivation reduces to a problem in which there are only two types of player. In this case, players of type 1 and 2 are grouped together to form a type whose initial frequency is $p_1 + p_2$ and value $\frac{p_1v_1+p_2v_2}{p_1+p_2}$. The derivation of such equilibria was considered in Ramsey [21]. The equilibrium condition in this reduced problem is $r_1(t^*_{1,3}, \pi^*) = 1$. Note, however, that for the unreduced problem, it is necessary to check the additional equilibrium

condition stating that initially type 1 searchers should accept type 2 searchers, i.e. $r_1(0;\pi^*) \leq v_2$.

From Eq. (3), when $t < t_{1,3}$ the rates at which prospective partners are found under such a strategy profile is given by

$$\frac{dp_i(t;\pi)}{dt} = -p_i(t;\pi)[p_1(t;\pi)+p_2(t;\pi)],\ \ i \in \{1,2\};\ \ \frac{dp_3(t;\pi)}{dt} = -[p_3(t;\pi)]^2. \tag{9}$$

Note that $p_2(t;\pi) = k_2 p_1(t;\pi)$, where from the boundary condition at $t = 0$, $k_2 = \frac{p_2}{p_1}$. Solving the system of equations given by (9), it follows that

$$p_i(t;\pi) = \frac{p_i}{(p_1+p_2)t+1},\quad i \in \{1,2\};\quad p_3(t;\pi) = \frac{p_3}{p_3 t+1}. \tag{10}$$

When $t > t_{1,3}$, this set of differential equations is given by Eq. (7). Again $p_2(t;\pi) = k_2 p_1(t;\pi)$. Also, $p_3(t;\pi) = k_3 p_1(t;\pi)$, where k_3 is calculated from the boundary condition at $t = t_{1,3}$ using the set of equations given by (10), i.e.

$$k_3 = \frac{p_3(t_{1,3};\pi)}{p_1(t_{1,3};\pi)} = \frac{p_3[(p_1+p_2)t_{1,3}+1]}{p_1[p_3 t_{1,3}+1]}.$$

Solving the system of differential equations given by (7), based on the continuity of the functions p_i, we obtain that for $t > t_{1,3}$

$$p_1(t;\pi) = \frac{1}{(1+k_2+k_3)t+c_1};\quad p_i(t;\pi) = \frac{k_i}{(1+k_2+k_3)t+c_1},\quad i \in \{2,3\}, \tag{11}$$

where $c_1 = \frac{1}{p_1} - k_3 t_{1,3}$. The expected value of a prospective partner when $t > t_{1,3}$ is given by

$$\overline{v} = \frac{v_1 + k_2 v_2 + k_3 v_3}{1+k_2+k_3} = \frac{[p_3 t_{1,3}+1][v_1 p_1 + v_2 p_2] + p_3[(p_1+p_2)t_{1,3}+1]}{[p_3 t_{1,3}+1][p_1+p_2] + p_3[(p_1+p_2)t_{1,3}+1]}.$$

From Eq. (5) and the equilibrium condition, $t^*_{1,3}$ satisfies

$$\begin{aligned} 1 &= \overline{v}\int_{t^*_{1,3}}^{100} \sum_{i=1}^{3} p_i(t;\pi^*) \exp\left[-\int_{t^*_{1,3}}^{t}\left\{\gamma + \sum_{i=1}^{3} p_i(s;\pi^*)\right\} ds\right] dt. \\ &= \overline{v}\int_{t^*_{1,3}}^{100} \frac{(1+k_2+k_3)[(1+k_2+k_3)t^*_{1,3}+c_1]\exp[-\gamma(t-t^*_{1,3})]}{[(1+k_2+k_3)t+c_1)]^2} dt. \end{aligned} \tag{12}$$

This equation was solved numerically using a program written in R. The value of $r_1(t_{1,3};\pi)$ was approximated over a dense grid of values of $t_{1,3}$ (note that π is defined by $t_{1,3}$, thus as $t_{1,3}$ varies, so does π). This procedure also checked the other

necessary condition, $r_1(0;\pi^*) \le v_2$. Considering the probability that a type 1 player does not find a partner before time $t^*_{1,3}$ and his/her expected reward from that time onwards ($v_3 = 1$), it follows that

$$r_1(0;\pi^*) = \frac{v_1 p_1 + v_2 p_2}{p_1 + p_2} \int_0^{t^*_{1,3}} \frac{(p_1+p_2)\exp(-\gamma t)}{[(p_1+p_2)t+1]^2} dt + \frac{\exp(-\gamma t^*_{1,3})}{(p_1+p_2)t^*_{1,3}+1}.$$

In the case of Example 1, such an equilibrium exists when $\gamma \ge \gamma_{2,1}$, where $\gamma_{2,1} \approx 0.0245$ satisfies the equation $r_1(0;\pi^*) = v_2$. Numerical results indicate that $r_1(t_{1,3};\pi)$ has at most a single maximum point and the maximum value of the function is decreasing in γ. Hence, there exists an equilibrium of this form when $\max_{t_{1,3}\in[0,100]} r_1(t_{1,3};\pi) \ge 1$. Solving this inequality numerically with respect to γ, such an equilibrium exists if $\gamma \le \gamma_{3,1}$, where $\gamma_{3,1} \approx 0.4755$. When $\gamma \in [\gamma_{2,1}, \gamma_{1,1}) \approx [0.0245, 0.4575)$, then there is exactly one solution of $r_1(t_{1,3};\pi) = 1$, i.e. there is a unique equilibrium of this form. If $\gamma \in (\gamma_{1,1}, \gamma_{3,1}) \approx (0.4575, 0.4755)$, there exist two positive solutions of $r_1(t_{1,3};\pi) = 1$ and, in addition, random mating is an equilibrium strategy profile. Hence, three equilibria exist for such discount rates. The stability of such equilibria based on the concept of a neighbourhood invasion strategy (NIS) (see Apaloo [4]), will be considered in Sect. 5.6. The equilibrium switching times are illustrated in Fig. 1. The graph on the left illustratres the equilibrium switching times when there is a unique equilibrium. The graph on the right presents the equilibrium switching times when multiple equilibria exist (the lower curve gives the Nash

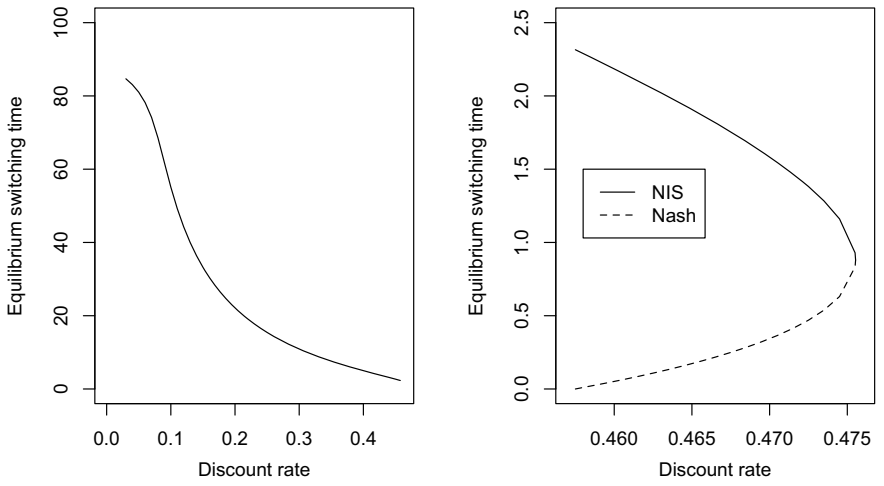

Fig. 1 Equilibrium switching times, $t^*_{1,3}$ for Example 1, $v_1 = 36$, $v_2 = 6$, $v_3 = 1$, $p_1 = 0.01$, $p_2 = 0.09$, $p_3 = 0.9$, as a function of the discount rate, γ, when type 1 searchers always accept prospective partners of type 2. Left: unique equilibrium switching time, $\gamma \in [0.0245, 0.4575)$ Right: close up of solutions when multiple equilibria exist, $\gamma \in (0.4575, 0.4755)$—see also Sect. 5.6

equilibrium switching time which does not satisfy the stronger condition based on the concept of an NIS).

In the case of Example 2, based on a similar approach, such an equilibrium exists if $\gamma \in (\gamma_{2,2}, \gamma_{1,2}) \approx (1.0371, 1.1905)$. Numerical calculations indicate that, for fixed γ, $r_1(t_{1,3}; \pi)$ is decreasing in $t_{1,3}$. Hence, there is no region in which there exist multiple equilibria, including random mating as one.

5.3 Two Switching Times

Such equilibria are described by two parameters $t^*_{1,2}$ and $t^*_{1,3}$. Consider a strategy profile of this form with switching times $t_{1,2}$ and $t_{1,3}$. From Eq. (3), for $t < t_{1,2}$ the differential equations determining the dynamics of the game are

$$\frac{dp_i(t;\pi)}{dt} = -[p_i(t;\pi)]^2, \qquad i \in \{1, 2, 3\}. \tag{13}$$

Solving these differential equations using the boundary conditions at $t = 0$, we obtain

$$p_i(t;\pi) = \frac{p_i}{p_i t + 1}, \quad i \in \{1, 2, 3\}. \tag{14}$$

For $t_{1,2} < t < t_{1,3}$, the system of differential equations determining the dynamics of the game is given by (9). Solving this system of equations using the boundary conditions at $t = t_{1,2}$, $p_3(t;\pi)$ is given by Eq. (14) and

$$p_1(t;\pi) = \frac{1}{(1+k_2)t + c_2}, \qquad p_2(t;\pi) = \frac{k_2}{(1+k_2)t + c_2},$$

where

$$k_2 = \frac{p_2(t_{1,2};\pi)}{p_1(t_{1,2};\pi)} = \frac{p_2[p_1 t_{1,2} + 1]}{p_1[p_2 t_{1,2} + 1]}; \qquad c_2 = \frac{1}{p_1} - k_2 t_{1,2}.$$

For $t > t_{1,3}$, the differential equations determining the dynamics of the game are given by (7). Solving these equations using the boundary conditions at $t = t_{1,3}$, we obtain

$$p_1(t;\pi) = \frac{1}{(1+k_2+k_3)t + c_1}; \quad p_i(t;\pi) = \frac{k_i}{(1+k_2+k_3)t + c_1}, \quad i \in \{2, 3\},$$

where

$$k_3 = \frac{p_3(t_{1,3};\pi)}{p_1(t_{1,3};\pi)} = \frac{p_3[(1+k_2)t_{1,3} + c_2]}{p_3 t_{1,3} + 1}; \qquad c_1 = c_2 - k_3 t_{1,3}.$$

Such an equilibrium satisfies $r_1(t^*_{1,3};\pi^*)=1$ and $r_1(t^*_{1,2};\pi^*)=v_2$. The first condition corresponds to Eq. (12). Considering whether or not a searcher of type 1 forms a partnership in the time interval $(t^*_{1,2}, t^*_{1,3})$ and setting $\bar{v}_2 = \frac{v_1+k_2v_2}{1+k_2}$, it follows from the second condition that

$$r_1(t_{1,2};\pi^*) = \bar{v}_2\int_{t^*_{1,2}}^{t^*_{1,3}}[p_1(t;\pi^*)+p_2(t;\pi^*)]\exp\left[-\int_{t^*_{1,2}}^{t}[\gamma+p_1(s;\pi^*)+p_2(s;\pi^*)]ds\right]dt+$$
$$+\frac{\exp[-\gamma(t^*_{1,3}-t^*_{1,2})]p_1(t^*_{1,3};\pi^*)}{p_1(t^*_{1,2};\pi^*)} = v_2. \tag{15}$$

In addition, a type 2 player should reject a prospective partner of type 3 at any time t for $t<t^*_{1,2}$, i.e. $r_2(t;\pi^*)>v_3, \forall t<t^*_{1,2}$. Conditioning on whether such a searcher finds a partner before time $t^*_{1,2}$, it follows from this that for any $t<t^*_{1,2}$

$$v_3 \le v_2\int_t^{t^*_{1,2}} p_2(s;\pi^*)\exp\left[-\int_t^s\{\gamma+p_2(\tau;\pi^*)\}d\tau\right]ds+$$
$$+\frac{v_2\exp[-\gamma(t^*_{1,2}-t)]p_2(t^*_{1,2};\pi^*)}{p_2(t;\pi^*)}. \tag{16}$$

Such equilibria were estimated by solving Eqs. (12) and (15). First, $t_{1,2}$ was varied over a grid of values over the interval [0, 100) with step length 0.1 to obtain an initial estimate of any Nash equilibria and then a fine grid search was used. For a given value of $t_{1,2}$, the resulting subgame defined for $t \ge t_{1,2}$ was solved by finding the value of $t_{1,3}$ satisfying $r_1(t_{1,3};\pi)=1$. This sub-procedure is analogous to the procedure described in Sect. 5.2. The equilibrium condition given by Inequality (16) was then checked by numerical calculation.

Considering Example 1, such an equilibrium exists when $\gamma \le \gamma_{4,1} \approx 0.0255$. This bound was estimated by finding the value of γ for which $r_1(0;\pi^*)=v_2$ using the method of bisection. Note that multiple equilibria occur when $\gamma \in (\gamma_{2,1}, \gamma_{4,1}) \approx (0.0245, 0.0255)$. Table 2 gives numerical results for various discount rates.

Now consider Example 2. Such an equilibrium exists if the discount rate is slightly less than $\gamma_{2,2}$. For such discount rates, type 1 players start accepting prospective

Table 2 Switching times at equilibrium for Example 1 ($v_1=36$, $v_2=6$, $v_3=1$, $p_1=0.01$, $p_2=0.09$, $p_3=0.9$), when the equilibrium is given by two parameters

Discount rate, γ	$t^*_{1,2}$ Equilibrium 1	$t^*_{1,3}$ Equilibrium 1	$t^*_{1,2}$ Equilibrium 2	$t^*_{1,3}$ Equilibrium 2
0	66.6642	94.4415	–	–
0.01	58.1484	93.8638	–	–
0.02	39.7536	92.4862	–	–
0.0245	0.1530	85.4398	20.8199	90.4273
0.025	2.2276	86.2493	17.1265	89.8591

Table 3 Switching times at equilibrium for Example 2 ($v_1 = 6$, $v_2 = 1.1$, $v_3 = 1$, $p_1 = p_2 = p_3 = 1/3$), when the equilibrium is given by two parameters $t^*_{1,2}, t^*_{1,3}$

Discount rate γ	$t^*_{1,2}$	$t^*_{1,3}$	Discount rate γ	$t^*_{1,2}$	$t^*_{1,3}$
0	81.1167	82.8451	1.005	0.0964	0.3178
0.001	80.9160	82.6727	1.015	0.0661	0.3011
0.002	80.7100	82.4964	1.025	0.0362	0.2846
0.003	80.4982	82.3014	1.035	0.0066	0.2685

partners of type 2 at some positive, but relatively small, time. Hence, it pays type 2 players not to pair with type 3 players initially in the hope of pairing with a type 1 player. This is the case when $r_2(0; \pi^*) \geq 1$. Secondly, suppose that the discount rate is zero and that type 1 players do not initially accept prospective partners of other types (which is expected since type 1 players are common and much more attractive than other prospective partners). Based on Condition (16), the expected reward of a type 2 player at equilibrium given that he/she finds a partner before time $t^*_{1,2}$ is v_2 (type 2 players only pair with other individuals of type 2 and the reward is not discounted). Given that a type 2 player is still searching at time $t^*_{1,2}$, then his/her expected reward from future search is $r_1(t^*_{1,2}; \pi^*)$, which is by definition v_2. Hence, for any $t < t^*_{1,2}$, the future expected reward of a type 2 player at equilibrium must be v_2. As γ increases, the minimum value of $r_2(t; \pi^*)$ on the interval $[0, t^*_{1,2})$ will decrease. Hence, the equilibrium will be defined by two parameters, $t^*_{1,2}$ and $t^*_{1,3}$, for discount rates close to zero. This holds when $\min_{t \in [0, t^*_{1,2})} r_2(t; \pi^*) \geq 1$.

Numerical calculations indicate that the equilibrium is of this form when $\gamma \in (\gamma_{3,2}, \gamma_{2,2}) \approx (1.0050, 1.0371)$ and $\gamma \leq \gamma_{4,2} \approx 0.0032$. Table 3 gives estimates of the equilibria for such discount rates.

5.4 *Three Switching Times*

Such an equilibrium is defined by three parameters: $t^{s,*}_{2,3}$, $t^*_{1,2}$ and $t^*_{1,3}$, where $t^{s,*}_{2,3} < t^*_{1,2} < t^*_{1,3}$. Consider a strategy profile of this form with switching times $t^s_{2,3}$, $t_{1,3}$ and $t_{2,3}$. From Eq. (3), for $t < t^s_{2,3}$,

$$\frac{dp_1(t;\pi)}{dt} = -[p_1(t;\pi)]^2; \quad \frac{dp_i(t;\pi)}{dt} = -p_i(t;\pi)[p_2(t;\pi) + p_3(t;\pi)], \quad i \in \{2,3\}. \tag{17}$$

Hence, on this interval $p_3(t;\pi) = k_{3,2}\, p_2(t;\pi)$, where $k_{3,2} = \frac{p_3}{p_2}$. Using the boundary conditions at $t = 0$, solving this system leads to

$$p_1(t;\pi) = \frac{p_1}{p_1 t + 1}; \quad p_i(t;\pi) = \frac{p_i}{(p_2 + p_3)t + 1}, \quad i \in \{2, 3\}. \tag{18}$$

For $t^s_{2,3} < t < t_{1,2}$, the system of differential equations describing the dynamics of the game are given by (13). Solving this system of differential equations using the boundary conditions at $t = t^s_{2,3}$, $p_1(t;\pi)$ is as given in (18). In addition,

$$p_2(t;\pi) = \frac{1}{t + c_4}; \quad p_3(t;\pi) = \frac{1}{t + c_3}, \tag{19}$$

where $c_4 = k_{3,2}t^s_{2,3} + \frac{1}{p_2}$; $\quad c_3 = \frac{t^s_{2,3}}{k_{3,2}} + \frac{1}{p_3}$.

When $t_{1,2} < t < t_{1,3}$, the differential equations determining the game's dynamics are given by (9). Using the boundary conditions at $t = t_{1,2}$, we obtain

$$p_1(t;\pi) = \frac{1}{(1 + k_2)t + c_2}; \quad p_2(t;\pi) = \frac{k_2}{(1 + k_2)t + c_2},$$

where $k_2 = \frac{p_2(t_{1,2};\pi)}{p_1(t_{1,2};\pi)} = \frac{p_1 t_{1,2}+1}{p_1[t_{1,2}+c_4]}$ and $c_2 = \frac{1}{p_1} - k_2 t_{1,2}$. Note that $p_3(t;\pi)$ is given by the relevant equation in (19).

For $t > t_{1,3}$, the differential equations determining the dynamics of the game are given by (7). Using the boundary conditions at $t = t_{1,3}$, it follows that

$$p_1(t;\pi) = \frac{1}{(1 + k_2 + k_3)t + c_1}; \quad p_i(t;\pi) = \frac{k_i}{(1 + k_2 + k_3)t + c_1}, \quad i \in \{2, 3\},$$

where $k_3 = \frac{p_3(t_{1,3};\pi)}{p_1(t_{1,3};\pi)} = \frac{(1+k_2)t_{1,3}+c_2}{t_{1,3}+c_3}$; $\quad c_1 = c_2 - k_3 t_{1,3}$. The necessary and sufficient conditions for such an equilibrium are: 1) $r_1(t^*_{1,3};\pi^*) = 1$, 2) $r_1(t^*_{1,2};\pi^*) = v_2$, 3) $r_2(t^{s,*}_{2,3};\pi^*) = 1$ and 4) $r_2(0;\pi^*) \le 1$. The first two conditions are equivalent to Eqs. (12) and (15), respectively.

The third condition is equivalent to

$$r_2(t^{s,*}_{2,3};\pi^*) = v_2 \int_{t^{s,*}_{2,3}}^{t^*_{1,2}} p_2(t;\pi^*) \exp\left[-\int_{t^{s,*}_{2,3}}^{t} \{\gamma + p_2(t;\pi^*)\} ds\right] dt + \\ + \frac{v_2 \exp[-\gamma(t^*_{1,2} - t^{s,*}_{2,3})] p_2(t^*_{1,2};\pi^*)}{p_2(t^{s,*}_{2,3};\pi^*)} = 1. \tag{20}$$

From Eq. (20), $r_2(t^{s,*}_{2,3};\pi^*) > v_2 \exp[-\gamma(t^*_{1,2} - t^{s,*}_{2,3})] > v_2 e^{-100\gamma}$. Hence, for such an equilibrium to exist, $v_2 e^{-100\gamma} \le 1$. This leads to $\gamma \ge \ln(v_2)/100$. For Example 1, this gives $\gamma \ge \ln(6)/100 \approx 0.0179$. Also, the discount factor must be small enough for type 1 players to initially only pair with other type 1 players. The previous section indicated that this requires $\gamma \le \gamma_{4,1} \approx 0.0255$. Hence, if such an equilibrium exists for a game corresponding to Example 1, the discount rate must belong to a narrow interval. In addition, the lower bound on γ derived above is not expected to be tight. Given these facts, it is unsurprising that no such equilibrium was found for a game corresponding to Example 1.

Table 4 Equilibria for Example 2 ($v_1 = 6$, $v_2 = 1.1$, $v_3 = 1$, $p_1 = p_2 = p_3 = 1/3$), when an equilibrium is given by three switching times $t^{s,*}_{2,3}, t^*_{1,2}, t^*_{1,3}$

Discount rate γ	$t^{s,*}_{2,3}$	$t^*_{1,2}$	$t^*_{1,3}$	Discount rate γ	$t^{s,*}_{2,3}$	$t^*_{1,2}$	$t^*_{1,3}$
0.01	69.15	79.02	81.07	0.3	7.78	8.10	9.04
0.02	71.41	76.26	78.74	0.4	5.04	5.28	5.97
0.05	58.13	60.05	64.50	0.6	2.28	2.44	2.87
0.1	29.67	30.63	33.58	0.8	0.88	1.00	1.30
0.2	13.26	13.74	15.19	1.0	0.01	0.11	0.33

In Example 2, such an equilibrium exists if $\gamma \in (\gamma_{5,2}, \gamma_{3,2}) \approx (0.0094, 1.0050)$, where $\gamma_{3,2}$ and $\gamma_{5,2}$ are solutions of the equation $r_2(0, \pi^*) = 1$. Table 4 presents the equilibrium for such values of the discount rate. A very rough estimate of the equilibrium is obtained by assuming that all the switching times are integers and minimizing the Euclidean distance between the vectors $[r_1(t_{1,3}; \pi), r_1(t_{1,2}; \pi), r_2(t^s_{2,3}; \pi)]$ and $[1, v_2, 1]$. This is followed by a local search over a denser grid of parameter values.

5.5 *Four Switching Times*

Such an equilibrium is described by 1) $t^*_{2,3}$, 2) $t^{s,*}_{2,3}$, 3) $t^*_{1,2}$ and 4) $t^*_{1,3}$, where $t^*_{2,3} < t^{s,*}_{2,3} < t^*_{1,2} < t^*_{1,3}$. Consider a strategy profile of the same form, where the switching times are given by $t_{2,3}$, $t^s_{2,3}$, $t_{1,2}$ and $t_{1,3}$, respectively. For $t < t_{2,3}$, since players only pair with those of the same type, the rates at which prospective partners are found are given by the set of equations in (14).

For $t > t_{2,3}$, the mating patterns evolve analogously to the equilibrium described in Sect. 5.3. Hence, on the intervals a) $t_{2,3} < t < t^s_{2,3}$, b) $t^s_{2,3} < t < t_{1,2}$ and c) $t_{1,2} < t < t_{1,3}$, the systems of differential equations determining the dynamics of the game are given by the set of equations in (17), (13) and (9), respectively. Solving these sets of differential equations, we obtain

$$p_1(t;\pi) = \begin{cases} \frac{p_1}{p_1 t+1}, & t \le t_{1,2} \\ \frac{1}{(1+k_2)t+c_2}, & t_{1,2} < t < t_{1,3} \end{cases}$$

$$p_2(t;\pi) = \begin{cases} \frac{1}{(1+k_{3,2})t+c_5}, & t_{2,3} < t < t^s_{2,3} \\ \frac{1}{t+c_4}, & t^s_{2,3} < t < t_{1,2} \\ \frac{k_2}{(1+k_2)t+c_2}, & t_{1,2} < t < t_{1,3} \end{cases}$$

$$p_3(t;\pi) = \begin{cases} \frac{k_{3,2}}{(1+k_{3,2})t+c_5}, & t_{2,3} < t < t^s_{2,3} \\ \frac{1}{t+c_3}, & t^s_{2,3} < t < t_{1,3} \end{cases},$$

Table 5 Equilibria for Example 2 ($v_1 = 6$, $v_2 = 1.1$, $v_3 = 1$, $p_1 = p_2 = p_3 = 1/3$), when an equilibrium is given by four switching times $t^*_{2,3}, t^{s,*}_{2,3}, t^*_{1,2}, t^*_{1,3}$

Discount rate γ	$t^*_{2,3}$	$t^{s,*}_{2,3}$	$t^*_{1,2}$	$t^*_{1,3}$
0.004	7.0	53.0	80.3	82.2
0.006	2.4	62.8	79.9	81.8
0.008	0.7	67.1	79.5	81.5
0.009	0.2	68.5	79.3	81.3

where $k_2 = \frac{p_2(t_{1,2};\pi)}{p_1(t_{1,2};\pi)}$, $c_2 = \frac{1}{p_1} - k_2 t_{1,2}$, $k_{3,2} = \frac{p_3(t_{2,3};\pi)}{p_2(t_{2,3};\pi)}$, $c_5 = \frac{1}{p_2} - k_{3,2} t_{2,3}$, $c_4 = c_5 + k_{3,2} t^s_{2,3}$, $c_3 = \frac{t^s_{2,3} + c_5}{k_{3,2}}$.

For $t > t_{1,3}$, the dynamics of the game are given by Eq. (11), where $c_1 = c_2 - k_3 t_{1,3}$.

The four equilibrium conditions are: (1) $r_1(t^*_{1,3}; \pi^*) = 1$, (2) $r_1(t^*_{1,2}; \pi^*) = v_2$, (3) $r_2(t^{s,*}_{2,3}; \pi^*) = 1$ and 4) $r_2(t^*_{2,3}; \pi^*) = 1$. The first three conditions correspond to Eqs. (12), (15) and (20). The fourth condition corresponds to

$$r_2(t^*_{2,3}; \pi^*) = \bar{v}_{2,3} \int_{t^*_{2,3}}^{t^{s,*}_{2,3}} [p_2(t; \pi^*) + p_3(t; \pi^*)] \exp\left[-\int_{t^*_{2,3}}^{t} [\gamma + p_2(s; \pi^*) + p_3(s; \pi^*)] ds \right] dt + \\ + \frac{\exp[-\gamma(t^{s,*}_{2,3} - t^*_{2,3})] p_2(t^{s,*}_{2,3}; \pi^*)}{p_2(t^*_{2,3}; \pi^*)} = 1,$$

where $\bar{v}_{2,3} = \frac{v_2 + k_{3,2}}{1 + k_{3,2}}$. Equilibria were estimated using a procedure analogous to the estimation of equilibria defined by three switching times. As mentioned above, no such equilibria exist for Example 1. Numerical results for Example 2 are presented in Table 5.

5.6 *Multiple Equilibria*

Ramsey [21] found multiple Nash equilibria in games of this type when there are only two types of prospective partner. In such games, a Nash equilibrium which does not correspond to random mating is defined by one switching time. The conditions required for this switching time to define a neighbourhood invader strategy, NIS, (a stronger condition introduced by Apaloo [4]) were also considered. In terms of a single strategy, a strategy π^* is an NIS if and only if when the relevant population use a strategy π sufficiently close to π^*, then selection favours individuals using π^* rather than π.

The selection pressure on a component strategy of a strategy profile depends on the other strategies in the profile. From another point of view, the selection pressure on a particular switching time depends on the other switching times being used.

For this reason, we will only look at the stability properties of switching times in isolation from each other (a weaker condition). The equilibrium switching time $t^*_{1,2}$ is only associated with the strategy of type 1 players. The switching times $t^*_{2,3}$ and $t^{s,*}_{2,3}$ are only associated with the strategy of type 2 players. The switching time $t^*_{1,3}$ is associated with the strategy of players of both type 1 and type 2. Consider the Nash equilibrium given by the set of switching times $(t^*_{2,3}, t^{s,*}_{2,3}, t^*_{1,2}, t^*_{1,3})$. The switching time $t^*_{1,3}$ is said to be a neigbourhood invader (NI) when the following condition is satisfied: when the other switching times are unchanged and the switching time $t_{1,3}$ is sufficiently close to $t^*_{1,3}$, then selection favours searchers of types 1 and 2 (those whose strategy is at least partially defined by $t_{1,3}$) who use the switching time $t^*_{1,3}$ rather than $t_{1,3}$. This property can be defined analogously for the remaining switching times.

Considering Example 1, when $\gamma \in (\gamma_{1,1}, \gamma_{3,1}) \approx (0.4575, 0.4755)$ there are two positive solutions of the equation $r_1(t_{1,3}; \pi) = 1$. Let $t^{*,i}_{1,3}$ denote the i-th smallest positive solution of $r_1(t_{1,3}; \pi) = 1$. Numerical calculations indicate that $r_1(t_{1,3}; \pi)$ 'upcrosses' the value 1 at $t^{*,1}_{1,3}$ and 'downcrosses' at $t^{*,2}_{1,3}$. It follows that when $t_{1,3}$ is slightly larger than $t^{*,1}_{1,3}$, then selection will favour searchers of type 1 (or type 2) who use a slightly larger switching time than $t_{1,3}$ rather than a slightly smaller one. Hence, the switching time $t^{*,1}_{1,3}$ is not an NI. On the other hand, when $t_{1,3}$ is very similar to $t^{*,2}_{1,3}$, then selection favours individuals of type 1 and 2 who use $t^{*,2}_{1,3}$ as a switching time. It follows that the switching time $t^{*,2}_{1,3}$ is an NI. Finally, since $r_1(0; \pi) < 1$ for random mating if $\gamma > \gamma_{1,1}$, when $t_{1,3}$ is sufficiently close to zero, then in this case an optimally individual of type 1 or 2 should accept any prospective partner. Hence, in this case $t_{1,3} = 0$ is an NI.

When $\gamma \in (\gamma_{2,1}, \gamma_{4,1}) \approx (0.0245, 0.0255)$, arguing as above, when $t_{1,2}$ is close to 0 and $t^*_{1,3}$ is the equilibrium switching time corresponding to $t^*_{1,2} = 0$, then selection favours type 1 individuals who always accept prospective partners of type 2. Hence, $t^*_{1,2} = 0$ is an NI. Setting $t^*_{1,3} = t^{*,1}_{1,3}$, the function $r_1(t_{1,2}; \pi)$ upcrosses the value v_2 at $t^{*,1}_{1,2}$. However, when $t^*_{1,3} = t^{*,2}_{1,3}$ the function $r_1(t_{1,2}; \pi)$ downcrosses v_2 at $t^{*,2}_{1,2}$. Hence, $t^{*,2}_{1,2}$ is an NI switching time, but $t^{*,1}_{1,2}$ is not.

If all the switching times satisfy this NI property, then one could say that the corresponding strategy is NIS. However, this is a weaker concept than presented by Apaloo [4], as simultaneous changes of switching times are not considered.

6 Conclusion

This article has considered a partnership formation game with scramble competition in which there is a continuum of players and the attractiveness of a prospective partner takes one of n possible values. The sex ratio is equal to one and the distribution of the values of partners is independent of sex. Some general results regarding Nash equilibria were given for the mixing population model, according to which it is assumed that the rate at which prospective partners are found is proportional to the fraction

of individuals who are still searching for a partner. A full characterization of the possible equilibria in the case where the attractiveness of prospective partners takes one of three possible values was presented. Such an equilibrium can be described by a set of between zero and four switching times, where the case 'zero switching times' corresponds to random mating. Two examples were presented to illustrate each type of equilibria. It was shown that multiple Nash equilibria are possible and the stability properties of these equilibria were considered from the point of view of the concept of neighbourhood invader strategy (see Apaloo [4]).

Except in the case of random mating, equilibria were estimated using search procedures based on a grid over the space of switching times. When an equilibrium is described by four switching times, the initial estimate assumes that the switching times are integers (there are ${}_{100}C_4$ such strategy profiles) and then uses a finer grid for local search. The running time of a program written in R was about 20 min using a 1.4 GHz Intel Core i5 processor with 4 GB of memory. When attractiveness takes a larger number of possible values, it is expected that the number of switching times possible at equilibrium grows exponentially. To solve more complex games of this form, other methods of solution, such as policy iteration or value iteration, should be considered. However, such approaches make it more difficult to examine the phenomenon of multiple equilibria.

Searchers of intermediate attractiveness do not always become less choosy as time progresses. Equilibria exist where such searchers initially accept (or start accepting) prospective partners of low attractiveness, but then stop accepting them if players of high attractiveness will start accepting those of intermediate attractiveness in the near future. For such an equilibrium to exist, the value of players of low attractiveness should be similar to the value of prospective partners of intermediate attractiveness. In such cases, either the period of time over which searchers of intermediate attractiveness become more choosy is very short or the discount rate is very low, which means that the expected reward from future search of an individual of intermediate attractiveness is always close to the value of a prospective partner of low attractiveness and so the selective pressure on whether to accept or reject a partner of low attractiveness is relatively small.

One avenue for future research would be to restrict the set of strategy profiles to those where players become less choosy over time. This would greatly simplify the form of 'equilibria' and from a practical point of view might be more realistic. Considering such a game as a stopping game, it is unclear what conditions should be satisfied by the future reward functions. However, such an approach is definitely appropriate in games where rewards are not discounted over time. For example, suppose an individual of type i is not initially acceptable to a searcher of type 1. By accepting only individuals of type i when $t < t_{1,i}$ and behaving in the same way as an individual of type 1 when $t \geq t_{1,i}$, where $t_{1,i}$ is the time at which the most attractive searchers start to accept those of type i, it is clear from the equilibrium conditions that such an individual has an expected reward of v_i and becomes less choosy as time progresses. Extending this argument, each searcher should become less choosy as time progresses (individuals who are always acceptable to those of type 1 should always behave in the same way as individuals of type 1 and hence

become less choosy over time). Hence, such an equilibrium can be described by at most $n - 1$ parameters.

The phenomenon of multiple equilibria should also be investigated. If multiple equilibria exist, then when searchers are not choosy, it pays an individual also not to be choosy and when searchers are relatively choosy, it pays (at least attractive searchers) to be choosy. It is possible that a policy iteration algorithm could be used to find 'a least choosy equilibrium' and a 'most choosy equilibrium'. The first equilibrium would be found by starting a policy iteration algorithm from a strategy profile where each searcher accepts any prospective partner. The second equilibrium could be found, for example, by starting a policy iteration algorithm from a strategy profile where searchers use the equilibrium searching rules in the game where the rates at which prospective partners of a given type are fixed. In such a game, type 1 searchers face a classical one-sided search problem for which the optimal rule can be found by recursion. The optimal rule of each successive type of searcher given the strategies of more attractive individuals could then be found in a similar way.

Acknowledgments This research is supported by the Polish National Centre for Science on the basis of Grant No. DEC-2015/17/B/ST6/01868: 'Stopping methods for the analysis of chosen algorithms'.

References

1. Alpern, S., Katrantzi I. Equilibria of two-sided matching games with common preferences. European Journal of Operational Research, **196** (3), 1214-1222 (2009).
2. Alpern, S., Reyniers, D.: Strategic mating with homotypic preferences. Journal of Theoretical Biology, **198** (1), 71-88 (1999).
3. Alpern, S., Reyniers, D.: Strategic mating with common preferences. Journal of Theoretical Biology, **237**, 337-354 (2005).
4. Apaloo, J.: Revisiting strategic models of evolution: the Concept of neighborhood invader strategies. Theoretical Population Biology, **52**, 71-77 (1997).
5. Burdett, K., Coles, M. G.: Long-term partnership formation: Marriage and employment. The Economic Journal, **109**, 307-334 (1999).
6. Chow, Y. S. Great expectations. The theory of optimal stopping. Houghton Mifflin, Boston, MA (1971).
7. Collins, E. J., McNamara, J. M.: The job-search problem with competition: an evolutionarily stable strategy. Advances in Applied Probability, **25**, 314-333 (1993).
8. Courtiol, A., Etienne, L., Feron, R., Godelle, B., Rousset, F.: The evolution of mutual mate choice under direct benefits. The American Naturalist, **188**(5), 521-538 (2016).
9. Dechaume-Moncharmont, F. X., Brom, T., Cézilly, F.: Opportunity costs resulting from scramble competition within the choosy sex severely impair mate choosiness. Animal Behavior, **114**, 249-260 (2016).
10. Etienne, L., Rousset, F., Godelle, B., Courtiol, A.: How choosy should I be? The relative searching time predicts evolution of choosiness under direct sexual selection. Proceedings of the Royal Society B, **281**, 20140190 (2014). https://doi.org/10.1098/rspb.2014.0190.
11. Janetos, A. C.: Strategies of female mate choice: a theoretical analysis. Behavioral and Ecological Sociobiology, **7**, 107-112 (1980).
12. Johnstone, R. A.: The tactics of mutual mate choice and competitive search. Behavioral and Ecological Sociobiology, **40**, 51-59 (1997).

13. Mazalov, V., Falko, A. Nash equilibrium in two-sided mate choice problem. International Game Theory Review, **10**(4), 421-435 (2008).
14. McNamara, J. M., Collins, E. J.: The job search problem as an employer-candidate game. Journal of Applied Probability, **28**, 815-827 (1990).
15. McNamara, J. M., Szekely, T., Webb, J. N., Houston, A. I.: A dynamic game-theoretic model of parental care. Journal of Theoretical Biology, **205**(4), 605-623 (2000).
16. Parker, G. A.: Mate quality and mating decisions. In: Bateson P. (ed.) Mate Choice, pp. 227-256. Cambridge University Press, Cambridge, UK (1983).
17. Piessens, R., de Doncker-Kapenga, E., Uberhuber, C., Kahaner, D.: Quadpack: a Subroutine Package for Automatic Integration, Vol. 1. Springer Science & Business Media, Berlin (2012).
18. Priklopil, T., Kisdi, E., Gyllenberg, M.: Evolutionarily stable mating decisions for sequentially searching females and the stability of reproductive isolation by assortative mating. Evolution, **69**(4), 1015-1026 (2015).
19. Ramsey, D. M.: A large population job search game with discrete time. European Journal of Operational Research, **188**, 586-602 (2008).
20. Ramsey, D. M.: Partnership formation based on multiple traits. European Journal of Operational Research, **216** (3), 624-637 (2012)..
21. Ramsey, D. M.: On a large population partnership formation game with continuous time. Contributions to Game Theory and Management, **8**, 268-277 (2015).
22. Ramsey, D. M.: A Large Population Partnership Formation Game with Associative Preferences and Continuous Time. Mathematica Applicanda, **46**(2), 173-196, (2018).
23. Real, L. A.: Search theory and mate choice. I. Models of single-sex discriminination. American Naturalist, **136**, 376-404 (1990)
24. Real, L. A.: Search theory and mate choice. II. Mutual interaction, assortative mating, and equilibrium variation in male and female fitness. American Naturalist, **138**, 901-917 (1991).
25. Smith, L.: The marriage model with search frictions. Journal of Political Economy, **114**, 1124-1144 (2006).
26. Stigler, G. J.: The economics of information. Journal of Political Economy, **69**, 213-225 (1961).

The Replicator Dynamics for Games in Metric Spaces: Finite Approximations

Saul Mendoza-Palacios and Onésimo Hernández-Lerma

1 Introduction

In this paper, we are interested in evolutionary games, in which the interaction of strategies is studied as a dynamical system. We are interested in the special case in which the strategies' interactions follow a specific dynamical system known as the replicator dynamics.

An evolutionary game is said to be *symmetric* if there are two players only and, furthermore, they have the same strategy sets and the same payoff functions. This type of game models interactions of the strategies of a single population. In contrast, an *asymmetric* evolutionary game, also known as *multipopulation games*, is a game with a finite set of players (or populations) each of which has a different set of strategies and different payoff functions.

In our model, the pure strategies set of each player (or population) is a metric space and consequently the replicator dynamics lives in a Banach space (a space of finite signed measures). In particular, if we have n players each of which has m_i strategies, for $i = 1, \ldots, n$, then the replicator dynamics is in $\mathbb{R}^m$, where $m = \sum_{i=1}^{n} m_i$.

The main goal of this paper is to establish conditions under which a finite-dimensional dynamical system approximates the replicator dynamics for games with strategies in metric spaces. In this manner, we can use numerical analysis techniques for finite-dimensional differential equations to approximate a solution to the replicator dynamics, which lives in an infinite-dimensional Banach space. This is important because it will allow us to study games with pure strategies in metric spaces such as models in oligopoly theory, international trade theory, war of attrition, and public goods, among others. To achieve this goal, we first present a finite-dimensional

S. Mendoza-Palacios (✉)
Economic Studies Center of El Colegio de México, Carretera Picacho Ajusco 20, Ampliación Fuentes del Pedregal, 14110 Tlapan, México city, Mexico
e-mail: smendoza@colmex.mx

O. Hernández-Lerma
Mathematics Department, CINVESTAV-IPN, A. Postal 14-740, 07000 México City, Mexico
e-mail: ohernand@math.cinvestav.mx

D. M. Ramsey and J. Renault (eds.), *Advances in Dynamic Games*,
Annals of the International Society of Dynamic Games 17,
https://doi.org/10.1007/978-3-030-56534-3_7

approximation technique for games in metric spaces and we give a proposal of a finite-dimensional dynamical system to approximate evolutionary dynamics in a Banach space, see Sect. 4. After, in Sects. 5 and 6, we establish general approximation theorems for the replicator dynamics in metric spaces and use these results for a finite-dimensional approximation given in Sect. 4, see Notes 1 and 3.

Oechssler and Riedel [24] propose two approximation theorems for symmetric games. The first theorem establishes the proximity in the strong topology of two paths generated by two dynamical systems (the original model and a discrete approximation of the model) with the same initial conditions. The second theorem establishes the proximity in the weak topology of two paths with different initial conditions, and these paths satisfy the same differential equation.

We propose here two approximation results with hypotheses less restrictive than those by Oechssler and Riedel [24]. Our approximation theorems extend the results in [24]. In our case, the approximation theorems are for symmetric and asymmetric games. Also, we establish the proximity of two paths generated by two different dynamical systems (the original model and a discrete approximation model) with different initial conditions. In addition, our approximation results are studied in the strong topology using the norm of total variation, and also in the weak topology using the Kantorovich–Rubinstein metric. This last point is important because the initial conditions and the paths (by consequence) of the original dynamics model and the finite-dimensional dynamic approximation may be very far between them (both initial conditions and paths) in terms of the strong topology, but very close between them in terms of the weak topology.

These approximations require different hypotheses. The first approximation theorem, Theorem 1, requires a proximity in the strong topology of the two initial conditions, and it only requires that the payoff functions for the original model be bounded. The second approximation result, Theorem 2, weakens the hypothesis of proximity of the two initial conditions (it only imposes a condition of proximity in the weak topology), but it requires that the payoff functions for the original model be Lipschitz continuous.

There are several publications on the replicator dynamics in games with strategies in metric spaces. For instance, conditions for the existence of solutions, as in Bomze [4], Oechssler and Riedel [23], Cleveland and Ackleh [7], Mendoza-Palacios and Hernández-Lerma [21] (for asymmetric games). Similarly, conditions for dynamic stability, as in Bomze [3], Oechssler and Riedel [23, 24], Eshel and Sansone [9], Veelen and Spreij [30], Cressman and Hofbauer [8], Mendoza-Palacios and Hernández-Lerma [21, 22].

The paper is organized as follows. Section 2 presents notation and technical requirements. Section 3 describes the replicator dynamics and its relation to evolutionary games. Some important technical issues are also summarized. Section 4 introduces a finite-dimensional game to approximate evolutionary games in a Banach space. Section 5 establishes an approximation theorem for the replicator dynamics on measure spaces by means of dynamical systems in finite-dimensional spaces. The distance for this first approximation is the total variation norm. Section 6 establishes an approximation theorem using the Kantorovich–Rubinstein metric. Section 7 pro-

poses an example to illustrate our results. We conclude in Sect. 8 with some general comments on possible extensions. An appendix contains results of some technical facts.

2 Technical Preliminaries

2.1 Spaces of Signed Measures

Consider a separable metric space (A, ϑ) and its Borel σ-algebra $\mathcal{B}(A)$. Let $\mathbb{M}(A)$ be the Banach space of finite signed measures μ on $\mathcal{B}(A)$ endowed with the total variation norm

$$\|\mu\| := \sup_{\|f\| \leq 1} \left| \int_A f(a)\mu(da) \right| = |\mu|(A). \tag{1}$$

The supremum in (1) is taken over functions in the Banach space $\mathbb{B}(A)$ of real-valued bounded measurable functions on A, endowed with the supremum norm

$$\|f\| := \sup_{a \in A} |f(a)|. \tag{2}$$

Consider the subset $\mathbb{C}(A) \subset \mathbb{B}(A)$ of all real-valued continuous and bounded functions on A. Consider the dual pair $(\mathbb{C}(A), \mathbb{M}(A))$ given by the bilinear form $\langle \cdot, \cdot \rangle : \mathbb{C}(A) \times \mathbb{M}(A) \to \mathbb{R}$

$$\langle g, \mu \rangle = \int_A g(a)\mu(da). \tag{3}$$

We consider the *weak topology* on $\mathbb{M}(A)$ (induced by $\mathbb{C}(A)$), i.e., the topology under which all elements of $\mathbb{C}(A)$ when regarded as linear functionals $\langle g, \cdot \rangle$ on $\mathbb{M}(A)$ are continuous.

2.2 The Kantorovich–Rubinstein Metric

There are many metrics that metrize the weak topology on $\mathbb{P}(A)$. Here we use the Kantorovich–Rubinstein metric. Let (A, ϑ) be a separable metric space, and $\mathbb{P}(A)$ the set of probability measure on A. For any $\mu, \nu \in \mathbb{P}(A)$ we define the **the Kantorovich–Rubinstein metric** r_{kr} as

$$r_{kr}(\mu, \nu) := \sup_{f \in \mathbb{L}(A)} \left\{ \int_A f(a)\mu(da) - \int_A f(a)\nu(da) \ : \ \|f\|_L \leq 1 \right\}, \tag{4}$$

where $(\mathbb{L}(A), \|\cdot\|_L)$ is the space of continuous real-valued functions on A that satisfy the Lipschitz condition

$$\|f\|_L := \sup\left\{|f(a) - f(b)|/\vartheta(a,b),\ \ a,b \in A,\ a \neq b\right\} < \infty. \tag{5}$$

Let a_0 be a fixed point in A, and

$$\mathbb{M}_K(A) := \left\{\mu \in \mathbb{M}(A) : \sup_{f\in\mathbb{L}(A)} \int_A |f(a)|\mu(da) < \infty\right\}.$$

The Kantorovich–Rubinstein metric r_{kr} can be extended as a norm on $\mathbb{M}_K(A)$ defined as

$$\|\mu\|_{kr} := |\mu(A)| + \sup_{f\in\mathbb{L}(A)} \left\{\int_A f(a)\mu(da) \ :\ \|f\|_L \le 1,\ f(a_0) = 0\right\} \tag{6}$$

for any μ in $\mathbb{M}_K(A)$ (see Bogachev [2], Chap. 8).

Remark 1 Note that for any $\mu, \nu \in \mathbb{P}(A)$, $r_{kr}(\mu,\nu) = \|\mu - \nu\|_{kr}$. Indeed if $\mu, \nu \in \mathbb{P}(A)$, then

$$\sup_{f\in\mathbb{L}(A)} \left\{\int_A f(a)\mu(da) - \int_A f(a)\nu(da) \ :\ \|f\|_L \le 1\right\}$$

$$= \sup_{f\in\mathbb{L}(A)} \left\{\int_A [f(a) - f(a_0)]\mu(da) - \int_A [f(a) - f(a_0)]\nu(da) \ :\ \|f\|_L \le 1\right\}$$

$$= \sup_{g\in\mathbb{L}(A)} \left\{\int_A g(a)\mu(da) - \int_A g(a)\nu(da) \ :\ \|g\|_L \le 1,\ g(a_0) = 0\right\}.$$

2.3 *Product Spaces*

Consider two separable metric spaces X and Y with their Borel σ-algebras $\mathcal{B}(X)$ and $\mathcal{B}(Y)$. We denote by $\mathcal{B}(X) \times \mathcal{B}(Y)$ the product σ-algebra on $X \times Y$. For $\mu \in \mathbb{M}(X)$ and $\nu \in \mathbb{M}(Y)$, we denote their product by $\mu \times \nu$ and it holds that

$$\|\mu \times \nu\| \le \|\mu\|\|\nu\|. \tag{7}$$

As a consequence, $\mu \times \nu$ is in $\mathbb{M}(X \times Y)$ (see by example Heidergott and Leahu [11], Lemma 4.2.).

Now consider a finite family of metric spaces $\{X_i\}_{i=1}^n$ and their σ-algebras $\mathcal{B}(X_i)$, as well as the Banach spaces $(\mathbb{M}(X_i), \|\cdot\|)$ and $(\mathbb{M}_K(X_i), \|\cdot\|_{kr})$. For $i = 1, \ldots, n$, let $\mu_i \in \mathbb{M}(X_i)$ and consider the elements $\mu = (\mu_1, ..., \mu_n)$ in the product space $\mathbb{M}(X_1) \times ... \times \mathbb{M}(X_n)$ with the norm

$$\|\mu\|_\infty := \max_{1\le i\le n} \|\mu_i\| < \infty. \tag{8}$$

These elements form the Banach space $(\mathbb{M}(X_1) \times ... \times \mathbb{M}(X_n), \|\cdot\|_\infty)$. We can similarly define the Banach space $(\mathbb{M}_K(X_1) \times ... \times \mathbb{M}_K(X_n), \|\cdot\|_\infty^{kr})$, where

$$\|\mu\|_\infty^{kr} := \max_{1\le i\le n} \|\mu_i\|_{kr} < \infty. \tag{9}$$

2.4 Differentiability

Definition 1 Let A be a separable metric space. We say that a mapping $\mu : [0, \infty) \to \mathbb{M}(A)$ is strongly differentiable if there exists $\mu'(t) \in \mathbb{M}(A)$ such that, for every $t > 0$,

$$\lim_{\epsilon\to 0} \left\| \frac{\mu(t+\epsilon) - \mu(t)}{\epsilon} - \mu'(t) \right\| = 0. \tag{10}$$

Note that, by (1), the left-hand side in (10) can be expressed more explicitly as

$$\lim_{\epsilon\to 0} \sup_{\|g\|\le 1} \left| \frac{1}{\epsilon} \left[\int_A g(a)\mu(t+\epsilon, da) - \int_A g(a)\mu(t, da) \right] - \int_A g(a)\mu'(t, da) \right|.$$

The signed measure μ' in (10) is called the strong derivative of μ.

For weak differentiability, see Remark 3.

3 The Replicator Dynamics and Evolutionary Games

3.1 Asymmetric Evolutionary Games

Let $I := \{1, 2, \ldots, n\}$ be the set of different species (or players). Each individual of the species $i \in I$ can choose a single element a_i in a set of characteristics (strategies or actions) A_i, which is a separable metric space. For every $i \in I$ and every vector $a := (a_1, ..., a_n)$ in the Cartesian product $A := A_1 \times ... \times A_n$, we write a as (a_i, a_{-i}) where $a_{-i} := (a_1, ..., a_{i-1}, a_{i+1}, ..., a_n)$ is in

$$A_{-i} := A_1 \times ... \times A_{i-1} \times A_{i+1} \times ... \times A_n.$$

For each $i \in I$, let $\mathcal{B}(A_i)$ be the Borel σ-algebra of A_i and $\mathbb{P}(A_i)$ the set of probability measures on A_i, also known as the set of *mixed strategies*. A probability measure $\mu_i \in \mathbb{P}(A_i)$ assigns a population distribution over the action set A_i of the species i.

Finally, for each species i we assign a payoff function $J_i : \mathbb{P}(A_1) \times ... \times \mathbb{P}(A_n) \to \mathbb{R}$ that explains the interrelation with the population of other species, and which is defined as

$$J_i(\mu_1, ..., \mu_n) := \int_{A_1} ... \int_{A_n} U_i(a_1, ..., a_n)\mu_n(da_n)...\mu_1(da_1), \tag{11}$$

where $U_i : A_1 \times ... \times A_n \to \mathbb{R}$ is a given measurable function.

For every $i \in I$ and every vector $\mu := (\mu_1, ..., \mu_n)$ in $\mathbb{P}(A_1) \times ... \times \mathbb{P}(A_n)$, we sometimes write μ as (μ_i, μ_{-i}), where $\mu_{-i} := (\mu_1, ..., \mu_{i-1}, \mu_{i+1}, ..., \mu_n)$ is in $\mathbb{P}(A_1) \times ... \times \mathbb{P}(A_{i-1}) \times \mathbb{P}(A_{i+1}) \times ... \times \mathbb{P}(A_n)$. If $\delta_{\{a_i\}}$ is a probability measure concentrated at $a_i \in A_i$, the vector $(\delta_{\{a_i\}}, \mu_{-i})$ is written as (a_i, μ_{-i}), and so

$$J_i(\delta_{\{a_i\}}, \mu_{-i}) = J_i(a_i, \mu_{-i}). \tag{12}$$

In particular, (11) yields

$$J_i(\mu_i, \mu_{-i}) := \int_{A_i} J_i(a_i, \mu_{-i})\mu_i(da_i). \tag{13}$$

In an evolutionary game, the dynamics of the strategies is determined by a system of differential equations of the form

$$\mu_i'(t) = F_i(\mu_1(t), ..., \mu_n(t)) \quad \forall\ i \in I, \quad t \geq 0, \tag{14}$$

with some initial condition $\mu_i(0) = \mu_{i,0}$ for each $i \in I$. The notation $\mu_i'(t)$ represents the strong derivative of $\mu_i(t)$ in the Banach space $\mathbb{M}(A_i)$ (see Definition 1). For each $i \in I$, $F_i(\cdot)$ is a mapping

$$F_i : \mathbb{P}(A_1) \times ... \times \mathbb{P}(A_n) \to \mathbb{M}(A_i).$$

Let

$$F : \mathbb{P}(A_1) \times ... \times \mathbb{P}(A_n) \to \mathbb{M}(A_1) \times ... \times \mathbb{M}(A_n)$$

be such that $F(\mu) := (F_1(\mu), ..., F_n(\mu))$, and consider the vector

$$\mu'(t) := (\mu_1'(t), ..., \mu_n'(t)).$$

Hence, the system (14) can be expressed as

$$\mu'(t) = F(\mu(t)), \tag{15}$$

and we can see that the system lives in the Cartesian product of signed measures

$$\mathbb{M}(A_1) \times ... \times \mathbb{M}(A_n),$$

which is a Banach space with norm as in (8).

More explicitly, we may write (14) as

$$\mu_i'(t, E_i) = F_i(\mu(t), E_i) \quad \forall\, i \in I,\ E_i \in \mathcal{B}(A_i),\ t \geq 0, \tag{16}$$

where $\mu_i'(t, E_i)$ and $F_i(\mu(t), E_i)$ denote the signed measures $\mu_i'(t)$ and $F_i(\mu(t))$ valued at $E_i \in \mathcal{B}(A_i)$.

We shall be working with a special class of asymmetric evolutionary games which can be described as

$$\Big[I, \Big\{\mathbb{P}(A_i)\Big\}_{i\in I}, \Big\{J_i(\cdot)\Big\}_{i\in I}, \Big\{\mu_i'(t) = F_i(\mu(t))\Big\}_{i\in I}\Big], \tag{17}$$

where

(i) $I = \{1, ..., n\}$ is the finite set of players;
(ii) for each player $i \in I$ we have a set $\mathbb{P}(A_i)$ of mixed actions and a payoff function $J_i : \mathbb{P}(A_1) \times ... \times \mathbb{P}(A_n) \to \mathbb{R}$ (as in (12)); and
(iii) the replicator function $F_i(\mu(t))$, where

$$F_i(\mu(t), E_i) := \int_{E_i} \Big[J_i(a_i, \mu_{-i}(t)) - J_i(\mu_i(t), \mu_{-i}(t))\Big]\mu_i(t, da_i). \tag{18}$$

Conditions for the existence of solutions and dynamic stability for asymmetric games are given, for instance, by Mendoza-Palacios and Hernández-Lerma [21], Theorems 4.3 and 4.5.

3.2 *The Symmetric Case*

We can obtain from (17) a *symmetric* evolutionary game when $I := \{1, 2\}$ and the sets of actions and payoff functions are the same for both players, i.e., $A = A_1 = A_2$ and $U(a, b) = U_1(a, b) = U_2(b, a)$, for all $a, b \in A$. As a consequence, the sets of mixed actions and the expected payoff functions are the same for both players, that is, $\mathbb{P}(A) = \mathbb{P}(A_1) = \mathbb{P}(A_2)$ and $J(\mu, \nu) = J_1(\mu, \nu) = J_2(\nu, \mu)$ for all $\mu, \nu \in \mathbb{P}(A)$. This kind of model determines the dynamic interaction of strategies of a unique species through the replicator dynamics $\mu'(t) = F(\mu(t))$, where $F : \mathbb{P}(A) \to \mathbb{M}(A)$ is given by

$$F(\mu(t), E) := \int_E \Big[J(a, \mu(t)) - J(\mu(t), \mu(t))\Big]\mu(t, da)\ \ \forall E \in \mathcal{B}(A). \tag{19}$$

As in (17), we can describe a symmetric evolutionary game in a compact form as

$$\left[I = \{1, 2\},\ \ \mathbb{P}(A),\ \ J(\cdot),\ \ \mu'(t) = F(\mu(t))\right]. \tag{20}$$

There are several papers on the replicator dynamics in symmetric games with strategies in metric spaces. In particular, for conditions on the existence of solutions, see, for instance, Bomze [4], Oechssler and Riedel [23], Cleveland and Ackleh [7]. Similarly, conditions for dynamic stability are given by Bomze [3], Oechssler and Riedel [23, 24], Eshel and Sansone [9], Veelen and Spreij [30], Cressman and Hofbauer [8], Mendoza-Palacios and Hernández-Lerma [22], among others.

4 Discrete Approximations to the Replicator Dynamics

To obtain a finite-dimensional approximation of the replicator dynamics (15) (with $F_i(\cdot)$ in (18)), for an asymmetric (17) (or symmetric (20)) model, we can apply the following Theorems 1 and 2 to a discrete approximation of the payoff functions U_i and the initial probability measures $\mu_{i,0}$, for i in I. For some approximation techniques for the payoff function in games, see Bishop and Cannings [1], Simon [29].

4.1 Games with Strategies in an Real Interval

Oechssler and Riedel [24] propose a finite approximation for a symmetric game. Following [24], consider an asymmetric game (17) where, for every i in I, $A_i = [c_{i,1}, c_{i,2}]$ (for some real numbers with $c_{i,1} < c_{i,2}$) and U_i is a real-valued bounded function. For every i in I, consider the partition $P_{k_i} := \{\xi_{m_i}\}_{m_i=0}^{2^{k_i}-1}$ over A_i, where

$$\xi_{m_i} := [a_{m_i}, a_{m_i+1}),\ \ a_{m_i} = c_{i,1} + \frac{m_i[c_{i,2} - c_{i,1}]}{2^{k_i}},$$

for $m_i = 0, 1, ..., 2^{k_i} - 1$ and $\xi_{2^{k_i}-1} := [a_{2^{k_i}-1}, c_{i,2}]$. For every i in I, the discrete approximation to U_i is given by the function

$$U_{k_i}(x_1, ..., x_i, ..., x_n) := U_i(a_{m_1}, ..a_{m_i}, ..., a_{m_n}),$$

if $(x_1, ..., x_i, ..., x_n)$ is in $\xi_{m_1} \times \cdots \times \xi_{m_i} \times \cdots \times \xi_{m_n}$. Also, for each i in I we approximate a probability measure $\mu_i \in \mathbb{P}(A_i)$ by a discrete probability distribution μ_{k_i} on the partition set P_{k_i}. Then we can write the approximation to the payoff function (11) as

$$J_{k_i}(\mu_{k_1}, ..., \mu_{k_n}) := \sum_{\xi_{m_1} \in P_{k_1}} ... \sum_{\xi_{m_n} \in P_{k_n}} U_i(a_{m_1}, ..., a_{m_n}) \mu_{k_n}(\xi_{m_n}) \cdots \mu_{k_1}(\xi_{m_1}). \quad (21)$$

For every $i \in I$ and every vector $\mu_k := (\mu_{k_1}, ..., \mu_{k_n})$ in $\mathbb{P}(P_{k_1}) \times ... \times \mathbb{P}(P_{k_n})$, we write μ_k as (μ_{k_i}, μ_{-k_i}), where $\mu_{k_{-i}} := (\mu_{k_1}, ..., \mu_{k_{i-1}}, \mu_{k_{i+1}}, ..., \mu_{k_n})$ is in $\mathbb{P}(P_{k_1}) \times ... \times \mathbb{P}(P_{k_{i-1}}) \times \mathbb{P}(P_{k_{i+1}}) \times ... \times \mathbb{P}(P_{k_n})$. If $\delta_{\{\xi_{m_i}\}}$ is a probability measure concentrated at $\xi_{m_i} \in P_{k_i}$, the vector $(\delta_{\{\xi_{m_i}\}}, \mu_{-i})$ is written as (a_{m_i}, μ_{-i}), and so

$$J_{k_i}(\delta_{\{\xi_{m_i}\}}, \mu_{k_{-i}}) = J_{k_i}(a_{m_i}, \mu_{k_{-i}}). \quad (22)$$

In particular, (21) yields

$$J_{k_i}(\mu_{k_i}, \mu_{k_{-i}}) := \sum_{\xi_{m_i} \in P_{k_i}} J_{k_i}(a_{m_i}, \mu_{k_{-i}}) \mu_{k_i}(\xi_{m_i}). \quad (23)$$

Note that $\mu_k := (\mu_{k_1}, ..., \mu_{k_n})$ in $\mathbb{P}(P_{k_1}) \times ... \times \mathbb{P}(P_{k_n})$ is a vector of measures in $\mathbb{P}(A_1) \times ... \times \mathbb{P}(A_n)$. Then for any $i \in I$ and $E_i \in \mathcal{B}(A_i) \cap P_{k_i}$, the replicator induced by $\{U_{k_i}\}_{i \in I}$ has the form,

$$\mu'_{k_i}(t, E_i) = \sum_{\xi_{m_i} \in E_i \cap P_{k_i}} \Big[J_{k_i}(a_{m_{k_i}}, \mu_{k_{-i}}(t)) - J_{k_i}(\mu_{k_i}(t), \mu_{k_{-i}}(t)) \Big] \mu_{k_i}(t, \xi_{m_i}), \quad (24)$$

which is equivalent to the system of differential equations in $\mathbb{R}^{2^{k_1}+...+2^{k_n}}$ of the form:

$$\mu'_{k_i}(t, \xi_{m_i}) = \Big[J_{k_i}(a_{m_i}, \mu_{k_{-i}}(t)) - J_{k_i}(\mu_{k_i}(t), \mu_{k_{-i}}(t)) \Big] \mu_{k_i}(t, \xi_{m_i}), \quad (25)$$

for $i = 1, 2, \ldots, n$ and $m_i = 0, 1, \ldots, 2^{ki} - 1$, with initial condition $\{\mu_{k_i,0}(\xi_{m_i})\}_{m_i=0}^{2^{ki-1}}$.

Hence, using Theorem 1 or Theorem 2, we can approximate (14), (15) (with $F_i(\cdot)$ as (18)) by a system of differential equations in $\mathbb{R}^{2^{k_1}+...+2^{k_n}}$ of the form (25).

4.2 *Games with Strategies in Compact Metric Spaces*

Similarly as in Sect. 4.1, consider an asymmetric game (17) where, for every i in I, A_i is a compact metric space and U_i is a real-valued bounded function. For every i in I, consider the partition $P_{k_i} := \{A_{m_i}\}_{m_i=0}^{2^{k_i}-1}$ over A_i. For every i in I and a fixed profile $(a_{m_1}, ..a_{m_i}, ..., a_{m_n}) \in A_{m_1} \times \cdots \times A_{m_i} \times \cdots \times A_{m_n}$, the discrete approximation to U_i is given by the function

$$U_{k_i}(x_1, ..., x_i, ..., x_n) := U_i(a_{m_1}, ..a_{m_i}, ..., a_{m_n}),$$

if $(x_1, ..., x_i, ..., x_n)$ is in $A_{m_1} \times \cdots \times A_{m_i} \times \cdots \times A_{m_n}$. If for each i in I we can approximate any probability measure $\mu_i \in \mathbb{P}(A_i)$ by a discrete probability distribution μ_{k_i} on the partition set P_{k_i}, then we can write the approximation to the payoff function (11) as

$$J_{k_i}(\mu_{k_1}, ..., \mu_{k_n}) := \sum_{A_{m_1} \in P_{k_1}} ... \sum_{A_{m_n} \in P_{k_n}} U_i(a_{m_1}, ..., a_{m_n}) \mu_{k_n}(A_{m_n}) \cdots \mu_{k_1}(A_{m_1}). \quad (26)$$

For every $i \in I$ and every vector $\mu_k := (\mu_{k_1}, ..., \mu_{k_n})$ in $\mathbb{P}(P_{k_1}) \times ... \times \mathbb{P}(P_{k_n})$, we write μ_k as (μ_{k_i}, μ_{-k_i}), where $\mu_{k_{-i}} := (\mu_{k_1}, ..., \mu_{k_{i-1}}, \mu_{k_{i+1}}, ..., \mu_{k_n})$ is in $\mathbb{P}(P_{k_1}) \times ... \times \mathbb{P}(P_{k_{i-1}}) \times \mathbb{P}(P_{k_{i+1}}) \times ... \times \mathbb{P}(P_{k_n})$. Note that $\mu_k := (\mu_{k_1}, ..., \mu_{k_n})$ in $\mathbb{P}(P_{k_1}) \times ... \times \mathbb{P}(P_{k_n})$ is a vector of measures in $\mathbb{P}(A_1) \times ... \times \mathbb{P}(A_n)$. Then for any $i \in I$ and $E_i \in \mathcal{B}(A_i) \cap P_{k_i}$, the replicator induced by $\{U_{k_i}\}_{i \in I}$ has the following form:

$$\mu'_{k_i}(t, E_i) = \sum_{A_{m_i} \in E_i \cap P_{k_i}} \Big[J_{k_i}(a_{m_{k_i}}, \mu_{k_{-i}}(t)) - J_{k_i}(\mu_{k_i}(t), \mu_{k_{-i}}(t)) \Big] \mu_{k_i}(t, A_{m_i}), \quad (27)$$

which is equivalent to the system of differential equations in $\mathbb{R}^{2^{k_1}+...+2^{k_n}}$ of the form:

$$\mu'_{k_i}(t, A_{m_i}) = \Big[J_{k_i}(a_{m_i}, \mu_{k_{-i}}(t)) - J_{k_i}(\mu_{k_i}(t), \mu_{k_{-i}}(t)) \Big] \mu_{k_i}(t, A_{m_i}), \quad (28)$$

for $i = 1, 2, \ldots, n$ and $m_i = 0, 1, \ldots, 2^{k_i} - 1$, with initial condition $\{\mu_{k_i,0}(A_{m_i})\}_{m_i=0}^{2^{k_i}-1}$.

As in Sect. 4.1, using Theorem 1 or Theorem 2, we can approximate (14), (15) (with $F_i(\cdot)$ as (18)) by a system of differential equations in $\mathbb{R}^{2^{k_1}+...+2^{k_n}}$.

5 An Approximation Theorem in the Strong Form

In this section, we provide an approximation theorem that gives conditions under which we can approximate (14), (15) (with $F_i(\cdot)$ as in (18)) by a finite-dimensional dynamical system of the form (25) under the total variation norm (1).

The proof of this theorem uses the following two lemmas, which are proved in the appendix.

Lemma 1 *For each i in I, let A_i be a separable metric space. If each map $\mu_i : [0, \infty) \to \mathbb{M}(A_i)$ is* strongly differentiable*, then*

$$\frac{d\|\mu(t)\|_\infty}{dt} \leq \|\mu'(t)\|_\infty.$$

Proof See Appendix.

Lemma 2 *For each i in I, let A_i be a separable metric space and let $F(\cdot)$ be as in (14), (15) (with F_i as in (18)). Suppose that for each i in I the payoff function $U_i(\cdot)$*

in (18) is bounded. Then

$$\|F(\nu) - F(\mu)\|_\infty \leq Q\|\nu - \mu\|_\infty \quad \forall \mu, \nu \in \mathbb{P}(A_1) \times ... \times \mathbb{P}(A_n), \tag{29}$$

where $Q := (2n+1)H$ *and* $H := \max_{i \in I} \|U_i\|$.

Proof See Appendix.

Theorem 1 *For each* i *in* I, *let* A_i *be a separable metric space and let* $U_i, U_i^\epsilon : A_1 \times ... \times A_n \to \mathbb{R}$ *be bounded functions such that* $\max_{i \in I} \|U_i - U_i^\epsilon\| < \epsilon$, *where* $\|\cdot\|$ *is the sup norm in (2). Consider the replicator dynamics induced by* $\{U_i\}_{i=1}^n$ *and* $\{U_i^\epsilon\}_{i=1}^n$, *i.e.,*

$$\mu_i'(t, E_i) = \int_{E_i} \Big[J_i(a_i, \mu_{-i}(t)) - J_i(\mu_i(t), \mu_{-i}(t)) \Big] \mu_i(t, da_i), \tag{30}$$

$$\nu_i'(t, E_i) = \int_{E_i} \Big[J_i^\epsilon(a_i, \nu_{-i}(t)) - J_i^\epsilon(\nu_i(t), \nu_{-i}(t)) \Big] \nu_i(t, da_i), \tag{31}$$

for each $i \in I$, $E \in \mathcal{B}(A_i)$, *and* $t \geq 0$. *If* $\mu(\cdot)$ *and* $\nu(\cdot)$ *are solutions of (30) and (31), respectively, with initial conditions* $\mu(0) = \mu_0$ *and* $\nu(0) = \nu_0$, *then for* $T < \infty$

$$\sup_{t \in [0,T]} \|\mu(t) - \nu(t)\|_\infty < \|\mu_0 - \nu_0\|_\infty e^{QT} + 2\epsilon \left(e^{QT} - \frac{1}{Q} \right). \tag{32}$$

where $Q := (2n+1)H$ *and* $H := \max_{i \in I} \|U_i\|$.

Proof For each i in I and $t \geq 0$, let

$$\beta_i(a_i|\mu) := J_i(a_i, \mu_{-i}) - J_i(\mu_i, \mu_{-i}), \quad \beta_i^\epsilon(a_i|\nu_i) := J_i^\epsilon(a_i, \nu_{-i}) - J_i^\epsilon(\nu_i, \nu_{-i}),$$

and

$$F_i(\mu, E_i) := \int_{E_i} \beta_i(a_i|\mu)\mu_i(da_i), \qquad F_i^\epsilon(\nu, E_i) := \int_{E_i} \beta_i^\epsilon(a_i|\nu)\nu_i(da_i).$$

Since U_i is bounded, by Lemma 2 there exists $Q > 0$ such that

$$\|F(\nu) - F(\mu)\|_\infty \leq Q\|\nu - \mu\|_\infty \quad \forall \mu, \nu \in \mathbb{P}(A_1) \times ... \times \mathbb{P}(A_n). \tag{33}$$

Actually, $Q := (2n+1)H$ and $H := \max_{i \in I} \|U_i\|$. We also have that, for all $i \in I$ and $\nu \in \mathbb{P}(A_1) \times ... \times \mathbb{P}(A_n)$,

$$\|F_i(\nu) - F_i^\epsilon(\nu)\| \leq \int_{A_i} |\beta_i(a_i|\nu) - \beta_i^\epsilon(a_i|\nu)|\nu_i(da_i) \leq 2\|U_i - U_i^\epsilon\| \leq 2\epsilon,$$

so

$$\|F(\nu) - F^{\epsilon}(\nu)\|_{\infty} \leq 2\epsilon. \tag{34}$$

By Lemma 1 and (33), (34), we have

$$\begin{aligned}\frac{d\|\mu(t) - \nu(t)\|_{\infty}}{dt} &\leq \|\mu'(t) - \nu'(t)\|_{\infty} \\ &= \|F(\mu(t)) - F^{\epsilon}(\nu(t))\|_{\infty} \\ &\leq \|F(\mu(t)) - F(\nu(t))\|_{\infty} + \|F(\nu(t)) - F^{\epsilon}(\nu(t))\|_{\infty} \\ &\leq Q\|\mu(t) - \nu(t)\|_{\infty} + 2\epsilon.\end{aligned}$$

Then

$$\frac{d\|\mu(t) - \nu(t)\|_{\infty}}{dt} - Q\|\mu(t) - \nu(t)\|_{\infty} \leq 2\epsilon.$$

Multiplying by e^{-Qt} we get

$$\frac{d\|\mu(t) - \nu(t)\|_{\infty}e^{-Qt}}{dt} - Q\|\mu(t) - \nu(t)\|_{\infty}e^{-Qt} \leq 2\epsilon e^{-Qt},$$

and integrating in the interval $[0, t]$, where $t \leq T$, we get

$$\|\mu(t) - \nu(t)\|_{\infty}e^{-Qt} - \|\mu_0 - \nu_0\|_{\infty}e^{-Q0} \leq 2\epsilon\left(\frac{1 - e^{-Qt}}{Q}\right).$$

Then for all $t \in [0, T]$

$$\begin{aligned}\|\mu(t) - \nu(t)\|_{\infty} &= \|\mu_0 - \nu_0\|_{\infty}e^{Qt} + 2\epsilon\left(\frac{e^{Qt} - 1}{Q}\right) \\ &\leq \|\mu_0 - \nu_0\|_{\infty}e^{QT} + 2\epsilon\left(\frac{e^{QT} - 1}{Q}\right),\end{aligned}$$

which yields (32). □

Remark 2 The last argument in the proof of Theorem 1 is a particular case of the well-known Gronwall–Bellman inequality: If $f(\cdot)$ is nonnegative and $f'(t) \leq Qf(t) + c$ for all $t \geq 0$, where Q and c are nonnegative constants, then

$$f(t) \leq f(0)e^{Qt} + cQ^{-1}(e^{Qt} - 1) \text{ for all } t \geq 0.$$

For the reader's convenience, we included the proof here. □

Note 1 As in Sects. 4.1 and 4.2, consider a game with strategies in compact metric spaces. For each player $i \in I$ consider a partition P_{k_i} of A_i and suppose that the initial

condition $\mu_{i,0} \in \mathbb{P}(A_i)$ of (30) can be approximated in the variation norm by a discrete probability distribution $\mu_{k_i,0} \in \mathbb{P}(P_{k_i})$. Then for any $i \in I$ and $E_i \in \mathcal{B}(A_i) \cap P_{k_i}$, (31) can be written as (27) (or (24)), with U_i^{ϵ} as (26) (or (21)). So, in this particular case, (30) can be approximated by a system of differential equations in $\mathbb{R}^{2^{k_1}+\ldots+2^{k_n}}$ of the form (28).

Note 2 For the existence of the replicator dynamic, only the boundedness of the payoff functions is necessary (see Sect. 4 in [21]). So, the hypothesis of compactness on the set of strategies is not necessary in Theorem 1. Hence, the hypothesis of compactness on the set of strategies is also not necessary to approximate (30) by a finite-dimensional dynamical system. For example, it is sufficient that there exists a discrete probability distribution with finite values for any probability distribution over the set of strategies. For this last case, it is enough that for each $i \in I$, let A_i be a separable metric space, see Theorem 6.3, p. 44 in [26]. However, the compactness on the set of strategies ensures the existence of Nash equilibrium.

Corollary 1 *Let us assume the hypotheses of Theorem 1. Suppose that for each i in I, there exists a sequence of functions $\{U_i^{\epsilon_n}\}_{n=1}^{\infty}$ and probability measure vectors $\{\nu^n\}_{n=1}^{\infty}$ such that $\max_{i\in I} \|U_i - U_i^{\epsilon_n}\| \to 0$ and $\|\mu_0 - \nu_0^n\|_\infty \to 0$. If $\mu(\cdot)$ and $\nu^n(\cdot)$ are solutions of (30) and (31), respectively, with initial conditions $\mu(0) = \mu_0$ and $\nu^n(0) = \nu_0^n$, then for $T < \infty$,*

$$\lim_{n\to\infty} \sup_{t\in[0,T]} \|\mu(t) - \nu_n(t)\|_\infty = 0.$$

6 An Approximation Theorem in the Weak Form

The next approximation result, Theorem 2, establishes the proximity of two paths generated by two different dynamical systems (the original model and a discrete approximating model) with different initial conditions, under the weak topology. To this end we use the Kantorovich–Rubinstein norm $\|\cdot\|_{kr}$ on $\mathbb{M}(A)$, which metrizes the weak topology.

Remark 3 Let A be a separable metric space. We say that a mapping $\mu : [0, \infty) \to \mathbb{M}(A)$ is weakly differentiable if there exists $\mu'(t) \in \mathbb{M}(A)$ such that for every $t > 0$ and $g \in \mathbb{C}(A)$

$$\lim_{\epsilon\to 0} \frac{1}{\epsilon}\left[\int_A g(a)\mu(t+\epsilon, da) - \int_A g(a)\mu(t, da)\right] = \int_A g(a)\mu'(t, da). \tag{35}$$

If $\|\cdot\|_{k,r}$ is the Kantorovich–Rubinstein metric in (4), then (35) is equivalent to

$$\lim_{\epsilon\to 0} \left\| \frac{\mu(t+\epsilon) - \mu(t)}{\epsilon} - \mu'(t) \right\|_{kr} = 0. \tag{36}$$

Moreover if $\mu'(t)$ is the strong derivative of $\mu(t)$, then it is also the weak derivative of $\mu(t)$. Conversely, if $\mu'(t)$ is the weak derivative of $\mu(t)$ and $\mu(t)$ is continuous in t with the norm (1), then it is the strong derivative of $\mu(t)$. (See Heidergott, Hordijk, and Leahu [11].)

Lemma 3 *For each i in I, let A_i be a separable metric space. If each map $\mu_i : [0, \infty) \to \mathbb{M}(A_i)$ is* strongly differentiable*, then*

$$\frac{d\|\mu(t)\|_\infty^{kr}}{dt} \leq \|\mu'(t)\|_\infty^{kr}.$$

Proof The proof is similar to that of Lemma 1. □

Lemma 4 *For each i in I, consider a bounded separable metric space (A_i, ϑ_i) (with diameter $C_i > 0$) and the metric space $(A_1 \times ... \times A_n, \vartheta^*)$, where $\vartheta^*(a, b) = \max_{i \in I}\{\vartheta_i(a_i, b_i)\}$ for any a, b in $A_1 \times ... \times A_n$. Let $F(\cdot)$ be as in (14), (15) (with F_i as in (18)). For each i in I, suppose that the payoff function $U_i(\cdot)$ in (11) is bounded and satisfies that $\|U_i\|_L < \infty$. Then there exists $Q > 0$ such that*

$$\|F(\nu) - F(\mu)\|_\infty^{kr} \leq Q\|\nu - \mu\|_\infty^{kr} \tag{37}$$

for all $\mu, \nu \in \mathbb{P}(A_1) \times ... \times \mathbb{P}(A_n) \cap \mathbb{M}_K(A_1) \times ... \times \mathbb{M}_K(A_n)$, where $Q := [2H + (2n-1)CH_L]$, $H := \max_{i \in I} \|U_i\|$, $H_L := \max_{i \in I} \|U_i\|_L$, and $C := \max_{i \in I} C_i$.

Proof See Appendix.

Theorem 2 *For each i in I, let (A_i, ϑ_i) be a bounded separable metric space (with diameter $C_i > 0$), and $U_i, U_i^\epsilon : A_1 \times ... \times A_n \to \mathbb{R}$ be two bounded functions such that $\max_{i \in I} \|U_i - U_i^\epsilon\| < \epsilon$.. For each i in I, suppose that $\|U_i\|_L < \infty$ and consider the replicator dynamics induced by $\{U_i\}_{i=1}^n$ and $\{U_i^\epsilon\}_{i=1}^n$, as in (30) and (31). If $\mu(\cdot)$ and $\nu(\cdot)$ are solutions of (30) and (31), respectively, with initial conditions $\mu(0) = \mu_0$ and $\nu(0) = \nu_0$, then for $T < \infty$*

$$\sup_{t \in [0,T]} \|\mu(t) - \nu(t)\|_\infty^{kr} < \|\mu_0 - \nu_0\|_\infty^{kr} e^{QT} + 2\epsilon\left(e^{QT} - \frac{1}{Q}\right). \tag{38}$$

where $Q := [2H + (2n-1)CH_L]$, $H := \max_{i \in I} \|U_i\|$, $H_L := \max_{i \in I} \|U_i\|_L$, and $C := \max_{i \in I} C_i$.

Proof For each i in I and $t \geq 0$, let

$$\beta_i(a_i|\mu) := J_i(a_i, \mu_i) - J_i(\mu_i, \mu_{-i}), \quad \beta_i^\epsilon(a_i|\nu_i) := J_i^\epsilon(a_i, \nu_{-i}) - J_i^\epsilon(\nu_i, \nu_{-i}),$$

and

$$F_i(\mu, E_i) := \int_{E_i} \beta_i(a_i|\mu)\mu_i(da_i), \qquad F_i^\epsilon(\nu, E_i) := \int_{E_i} \beta_i^\epsilon(a_i|\nu)\nu_i(da_i).$$

By Lemma 4 there exists $Q > 0$ such that

$$\|F(\nu) - F(\mu)\|_\infty^{kr} \le Q\|\nu - \mu\|_\infty^{kr} \tag{39}$$

for all $\mu, \nu \in \mathbb{P}(A_1) \times ... \times \mathbb{P}(A_n) \cap \mathbb{M}_K(A_1) \times ... \times \mathbb{M}_K(A_n)$. Actually, $Q := [2H + (2n-1)CH_L], H := \max_{i\in I} \|U_i\|, H_L := \max_{i\in I} \|U_i\|_L$, and $C := \max_{i\in I} C_i$.

We also have that, for all i, in I and

$$\nu \in \mathbb{P}(A_1) \times ... \times \mathbb{P}(A_n) \cap \mathbb{M}_K(A_1) \times ... \times \mathbb{M}_K(A_n),$$

$$\begin{aligned}
\|F_i(\nu) - F_i^\epsilon(\nu)\|_{kr} &\le \sup_{\substack{\|f\|_L \le 1 \\ f(a_i^0)=0}} \int_{A_i} f(a_i)|\beta_i(a_i|\nu) - \beta_i^\epsilon(a_i|\nu)|\nu_i(da_i) \\
&\le 2\|U_i - U_i^\epsilon\| \sup_{\substack{\|f\|_L \le 1 \\ f(a_i^0)=0}} \int_{A_i} f(a_i)\nu_i(da_i) \\
&\le 2C\epsilon.
\end{aligned}$$

Then[1]

$$\|F(\nu) - F^\epsilon(\nu)\|_\infty^{kr} \le 2C\epsilon. \tag{40}$$

By Lemma 3 and (39), (40) we have

$$\begin{aligned}
\frac{d\|\mu(t) - \nu(t)\|_\infty^{kr}}{dt} &\le \|\mu'(t) - \nu'(t)\|_\infty^{kr} \\
&= \|F(\mu(t)) - F^\epsilon(\nu(t))\|_\infty^{kr} \\
&\le \|F(\mu(t)) - F(\nu(t))\|_\infty^{kr} + \|F(\nu(t)) - F^\epsilon(\nu(t))\|_\infty^{kr} \\
&\le Q\|\mu(t) - \nu(t)\|_\infty^{kr} + 2C\epsilon.
\end{aligned}$$

(See Remark 2 after Theorem 1.) The rest of the proof is similar to that done in Theorem 1. □

Note 3 As in Sects. 4.1 and 4.2, consider a game with strategies in compact metric spaces. For each player $i \in I$ let $\|U_i\|_L < \infty$ and consider a partition P_{k_i} of A_i.

[1] Note that if f satisfies that $\|f\|_L \le 1$ and $f(a_i^0) = 0$, then $f(a_i) \le \vartheta_i(a_i, a_i^0) \le C_i$ for all $a_i \in A_i$. Therefore $\sup_{\substack{\|f\|_L \le 1 \\ f(a_i^0)=0}} \int_{A_i} f(a_i)\nu_i(da_i) \le C$.

Suppose that the initial condition $\mu_{i,0} \in \mathbb{P}(A_i)$ of (30) can be approximated in the weak form by a discrete probability distribution $\mu_{k_i,0} \in \mathbb{P}(P_{k_i})$, then for any $i \in I$ and $E_i \in \mathcal{B}(A_i) \cap P_{k_i}$, (31) can be written as (27) (or (24)), with U_i^{ϵ} as (26) (or (21)). So, in this particular case, (30) can be approximated by a system of differential equations in $\mathbb{R}^{2^{k_1}+\cdots+2^{k_n}}$ of the form (28).

Corollary 2 *Let us assume the hypotheses of Theorem 2. Suppose that for each i in I, there exist a sequences of functions $\{U_i^{\epsilon_n}\}_{n=1}^{\infty}$ and of vectors of probability measures $\{\nu^n\}_{n=1}^{\infty}$ such that $\max_{i\in I} \|U_i - U_i^{\epsilon_n}\| \to 0$ and $\|\mu_0 - \nu_0^n\|_{\infty}^{kr} \to 0$. If $\mu(\cdot)$ and $\nu^n(\cdot)$ are solutions of (30) and (31), respectively, with initial conditions $\mu(0) = \mu_0$ and $\nu^n(0) = \nu_0^n$, then, for $T < \infty$,*

$$\lim_{n\to\infty} \sup_{t\in[0,T]} \|\mu(t) - \nu_n(t)\|_{\infty}^{kr} = 0.$$

7 Examples

7.1 A Linear-Quadratic Model: Symmetric Case

In this subsection, we consider a symmetric game in which we have two players with the following payoff function:

$$U(x, y) = -ax^2 - bxy + cx + dy, \tag{41}$$

with $a, b, c > 0$ and d any real number.

Let $A = [0, M]$, for $M > 0$, be the strategy set. If $2c(a - b) > 0$ and $4a^2 - b^2 > 0$, then we have an interior Nash equilibrium strategy (NES)

$$x^* = \frac{2c(a-b)}{4a^2 - b^2}.$$

Let $\mu(t)$ be the solution of the symmetric replicator dynamics induced by (41). Then if the initial condition is such that $\mu_0(x*) > 0$, we have that $\mu(t) \to \delta_{x^*}$ in distribution (see, [21–23]).

Consider a game where $a = 2,\ b = 1,\ c = 5,\ d = 1,\ M = 2$. For this game, the payoff function (41) is bounded Lipschitz and by Theorem 2 we can approximate the replicator dynamics by a finite-dimensional dynamical system of the form (25) under the Kantorovich–Rubinstein norm. Figure 1 shows a numerical approximation for this game where the Nash equilibrium is $x^* = 1$. For this numerical approximation, we consider a partition with 100 elements with the same size and use the forward Euler method for solving ordinary differential equations. We consider the uniform distribution as initial condition. We show the distribution for the times 0, 1000, and 2000.

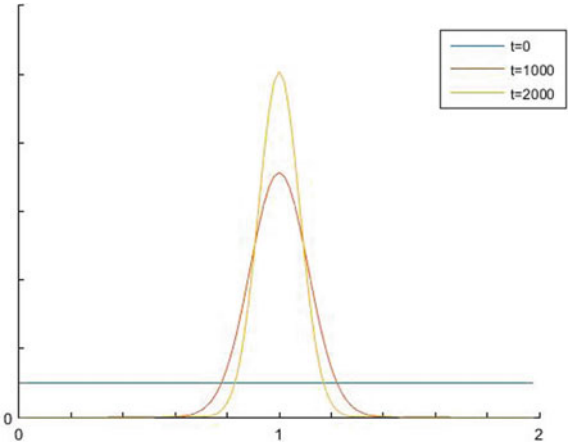

Fig. 1 Linear Quadratic Model: Symmetric Case

Note that, under the strong norm, the Nash equilibrium $x^* = 1$ cannot be approximated by any probability measure with continuous density function.

7.2 Graduated Risk Game

The graduated risk game is a symmetric game (proposed by Maynard Smith and Parker [20]), where two players compete for a resource of value $v > 0$. Each player selects the "level of aggression" for the game. This "level of aggression" is captured by a probability distribution $x \in [0, 1]$, where x is the probability that neither player is injured, and $\frac{1}{2}(1 - x)$ is the probability that player one (or player two) is injured. If the player is injured its payoff is $v - c$ (with $c > 0$), and hence the expected payoff for the player is

$$U(x, y) = \begin{cases} vy + \frac{v-c}{2}(1 - y) & \text{if } y > x, \\ \frac{v-c}{2}(1 - x) & \text{if } y \leq x, \end{cases} \tag{42}$$

where x and y are the "levels of aggression" selected by the player and her opponent, respectively.

If $v < c$, this game has a Nash equilibrium strategy with the density function

$$\frac{d\mu^*(x)}{dx} = \frac{\alpha - 1}{2} x^{\frac{\alpha-3}{2}}, \tag{43}$$

where $\alpha = \frac{c}{v}$ (see Maynard Smith and Parker [20], and Bishop and Cannings [1]).

Let $\mu(t)$ be the solution of the symmetric replicator dynamics induced by (42). Then, for any initial condition μ_0 with support $[0, 1]$, we have that $\mu(t) \to \delta_{x^*}$ in distribution (see [22]).

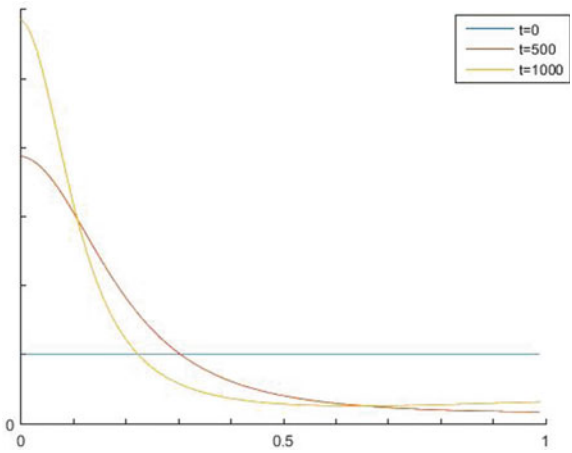

Fig. 2 Graduate Risk Game: Case $c = 10$; $v = 6 : 5$

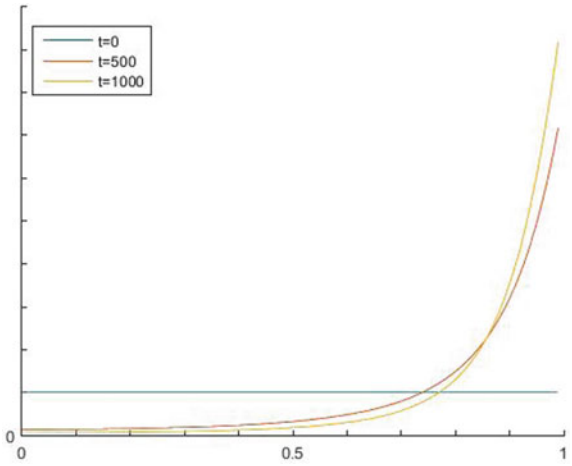

Fig. 3 Graduate Risk Game: Case $c = 10$; $v = 0 : 5$

Consider a game where $c = 10,\ v = 6.5$. For this game, the payoff function (42) is bounded, and by Theorem 1 we can approximate the replicator dynamics by a finite-dimensional dynamical system of the form (25) under the strong norm (1). Figure 2 shows a numerical approximation for this game. For this numerical approximation, we consider a partition with 100 elements with the same size, and use the forward Euler method for solving ordinary differential equations. We consider the uniform distribution as initial condition. We show the distribution for the times 0, 500, and 1000.

In the same way, Fig. 3 shows a numerical approximation for a game where $c = 10,\ v = 0.5$. For this numerical approximation, we consider a partition with 100 elements with the same size, and use the forward Euler method for solving ordinary differential equations. We consider the uniform distribution as initial condition. We show the distribution for the times 0, 500, and 1000.

8 Comments

In this paper, we introduced a model of asymmetric evolutionary games with strategies on measurable spaces. The model can be reduced, of course, to the symmetric case. We established conditions to approximate the replicator dynamics in a measure space by a sequence of dynamical systems on finite spaces. Finally, we presented two examples. The first one may be applicable to oligopoly models, theory of international trade, and public good models. The second example deals with a graduated risk game.

There are many questions, however, that remain open. For instance, the replicator dynamics has been studied in other general spaces without direct applications in game theory such as Kravvaritis et al. [15–18], and Papanicolaou and Smyrlis [25] studied conditions for stability and examples for these general cases. These extensions may be applicable in areas such as migration, regional sciences, and spatial economics (see Fujita et al. [10] Chaps. 5 and 6). An open question: can we establish conditions to approximate the replicator dynamics for general spaces by a sequence of dynamical systems on finite spaces?

In the theory of evolutionary games, there are several interesting dynamics, for instance, the imitation dynamics, the monotone-selection dynamics, the best-response dynamics, the Brown–von Neumann–Nash dynamics, and so forth (see, for instance, Hofbauer and Sigmund [13, 14], Sandholm [28]). Some of this evolutionary dynamics have been extended to games with strategies in a space of probability measures. For instance, Hofbauer et al. [12] extend the Brown–von Neumann–Nash dynamics; Lahkar and Riedel extend the logit dynamics [19]. These publications establish conditions for the existence of solutions and the stability of the corresponding dynamical systems. Cheung proposes a general theory for pairwise comparison dynamics [5] and for imitative dynamics [6]. Ruijgrok and Ruijgrok [27] extend the replicator dynamics with a mutation term. An open question: can we establish conditions to approximate other evolutionary dynamics for measurable spaces by a sequence of dynamical systems on finite spaces?

Acknowledgment This research was partially supported by the Fondo SEP-CINVESTAV grant FIDSC 2018/196.

Appendix: Proof of Lemmas

For the proof of Lemmas 2 and 4, it is convenient to rewrite (11) as

$$\mathcal{I}_{(\mu_1,\ldots,\mu_n)}U_i := \int_{A_1} \ldots \int_{A_n} U_i(a_1, \ldots, a_n)\mu_n(da_n)\ldots\mu_1(da_1). \tag{44}$$

Hence (12) becomes

$$J_i(a_i, \mu_{-i}) = \int_{A_{-i}} U_i(a_i, a_{-i})\mu_{-i}(da_{-i}) \qquad (45)$$
$$= \mathcal{I}_{(\mu_1,\ldots,\mu_{i-1},\mu_{i+1},\ldots,\mu_n)} U_i(a_i).$$

Proof of Lemma 1

We have the following inequalities:

$$\begin{aligned}
\frac{d\|\mu(t)\|_\infty}{dt} &= \frac{d}{dt}\max_{i\in I}[\|\mu_i(t)\|] \\
&= \lim_{\epsilon\to 0}\frac{1}{\epsilon}\left[\max_{i\in I}[\|\mu_i(t+\epsilon)\|] - \max_{i\in I}[\|\mu_i(t)\|]\right] \\
&\le \lim_{\epsilon\to 0}\frac{1}{\epsilon}\left[\max_{i\in I}[\|\mu_i(t+\epsilon)\| - \|\mu_i(t)\|]\right] \\
&\le \lim_{\epsilon\to 0}\frac{1}{\epsilon}\left[\max_{i\in I}[\|\mu_i(t+\epsilon) - \mu_i(t)\|]\right] \\
&= \max_{i\in I}\left[\lim_{\epsilon\to 0}\left\|\frac{\mu_i(t+\epsilon)-\mu_i(t)}{\epsilon}\right\|\right] \\
&= \max_{i\in I}\left[\|\mu_i'(t)\|\right] \\
&= \|\mu'(t)\|.
\end{aligned}$$

□

Proof of Lemma 2

For any i in I and μ, ν in $\mathbb{P}(A_1)\times\ldots\times\mathbb{P}(A_1)$, using (44) we obtain

$$\begin{aligned}
&\left|\int_A U_i(a)\eta(da) - \int_A U_i(a)\nu(da)\right| \\
&\quad\le |\mathcal{I}_{(\eta_1,\eta_2,\ldots,\eta_n)}U_i - \mathcal{I}_{(\nu_1,\eta_2,\ldots,\eta_n)}U_i| \\
&\qquad + |\mathcal{I}_{(\nu_1,\eta_2,\eta_3,\ldots,\eta_n)}U_i - \mathcal{I}_{(\nu_1,\nu_2,\eta_3,\ldots,\eta_n)}U_i| \\
&\qquad + \ \ldots \\
&\qquad + |\mathcal{I}_{(\nu_1,\ldots,\nu_{n-2},\eta_{n-1},\eta_n)}U_i - \mathcal{I}_{(\nu_1,\ldots,\nu_{n-2},\nu_{n-1},\eta_n)}U_i| \\
&\qquad + |\mathcal{I}_{(\nu_1,\ldots,\nu_{n-1},\eta_n)}U_i - \mathcal{I}_{(\nu_1,\ldots,\nu_{n-1},\nu_n)}U_i| \\
&\quad\le \|U_i\|\|\eta_2\times\ldots.\times\eta_n\|\|\eta_1-\nu_1\| \\
&\qquad + \|U_i\|\|\nu_1\times\eta_3\times\ldots\times\eta_n\|\|\eta_2-\nu_2\| \\
&\qquad + \ \ldots \\
&\qquad + \|U_i\|\|\nu_1\times\ldots\times\nu_{n-2}\times\eta_n\|\|\eta_{n-1}-\nu_{n-1}\|
\end{aligned}$$

$$
\begin{aligned}
&+ \|U_i\| \|\nu_1 \times .... \times \nu_{n-1}\| \|\eta_n - \nu_n\| \\
&\leq n \|U_i\| \max_{j \in I} \|\eta_j - \nu_j\|. \qquad (46)
\end{aligned}
$$

Similarly, using (45),

$$
|J_i(a_i, \mu_{-i}) - J_i(a_i, \nu_{-i})| \leq (n-1)\|U_i\| \|\mu - \nu\|_\infty. \qquad (47)
$$

Using (46) and (47), we have

$$
\begin{aligned}
\|F_i(\mu) - F_i(\nu)\|_\infty &= \sup_{\|f\| \leq 1} \int_{A_i} f(a_i)[F_i(\mu) - F_i(\nu)](da_i) \\
&\leq \sup_{\|f\| \leq 1} \int_{A_i} f(a_i)|J_i(a_i, \mu_{-i})|[\mu_i - \nu_i](da) \\
&\quad + \sup_{\|f\| \leq 1} \int_{A_i} f(a_i)|J_i(a_i, \mu_{-i}) - J_i(a_i, \nu_{-i})|\nu_i(da) \\
&\quad + \sup_{\|f\| \leq 1} \int_{A} f(a_i)|J_i(\mu_i, \mu_{-i})|[\nu_i - \mu_i](da) \\
&\quad + \sup_{\|f\| \leq 1} \int_{A} f(a_i)|J_i(\nu_i, \nu_{-i}) - J(\mu_i, \mu_{-i})|\nu_i(da) \\
&\leq \|U_i\| \|\mu_i - \nu_i\| + (n-1)\|U_i\| \|\mu - \nu\|_\infty \|\nu_i\| \\
&\quad + \|U_i\| \|\mu_i - \nu_i\| + n\|U_i\| \|\mu - \nu\|_\infty \|\nu_i\| \\
&\leq H\|\mu - \nu\|_\infty + (n-1)H\|\mu - \nu\|_\infty + H\|\mu - \nu\|_\infty + nH\|\mu - \nu\|_\infty \\
&= (2n+1)H\|\mu - \nu\|_\infty,
\end{aligned}
$$

where $H := \max_{i \in I} \|U_i\|$. □

Proof of Lemma 4

For any i and j in I and a_{-j} in A_{-j} let

$$
\|U_i(\cdot, a_{-j})\|_L := \sup_{a_j, b_j \in A_j} \frac{|U_i(a_j, a_{-j}) - U_i(b_j, a_{-j})|}{\vartheta^*((a_j, a_{-j}), (b_j, a_{-j}))} \leq \|U_i\|_L, \quad \text{and}
$$

$$
U_i^j := \frac{U_i(a_j, a_{-j})}{\|U_i(\cdot, a_{-j})\|_L}.
$$

Then for any i in I and μ, ν in $\mathbb{P}(A_1) \times ... \times \mathbb{P}(A_1)$, using (44) we see that

$$\left|\int_A U_i(a)\eta(da) - \int_A U_i(a)\nu(da)\right|$$

$$\begin{aligned}
&\leq \|U_i(\cdot, a_{-1})\|_L |\mathcal{I}_{(\eta_1,\eta_2,\ldots,\eta_n)} U_i^1 - \mathcal{I}_{(\nu_1,\eta_2,\ldots,\eta_n)} U_i^1| \\
&\quad + \|U_i(\cdot, a_{-2})\|_L |\mathcal{I}_{(\nu_1,\eta_2,\eta_3,\ldots,\eta_n)} U_i^2 - \mathcal{I}_{(\nu_1,\nu_2,\eta_3,\ldots,\eta_n)} U_i^2| \\
&\quad + \ \ldots \\
&\quad + \|U_i(\cdot, a_{-(n-1)})\|_L |\mathcal{I}_{(\nu_1,\ldots,\nu_{n-2},\eta_{n-1},\eta_n)} U_i^{n-1} - \mathcal{I}_{(\nu_1,\ldots,\nu_{n-2},\nu_{n-1},\eta_n)} U_i^{n-1}| \\
&\quad + \|U_i(\cdot, a_{-n})\|_L |\mathcal{I}_{(\nu_1,\ldots,\nu_{n-1},\eta_n)} U_i^n - \mathcal{I}_{(\nu_1,\ldots,\nu_{n-1},\nu_n)} U_i^n| \\
&\leq \|U_i\|_L \|\eta_2 \times \ldots. \times \eta_n\| \|\eta_1 - \nu_1\|_{kr} \\
&\quad + \|U_i\|_L \|\nu_1 \times \eta_3 \times \ldots \times \eta_n\| \|\eta_2 - \nu_2\|_{kr} \\
&\quad + \ \ldots \\
&\quad + \|U_i\|_L \|\nu_1 \times \ldots \times \nu_{n-2} \times \eta_n\| \|\eta_{n-1} - \nu_{n-1}\|_{kr} \\
&\quad + \|U_i\|_L \|\nu_1 \times \ldots. \times \nu_{n-1}\| \|\eta_n - \nu_n\|_{kr} \\
&\leq n\|U_i\|_L \|\eta_j - \nu_j\|_\infty^{kr}. \qquad (48)
\end{aligned}$$

Similarly, using (45),

$$|J_i(a_i, \mu_{-i}) - J_i(a_i, \nu_{-i})| \leq (n-1)\|U_i\|_L \|\mu - \nu\|_\infty^{kr}. \qquad (49)$$

Using (48) and (49) we have

$$\|F_i(\mu) - F_i(\nu)\|_{kr}$$

$$\begin{aligned}
&= \sup_{\substack{\|f\|_L \leq 1 \\ f(a_0)=0}} \int_{A_i} f(a_i)[F_i(\mu) - F_i(\nu)](da_i) \\
&\leq \sup_{\substack{\|f\|_L \leq 1 \\ f(a_0)=0}} \int_{A_i} f(a_i)|J_i(a_i, \mu_{-i})|[\mu_i - \nu_i](da) \\
&\quad + \sup_{\substack{\|f\|_L \leq 1 \\ f(a_0)=0}} \int_{A_i} f(a_i)|J_i(a_i, \mu_{-i}) - J_i(a_i, \nu_{-i})|\nu_i(da) \\
&\quad + \sup_{\substack{\|f\|_L \leq 1 \\ f(a_0)=0}} \int_{A} f(a_i)|J_i(\mu_i, \mu_{-i})|[\nu_i - \mu_i](da) \\
&\quad + \sup_{\substack{\|f\|_L \leq 1 \\ f(a_0)=0}} \int_{A} f(a_i)|J_i(\nu_i, \nu_{-i}) - J(\mu_i, \mu_{-i})|\nu_i(da) \\
&\leq \|U_i\| \|\mu_i - \nu_i\|_{kr} + (n-1)\|U_i\|_L \|\mu - \nu\|_\infty^{kr} \sup_{\substack{\|f\|_L \leq 1 \\ f(a_0)=0}} \int_{A_i} f(a_i)\nu_i(da_i)
\end{aligned}$$

$$+ \|U_i\|\|\mu_i - \nu_i\|_{kr} + n\|U_i\|_L\|\mu - \nu\|_\infty^{kr} \sup_{\substack{\|f\|_L \le 1 \\ f(a_0)=0}} \int_{A_i} f(a_i)\nu_i(da_i)$$

$$\le 2H\|\mu - \nu\|_\infty^{kr} + (2n-1)H_L\|\mu - \nu\|_\infty^{kr} C_i$$

$$= [2H + (2n-1)CH_L]\|\mu - \nu\|_\infty,$$

where $H := \max_{i\in I} \|U_i\|$, $H_L := \max_{i\in I} \|U_i\|_L$, and $C := \max_{i\in I} C_i$. □

References

1. D. Bishop and C. Cannings. A generalized war of attrition. *Journal of Theoretical Biology*, 70(1):85–124, 1978.
2. V. I. Bogachev. *Measure theory*, volume 2. Berlin, 2007.
3. I. M. Bomze. Dynamical aspects of evolutionary stability. *Monatshefte für Mathematik*, 110(3-4):189–206, 1990.
4. I. M. Bomze. Cross entropy minimization in uninvadable states of complex populations. *Journal of Mathematical Biology*, 30(1):73–87, 1991.
5. M.-W. Cheung. Pairwise comparison dynamics for games with continuous strategy space. *Journal of Economic Theory*, 153:344–375, 2014.
6. M.-W. Cheung. Imitative dynamics for games with continuous strategy space. *Games and Economic Behavior*, 99:206–223, 2016.
7. J. Cleveland and A. S. Ackleh. Evolutionary game theory on measure spaces: well-posedness. *Nonlinear Analysis: Real World Applications*, 14(1):785–797, 2013.
8. R. Cressman and J. Hofbauer. Measure dynamics on a one-dimensional continuous trait space: theoretical foundations for adaptive dynamics. *Theoretical Population Biology*, 67(1):47–59, 2005.
9. I. Eshel and E. Sansone. Evolutionary and dynamic stability in continuous population games. *Journal of Mathematical Biology*, 46(5):445–459, 2003.
10. M. Fujita, P. R. Krugman, and A. J. Venables. *The spatial economy: cities, regions, and international trade*. MIT press, 2001.
11. B. Heidergott and H. Leahu. Weak differentiability of product measures. *Mathematics of Operations Research*, 35(1):27–51, 2010.
12. J. Hofbauer, J. Oechssler, and F. Riedel. Brown–von neumann–nash dynamics: The continuous strategy case. *Games and Economic Behavior*, 65(2):406–429, 2009.
13. J. Hofbauer and K. Sigmund. *Evolutionary games and population dynamics*. Cambridge University Press, Cambridge, 1998.
14. J. Hofbauer and K. Sigmund. Evolutionary game dynamics. *Bulletin of the American Mathematical Society*, 40(4):479–519, 2003.
15. D. Kravvaritis, V. Papanicolaou, A. Xepapadeas, and A. Yannacopoulos. On a class of operator equations arising in infinite dimensional replicator dynamics. *Nonlinear Analysis: Real World Applications*, 11(4):2537–2556, 2010.
16. D. Kravvaritis, V. Papanicolaou, T. Xepapadeas, and A. Yannacopoulos. A class of infinite dimensional replicator dynamics. In *Dynamics, Games and Science*, volume I, pages 529–532. Springer, 2011.
17. D. Kravvaritis and V. G. Papanicolaou. Singular equilibrium solutions for a replicator dynamics model. *Electronic Journal of Differential Equations*, 2011(87):1–8, 2011.
18. D. Kravvaritis, V. G. Papanicolaou, and A. N. Yannacopoulos. Similarity solutions for a replicator dynamics equation. *Indiana University Mathematics Journal*, 57(4):1929–1945, 2008.
19. R. Lahkar and F. Riedel. The logit dynamic for games with continuous strategy sets. *Games and Economic Behavior*, 2015.

20. J. Maynard Smith and G. A. Parker. The logic of asymmetric contests. *Animal Behaviour*, 24(1):159–175, 1976.
21. S. Mendoza-Palacios and O. Hernández-Lerma. Evolutionary dynamics on measurable strategy spaces: asymmetric games. *Journal of Differential Equations*, 259(11):5709–5733, 2015.
22. S. Mendoza-Palacios and O. Hernández-Lerma. Stability of the replicator dynamics for games in metric spaces. *Journal of Dynamics and Games*, 4(4):–, 2017.
23. J. Oechssler and F. Riedel. Evolutionary dynamics on infinite strategy spaces. *Economic Theory*, 17(1):141–162, 2001.
24. J. Oechssler and F. Riedel. On the dynamic foundation of evolutionary stability in continuous models. *Journal of Economic Theory*, 107(2):223–252, 2002.
25. V. G. Papanicolaou and G. Smyrlis. Similarity solutions for a multi-dimensional replicator dynamics equation. *Nonlinear Analysis: Theory, Methods & Applications*, 71(7):3185–3196, 2009.
26. K. R. Parthasarathy. *Probability measures on metric spaces*. Academic Press, New York, 1967.
27. M. Ruijgrok and T. W. Ruijgrok. An effective replicator equation for games with a continuous strategy set. *Dynamic Games and Applications*, pages 157–179, 2015.
28. W. H. Sandholm. *Population games and evolutionary dynamics*. MIT press, 2010.
29. L. K. Simon. Games with discontinuous payoffs. *The Review of Economic Studies*, 54(4):569–597, 1987.
30. M. Van Veelen and P. Spreij. Evolution in games with a continuous action space. *Economic Theory*, 39(3):355–376, 2009.

Eco-evolutionary Spatial Dynamics of Nonlinear Social Dilemmas

Chaitanya S. Gokhale and Hye Jin Park

1 Introduction

The most significant impact of evolutionary game theory has been in the field of social evolution. When an individual's action results in a conflict between the individual and the group benefit, a social dilemma arises. Social dilemmas can be captured by the two-player prisoners dilemma game [6] and its multiplayer version, the public goods game [8, 17, 24]. The domain of public goods games ranges from behavioural economists, cognitive scientists, psychologists, to biologists given the ubiquity of multiplayer interactions in nature. Situations impossible in two-player games can occur in multiplayer games, which can lead to drastically different evolutionary outcomes [7, 14, 35, 39, 44, 52].

In public goods games, while cooperation raises the group benefit, cooperators themselves get less benefit than defectors. The group benefit typically increases linearly with the number of cooperators in the group. However, in the context of helping behaviour, reference [10] discusses a case where each additional cooperator in the group provides more benefit than the previous (superadditivity of benefit). The approach has been further generalised using a particular nonlinear function where the additional cooperators can provide not only more (synergy) but also less (discounting) benefit than the previous cooperator [20]. The study [5] presents an excellent review of the use and importance of nonlinear public goods game.

The nonlinear public goods game as proposed in [20] has been extended in [13] to include population dynamics. In ecological public goods games, the total density of cooperators and defectors changes, effectively changing the interaction group

C. S. Gokhale (✉)
Research Group for Theoretical Models of Eco-evolutionary Dynamics, Department of Evolutionary Theory, Max Planck Institute for Evolutionary Biology, August Thienemann Str-2, 24306 Plön, Germany
e-mail: gokhale@evolbio.mpg.de

H. J. Park
Department of Evolutionary Theory, Max Planck Institute for Evolutionary Biology, August Thienemann Str-2, 24306 Plön, Germany

D. M. Ramsey and J. Renault (eds.), *Advances in Dynamic Games*,
Annals of the International Society of Dynamic Games 17,
https://doi.org/10.1007/978-3-030-56534-3_8

size. Changes in group size have been shown to result in a stable coexistence of cooperators and defectors [19, 30, 38]. A spatial version of ecological public goods games, where multiple populations of cooperators and defectors are present on a lattice and connected by diffusion, can promote cooperation [53]. The spread of cooperation, in such a case, is possible by a variety of pattern-forming processes.

They use of spatially extended system in different forms such as grouping, explicit space and deme structures, and other ways of limiting interactions have been studied for long [18, 33, 40, 45, 47, 55]. In particular, in [29], the authors provide conditions for strategy selection in nonlinear games about population structure coefficients. The study cited above by [53] while incorporating ecological dynamics focusses solely on linear public goods games.

Previously we have combined a linear social dilemma with density-dependent diffusion coefficients [12, 37]. Including a dynamic diffusion coefficient comes closer to analysing real movements seen across species from bacteria to humans [16, 23, 27, 28, 32, 34, 43]. Incorporating aspects of ecological games as in [19], spatial dynamics per [53] and nonlinear social dilemmas from [13] we develop our previous approach in this study to nonlinear social dilemmas.

We begin by introducing nonlinearity in the payoff function of the social dilemma, including population dynamics. Then we include simple diffusion dynamics and analyse the resulting spatial patterns. For the parameter set comprising of the diffusion coefficients and the multiplication factor, we can observe the extinction, heterogenous or homogenous non-extinction patterns. Under certain simplifying assumptions, we can also characterise the stability of the fixed point and discuss the dynamics of the Hopf-bifurcation transition and the phase boundary between heterogenous- and homogenous-patterned phases. Overall, our results suggest that the spatial patterns while remaining in the same regions relative to each other in the parameter space, synergy and discounting effects shift the boundaries including the phase boundary between extinction and surviving phases. For synergy, the extinction region shrinks as the effective benefit increases resulting in an increased possibility of cooperator persistence. For discounting, however, the extinction region expands. Crucially, the change in the extinction region is not symmetric for synergy and discounting. The above asymmetry is due to the asymmetries in the nonlinear function that we employ for calculating the benefit. The development will help contrast the results with the work of [53] and relates our work to realistic public goods scenarios where the contributions often have a nonlinear impact [9].

2 Model and Results

2.1 Nonlinear Public Goods Game

Complexity of evolutionary games increases as we move from two-player games to multiplayer games [14]. A similar trend ensues as we move from linear public

goods games to nonlinear payoff structures [5]. One of the ways of moving from linear to nonlinear multiplayer games is given in [20]. To introduce this method in our notational form, we will first derive the payoffs in a linear setting.

In the classical version of the public goods game (PGG), the cooperators invest c to the common pool while the defectors contribute nothing. The value of the pool increases by a certain multiplication factor r, $1 < r < N$, where N is the group size. The amplified returns are equally distributed to all the N players in the game. For such a setting, the payoffs for cooperators and defectors are given by

$$\begin{aligned} P_D(m) &= \frac{rcm}{N}, \\ P_C(m) &= \frac{rcm}{N} - c, \end{aligned} \tag{1}$$

where m is the number of cooperators in the group. The nonlinearity in the payoffs can be introduced by the parameter Ω as in [20],

$$\begin{aligned} P_D(m) &= \frac{rc}{N}(1 + \Omega + \Omega^2 + \ldots + \Omega^{m-1}) = \frac{rc}{N}\frac{1-\Omega^m}{1-\Omega}, \\ P_C(m) &= P_D(m) - c = \frac{rc}{N}\Omega(1 + \Omega + \ldots + \Omega^{m-2}) + \frac{rc}{N} - c. \end{aligned} \tag{2}$$

If $\Omega > 1$ every additional cooperator contributes more than the previous, thus providing a synergistic effect. If $\Omega < 1$ then every additional cooperator contributes less than the previous, thus saturating the benefits and providing a discounting effect. The linear version of the PGG can be recovered by setting $\Omega = 1$.

As in [19] besides the evolutionary dynamics (change in the frequency of cooperators over time), we are also interested in the ecological dynamics (change in the population density over time). This system analysed in [19, 21] is briefly reintroduced in our notation for later extension. We characterise the densities of cooperators and defectors in the population as u and v. Thus $0 \leq u + v \leq 1$ and the empty space is given by $w = 1 - u - v$. Low population density means that it is hard to encounter other individuals and accordingly hard to interact with them. Hence, the group size N, the maximum group size, in this case, is not always reachable. Instead, S individuals form an interacting group. With fixed N the interacting group size S is bounded, $S \leq N$, and the probability $p(S; N)$ of interacting with $S - 1$ individuals is depending on the total population density $u + v = 1 - w$. When we consider the focal individual, the probability $p(S; N)$ of interacting with $S - 1$ individuals among a maximum group of size $N - 1$ individuals (excluding the focal individual),

$$p(S; N) = \binom{N-1}{S-1}(1-w)^{S-1}w^{N-S}. \tag{3}$$

Then, the average payoffs for defectors and cooperators, f_D and f_C, are given as

$$f_D = \sum_{S=2}^{N} p(S; N)\overline{P_D}(S),$$
$$f_C = \sum_{S=2}^{N} p(S; N)\overline{P_C}(S), \tag{4}$$

where $\overline{P_D}(S)$ and $\overline{P_C}(S)$ are the expected payoffs for defectors and cooperators at a given S. The sum for the group sizes S starts at two as for a social dilemma there need to be at least two interacting individuals.

To derive the expected payoffs, we first need to assess the probability of having a certain number of cooperators m in a group of size $S-1$ which is given by $p_c(m; S)$,

$$p_c(m; S) = \binom{S-1}{m} \left(\frac{u}{1-w}\right)^m \left(\frac{v}{1-w}\right)^{S-1-m}. \tag{5}$$

Thus, the payoffs in Eq. (2) are weighted with the probability of there being m cooperators, giving us the expected payoffs,

$$\overline{P_D}(S) = \sum_{m=0}^{S-1} p_c(m; S)P_D(m),$$
$$\overline{P_C}(S) = \sum_{m=0}^{S-1} p_c(m; S)P_C(m+1). \tag{6}$$

The average payoffs f_D and f_C are thus given by

$$f_D = \frac{r}{N}\frac{1}{1-w-u(1-\Omega)}\left[\frac{(u(\Omega-1)+1)^N-1}{\Omega-1} - \frac{u(1-w^N)}{1-w}\right],$$
$$f_C = f_D - 1 - (r-1)w^{N-1} + \frac{r}{N}\frac{(1-u(1-\Omega))^N - w^N}{1-w-u(1-\Omega)}, \tag{7}$$

where the investment cost has been set to $c = 1$ without loss of generality. Again, the linear version of the PGG can be recovered by setting $\Omega = 1$,

$$f_D = \frac{ru}{1-w}\left[1 - \frac{(1-w^N)}{N(1-w)}\right],$$
$$f_C = f_D - 1 - (r-1)w^{N-1} + \frac{r}{N}\frac{1-w^N}{1-w}. \tag{8}$$

2.2 *Spatial Nonlinear Public Goods Games*

For tracing the population dynamics, we are interested in the change in the densities of cooperators and defectors over time. Both cooperators and defectors are assumed to have a baseline birth rate of b and death rate of d. Growth is possible only when

there is empty space available, i.e. $w > 0$. We track the densities of cooperators and defectors by an extension of the replicator dynamics [19, 22, 48],

$$\begin{aligned} \dot{u} &= u[w(f_C + b) - d], \\ \dot{v} &= v[w(f_D + b) - d]. \end{aligned} \tag{9}$$

To include spatial dynamics in the above system, we assume that a population of cooperators and defectors resides in a given patch. Game interactions only occur within patches, and the individuals can move adjacent patches. The patches live in a two-dimensional space connected in the form of a regular lattice. Taking a continuum limit, we obtain the differential equations with constant diffusion coefficients for cooperators D_c and defectors D_d,

$$\begin{aligned} \dot{u} &= D_c \nabla^2 u + u[w(f_C + b) - d], \\ \dot{v} &= D_d \nabla^2 v + v[w(f_D + b) - d]. \end{aligned} \tag{10}$$

At the boundaries, there is no in- and out-flux. As in classical activator-inhibitor systems, the different ratio of the diffusion coefficients $D = D_d/D_c$ can generate various patterns from coexistence, extinction as well as chaos [53].

Nonlinearity in PGG is implemented by $\Omega \neq 1$. Previous work shows that the introduction of Ω is enriching the dynamics [13, 20]. Synergy ($\Omega > 1$) enhances cooperation while discounting ($\Omega < 1$) suppresses it. Accordingly, synergy and discounting with a multiplication factor r can map into the linear game with the higher or lower multiplication factor r', respectively: $r' > r$ for synergy and $r' < r$ for discounting. We call r' as the effective multiplication factor. As shown in Fig. 1, for synergy effect ($\Omega = 1.1$), we can find a chaotic coexistence of cooperators and defectors. The same parameter for a linear case ($\Omega = 1.0$) resulted in total extinction of the population [53]. In the linear case, chaotic patterns were observed for r values larger than that of extinction patterns. Thus, our observation implies the mechanism of how synergy works by effectively increasing r value.

The change in the resulting patterns due to synergy or discounting is not limited to extinction or chaos but is a general feature of the nonlinearity in payoffs. To illustrate this change, we show how a stable pattern under linear PGG ($\Omega = 1$) can change the shape under discounting or synergy in Fig. 2. Such changes in the final structure happen all over the parameter space. To confirm this tendency, we examine the spatial patterns for various parameters and find five phases, same as in the linear PGG case [53] but now with shifted phase boundaries (see Fig. 3). The effective multiplication factor r' increases with an increasing Ω, and thus the location of the Hopf bifurcation also shifts. As a result of shifting r_{Hopf}, extinction region is reduced in the parameter space with synergy effect. We thus focus our attention on the Hopf-bifurcation point r_{Hopf}.

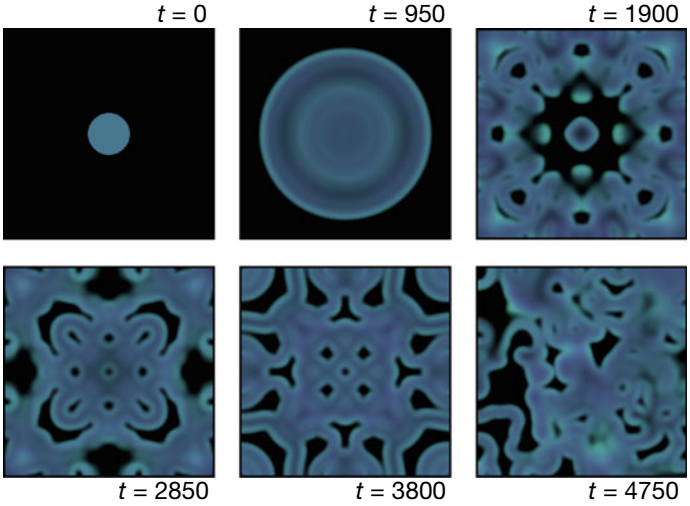

Fig. 1 Pattern formation on the two-dimensional square lattice. We observe the chaotic pattern for $\Omega = 1.1$ (synergy effect) where extinction comes out with $\Omega = 1$ [53]. Mint green and Fuchsia pink colours represent the cooperator and defector densities, respectively. For a full explanation of the colour scheme, we refer to the appendix. Black indicates no individual on the site, whereas blue appears when the ratio of cooperators and defectors is the same. For a system of size L, initially, a disc with radius $L/10$ at the centre is occupied by cooperator and defector with densities 0.1. We use multiplication factor $r = 2.2$ and diffusion coefficient ratio $D = 2$. Throughout the paper, for simulations, we used the system size $L = 283$, $dt = 0.1$ and $dx = 1.4$ with the Crank–Nicolson algorithm

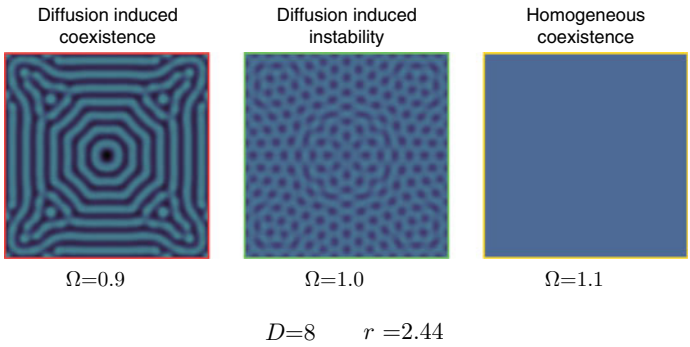

Fig. 2 Synergy and discounting effects on pattern formation. We get the different patterns under discounting and synergy effects distinct from the linear PGG game at a given the same parameter set. While diffusion-induced instability is observed in the linear PGG, the discounting effect makes diffusion-induced coexistence pattern implying that the discounting effect makes the Hopf-bifurcation point shift to the larger value. Under the synergy effect, on the contrary, we obtain the opposite trend observing the homogenous coexistence pattern. In the linear PGG, the homogenous patterns are observed in higher multiplication factor r, implying the shift of r_{Hopf} to the smaller value under the synergy effect

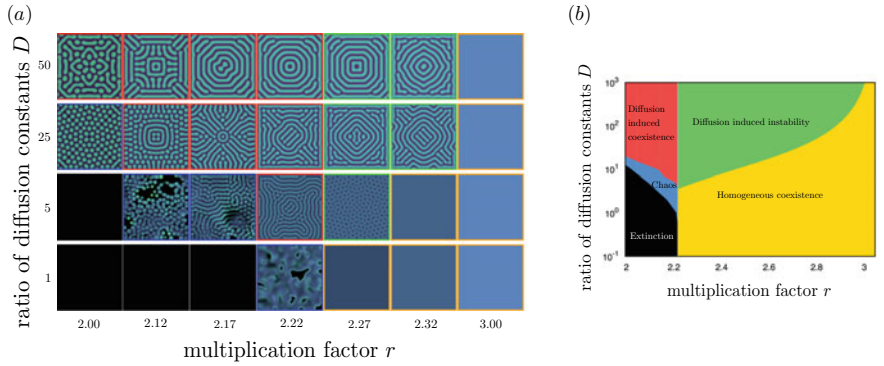

Fig. 3 Spatial patterns and corresponding phase diagram for $\Omega = 1.1$. There are five phases (framed using different colours), extinction (black), chaos (blue), diffusion-induced coexistence (red), diffusion-induced instability (green) and homogeneous coexistence (orange). The Hopf-bifurcation point $r_{\mathrm{Hopf}} \simeq 2.2208$ and the boundary between diffusion-induced instability and homogeneous coexistence are analytically calculated, while the other boundaries are from the simulation results. All boundaries and r_{Hopf} shift to the left, indicating that the multiplication factor r with the synergy maps into the higher multiplication factor r' in the linear game

2.2.1 Hopf Bifuraction in Nonlinear PGG

We find the Hopf-bifurcation point r_{Hopf} for various Ω values using Eq. (7). The effective multiplication factor r' increases as Ω increases, and thus r_{Hopf} is monotonically decreasing with Ω as in Fig. 4a. The tangential line at $\Omega = 1$

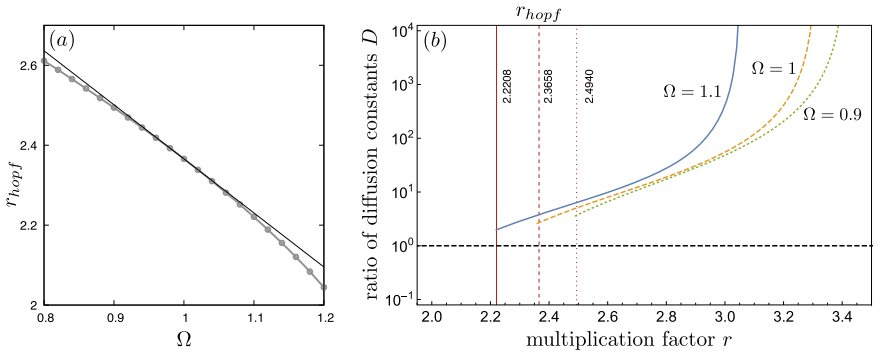

Fig. 4 Hopf-bifurcation points in Ω and **shift of the phase boundary. a** The Hopf-bifurcation point r_{Hopf} for various Ω (solid line with points). Synergy ($\Omega > 1$) decreases r_{Hopf} while discounting ($\Omega < 1$) increases r_{Hopf}. By decreasing r_{Hopf}, the surviving region is extended in the parameter space. The solid line without points is a tangential line at $\Omega = 1$. **b** The phase boundaries between diffusion-induced instability and homogeneous coexistence phases are also examined for various Ω. Since r_{Hopf} increases with a decreasing Ω, the boundaries also move to the right

is drawn for comparing the effects of synergy and discounting. If we focus on the differences between the tangent and r_{Hopf} line, synergy changes r_{Hopf} more dramatically than discounting. Synergy and discounting effects originate from $1 + (1 \pm \Delta\Omega) + (1 \pm \Delta\Omega)^2 + \cdots + (1 \pm \Delta\Omega)^{m-1}$ in Eq. (2), where $\Delta\Omega > 0$ and plus and minus signs for synergy and discounting, respectively. Straightforwardly, the difference between 1 and $(1 + \Delta\Omega)^k$ is larger than that of $(1 - \Delta\Omega)^k$ for $k > 2$. Hence, the nonlinear PGG itself gives different Δr_{Hopf} for the same $\Delta\Omega$.

2.2.2 Criterion for Diffusion-Induced Instability

Since Ω changes r' value, the phase boundary also moves. By using the linear stability analysis, we find phase boundaries between diffusion-induced instability and homogeneous coexistence phases in r-D space shown in Fig. 4b. To do that, we introduce new notations, and two reaction–diffusion equations in Eq. (10) can be written as

$$\partial_t \mathbf{u} = \mathbf{D}\nabla^2\mathbf{u} + \mathbf{R}(\mathbf{u}), \tag{11}$$

with density vector $\mathbf{u} = (u, v)^T$ and matrix $\mathbf{D} = \begin{pmatrix} D_c & 0 \\ 0 & D_d \end{pmatrix}$. Elements of the vector $\mathbf{R}(\mathbf{u}) = \begin{pmatrix} g(u,v) \\ h(u,v) \end{pmatrix}$ indicate reaction terms for each density which is the second terms in Eq. (10). Without diffusion, the differential equations have homogeneous solution $\mathbf{u}_0 = (u_0, v_0)^T$ where $g(u_0, v_0) = h(u_0, v_0) = 0$. We assume that the solution is a fixed point, and examine its stability under diffusion.

If we consider small perturbation $\tilde{\mathbf{u}}$ from the homogeneous solution, $\mathbf{u} \cong \mathbf{u}_0 + \tilde{\mathbf{u}}$, we get the relation,

$$\partial_t \tilde{\mathbf{u}} = \mathbf{D}\nabla^2\tilde{\mathbf{u}} + \mathbf{J}\tilde{\mathbf{u}}, \tag{12}$$

where $\mathbf{J} = (\partial\mathbf{R}/\partial\mathbf{u})_{\mathbf{u}_0} \equiv \left.\begin{pmatrix} g_u & g_v \\ h_u & h_v \end{pmatrix}\right|_{\mathbf{u}_0}$. Subscripts of the g and h mean partial derivative of that variable, e.g. g_u means $\partial g/\partial u$. Decomposing $\tilde{\mathbf{u}} = \sum_k \mathbf{a}_k e^{i\mathbf{k}\mathbf{r}}$ based on propagation wave number k gives us relation $\dot{\mathbf{a}}_k = \mathbf{B}\mathbf{a}_k$ where $\mathbf{B} \equiv \mathbf{J} - k^2\mathbf{D}$. Therefore, the stability of the homogeneous solution can be examined by the matrix $\mathbf{B}$. Note that $\text{Tr}(\mathbf{B}) < 0$ is guaranteed because $\text{Tr}(\mathbf{J}) < 0$. Hence, if the determinant of $\mathbf{B}$ is smaller than zero [$\det(\mathbf{B}) < 0$], it means one of the eigenvalues of the matrix $\mathbf{B}$ is positive. The homogeneous solution becomes unstable and Turing patterns appear.

The condition for $\det(\mathbf{B}) < 0$ is given by

$$\left(\frac{g_u}{D_c} + \frac{h_v}{D_d}\right)^2 > \frac{4\det(\mathbf{J})}{D_c D_d}. \tag{13}$$

It can be rewritten as following form:

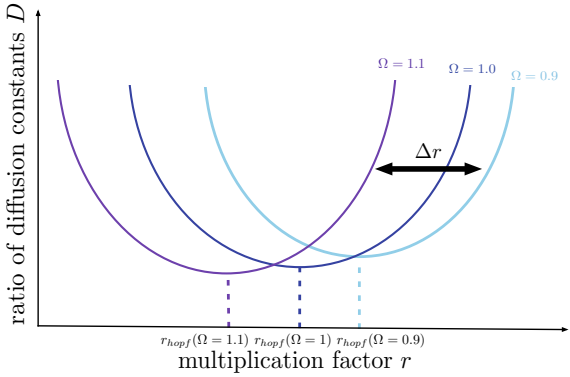

Fig. 5 Schematic figure for expected shift of phase boundaries. According to the change of r_{Hopf}, over all phase boundaries may shift together at the same direction. As we have seen in Fig. 4b, the phase boundaries with r_{Hopf} move to the right with discounting effect and move to the left with synergy effect, respectively. Accordingly, the surviving region in the parameter space expands with synergy effect while it shrinks with discounting effect

$$\frac{D_d}{D_c} > \frac{g_u h_v - 2g_v h_u + 2\sqrt{-g_v h_u \det(\mathbf{J})}}{g_u^2}. \tag{14}$$

With our model parameters this inequality is equivalent to

$$D > \frac{v}{u}\frac{1}{C_u^2}\left[C_u D_v - 2C_v D_u\left(1 - \sqrt{C_v D_u E}\right)\right]\Big|_{u=u^*, v=v^*}, \tag{15}$$

where u^* and v^* are values at the fixed point. The symbols indicate

$$\begin{pmatrix} C_u & C_v \\ D_u & D_v \end{pmatrix} = \begin{pmatrix} d - w^2\partial_u f_C & d - w^2\partial_v f_C \\ d - w^2\partial_u f_D & d - w^2\partial_v f_D \end{pmatrix}, \tag{16}$$

$$E = C_v\partial_u f_D - C_u\partial_v f_D + d\partial_u f_C - d\partial_v f_C,$$

with $\partial_x y = \frac{\partial y}{\partial x}$. If the above criterion is satisfied, the stable fixed point predicted without diffusion becomes unstable with diffusion (Fig. 5).

3 Discussion

Linear public goods game is a useful approximation of the real nonlinearities in social dilemmas from microbes to macro-life [15, 36, 49] with applications such as in antibiotic resistance [25] as well as cancer [1]. However, taking nonlinearities into account might show different resulting outcomes from naive expectations [13].

Especially, nonlinearities in interactions have a profound effect in ecology when it comes to fecundity and avoiding predation [56, 57]. In this manuscript, we have extended the analysis of spatial public goods games beyond the traditional linear public goods games.

The benefits, in our case, accumulate in a nonlinear fashion in the number of cooperators in the group. Each cooperator can provide a larger benefit than the last one as the number of cooperators increases (resulting in a synergy), or each cooperator provides a smaller benefit than the previous one (thus leading to discounting) [20]. Such an extension to public goods game was proposed very early on by [10]. Termed as superadditivity in benefits, extending from this particular model framework, we can visualise nonlinearities in costs as well, a concept not yet dealt with. Again, such economies of scale [9] can be justified in both bacterial and human interactions as proxies for quorum sensing (or quenching) or accruing of wealth (or austerity) [3, 4, 40].

We show that including such nonlinearities in the benefit function affects the effective rate of return from the public goods game, irrespective of the types of diffusion dynamics. With spatial dynamics, synergy increases the effective rate of return on the investment and expands the region in the parameter space where survival of the population is possible. This itself may make cooperation a favourable strategy. Besides the trivial observation that synergy helps cooperators, we show that as we move symmetrically away from the linear case towards more synergy or discounting, the change in the eventual dynamics is not symmetric. It would be interesting to check if the asymmetry holds for different designs of benefit functions.

We used the particular functional form of the benefit function, including nonlinearities in payoffs [20]. However, there are various ways of including nonlinearities in the benefit function [4, 7, 40]. The model considered in [40] extends the results of [20] to games between relatives. Furthermore, [40] has described the relationships between different nonlinear social dilemma models with a variety of benefit functions. Also these nonlinear social dilemmas have been analysed in a structured population [29, 40, 41]. However, previous studies have focused on the approach presented in [46], which provide a criterion for strategy selection rather than explicitly positioning the populations on a grid and including diffusion. When studying games in structured populations, often a network structure is considered [2, 42]. The role of network connectivity is determined to be critical for the eventual evolutionary outcome [41, 50, 51] and some structures can result in hindering the evolution of cooperation as well [26]. In contrast, our approach focuses more on the ecological framework but not in network structures. We take into account not only the changes in frequencies of cooperators and defectors but also the population dynamics, which is usually missed in a network approach. While both approaches make evolutionary games ecologically explicit, the models are thoroughly different in their setup and implementation.

The importance of including ecology in evolutionary games has been known for long, but the complexity that it generates has prevented it from garnering widespread attention [11]. Seasonal variations in the rate of return radically change the selection pressures on cooperation and defection. Changes in the ecology may not feedback

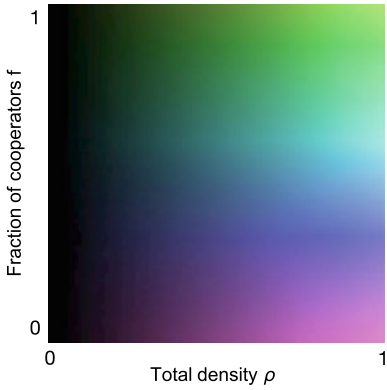

Fig. 6 The exact colour scheme developed for colouring the patterns. Each patch in a pattern is coloured using this palette by choosing the corresponding f and ρ values. For brightness we used Eq. (17) with $a = 15$

directly to the frequencies of cooperators and defectors but on to a variable in benefit–cost functions. If the variable affects the frequency of cooperators and defectors (or even the group size) in a nonlinear fashion, then the results are not trivial [13, 38]. Thus, even a simple connection between evolutionary and ecological dynamics may already generate rich dynamics [31, 54], and the feedback between the two is often already convoluted. Similar to [12, 37], it is possible to include feedback between the population dynamics and diffusion here, but together with a nonlinear social dilemma, we envision that the formal analysis and the computational implementation will be a considerable challenge.

Acknowledgments We thank Christoph Hauert for comments and suggestions in improving an early version of the manuscript. The authors thank the constructive comments of the reviewers. Both authors acknowledge generous support from the Max Planck Society.

Appendix

Colour Coding

Similar to the colour coding used in [37] we use mint green (colour code: #A7FF70) and Fuchsia pink (colour code: #FF8AF3) colours for denoting the cooperator and defector densities, respectively, for each type. The colour spectrum and saturation is determined by the ratio of cooperators to defectors which results in the Maya blue colour for equal densities of cooperators and defectors. For convenience, we use HSB colour space which is a cylindrical coordinate system $(r, \theta, h) =$ (saturation, hue, brightness). The radius of circle r indicates saturation or the colour whereas θ helps us transform the RGB space to HSB. The total density of the population $\rho = u + v$ is represented by the brightness h of the colour. For better visualisation, we formulate the brightness h as

$$\frac{\log a\rho + 1}{\log a + 1}, \tag{17}$$

where a control parameter a (> -1 and $\neq 0$) (see Fig. 6). The complete colour scheme so developed passes the standard tests for colour blindness.

References

1. Aktipis A (2016) Principles of cooperation across systems: from human sharing to multicellularity and cancer. Evolutionary Applications 9(1):17–36
2. Allen B, Lipper G, Chen YT, Fotouhi B, Nowak MA, Yau ST (2017) Evolutionary dynamics on any population structure. Nature 544:227–230
3. Archetti M (2009) Cooperation as a volunteer's dilemma and the strategy of conflict in public goods games. Journal of Evolutionary Biology 11:2192–2200
4. Archetti M, Scheuring I (2011) Co-existence of cooperation and defection in public goods games. Evolution 65(4):1140–1148
5. Archetti M, Scheuring I (2012) Review: Game theory of public goods in one-shot social dilemmas without assortment. Journal of Theoretical Biology 299(0):9–20
6. Axelrod R (1984) The evolution of cooperation. Basic Books, New York, NY
7. Bach LA, Helvik T, Christiansen FB (2006) The evolution of n-player cooperation - threshold games and ESS bifurcations. Journal of Theoretical Biology 238:426–434
8. Binmore KG (1994) Playing fair: game theory and the social contract. MIT Press, Cambridge
9. Dawes RM, Orbell JM, Simmons RT, Van De Kragt AJC (1986) Organizing groups for collective action. The American Political Science Review 80(4):1171–1185
10. Eshel I, Motro U (1988) The Three Brothers' Problem: Kin Selection with More than One Potential Helper. 1. The Case of Immediate Help. The American Naturalist 132(4):550–566
11. Estrela S, Libby E, Van Cleve J, Débarre F, Deforet M, Harcombe WR, Peña J, Brown SP, Hochberg ME (2018) Environmentally Mediated Social Dilemmas. Trends in Ecology & Evolution 34(1):6–18
12. Funk F, Hauert C (2019) Directed migration shapes cooperation in spatial ecological public goods games. PLOS Computational Biology 15(8):1–14
13. Gokhale CS, Hauert C (2016) Eco-evolutionary dynamics of social dilemmas. Theoretical Population Biology 111:28–42
14. Gokhale CS, Traulsen A (2010) Evolutionary games in the multiverse. Proceedings of the National Academy of Sciences USA 107:5500–5504
15. Gore J, Youk H, van Oudenaarden A (2009) Snowdrift game dynamics and facultative cheating in yeast. Nature 459:253–256
16. Grauwin S, Bertin E, Lemoy R, Jensen P (2009) Competition between collective and individual dynamics. Proceedings of the National Academy of Sciences of the United States of America 106(49):20,622–20,626
17. Hardin G (1968) The tragedy of the commons. Science 162:1243–1248
18. Hauert C, Imhof L (2012) Evolutionary games in deme structured, finite populations. Journal of Theoretical Biology 299:106–112
19. Hauert C, Holmes M, Doebeli M (2006a) Evolutionary games and population dynamics: maintenance of cooperation in public goods games. Proceedings of the Royal Society B 273:2565–2570
20. Hauert C, Michor F, Nowak MA, Doebeli M (2006b) Synergy and discounting of cooperation in social dilemmas. Journal of Theoretical Biology 239:195–202
21. Hauert C, Yuichiro Wakano J, Doebeli M (2008) Ecological public goods games: cooperation and bifurcation. Theoretical Population Biology 73:257–263

22. Hofbauer J, Sigmund K (1998) Evolutionary Games and Population Dynamics. Cambridge University Press, Cambridge, UK
23. Kawasaki K, Mochizuki A, Matsushita M, Umeda T, Shigesada N (1997) Modeling spatio-temporal patterns generated by bacillus subtilis. Journal of Theoretical Biology 188:177–185
24. Kollock P (1998) Social dilemmas: The anatomy of cooperation. Annual Review of Sociology 24:183–214
25. Lee HH, Molla MN, Cantor CR, Collins JJ (2010) Bacterial charity work leads to population-wide resistance. Nature 467(7311):82–85
26. Li A, Broom M, Du J, Wang L (2016) Evolutionary dynamics of general group interactions in structured populations. Physical Review E 93(2):022,407
27. Loe LE, Mysterud A, Veiberg V, Langvatn R (2009) Negative density-dependent emigration of males in an increasing red deer population. Proc R Soc B 276:2581–2587
28. Lou Y, Martínez S (2009) Evolution of cross-diffusion and self-diffusion. Journal of Biological Dynamics 3(4):410–429
29. McAvoy A, Hauert C (2016) Structure coefficients and strategy selection in multiplayer games. Journal of Mathematical Biology pp 1–36
30. McAvoy A, Fraiman N, Hauert C, Wakeley J, Nowak MA (2018) Public goods games in populations with fluctuating size. Theoretical Population Biology 121:72–84, https://doi.org/10.1016/j.tpb.2018.01.004
31. McNamara JM (2013) Towards a richer evolutionary game theory. Journal of The Royal Society Interface 10:20130,544
32. Ohgiwari M, Matsushita M, Matsuyama T (1992) Morphological changes in growth phenomena of bacterial colony patterns. J Phys Soc Jap 61:816–822
33. Ohtsuki H, Pacheco J, Nowak MA (2007) Evolutionary graph theory: Breaking the symmetry between interaction and replacement. Journal of Theoretical Biology 246:681–694
34. Okubo A, Levin SA (1980) Diffusion and Ecological Problems: Mathematical Models. Springerr-Verlag
35. Pacheco JM, Santos FC, Souza MO, Skyrms B (2009) Evolutionary dynamics of collective action in n-person stag hunt dilemmas. Proceedings of the Royal Society B 276:315–321
36. Packer C, Ruttan L (1988) The evolution of cooperative hunting. The American Naturalist 132:159–198
37. Park HJ, Gokhale CS (2019) Ecological feedback on diffusion dynamics. Journal of the Royal Society Open Science 6:181,273
38. Peña J (2012) Group size diversity in public goods games. Evolution 66:623–636
39. Peña J, Lehmann L, Nöldeke G (2014) Gains from switching and evolutionary stability in multi-player matrix games. Journal of Theoretical Biology 346:23–33
40. Peña J, Nöldeke G, Lehmann L (2015) Evolutionary dynamics of collective action in spatially structured populations. Journal of Theoretical Biology 382:122–136
41. Peña J, Wu B, Arranz J, Traulsen A (2016) Evolutionary games of multiplayer cooperation on graphs. PLoS Computational Biology 12(8):1–15
42. Santos FC, Pacheco JM, Lenaerts T (2006) Evolutionary dynamics of social dilemmas in structured heterogeneous populations. Proceedings of the National Academy of Sciences USA 103:3490–3494
43. Shigesada N, Kawasaki K, Teramoto E (1979) Spatial segregation of interacting species. Journal of Theoretical Biology 79(1):83–99
44. Souza MO, Pacheco JM, Santos FC (2009) Evolution of cooperation under n-person snowdrift games. Journal of Theoretical Biology 260:581–588
45. Tarnita CE, Antal T, Ohtsuki H, Nowak MA (2009a) Evolutionary dynamics in set structured populations. Proceedings of the National Academy of Sciences USA 106:8601–8604
46. Tarnita CE, Ohtsuki H, Antal T, Fu F, Nowak MA (2009b) Strategy selection in structured populations. Journal of Theoretical Biology 259:570–581
47. Tarnita CE, Wage N, Nowak MA (2011) Multiple strategies in structured populations. Proceedings of the National Academy of Sciences USA 108:2334–2337

48. Taylor PD, Jonker LB (1978) Evolutionarily stable strategies and game dynamics. Mathematical Biosciences 40:145–156
49. Turner PE, Chao L (1999) Prisoner's Dilemma in an RNA virus. Nature 398:441–443
50. van Veelen M, Nowak MA (2012) Multi-player games on the cycle. Journal of Theoretical Biology 292:116–128
51. van Veelen M, García J, Rand DG, Nowak MA (2012) Direct reciprocity in structured populations. Proceedings of the National Academy of Sciences USA 109:9929–9934
52. Venkateswaran VR, Gokhale CS (2019) Evolutionary dynamics of complex multiple games. Proceedings of the Royal Society B: Biological Sciences 286(1905):20190,900
53. Wakano JY, Nowak MA, Hauert C (2009) Spatial dynamics of ecological public goods. Proceedings of the National Academy of Sciences USA 106:7910–7914
54. Weitz JS, Eksin C, Paarporn K, Brown SP, Ratcliff WC (2016) An oscillating tragedy of the commons in replicator dynamics with game-environment feedback. Proceedings of the National Academy of Sciences of the United States of America 113(47):E7518–E7525
55. Wright S (1930) The genetical theory of natural selection. Journal of Heredity 21:349–356
56. Wrona FJ, Jamieson Dixon RW (1991) Group Size and Predation Risk: A Field Analysis of Encounter and Dilution Effects. The American Naturalist 137(2):186–201
57. Zöttl M, Frommen JG, Taborsky M (2013) Group size adjustment to ecological demand in a cooperative breeder. Proceedings of the Royal Society B: Biological Sciences 280(1756):20122,772

Applications to Economics

Heuristic Optimization for Multi-Depot Vehicle Routing Problem in ATM Network Model

Valeria Platonova, Elena Gubar, and Saku Kukkonen

1 Introduction

This work is inspired by a real-life optimization problem, which is generally based on the distribution of goods, traffic planning, and management. The modern metropolitan environment cannot be imagined without facilities such as ATM networks. One of the most actual problems in the ATM network of the bank is cash flow optimization and organization of uninterrupted work. The current paper considers the problem in which a set of geographically dispersed ATMs with known requirements must be serviced with a heterogenous fleet of money collector teams stationed in the depots with the objective of minimizing the total distribution costs. Metropolitan banks typically come across the problem of long distances between encashment centers, depots, and ATMs, particularly in the situations where several ATMs are to be located in remote districts of the city. Generally speaking, client support and servicing the ATM network can be costly: it takes employees time to supervise the network and make decisions on managing the cash flow efficiently and it also involves high operating costs (i.e., financial, transport, etc.). The servicing costs of the bank can be reduced through the implementation of an appropriate encashment strategy and optimizing encashment routes in ATM network. In the previous study [14], the combined framework has been considered where the optimal encashment routes were designed based on the statistical prediction of money demand in the ATM network.

V. Platonova
Intermedia Ltd, Sunnyvale, CA, USA
e-mail: vplatonova@intermedia.net

E. Gubar (✉)
Faculty of Applied Mathematics and Control Processes,
St. Petersburg State University, St Petersburg, Russia
e-mail: e.gubar@spbu.ru

S. Kukkonen
Machine Learning Group, School of Computing,
University of Eastern Finland, Joensuu, Finland
e-mail: saku.kukkonen@uef.fi

D. M. Ramsey and J. Renault (eds.), *Advances in Dynamic Games*,
Annals of the International Society of Dynamic Games 17,
https://doi.org/10.1007/978-3-030-56534-3_9

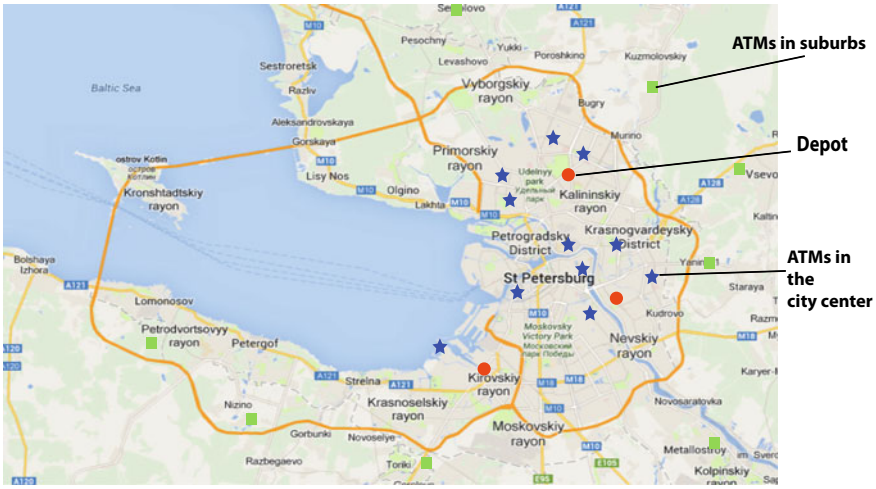

Fig. 1 An example of location of encashment centers and ATMs for one bank in St.Petersburg

However, the research takes into account the Capacitated Vehicle Routing Problem (CVRP) with only one depot. The problem of remote locations inevitably leads to the increase in servicing costs and thus requires a new approach to develop for new depots. Figure 1 illustrates an example of encashment centers and ATMs location in St.Petersburg and the neighboring districts. The picture enables to consider the necessity of establishing new depots and optimization of encashment routes.

The foregoing discussion stipulates the necessity of considering the complex problem of encashment process in the bank with many banking branches and ATM network dispersed across a large area as a composition of several modified Capacitated Vehicle Routing Problems (CVRP). This model is a widely used extension of the Vehicle Routing Problem (VRP), which have been one of the key models in the optimization studies, since it was proposed by Dantzig in [11]. Recently, the VRP has been one of the most studied problems in the combinatorial optimization of cargo, passenger traffic, and logistics, which can be explained by its great relevance for real-life applications as well as its being one of the most challenging combinatorial optimization tasks. In the classical VRP, CVRP routes are constructed starting from one common vertex to multiple geographically dispersed customers and service them with the minimum total cost. Today minimization of operational costs without quality and safety lapses is considered to be one of the most important objectives. This tendency has attracted considerable attention in the recent years, see in [10, 15, 21]. The main objective of the study is to adapt and consider the possibilities of applying well-known transportation (logistics) models together with approved optimization methods as a solution to the problems arising in banking sphere, particularly during encashment process. This study can be considered, on the one hand, as a research project that is aimed at examining the possibilities of applying various techniques to solve problems related to complex transportation models, and, on the other hand, if

the paper can be considered as a case study of an encashment process in one bank of St. Petersburg, taking into account the real-life traffic conditions.

The logistics problem concerned marks out two possible approaches: the first one is the optimization of the location of depot (encashment centers) over the feasible area and evaluation of the ATMs availability and construction/opening a new depot, the second, calculation of the optimal or nearly optimal routes from to existing depots. Previous studies have presented a wide range of different optimization methods for transportation models that lead to the necessity of selecting of relevant techniques for the problems considered. We have opted for the Multi-Depot Location Routing Problem (MDLRP) and Multi-Depot Vehicle Routing Problem (MDVRP). On the one hand, these two models are widely applied nowadays, but on the other hand they can be modified according to the real-life problem concerned. The MDVRP presents a generalization of the vehicle routing problem, where vehicles depart from and arrive to one of multiple depots. Furthermore, it is necessary to mark which depot the money collector teams visit, additionally to the definition of the vehicles routes. The MDVRP simultaneously defines the service areas of each depot and establishes the associated vehicle routes [28].

It is more cost efficient for a bank to have several encashment centers, which are located in different districts of the city. Therefore, the problem of encashment of the ATMs network can be described through a complex model which combines Multi-Depot Location Routing Problem and Multi-Depot Vehicle Routing Problem. In the current study, we use Cluster First-Route Second approach to find a solution to the considered optimization tasks. Thus, in this paper we propose two-stage process to solve the MDLRP. On the first stage, a feasible solution is obtained using the Clarke–Wright algorithm [7]. The second stage includes defining the optimal locations of encashment centers through the method of Super-ATMs [26] and the construction of a heuristic solution using evolutionary computation (EC) [13].

The constructive heuristics have been considered as one of the most convenient and efficient methods to solve the VRP and its modifications. Evolutionary computation is a stochastic approach to global optimization. Although evolutionary computation does not guarantee finding the optimum, it can often find a good solution even to hard problems. The problem discussed in this paper is basically a modification of the traveling salesman problem which is suitable for evolutionary computation.

Solving the MDLRP by using the method of Super-ATMs enables clustering the ATM network according to the distance between them and the nearest encashment center. This process helps to reduce transportation servicing costs of ATMs in remote districts of the city. However, the introduction of a new encashment center complicates the solution as it generates new subproblems where each of them should satisfy all constraints of the initial routing problem. The solution of the MDLRP provides a depot location plan. As soon as a new distinct location plan is found, the set of routes from the depots can be defined. At this stage, the MDVRP formulation can be used for defining the optimal routes of money collector teams. The MDVRP belongs to the class of NP-hard optimization problems, hence it is very difficult to receive the optimal solution for a large amount of units [2, 3].

Routing problems concern a vast range of real-life problems, which makes it a widely discussed subject nowadays. Numerous research studies have been dedicated to developing and improving new and existing algorithms for solving such problems [8, 31, 34]. The key objective of improving the algorithm is to obtain better solutions, as well as to increase the efficiency of the algorithm and avoid premature convergence. For example, in [6], Carlsson considered two heuristic methods for solving the MDVRP. The first method is based on the technique of linear programming with global improvements. The second method is based on the asymptotic optimality. As a solution to the problem, Nallusamy, in his turn, has proposed clustering at the first stage [24]. This technique allows to divide the serviced territory into several areas with a given number of vehicles, hence the original problem is also divided into several subproblems such as the VRP, each of them has a feasible solution, which was optimized using a genetic algorithm (GA) (one form of evolutionary computation). The paper by Crevier [8] introduces the concept of an intermediate depot. This depot is a station where vehicles refill their resources. The paper considers the combined heuristic method based on tabu search algorithm and integrates programming algorithms into solving subproblems. A project of networking and emerging optimization has been dedicated to the study of the VRP [22]. The work of [30] represents a case study of the VRP problem in a distribution company. The paper [28] concerns a two-commodity flow formulation for the MDVRP considering a heterogeneous vehicle fleet and maximum routing time.

In the current paper, the method of improving the encashment process in the ATM network is proposed taking into account the real-life traffic conditions in St.Petersburg and the neighboring districts.

In our study, we focus on the joint optimization problem, which includes MDLRP and MDVRP models for defining the location of new depots and optimal circular routes from the existing depots. The solution method of MDVRP has been developed using two different evolutionary computation approaches and is illustrated through geo-location of ATMs network on the map of St.Petersburg and the suburbs including the valid delivery costs.

The paper is structured as follows. Section 2 represents the formulation of the MDLRP and its adaptation to the network of ATMs. Section 3 describes method of solving the MDLRP. Section 4 includes the formulation of the MDVRP for ATM network. Section 5 focuses on two specific approaches of solving the MDLRP and the MDVRP. Section 6 provides a numerical example. Section 7 concludes the paper and outlines the future research prospects.

2 Multi-Depot Location Routing Problem (MDLRP)

The paper considers a problem in which a set of geographically dispersed ATMs must be served with a fleet of money collector teams stationed in the several encashment centers of the bank. This problem is a modification of the original vehicle routing problem (VRP), proposed by Dantzig in 1959 [11], which has a simple interpretation:

a set of service vehicles need to visit all customers in a geographical region with the minimum cost. In our study, we use the extensions of this basic formulation, where, firstly, it is necessary to define the location of depots with minimal costs. Secondly, the ATMs which are located in different clusters are serviced by a fleet of homogeneous vehicles with the minimal costs. To define the optimization problem of the encashment process with minimum operational costs, the MDLRP and the MDVRP have been integrated. According to [6, 16], vehicle capacity and traveling costs are minimized subject to vehicle capacity constraints as well as the depot opening-closing is defined by MDLRP.

This formulation helps to define the optimal location of the encashment centers to cover all the city's central districts and remote suburbs. After obtaining the optimal location of depots, the routes for collector teams can be found using the MDVRP [8]. In this case, received depots are fixed and used as an input data to the MDVRP. Solutions of Multi-Depots Vehicle Routing problem help to define feasible routes for a set of homogeneous vehicles that make up a vehicle fleet. The routes are planned according to the minimization of travel costs for each of the routes. Each route begins and ends at the depot and contains a subset of stops for servicing ATMs. A solution to this problem is feasible if the vehicle capacity on each route is not exceeded and all stops are located within this route. The simplest formulation of the MDVRP stipulates no lower and upper bounds for the length of each route. The MDVRP shall satisfy the next conditions:

- The objective is to minimize the costs of each of the routes;
- A solution to this problem is feasible if the vehicle capacity on each route is not exceeded and all stops are located within this route;
- Each route starts and ends at the same depot;
- Each ATM is serviced once;
- A fleet of vehicles consists of homogeneous cars with the same capacity;
- Each depot should have a sufficient amount of money so that the encashment process remains uninterrupted.

A network of ATM contains two subsets: I is a set of encashment centers (depots) belonging to the bank and J is a set of ATMs, where $i \in I$ is the variable which defines the index of encashment centers of the bank and $j \in J$ is the index of each ATM. The money collector teams, which are located in depots, have a set of vehicles denoted as K, where $k \in K$ is a route index, Q_k is the capacity of vehicle k with the given route k. F is a variable that shows the delivery costs for each money collector team. A subset of ATMs, in its turn, can be divided into two parts: firstly, there is a group of ATMs, which has been already serviced and secondly, there is a group of ATMs, that needs to be serviced. The set of unserviced ATMs will be denoted as S.

Lets denote N as the number of vehicles and L as the number of ATMs. We set M as the number of all encashment centers (depots). Variable Z ($Z \subset M$) corresponds with the number of depots which already exist and operate. The introduction of a new encashment center leads to additional costs O_i, for each i, $C = \{c_{ij}\}$ is a distance matrix, the associated variable $c^* = \{c^*_{ij}\}$ is calculated based on the distance c_{ij} and shows the costs for each route. As in [14], it is assumed that variable d_j corresponds

with the demand for cash cartridges for each ATM j, and V_i is the amount of cartridges which are kept in the i-th encashment center of the bank. The artificial variable y_i is binary that has been introduced to show whether an encashment center i is closed or not;

$$y_i = \begin{cases} 1, \text{ if depot } i \text{ is fictitious,} \\ 0, \text{ if depot } i \text{ exists.} \end{cases}$$

- x_{ijk} is a binary variable, which shows that vehicle k starts from depot i and then moves to ATM j.

$$x_{ijk} = \begin{cases} 1, \text{ if } i \text{ immediately precedes } j \text{ on route } k, i \in I, j \in J, k \in K; \\ 0, \text{ otherwise.} \end{cases}$$

- x_{jik} is binary variable, which shows that a vehicle k finishes in the encashment center i:

$$x_{jik} = \begin{cases} 1, \text{ if } j \text{ immediately precedes } i \text{ on route } k, i \in I, j \in J, k \in K; \\ 0, \text{ otherwise.} \end{cases}$$

- an artificial variable m_{ik} shows that each route k starts and finishes in the same encashment center i.

$$m_{ik} : \forall i \in I, \ \forall k \in K, \ m_{ik} = x_{ijk} + x_{jik}.$$

- x_{jlk} is binary variable, which shows that vehicle k after servicing ATM j moves to ATM l on the same route:

$$x_{jlk} = \begin{cases} 1, \text{ if } j \text{ immediately precedes } l \text{ on route } k, j, l \in S, k \in K; \\ 0, \text{ otherwise.} \end{cases}$$

- z_{ij} is binary variable, which shows consolidation of ATM j and depot i:

$$z_{ij} = \begin{cases} 1, \text{ if ATM } j \text{ belongs to depot } i; \\ 0, \text{ otherwise.} \end{cases}$$

Formally, a definition of a route based on the notations that were introduced before (Fig. 2).

Definition 1 Route is a set of vertices $x_{ijk}, x_{jlk}, x_{jik}$, which show that each ATM should be serviced only once and a team of money collectors starts and finishes in the same encashment center of the bank [28]. Capacity of the vehicles and amount of money in ATMs should satisfy to all restrictions for i-th department (see [8, 15, 32]).

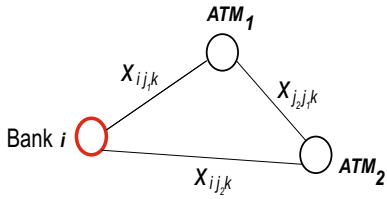

Fig. 2 An example of route from a depot to ATM: $i - j_1 - j_2 - i$

Based on these notations, the definition of the objective function and constraints are:

$$min\Bigg(\sum_{i\in I}\sum_{j\in J}\sum_{k\in K} c_{ij}x_{ijk} + \sum_{j,l\in J}\sum_{k\in K} c_{jl}x_{jlk} + \sum_{i\in I}\sum_{j\in J}\sum_{k\in K} c_{ji}x_{jik} + \\ + F\Big(\sum_{i\in I}\sum_{j\in J}\sum_{k\in K} x_{ijk} + \sum_{j,l\in J}\sum_{k\in K} x_{jlk} + \sum_{i\in I}\sum_{j\in J}\sum_{k\in K} x_{jik}\Big) + \sum_{i\in I} O_i y_i\Bigg); \tag{1}$$

together with constraints:

$$\sum_{k\in K}\sum_{i\in I} m_{ik} = \sum_{i\in I}\sum_{k\in K}(x_{ijk} + x_{jik}) = 2, j \in J; \tag{2}$$

$$\sum_{i\in I}\sum_{j\in J} x_{ijk} = 1, k \in K; \tag{3}$$

$$\sum_{j\in J, l\in S} x_{jlk} \le 1, S \subseteq J, k \in K; \tag{4}$$

$$\sum_{j\in J} d_j \left(\sum_{i\in I} x_{ijk} + \sum_{j,l\in J} x_{jlk}\right) \le Q_k, k \in K; \tag{5}$$

$$\sum_{i\in S}\sum_{j\in S} x_{ijk} \le |S| - 1, \forall \mathrm{S} \subseteq \mathrm{J}, k \in K; \tag{6}$$

$$\sum_{j,l\in J} x_{jlk} - \sum_{j,l\in J} x_{ljk} \ne 0, k \in K; \tag{7}$$

$$\sum_{j\in J} d_j z_{ij} \le V_i, i \in I; \tag{8}$$

$$-z_{ij} + \sum_{u\in I\cup J} (x_{iuk} + x_{ujk}) \le 1, \mathrm{i} \in \mathrm{I}, \mathrm{j} \in \mathrm{J}, k \in K; \tag{9}$$

$$\begin{aligned} &x_{ijk} \in \{0, 1\}, i \in I, j \in J, k \in K \\ &z_{ij} \in \{0, 1\}, i \in I, j \in J \\ &y_i \in \{0, 1\}, i \in I. \end{aligned} \tag{10}$$

Expression (1) is the objective function which minimizes the total distance of all given vehicles. Constraint (2) guarantees that the route starts and finishes in the same encashment center. Constraints (3) and (4) show that to each ATM is assigned to only one route; (5) is a capacity constraint for a given set of vehicles; (6) gives the new sub-tour elimination constraint set; (7) represents that the route between an ATM i and j is asymmetric; (8) is the capacity constraints for the given depots; Constraint (9) demonstrates that each route should be served only once; Definitions in (10) specify that each collector team can be assigned to a depot only if a route from the depot to an ATM is available.

3 Solving Methods of the Multi-Depot Location Routing Problem (MDLRP)

According to the previous discussions, in a large city, the optimal location of depots decreases the servicing costs of encashment process of ATM network significantly. At the first stage of our framework, the optimal place to establish new encashment centers is defined or the subnetwork which is operated by the corresponding depot should be reorganized. The aforementioned MDLRP considers several encashment centers, where some centers already exist and some centers are virtual. The solution of the MDLRP can be found according to the next iterative process.

1. Firstly, we form a cluster which contains an encashment center and neighboring ATMs through comparing the distance between them. As a result, several subnetworks are received, each of them includes one depot and a set of ATMs. For each cluster we can find optimal or heuristic optimal routes for encashment teams. For example, clustering for two depots A and B follows the next rules:

   - if $D(j, A) < D(j, B)$, then j-th ATM belongs to depot A;
   - if $D(j, A) > D(j, B)$, then j-th ATM belongs to depot B;
   - if $D(j, A) = D(j, B)$, then j-th ATM belongs to depot A or B,

   where $D(j, A)$, $D(j, B)$ are distances between ATM j and depot A and B, correspondingly. If numbers of depots $M \geq 2$, then clustering follows the same rule [12]. Hence we divide a large problem into several simple subproblems according to the number of depots. This procedure enables reducing the total number of routes, which satisfy the capacity of bank's encashment centers and minimize the costs of servicing. After the clustering is completed, we focus on two subproblems: optimization of encashment routes of depot A and B separately.

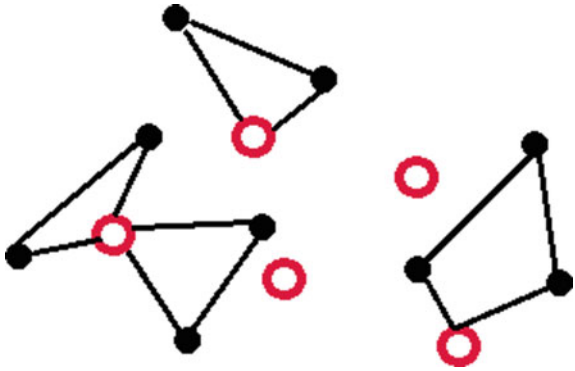

Fig. 3 Feasible solution. Here empty dots are depots and black dots are ATMs

On the first stage, we use a method called Super-ATMs, which was proposed in [26], to reduce a number of variables. The Super-ATMs algorithm contains the following steps:

- It is supposed that there are several presumed places to open a new encashment center. Then we find a feasible solution of the original system (1)–(10) by any heuristic algorithm, for example, by Clarke and Wright [7], taking into account all the possible locations of the encashment centers;
- exclude all encashment centers from the constructed routes;
- collect ATMs of each route into Super-ATM;
- construct new routes, using Super-ATMs and encashment centers;
- for each constructed route Super-ATM is divided into new sub-routes thus we obtain a new solution.

We illustrate the stages of Super-ATMs algorithm in Figs. 3, 4, 5, 6 and 7.

2. On the second stage, the set feasible routes that were obtained at the stage 1 are used as an initial solution, where each ATM is serviced by a certain vehicle. Hence, the number of such routes coincide to the number of ATMs. To construct a feasible solution, for each of the subproblems, the Clarke–Wright method is used.

Below the mathematical formulation of the MDLRP with the concept of Super-ATMs is presented:

$$min\left(\sum_{i\in I} O_i y_i + \sum_{i\in I}\sum_{h\in H} C_{ih}X_{ih}\right) \tag{11}$$

$$\sum_{i\in I} X_{ih} = 1, \quad h \in H; \tag{12}$$

$$\sum_{h\in H} D_h X_{ih} \leq V_i y_i, \, i \in I; \tag{13}$$

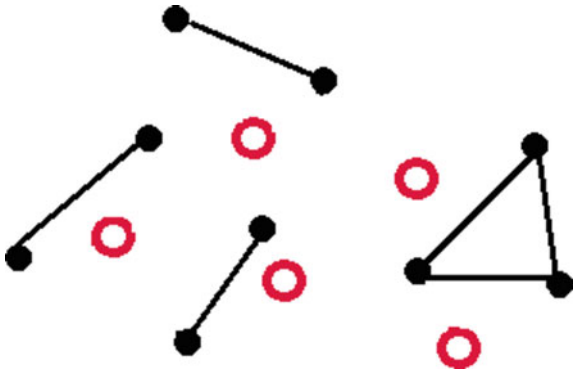

Fig. 4 Excluding encashment centers from constructed routes

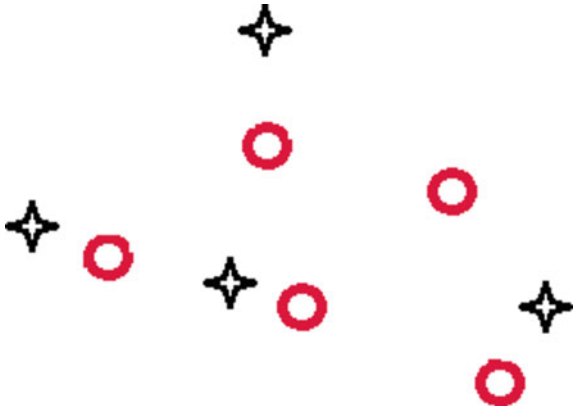

Fig. 5 Recombination of a set of ATM of each route into Super-ATMs. Stars are Super-ATMs, empty dots are depots

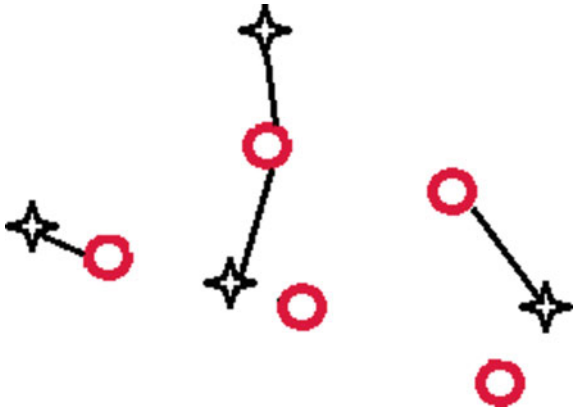

Fig. 6 Constructing of new routes between Super-ATMs and initial depots

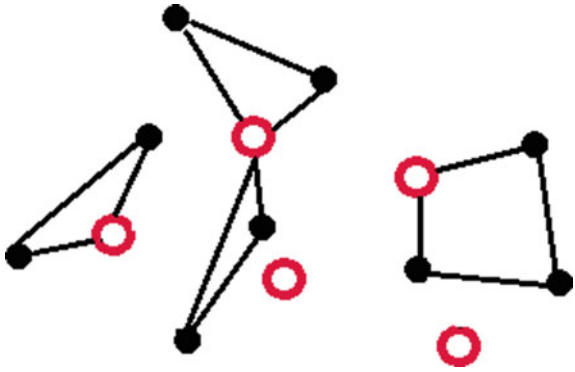

Fig. 7 Disconnection of Super-ATMs and constructing new sub-routes

$$X_{ih} \in \{0, 1\}, \quad i \in I, h \in H, \tag{14}$$

$$y_i \in \{0, 1\}, \quad i \in I. \tag{15}$$

Here variable D_h is the aggregated demand of ATMs, which corresponds to Super-ATMs denoted as h, H is a set of Super-ATMs; the binary variable X_{ih} represents whether Super-ATM h is grouped with encashment center i;

$$X_{ih} = \begin{cases} 1, & \text{if encashment center } i \text{ is grouped with Super-ATMs } h, i \in I, h \in H; \\ 0, & \text{otherwise.} \end{cases}$$

Additional encashment center is grouped with the neighboring Super-ATM through comparing the distances between them. The distance from the encashment center to some Super-ATMs is approximately equal to $\widehat{h}$ (here $\widehat{h}$ is the average sum of distances from this encashment center to each ATM which is included into Super-ATMs). Value O_h is the additional costs generated by the distance $\widehat{h}$.

In contrast to the original MDLRP in (1)–(10), in considered modification, the number of constraints is significantly reduced since the constraints (5), (6), (7), and (9) are not used. Whereas they do not impact on the solution of the problem, constraints (2), (3), and (4) are replaced by (12), and (9) is replaced by (13). The replacement guarantees that Super-ATMs can be combined only with the open encashment centers, which have sufficient amount cash cartridges. After using the Super-ATMs method, we received the optimal locations of encashment, thereafter the original problem is transformed to the MDVRP.

4 Multi-Depot Vehicle Routing Problem (MDVRP)

After obtaining the optimal location of depots, we construct the routes for money collector teams in the second part of the initial framework. Let $G = (V, E)$ be an undirected complete graph, where V is a vertex set and E is an edge set. The vertex set V is partitioned into a subset of encashments centers $I = 1, \ldots, m$ and a subset of ATMs $J = 1, \ldots, n$. Each ATM $j \in J$ has a nonnegative demand d_j and a nonnegative service time δ_j. A service time $\delta_i = 0$, corresponds to each depot $i \in I$, shows that not all depots are necessarily used in the MDVRP. A set of k identical vehicles, each with capacity Q, is available in each depot i. Each edge $(i, j) \in E$ is associated with nonnegative traveling costs c_{ij}. The objective of the MDVRP is to define the routes which satisfy the demand of the ATMs with the minimal servicing costs. The MDVRP is subject to the following constraints [6, 28, 34]:

- Each route should start and finish at the same depot;
- Each ATM should be visited exactly once on one route;
- The total demand of each route should not exceed the vehicle capacity Q;
- The number of routes from each depot should not exceed the value of k.
- The total distance of each route should not exceed a given value D.

Mathematical formulation of the MDVRP follows the model from (1)–(10); however, we use a new objective function:

$$min\Bigg(\sum_{i\in I}\sum_{j\in J}\sum_{k\in K} c_{ij}x_{ijk} + \sum_{j,l\in J}\sum_{k\in K} c_{jl}x_{jlk} + \sum_{i\in I}\sum_{j\in J}\sum_{k\in K} c_{ji}x_{jik} + \\ + F\Big(\sum_{i\in I}\sum_{j\in J}\sum_{k\in K} x_{ijk} + \sum_{j,l\in J}\sum_{k\in K} x_{jlk} + \sum_{i\in I}\sum_{j\in J}\sum_{k\in K} x_{jik}\Big)\Bigg). \tag{16}$$

5 Solution Methods for MDVRP

Evolutionary Algorithms (EAs) are population-based stochastic methods that are inspired by Darwin's Theory of Evolution [13]. EAs are most often applied for optimization, since EAs have minimal demand for the problem in hand, and EAs have shown their good performance in solving many hard problems. Different types of EAs have been developed and Genetic Algorithms (GAs) are one of the historical main branches of EAs. Genetic Algorithms are in all application domains traditionally use to solve different modification of VRP [4, 17]. The usage of EAs has become increasingly popular in the last few years and performs good results in optimization of VRP and its modification. In the previous studies [19, 23, 24, 32] various algorithms were developed to find the optimal or good solutions, depending on the dimension of the problem. Originally, GAs used binary numbers for coding variables. Later also other values such as integers and real numbers have been used as variable values.

In GA, a random population of individuals is first created. Then this population undergoes changes and selection based on goodness of individuals that guides the evolution. Two main genetic operators with a GA are crossover and mutation. In crossover, two individuals are mixed to obtain two new individuals. In mutation, one individual undergo a little change.

GAs as other EAs did not guarantee finding the optimal solution (that would be quite impossible in general case), but they are often able to find good solutions. A disadvantage of EAs is that they need lots of calculations compared to some problem-specific methods. On the other hand, EAs are easy to parallelize thus parallel computation can be applied for calculations.

5.1 Genetic Algorithm 1

In the current section, the Clarke and Wright method is used to find a feasible solution for the problem and then the modified GA is applied to improve the received feasible solution. However, despite the considered case study has low problem size, we turn to genetic algorithm to improve a feasible solution. This approach allows scaling our method to the problems with a larger dimension. Thus, we use GA as a basic method of solving the MDVRP for each encashment center. GA is a heuristic method, which provides more effective solutions than some other classical optimization methods, such as branch and bound, or the simulated annealing. The algorithm is based on the natural selection and adaptive mechanism. In Fig. 8, we show the main steps of computation [13].

Usually, genetic algorithm includes several required stages: representation of the problem, definition of the initial population, selection of parent individuals for future evaluation, applying of crossover operator, mutation procedure and finally the survival selection of the best offsprings (Figs. 9 and 10).

Definition 2 Chromosome (sometimes it is called a genome) is a set of parameters which defines the proposed solution to the problem that the GA1 is trying to solve. The chromosome is often represented as a simple string.

Definition 3 Gene is a part of chromosome. A gene contains a part of solution such as each variable x_{ijk} shows if ATM j is included in a route of vehicle k or not.

Definition 4 Crossover operator is a genetic operator that combines two chromosomes (parents) to produce a new chromosome (children) with crossover with some probability

In the current chapter, we use a modified single-point crossover which satisfies following conditions [5]:

- Randomly choose two chromosomes, which describe routes starting from any depot;

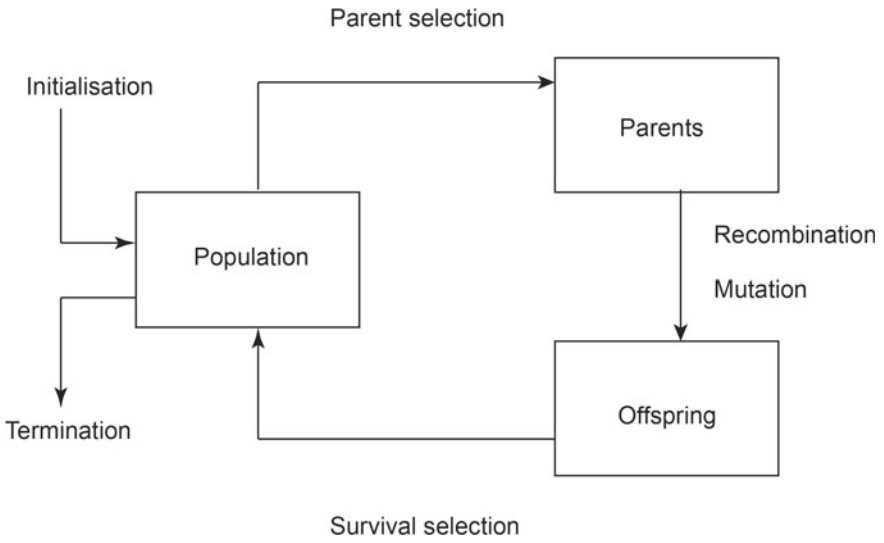

Fig. 8 Sheme of evolutionary algorithm

X_{A11}	X_{121}	X_{2A1}	
1	1	1	1
A	1	2	A

Fig. 9 An example of chromosome. Route $A - 1 - 2 - A$ represented as a chromosome, where variables of genes are $x_{A11} = 1$; $x_{121} = 1$; $x_{2A1} = 1$

X_{A11}	X_{121}	X_{2A1}	
1	1	0	1
A	1	2	A

Fig. 10 An example of chromosome. Route $A - 1 - A$ represented as a chromosome, where gene-variables are $x_{A11} = 1$; $x_{121} = 1$

- A single-point, called a breaking point, is randomly defined in each chromosome;
- Each chromosome is divided into two parts in the breaking point and two chromosomes exchange their parts before or after breaking point. Hence as a result, we receive two new chromosomes and each depot gets two new routes;
- Calculate new value of the objective function;

Definition 5 Mutation operator helps to avoid the appearance of a uniform population. This operator randomly changes or alters one or more gene values at randomly selected locations in a chromosome with a mutation probability.

We randomly choose any variable (gen) x_{ijk} of chromosome and change its value to any other possible value, i.e., if we have 0 then it becomes 1. As an example, we consider a chromosome which consists of six genes: 101101. Mutation of this chromosome can be **0**01101 or 10**0**101, if only one gene is changed, if two genes are altered then **01**1101 or 1011**10**.

Definition 6 Selection operator guides evolution to right direction by promoting better solutions.

5.2 Genetic Algorithm 2

Another GA approach for the MDVRP is to consider the whole routing problem as one big traveling salesman problem with an exception that there are multiple depots that can serve as starting and ending points for sub-routes. Since in traveling salesman problem a solution is the permutation of different locations, permutation of locations indexes is a natural way of coding when GA is applied for the MDVRP. Several different ways of performing crossover and mutation with permutation coding have been developed especially targeted for traveling salesman problem [4, 13, 17].

6 Numerical Simulations

In this section, the results of application of clustering method and two genetic algorithms GA1 and GA2 are presented, based on the ATM subnetwork of a bank from St.Petersburg. We consider a subset of ATMs, which contains 99 ATMs, located in the city center and the remote suburbs. Special cartographic sources such as QGIS 2.2; Topplan, [33]; Google maps; ArcGis [1], the Google Distance Matrix API are used to illustrate the results of simulations. We form a distance matrix 109×109, which includes 10 depots and 99 ATMs. All distances correspond to real-life locations in the city's central districts and remote suburbs of St.Petersburg. The results of computation are presented in Appendix 2. The received routes of the money collector teams are depicted on the city-map, base on the coordinates for 20 ATMs and 4 depots. The matrix of distances is presented in Appendix 1. To simplify the representation of the computation results, we additionally suppose that the bank receives a claim for servicing of 20 ATMs. This claim includes four encashment centers with money collector teams. The notations and addresses of depots are

- open depot: ***A***(Vereiskaya st. 16, A), ***B***(Bukharestskaya st. 23);
- fictitious depots: ***C***(Oleca Dundich St. 34), ***D***(Marata st. 65).

The list of addresses of ATMs included in the claim for servicing is presented in Appendix 1.

Firstly, a solution for this subnetwork of 20 × 20 ATMs is found by using the method of Super-ATMs. At the first stage, the optimal location of encashment centers is obtained, such as servicing costs are minimized and constraints (2)–(10) are satisfied. As in [14], we assume that every ATM contains $d_i = 4$ cash cartridges and capacity of every vehicle is $Q = 16$. Distances between depots and ATMs are presented in Fig. 14. In the example, we take into account the cost of technical and human resources separately, because its allocation can affect on the bank's decision about the effectiveness of the used optimization approach. To calculate the servicing costs we assess costs per 1 km of route and one working day of collector team. Following the statistical data we use following values: cost of gasoline is about 30 rubles/liter, every vehicle consumes 1 l of gasoline per 10 km, hence the costs of 1 km is 3 rubles. In dynamics, fuel costs impact on the total cost of the encashment process if a number of serviced ATMs will increase. Each money collector team includes driver, security guard, and a cashier. Average salaries for these positions in St. Petersburg are 20 000 rubles/month, 27 000 rubles/month, and 30 000 rubles/month, respectively. We assume that the work schedule of collection team is 2/2 (two working day/two days of rest) then the cost of one working day is about 5500 rubles. The solution of the framework consists of two stages:

Stages:
(1) First, we combine encashment centers and its neighboring ATMs taking into account the distance matrix:

- depot A: 15, 19, 20.
- depot B: 3, 4, 6, 7, 9, 10, 13, 14, 18.
- depot C: 1, 2, 8, 12, 16, 17.
- depot D: 5, 11.

Following the Clarke–Write algorithm, we find a feasible solution for 4 encashment centers: $A-15-19-20-A$; $B-18-4-9-3-B$; $B-13-14-6-B$; $B-7-10-B$; $C-17-16-8-2-C$; $C-1-12-C$; $D-5-11-D$.

(2) On the second stage, the Super-ATMs method is applied, according to it we exclude encashment centers from the routes and merge ATMs into seven Super-ATMs:

- **a** = 15–19–20; **b** = 18–4–9–3; **c** = 13–14–6;
- **d** = 7–10; **e** = 17–16–8–2; **f** = 1–12; **j** = 5–11.

Received solution shows that depot D is connected with two ATMs, but it is closer to depot A than ATMs 5 and 11 should be connected with the depot A. Depot B is connected with ATMs 18, 4, 9, 3, 13, 14, 6, 7, 10. Depot C is grouped with ATMs 17, 16, 8, 2, 1, 12. Thus for the considered subset of ATMs, the opening of depots B and C is the optimal solution.

Hence, the solution of MDLRP problem is the following: $A-15-19-20-A-5-11-A$; $B-18-4-9-3-B-13-14-6-B-7-10-B$; $C-17-16-8-2-C-1-12-C$.

Further, GA1 is applied to improve the feasible solution. Then the distances from depots to Super-ATMs are defined as the average of the sum of distances from each

Table 1 The average distance between depot and Super-ATMs

Variable	Distance	Variable	Distance	Variable	Distance	Variable	Distance
X_{Aa}	5.76	X_{Ab}	11.675	X_{Ac}	8.3	X_{Ad}	6.7
X_{Ba}	11.1	X_{Bb}	10.05	X_{Bc}	5.73	X_{Bd}	4.55
X_{Ca}	15.9	X_{Cb}	11.225	X_{Cc}	8.93	X_{Cd}	9.2
X_{Da}	6.2	X_{Db}	11.775	X_{Dc}	8.5	X_{Dd}	6.5

Table 2 The average distance between depot and Super-ATMs

Variable	Distance	Variable	Distance	Variable	Distance
X_{Ae}	5.76	X_{Af}	11.675	X_{Aj}	8.3
X_{Be}	11.1	X_{Bf}	10.05	X_{Bj}	5.73
X_{Ce}	15.9	X_{Cf}	11.225	X_{Cj}	8.93
X_{De}	6.2	X_{Df}	11.775	X_{Dj}	8.5

Table 3 The shortest distances between depots and Super-ATMs

Super-ATMs	Variable	Minimum distance
a	X_{Aa}	5.76
b	X_{Bb}	10.05
c	X_{Bc}	5.75
d	X_{Bd}	4.55
e	X_{Ce}	9.95
f	X_{Cf}	4.4
j	X_{Dj}	2.75

ATM to Super-ATMs. In Tables 1, 2 variables X_{Aa}–X_{Dj} represent the average distance between depot and Super-ATMs, for example, X_{Aa} is the distance between depot A and Super-ATMs a.

Thus, the number of constraints is reduced, which simplifies solving of the problem and finding the shortest distances between a depot and Super-ATMs (Table 3).

GA1 gives the next solution: $A-5-11-15-19-A$; $B-4-16-17-18-B-10-20-13-6-B$, $B-14-3-9-8-B$; $C-12-1-2-8-16-17-C$, where total length is 114.7 km and costs are 17 000 rubles. Figure 11 represents the routes of money collector teams from depots A on the map of the streets.

Applying the second GA2, we obtain a slightly different solution: $B-4-6-17-18-B-10-20-13-6-B-14-3-8-9-B$, $C-12-1-2-8-16-17-C$, $D-5-11-15-19-D$, where total length of encashment routes is 113.5 km and costs are 16 800 rubles. Figures 11, 12, 13, 16, 17, 18, 19 and 20 show an influence of the transportation system of St.Petersburgs on the solutions.

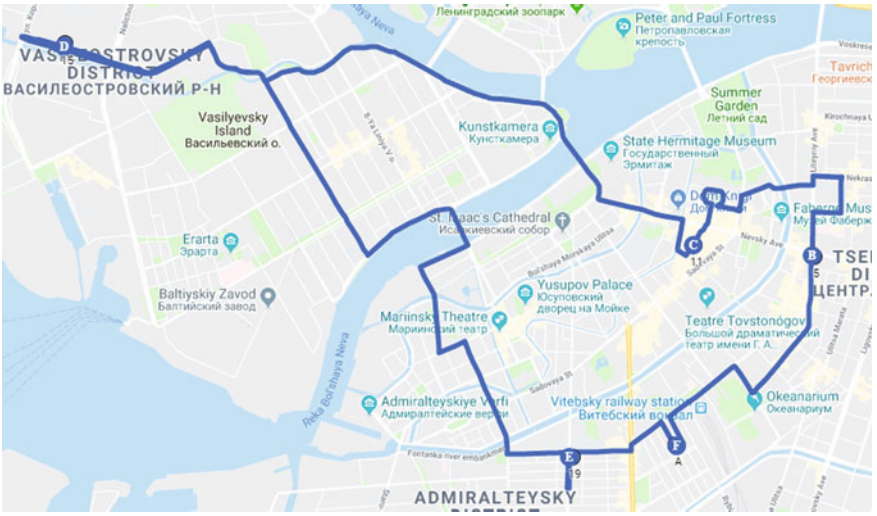

Fig. 11 Routes for depot A. $A-5-11-15-19-A$, route length is 28.4 km

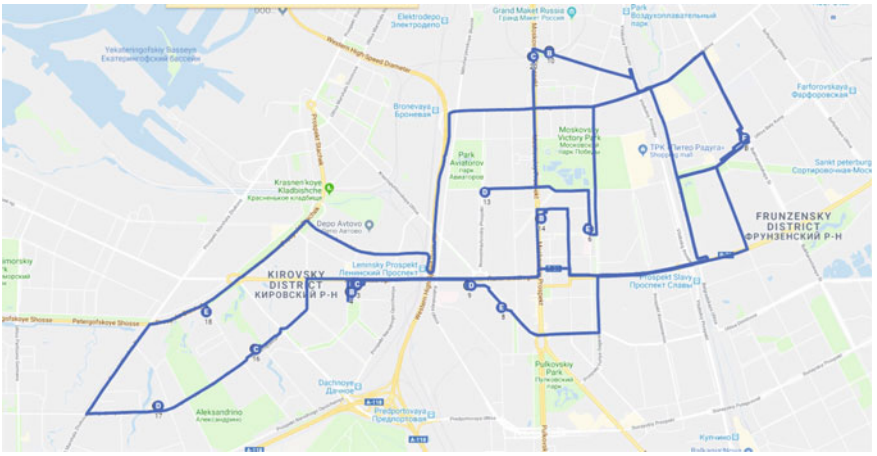

Fig. 12 Routes for depot B. $B-4-16-17-18-B$, $B-10-20-13-6-B$, $B-14-3-9-8-B$, route length is 67.3 km

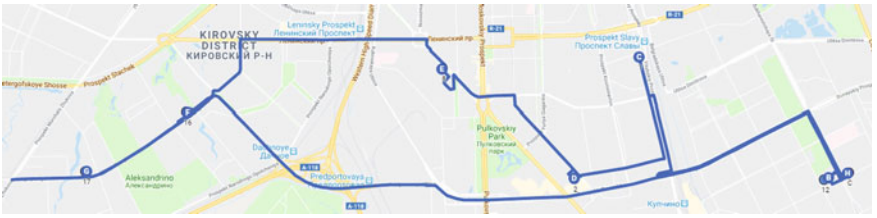

Fig. 13 Routes for depot C. $C-12-1-2-8-16-17-C$, route length is 19 km

Figure 11 represents routes from depot *A*. Figures 16, 17, 18 and 19 in Appendix 4 represent the routes which are similar for the solutions of GA1 and GA2. Figure 20 shows the routes correspond to the depot *D*.

7 Conclusion and Discussion

The paper represents the two-stage encashment problem solution consisting of adaptation of Multi-Depot Location Routing Problem for defining the optimal location of the encashment at the first stage and application of Multi-Depot Vehicle Routing Problem for the construction of routes though ATM subnetworks at the second stage.

We consider the modified routing model which incorporates the problem of optimal location of the encashment centers (depots) and the multi-depot vehicle routing problem. This approach allows receiving a solution of routing problem with large number of serviced ATMs by clustering them into different depots. As it was presented in the previous research studies, the scope of the problem leads to necessity of application of different numerical methods to receive a satisfactory solution. To solve the entire problem, we have used the Super-ATMs method to define the location of encashment centers and evolutionary computation to calculate the better routes in serviced areas of each encashment center. Here we use and compare two different genetic algorithms to receive routes for the network of 99 ATMs and 10 depots. The results show an insignificant difference between the results of GA1 and GA2 with a smaller problem instance, but with the bigger instance, GA2 has given a significantly better solution. The distance received by GA1 exceeds the distance obtained by GA2 by 18% in case of a large network of ATMs.

The recent studies [9, 25, 29] concerning the solution of this routing optimization problem have shown that game theoretical approach is also applicable in construction of the optimal distribution of nodes between depots as well as optimal routes between nodes in each cluster. Hereby, the problem can be solved using two-stage method: the game between encashment centers for designing the own subnetworks of ATMs and the routing game inside each cluster for defining the optimal traffic flow to encashment teams. At the first stage, we can formulate a game of grand players (depots) pursuing their aims. The aim of a player is to enlarge his/her subnetwork by adding new ATMs for increasing profit from ATMs. This triggers the competition for the items from the total set of ATMs between the encashment centers. As it was mentioned previously, in such a big city as St.Petersburg the distance between ATMs and encashment centers is large. Consequently, the conjunction of each new ATM increases the maintenance costs of subnetwork, since costs of service depend on the distances between nodes in the network.

Therefore, each encashment center shall find a compromised solution between connecting the maximum number of ATMs into the network and keeping the minimal servicing costs. Furthermore, the strategy of a player (an encashment center) can be defined as a selection of ATMs which can be connected to the network with the minimal servicing costs. In other words, we can consider an iteration process where

on each step player estimates the distance between the existing subnetwork and the nearest neighbors and makes a decision on a new unit.

Minimization of the total costs for maintenance of the subnetwork leads to the restriction of the maximum number of nodes in each subnetwork. Thus, we can define the payoff of the players as the function which depends on the difference between profit and the costs of servicing of ATMs subnetwork.

At the second stage, we can formulate a routing game between money collector teams inside each of the designed subnetworks. In this game, the set of players consists of money collector teams. Each team starts and finishes its route in the corresponding depot and plans a circle route with the minimal cost. We can define a strategy set of each player as a set of routes between their initial and final locations.

As optimality principles in the game between depots and routing games inside subnetworks we can use the Nash or Wardrop equilibriums, respectively. Equilibrium concept provides us with the possibility of taking into account individual preferences of the encashment centers. Moreover, the routing game can imply the detailed analysis of two additional subcases: in the first case the routes are planned in accordance with the principle of minimizing the route costs, while in the second, players take into account the cost of all routes in the subnetwork which results in obtaining the state of social optimum. According to this, further research studies can discuss social and individual preferences of the grand players as well as estimation of different strategies of the route planning of money collector teams.

Additionally, the game of competition between depots will also be discussed from the cooperative point of view by considering the tendency of consolidation between different branch offices of the banks. This new formulation of the problem allows us to compare different approaches and their application to large dimensional problem. As far as the considered complex optimization problem covers not only an encashment process but also includes an ensemble of various logistic tasks, therefore various techniques can be applied to solve the VRP and its different modifications such as CVRP, MDLRP, and MDVRP [22, 28].

Another approach which can be used to solve the proposed complex optimization problem of encashment is the dynamic programming (DP). Previous research studies have offered the possibility of application of this approach to the VRP and the CVRP, for example, in [18], the extension of the DP algorithm was introduced, where authors notice the difficulties in applying the methods to real-life problems. In [20], the MDVRP as a deterministic dynamic programming with finite state and action space has been considered. In the current framework, the DP algorithm can be used at the second stage of the optimization process as a method of constructing the giant tour inside the clusters of ATMs belonging to one depot. However, according to [18], the DP algorithm does not run in practically acceptable computation times for problem instances of realistic sizes. The application of the method is restricted by the maximum number of states and the number of state expansions of a single state. Despite this, the application of the DP algorithm to our problem provides the results which can be the subject for further research devoted to the comparison of the computational complexity of the methods discussed.

Acknowledgments We are really grateful to Svetlana Medvedeva for many helpful suggestions and constructive comments. The third author wants to acknowledge the support of the Academy of Finland.

Appendix 1

A list of ATMs included in the claim of servicing: Vitebskiy av., 53/4; Zvezdnaya st., 6; Leninskiy av., 129; Novatorov blvd., 11/2; Nevskiy av, 49; Gagarina av., 27; Kosmonavtov av., 28; Krasnoputilovskaya st., 121; Leninskiy av, 151; Koli Tomchaka st., 27; Dumskaya st., 4; Bukharestskaya st, 89; Basseynaya st., 17; Moskovskiy av., 200; Novosmolenskaya emb., 1/3; Veteranov av., 43; Veteranov av., 89; Leni Golikova st., 3; Izmaylovskiy av., 4; Moskovskiy av., 133 (Figs. 14, 15).

Appendix 2

In the current case study we apply both modification of genetic algorithms GA1 and GA 2 respectively for the problem of 109 × 109, where we have 10 depots and 99 ATMs. By using GA1 we obtain

- $A - 11 - 35 - 64 - A$, $A - 16 - 31 - 4 - A$, length is 78.467 km;

	1	2	3	4	5	6	7	8	9	10	11	12
1	0	3,6	6,7	6,6	12,7	4,7	3	5,5	6,2	7,1	13,2	5,4
2	3,9	0	5,8	5,7	13,6	3,8	3,6	4,6	5,7	8,4	13,8	4,9
3	6,4	5,8	0	4,5	13,1	5,1	6,6	2,6	1,7	7,9	13,2	10,1
4	6,6	5,2	4,8	0	12,6	5,5	7,1	3,1	2,2	8,3	12,4	10,6
5	12,5	13,9	13,5	12,6	0	10,5	10	12,2	13,7	7,3	3,3	13,1
6	4,7	3,8	5,1	5,8	10,7	0	2	3,7	5,1	5,2	10,5	7,1
7	3,2	3,4	6,9	7,9	10,2	2,2	0	5	6,9	5,5	10,8	6,2
8	5,1	4	2,2	3,4	12,2	3,7	5,2	0	3,2	6,9	12,2	7,6
9	6,2	5,7	1,7	2,2	14,1	5,1	6,4	3,5	0	6,2	11,5	8,4
10	7,1	9,1	7,7	8,3	7,8	5,8	5,5	6,9	6,4	0	7	9,7
11	13,5	14	13,4	12,8	3,5	10,8	10,8	12,2	11,2	7,2	0	14,8
12	5	4,9	10,1	10,2	13,1	7,5	5,8	7,4	8,8	10	15	0
13	6,2	5,2	3,4	4,2	9,7	2,4	2,7	2,3	2,2	3,5	8,6	10,1
14	4,4	4,4	3,6	4,5	11,4	1,1	2,9	2,2	2	4,5	10,1	8,8
15	20,4	20,9	18,5	16,2	10,3	16,8	17,9	16,8	16,8	13,7	9,2	22,1
16	10,2	9,3	4,5	4,1	16,1	8,1	10,2	7,1	5,7	9,5	15,7	19,2
17	12,2	11,2	6,4	5,8	18,2	10	11,2	8,4	8,1	11,8	17	16,7
18	9	8,5	5,9	3,4	15,5	7,3	8,5	5,5	5,4	9,1	14,9	12,8
19	12,6	11,1	10,1	8,9	5,7	9,3	9,6	8,2	8,4	5,8	3,5	14,3
20	9	9,1	8,9	8,4	6,8	5,4	6,1	7,8	7,1	0,5	5,8	12,3
A	11,2	10,2	10,7	10,8	3,6	7,9	8,4	9,9	11,2	4,9	3,6	15,7
B	6,8	8,7	9,7	10,5	8,5	5,3	5,1	9,2	8	4,1	9,8	6,8
C	6,9	5,6	10,9	11,5	17,6	7,9	6,9	7,9	10,4	12,5	16,8	2,1
D	9,2	8,7	12	11,2	2,2	8,5	8,1	10,8	10,5	5	3,5	11,2

Fig. 14 Matrix of distances C for 30 ATM and 4 encashment center

13	14	15	16	17	18	19	20	A	B	C	D
5,9	4,8	20,1	10,2	11,9	9	12,9	9,4	11,7	6,8	6,8	8,9
5	4,5	20,5	9,3	11	8,2	11,4	9,1	10,7	8,7	5,5	11,8
3,7	3,8	18	4,5	6,4	5,7	10,1	8,6	10,5	9,7	10,6	11,2
4,2	4,2	16,4	4,1	5,8	3	8,9	8,4	10,6	10,2	11,2	11,4
9,6	11,2	10,3	16,1	17,9	15,8	5,9	6,8	3,4	8	17,6	2
2,6	1,2	17,2	8,3	10,1	7,3	9,3	5,8	7,7	5,3	7,9	8,1
2,9	2,9	17,5	9,7	11,4	8,5	9,6	6,3	8,8	5	6,6	8
2,3	2,9	16,6	6,6	8,4	5,5	8,7	7,6	9,5	9,6	7,9	10,8
2	2	16,2	6,3	8	5,2	8,4	6,8	11	8	10,1	10,5
3,3	4,5	13,7	9,8	11,6	9,4	5,8	0,5	4,6	4,1	11,8	5
8,8	10,3	9	15,3	17	14,9	3	6	3,6	9,8	16,2	3,5
10,2	8,4	22,1	18,4	16,2	13,4	14,3	12,3	15,4	6,4	2	11,9
0	2,6	16,2	7,2	8,9	6	8,4	4,9	6,9	6,1	10	8,2
2,4	0	16	8	9,7	6,9	8,1	4,6	10,3	5,8	8,9	9,2
16,2	16,2	0	19,3	21,1	18,2	9,9	14,1	10,2	18	22	10,2
7,8	8	18,5	0	1,7	1,2	11	12,4	13,4	13,6	11,8	13,3
9,4	9,4	21	1,6	0	4	13,5	14,9	15,9	16	14,6	15,2
6,1	6,2	18,4	1,4	4,1	0	9,8	11,2	14,6	12,3	13	14
8,6	8,1	9,9	11	13,7	9,6	0	4,3	2,6	10,4	15,5	2,8
4,9	5	14,1	12,4	14,9	11,4	4,5	0	4,5	4,9	10,2	5,6
6,7	10,5	10,4	13,8	15,9	14,4	2,4	4,1	0	7,4	12,8	2,1
6,1	5,8	17,8	13,6	16,4	12,3	10,4	4,5	7,8	0	6,2	6,4
10,2	8,2	22,1	11,4	14,2	13,2	15,9	9,8	12,9	6,4	0	13,8
8	9,2	10	13,5	15,2	14	2,9	5,4	2,4	6,2	12,2	0

Fig. 15 Matrix of distances C for 30 ATM and 4 encashment center

- $B-42-70-80-B, B-46-12-14-2-B, B-56-62-21-37-B$, $B-60-18-36-71-B$, length is 86.149 km;
- $C-42-85-13-61-C$, $C-81-44-C$, length is 39.988 km;
- $D-22-24-47-D$, $D-39-38-6-D$, $D-75-72-17-10-D$, $D-82-5-89-66-D$, length is 87.649 km;
- $E-8-15-25-73-E$, $E-83-84-74-79-E$, $E-86-59-87-E$, length is 65.516 km;
- $F-3-41-48-F$, $F-54-69-58-88-F$, length is 42.953 km;
- $G-7-77-20-G$, $G-63-26-G$, length is 39.801 km;
- $H-52-76-32-68-H$, length is 27.390 km;
- $I-27-57-55-65-I$, $I-49-40-19-9-I$, $I-51-23-45-34-I, I-78-I$, length is 112.126 km;
- $J-28-30-50-1-J, J-53-33-29-67-J$, length is 47.477 km.

Total distance is 627.516 km and costs are 56883 rubles.

By GA2 approach we receive the next solution:

- $A-72-1-38-7-A, A-19-56-A; A-77-20-84-29-A$;
- $B-59-10-40-4-B$
- $C-85-36-17-41-C$;
- $G-8-21-14-46-G$;
- $E-74-26-71-35-E$;
- $D-18-30-D; D-87-78-88-6-D$;

- $D-58-89-49-13-D$;
- $D-44-76-5-50-D$, $D-23-63-82-73-D$;
- $E-42-34-65-E$;
- $E-9-53-61-54-E$; $E-64-69-37-51-E$,
- $G-60-63-57-75-G$;
- $H-43-45-67-33-H$;
- $H-16-H$, $H-66-81-28-3-H$, $H-22-12-15-52-H$;
- $H-27-90-31-68-H$;
- $H-32-24-H$, $H-39-2-80-83-H$;
- $H-48-25-47-11-H$.

Total distance is 452.119 km and costs are 39857 rubles.

From the computation we can see that the total distance on the routes for money collector teams received by GA2 are shorter that total distance received by GA1 for 18%.

Appendix 3

The savings algorithm is a heuristic algorithm, and therefore it does not provide an optimal solution to the problem with certainty. However it often gives a relatively good solution. The basic savings concept depicts the cost savings obtained by joining small routes into more large route. Consider the depot D and n demand points. Suppose that initially the solution to the VRP consists of using n vehicles and dispatching one vehicle to each one of the n demand points. The total tour length of this solution is, $2\sum_{i=1}^{n} d(D,i)$. If now we use a single vehicle to serve two points, say i and j, on a single trip, the total distance traveled is reduced by the amount

$$S_{ij} = c_{i0} + c_{0j} - c_{ij}.$$

Stage 1. Calculate the savings $S_{ij} = d(D,i) + d(D,j) - d(i,j)$ for every pair (i,j) of demand points.

Stage 2. Rank the savings S_{ij} and list them in descending order of magnitude. This creates the "savings list." Process the savings list beginning with the topmost entry in the list (the largest S_{ij}).

Stage 3. For the savings S_{ij} under consideration, include link (i,j) in a route if no route constraints will be violated through the inclusion of (i,j) in a route, and if:

a. Either, neither i nor j have already been assigned to a route, in which case a new route is initiated including both i and j.
b. Or, exactly one of the two points (i or j) has already been included in an existing route and that point is not interior to that route (a point is interior to a route if it is not adjacent to the depot D in the order of traversal of points), in which case the link (i, j) is added to that same route.
c. Or, both i and j have already been included in two different existing routes and neither point is interior to its route, in which case the two routes are merged.

Stage 4. If the savings list S_{ij} has not been exhausted, return to Stage 3, processing the next entry in the list; otherwise, stop: the solution to the VRP consists of the routes created during Stage 3. (Any points that have not been assigned to a route during Stage 3 must each be served by a vehicle route that begins at the depot D visits the unassigned point and returns to D.)

Appendix 4

See Figs. 16, 17, 18, 19, 20.

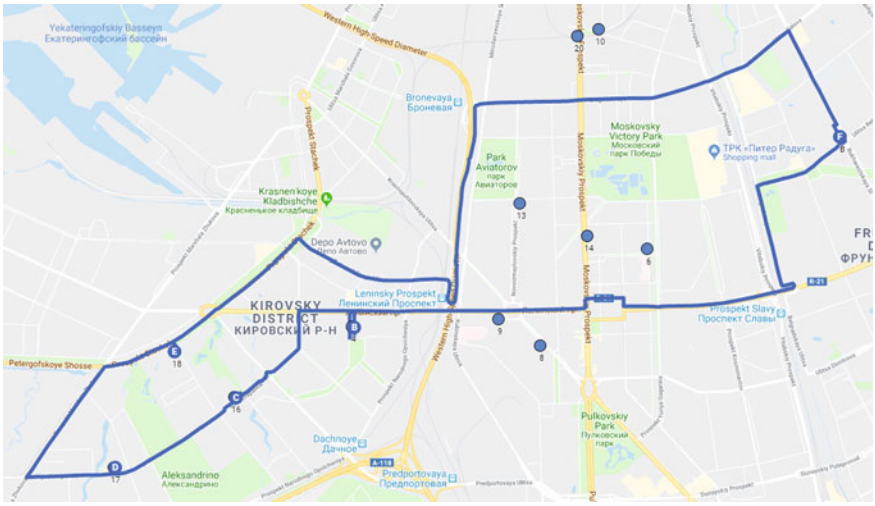

Fig. 16 Routes for depot B. $B - 4 - 16 - 17 - 18 - B$. Length of route is 31.4 km

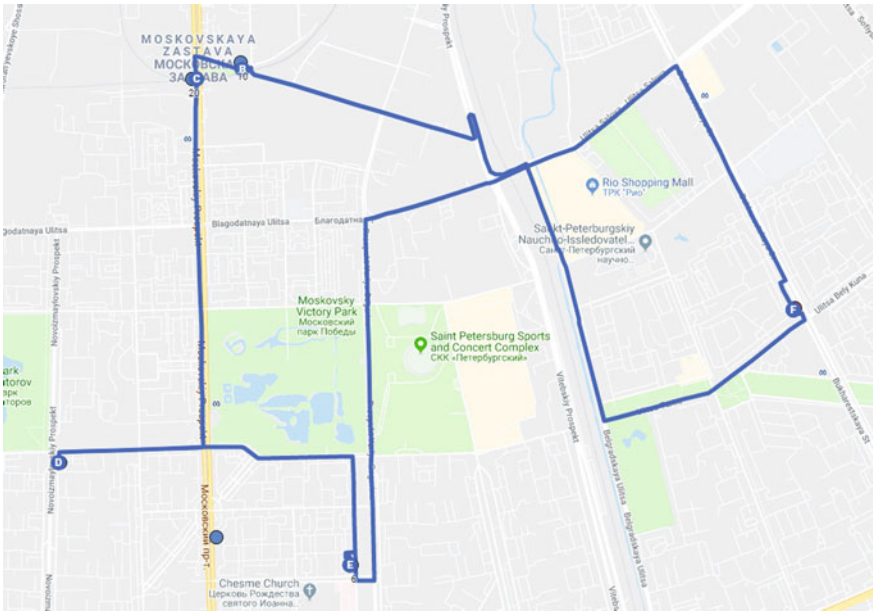

Fig. 17 Routes for depot B. $B - 10 - 20 - 13 - 6 - B$. Length of route is 16 km

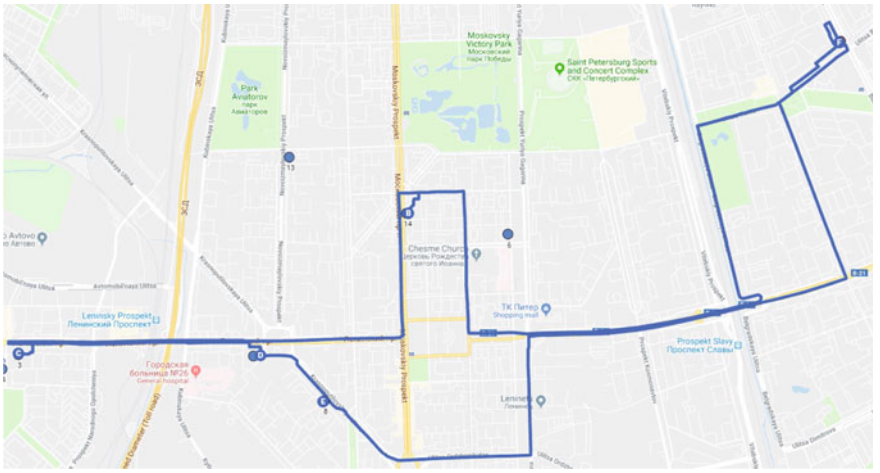

Fig. 18 Routes for depot B. $B - 14 - 3 - 9 - 8 - B$. Length of route is 19.9 km

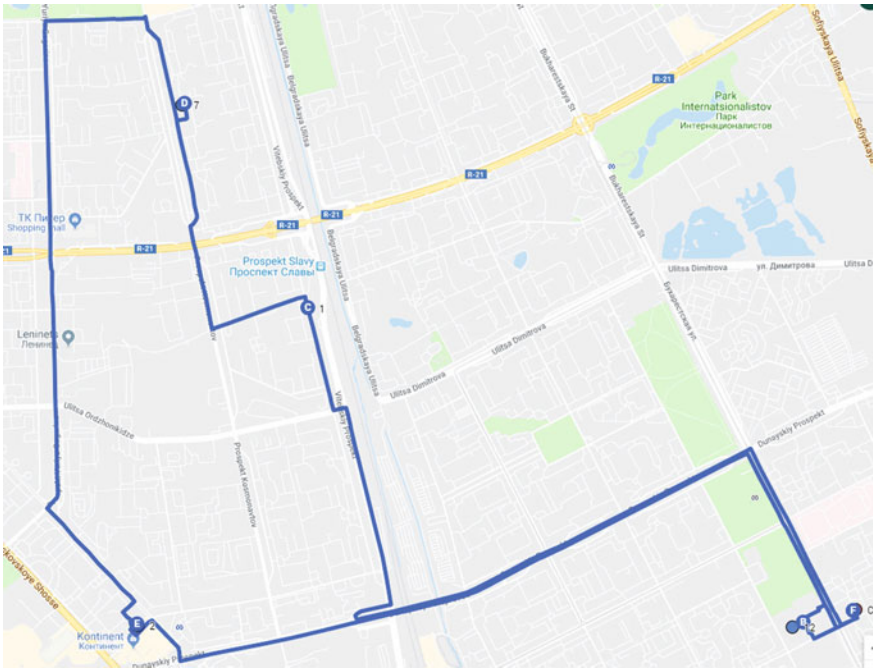

Fig. 19 Routes for depot C. $C - 12 - 1 - 7 - 2 - C$. Length of route is 19 km

Fig. 20 Routes for depot D. $D - 5 - 11 - 15 - 19 - D$. Route length is 27.2 km

References

1. ArcGis Resource Center.: Working with spatial references. ArcObjects Help for .NET developers.
2. Arnold, F., Gendreau, M., Sorensen, K.: Efficiently solving very large-scale routing problems. Comp. & Oper. Res. **107**, 32–42 (2019)
3. Arora, S.: Approximation schemes for NP-hard geometric optimization problems: a survey. Math. Prog. **97**, 1, 43–69 (2003)
4. Baker, B. M., Ayechew, M. A.: A genetic algorithm for the vehicle routing problem. Comp. & Oper. Res. **30**, 5, 787–800 (2003)
5. Bentley, P. J. and Wakefield, J. P. Hierarchical Crossover in Genetic Algorithms. In: Proceedings of the 1st On-line Workshop on Soft Computing (WSC1), Nagoya University, Japan (1996)
6. Carlsson, J. , Dongdong, G., Subramaniam, A., Wu, A., Yek, Y.: Solving Min-Max Multi-Depot Vehicle Routing Problem. Fields Institute Communications, **55**. (2009)
7. Clarke, G., Wright, J.: Scheduling of vehicles from a central depot to a number of delivery points. Oper. Res. **12**, 4, 568–581 (1964)
8. Crevier, B., Cordeau, J., Laporte, G.: The multi–depot vehicle routing problem with inter–depot routes. E. J. of Oper. Res. **176**, 756 –773 (2007)
9. Chkhartishvili, A. G., Gubanov, D. A., Novikov, D. A.: Social Networks: Models of Information Influence, Control and Confrontation. Springer, Heidelberg (2019)
10. Christofides, N., Mingozzi, A., Toth, P.: Exact Algorithms for the Vehicle Routing Problem, Based on Spanning Tree and Shortest Path Relaxations. Math. Prog. **20**, 255–282 (1981)
11. Dantzig G.B., Ramser, J.H.: The truck dispatching problem. Manag. Sci. **6**, 60, Vol. 80–91 (1959)
12. Dondo, R., Cerda, J.: A cluster–based optimization approach for the multi-depot heterogeneous fleet vehicle routing problem with time windows. E. J. of Oper. Res. **176**, 1478–1507 (2007)
13. Eiben, A. E., Smith, J. E.: Introduction to Evolutionary Computing. Springer (2003)
14. Gubar, E. A., Merzlyakova, J. D., Zubareva, M. L.: Cash flow optimization in ATMs network model. Contrib. to Game Theory and Manag. **4**, 213–223 (2011)
15. Hall, R. W.: Handbook of Transportation Science. Springer, 741 (2003)
16. Laporte, G., Nobert, Y., Taillefer, S.: Solving a family of multi-depot vehicle routing and location-routing problems. Transp. Sci. **22**, 161–172 (1988).
17. Hoa, W. Hob, G. T. S., Jib, P., Laub, H. C. W.: A hybrid genetic algorithm for the multi-depot vehicle routing problem. Engin. App. of Artificial Intell. **21**, 4, 548–557 (2008)
18. Kok A.L., Meyer C. M., Kopfer H., Schutten J. M. J.: Dynamic Programming Algorithm for the Vehicle Routing Problem with Time Windows and EC Social Legislation. Transp. Sc. **44**, No. 4. 429–553 (2010).
19. Larranaga, P., Kuijpers, C. M. H., Murga, R. H., Inza, I., Dizdarevic, S.: Genetic Algorithms for the Travelling Salesman Problem: A Review of Representations and Operators. Art. Intell. Rev. **13**, 2, 129–170 (1999)
20. Lee, C.-G., Epelman M., White Ch. C. and Bozer Ya. A.: A shortest path approach to the multiple-vehicle routing problem with split pick-ups. **40**, 4, 265–284 (2006)
21. Lysgaard, J., Letchford, A., Eglese, R. A New Branch-and-Cut Algorithm for the Capacitated Vehicle Routing Problem. Math. Program., Ser. A **100**, 423–445 (2004)
22. Vehicle Routing Problem | NEO Research Group. 2013. http://neo.lcc.uma.es/vrp/
23. Nagy G., Salhi S.: Heuristic algorithms for single and multiple depot vehicle routing problems with pickups and deliveries. European Journal of Operational Research. **162**, 126–141 (2005)
24. Nallusamy, R., Duraiswamy, K., Dhanalaksmi, R., Parthiban, P.: Optimization of Multiple Vehicle Routing Problems using approximation algorithms. International Journal of Engineering Science and Technology. **1**(3). 129–135 (2009)
25. Paltseva D. A., Parfyonov A. P.: Atomic routing game with capacity constraints, Mat. Teor. Igr Pril., **10**, 1, 65–82, (2018).

26. Prins, C., Prodhon, C., Ruiz, A., Soriano, P., Calvo, R. W.: Solving the Capacitated Location-Routing Problem by a Cooperative Lagrangean Relaxation-Granular Tabu Search Heuristic. Transp. Sc., **41**, 4, 470–483 (2007)
27. Platonova V., Gubar E.: Multi-depots location routing problem in ATM's network. In: The XLIV annual international conference Control Processes and Stability (CPS'13). Saint-Petersburg, 644–650 (2013)
28. Ramos T. R. P., Gomes M.I. and Barbosa Póvoa A.P.: Multi-depot vehicle routing problem: a comparative study of alternative formulations. Int. J. of Log. Res. and App., Taylor & Francis 0, pp. 1–18, (2019) https://doi.org/10.1080/13675567.2019.1630374
29. Roughgarden, T.: Routing Games. In N. Nisan, T. Roughgarden, E. Tardos, & V. Vazirani (Eds.), Algorithmic Game Theory. Cambridge: Cambridge University Press. 461–486 (2007) doi:https://doi.org/10.1017/CBO9780511800481.020
30. Santana R.M.: Heuristic algorithms and Variants of the Vehicle Routing Problem for a Distribution Company: A Case Study. In: The European Master's Program in Computational Logic Master's Thesis. Facultade de Ciencias e tecnologis Universidade Nova de Lisboa (2016)
31. Shchegryaev A., Zakharov V.: Multi-period cooperative vehicle routing games. Contrib. to Game Theory and Management. **7**, 349–359 (2014)
32. Wu, T.-H., Low, Ch., Bai, J.-W.: Heuristic solutions to multi-depot location-routing problems. Comp. and oper. res. **29**, 1393–1415 (2002)
33. Topplan, http://www.topplan.ru/
34. Velasquez, J., W., E., Heuristic Algorithms for the Capacitated Location-Routing Problem and the Multi-Depot Vehicle Routing Problem. 4OR, A Quar. J. Oper. Res. Springer, Berlin, **12**, 1, 99–100 (2014)

Load Balancing Congestion Games and Their Asymptotic Behavior

Eitan Altman, Corinne Touati, Nisha Mishra, and Hisao Kameda

1 Introduction

A central question in routing games has been to establish conditions for the uniqueness of the equilibria, either in terms of the network topology or in terms of the costs. A survey on these issues is given in [1].

The question of uniqueness of equilibria has been studied in two different frameworks. The first, which we call **F1**, is the *non-atomic routing* introduced by Wardrop on 1952 in the context of road traffic in which each player (car) is infinitesimally small; a single car has a negligible impact on the congestion. Each car wishes to minimize its expected delay. Under arbitrary topology, such games are known to have a convex potential and thus have a unique equilibrium [2]. The second framework, denoted by **F2**, is *splittable atomic games*. There are finitely many players, each controlling the route of a population of individuals. This type of games have already been studied in the context of road traffic by Haurie and Marcotte [3] but have become central in the telecom community to model routing decisions of Internet Service Providers that can decide how to split the traffic of their subscribers among various routes so as to minimize network congestion [4].

E. Altman (✉)
1. INRIA, University Cote d'Azur 2. LIA, Avignon University, and 3. LINCS, Paris, France
e-mail: Eitan.Altman@inria.fr

C. Touati · N. Mishra
INRIA and CNRS, LIG, Univrsity of Grenobles, Saint-Martin-d'Héres, France
e-mail: Corinne.Touati@inria.fr

N. Mishra
e-mail: Nisha.Mishra@inria.fr

H. Kameda
Hisao Kameda, University of Tsukuba, Tsukuba, Japan
e-mail: kameda@cs.tsukuba.ac.jp

D. M. Ramsey and J. Renault (eds.), *Advances in Dynamic Games*,
Annals of the International Society of Dynamic Games 17,
https://doi.org/10.1007/978-3-030-56534-3_10

In this paper, we study properties of equilibria in two other frameworks of routing games which exhibit surprising behavior. The first, which we call **F3**, known as *congestion games* [5], consists of atomic players with non-splittable traffic: each player has to decide on the path to be followed by for its traffic and cannot split the traffic among various paths. This is a non-splittable framework. We further introduce a new semi-splittable framework, denoted by **F4**, in which each of several players has an integer number of connections to route. It can choose different routes for different connections but there is a constraint that the traffic of a connection cannot be split. In the case where each player controls the route of a single connection and all connections have the same size, this reduces to the congestion game of Rosenthal [5].

We consider in this paper routing games with additive costs (i.e., the cost of a path equals to the sum of costs of the links over the path) and the cost of a link is assumed to be convex increasing in the total flow in the link. The main goal of this paper is to study a particular symmetric game of this type in a simple topology consisting of three nodes and three links. We focus both on the uniqueness issue as well as on other properties of the equilibria.

This game has already been studied within the two frameworks **F1**-**F2** that we mentioned above. In both frameworks it was shown [6] to have a unique equilibrium. Our first finding is that in frameworks **F3** and **F4** there is a multitude of equilibria. The price of stability is thus different from the price of anarchy and we compute both. We show the uniqueness of the equilibrium in the limit as the number of players N grows to infinity extending known results [3] from framework **F2** to the new frameworks. In framework **F2** uniqueness is in fact achieved not only for the limiting games but also for all N large enough. We show that this *is not the case* for **F3**-**F4**: for any finite N there may be several equilibria. We show however in **F3** that the whole set of equilibria corresponding to a given N converge to the singleton corresponding to the equilibrium in **F1** as $N \to \infty$. We finally show a surprising property of **F4** that exhibits non-symmetric equilibria in our symmetric network example while under **F1**, **F2**, and **F3** there are no asymmetric equilibria.

The structure of the paper is as follows. We first introduce the model and the notations used in the study, we then move on to the properties of frameworks **F3** (Sect. 3) and **F4** (Sect. 4) and their relation to frameworks **F1** and **F2**. We include in the Appendix the proofs of the theorems and propositions of the paper.

2 Model and Notations

We shall use throughout the term *atomic game* to denote situations in which decisions of a player have an impact on other players' utility. It is *non-atomic* when players are infinitesimally small and are viewed like a fluid of players, such that a single player has a negligible impact on the utility of other players.

We consider a system of three nodes (A, B and C) with two incoming traffic sources (respectively, from node A and B) and an exit node C. There are a total of N connections originating from each one of the sources. Each connection can either be

Fig. 1 Physical system

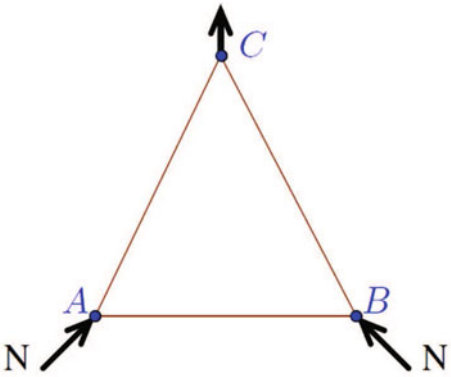

sent directly to node C or rerouted via the remaining node. The system is illustrated in Fig. 1.

This model has been used to model load balancing issues in computer networks, see [6] and references therein. Jobs arrive to two computing centers represented by nodes A and B. A job can be processed locally at the node where it arrives or it may be forwarded to the other node incurring further communication delay. The costs of links $[AC]$ and $[BC]$ represent the processing delays of jobs processed at nodes A and B, respectively. Once processed, the jobs leave the system. A connection is a collection of jobs with similar characteristics (e.g., belonging to the same application).

We introduce the following notations:

- A link between two nodes, say A and B, is denoted by $[AB]$. Our considered system has three links $[AB]$, $[BC]$ and $[AC]$.
- A route is simply referred by a sequence of nodes. Hence, the system has four types of connections (routes): two originating from node A (route AC and ABC) and two originating from node B (route BC and BAC).

Further, in the following, n_{AC}, n_{BC}, n_{ABC}, and n_{BAC} will refer to the number of connections routed via the different routes while $n[AC]$, $n[BC]$ and $n[AB]$ will refer to the number of connections on each subsequent link. By conservation law, we have

$$n_{AC} + n_{ABC} = n_{BC} + n_{BAC} = N$$

$$and \begin{cases} n[AC] = n_{AC} + n_{BAC}, \\ n[BC] = n_{ABC} + n_{BC}, \\ n[AB] = n_{BAC} + n_{ABC}. \end{cases}$$

For each route r, we also define the fraction (among N) of flow using it, i.e., $f_r = n_r/N$. The conservation law becomes $f_{AC} + f_{ABC} = f_{BC} + f_{BAC} = 1$.

Finally, the performance measure considered in this work is the cost (delay) of connections experienced on their route. We consider a simple model in which the cost is additive (i.e., the cost of a connection on a route is simply taken as the sum of

delays experienced by the connection over the links that constitute this route). The link costs are given by

$$\begin{cases} C_{[AB]} = a(f_{BAC} + f_{ABC}), \\ C_{[AC]} = b(f_{BAC} + f_{AC}), \\ C_{[BC]} = b(f_{BC} + f_{ABC}), \end{cases}$$

where $a(.)$ and $b(.)$ are some functions of the corresponding fractions of link flows. The path costs are given by

$$C_{AB} = C_{[AB]},\ C_{ABC} = C_{[AB]} + C_{[BC]},$$
$$C_{BC} = C_{[BC]},\ C_{BAC} = C_{[AB]} + C_{[AC]}.$$

The cost for a user in frameworks F2-F4 is the average of path costs weighted by the fraction that the player sends over each of the paths. For framework F3 a single packet is sent by each player so the cost for the player is the cost for the path that it takes.

We shall frequently assume that the costs on each link are linear with coefficient α/N on link $[AB]$ and coefficient β/N on link $[AC]$ and $[BC]$, i.e., for some positive constants α and β we have

$$\begin{cases} C_{[AB]} = \dfrac{\alpha}{N}(f_{BAC} + f_{ABC}), \\ C_{[AC]} = \dfrac{\beta}{N}(f_{BAC} + f_{AC}), \\ C_{[BC]} = \dfrac{\beta}{N}(f_{BC} + f_{ABC}). \end{cases}$$

We restrict our study to the (pure) Nash equilibria which we express in terms of the corresponding flows marked by a star. By conservation law, the equilibria are uniquely determined by the specification of f^*_{ABC} and f^*_{BAC} (or equivalently n^*_{ABC} and n^*_{BAC}).

The main contribution of the paper is the study of the above network within the following two types of decision models. In the first (**F3**), the decision is taken at the connection level (Sect. 3), i.e., each connection has its own decision-maker that seeks to minimize the connection's cost, and the connection cannot be split into different routes. In the second (**F4**), (Sect. 4) each one of the two source nodes decides on the routing of all the connections originating there. Each connection of a given source node (either A or B) can be routed independently but a connection cannot be split into different routes. We hence refer to **F4** this semi-splittable framework. Note that the two approaches (**F3** and **F4**) coincide when there is only $N = 1$ connection at each source, which we also detail later. We shall relate frameworks **F3** and **F4** to the frameworks **F1** and **F2** obtained as limits as the number of connections grows to infinity.

3 Atomic Non-splittable (F3 Framework) Case and Its Non-atomic Limit (F1 Framework)

We consider here the case where each $2N$ players connection belongs to an individual user acting selfishly.

We first show that for fixed parameters, the game may have several equilibria, all of which are symmetric for any number of players. The number of distinct equilibria can be made arbitrarily large by an appropriate choice of functions a and b.

We then show properties of the limiting game obtained as the number of players increases to infinity.

3.1 Non-uniqueness of the Equilibrium

Theorem 1 *Assume that a is non-negative and non-decreasing and that b is increasing. Then any equilibrium is symmetric, i.e.,* $f^*_{BAC} = f^*_{ABC}$. *Routing a fraction* $2x$ *players (x from A and x from B) to indirect links is an equilibrium if and only if*

$$a(2x) \leq b(1 + 1/N) - b(1) \tag{1}$$

Proof Consider an equilibrium (f^*_{ABC}, f^*_{BAC}). We first show that the equilibrium is symmetric. Assume on the contrary that $f^*_{ABC} > f^*_{BAC}$. Since the demands are the same this implies that $f^*_{BC} > f^*_{AC}$ and the total flow on link BC is strictly larger than the flow on link AC. But then, any player that takes the route ABC (note that by assumption there is at least one such player) would strictly decrease its cost if it deviates to the direct path AC. This contradicts the assumption of equilibrium. Hence $f^*_{ABC} = f^*_{BAC}$ and $f^*_{BC} = f^*_{AC}$.

At equilibrium a player that takes the direct path cannot gain by deviating. Thus a routing multistrategy is an equilibrium if and only if a player that takes the indirect path cannot strictly decrease its cost by deviation. Equivalently, routing a fraction x of players via the indirect link is an equilibrium if and only if $b(1) + a(2x) \leq b(1 + 1/N)$, which implies the Theorem. □

We shall call a multipolicy that routes k connections to each of the indirect path a "k-policy".

Corollary 1 *Assume that* $a(x)$ *and* $b(x)$ *are increasing in* x. *Then, (i) if for some k, the k-policy is an equilibrium then for any* $j < k$, *the j-policy is also equilibrium. (ii) If for some N, a k-policy is an equilibrium then it is also an equilibrium for smaller values of N.*

We calculate the number of equilibria for different cost functions. Let k be the solution of Eq. (1) obtained with equality. Hence the number of equilibria is $\lfloor k \rfloor + 1$.

We have the following cases:

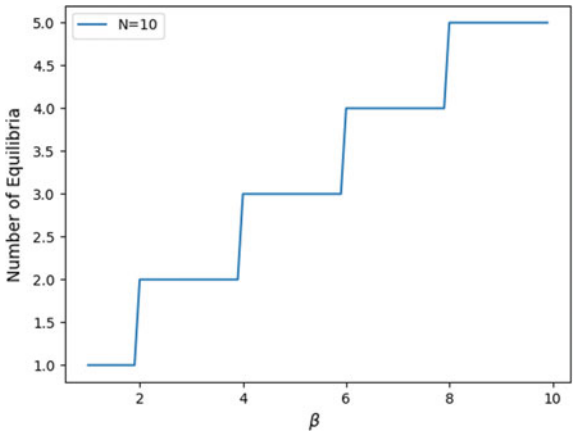

Fig. 2 Variation of the number of equilibria with respect to β (for $\alpha = 1$)

- When $b(x) = \beta x$ and $a(x) = \alpha x$, then Condition (1) reduces to

$$x \leq \frac{\beta}{2N\alpha}.$$

So the number of equilibria is $\lfloor \frac{\beta}{2\alpha} \rfloor + 1$.
The plot of the number of equilibria with respect to β for $\alpha = 1$ and $N = 10$ is given in Fig. 2.
We have the following observations:

1. The number of equilibria does not depend on the number N of players.
2. The number of equilibria increases as the cost function β increases for constant value of α.

- When the cost function on the direct link is linear, i.e., $b(x) = \beta x$ and indirect link is non-linear and is of the form $a(x) = x^{\ell}$ for $\ell \geq 0$, then Condition (1) reduces to

$$x \leq \frac{1}{2}\left(\frac{\beta}{N}\right)^{\frac{1}{\ell}}.$$

So the number of equilibria is $\left\lfloor \frac{N}{2}\left(\frac{\beta}{N}\right)^{\frac{1}{\ell}} \right\rfloor + 1$.
The plot of the number of equilibria with respect to ℓ for $\beta = 1$ is shown in Fig. 3.
We have the following observations:

1. The number of equilibria depends on the number of players, N. It increases with N for $\ell > 1$ and decreases in N for $\ell < 1$.
2. The number of equilibria increases in the power factor ℓ.

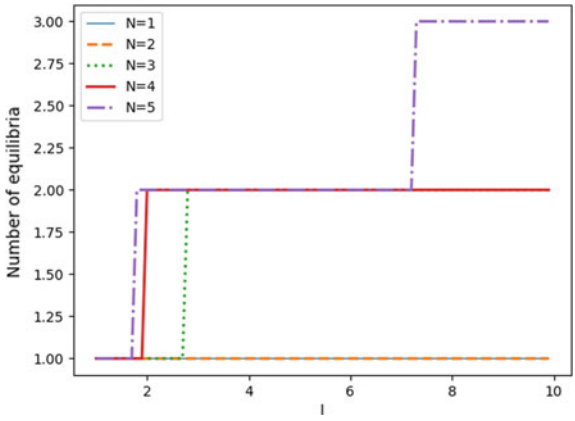

Fig. 3 Variation of the number of equilibria with respect to ℓ (for $\beta = 1$)

Remark 1 Consider the special case that $a = 0$. The problem is the equivalent to routing on parallel links. Now assume that b is decreasing. Then the only equilibria are (i) send no flow through AC and (ii) send no flow through BC.

Corollary 2 *Assume that the derivative $a'(0)$ of a at zero and the derivative $b'(1)$ of b at 1 exist. Then for large enough N, the k-policy is an equilibrium if*

$$2ka'(0) < b'(1)$$

If moreover, b is convex and a concave (not necessarily strictly), then the above holds for every n. If the opposite inequality holds above then for all n large enough the k policy is not an equilibrium.

Proof The first part follows from (1). The second part follows from the fact that the slope $(f(x + y) - f(x))/y$ of a function increases in y if the function is convex and decreases in y if it is concave. □

3.2 The Potential and Asymptotic Uniqueness

When the number of players N grows to infinity, the limiting game becomes a non-atomic game with a potential [7] defined by

$$F_\infty(f_{ABC}, f_{BAC}) = \int_0^{r_1} a(s)ds + \int_0^{r_2} b(s)ds + \int_0^{r_3} b(s)ds,$$

where $r_1 = f_{ABC} + f_{BAC}, r_2 = 1 - f_{ABC} + f_{BAC}$ and $r_3 = 1 + f_{ABC} - f_{BAC}$. In the special case of linear cost of the form $a(x) = \alpha x, b(x) = \beta x$, the above potential is equivalent to the following one (upto a constant)

$$F_\infty(f_{ABC}, f_{BAC}) \tag{2}$$

$$= \beta(f_{ABC} - f_{BAC})^2 + \frac{\alpha}{2}(f_{ABC} + f_{BAC})^2.$$

Hence we have the following:

Proposition 1 *If a and b are strictly increasing then the non-atomic game (framework* **F1***) has a unique Nash equilibrium, which is* $f^*_{ABC} = f^*_{BAC} = 0$.

Uniqueness of the equilibrium was shown to hold in [8, 9] under different conditions. More general topological settings are considered and more general definition of players. Yet it is assumed there that the costs are continuously differentiable which we do not assume here.

To show the uniqueness of the equilibrium in the limiting game, we make use of the fact that the limiting game has a potential which is convex. Yet, not only the limiting game has a potential, but also the original one, as we conclude from next theorem, whose proof is a direct application of [5].

Theorem 2 *For any finite number of players, the game (in framework F3) is a potential game [10] with the potential function up to a constant:*

$$F(f_{ABC}, f_{BAC}) =$$

$$\sum_{i=0}^{Nr_1} a(i) + \sum_{i=0}^{Nr_2} b(i) + \sum_{i=0}^{Nr_3} b(i). \tag{3}$$

For the case of linear costs this gives

$$\begin{aligned} F(f_{ABC}, f_{BAC}) &= \beta N^2 (f_{ABC} - f_{BAC})^2 \\ &+ \frac{\alpha N^2}{2} (f_{ABC} + f_{BAC})(f_{ABC} + f_{BAC} + 1/N). \end{aligned} \tag{4}$$

Note that unlike the framework **F1** of non-atomic games, the fact that the game has a potential which is convex over the action set does not imply uniqueness. The reason for that is that in congestion games, the action space over which the potential is minimized is not a convex set (due to the non-splittable nature) so that it may have several local minima, each corresponding to another equilibrium, whereas a for a convex function over the Euclidean space, there is a unique local minimum which is also a global minimum of the function (and thus an equilibrium of the game).

3.3 Efficiency

Proposition 1 implies that

Theorem 3 *In the non-atomic setting,* **F1***, the only Nash equilibrium is also the social optimum (i.e., the point minimizing the sum of costs of all players) of the system.*

Proof The sum of costs of all players is

$$\begin{aligned} & f_{ABC}C_{ABC} + f_{AC}C_{AC} + f_{BAC}C_{BAC} + f_{BC}C_{BC} \\ &= (f_{ABC} + f_{BAC})a(f_{ABC} + f_{BAC}) + f_{ABC}b(f_{BC} + f_{ABC}) \\ &+ f_{AC}b(f_{AC} + f_{BAC}) + f_{BAC}b(f_{AC} + f_{BAC}) \\ &+ f_{BC}b(f_{ABC} + f_{BC}). \end{aligned} \tag{5}$$

The minimum is hence obtained for $(f_{ABC}, f_{BAC}) = (0, 0)$. □

See [8, 9] for related results. Since the game possesses several equilibria, we can expect the PoA (Price of Anarchy—the largest ratio between the sum of costs at an equilibrium and the sum of costs at the social optimum) and PoS (Price of Stability—the smallest corresponding ratio) to be different.

Let k^* be the largest integer such that $x^* = k^*/N$ satisfies Eq. (1). Then the equilibrium $(\hat{x}^*, \hat{x}^*)$ with largest cost corresponds to this k.

Theorem 4 *The price of stability of the game is* 1 *and the price of anarchy is*

$$PoA = \frac{x^* a(2x^*)}{b(1)} + 1$$

with $x^* = f^*_{ABC} = f^*_{BAC}$.

Proof According to Theorem 1 we may restrict to symmetric equilibria, i.e., $n^*_{ABC} = n^*_{BAC}$, then $f^*_{ABC} = f^*_{BAC} = x^*$. So the sum of costs of all the players becomes $2x^* a(2x^*) + 2b(1)$.

The sum of costs at social optimum is $2b(1)$, i.e., at $x^* = 0$.

The price of anarchy is equal to the largest ratio between the sum of costs at an equilibrium to the sum of costs at social optimum. So $PoA = \frac{2x^* a(2x^*)+2b(1)}{2b(1}$. Hence the result. □

Note: Substituting $x^* = k^*/N$, the price of anarchy becomes,

$$PoA = \frac{k^*}{Nb(1)} a\left(\frac{2k^*}{N}\right) + 1.$$

We look into different cases of cost functions and calculate the price of anarchy using the value of x and the theorem.

We have the following cases:

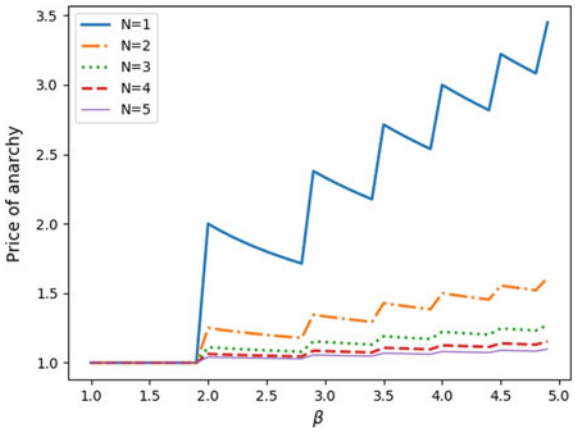

Fig. 4 Variation of the price of anarchy with respect to β (for $\alpha = 1$)

- When the cost function on both the direct and indirect link is linear and is of the form $b(x) = \beta x$ and $a(x) = \alpha x$, then $PoA \leq \frac{\beta}{2\alpha N^2} + 1$. The exact value of price of anarchy can be obtained by substituting the exact value of k. So,

$$PoA = \frac{2\alpha}{N^2\beta}\left\lfloor \frac{\beta}{2\alpha} \right\rfloor^2 + 1.$$

The plot of the PoA with respect to varying β for a constant $\alpha = 1$ is shown in Fig. 4.
We have the following observations

1. As the number of player increases, the PoA decreases.
2. For large N, the price of anarchy may asymptotically reach 1.
3. The PoA increases as the cost function β increases.
4. If $\beta > 2\alpha$, the PoA never becomes 1 for any value of N.

- When the cost function on the direct link is linear, i.e., $b(x) = \beta x$ and the cost of the indirect link is non-linear and is of the form $a(x) = x^\ell$ for $l \geq 0$, then the exact value of price of anarchy can be obtained by substituting the exact value of k. So,

$$PoA = \frac{2^\ell}{\beta N^{\ell+1}}\left\lfloor \frac{N}{2}\left(\frac{\beta}{N}\right)^{\frac{1}{\ell}} \right\rfloor^{\ell+1} + 1.$$

The plot of the PoA with respect to varying ℓ for a constant $\beta = 1$ is given in Fig. 5.
We have the following observations from the graph:

1. There is no monotonicity in the graph with either respect to the number of players or with the power factor l.
2. If $\beta < 2^\ell N^{1-\ell}$, the PoA becomes 1.

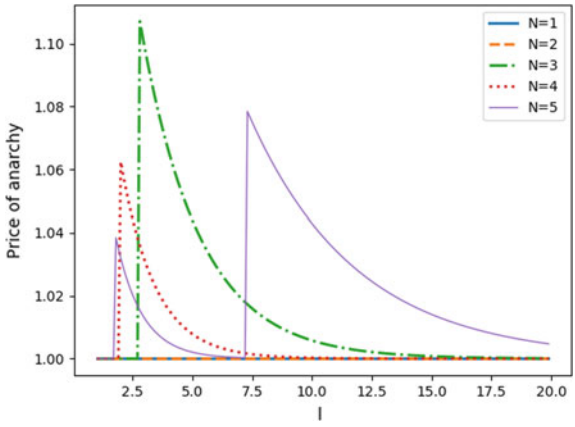

Fig. 5 Variation of the number of equilibria with respect to ℓ (for $\beta = 1$)

3. For large ℓ, the PoA again becomes 1.
4. For $N = 1, 2$, the PoA is 1 for all values of ℓ.

We also make the following observations:
(i) In the splittable atomic games studied in [6] the PoA was shown to be greater than one for a sufficiently small number of players (smaller than some threshold) and was 1 for all large enough number of players (larger than the same threshold). Here for any number of players, the PoS is 1 and the PoA is greater than 1.
(ii) The PoA decreases in N and tends to 1 as N tends to infinity, the case of splittable games.
(iii) We have shown that the PoA is unbounded: for any real value K and any number of players, one can choose the cost parameters a and b so that the PoA exceeds K. This corresponds to what was observed in splittable games [8] and contrasts with the non-atomic setting [11, 12].

4 Atomic Semi-splittable Case and Its Splittable Limit (F4 Framework)

We restrict in the rest of the paper to the linear cost. The game can be expressed as a 2-player matrix game where each player (i.e., each source node A and B) has $N + 1$ possible actions, for each of the $N + 1$ possible values of f_{ABC} and f_{BAC}, respectively.

The utility for player A is

$$\begin{aligned} U_A(f_{ABC}, f_{BAC}) &= f_{AC}C_{AC} + f_{ABC}C_{ABC} \\ &= b - bf_{ABC} + bf_{BAC} \\ &\quad +(a-2b)f_{ABC}f_{BAC} + (a+2b)f_{ABC}^2. \end{aligned} \tag{6}$$

Similarly, for player B:

$$\begin{aligned} U_B(f_{ABC}, f_{BAC}) &= f_{BC}C_{BC} + f_{BAC}C_{BAC} \\ &= b - bf_{BAC} + bf_{ABC} \\ &\quad +(a-2b)f_{BAC}f_{ABC} + (a+2b)f_{BAC}^2. \end{aligned} \tag{7}$$

Note that

$$\frac{\partial U_A}{\partial f_{ABC}} = -b + (a-2b)f_{BAC} + 2(a+2b)f_{ABC}$$

$$and\ \frac{\partial U_B}{\partial f_{BAC}} = -b + (a-2b)f_{ABC} + 2(a+2b)f_{BAC}.$$

Hence $\frac{\partial^2 U_A}{\partial f_{ABC}^2} = 2(a+2b) = \frac{\partial^2 U_B}{\partial f_{BAC}^2}$. Therefore, both $u_A : f_{ABC} \mapsto U_A(f_{ABC}, f_{BAC})$ and $u_B : f_{BAC} \mapsto U_B(f_{ABC}, f_{BAC})$ are (strictly) convex functions. This means that for each action of one player, there would be a unique best response to the second player if its action space was the interval $(0, 1)$. Hence, for the limit case (when $N \to \infty$), the best response is unique. In contrast, for any finite value of N, there are either 1 or 2 possible best responses which are the discrete optima of functions $u_A : f_{ABC} \mapsto U_A(f_{ABC}, f_{BAC})$ and $u_B : f_{BAC} \mapsto U_B(f_{ABC}, f_{BAC})$. We will however show that in the finite case, there may be up to $2 \times 2 = 4$ Nash equilibria while in the limit case the equilibrium is always unique.

4.1 Efficiency

Note that the total cost of the players is

$$\begin{aligned} &\Sigma(f_{ABC}, f_{BAC}) = U_A(f_{ABC}, f_{BAC}) + U_B(f_{ABC}, f_{BAC}) \\ &= 2b + 2(a-2b)f_{ABC}f_{BAC} + (a+2b)(f_{ABC}^2 + f_{BAC}^2) \\ &= 2b + a(f_{ABC} + f_{BAC})^2 + 2b(f_{ABC} - f_{BAC})^2 \\ &\geq 2b. \end{aligned}$$

Further, note that $\Sigma = 2(F_\infty + b)$. Hence Σ is strictly convex. Also $\Sigma(0, 0) = 2b$. Therefore $(0, 0)$ is the (unique) social optimum of the system. Yet, for sufficiently large N (that is, as soon as we add enough flexibility in the players' strategies), this is not a Nash equilibrium, as stated in the following theorem:

Theorem 5 *The point* $(f_{ABC}, f_{BAC}) = (0, 0)$ *is a Nash equilibrium if and only if* $N \leq (a/b) + 2$.

Proof By symmetry and as $u_A : f_{ABC} \mapsto U_A(f_{ABC}, f_{BAC})$ is convex, then $(0, 0)$ is a Nash equilibrium iff $U_A(0, 0) \leq U_A(1/N, 0) = b - b/N + (a+2b)/N^2$ which leads to the conclusion. □

Also, we can bound the total cost by

$$\begin{aligned}
&\Sigma(f_{ABC}, f_{BAC}) = \\
&= 2b + 2(a-2b) f_{ABC} f_{BAC} + (a+2b)(f_{ABC}^2 + f_{BAC}^2) \\
&\leq 2b + (a-2b)(f_{ABC}^2 + f_{BAC}^2) + (a+2b)(f_{ABC}^2 + f_{BAC}^2) \\
&\leq 2b + 2a(f_{ABC}^2 + f_{BAC}^2) \\
&\leq 2b + 4a.
\end{aligned}$$

This bound is attained at $\Sigma(1,1) = 2b + 2(a-2b) + 2(a+2b) = 4a + 2b$. Yet, it is not obtained at the Nash equilibrium for sufficiently large values of N:

Theorem 6 $(1,1)$ *is a Nash equilibrium if and only if* $N \leq \dfrac{2b+a}{3a+b}$.

Proof We have $U_A(1,1) = b + 2a$ and

$$U_A(1 - 1/N, 1) = 2a + b - 3a/N - b/N + 2b/N^2 + a/N^2.$$

Therefore $U_A(1-1/N,1) \geq U_A(1,1) \Leftrightarrow 2b + a \geq (3a+b)N$. The conclusion follows by convexity. □

Therefore, for $N \geq \max(\dfrac{a}{b} + 2, \dfrac{2b+a}{3a+b})$ the Nash equilibria are neither optimal nor worse-case strategies of the game.

4.2 Case of $N = 1$

In case of $N = 1$ (one flow arrives at each source node and there are thus two players) the two approach coincides: the atomic non-splittable case (**F3**) is also a semi-splittable atomic game (**F4**). f_{ABC} and f_{BAC} take values in $\{\{0\}, \{1\}\}$. From Eqs. 6 and 7, the matrix game can be written

$$\begin{pmatrix} (b,\ b) & (2b,\ a+2b) \\ (a+2b,\ 2b) & (2a+b,\ 2a+b) \end{pmatrix} \tag{8}$$

and the potential of Eq. 4 becomes

$$\begin{pmatrix} 0 & a+b \\ a+b & 3a \end{pmatrix}.$$

Then, assuming that either a or b is non-null, we get that $(0,0)$ is always a Nash equilibrium and that $(1,1)$ is a Nash equilibrium if and only if $3a \leq a + b$, i.e., $2a < b$.

We next consider any integer N and identify another surprising feature of the equilibrium. We show that depending on the sign of $a - 2b$, non-symmetric equilibria

arise in our symmetric game. In all frameworks other than the semi-splittable games there are only symmetric equilibria in this game. We shall show however that in the limit (as N grows to infinity), the limiting game has a single equilibrium.

4.3 Case $a - 2b < 0$

In this case, there may be multiple equilibria, as shown in the following example.

Example 1 Consider $a = 1$, $b = 3$, and $N = 4$, then the cost matrices are given below, with the two Nash equilibria of the game represented in bold letters:

$$U_A = \frac{1}{16}\begin{pmatrix} 48 & 60 & 72 & 84 & 96 \\ 43 & \mathbf{50} & 57 & 64 & 71 \\ 52 & 54 & \mathbf{56} & 58 & 60 \\ 75 & 72 & 69 & 66 & 63 \\ 112 & 104 & 96 & 88 & 80 \end{pmatrix}, \text{ and}$$

$$U_B = \frac{1}{16}\begin{pmatrix} 48 & 43 & 52 & 75 & 112 \\ 60 & \mathbf{50} & 54 & 72 & 104 \\ 72 & 57 & \mathbf{56} & 69 & 96 \\ 84 & 64 & 58 & 66 & 88 \\ 96 & 71 & 60 & 63 & 80 \end{pmatrix}.$$

Note that due to the shape of U_A and U_B the cost matrices of the game are transpose of each other. Therefore in the following, we shall only give matrix U_A.

We have the following theorem:

Theorem 7 *All Nash equilibria are symmetric, i.e.,*

$$f^*_{ABC} = f^*_{BAC}.$$

The proof is given in Appendix 1.

4.4 Case $a = 2b$ (with $a > 0$)

When $a = 2b$, we shall show that some non-symmetric equilibria exist.

Theorem 8 *If $a = 2b$, there are exactly either* 1 *or* 4 *Nash equilibria. For any N, let $\overline{N} = \lfloor N/8 \rfloor$.*

- *If $N \bmod 8 = 4$, there are* 4 *equilibria (n^*_{ABC}, n^*_{BAC}), which are $(\overline{N}, \overline{N})$, $(\overline{N}+1, \overline{N})$, $(\overline{N}, \overline{N}+1)$ and $(\overline{N}+1, \overline{N}+1)$.*

- *Otherwise, there is a unique equilibrium, which is* $(\overline{N}, \overline{N})$ *if* $N \bmod 8 < 4$ *or* $(\overline{N}+1, \overline{N}+1)$ *if* $N \bmod 8 > 4$.

Proof The Nash equilibria are the optimal points for both u_A and u_B. They are therefore either interior or boundary points (i.e., either f_{ABC} or f_{BAC} are in 0, 1). We detail the interior point cases in Appendix 1. The rest of the proof derives directly from the definition of $\frac{\partial U_A}{\partial f_{ABC}}$ and $\frac{\partial U_B}{\partial f_{BAC}}$. Indeed:

$$\frac{\partial U_A}{\partial f_{ABC}} = (a-2b) f_{BAC} + 2(2b+a) f_{ABC} - b = 8b f_{ABC} - b$$

$$\frac{\partial U_B}{\partial f_{BAC}} = (a-2b) f_{ABC} + 2(a+2b) f_{BAC} - b = 8b f_{BAC} - b.$$

Both are minimum for $1/8$. Therefore, it is attained if N is a multiple of 8. Otherwise, the best response of each player is either $\lfloor N/8 \rfloor / N$ if $N \bmod 8 \leq 3$ or $\lceil N/8 \rceil / N$ if $N \bmod 8 \geq 5$. If $N \bmod 8 = 4$, then each player has 2 best responses which are $\frac{1}{N}\frac{N-4}{8}$ and $\frac{1}{N}\frac{N+4}{8}$. Then, one can check that the boundary points follow the law of Theorem 11 when $\overline{N} = \lfloor N/8 \rfloor = 0$. □

4.5 Case $a - 2b > 0$

Theorem 9 *If* $a - 2b > 0$, *there are exactly either* 1, 2, *or* 3 *Nash equilibria. Let* $\alpha = \frac{a+2b}{3a+2b}$, $\beta = \frac{2a}{3a+2b}$ *and* $\gamma = \frac{b}{3a+2b}$.

Define further $\widetilde{N} = \lfloor N\gamma \rfloor$ *and* $z(N) = N\gamma - \widetilde{N}$. *The equilibria are of the form*

- *Either* $(\widetilde{N}, \widetilde{N})$, $(\widetilde{N}+1, \widetilde{N})$, $(\widetilde{N}, \widetilde{N}+1)$
  if N *is such that* $z(N) = \alpha$ *(mode 3-A in Fig. 6).*
- *Or* $(\widetilde{N}+1, \widetilde{N}+1)$, $(\widetilde{N}+1, \widetilde{N})$, $(\widetilde{N}, \widetilde{N}+1)$ *if* N *is such that* $z(N) = \beta$ *(mode 3-B).*
- *Or* $(\widetilde{N}, \widetilde{N}+1)$, $(\widetilde{N}+1, \widetilde{N})$
  if N *is such that* $\alpha < z(N) < \beta$ *(mode 2)*
- *Or* $(\widetilde{N}, \widetilde{N})$
  if N *is such that* $\beta < z(N) < \alpha + 1$ *(mode 1).*

We illustrate the different modes in the following example.

Example 2 Suppose that $a = 10$ and $b = 3$ (we represent only the part of the matrices corresponding to $1/N \leq f_{ABC}, f_{BAC} \leq 4/N$).

If $N = 24$, there are 3 Nash equilibria:

- *Either* $(\widetilde{N},\widetilde{N})$, $(\widetilde{N}+1,\widetilde{N})$, $(\widetilde{N},\widetilde{N}+1)$
  if N is such that $z(N)=\alpha$ *(mode 3-A in Figure 6)*
- *Or* $(\widetilde{N}+1,\widetilde{N}+1)$, $(\widetilde{N}+1,\widetilde{N})$, $(\widetilde{N},\widetilde{N}+1)$ *if N is such that* $z(N)=\beta$ *(mode 3-B)*
- *Or* $(\widetilde{N},\widetilde{N}+1)$, $(\widetilde{N}+1,\widetilde{N})$
  if N is such that $\alpha<z(N)<\beta$ *(mode 2)*
- *Or* $(\widetilde{N},\widetilde{N})$
  if N is such that $\beta<z(N)<\alpha+1$ *(mode 1).*

Fig. 6 Different modes according to different values of N

1152 1200 1248 1296
1118 **1172** **1226** 1280
1112 **1172** 1232 1292
1134 1200 1266 1332

If $N=26$, there are 2 Nash equilibria:

1352 1404 1456 1508
1314 1372 **1430** 1488
1304 **1368** 1432 1496
1322 1392 1462 1532

If $N=27$, there are 3 Nash equilibria:

1458 1512 1566 1620
1418 1478 **1538** 1598
1406 **1472** **1538** 1604
1422 1494 1566 1638

If $N=28$, there is a single Nash equilibrium:

1568 1624 1680 1736
1526 1588 1650 1712
1512 1580 **1648** 1716
1526 1600 1674 1748

4.6 Limit Case: Perfectly Splittable Sessions

We focus here in the limit case where $N\to+\infty$.

Theorem 10 *There exists a unique Nash equilibrium and it is such that*

$$f^*_{BAC} = f^*_{ABC} = \frac{b}{3a + 2b}.$$

Proof Note that $\frac{\partial U_A}{\partial f_{ABC}}(1) > 0$ and $\frac{\partial U_B}{\partial f_{BAC}}(1) > 0$. If $f_{ABC} = 0$ then $f_{BAC} = \frac{b}{2a + 4b}$ which implies that $-b + \frac{b(a - 2b)}{2a + 4b} \geq 0$, which further implies that $-a - 6b > 0$ which is impossible. Hence $f_{ABC} > 0$. Similarly $f_{BAC} > 0$ which concludes the proof. □

Recall that the optimum sum (social optimum) is given by $(0, 0)$ and that the worse case is given by $(1, 1)$. Hence, regardless of the values of a and b, at the limit case, we observe that there is a unique Nash equilibrium, that is symmetric, and is neither optimal (as opposed to **F3**), nor the worst case scenario. The price of anarchy is then:

$$PoA = PoS = \frac{2b + 2f^{*^2}_{ABC}a}{2b} = 1 + \frac{ab}{(3a + 2b)^2}.$$

5 Conclusions

We revisited in this paper a load balancing problem within a non-cooperative routing game framework. This model had already received much attention in the past within some classical frameworks (the Wardrop equilibrium analysis and the atomic splittable routing game framework). We studied this game under other frameworks—the non-splittable atomic game (known as congestion game) as well as a the semi-splittable framework. We have identified many surprising features of equilibria in both frameworks. We showed that unlike the previously studied frameworks, there is no uniqueness of equilibrium, and non-symmetric equilibria may appear (depending on the parameters). For each of the frameworks, we identified the different equilibria and provided some of their properties. We also provided an efficiency analysis in terms of price of anarchy and price of stability. In the future we plan to investigate more general cost structures and topologies.

Appendix 1

Proof of Theorem 7

Suppose that (f^*_{ABC}, f^*_{BAC}) is a Nash equilibrium with $f^*_{ABC} \neq f^*_{BAC}$. Then, by definition:

$$U_A(f^*_{ABC}, f^*_{BAC}) \leq U_A(f^*_{BAC}, f^*_{BAC}) \text{and}$$
$$U_B(f^*_{ABC}, f^*_{BAC}) \leq U_B(f^*_{ABC}, f^*_{ABC}),$$

which gives, after some manipulations,

$$\begin{cases} (a-2b) f^*_{ABC} f^*_{BAC} \leq \\ \qquad 2a f^{*2}_{BAC} + b f^*_{ABC} - b f_{BAC} - (a+2b) f^{*2}_{ABC} \\ (a-2b) f^*_{ABC} f^*_{BAC} \leq \\ \qquad 2a f^{*2}_{ABC} + b f^*_{BAC} - b f^*_{ABC} - (a+2b) f^{*2}_{BAC}. \end{cases}$$

Therefore $2(a-2b) f^*_{ABC} f^*_{BAC} \leq (a-2b)(f^{*2}_{ABC} + f^{*2}_{BAC})$ and hence $0 \leq (a-2b)(f^*_{ABC} - f^*_{BAC})^2$ which is impossible.

Boundary Equilibria When a = 2b

Theorem 11 *If $a = 2b$, there exists a single Nash equilibrium of the form $(0,\ f^*_{BAC})$ and $(f^*_{BAC}, 0)$ with f^*_{BAC} non-null. It is obtained for $N = 4$ and $f^*_{BAC} = 1/4$. The points $(0, 0)$ are Nash equilibria if and only if $N \leq 4$. Further, there are no equilibrium of the form $(f_{ABC}, 1)$ or $(1, f_{BAC})$.*

Proof We first study the equilibria of the form $(0,\ f_{ABC})$. $(0, \gamma)$ is a Nash equilibrium iff

$$\begin{cases} U_A(0,\gamma) \leq U_A\left(\frac{1}{N}, \gamma\right) \\ U_B(0,\gamma) \leq U_B\left(0, \gamma + \frac{1}{N}\right) \\ U_B(0,\gamma) \leq U_B\left(0, \gamma - \frac{1}{N}\right) \end{cases} \Leftrightarrow \begin{cases} b \leq \dfrac{2b+a}{N} \\ b \leq (a+2b)(2\gamma + \dfrac{1}{N}) \\ b \geq (a+2b)(2\gamma - \dfrac{1}{N}) \end{cases}$$

$$\Leftrightarrow \begin{cases} 1 \leq \dfrac{4}{N} \\ 1 \leq 4(2\gamma + \dfrac{1}{N}) \\ 1 \geq 4(2\gamma - 1/N) \end{cases} \Leftrightarrow \begin{cases} N \leq 4 \\ \dfrac{N/8 - 1/2}{N} \leq \gamma \\ \qquad\qquad \leq \dfrac{N/8 + 1/2}{N}. \end{cases} \tag{9}$$

If $N \leq 3$ then $N/8 + 1/2 \leq 7/8 < 1$ which cannot be obtained by the player otherwise than in 0. For $N = 4$, the second inequality becomes $0 \leq \gamma \leq \frac{1}{4}$ which hence leads to the only non-null Nash equilibrium.

We next study the potential equilibria of the form $(f_{ABC}, 1)$. Let $(\gamma, 1)$ be a Nash equilibrium. Then $U_B(\gamma, 1) \leq U_B(\gamma, 1 - 1/N)$. Then

$$\begin{aligned} & b\gamma + a + 2b \leq b - b(1-1/N) + b\gamma + (a+2b)(1-1/N)^2 \\ & \Rightarrow a + 2b \leq b/N + (a+2b)(1 + 1/N^2 - 2/N) \\ & \Rightarrow 0 \leq b + (a+2b)(1/N - 2) \\ & \Rightarrow 2a + 3b \leq (a+2b)/N \Rightarrow N \leq 1/4. \end{aligned}$$

□

Boundary Equilibria When $a - 2b > 0$

Theorem 12 $(0, \alpha)$ *and* $(\alpha, 0)$ *are Nash equilibria iff:*

$$\frac{b}{a-2b} - \frac{1}{N}\frac{a+2b}{a-2b} \leq \alpha \leq \frac{b}{2(a+2b)} + \frac{1}{2N}.$$

Further, there are no Nash equilibrium of the form $(A, 1)$.

Proof We first focus on the Nash equilibria of the form $(0, A)$. Since $U_A(., f_{BAC})$ and $U_B(f_{ABC}, .)$ are convex, $(0, \gamma)$ is a Nash equilibrium iff

$$\begin{cases} U_A(0,\gamma) \leq U_A\left(\frac{1}{N}, \gamma\right) \\ U_B(0,\gamma) \leq U_B\left(0, \gamma + \frac{1}{N}\right) \\ U_B(0,\gamma) \leq U_B\left(0, \gamma - \frac{1}{N}\right) \end{cases}$$

$$\Leftrightarrow \begin{cases} b \leq (a-2b)\gamma + \frac{2b+a}{N} \\ b \leq (a+2b)(2\gamma + \frac{1}{N}) \\ b \geq (a+2b)(2\gamma - \frac{1}{N}) \end{cases} \Leftrightarrow \begin{cases} \gamma \geq \frac{bN-2b-a}{N(a-2b)} \\ \gamma \geq \frac{bN-a-2b}{2N(a+2b)} \\ \gamma \leq \frac{bN+a+2b}{2N(a+2b)} \end{cases}$$

But $\frac{bN-2b-a}{N(a-2b)} \geq \frac{bN-a-2b}{2N(a+2b)}$ which concludes the proof. and hence $\frac{bN-a-2b}{2N(a+2b)} \leq \gamma \leq \frac{bN+a+2b}{2N(a+2b)}$.

We now study the potential equilibria of the form $(A, 1)$. Let $(A, 1)$ be a Nash equilibrium. Then $U_B(A, 1) \leq U_B(A, 1 - 1/N)$. Then

$$\begin{aligned} -b + (a-2b)A + (a+2b) &\leq -b(1-1/N) \\ &\quad +(a-2b)A(1-1/N) + (a+2b)(1-1/N)^2 \end{aligned}$$

$$\Rightarrow 0 \leq b - (a-2b)A + (a+2b)(-2+1/N)$$

$$\Rightarrow (a-2b)A \leq -2a - 3b + (a+2b)/N \Rightarrow$$

$$\Rightarrow 2a + 3b \leq (a-2b)A + 2a + 3b \leq (a+2b)/N$$

.

But $2a + 3b \leq (a+2b)/N \Rightarrow N \leq \frac{a+2b}{2a+3b} < 1.$ □

Proof of Theorem 9

We first start by showing that there are at most 4 interior Nash equilibria and that they are of the form: (A, A),$(A+1, A)$,$(A, A+1)$,$(A+1, A+1)$.

Proof Let f_{ABC}, f_{BAC} be a Nash equilibrium in the interior (i.e., $0 < f_{ABC} < 1$ and $0 < f_{BAC} < 1$). Then f_{ABC} and f_{BAC} are the (discrete) minimizers of $x \mapsto U_A(x, f_{BAC})$ and $x \mapsto U_B(f_{ABC}, x)$, respectively. Further:

$$\begin{cases} \dfrac{\partial U_A}{\partial f_{ABC}} = -b + (a-2b) f_{BAC} + 2(2b+a) f_{ABC} \\ \dfrac{\partial U_B}{\partial f_{BAC}} = -b + (a-2b) f_{ABC} + 2(a+2b) f_{BAC} \end{cases}$$

The optimum values are therefore, respectively:

$$x_A = \frac{b - \theta f_{BAC}}{\lambda} \text{ and } x_B = \frac{b - \theta f_{ABC}}{\lambda}$$

with $\lambda = 2(2b+a)$ and $\theta = a - 2b$. Therefore:

$$\begin{cases} x_A - 1/(2N) \le f_{ABC} \le x_A + 1/(2N), \\ x_B - 1/(2N) \le f_{BAC} \le x_B + 1/(2N). \end{cases}$$

Hence

$$\frac{b}{\lambda} - \frac{\theta}{\lambda}\left(\frac{b}{\lambda} - \frac{\theta}{\lambda} f_{ABC} + \frac{1}{2N}\right) - \frac{1}{2N} \le f_{ABC} \le \frac{1}{2N} + \frac{b}{\lambda} - \frac{\theta}{\lambda}\left(\frac{b}{\lambda} - \frac{\theta}{\lambda} f_{ABC} - \frac{1}{2N}\right).$$

Then

$$\frac{b}{\lambda+\theta} - \frac{\lambda}{2N(\lambda-\theta)} \le f_{ABC} \le \frac{\lambda}{2N(\lambda-\theta)} + \frac{b}{\lambda+\theta}.$$

Then $\dfrac{b}{\lambda+\theta} = \dfrac{b}{2b+3a}$, $\dfrac{\lambda}{2N(\lambda-\theta)} = \dfrac{4b+2a}{2N(6b+a)}$ and $\dfrac{\lambda}{2N(\lambda-\theta)} = \dfrac{2(a+2b)}{2N(6b+a)}$, which gives

$$\frac{b}{2b+3a} - \frac{a+2b}{N(6b+a)} \le f_{ABC} \le \frac{2b+a}{N(6b+a)} + \frac{b}{2b+3a}.$$

Similarly, we have

$$\frac{b}{2b+3a} - \frac{(2b+a)}{N(6b+a)} \le f_{BAC} \le \frac{b}{2b+3a} + \frac{2b+a}{N(6b+a)}.$$

Note that $\frac{1}{2} < \frac{2b+a}{6b+a} < 1$. Therefore there are either 1 or 2 possible values, which are identical for f_{ABC} and f_{BAC}. There are therefore 4 possible equilibria. □

Now, the potential equilibria are of the form (A, A), $(A, A+1)$, $(A+1, A)$, and $(A+1, A+1)$. By symmetry, note that if $(A, A+1)$ is a Nash equilibrium, then $(A+1, A)$ also is. The following lemma reduces the number of combinations of equilibria:

Lemma 1 *If (A, A) is a Nash equilibrium then $(A+1, A+1)$ is not a Nash equilibrium.*

Proof Suppose that (A, A) and $(A+1, A+1)$ are two Nash equilibria. Then $U_A(A, A) \leq U_A(A+1, A)$ and $U_A(A+1, A+1) \leq U_A(A, A+1)$, which implies

$$\begin{cases} -bAN + (a-2b)A^2 + (2b+a)A^2 \leq \\ \quad -b(A+1)N + (a-2b)A(A+1) + (2b+a)(A+1)^2 \\ -b(A+1)N + (a-2b)(A+1)^2 + (2b+a)(A+1)^2 \leq \\ \qquad\qquad -bAN + (a-2b)A(A+1) + (2b+a)A^2 \end{cases}$$

$$\Rightarrow \begin{cases} bN \leq (a-2b)A + (2b+a)(2A+1) \\ (a-2b)(A+1) + (2b+a)(2A+1) \leq bN \end{cases}$$

$$\Rightarrow (a-2b)(A+1) \leq bN - (2b+a)(2A+1) \leq (a-2b)A$$

.

Hence $(a-2b)(A+1) \leq (a-2b)A$ and therefore $a - 2b \leq 0$ which is impossible. □

Therefore the different possible combinations are mode 1, mode 2, mode 3-A, and mode 3-B in Fig. 6).

We first start by the occurrence of mode 3-A:

Lemma 2 *Suppose that $a - 2b > 0$. Suppose that (A, A) and $(A+1, A)$ are two Nash equilibria. Then*

$$A = \frac{bN - 2b - a}{3a + 2b}.$$

Proof Suppose that (A, A) and $(A+1, A)$ are two Nash equilibria. Then necessarily $U_A(A, A) = U_A(A+1, A)$. Hence

$$\begin{aligned} &-bAN + (a-2b)A^2 + (2b+a)A^2 \\ &= -b(A+1)N + (a-2b)A(A+1) + (2b+a)(A+1)^2 \end{aligned}$$

i.e.,

$$bN = (a-2b)A + (2b+a)(2A+1) \Rightarrow bN - 2b - a = (3a+2b)A$$

which leads to the conclusion. □

Hence, the system is in mode 3-A iff $bN - 2b - a$ is divisible by $3a + 2b$ or in other words, if N is of the form $[(3a + 2b)K + 2a]/b$ for some integer K.

We then move on to Mode 3-B:

Lemma 3 *Suppose that* $a - 2b > 0$. *Suppose that* $(A + 1, A + 1)$ *and* $(A + 1, A)$ *are two Nash equilibria. Then*

$$A = \frac{bN - 2a}{3a + 2b}.$$

Proof Suppose that $(A + 1, A + 1)$ and $(A, A + 1)$ are two Nash equilibria, then $U_1(A + 1, A + 1) = U_1(A, A + 1)$. This implies

$$\begin{aligned} -Nb(A+1) + (a-2b)(A+1)^2 + (2b+a)(A+1)^2 = \\ -NbA + (a-2b)A(A+1) + (2b+a)A^2 \end{aligned}$$

$$\Rightarrow (a-2b)(A+1) + (2b+a)(2A+1) = Nb$$

$$\Rightarrow (3a+2b)A = Nb - 2a$$

which concludes the proof. □

Hence, the system is in mode 3-B iff $bN - 2a$ is divisible by $3a + 2b$ or in other words, if N is of the form $[(3a + 2b)K + 2b + a]/b$ for some integer K.

Finally, for Mode 2:

Lemma 4 *Suppose that* $a - 2b > 0$. *Suppose that* $(A, A + 1)$ *and* $(A + 1, A)$ *are only two Nash equilibria. Then*

$$(3a + 2b)A + 2b + a < bN < (3a + 2b)A + 2a.$$

Proof Suppose that $(A, A + 1)$ and $(A + 1, A)$ are two Nash equilibria, then:

$$\begin{aligned} &U_A(A, A+1) \leq U_A(A+1, A+1) \text{and} \\ &U_A(A+1, A) \leq U_A(A, A), \end{aligned}$$

i.e.,

$$\begin{cases} bN \leq (3a+2b)A + 2a \\ (3a+2b)A + 2b + a \leq bN \end{cases}$$

The conclusion comes from Lemmas 2 and 3, since neither (A, A) nor $(A + 1, A + 1)$ are Nash equilibria. □

Finally the system is in mode 1 if it is not in any other modes. One can then check that the boundary cases found in Theorem 12 correspond to the case where $A = 0$ which concludes the proof.

References

1. N. Shimkin, "A survey of uniqueness results for selfish routing," in *Proc. of the International Conference on Network Control and Optimization (NetCoop)*, L. N. in Computer Science 4465, Ed., 2007, pp. 33–42.
2. M. Beckmann, C. McGuire, and C. Winsten, *Studies in the Economics of Transportation*. New Haven: Yale University Press, 1956.
3. A. Haurie and P. Marcotte, "On the relationship between Nash-Cournot and Wardrop equilibria," *Networks*, vol. 15, no. 3, 1985.
4. A. Orda, R. Rom, and N. Shimkin, "Competitive routing in multiuser communication networks," *IEEE/ACM Trans. Netw.*, vol. 1, no. 5, pp. 510–521, 1993.
5. R. W. Rosenthal, "A class of games possessing pure-strategy Nash equilibria," *International Journal of Game Theory*, vol. 2, pp. 65–67, 1973.
6. E. Altman, H. Kameda, and Y. Hosokawa, "Nash equilibria in load balancing in distributed computer systems," *International Game Theory Review (IGTR)*, vol. 4, no. 2, pp. 91–100, 2002.
7. M. Beckmann, C. McGuire, and C. Winsten, N. H. Y. U. Press, Ed., 1956.
8. H. Kameda and O. Pourtallier, "Paradoxes in distributed decisions on optimal load balancing for networks of homogeneous computers," *J. ACM*, vol. 49, no. 3, pp. 407–433, 2002.
9. H. Kameda, E. Altman, and O. Pourtallier, "A mixed optimum in symmetric distributed computer systems," *IEEE Trans. Automatic Control*, vol. 53, pp. 631–635, 2008.
10. D. Monderer and L. S. Shapley, "Potential games," *Games and economic behavior*, vol. 14, no. 1, pp. 124–143, 1996.
11. T. Roughgarden, *Selfish routing and the price of anarchy*. MIT Press, 2006.
12. H. Lin, T. Roughgarden, É. Tardos and A. Walkover, Stronger Bounds on Braess Paradox and the Maximum Latency of Selfish Routing, *SIAM J. Discrete Math.*, **25**(4), pp. 1667–1686, 2011.

Non-deceptive Counterfeiting and Consumer Welfare: A Differential Game Approach

Bertrand Crettez, Naila Hayek, and Georges Zaccour

1 Introduction

Grossman and Shapiro [14, 15] define counterfeiting as illegally copying genuine goods with a brand name, whereas Cordell et al. [8] state that "Any unauthorized manufacturing of goods whose special characteristics are protected as intellectual property rights (trademarks, patents and copyrights) constitutes product counterfeiting."As clearly shown by the numbers to follow, the worldwide magnitude of this illegal activity is simply astonishing. According to Levin [24], American businesses and industries lose approximately $200 billion in revenues annually due to counterfeits, and on a broader scale, counterfeit goods account for more than half a trillion dollars each year.[1] Research analysts estimate that the number of jobs lost worldwide to counterfeit black markets is approximately 2.5 million with 750,000 of them being located in the United States (Levin, ibid) and 300,000 in Europe (Eisend and

[1] See also A. Sowder, "The Harmful Effects of Counterfeit Goods", Athens State University, http://www.athens.edu/business-journal/spring-2013/asowder-couterfeit/.

We thank a referee for helpful remarks on a previous version of this work. The third author's research is supported by NSERC Canada, grant RGPIN-2016-04975 and was partially conducted during his stay at CRED, Université Panthéon-Assas Paris II.

B. Crettez (✉) · N. Hayek
Université Panthéon-Assas, Paris II, CRED, France
e-mail: bertrand.crettez@u-paris2.fr

N. Hayek
e-mail: naila.hayek@u-paris2.fr

G. Zaccour
GERAD, HEC Montréal, Montréal, Canada
e-mail: georges.zaccour@gerad.ca

D. M. Ramsey and J. Renault (eds.), *Advances in Dynamic Games*,
Annals of the International Society of Dynamic Games 17,
https://doi.org/10.1007/978-3-030-56534-3_11

Schichert-Guler [13]). Even though they are already impressive, these figures probably do not tell the whole story. For instance, it may well be that by violating property rights, counterfeiting discourages the owners from investing in improving the quality of their products, which undoubtedly has a private and a social cost.[2]

It is natural to wonder how to efficiently combat and deter counterfeiting, and one can distinguish between private and public efforts. Public enforcement of property rights has often relied on the seizure of counterfeit goods, which is prescribed in the commercial laws of many countries. For instance, more than 40 million counterfeit products were seized at the European Union's external border in 2012: their equivalent value in genuine products is nearly €1 billion.[3,4] In addition to confiscation, authorities can find anyone producing or trading (in) fake goods.[5] Designing fines involves two decisions. The first pertains to determining of the fines' values, and the second relates to how the proceeds of the fines are used. As regards the first issue, the penalty for counterfeiting is often set as a function of the price charged by the intellectual property right (henceforth IPR) holder. To illustrate, in the U.S., the Anti-counterfeiting Consumer Protection Act of 1996, S. 1136, provides civil fines pegged to the value of genuine goods. The fines are often rebated to the producers of the genuine goods. For instance, in June 2008, a French Court "ordered e-Bay to pay $63 million in damages to units of the Paris-based luxury goods mammoth LVMH, after agreeing that the site had facilitated the sale of counterfeit versions of its high-end products, particularly Louis Vuitton luggage..."[6].

Another important issue when it comes to deterring counterfeiting is whether consumers of fake products should be fined as well (in addition to being exposed to seizure). This depends on whether consumers are victims of counterfeiting or whether know perfectly well that the products they are buying are imitations. One can argue that punishing the purchase of counterfeit products would deter the illegal trade of such goods. For example, in Italy, purchasing counterfeit products is considered a

[2]Staake et al. (2009) provides a comprehensive literature review and discusses the existing body of research on the structures and mechanisms of counterfeit trade before 2010.

[3]See T. Bashir: http://brandandcommercial.com/articles/show/brand-building/214/counterfeiting-the-challenge-to-brand-owners-and-manufacturers1.

[4]Interestingly, the law can even specify what to do with the confiscated products. In the US case, the law gives the Customs Service four options regarding the uses of the seized goods at the border, namely: reexportation of the goods, donation to charity, destruction, or turning them to the General Services Administration for relabeling and sale (see Grossman and Shapiro, p. 72 [14]).

[5]There can be either monetary or non-monetary sanctions. There are other policies that prevent counterfeiting. For instance, a tariff on copying devices may prevent copyright infringement when the copying cost is relatively low and the tariff raises the effective copying cost. The Copyright Board of Canada has the power to impose tariffs on copying devices (subject to the approval of the Supreme Court of Canada).

[6]Pocketing, i.e., rebating fines to the producers of the genuine goods, affects their production decisions. When fines imposed on counterfeiters are pegged to the price of the genuine items, a luxury monopolist can find counterfeiting profitable (in comparison to the case where IPRs are completely enforced) by raising its selling price (Yao [35]). This result is also obtained by Di Liddo [12] in the case where the genuine firm can pocket fines not necessarily pegged to the price of its product.

crime. Buyers of counterfeit goods are given on-the-spot fines of up to 10,000 euros. In France, the maximum fine for buying fake goods is 300,000 euros or three years in jail.[7] In other countries, like the US or the UK, authorities target those who trade in fake goods, but refrain from criminalizing consumers who buy them. A possible drawback of prosecuting consumers of fake products is reducing the incentive of consumers to buy genuine products when they cannot distinguish between fake items and the genuine product [36].

Private enforcement of property rights can essentially take two forms, namely, policing and policies by their owners. Qian [28] notes that the luxury house LVMH assigns approximately 60 full-time employees to anti-counterfeiting, working in collaboration with a wide network of outside investigators and a team of lawyers, and that it spent more than 16 million dollars on investigations and legal fees in 2004 alone. In terms of policies, a number of anti-counterfeiting strategies have been recommended by numerous researchers. For instance, Chaudhry and Zimmerman [7] suggest aggressively cutting prices, providing financial incentives to distributors so they will reject counterfeits, and educating consumers about the harmful effects of fake goods. Shultz and Saporito [32] propose ten anti-counterfeiting strategies, among them, advertising as a tool to differentiate real products from phony ones, pricing to influence demand; and finally, involvement in coalitions with organizations that have similar intellectual property right (IPR) interests.

This paper looks at how the entry of a counterfeiter on the market affects the legal firm's pricing and advertising strategies and profits when there is no public nor private enforcement of property rights. The rationale for focusing on price and advertising is straightforward. First, it is probably the high margin, that is, the difference between the price and the (comparatively very low) production cost that makes counterfeiting financially attractive. Second, the high willingness-to-pay by consumers is driven by the brand image or reputation, and this asset is built through advertising, and of course, through other features such as design, quality, etc. Third, public enforcement of property rights is often lax or imperfect and not all legal firms can afford private enforcement policies. In such a setting, fining the consumption of fake products would be especially relevant if counterfeiting were actually detrimental to both the legal firm and the consumers.

To the best of our knowledge, excepting Buratto et al. [4], Crettez et al. [10], and Biancardi et al. [3] there are no papers analyzing brand quality dynamics in the presence of counterfeiting. To be sure, the impact of counterfeiting and piracy on brand reputation (and quality) has already been analyzed—see, for instance, Banerjee [2], Qian [28], Qian et al. [29], Zhang [37], and the review by Di Liddo [11]. But in these contributions, the analysis is restricted to a two-period setup (or a static setting). By contrast, the present paper, like Buratto et al. (ibid), Crettez et al. (ibid), and Biancardi et al. (ibid) considers a continuous time framework, which allows us to study how the genuine firm's strategic decisions regarding pricing and advertising change with the date of the counterfeiter's arrival and the parameters describing the

[7]Cox and Collins [9], which focuses on music and movie piracies in Finland, derives a demand function for pirated products that take into account the expected cost of punishment.

dynamics of its brand reputation. Moreover, our framework allows us to study the dynamics of brand reputation before as well as after the counterfeiter's entry.[8] We will later highlight the differences between Buratto et al. and Crettez et al. papers and ours. We shall answer the following research questions:

1. How does the counterfeiter's entry affect the legal firm's pricing and advertising decisions?
2. Are there conditions under which the legal firm benefits from counterfeiting?
3. Does the consumer benefit from counterfeiting?

In a nutshell, our results are as follows: First, we obtain that counterfeiting influences pricing and advertising strategies before and after entry occurs. The legal firm decreases its price and advertising investments in the counterfeiting scenarios. This leads to a loss in a long-term brand equity, that is, counterfeiting has a long-lasting effect on the legal firm even when the counterfeiter stops. This result contradicts some findings in the literature, according to which counterfeiting may stimulate innovation or the quality of the genuine good through product differentiation (e.g., Banerjee [2], Qian [28], Qian et al. [29], Zhang et al. [37]). A common feature of these results is that the legal firm is able to sustainably differentiate the quality of its product from that of the counterfeiters. This, however, possibly overlooks the case where the counterfeiters interact *repeatedly* with the legal firm. In such a case, it makes sense for counterfeiters to react to the differentiation efforts of the legal firm by adapting their own products. By construction, our analysis captures the repeated interactions between the genuine firm and the counterfeiter and illustrates the relevance of a differentiable game approach to counterfeiting.

Second, we show that while under no circumstances will counterfeiting be welcomed by a legal firm, there are indeed circumstances under which the consumer benefits from this illegal trade (the decrease in the price of the genuine good compensates for the decrease in the brand reputation of this good). This result can serve as a rationale for not fining consumers of fake products.

The rest of the paper is organized as follows: In Sect. 2, we introduce the model and present the two considered scenarios. In Sect 3, the optimal strategies and outcomes are determined in the no-counterfeiting scenario, which is our benchmark. In Sect. 4, we characterize the equilibrium strategies and payoffs in the counterfeiting scenario; and in Sect. 5, we compare the results of the two scenarios. Section 6 briefly concludes.

[8] Our approach also differs from that of dynamic general equilibrium models, which study innovation in the case where intellectual property rights are poorly protected (see, e.g., Suzuki [34]). An important difference between these models and the present paper is that we pay more attention to the brand reputation and to the nature of the imperfect competition between the genuine firm and the counterfeiter.

2 Model

We consider a planning horizon $[0, T]$, with time t running continuously. The initial date corresponds to the launch of a new product by an established legal manufacturer, player l, and T to the end of the selling season. After T, the product loses its appeal because of, e.g., a change of season for fashion apparel, or the arrival of a new version of software. At an **exogenously given** intermediate date $\mathcal{E} \in (0, T]$ a counterfeiter, player c, enters the market and offers a fake product, which performs the same functions as the legal product, e.g., typing a scientific paper in the case of software. Denote by $p_l(t)$ the price of the manufacturer's product at time $t \in [0, T]$ and by $p_c(t)$ the price of the copied product at $t \in [\mathcal{E}, T]$.

Denote by $R(t)$ the manufacturer's brand reputation, to which we can also refer as goodwill or brand equity. In the absence of counterfeiting, the demand for the legal firm is given by

$$q_l(t) = \max\left\{0, \tilde{\delta}_l\sqrt{R(t)} - \tilde{\beta}_l p_l(t)\right\}, \quad t \in [0, T],$$

and in the scenario with counterfeiting the demand functions for the legal firm and the counterfeiter are given by

$$q_{l1}(t) = \max\left\{0, \tilde{\delta}_l\sqrt{R(t)} - \tilde{\beta}_l p_{l1}(t)\right\}, \qquad t \in [0, \mathcal{E}), \tag{1}$$

$$q_{l2}(t) = \max\left\{0, \delta_l\sqrt{R(t)} - \beta_l p_{l2}(t) + \gamma p_c(t)\right\}, \quad t \in [\mathcal{E}, T], \tag{2}$$

$$q_c(t) = \max\left\{0, \delta_c\sqrt{R(t)} - \beta_c p_c(t) + \gamma p_{l2}(t)\right\}, \quad t \in [\mathcal{E}, T], \tag{3}$$

where $\tilde{\delta}_l, \delta_l, \delta_c$ and $\beta_j, j \in \{l, c\}$ are positive parameters and $\gamma \geq 0$ with $\beta_j > \gamma$, that is, the direct-price effect is larger than the cross-price effect.[9] The subscripts 1 and 2 are used to distinguish between the two periods, that is, before and after the counterfeiter's entry.

Remark 1 The fake product is non-deceptive, meaning that the buyer knows perfectly well that the product is not genuine. To illustrate, think of a consumer purchasing an illegal copy of software on the Internet, or a tourist buying a Lancel bag from a street seller in Paris.

We make the following comments on the above demand functions:

1. We show in Appendix 1 that these demand functions are obtained at each date by maximizing the following consumer's utility function:

$$U(q_l, q_c, y) = \sigma_l\sqrt{R}q_l + \sigma_c\sqrt{R}q_c - \frac{\kappa_l q_l^2}{2} - \frac{\kappa_c q_c^2}{2} - \psi q_l q_c + y,$$

[9] To study the interactions between firms in a dynamic setting it is most convenient to use linear demand function (see, i.e., Cellini and Lambertini [6]).

subject to the budget constraint given by

$$p_l q_l + p_c q_c + y = I,$$

where: y is a composite good; I the consumer's income; and σ_l, σ_c, ψ, κ_l and κ_c are positive parameters. The derivation of demand functions from utility maximization provides a micro-foundation for the specifications in (1)–(3).[10] Assuming that the set of consumers can be represented by a single consumer at each date is probably the simplest setting that allows us to the study the welfare effects of counterfeiting.[11]

2. The demands for the genuine product, with and without the presence of a fake good, are structurally different, that is, $\tilde{\delta}_l \neq \delta_l$ and $\tilde{\beta}_l \neq \beta_l$, with $\tilde{\delta}_l > \delta_l$ and $\tilde{\beta}_l < \beta_l$. Put differently, setting $p_c(t) = 0$ in the duopoly market does not yield the demand in the monopoly market.
3. The demand functions have the familiar affine shape, with, however, the additional feature that the market potential is not a given constant but depends positively on the brand reputation. The square root function is to account for marginal decreasing returns in reputation.
4. As expected, each demand is decreasing in own price and increasing in competitor's price.

The manufacturer can increase the brand reputation by investing in advertising. The evolution of the brand's reputation is described by the following linear differential equation:

$$\dot{R}(t) = ka(t) - \sigma R(t), \; R(0) = R_0 > 0, \tag{4}$$

where $a(t)$ is the advertising effort of the legal producer at time $t, k > 0$ is an efficiency parameter, and σ is the decay rate.[12] Following a substantial literature in both optimal control and differential games (see, e.g., the book by Jørgensen and

[10] A similar approach can be founded in Lai and Chang [22].

[11] By contrast with the vertical product differentiation model used in several papers in the literature (see *inter alia* Banerjee [1], Di Liddo [12], Zhang et al. [37]), in our approach the "representative consumer"buys both the genuine and the fake product. It is possible, however, to give an alternative derivation of the linear demand functions and the quadratic objective under which some consumers do not buy any product, some consumers buy the two kinds of products and some other consumers buy one kind of good only (see Martin [26]). A general discussion of demand functions can be found in Huang et al. [20] (see especially Sect. 2.2). The fact that some consumers buy both genuine goods and counterfeits, is documented, e.g., in Kapferer and Michaut [21] or Stöttinger and Penz [33]. Thus, it seems acceptable to assume that the *representative* consumer buys both the genuine good and the counterfeit.

[12] We do not take into account word-of-mouth communication effects (see Remark 2 below). For instance, Givon et al. [17] studies on an innovation diffusion model where pirates play an important role in converting potential users into users and even buyers of the software (they show that this effect was at work in the diffusion on spreadsheets and word processors during the 1990s in the United Kingdom). Peres et al. [27] review the literature on innovation diffusion that, in addition to word-of-mouth communications, incorporates network externalities and social signals.

Zaccour [23] and the survey by Huang et al. [19]), we suppose that the advertising cost is convex increasing and given by the quadratic function

$$C_l(a) = \frac{\omega}{2} a^2(t),$$

where ω is a positive parameter. Further, we suppose that the marginal production costs of both players are constant and we set them equal to zero. This is not a severe assumption as adding costs will have only a quantitative impact on the results without altering the qualitative insights.

The legal producer maximizes its stream of profit over the planning horizon. [13] Its optimization problem is defined as follows:

$$\begin{aligned}\max_{p_{l1}(t),\, p_{l2}(t),\, a_1(t),\, a_2(t)} \Pi_l = \Bigg[& \int_0^{\mathcal{E}} \left(p_{l1}(t) \left(\tilde{\delta}_l \sqrt{R(t)} - \tilde{\beta}_l p_{l1}(t) \right) - \frac{\omega}{2} a_1^2(t) \right) dt + \\ & \int_{\mathcal{E}}^{T} \left(p_{l2}(t) \left(\delta_l \sqrt{R(t)} - \beta_l p_{l2}(t) + \gamma p_c(t) \right) - \frac{\omega}{2} a_2^2(t) \right) dt \Bigg] \\ & + S(R(T)), \\ & \text{subject to (4)},\end{aligned} \tag{5}$$

where $S(R(T))$ is the salvage value of the brand at T, which captures the potential future payoffs that the manufacturer can derive from other products having the same brand name. We suppose that the salvage value can be well approximated by a linear function, that is, $S(R(T)) = sR(T)$. Clearly, this is a simplifying assumption and there is no conceptual difficulty in adopting a non-linear salvage value. However, retaining a non-linear function would come at the cost of complicating considerably the computations, without adding any qualitative gain in terms of our research questions.

The counterfeiter's optimization problem is given by

$$\max_{p_c(t)} \Pi_c = \int_{\mathcal{E}}^{T} p_c(t) \left(\delta_c \sqrt{R(t)} - \beta_c p_c(t) + \gamma p_{l2}(t) \right) dt, \quad t \in [\mathcal{E}, T]. \tag{6}$$

As the counterfeiter's decision does not affect the dynamics, its optimization problem is equivalent to solving the following static one:

$$\max_{p_c(t)} \pi_c = \max_{p_c(t)} p_c(t) \left(\delta_c \sqrt{R(t)} - \beta_c p_c(t) + \gamma p_{l2}(t) \right), \quad \forall t \in [\mathcal{E}, T].$$

To address our research questions, we shall characterize and compare the solutions in the following two scenarios:

[13] As the producer's problem is defined on a short horizon, we do not include a discount factor in the objective functional.

No Counterfeiting. The product cannot be copied and the only demand is legal. The manufacturer then solves the following optimal control problem:

$$\max_{p_l(t),\, a(t)} \Pi_l^{\mathcal{N}} = \max_{p_l(t),\, a(t)} \int_0^T \left(p_l(t) \left(\tilde{\delta}_l \sqrt{R(t)} - \tilde{\beta}_l p_l(t) \right) - \frac{\omega}{2} a^2(t) \right) dt + sR(T), \tag{7}$$

$$\dot{R}(t) = ka(t) - \sigma R(t), \; R(0) = R_0,$$

where the superscript $\mathcal{N}$ refers to no counterfeiting. This is our benchmark scenario, which corresponds either to a situation where the product life cycle is so short that illegal producers do not have enough time to enter the market or to a case where the institutions acting against counterfeiting are highly efficient.

Counterfeiting. Entry of the illegal producer occurs at time $\mathcal{E} \leq T$. The counterfeiter and the manufacturer play a finite-horizon differential game during the time interval $[\mathcal{E}, T]$. The manufacturer maximizes

$$\Pi_{l2}^{\mathcal{C}} = \int_{\mathcal{E}}^T \left(p_{l2}(t) \left(\delta_l \sqrt{R(t)} - \beta_l p_{l2}(t) + \gamma p_c(t) \right) - \frac{\omega}{2} a_2^2(t) \right) dt + sR(T),$$
subject to (4) and $R(\mathcal{E})$,

and the counterfeiter maximizes (6). A Nash equilibrium will be sought and the equilibrium state and strategy will be superscripted with $\mathcal{C}$ (for counterfeiting). To this Nash equilibrium we will associate a value function W_l to the manufacturer problem over the horizon $[\mathcal{E}, T]$. Next, we solve the following maximization problem over the horizon $[0, \mathcal{E}]$:

$$\Pi_{l1}^{\mathcal{C}} = \int_0^{\mathcal{E}} \left(p_{l1}(t) \left(\tilde{\delta}_l \sqrt{R(t)} - \tilde{\beta}_l p_{l1}(t) \right) - \frac{\omega}{2} a_1^2(t) \right) dt + W_l(\mathcal{E}, R(\mathcal{E})).$$

By comparing the outcomes of the two scenarios, we will be able to measure the impact of counterfeiting on the manufacturer's profit and on the consumer. We henceforth omit the time argument when no ambiguity may arise.

Remark 2 The closest papers to ours are Buratto et al. [4], Crettez et al. [10], Biancardi et al. [3] and we wish to point out the following important differences between these three contributions. With respect to Buratto et al. (ibid): (i) The demand functions are different. In particular, in Buratto et al. [4] the demand functions are structurally the same with and without counterfeiting. (ii) The demand functions adopted here are micro-founded. (iii) The dynamics are different in two respects. First, in Buratto et al., the illegal firm also advertises the product, which increases the reputation of the legal brand. Here, the counterfeiter does not engage in such activities, which is probably more in line with what is observed empirically. Second, our dynamics include a decay rate to account for consumer forgetting. (iv) The

strategies in the counterfeiting scenario are feedback, which is conceptually more attractive than open-loop strategies. (v) And lastly, here, all results are analytical. The main result obtained in Buratto et al. is that counterfeiting can increase the legal firm's profit, notably if the later can benefit from the advertising chosen by the counterfeiter. We obtain a different conclusion. With respect to Crettez et al. (ibid): (i) The demand function is slightly different. (ii) The present paper deals with counterfeiting whereas Crettez et al. (ibid) also consider imitation more broadly conceived (e.g., knockoffs). (iii) Crettez et al. assume that the evolution of the incumbent's brand reputation also depends on the entrant's sales during the duopoly period. They notably show that the incumbent will price and advertise at a lower level before entry, independently on whether the entrant will harm or not its brand reputation. Here, as was mentioned above, we do not consider dilution or promotion effects. This is because we are interested in the welfare effects of counterfeiting. For instance, it is clear that in the presence of dilution or promotion effects, counterfeiting can be either welfare decreasing or welfare increasing. To better understand the welfare effects of counterfeiting, we concentrate on the case where counterfeiting has neutral effects on brand reputation.[14] With respect to Biancardi et al. (ibid): (i) The demand functions are different (in Biancardi et al. the demand functions are not micro-funded and they are assumed to be proportional to the brand reputation). (ii) In contrast with the present paper, Biancardi et al. pay attention to the case where whenever the counterfeiters are caught, they are forced to pay a fine proportional to the quantity sold which is related to the legal firm. (iii) The authors carry out a numerical analysis of a feedback-Nash equilibrium and show that under specific values for the parameters of the model, the genuine producer can be better off in the presence of counterfeiting rather than in its absence.

3 No Counterfeiting

In this section, we characterize the optimal solution in the absence of counterfeiting and derive some properties.

Denote by $V_l\left(t, R\left(t\right)\right) : [0, T] \times \mathbb{R}_+ \rightarrow \mathbb{R}_+$ the value function of the legal firm.[15] The following proposition provides the optimal solution.

[14] According to Qian [28] "counterfeits have both advertising effects for a brand and substitution effects for authentic products, additionally the effects linger for some years. The advertising effect dominates the substitution effect for high-end authentic-product sales, and the substitution effect the advertising effect for low-end product sales. Our model refers to the case where these two effects are small. ".

[15] As a reminder, the value function gives the optimal payoff that can be obtained from $(t, R\left(t\right))$, assuming that optimal policies are followed.

Proposition 1 *In the absence of counterfeiting, the optimal pricing and advertising policies are given by*

$$p_l^{\mathcal{N}}(t, R(t)) = p_l^{\mathcal{N}}(R(t)) = \frac{\tilde{\delta}_l}{2\tilde{\beta}_l}\sqrt{R(t)}, \tag{8}$$

$$a^{\mathcal{N}}(t, R(t)) = a^{\mathcal{N}}(t) = \frac{k}{4\sigma\tilde{\beta}_l\omega}(\tilde{\delta}_l^2 + (4\sigma\tilde{\beta}_l s - \tilde{\delta}_l^2)e^{\sigma(t-T)}), \tag{9}$$

and the brand's reputation trajectory by

$$R^{\mathcal{N}}(t) = R_0 e^{-\sigma t} + \frac{k^2}{\omega}\frac{4\sigma\tilde{\beta}_l s - \tilde{\delta}_l^2}{8\sigma^2\tilde{\beta}_l}\left(e^{\sigma(t-T)} - e^{-\sigma(T+t)}\right) + \frac{k^2}{\omega}\frac{\tilde{\delta}_l^2}{4\sigma^2\tilde{\beta}_l}\left(1 - e^{-\sigma t}\right). \tag{10}$$

Proof See Appendix 2. □

The above proposition calls for the following remarks. First, it is easy to see that the advertising level is strictly positive at each instant of time, which, along with the assumption that $R_0 > 0$, implies that $R^{\mathcal{N}}(t)$ is strictly positive for all $t \in [0, T]$. Consequently, the price is also strictly positive, and hence, the solution is indeed interior. Second, from the proof in Appendix 2, we see that the optimal advertising effort is dictated by the familiar rule of marginal cost (given by wa) equals marginal revenue, which is measured by $k\frac{\partial V_l}{\partial R}$, that is, the marginal efficiency of advertising in raising reputation times the shadow price of the brand's reputation, measured by the derivative of the value function with respect to reputation. Third, the firm adopts a pricing policy that follows reputation: the higher the reputation, the higher the price. This is observed empirically and is due to the fact that the market potential is increasing in the brand's reputation. Finally, the strategies vary as follows with the different parameter values:

$$\begin{array}{cccccccc} & \tilde{\delta}_l & \tilde{\beta}_l & k & \sigma & \omega & s \\ p_l^{\mathcal{N}} & + & - & & & & \\ a^{\mathcal{N}} & + & - & + & - & - & +. \end{array}$$

We note that the price only depends on the demand function parameters, namely, $\tilde{\delta}_l$ and $\tilde{\beta}_l$, and is increasing in market size parameter $\tilde{\delta}_l$ and decreasing in consumer's sensitivity to price $\tilde{\beta}_l$. Advertising expenditures increase with $\tilde{\delta}_l$, with advertising efficiency k, and with the marginal salvage value of reputation s, and they decrease with advertising cost ω, with the decay rate σ and the consumer's sensitivity to price $\tilde{\beta}_l$. These results are fairly intuitive.

Proposition 2 *The optimal advertising policy is monotonically decreasing over time if, and only if,* $s \leq \frac{\tilde{\delta}_l^2}{4\sigma\tilde{\beta}_l}$.

Proof It suffices to compute

$$\dot{a}^{\mathcal{N}}(t) = \frac{ke^{\sigma(t-T)}}{4\tilde{\beta}_l\omega}\left(-\tilde{\delta}_l^2 + 4\sigma\tilde{\beta}_l s\right),$$

to get the result. □

The intuition behind this result is as follows: if the marginal value of the brand reputation at the end of the planning horizon is sufficiently low, then the firm should start by advertising at a relatively high level and decrease it over time. Early investments in advertising allow the firm to benefit from a high reputation for a longer period of time. In particular, if the salvage value is zero, then the condition in the above proposition will always be satisfied.

The evolution of the price over time follows the evolution of reputation. Indeed,

$$\dot{p}_l^{\mathcal{N}}(R(t)) = \frac{\tilde{\delta}_l \dot{R}(t)}{4\tilde{\beta}_l\sqrt{R(t)}}.$$

It can be easily verified that

$$\dot{R}^{\mathcal{N}}(t) \geq 0 \Leftrightarrow s \geq \frac{8\sigma^2\tilde{\beta}_l\omega R_0 e^{-\sigma t} - k^2\tilde{\delta}_l^2\left(2e^{-\sigma t} - e^{\sigma(t-T)} - e^{-\sigma(T+t)}\right)}{4\sigma\tilde{\beta}_l k^2\left(e^{\sigma(t-T)} + e^{-\sigma(T+t)}\right)}.$$

The above inequality, which involves all the model's parameters, states that, for the reputation to be increasing over time, the marginal salvage value must be high enough. Note that if the brand enjoys a large initial reputation value R_0 or if the advertising cost ω is high, then the condition becomes harder to satisfy. On the other hand, the condition is easier to satisfy when the advertising efficiency k is high.

It is shown in Appendix 2 that the value function is linear and given by

$$V_l(t, R(t)) = z(t)R(t) + y(t),$$

where

$$z(t) = \frac{\tilde{\delta}_l^2}{4\sigma\tilde{\beta}_l} + \frac{4\sigma\tilde{\beta}_l s - \tilde{\delta}_l^2}{4\sigma\tilde{\beta}_l}e^{\sigma(t-T)},$$

$$y(t) = \frac{k^2}{16\sigma^3\omega\tilde{\beta}_l^2}\left(\frac{\tilde{\sigma\delta}_l^4}{2}(T-t) + \tilde{\delta}_l^2(4\sigma\tilde{\beta}_l s - \tilde{\delta}_l^2)(1-e^{\sigma(t-T)}) + \frac{(4\sigma\tilde{\beta}_l s - \tilde{\delta}_l^2)^2}{4}(1-e^{2\sigma(t-T)})\right).$$

Proposition 3 *The coefficients $z(t)$ and $y(t)$ are nonnegative for all $t \in [0, T]$.*

Proof The coefficient $z(t)$ is clearly strictly positive for all $t \in [0, T]$. To show that $y(t) \geq 0$ for all t, it suffices to note that its derivative over time

$$\dot{y}(t) = -\frac{k^2}{32\sigma^2\omega\tilde{\beta}_l^2}\left(\tilde{\delta}_l^2 + \left(4\sigma\tilde{\beta}_l s - \tilde{\delta}_l^2\right)e^{\sigma(t-T)}\right)^2$$

is strictly negative and that $y(T) = 0$. □

The implications of the above proposition are as follows: (i) the value function is strictly increasing in reputation; and (ii) even if the firm is new, that is, if its reputation at initial instant of time is zero, it can still secure a nonnegative profit.

In the absence of counterfeiting, the legal firm's payoff over the whole planning horizon is given by

$$V_l(0, R_0) = \left(\frac{\tilde{\delta}_l^2}{4\sigma\tilde{\beta}_l} + \frac{4\sigma\tilde{\beta}_l s - \tilde{\delta}_l^2}{4\sigma\tilde{\beta}_l}e^{-\sigma T}\right)R_0 + \frac{k^2}{16\sigma^3\omega\tilde{\beta}_l^2}\left(\frac{\tilde{\sigma\delta}_l^4}{2}T + \tilde{\delta}_l^2(4\sigma\tilde{\beta}_l s - \tilde{\delta}_l^2)(1 - e^{-\sigma T}) + \frac{(4\sigma\tilde{\beta}_l s - \tilde{\delta}_l^2)^2}{4}(1 - e^{-2\sigma T})\right). \tag{11}$$

This value will be compared to the total profit that the legal firm obtains in the presence of counterfeiting. Finally, the reputation of the legal firm by the terminal planning date is

$$R^{\mathcal{N}}(T) = R_0 e^{-\sigma T} + \frac{k^2}{\omega}\frac{4\sigma\tilde{\beta}_l s - \tilde{\delta}_l^2}{8\sigma^2\tilde{\beta}_l}\left(1 - e^{-2\sigma T)}\right) + \frac{k^2}{\omega}\frac{\tilde{\delta}_l^2}{4\sigma^2\tilde{\beta}_l}\left(1 - e^{-\sigma T}\right).$$

4 Counterfeiting

The manufacturer's optimization problem is in two stages: between 0 and $\mathcal{E}$, it is a dynamic optimization problem with the solution being (qualitatively) similar to the problem without counterfeiting; between $\mathcal{E}$ and T, the two agents play a noncooperative game and a Nash equilibrium is sought. To obtain a subgame-perfect Nash equilibrium (SPNE) in the two-stage problem, we first solve the second stage with $R^{\mathcal{C}}(\mathcal{E})$ as the initial value of the brand's reputation.

4.1 The Duopoly Equilibrium

In this second-stage game, the counterfeiter solves the following static optimization problem:

$$\max_{p_c(t)} p_c(t)\left(\delta_c\sqrt{R(t)} - \beta_c p_c(t) + \gamma p_{l2}(t)\right), \quad \forall t \in [\mathcal{E}, T],$$

while the legal firm solves

$$\Pi_{l2}^{\mathcal{C}} = \max_{p_{l2}(t),\, a_2(t)} \int_{\mathcal{E}}^{T} \left(p_{l2}(t) \left(\delta_l \sqrt{R(t)} - \beta_l p_{l2}(t) + \gamma p_c(t) \right) - \frac{\omega}{2} a_2^2(t) \right) dt + sR(T),$$
$$\text{subject to (4) and } R^{\mathcal{C}}(\mathcal{E}).$$

Denote by φ_i the strategy of player $i = l, c$. We assume that each player implements a feedback strategy that selects the control action according to the rule $u_i(t) = \varphi_i(t, R(t))$, where

$$u_l(t) = (p_{l2}(t), a_2(t)) \in \mathbb{R}_+^2 \text{ and } u_c(t) = (p_c(t)) \in \mathbb{R}_+.$$

This means that firm $i = l, c$ observes the state $(t, R(t))$ of the system and then chooses its action as prescribed by the decision rule φ_i.

Definition 1 A pair (φ_l, φ_c) of functions $\varphi_i : [\mathcal{E}, T] \times \mathbb{R}_+ \longrightarrow R^{m_i}$, $i = l, c$, is a feedback-Nash equilibrium if

$$\Pi_{l2}^{\mathcal{C}}(\varphi_l, \varphi_c) \geq \Pi_{l2}^{\mathcal{C}}(u_1, \varphi_c), \quad \forall u_l \in \mathbb{R}_+^2,$$
$$\Pi_c(\varphi_l, \varphi_c) \geq \Pi_c(\varphi_l, u_c), \quad \forall u_c \in \mathbb{R}_+.$$

To characterize a feedback-Nash equilibrium, denote by $W_l(t, R(t)) : [\mathcal{E}, T] \times \mathbb{R}_+ \to \mathbb{R}$ the legal firm's value function. The following proposition gives the equilibrium solution of the duopoly game.[16]

Proposition 4 *Assuming that the counterfeiter enters the market at date $\mathcal{E} \leq T$, then the feedback-Nash pricing and advertising strategies are given by*

$$p_{l2}^{\mathcal{C}}(t, R(t)) = p_{l2}^{\mathcal{C}}(R(t)) = \frac{2\beta_c\delta_l + \delta_c\gamma}{4\beta_c\beta_l - \gamma^2} \sqrt{R(t)}, \tag{12}$$

$$p_c^{\mathcal{C}}(t, R(t)) = p_c^{\mathcal{C}}(R(t)) = \frac{2\beta_l\delta_c + \delta_l\gamma}{4\beta_c\beta_l - \gamma^2} \sqrt{R(t)}, \tag{13}$$

$$a_2^{\mathcal{C}}(t, R(t)) = a_2^{\mathcal{C}}(t) = \frac{k}{\omega} \left(\Gamma + (s - \Gamma) e^{-\sigma(T-t)} \right), \tag{14}$$

where

$$\Gamma = \frac{\beta_l}{\sigma} \left(\frac{2\beta_c\delta_l + \delta_c\gamma}{4\beta_c\beta_l - \gamma^2} \right)^2 > 0.$$

[16] See Haurie et al. [18] for details on determining a feedback-Nash equilibrium in differential games.

The reputation trajectory is given by

$$R_2^{\mathcal{C}}(t) = R(\mathcal{E})\, e^{-\sigma(t-\mathcal{E})} + \frac{k^2\Gamma}{\sigma\omega}\left(1 - e^{-\sigma(t-\mathcal{E})}\right) + \frac{k^2(s-\Gamma)}{2\sigma\omega}\left(1 - e^{-2\sigma(t-\mathcal{E})}\right) e^{-\sigma(T-t)}. \tag{15}$$

Proof See Appendix 2 □

The results in the above proposition deserve the following comments. First, by the same arguments provided after Proposition 1, it is easy to verify that the equilibrium solution is indeed interior.

Second, the pricing policies are increasing in the legal firm's reputation and are invariant over time, that is, the time dependency is only through the reputation value. Interestingly, the ratio of the two prices is constant, that is, independent of the state R and of time. Indeed,

$$\frac{p_{l2}^{\mathcal{C}}(R(t))}{p_c^{\mathcal{C}}(R(t))} = \frac{2\beta_c\delta_l + \delta_c\gamma}{2\beta_l\delta_c + \delta_l\gamma}.$$

It is shown in Appendix 1 that the assumptions made on the utility function imply that the above ratio is always larger than one, which means that the price of the genuine product is always higher than the price of the fake one. Clearly, this is in line with what is observed in the market.

Third, the advertising policy is again determined by equating the marginal cost ωa to the marginal revenue given by $k\frac{\partial W_l}{\partial R}$ and is monotonically decreasing over time if $s \leq \Gamma$. Further, because the advertising policy is independent of $R(t)$ and of the counterfeiter's entry date, it may appear at first glance that the legal firm's advertising policy is not affected by entry. This is clearly not the case since advertising depends on Γ, which involves the counterfeiter's parameters, i.e., β_c and γ.

Finally, we show in Appendix 2 that the value function of the second-stage problem is linear and given by

$$W_l(t, R(t)) = x(t)\, R(t) + v(t),$$

where

$$x(t) = \Gamma + (s-\Gamma)\, e^{-\sigma(T-t)}, \tag{16}$$

$$v(t) = \frac{k^2}{2\omega}\left(\Gamma^2(T-t) + \frac{(s-\Gamma)^2}{2\sigma}(1 - e^{2\sigma(t-T)}) + \frac{2\Gamma(s-\Gamma)}{\sigma}(1 - e^{\sigma(t-T)})\right). \tag{17}$$

4.2 The First-Stage Optimal Solution

Inserting the equilibrium strategies $p_c^{\mathcal{C}}, p_l^{\mathcal{C}}$ and $a^{\mathcal{C}}$ in the legal firm's second-stage profit ultimately yields a function that depends on the reputation value at counterfeiter's entry time $\mathcal{E}$, which we denote by $W_l\left(\mathcal{E}, R\left(\mathcal{E}\right)\right)$. This function is the salvage value in the first-stage optimization problem of the legal firm, which is,

$$\max_{p_{l1}(t),\, a_1(t)} \Pi_l^{\mathcal{C}} = \int_0^{\mathcal{E}} \left(p_{l1}\left(t\right)\left(\tilde{\delta}_l\sqrt{R\left(t\right)} - \tilde{\beta}_l p_{l1}\left(t\right)\right) - \frac{\omega}{2}a_1^2\left(t\right)\right) dt + W_l(\mathcal{E}, R\left(\mathcal{E}\right))$$

subject to the reputation dynamics

$$\dot{R}\left(t\right) = ka_1\left(t\right) - \sigma R\left(t\right),\ R\left(0\right) = R_0.$$

Observe that this optimization problem is very similar to the one solved in the scenario without counterfeiting. The main difference is the duration of the planning horizon and of the transversality condition. Adapting the proof of Proposition 1, we get the following optimal solution on $[0, \mathcal{E}]$:

Proposition 5 *The optimal pricing and advertising policies are given by*

$$p_{l1}^{\mathcal{C}}\left(t, R_1\left(t\right)\right) = p_{l1}^{\mathcal{C}}\left(R_1\left(t\right)\right) = \frac{\tilde{\delta}_l}{2\tilde{\beta}_l}\sqrt{R_1\left(t\right)},$$

$$a_1^{\mathcal{C}}\left(t, R_1\left(t\right)\right) = a_1^{\mathcal{C}}\left(t\right) = \frac{k}{4\sigma\tilde{\beta}_l\omega}\left(\tilde{\delta}_l^2\left(1 - e^{\sigma(t-\mathcal{E})}\right) + 4\sigma\tilde{\beta}_l(\Gamma + (s-\Gamma)\,e^{-\sigma(T-\mathcal{E})})e^{\sigma(t-\mathcal{E})}\right),$$

and the reputation stock by

$$R_1^{\mathcal{C}}\left(t\right) = R_0e^{-\sigma t} + \frac{k^2}{\omega}\frac{4\sigma\tilde{\beta}_l x(\mathcal{E}) - \tilde{\delta}_l^2}{8\sigma^2\tilde{\beta}_l}\left(e^{\sigma(t-\mathcal{E})} - e^{-\sigma(\mathcal{E}+t)}\right) + \frac{k^2}{\omega}\frac{\tilde{\delta}_l^2}{4\sigma^2\tilde{\beta}_l}\left(1 - e^{-\sigma t}\right).$$

Proof See Appendix 2. □

The same comments made after Proposition 1 remain valid, qualitatively speaking, and therefore there is no need to repeat them. Substituting for $x(\mathcal{E})$ in $R_1^{\mathcal{C}}\left(t\right)$ we obtain

$$R_1^{\mathcal{C}}\left(t\right) = R_0e^{-\sigma t} + \frac{k^2}{\omega}\frac{4\sigma\tilde{\beta}_l\left(\Gamma + (s-\Gamma)\,e^{-\sigma(T-\mathcal{E})}\right) - \tilde{\delta}_l^2}{8\sigma^2\tilde{\beta}_l}\left(e^{\sigma(t-\mathcal{E})} - e^{-\sigma(\mathcal{E}+t)}\right) + \frac{k^2}{\omega}\frac{\tilde{\delta}_l^2}{4\sigma^2\tilde{\beta}_l}\left(1 - e^{-\sigma t}\right), \tag{18}$$

and in particular, the following value for reputation at the counterfeiter's entry date:

$$R_1^{\mathcal{C}}\left(\mathcal{E}\right) = R_0e^{-\sigma\mathcal{E}} + \frac{k^2}{8\sigma^2\tilde{\beta}_l\omega}\left(\left(4\sigma\tilde{\beta}_l\left(\Gamma + (s-\Gamma)\,e^{-\sigma(T-\mathcal{E})}\right) - \tilde{\delta}_l^2\right)\left(1 - e^{-2\sigma\mathcal{E}}\right) + 2\tilde{\delta}_l^2\left(1 - e^{-\sigma\mathcal{E}}\right)\right).$$

The reputation by the end of the planning horizon is

$$R_2^{\mathcal{C}}(T) = R_1^{\mathcal{C}}(\mathcal{E})\, e^{-\sigma(T-\mathcal{E})} + \frac{k^2\Gamma}{\sigma\omega}\left(1 - e^{-\sigma(T-\mathcal{E})}\right) + \frac{k^2(s-\Gamma)}{2\sigma\omega}\left(1 - e^{-2\sigma(T-\mathcal{E})}\right).$$

It is shown in Appendix 2 that the first-stage value function $Z_l(t, R(t))$ is linear, that is,

$$Z_l(t, R(t)) = m(t)\, R(t) + n(t),$$

where the coefficients $m(t)$ and $n(t)$ are given by

$$\begin{aligned}
m(t) &= \frac{\tilde{\delta}_l^2}{4\sigma\tilde{\beta}_l} + \frac{4\sigma\tilde{\beta}_l x(\mathcal{E}) - \tilde{\delta}_l^2}{4\sigma\tilde{\beta}_l} e^{\sigma(t-\mathcal{E})},\\
n(t) &= -\frac{k^2}{4\sigma\omega}\left(\frac{\tilde{\delta}_l^4}{8\sigma\tilde{\beta}_l^2}t + \tilde{\delta}_l^2\left(\frac{4\sigma\tilde{\beta}_l x(\mathcal{E}) - \tilde{\delta}_l^2}{4\sigma^2\tilde{\beta}_l^2}e^{-\sigma\mathcal{E}}\right)e^{\sigma t} + \left(\frac{4\sigma\tilde{\beta}_l x(\mathcal{E}) - \tilde{\delta}_l^2}{4\sigma\tilde{\beta}_l}e^{-\sigma\mathcal{E}}\right)^2 e^{2\sigma t}\right)\\
&\quad + \frac{k^2}{16\sigma^3\omega\tilde{\beta}_l^2}\left(\frac{\sigma\tilde{\delta}_l^4}{2}\mathcal{E} + \tilde{\delta}_l^2(4\sigma\tilde{\beta}_l x(\mathcal{E}) - \tilde{\delta}_l^2) + \frac{(4\sigma\tilde{\beta}_l x(\mathcal{E}) - \tilde{\delta}_l^2)^2}{4}\right) + v(\mathcal{E}).
\end{aligned}$$

Note that the above coefficients involve $x(\mathcal{E})$ and $v(\mathcal{E})$, that is, the coefficients of the second-stage value function evaluated at entry time $\mathcal{E}$. As alluded to it earlier, $W_l(\mathcal{E}, R(\mathcal{E}))$ plays the role of a salvage value in the first-stage optimization problem of the legal firm. Substituting for $x(\mathcal{E})$ and $v(\mathcal{E})$, and next for $m(t)$ and $n(t)$ in $Z_l(t, R(t))$, we obtain the value function for the legal firm on $[0, \mathcal{E}]$, that is,

$$\begin{aligned}
Z_l(t, R(t)) = \frac{1}{4\sigma\tilde{\beta}_l}\left(\tilde{\delta}_l^2 + \Lambda e^{\sigma(t-\mathcal{E})}\right)R(t) + \frac{k^2\tilde{\delta}_l^4(\mathcal{E}-t)}{32\sigma^2\omega\tilde{\beta}_l^2}\\
+\frac{k^2\Lambda\left(1 - e^{\sigma(t-\mathcal{E})}\right)}{64\sigma^3\omega\tilde{\beta}_l^2}\left(4\tilde{\delta}_l^2 + \Lambda\left(1 + e^{\sigma(t-\mathcal{E})}\right)\right)\\
+\frac{k^2}{2\omega}\left(\Gamma^2(T-\mathcal{E}) + \frac{(s-\Gamma)^2}{2\sigma}(1 - e^{2\sigma(\mathcal{E}-T)}) + \frac{2\Gamma(s-\Gamma)}{\sigma}(1 - e^{\sigma(\mathcal{E}-T)})\right),
\end{aligned}$$

where

$$\Lambda = 4\sigma\tilde{\beta}_l\left(\Gamma + (s-\Gamma)\, e^{-\sigma(T-\mathcal{E})}\right) - \tilde{\delta}_l^2.$$

To obtain the total profit that the legal firm gets in the game with counterfeiting, it suffices to evaluate the above value function at $(0, R(0))$, which yields

$$\begin{aligned}
Z_l(0, R(0)) = \frac{1}{4\sigma\tilde{\beta}_l}\left(\tilde{\delta}_l^2 + \Lambda e^{-\sigma\mathcal{E}}\right)R_0 + \frac{k^2\tilde{\delta}_l^4\mathcal{E}}{32\sigma^2\omega\tilde{\beta}_l^2}\\
+\frac{k^2\Lambda\left(1 - e^{-\sigma\mathcal{E}}\right)}{64\sigma^3\omega\tilde{\beta}_l^2}\left(4\tilde{\delta}_l^2 + \Lambda\left(1 + e^{-\sigma\mathcal{E}}\right)\right)\\
+\frac{k^2}{2\omega}\left(\Gamma^2(T-\mathcal{E}) + \frac{(s-\Gamma)^2}{2\sigma}(1 - e^{2\sigma(\mathcal{E}-T)}) + \frac{2\Gamma(s-\Gamma)}{\sigma}(1 - e^{\sigma(\mathcal{E}-T)})\right). \qquad (19)
\end{aligned}$$

Before comparing the results of the two scenarios, it is of particular interest to look at is the impact of the counterfeiter's entry date on the legal firm's pricing and advertising policies and on the reputation of the brand. As we shall see, this impact hinges on the sign of the difference between the instantaneous (static) revenue of the legal firm without counterfeiting (which we denote by $r_l^{\mathcal{N}}(t)$) and its revenue with counterfeiting (denoted $r_l^{\mathcal{C}}(t)$) for any given reputation level $R(t)$. Substituting for $p_l^{\mathcal{N}}(t)$ from (8) and for $p_{l2}^{\mathcal{C}}(t)$ and $p_c^{\mathcal{C}}(t)$ from (12) and (13) in the relevant revenue functions, we get

$$r_l^{\mathcal{N}}(t) = p_l^{\mathcal{N}}(t)\left(\tilde{\delta}_l\sqrt{R(t)} - \tilde{\beta}_l p_l^{\mathcal{N}}(t)\right) = \frac{\tilde{\delta}_l^2}{4\tilde{\beta}_l}R(t),$$

$$r_l^{\mathcal{C}}(t) = \frac{\beta_l\left(2\beta_c\delta_l + \delta_c\gamma\right)^2}{\left(4\beta_c\beta_l - \gamma^2\right)^2}R(t).$$

We have the following result.

Lemma 1 *For any given reputation level $R(t)$, the revenue of the legal firm without counterfeiting $r_l^{\mathcal{N}}(t)$) is higher than its revenue with counterfeiting (denoted $r_l^{\mathcal{C}}(t)$). More formally, the following inequality holds true:*

$$\Delta = \frac{\tilde{\delta}_l^2}{4\tilde{\beta}_l} - \beta_l\left(\frac{2\beta_c\delta_l + \delta_c\gamma}{4\beta_c\beta_l - \gamma^2}\right)^2 > 0. \tag{20}$$

Proof See Appendix 2. □

The proof of the above lemma relies on the general result that in imperfect competition, firms realize higher profits when they compete in quantities à la Cournot than in prices à la Bertrand. This result also strongly depends on the micro-foundations for the demand functions.

Noting that Δ can also be written as

$$\Delta = \frac{1}{4\tilde{\beta}_l}\left(\tilde{\delta}_l^2 - 4\sigma\tilde{\beta}_l\Gamma\right),$$

the effect of the counterfeiter's entry date on the legal firm's pricing and advertising policies and on the reputation of the brand is given in the following result.

Proposition 6 *On $[0, \mathcal{E}]$, the legal firm's advertising, pricing, and reputation are increasing in the counterfeiter's entry date $\mathcal{E}$.*

Proof It suffices to compute the derivatives

$$\frac{\partial a_1^{\mathcal{C}}(t)}{\partial \mathcal{E}} = \frac{k}{\omega}\Delta e^{\sigma(t-\mathcal{E})},$$
$$\frac{\partial R_1^{\mathcal{C}}(t)}{\partial \mathcal{E}} = \frac{k^2}{2\sigma\omega}\left(e^{\sigma(t-\mathcal{E})} - e^{-\sigma(\mathcal{E}+t)}\right)\Delta,$$
$$\frac{\partial p_{l1}^{\mathcal{C}}(t)}{\partial \mathcal{E}} = \frac{\tilde{\delta}_l}{4\tilde{\beta}_l\sqrt{R_1(t)}}\frac{\partial R_1^{\mathcal{C}}(t)}{\partial \mathcal{E}},$$

and to use Lemma 1 to get the result. □

Intuitively, one would expect the price to be increasing in $\mathcal{E}$, as the need to face price competition is less urgent for the legal firm when the entry date is later. Further, during the monopoly period $[0, \mathcal{E}]$, the legal firm is the only beneficiary from advertising investment in reputation, and therefore, the later is the counterfeiter's entry date, the higher is the incentive to invest in advertising to raise the value of the (private good) reputation.

Remark 3 During the duopoly period $[\mathcal{E}, T]$, the advertising, reputation, and pricing trajectories vary as follows in terms of entry date $\mathcal{E}$:

$$\frac{\partial a_2^{\mathcal{C}}(t)}{\partial \mathcal{E}} = 0,$$
$$\frac{\partial R_2^{\mathcal{C}}(t)}{\partial \mathcal{E}} = \frac{k^2}{2\omega}e^{-\sigma(t-\mathcal{E})}\left(2e^{-\sigma(T-\mathcal{E})}s + \Gamma e^{-2\sigma\mathcal{E}}\left(1 - 2e^{-\sigma(T+\mathcal{E})}\right) + \frac{\tilde{\delta}_l^2}{4\sigma\tilde{\beta}_l} - \Gamma\right) > 0,$$
$$\frac{\partial p_{l2}^{\mathcal{C}}(t)}{\partial \mathcal{E}} = \frac{2\beta_c\delta_l + \delta_c\gamma}{4\beta_c\beta_l - \gamma^2}\frac{1}{2\sqrt{R(t)}}\frac{\partial R_2^{\mathcal{C}}(t)}{\partial \mathcal{E}} > 0.$$

The reputation and the counterfeiter's price are increasing with respect to the date of entry $\mathcal{E}$. As shown above, the later the date of entry, the higher the values of advertising and reputation *before* entry. Since reputation after $\mathcal{E}$ depends on the level achieved at this date, the later the date of entry, the higher the level of reputation *after* entry. And since the legal firm's price increases with its reputation, the later the entry date, the higher is this price. Observe also that advertising does not depend on the date of entry. This is because advertising does not depend on the legal firm's reputation but only on the date at which it is carried out and the final date (to put it differently, advertising does not depend on a state variable, which would take into account what happened at date $\mathcal{E}$). Notice that this property also holds for the case where there is no counterfeiting.

Of particular interest is the impact of the counterfeiter's entry date on the legal firm's total profit.

Proposition 7 *The impact of the counterfeiter's entry date on the legal firm's total profit is positive and given by*

$$\frac{\partial Z_l(0,R_0;\mathcal{E})}{\partial \mathcal{E}} = \pi_1\left(R_1^{\mathcal{C}}(\mathcal{E};\mathcal{E}), a_1^{\mathcal{C}}(\mathcal{E};\mathcal{E}), p_{l1}^{\mathcal{C}}(\mathcal{E};\mathcal{E})\right) - \pi_2\left(R_2^{\mathcal{C}}(\mathcal{E};\mathcal{E}), a_2^{\mathcal{C}}(\mathcal{E};\mathcal{E}), p_{l2}^{\mathcal{C}}(\mathcal{E};\mathcal{E})\right) > 0.$$

Proof See Appendix 2. □

The proposition first establishes that the impact of the counterfeiter's entry date on the legal firm's total profit is equal to the difference between the instantaneous profit of the legal firm just before the counterfeiter's entry, denoted by $\pi_1\left(R_1^{\mathcal{C}}(\mathcal{E};\mathcal{E}), a_1^{\mathcal{C}}(\mathcal{E};\mathcal{E}), p_{l1}^{\mathcal{C}}(\mathcal{E};\mathcal{E})\right)$, and its instantaneous profit just after the counterfeiter's entry, denoted by $\pi_2\left(R_2^{\mathcal{C}}(\mathcal{E};\mathcal{E}), a_2^{\mathcal{C}}(\mathcal{E};\mathcal{E}), p_{l2}^{\mathcal{C}}(\mathcal{E};\mathcal{E})\right)$.[17] Since $R_1^{\mathcal{C}}(\mathcal{E};\mathcal{E}) = R_2^{\mathcal{C}}(\mathcal{E};\mathcal{E})$, and since, from Lemma 1, we know that the instantaneous profit before entry is higher than the instantaneous profit after entry, we see that the earlier the counterfeiter enters the market, the greater is the legal firm's loss, which is intuitive, as entry changes the market from a monopoly to a duopoly.

Finally, as we assumed that the entry date is exogenous, it is of interest to check how the counterfeiter's equilibrium payoff varies with this parameter. The total counterfeiter's payoff is given by

$$\Pi_c^{\mathcal{E}} = \int_{\mathcal{E}}^{T} p_c(t)\left(\delta_c\sqrt{R(t)} - \beta_c p_c(t) + \gamma p_{l2}(t)\right)dt.$$

Substituting for the equilibrium values for $p_c(t)$and $p_{l2}(t)$ we get

$$\Pi_c^{\mathcal{C}} = \beta_c\left(\frac{2\beta_l\delta_c + \delta_l\gamma}{4\beta_c\beta_l - \gamma^2}\right)^2 \int_{\mathcal{E}}^{T} R(t)\,dt.$$

Taking the derivative with respect to $\mathcal{E}$, we have

$$\frac{\partial \Pi_c^{\mathcal{C}}}{\partial \mathcal{E}} = \beta_c\left(\frac{2\beta_l\delta_c + \delta_l\gamma}{4\beta_c\beta_l - \gamma^2}\right)^2 \frac{\partial\left(\int_{\mathcal{E}}^{T} R(t)\,dt\right)}{\partial \mathcal{E}},$$

$$\frac{\partial\left(\int_{\mathcal{E}}^{T} R(t)\,dt\right)}{\partial \mathcal{E}} = -R(\mathcal{E}) + \int_{\mathcal{E}}^{T} \frac{\partial R(t)}{\partial \mathcal{E}}dt.$$

The above equality has the following interpretation: On the one hand, an increase in $\mathcal{E}$ leads to the loss of the profit at date $\mathcal{E}$. On the other hand, from Remark 3, the value of the goodwill is higher at any date after $\mathcal{E}$, and so is the price of the legal firm. This directly increases the counterfeiter's demand.

[17] The argument $(\mathcal{E};\mathcal{E})$ of the reputation, advertising, and pricing variables is to specify that these variables depend on the entry date $\mathcal{E}$ and that this date is also a parameter.

Now, from Eq. (18) in the text, we have

$$R(\mathcal{E}) = R_1^{\mathcal{C}}(\mathcal{E}) = R_0 e^{-\sigma\mathcal{E}} + \frac{k^2}{8\sigma^2\tilde{\beta}_l\omega}\left(\left(4\sigma\tilde{\beta}_l\left(\Gamma + (s-\Gamma)e^{-\sigma(T-\mathcal{E})}\right) - \tilde{\delta}_l^2\right)\left(1 - e^{-2\sigma\mathcal{E}}\right) + 2\tilde{\delta}_l^2\left(1 - e^{-\sigma\mathcal{E}}\right)\right),$$

and from Remark 3, we know that

$$\frac{\partial R_2^{\mathcal{C}}(t)}{\partial\mathcal{E}} = \frac{k^2}{2\omega}e^{-\sigma(t-\mathcal{E})}\left(2e^{-\sigma(T-\mathcal{E})}s + \Gamma e^{-2\sigma\mathcal{E}}\left(1 - 2e^{-\sigma(T+\mathcal{E})}\right) + \frac{\tilde{\delta}_l^2}{4\sigma\tilde{\beta}_l} - \Gamma\right).$$

Therefore,

$$\int_{\mathcal{E}}^{T}\frac{\partial R_2^c}{\partial\mathcal{E}}dt = \frac{1 - e^{-\sigma(T-\mathcal{E})}}{\sigma}\frac{k^2}{2\omega}\left(2e^{-\sigma(T-\mathcal{E})}s + \Gamma e^{-2\sigma\mathcal{E}}\left(1 - 2e^{-\sigma(T+\mathcal{E})}\right) + \frac{\tilde{\delta}_l^2}{4\sigma\tilde{\beta}_l} - \Gamma\right).$$

After some algebra we find that

$$\frac{\partial\left(\int_{\mathcal{E}}^{T}R(t)\,dt\right)}{\partial\mathcal{E}} = -R_0e^{-\sigma\mathcal{E}} - \frac{sk^2}{2\omega\sigma}e^{-\sigma(T-\mathcal{E})}\left(2e^{-\sigma(T-\mathcal{E})} - e^{-2\sigma\mathcal{E}} - 1\right) \tag{21}$$

$$- \frac{k^2\tilde{\delta}_l^2}{8\omega\sigma^2\tilde{\beta}_l}\left(e^{-2\sigma\mathcal{E}} - 2e^{-\sigma\mathcal{E}} + e^{-\sigma(T-\mathcal{E})}\right) \tag{22}$$

$$- \frac{\Gamma k^2}{\omega\sigma}(1 - e^{-\sigma(T-\mathcal{E})})\left(1 - e^{-2\sigma\mathcal{E}} + e^{-3\sigma\mathcal{E}-\sigma T}\right). \tag{23}$$

The right-hand side of the above equation is highly non-linear in all model's parameters and cannot be utterly signed. However, we see that for an R_0 high enough, we have $\frac{\partial\left(\int_{\mathcal{E}}^{T}R(t)dt\right)}{\partial\mathcal{E}} < 0$, that is, the counterfeiter's equilibrium payoff is decreasing in the entry date.

5 Comparison

In this section, we compare the strategies and outcomes in the two scenarios. Further, we determine the cost of counterfeiting to the legal firm and to the consumer.

5.1 Profit Comparison

We shall first compare the advertising policies with and without counterfeiting.

Proposition 8 *The legal firm advertises more when there is no counterfeiting. That is, $a^{\mathcal{N}}(t) > a^{\mathcal{C}}(t)$, for all t in $[0, T]$*

Proof See Appendix 2. □

Before interpreting the above result, we shall next compare the trajectories of reputation and the prices in the two scenarios.

Proposition 9 *At each instant of time, the legal brand enjoys a higher reputation when there is no counterfeiting, and the legal firm sells throughout the whole planning horizon at a higher price. That is,* $R^{\mathcal{N}}(t) > R^{\mathcal{C}}(t)$, *and* $p_l^{\mathcal{N}}(t) > p_l^{\mathcal{C}}(t)$ *for all* t *in* $[0, T]$.

Proof See Appendix 2. □

Proposition 9 shows that the impact of entry on reputation is felt at any instant of time throughout the planning horizon, and not only after entry actually occurs. The fact that a counterfeiter will enter the market influences the advertising behavior of the legal firm during the monopoly period and this results in a loss of reputation even before entry takes place.

The interpretation of these results is as follows: Counterfeiting induces a competitive pressure on the legal firm pushing it to lower its price. Further, the legal firm invests less in advertising because the consequent reward, namely, a higher reputation and larger market size, is not fully appropriable in the counterfeiting scenario since the illegal firm benefits for free from the advertising investments and the brand's reputation. This is a typical case where the counterfeiter enjoys a positive externality without contributing at all to the building of reputation.

The above result differs from some of the findings in the literature, according to which counterfeiting may stimulate innovation or the quality of the genuine good (see Zhang et al. [37]). This occurs notably when there are network externalities and R&D competition (Banerjee [2]) or imperfect information (Qian [28], Qian et al. [29]). A common feature of these results is that the legal firm is able to sustainably differentiate the quality of its product from that of the counterfeiters. This, however, probably overlooks the case where the counterfeiters interact *repeatedly* with the legal firm. In such a case, it makes sense for counterfeiters to react to the differentiation efforts of the legal firm by adapting their own products. Here, we capture this reaction by assuming that the reputation of the genuine good always positively affects the reputation of the counterfeited product.

The following proposition shows that, for any given value of reputation $R(t)$, the legal firm obtains a higher total payoff in the no-counterfeiting case than in the counterfeiting scenario.

Proposition 10 *For any* $R(t)$ *and all* $t \in [\mathcal{E}, T]$, *we have* $W_l(t, R(t)) < V_l(t, R(t))$.

Proof See Appendix 2. □

The two preceding propositions imply the following corollary:

Corollary 1 *We have* $W_l(\mathcal{E}, R^{\mathcal{C}}(\mathcal{E})) < V_l(\mathcal{E}, R^{\mathcal{N}}(\mathcal{E}))$.

Proof From Proposition 10, we have

$$W_l(t, R^{\mathcal{C}}(t)) < V_l(t, R^{\mathcal{C}}(t))$$

and from Proposition 8, we have $R^{\mathcal{N}}(\mathcal{E}) > R^{\mathcal{C}}(\mathcal{E})$, so $W_l(\mathcal{E}, R^{\mathcal{C}}(\mathcal{E})) < V_l(\mathcal{E}, R^{\mathcal{N}}(\mathcal{E}))$. □

The impact of counterfeiting on total profit is given in the following result.

Proposition 11 *The total profit of the legal firm calculated by starting at any date t in* $[0, \mathcal{E}]$ *is higher in the absence of counterfeiting. That is,* $V_l(t, R^{\mathcal{N}}(t)) > Z_l(t, R^{\mathcal{C}}(t))$.

Proof Denote by $\left(R^{\mathcal{C}}(s), a^{\mathcal{C}}(s), p_l^{\mathcal{C}}(s)\right)$ the equilibrium trajectory in the presence of the counterfeiter and by $\pi_1\left(R^{\mathcal{C}}(s), a^{\mathcal{C}}(s), p_s^{\mathcal{C}}(s)\right)$ the corresponding instantaneous profit of the legal firm before the counterfeiter's entry. The total payoff that the legal firm realizes in the game starting at any t in $[0, \mathcal{E}]$ can be written as

$$\begin{aligned} Z_l\left(t, R^{\mathcal{C}}(t)\right) &= \int_t^{\mathcal{E}} \pi_1\left(p_l^{\mathcal{C}}(s), a^{\mathcal{C}}(s), R^{\mathcal{C}}(t)\right) ds + W_l(\mathcal{E}, R^{\mathcal{C}}(\mathcal{E})), \\ &\leq \int_t^{\mathcal{E}} \pi_1\left(p_l^{\mathcal{C}}(s), a^{\mathcal{C}}(s), R^{\mathcal{C}}(s)\right) ds + V_l(\mathcal{E}, R^{\mathcal{C}}(\mathcal{E})), \\ &\leq V_l(t, R^{\mathcal{N}}(t)). \end{aligned}$$

The first inequality is due to Proposition 10, and the second inequality follows from the optimality principle of dynamic programming. In particular, the total payoff in the whole game is higher in the absence of counterfeiting, that is, $Z_l(0, R_0) \leq V_l(0, R_0)$. □

Independently of the fact that counterfeiting is illegal, its very presence means competition for the legal firm, and consequently, the above result is not surprising. A relevant question is how much counterfeiting costs the legal firm and how this loss varies with the parameter values. The total loss is given by $\Delta\Pi = V_l(0, R(0)) - Z_l(0, R(0))$. We note that $\Delta\Pi$ is increasing in R_0, which means that a company having a high initial brand equity (or reputation) suffers more from counterfeiting than a firm with a lower value.[18]

The main message from the above comparisons is that counterfeiting is under no circumstances beneficial to the legal firm. Although these results sometimes involved complicated proofs, they are somewhat expected. If this were not the case, then legal firms would not invest much effort in deterring counterfeiting.[19] In the next subsection, we shift the focus from the firm to the consumer.

[18] This assertion can be established using Eqs. (11) and (16), and Lemma 1.

[19] See El Harbi and Grolleau [16], however, for a review of some cases where counterfeiting can be profit enhancing for the legal firm.

5.2 Consumer Welfare Comparison

Standard consumer measures of surplus are difficult to use here since, in our setting, there are two goods whose prices change over time. It is then better to study the welfare effect of counterfeiting by comparing the equilibrium value of the consumer's utility function with and without counterfeiting.

First, at any $t \in [0, \mathcal{E}]$, the consumer's optimization problem is

$$\max_{q_l} U(q_l, 0, y) = \sigma_l \sqrt{R} q_l - \frac{\kappa_l q_l^2}{2} + I - p_l q_l.$$

From the first-order optimality condition, we obtain $q_l = \frac{\sigma_l \sqrt{R}}{2\kappa_l}$ and, for any $t \in [0, \mathcal{E}]$, the equilibrium (indirect) utility value

$$U(q_l, 0, y) = \frac{\kappa_l}{2}(q_l)^2 + I.$$

The above expression is the same with and without counterfeiting (only the value of brand reputation and the quantity q_l are different). Knowing that the brand's reputation is lower under counterfeiting, we conclude unambiguously that the counterfeiter causes a loss in welfare even during the monopoly period, that is, even before it enters into play.

Now at any $t \in [\mathcal{E}, T]$, the consumer's optimization problem is

$$\max_{q_l, q_c} U(q_l, q_c, y) = \left(\sigma_l \sqrt{R} q_l + \sigma_c \sqrt{R} q_c - \frac{\kappa_l q_l^2}{2} - \frac{\kappa_c q_c^2}{2} - \psi q_l q_c + I - p_l q_l - p_c q_c \right).$$

Assuming an interior solution, we can show that the equilibrium value of the demand for the legal product and the counterfeit are, respectively, given as follows:

$$q_l^{\mathcal{C}} = \frac{\kappa_c \left(2\kappa_c \kappa_l \sigma_l - \psi \sigma_c \kappa_l - \psi^2 \sigma_l\right)}{\left(4\kappa_c \kappa_l - \psi^2\right)\left(\kappa_c \kappa_l - \psi^2\right)} \sqrt{R},$$

$$q_c^{\mathcal{C}} = \frac{\kappa_l \left(2\kappa_c \kappa_l \sigma_c - \psi \sigma_l \kappa_c - \psi^2 \sigma_c\right)}{\left(4\kappa_c \kappa_l - \psi^2\right)\left(\kappa_c \kappa_l - \psi^2\right)} \sqrt{R}.$$

Inserting these demands in $U(q_l, q_c, y)$, it is easy to show that the equilibrium value of the consumer (indirect) utility function can be written as $U(q_l^{\mathcal{C}}, q_c^{\mathcal{C}}, y^{\mathcal{C}}) = \chi^{\mathcal{C}} R^{\mathcal{C}}$, where

$$\chi^{\mathcal{C}} = \frac{\kappa_c^2 X_1^2 + \kappa_l^2 X_2^2 + 2\psi \kappa_c \kappa_l X_1 X_2}{2\left(4\kappa_c \kappa_l - \psi^2\right)^2 \left(\kappa_c \kappa_l - \psi^2\right)^2},$$

and

$$X_1 = \left(2\kappa_c\kappa_l\sigma_l - \psi\sigma_c\kappa_l - \psi^2\sigma_l\right),$$
$$X_2 = \left(2\kappa_c\kappa_l\sigma_c - \psi\sigma_l\kappa_c - \psi^2\sigma_c\right).$$

We first want to compare $\chi^{\mathcal{C}}$ with $\chi^{\mathcal{N}}$ where we recall that

$$\chi^{\mathcal{N}} = \frac{\sigma_l^2}{8\kappa_l}.$$

Assume that $R^{\mathcal{C}} = R^{\mathcal{N}} = R$. We know, of course, that this is false in equilibrium, but it does not matter as we are dealing with variables that are solutions to static optimization problems. We know that the equilibrium price of the legal good is higher without counterfeiting than with counterfeiting. Therefore, the equilibrium value of the consumer's utility function with counterfeiting is no lower (and indeed is higher) than this value when there is counterfeiting. This is because the consumer can always buy the same quantity of the legal good that he bought when there was no counterfeiting, at a *lower* price. Since his income is constant, he can also buy the fake good, and this increases his utility. This leads to the following:

Proposition 12 *We have* $\chi^{\mathcal{N}} < \chi^{\mathcal{C}}$.

The next result gives a sufficient condition for counterfeiting to be welfare improving for any $t \in [\mathcal{E}, T]$, that is, $\chi^{\mathcal{N}} R^{\mathcal{N}}(t) < \chi^{\mathcal{C}} R^{\mathcal{C}}(t)$.

Proposition 13 *There exists* $\underline{\omega}$*, such that, for all* ω*, such that* $\underline{\omega} \leq \omega$*, counterfeiting is welfare improving for all* t *in* $[\mathcal{E}, T]$.

Proof See Appendix 2. □

One explanation of this result is the following: When the advertising cost is high, the legal firm invests less in this activity, which results in a lower value for the brand's reputation, and consequently, the market size is smaller. This in turn increases competition between the two firms, and prices are lower, which is good news for the consumer. In this case, the positive effect of price competition on welfare more than compensates for the negative effect of the decrease in the legal firm's reputation (since accumulating reputation is costly, even in the absence of counterfeiting, the negative effect of counterfeiting on reputation is small).

Though counterfeiting may enhance consumer welfare on the interval $[\mathcal{E}, T]$, we have seen that counterfeiting is unambiguously welfare decreasing on the interval $[0, \mathcal{E}]$. The question of the global impact of counterfeiting on welfare is thus pending. The next result extends Proposition 13 to ensure that counterfeiting may improve consumer welfare on the whole horizon.

Proposition 14 *There exists $\underline{\omega}'$, such that, for all ω, such that $\underline{\omega}' \leq \omega$, counterfeiting is welfare improving* $[0, T]$ *in the sense that*

$$\int_0^T \chi^{\mathcal{N}} R^{\mathcal{N}}(t)dt < \int_0^{\mathcal{E}} \chi^{\mathcal{N}} R^{\mathcal{C}}(t)dt + \int_{\mathcal{E}}^T \chi^{\mathcal{C}} R^{\mathcal{C}} dt.$$

6 Concluding Remarks

To the best of our knowledge, this is the first attempt to analyze the impact of counterfeiting in a fully dynamic context with micro-founded demand functions. The decision variables, that is, price and advertising, are clearly the most relevant ones for well-known brands that eventually end up being copied by illegal producers. In one sentence, the main takeaway of our paper is that counterfeiting is under no circumstances beneficial to the legal producer, but it can suit consumers under some conditions. Further, we showed that brand equity is always lower in the presence of counterfeiting. This implies that this illegal activity has a really damaging effect on the legal firm over the long term.

This last effect clearly supports prosecuting counterfeiters, as it is currently done in many countries. By contrast, only a few countries like France and Italy penalize consumers who purchase counterfeits. Our finding that counterfeiting can benefit consumers suggests acting with caution with regard to the introduction of consumer liability.[20] That is because, it may be difficult to actually identify the goods for which counterfeiting is detrimental to consumers from the others.

As in any modeling effort, some simplifying assumptions have been made here, and it would clearly be advantageous to relax them in future work. First, we assumed that the counterfeiter's entry date is known, which in practice may be hard to predict precisely. It would not really be conceptually difficult to keep the same framework and consider a case where this date is random. However, one can expect this to potentially lead to equilibria that cannot be either fully characterized analytically or not be compared analytically.

Second, we have implicitly assumed that the legal producer cannot deter entry. In the absence of efficient institutions to combat counterfeiting, one intuitive option for private firms to prevent illegal producers from entering the market is to sell at a lower price to reduce the temptation of consumers to buy the illegal product (The assumption here is that the attractiveness of going illegal depends on the gap in prices.). For this to work, we minimally need to assume that the illegal producer faces a fixed cost. The relevance and the level of such cost is an empirical matter. Indeed, the fixed cost that needs to be paid to be able to start selling an illegal version of software is not the same as producing a fake *Lancel* bag.

[20] For a defense of consumer liability in the U.S., see, e.g., Orscheln [25] or Riso [30]. According to Orschel [25], in 1993, Ms. Chin, a representative for District 1 of New York City, proposed to adapt New York legislation to prosecute consumers for purchasing counterfeit goods. The proposal appears to be laid over.

Third, we assumed that the product is normal. An interesting question that we did not address is what would happen if the product had a network externality value. For instance, the value that a person derives from a video game may depend on the number of individuals in the person's circle who own the product. Here, the illegal demand may have a positive effect on the brand's reputation, that is, illegal demand works as an additional advertising activity that feeds the brand equity. In such a case, one expects very different results from those obtained here, and it is surely of interest to investigate such a context.

Appendix 1

Derivation of the Demand Functions

Assume that the utility function of the representative consumer is given by the following quadratic function:

$$U(q_l, q_c, y) = \sigma_l \sqrt{R} q_l + \sigma_c \sqrt{R} q_c - \frac{\kappa_l q_l^2}{2} - \frac{\kappa_c q_c^2}{2} - \psi q_l q_c + y,$$

where y is a composite good, and σ_l, σ_c, ψ, κ_l and κ_c are positive parameters, with

$$\sigma_l \kappa_c - \sigma_c \psi > 0, \tag{24}$$

$$\sigma_c \kappa_l - \sigma_l \psi > 0, \tag{25}$$

$$\psi > 0. \tag{26}$$

The budget constraint is given by

$$p_l q_l + p_c q_c + y = I.$$

Suppose now that there is no counterfeit good, i.e., $q_c = 0$. Then, the representative consumer solves the following problem:

$$\max_{q_l} \left(\sigma_l \sqrt{R} q_l - \frac{\kappa_l q_l^2}{2} + I - p_l q_l \right).$$

We easily find that the demand function is

$$q_l = \frac{\sigma_l \sqrt{R} - p_l}{\kappa_l}. \tag{27}$$

By contrast, when there *is* a counterfeiter, the representative consumer solves the following program:

$$\max_{q_l,q_c}\left(\sigma_l\sqrt{R}q_l+\sigma_c\sqrt{R}q_c-\frac{\kappa_l q_l^2}{2}-\frac{\kappa_c q_c^2}{2}-\psi q_l q_c+I-p_l q_l-p_c q_c\right).$$

Assuming an interior solution, then the first-order optimality conditions are given by

$$\sigma_l\sqrt{R}-\kappa_l q_l-\psi q_c-p_l=0, \tag{28}$$

$$\sigma_c\sqrt{R}-\kappa_c q_c-\psi q_l-p_c=0. \tag{29}$$

Solving for q_l and q_c, we obtain

$$q_l=\frac{\kappa_c\sigma_l\sqrt{R}-\psi\sigma_c\sqrt{R}-\kappa_c p_l+\psi p_c}{\kappa_l\kappa_c-\psi^2}, \tag{30}$$

$$q_c=\frac{\kappa_l\sigma_c\sqrt{R}-\psi\sigma_l\sqrt{R}-\kappa_l p_c+\psi p_l}{\kappa_l\kappa_c-\psi^2}. \tag{31}$$

We see at once that the demand functions for the legal good are structurally different in the two cases. Setting $p_c=0$ in (30) does not yield (27). We shall then assume that the demand functions for the legal good and the counterfeit good are given by the next expressions:

$$q_l(t)=\begin{cases}\tilde{\delta}_l\sqrt{R(t)}-\tilde{\beta}_l p_l(t), & t\in[0,\mathcal{E}),\\ \delta_l\sqrt{R(t)}-\beta_l p_l(t)+\gamma p_c(t), & t\in[\mathcal{E},T],\end{cases}$$

$$q_c(t)=\delta_c\sqrt{R(t)}-\beta_c p_c(t)+\gamma p_l(t), \quad t\in[\mathcal{E},T],$$

where $\beta_j>0$ and $\gamma\geq 0$, with $\beta_j>\gamma, j\in\{l,c\}$, and

$$\tilde{\delta}_l=\frac{\sigma_l}{\kappa_l},\quad \delta_l=\frac{\kappa_c\sigma_l-\psi\sigma_c}{\kappa_c\kappa_l-\psi^2},\quad \delta_c=\frac{\kappa_l\sigma_c-\psi_l\sigma_l}{\kappa_c\kappa_l-\psi^2},$$

$$\tilde{\beta}_l=\frac{1}{\kappa_l},\quad \beta_l=\frac{\kappa_c}{\kappa_c\kappa_l-\psi^2},\quad \beta_c=\frac{\kappa_l}{\kappa_c\kappa_l-\psi^2},\quad \gamma=\frac{\psi}{\kappa_c\kappa_l-\psi^2}.$$

We notice that

$$\delta_l=\frac{\kappa_c\sigma_l-\psi\sigma_c}{\kappa_c\kappa_l-\psi^2}<\tilde{\delta}_l=\frac{\sigma_l}{\kappa_l},$$

if and only if $\sigma_c\kappa_l-\sigma_l\psi>0$ which holds true by assumption.

Moreover, we have

$$\tilde{\beta}_l = \frac{1}{\kappa_l} < \beta_l = \frac{\kappa_c}{\kappa_c \kappa_l - \psi^2}.$$

To ensure that in equilibrium the price of the good produced by the legal firm is higher than the price of the counterfeit good, that is,

$$\frac{p_l^{\mathcal{C}}(R(t))}{p_c^{\mathcal{C}}(R(t))} = \frac{2\beta_c \delta_l + \delta_c \gamma}{2\beta_l \delta_c + \delta_l \gamma} > 1,$$

we assume that $\sigma_l - \sigma_c > 0$ and

$$\left(2\kappa_l \kappa_c - \psi^2\right)(\sigma_l - \sigma_c) + \psi(\kappa_c \sigma_l - \kappa_l \sigma_c) > 0.$$

Appendix 2

Proofs

Proof of Proposition 1

Denote by $V_l(t, R(t)) : [0, T] \times \mathbb{R}_+ \to \mathbb{R}_+$ the value function of the legal firm. The Hamilton-Jacobi-Bellman (HJB) equation reads as follows:

$$-\frac{\partial V_l}{\partial t}(t, R(t)) = \max_{p_l, a} \left(\left(p_l(t) \left(\tilde{\delta}_l \sqrt{R(t)} - \tilde{\beta}_l p_l(t) \right) - \frac{\omega}{2} a^2(t) \right) + \frac{\partial V_l}{\partial R}(t, R(t))(ka(t) - \sigma R(t)) \right).$$

Assuming an interior solution, the first-order optimality conditions are

$$\frac{\partial RHS}{\partial p_l} = \tilde{\delta}_l \sqrt{R} - 2\tilde{\beta}_l p_l = 0 \Leftrightarrow p_l = \frac{\tilde{\delta}_l}{2\tilde{\beta}_l} \sqrt{R},$$
$$\frac{\partial RHS}{\partial a} = -\omega a + k \frac{\partial V_l}{\partial R} = 0 \Leftrightarrow a = \frac{k}{\omega} \frac{\partial V_l}{\partial R}.$$

Substitute in the HJB equation to get

$$-\frac{\partial V_l}{\partial t} = \left(\frac{\tilde{\delta}_l}{2\tilde{\beta}_l} \sqrt{R(t)} \left(\tilde{\delta}_l \sqrt{R(t)} - \tilde{\beta}_l \frac{\tilde{\delta}_l}{2\tilde{\beta}_l} \sqrt{R(t)} \right) - \frac{\omega}{2} \left(\frac{k}{\omega} \frac{\partial V_l}{\partial R} \right)^2 \right) + \frac{\partial V_l}{\partial R} \left(k \frac{k}{\omega} \frac{\partial V_l}{\partial R} - \sigma R(t) \right),$$

which simplifies to

$$-\frac{\partial V_l}{\partial t}=\frac{\tilde{\delta}_l^2}{4\tilde{\beta}_l}R+\frac{k^2}{2\omega}\left(\frac{\partial V_l}{\partial R}\right)^2-\sigma R\frac{\partial V_l}{\partial R}. \tag{32}$$

Conjecture that the value function is linear, i.e.,

$$\begin{aligned} V_l\left(t,R\left(t\right)\right)&=z\left(t\right)R\left(t\right)+y\left(t\right),\\ V_l\left(T,R\left(T\right)\right)&=sR\left(T\right), \end{aligned}$$

where $z\left(t\right)$ and $y\left(t\right)$ are the coefficient to be identified. Substituting in (32) yields

$$-\left(\dot{z}R+\dot{y}\right)=\left(\frac{\tilde{\delta}_l^2}{4\tilde{\beta}_l}-\sigma z\right)R+\frac{k^2}{2\omega}z^2.$$

By identification, we have

$$\begin{aligned} -\dot{z}&=\frac{\tilde{\delta}_l^2}{4\tilde{\beta}_l}-\sigma z,\\ -\dot{y}\left(t\right)&=\frac{k^2}{2\omega}\left(z\left(t\right)\right)^2. \end{aligned}$$

Solving the two above differential equations, we obtain

$$z\left(t\right)=\frac{\tilde{\delta}_l^2}{4\sigma\tilde{\beta}_l}+C_1e^{\sigma t}, \tag{33}$$

$$y\left(t\right)=-\frac{k^2}{4\sigma\omega}\left(\frac{\tilde{\delta}_l^4}{8\sigma\tilde{\beta}_l^2}t+\frac{\tilde{\delta}_l^2C_1}{\sigma\tilde{\beta}_l}e^{\sigma t}+C_1^2e^{2\sigma t}\right)+C_2, \tag{34}$$

where C_1 and C_2 are integration constants.

Using the terminal condition

$$V_l\left(T,R\left(T\right)\right)=sR\left(T\right),$$

we conclude that

$$\begin{aligned} z\left(T\right)&=s,\\ y\left(T\right)&=0. \end{aligned}$$

Consequently,

$$z\left(T\right)=\frac{\tilde{\delta}_l^2}{4\sigma\tilde{\beta}_l}+C_1e^{\sigma T}=s\Leftrightarrow C_1=\frac{4\sigma\tilde{\beta}_ls-\tilde{\delta}_l^2}{4\sigma\tilde{\beta}_l}e^{-\sigma T}.$$

Further, we have

$$
\begin{aligned}
y(T) &= -\frac{k^2}{4\sigma\omega}\left(\frac{\tilde{\delta}_l^4}{8\sigma\tilde{\beta}_l^2}T + \frac{\tilde{\delta}_l^2 C_1}{\sigma\tilde{\beta}_l}e^{\sigma T} + C_1^2 e^{2\sigma T}\right) + C_2 = 0,\\
\frac{4\sigma\tilde{\beta}_l s - \tilde{\delta}_l^2}{4\sigma\tilde{\beta}_l}e^{-\sigma T} &= -\frac{k^2}{4\sigma\omega}\left(\frac{\tilde{\delta}_l^4}{8\sigma\tilde{\beta}_l^2}T + \frac{\tilde{\delta}_l^2\frac{4\sigma\tilde{\beta}_l s-\tilde{\delta}_l^2}{4\sigma\tilde{\beta}_l}e^{-\sigma T}}{\sigma\tilde{\beta}_l}e^{\sigma T} + (\frac{4\sigma\tilde{\beta}_l s - \tilde{\delta}_l^2}{4\sigma\tilde{\beta}_l}e^{-\sigma T})^2 e^{2\sigma T}\right) + C_2 = 0,\\
&\Leftrightarrow C_2 = \frac{k^2}{4\sigma\omega}\left(\frac{\tilde{\delta}_l^4}{8\sigma\tilde{\beta}_l^2}T + \tilde{\delta}_l^2\frac{4\sigma\tilde{\beta}_l s - \tilde{\delta}_l^2}{4\sigma^2\tilde{\beta}_l^2} + \left(\frac{4\sigma\tilde{\beta}_l s - \tilde{\delta}_l^2}{4\sigma\tilde{\beta}_l}\right)^2\right)\\
&= \frac{k^2}{16\sigma^3\omega\tilde{\beta}_l^2}\left(\frac{\tilde{\sigma\delta}_l^4}{2}T + \tilde{\delta}_l^2(4\sigma\tilde{\beta}_l s - \tilde{\delta}_l^2) + \frac{(4\sigma\tilde{\beta}_l s - \tilde{\delta}_l^2)^2}{4}\right)
\end{aligned}
$$

Substituting for C_1 and C_2 in (33) and (34) yields the values of $z(t)$ and $y(t)$ displayed p. 265. Now,

$$a = \frac{k}{\omega}\frac{\partial V_l}{\partial R} = \frac{k}{\omega}z(t) = \frac{k}{4\sigma\tilde{\beta}_l\omega}(\tilde{\delta}_l^2 + (4\sigma\tilde{\beta}_l s - \tilde{\delta}_l^2)e^{\sigma(t-T)}).$$

Inserting in the dynamics and solving the differential equation, we obtain the brand's reputation trajectory given in (10).

Substituting for $z(t)$ and $y(t)$ in $V_l(t, R(t))$ yields the following value:

$$
\begin{aligned}
V_l(t, R(t)) = &\left(\frac{\tilde{\delta}_l^2}{4\sigma\tilde{\beta}_l} + \frac{4\sigma\tilde{\beta}_l s - \tilde{\delta}_l^2}{4\sigma\tilde{\beta}_l}e^{\sigma(t-T)}\right)R(t)\\
&+\frac{k^2}{16\sigma^3\omega\tilde{\beta}_l^2}\left(\frac{\tilde{\sigma\delta}_l^4}{2}(T-t) + \tilde{\delta}_l^2(4\sigma\tilde{\beta}_l s - \tilde{\delta}_l^2)(1-e^{\sigma(t-T)})\right.\\
&\left.+\frac{(4\sigma\tilde{\beta}_l s - \tilde{\delta}_l^2)^2}{4}(1-e^{2\sigma(t-T)})\right).
\end{aligned}
$$

The total payoff is obtained by evaluating the above value function at $(0, R(0))$, that is,

$$
\begin{aligned}
V_l(0, R(0)) &= z(0)R(0) + y(0),\\
&= \left(\frac{\tilde{\delta}_l^2}{4\sigma\tilde{\beta}_l} + \frac{4\sigma\tilde{\beta}_l s - \tilde{\delta}_l^2}{4\sigma\tilde{\beta}_l}e^{-\sigma T}\right)R_0\\
&\quad+\frac{k^2}{16\sigma^3\omega\tilde{\beta}_l^2}\left(\frac{\tilde{\sigma\delta}_l^4}{2}T + \tilde{\delta}_l^2(4\sigma\tilde{\beta}_l s - \tilde{\delta}_l^2)(1-e^{-\sigma T}) + \frac{(4\sigma\tilde{\beta}_l s - \tilde{\delta}_l^2)^2}{4}(1-e^{-2\sigma T})\right).
\end{aligned}
$$

Payoff starting from $(\mathcal{E}, R(\mathcal{E}))$ is given by

$$V_l(\mathcal{E}, R(\mathcal{E})) = z(\mathcal{E}) R(\mathcal{E}) + y(\mathcal{E}).$$

Proof of Proposition 4

Denote by $W_l(t, R(t)) : [\mathcal{E}, T] \times \mathbb{R}_+ \to \mathbb{R}$ the legal firm's value function. The HJB equation of the legal firm is given by

$$-\frac{\partial W_l}{\partial t}(t, R(t)) = \max_{p_l, a} \left(\left(p_l(t) \left(\delta_l \sqrt{R(t)} - \beta_l p_l(t) + \gamma p_c(t) \right) - \frac{\omega}{2} a^2(t) \right) + \frac{\partial W_l}{\partial R}(t, R(t)) (ka(t) - \sigma R(t)) \right).$$

The counterfeiter's optimization problem is

$$\max_{p_c(t)} \pi_c(t) = \max_{p_c(t)} p_c(t) \left(\delta_c \sqrt{R(t)} - \beta_c p_c(t) + \gamma p_l(t) \right), \quad \forall t \in [\mathcal{E}, T].$$

Assuming an interior solution, the first-order equilibrium conditions are

$$\begin{aligned} \frac{\partial RHS}{\partial p_l} &= \delta_l \sqrt{R} - 2\beta_l p_l + \gamma p_c = 0, \\ \frac{\partial RHS}{\partial a} &= -\omega a + k \frac{\partial W_l}{\partial R} = 0, \\ \frac{\partial \pi_c}{\partial p_c} &= \delta_c \sqrt{R} - 2\beta_c p_c + \gamma p_l = 0 \Leftrightarrow p_c = \frac{\delta_c \sqrt{R} + \gamma p_l}{2\beta_c}, \end{aligned}$$

which is equivalent to (12), (13) and

$$a = \frac{k}{\omega} \frac{\partial W_l}{\partial R}.$$

Substituting in the HJB yields

$$-\frac{\partial W_l}{\partial t} = \beta_l \left(\frac{2\beta_c \delta_l + \delta_c \gamma}{4\beta_c \beta_l - \gamma^2} \right)^2 R + \frac{\omega}{2} \left(\frac{k}{\omega} \frac{\partial W_l}{\partial R} \right)^2 - \sigma R \frac{\partial W_l}{\partial R}. \tag{35}$$

Conjecture the following linear form for the value function:

$$W_l(t, R(t)) = x(t) R(t) + v(t),$$

then

$$a = \frac{k}{\omega}x,$$
$$\frac{\partial W_l}{\partial t} = \dot{x}R + \dot{v}.$$

Substituting in (35), we obtain

$$-(\dot{x}R + \dot{v}) = \left(\beta_l \left(\frac{2\beta_c\delta_l + \delta_c\gamma}{4\beta_c\beta_l - \gamma^2}\right)^2 - \sigma x\right) R + \frac{k^2x^2}{2\omega}.$$

By identification of terms in order of R, we have

$$-\dot{x} + \sigma x = \beta_l \left(\frac{2\beta_c\delta_l + \delta_c\gamma}{4\beta_c\beta_l - \gamma^2}\right)^2,$$
$$\dot{v} = -\frac{k^2}{2\omega}x^2.$$

Solving the two above differential equations, we get

$$x(t) = \Gamma + C_1 e^{\sigma t},$$
$$v(t) = -\frac{k^2}{2\omega}\left(\Gamma^2 t + \frac{C_1^2}{2\sigma}e^{2\sigma t} + \frac{2\Gamma C_1}{\sigma}e^{\sigma t}\right) + C_2,$$

where C_1 and C_2 are integration constants and

$$\Gamma = \frac{\beta_l}{\sigma}\left(\frac{2\beta_c\delta_l + \delta_c\gamma}{4\beta_c\beta_l - \gamma^2}\right)^2.$$

Using the boundary condition

$$W_l(T, R(T)) = sR(T)$$

yields

$$C_1 = (s - \Gamma)e^{-\sigma T},$$
$$C_2 = \frac{k^2}{2\omega}\left(\Gamma^2 T + \frac{(s-\Gamma)^2}{2\sigma} + \frac{2\Gamma(s-\Gamma)}{\sigma}\right),$$

and consequently we get the values of $x(t)$ and $v(t)$ given in (16) and (17). Recalling that $a = \frac{k}{\omega}x$, we then get (14).

Substituting for a in the dynamics and solving the differential equation with $R(\mathcal{E})$ as initial condition, we get the value of the reputation after entry given in (15).

Proof of Proposition 5

Denote by $Z_l(t, R(t)) : [0, T] \times \mathbb{R}_+ \to \mathbb{R}_+$ the value function of the legal firm. The Hamilton-Jacobi-Bellman (HJB) equation reads as follows:

$$-\frac{\partial Z_l}{\partial t}(t, R(t)) = \max_{p_l, a}\left(\left(p_l(t)\left(\tilde{\delta}_l\sqrt{R(t)} - \tilde{\beta}_l p_l(t)\right) - \frac{\omega}{2}a^2(t)\right) + \frac{\partial Z_l}{\partial R}(t, R(t))(ka(t) - \sigma R(t))\right).$$

Assuming an interior solution, the first-order optimality conditions are

$$\frac{\partial RHS}{\partial p_l} = \tilde{\delta}_l\sqrt{R} - 2\tilde{\beta}_l p_l = 0 \Leftrightarrow p_l = \frac{\tilde{\delta}_l}{2\tilde{\beta}_l}\sqrt{R},$$
$$\frac{\partial RHS}{\partial a} = -\omega a + k\frac{\partial Z_l}{\partial R} = 0 \Leftrightarrow a = \frac{k}{\omega}\frac{\partial Z_l}{\partial R}.$$

Substitute in the HJB equation to get

$$-\frac{\partial Z_l}{\partial t} = \frac{\tilde{\delta}_l}{2\tilde{\beta}_l}\sqrt{R(t)}\left(\tilde{\delta}_l\sqrt{R(t)} - \tilde{\beta}_l\frac{\tilde{\delta}_l}{2\tilde{\beta}_l}\sqrt{R(t)}\right) - \frac{\omega}{2}\left(\frac{k}{\omega}\frac{\partial Z_l}{\partial R}\right)^2 + \frac{\partial Z_l}{\partial R}\left(k\frac{k}{\omega}\frac{\partial Z_l}{\partial R} - \sigma R(t)\right),$$

which simplifies to

$$-\frac{\partial Z_l}{\partial t} = \frac{\tilde{\delta}_l^2}{4\tilde{\beta}_l}R + \frac{k^2}{2\omega}\left(\frac{\partial Z_l}{\partial R}\right)^2 - \sigma R\frac{\partial Z_l}{\partial R}. \tag{36}$$

Conjecture that the value function is linear, i.e.,

$$Z_l(t, R(t)) = m(t)R(t) + n(t),$$
$$Z_l(\mathcal{E}, R(\mathcal{E})) = W_l(\mathcal{E}, R(\mathcal{E})),$$

where $m(t)$ and $n(t)$ are the coefficients to be identified. Substituting in (36) yields

$$-(\dot{m}R + \dot{n}) = \left(\frac{\tilde{\delta}_l^2}{4\tilde{\beta}_l} - \sigma m\right)R + \frac{k^2}{2\omega}m^2.$$

By identification, we have

$$-\dot{m} = \frac{\tilde{\delta}_l^2}{4\tilde{\beta}_l} - \sigma m$$
$$-\dot{n} = \frac{k^2}{2\omega}m^2.$$

Solving the two above differential equations, we obtain

$$m(t) = \frac{\tilde{\delta}_l^2}{4\sigma\tilde{\beta}_l} + C_1 e^{\sigma t}, \tag{37}$$

$$n(t) = -\frac{k^2}{4\sigma\omega}\left(\frac{\tilde{\delta}_l^4}{8\sigma\tilde{\beta}_l^2}t + \frac{\tilde{\delta}_l^2 C_1}{\sigma\tilde{\beta}_l}e^{\sigma t} + C_1^2 e^{2\sigma t}\right) + C_2, \tag{38}$$

where C_1 and C_2 are integration constants.

Using the terminal condition

$$Z_l(\mathcal{E}, R(\mathcal{E})) = W_l(\mathcal{E}, R(\mathcal{E})) = x(\mathcal{E})R(\mathcal{E}) + v(\mathcal{E}),$$

we conclude that

$$m(\mathcal{E}) = x(\mathcal{E}) = \Gamma + (s-\Gamma)e^{-\sigma(T-\mathcal{E})},$$
$$n(\mathcal{E}) = v(\mathcal{E}) = \frac{k^2}{2\omega}\left(\Gamma^2(T-\mathcal{E}) + \frac{(s-\Gamma)^2}{2\sigma}(1-e^{2\sigma(\mathcal{E}-T)}) + \frac{2\Gamma(s-\Gamma)}{\sigma}(1-e^{\sigma(\mathcal{E}-T)})\right).$$

Consequently,

$$m(\mathcal{E}) = \frac{\tilde{\delta}_l^2}{4\sigma\tilde{\beta}_l} + C_1 e^{\sigma\mathcal{E}} = x(\mathcal{E}) \Leftrightarrow C_1 = \frac{4\sigma\tilde{\beta}_l x(\mathcal{E}) - \tilde{\delta}_l^2}{4\sigma\tilde{\beta}_l}e^{-\sigma\mathcal{E}}.$$

Further, we have

$$n(\mathcal{E}) = -\frac{k^2}{4\sigma\omega}\left(\frac{\tilde{\delta}_l^4}{8\sigma\tilde{\beta}_l^2}\mathcal{E} + \frac{\tilde{\delta}_l^2 C_1}{\sigma\tilde{\beta}_l}e^{\sigma\mathcal{E}} + C_1^2 e^{2\sigma\mathcal{E}}\right) + C_2 = v(\mathcal{E}),$$
$$= -\frac{k^2}{16\sigma^3\omega\tilde{\beta}_l^2}\left(\frac{\sigma\tilde{\delta}_l^4}{2}\mathcal{E} + \tilde{\delta}_l^2(4\sigma\tilde{\beta}_l x(\mathcal{E}) - \tilde{\delta}_l^2) + \frac{(4\sigma\tilde{\beta}_l x(\mathcal{E}) - \tilde{\delta}_l^2)^2}{4}\right) + C_2 = v(\mathcal{E}).$$

Substituting for C_1 and C_2 in (37) and (38) yields the values of $m(t)$ and $n(t)$ displayed page 270. Now,

$$a = \frac{k}{\omega}\frac{\partial Z_l}{\partial R} = \frac{k}{\omega}m(t) = \frac{k}{4\sigma\tilde{\beta}_l\omega}\left(\tilde{\delta}_l^2\left(1-e^{\sigma(t-\mathcal{E})}\right) + 4\sigma\tilde{\beta}_l x(\mathcal{E})e^{\sigma(t-\mathcal{E})}\right)$$

$$= \frac{k}{4\sigma\tilde{\beta}_l\omega}\left(\tilde{\delta}_l^2\left(1-e^{\sigma(t-\mathcal{E})}\right) + 4\sigma\tilde{\beta}_l(\Gamma + (s-\Gamma)e^{-\sigma(T-\mathcal{E})})e^{\sigma(t-\mathcal{E})}\right).$$

Inserting in the dynamics and solving the differential equation, we obtain the reputation trajectory given in Proposition 5.

Proof of Lemma 1

To prove the Lemma, we have to establish that the legal firm's profit in the monopoly case is higher than the profit under Bertrand competition. To do this, we shall rely on the micro-foundations of the demand functions. From Appendix 1, we know that when the consumptions of the three goods, q_l, q_c and y, are positive (where we recall that y is the composite good), the next conditions hold:

$$\sigma_l - \kappa_l q_l - \psi q_c = p_l, \tag{39}$$

$$\sigma_c - \kappa_l q_c - \psi q_l = p_c. \tag{40}$$

To derive the demand functions used in the paper, we have solved the consumer's maximization problem for quantities q_l and q_c (as a function of the prices) and we have studied the Bertrand competition case. We could also have considered Cournot competition where the legal firm (resp. the counterfeiter) maximizes $p_l q_l$ (resp. $p_c q_c$) with respect to q_l (resp. q_c), p_l and p_c being given by (39)–(40).

The quantities associated to a Cournot equilibrium satisfy the next conditions:

$$\sigma_l - 2\kappa_l q_l - \psi q_c = 0, \tag{41}$$

$$\sigma_c - 2\kappa_l q_c - \psi q_l = 0, \tag{42}$$

and are given by

$$\bar{q}_l = \frac{2\kappa_c \sigma_l - \psi \sigma_c}{4\kappa_c \kappa_l - \psi^2}, \tag{43}$$

$$\bar{q}_c = \frac{2\kappa_l \sigma_c - \psi \sigma_l}{4\kappa_c \kappa_l - \psi^2}. \tag{44}$$

Using Eqs. (39), (40), (41), and (42) we notice that, in a Cournot equilibrium,

$$\bar{p}_l = \kappa \bar{q}_l, \tag{45}$$

$$\bar{p}_c = \kappa \bar{q}_c. \tag{46}$$

- Now recall that, in the monopoly case, the demand for the legal product is obtained from the condition $\sigma_l - \kappa_l q_l - p_l = 0$. In this case, the legal firm chooses its price so as to maximize its profit $p_l q_l$, and we obtain that $q_c^* = \frac{\sigma_l}{2\kappa_l}$ and $p_l^* = \frac{\sigma_l}{2}$.
- Next, we shall rely on Proposition 1 of Singh and Vives [31], p. 549, which asserts that the profit of each firm under Cournot competition is higher than the profit obtained under Bertrand Competition (which is the case considered in the paper).
- We shall now prove that the monopoly profit is higher than the Cournot profit. To do this, we only have to show that $q_l^* > \bar{q}_l$ (see Eqs. (45) and (46)). But we can check that the condition $q_l^* > \bar{q}_l$, that is,

$$\frac{\sigma_l}{2\kappa_l} > \frac{2\kappa_c\sigma_l - \psi\sigma_c}{4\kappa_c\kappa_l - \psi^2} \tag{47}$$

is equivalent to

$$2\kappa_l\sigma_c > \sigma_l\psi.$$

This last condition is always met since we have assumed that $\kappa_l\sigma_c > \sigma_l\psi$. In the model's notation, the inequality in (47) corresponds to the inequality in the Lemma.

Proof of Proposition 7

By the dynamic programming optimality principle, we have, along an optimal path (here it is unique) for the legal firm, that

$$Z_l\,(0, R_0) = \int_0^{\mathcal{E}} \pi_1\left(R^{\mathcal{C}}(t;\mathcal{E}), a^{\mathcal{C}}(t;\mathcal{E}), p_l^{\mathcal{C}}(t;\mathcal{E})\right) dt + W_l(\mathcal{E}, R^{\mathcal{C}}(\mathcal{E};\mathcal{E})).$$

Notice that the optimal path $\left(R^{\mathcal{C}}(t;\mathcal{E}), a^{\mathcal{C}}(t;\mathcal{E}), p_l^{\mathcal{C}}(t;\mathcal{E})\right)$ a priori depends on $\mathcal{E}$.

Differentiating with respect to $\mathcal{E}$, we get

$$\frac{\partial Z_l(0,R_0;\mathcal{E})}{\partial\mathcal{E}} = \int_0^{\mathcal{E}} \left\{ \frac{\partial\pi_1}{\partial R}\frac{\partial R}{\partial\mathcal{E}} + \frac{\partial\pi_1}{\partial a}\frac{\partial a}{\partial\mathcal{E}} + \frac{\partial\pi_1}{\partial p_l}\left(\frac{\partial p_l}{\partial R}\frac{\partial R}{\partial\mathcal{E}} + \frac{\partial p_l}{\partial\mathcal{E}}\right)\right\} dt \tag{48}$$

$$+ \pi_1\left(R^{\mathcal{C}}(\mathcal{E};\mathcal{E}), a^{\mathcal{C}}(\mathcal{E};\mathcal{E}), p_l^{\mathcal{C}}(\mathcal{E};\mathcal{E})\right) + \frac{\partial W_l}{\partial t}(\mathcal{E}; R^{\mathcal{C}}(\mathcal{E};\mathcal{E})) + \frac{\partial W_l}{\partial R}\left(\frac{\partial R}{\partial t}(\mathcal{E};\mathcal{E}) + \frac{\partial R}{\partial\mathcal{E}}(\mathcal{E};\mathcal{E})\right). \tag{49}$$

Now, by the Pontryagin maximum principle, there exists an adjoint variable $\lambda(t;\mathcal{E})$, such that, for all t in $[0,\mathcal{E}]$, the (unique) optimal path $\left(R^{\mathcal{C}}(t;\mathcal{E}), a^{\mathcal{C}}(t;\mathcal{E}), p_l^{\mathcal{C}}(t;\mathcal{E})\right)$ maximizes the Hamiltonian

$$\pi_1(R(t), a(t), p_l(t)) + \lambda(t)[ka(t) - \sigma R(t)].$$

Moreover the adjoint variable $\lambda(t)$ also satisfies

$$\dot{\lambda}(t;\mathcal{E}) = -\left(\frac{\partial\pi_1}{\partial R} - \sigma\lambda(t,\mathcal{E})\right),$$

$$\lambda(\mathcal{E};\mathcal{E}) = \frac{\partial W_l}{\partial R}(\mathcal{E}; R^{\mathcal{C}}(\mathcal{E};\mathcal{E})).$$

Therefore, the next conditions must hold at each date t:

$$\frac{\partial\pi_1}{\partial a} + \lambda(t;\mathcal{E})k = 0, \tag{50}$$

$$\frac{\partial\pi_1}{\partial p_l} = 0. \tag{51}$$

Following an argument in the proof of the Dynamic Envelope Theorem (Th. 9.1, pp 233) in Caputo [5], we first differentiate the following dynamics equation:

$$\dot{R}(t,\mathcal{E}) = ka(t;\mathcal{E}) - \sigma R(t;\mathcal{E}),$$

with respect to $\mathcal{E}$ to obtain

$$\frac{\partial \dot{R}(t;\mathcal{E})}{\partial \mathcal{E}} = k\frac{\partial a(t;\mathcal{E})}{\partial \mathcal{E}} - \sigma\frac{\partial R(t,\mathcal{E})}{\partial \mathcal{E}}.$$

Let us now add the following quantity

$$\lambda(t,\mathcal{E})\left(k\frac{\partial a(t;\mathcal{E})}{\partial \mathcal{E}} - \sigma\frac{\partial R(t,\mathcal{E})}{\partial \mathcal{E}} - \frac{\partial \dot{R}(t;\mathcal{E})}{\partial \mathcal{E}}\right) = 0,$$

to the integrand of the integral in (48). Using (51) we get

$$\begin{aligned}\frac{\partial Z_l(0,R_0;\mathcal{E})}{\partial \mathcal{E}} = \int_0^{\mathcal{E}} \Bigg\{ &\frac{\partial \pi_1}{\partial R}\frac{\partial R}{\partial \mathcal{E}} + \frac{\partial \pi_1}{\partial a}\frac{\partial a}{\partial \mathcal{E}} \\ &+\lambda(t;\mathcal{E})\left(k\frac{\partial a(t;\mathcal{E})}{\partial \mathcal{E}} - \sigma\frac{\partial R(t,\mathcal{E})}{\partial \mathcal{E}} - \frac{\partial \dot{R}(t;\mathcal{E})}{\partial \mathcal{E}}\right)\Bigg\} dt \\ &+ \pi_1\left(R^{\mathcal{C}}(\mathcal{E};\mathcal{E}), a^{\mathcal{C}}(\mathcal{E};\mathcal{E}), p_l^{\mathcal{C}}(\mathcal{E};\mathcal{E})\right) \\ &+ \frac{\partial W_l}{\partial t}(\mathcal{E}; R(\mathcal{E};\mathcal{E})) + \frac{\partial W_l}{\partial R}\left(\frac{\partial R}{\partial t}(\mathcal{E};\mathcal{E}) + \frac{\partial R}{\partial \mathcal{E}}(\mathcal{E};\mathcal{E})\right)\end{aligned} \tag{52}$$

To simplify the above expression, we integrate

$$\int_0^{\mathcal{E}} \lambda(t;\mathcal{E})\frac{\partial \dot{R}(t;\mathcal{E})}{\partial \mathcal{E}} dt,$$

by parts to obtain

$$\int_0^{\mathcal{E}} \lambda(t,\mathcal{E})\frac{\partial \dot{R}(t;\mathcal{E})}{\partial \mathcal{E}} dt = \lambda(\mathcal{E};\mathcal{E})\frac{\partial R}{\partial \mathcal{E}}(\mathcal{E};\mathcal{E}) - \lambda(0;\mathcal{E})\frac{\partial R}{\partial \mathcal{E}}(0;\mathcal{E}) - \int_0^{\mathcal{E}} \dot{\lambda}(t,\mathcal{E})\frac{\partial R(t;\mathcal{E})}{\partial \mathcal{E}} dt.$$

We observe that: $\frac{\partial R}{\partial \mathcal{E}}(0;\mathcal{E}) = 0$. Substituting the above expression in (52) we get after a little algebra

$$\begin{aligned}\frac{\partial Z_l(0,R_0;\mathcal{E})}{\partial \mathcal{E}} = \int_0^{\mathcal{E}} &\left\{\left(\frac{\partial \pi_1}{\partial R} - \sigma\lambda(t;\mathcal{E}) + \dot{\lambda}(t;\mathcal{E})\right)\frac{\partial R}{\partial \mathcal{E}} + \left(\frac{\partial \pi_1}{\partial a} + k\lambda(t;\mathcal{E})\right)\frac{\partial a}{\partial \mathcal{E}}\right\} dt \\ &- \lambda(\mathcal{E};\mathcal{E})\frac{\partial R}{\partial \mathcal{E}}(\mathcal{E};\mathcal{E}) + \pi_1\left(R^{\mathcal{C}}(\mathcal{E};\mathcal{E}), a^{\mathcal{C}}(\mathcal{E};\mathcal{E}), p_l^{\mathcal{C}}(\mathcal{E};\mathcal{E})\right) \\ &+ \frac{\partial W_l}{\partial t}(\mathcal{E}; R^{\mathcal{C}}(\mathcal{E};\mathcal{E})) + \frac{\partial W_l}{\partial R}\left(\frac{\partial R}{\partial t}(\mathcal{E};\mathcal{E}) + \frac{\partial R}{\partial \mathcal{E}}(\mathcal{E};\mathcal{E})\right).\end{aligned} \tag{53}$$

Using the Pontryagin maximum principle (and notably the fact that $\lambda(\mathcal{E};\mathcal{E}) = \frac{\partial W_l}{\partial R}(\mathcal{E}; R^{\mathcal{C}}(\mathcal{E};\mathcal{E}))$) the above expression reduces to

$$\frac{\partial Z_l(0,R_0;\mathcal{E})}{\partial \mathcal{E}} = \pi_1\left(R^{\mathcal{C}}(\mathcal{E};\mathcal{E}), a^{\mathcal{C}}(\mathcal{E};\mathcal{E}), p_l^{\mathcal{C}}(\mathcal{E};\mathcal{E})\right) + \frac{\partial W_l}{\partial t}(\mathcal{E}; R^{\mathcal{C}}(\mathcal{E};\mathcal{E})) + \frac{\partial W_l}{\partial R}\frac{\partial R}{\partial t}(\mathcal{E};\mathcal{E}).$$

Now, we use the Hamilton-Jacobi-Bellman equation, which holds at date $\mathcal{E}$, that is,

$$-\frac{\partial W_l(\mathcal{E}, R^{\mathcal{C}}(\mathcal{E};\mathcal{E}))}{\partial t} = \pi_2\left(R^{\mathcal{C}}(\mathcal{E};\mathcal{E}), a^{\mathcal{C}}(\mathcal{E};\mathcal{E}), p_l^{\mathcal{C}}(\mathcal{E};\mathcal{E})\right) + \frac{\partial W_l(\mathcal{E}; R^{\mathcal{C}}(\mathcal{E};\mathcal{E}))}{\partial R}\dot{R}(\mathcal{E};\mathcal{E}).$$

Substituting the above equation in Eq. (53) yields

$$\frac{\partial Z_l(0,R_0;\mathcal{E})}{\partial \mathcal{E}} = \pi_1\left(R^{\mathcal{C}}(\mathcal{E};\mathcal{E}), a^{\mathcal{C}}(\mathcal{E};\mathcal{E}), p_l^{\mathcal{C}}(\mathcal{E};\mathcal{E})\right) - \pi_2\left(R^{\mathcal{C}}(\mathcal{E};\mathcal{E}), a^{\mathcal{C}}(\mathcal{E};\mathcal{E}), p_l^{\mathcal{C}}(\mathcal{E};\mathcal{E})\right).$$

A more direct route consists in directly computing $\frac{\partial Z_l(0,R_0;\mathcal{E})}{\partial \mathcal{E}}$. Indeed, we have

$$\begin{aligned}
\frac{\partial Z_l(0,R_0;\mathcal{E})}{\partial \mathcal{E}} &= \frac{1}{4\sigma\tilde{\beta}_l}\left(\Lambda' - \sigma\Lambda e^{-\sigma\mathcal{E}}\right)R_0 + \frac{k^2\tilde{\delta}_l^4}{32\sigma^2\omega\tilde{\beta}_l^2} + \frac{k^2\tilde{\delta}_l^2}{16\sigma^3\omega\tilde{\beta}_l^2}\left(\Lambda'\left(1-e^{-\sigma\mathcal{E}}\right) + \Lambda\sigma e^{-\sigma\mathcal{E}}\right)\\
&\quad + \frac{k^2}{64\sigma^3\omega\tilde{\beta}_l^2}\left(2\Lambda\Lambda'\left(1-e^{-2\sigma\mathcal{E}}\right) + \Lambda^2 2\sigma e^{-2\sigma\mathcal{E}}\right)\\
&\quad - \frac{k^2}{2\omega}\left(\Gamma + (s-\Gamma)e^{\sigma(\mathcal{E}-T)}\right)^2,\\
&= \frac{R_0}{4\sigma\tilde{\beta}_l}(\tilde{\delta}_l^2 - 4\sigma\tilde{\beta}_l\Gamma)e^{-\sigma\mathcal{E}} + \frac{k^2\tilde{\delta}_l^4}{32\sigma^2\omega\tilde{\beta}_l^2} + \frac{k^2\tilde{\delta}_l^2}{16\sigma^3\omega\tilde{\beta}_l^2}\left(\sigma(\Lambda+\tilde{\delta}_l^2 - 4\sigma\tilde{\beta}_l\Gamma) + \sigma(4\sigma\tilde{\beta}_l\Gamma - \tilde{\delta}_l^2)e^{-\sigma\mathcal{E}}\right),\\
&\quad + \frac{k^2\Lambda}{32\sigma^3\omega\tilde{\beta}_l^2}\left(\sigma(\Lambda+\tilde{\delta}_l^2 - 4\sigma\tilde{\beta}_l\Gamma) + \sigma(4\sigma\tilde{\beta}_l\Gamma - \tilde{\delta}_l^2)e^{-2\sigma\mathcal{E}}\right) - \frac{k^2}{32\sigma^2\omega\tilde{\beta}_l^2}(\Lambda+\tilde{\delta}_l^2)^2,\\
&= \frac{R_0}{4\sigma\tilde{\beta}_l}(\tilde{\delta}_l^2 - 4\sigma\tilde{\beta}_l\Gamma)e^{-\sigma\mathcal{E}} + \frac{k^2\tilde{\delta}_l^2}{16\sigma^3\omega\tilde{\beta}_l^2}\left(\sigma(\tilde{\delta}_l^2 - 4\sigma\tilde{\beta}_l\Gamma)(1-e^{-\sigma\mathcal{E}})\right)\\
&\quad + \frac{k^2\Lambda}{32\sigma^3\omega\tilde{\beta}_l^2}\left(\sigma(\tilde{\delta}_l^2 - 4\sigma\tilde{\beta}_l\Gamma)(1-e^{-2\sigma\mathcal{E}})\right),\\
&= \frac{R_0}{4\sigma\tilde{\beta}_l}(\tilde{\delta}_l^2 - 4\sigma\tilde{\beta}_l\Gamma)e^{-\sigma\mathcal{E}}\\
&\quad + \frac{k^2(\sigma(\tilde{\delta}_l^2 - 4\sigma\tilde{\beta}_l\Gamma)}{32\sigma^3\omega\tilde{\beta}_l^2}(4\sigma\tilde{\beta}_l\left(\Gamma + (s-\Gamma)e^{-\sigma(T-\mathcal{E})}\right)(1-e^{-2\sigma\mathcal{E}}) + \tilde{\delta}_l^2(1+e^{-2\sigma\mathcal{E}} - 2e^{-\sigma\mathcal{E}})) > 0.
\end{aligned}$$

Proof of Proposition 8

We must prove the statement for the two periods, that is, before and after entry of the counterfeiter.

During the interval $[0, \mathcal{E})$, the difference in advertising is given by

$$a^{\mathcal{N}}(t) - a_1^{\mathcal{C}}(t) = \frac{k\Delta}{\sigma\omega}\left(e^{\sigma(t-\mathcal{E})} - e^{\sigma(t-T)}\right) \geq 0.$$

During the interval $[\mathcal{E}, T]$, the difference in advertising is given by

$$a^{\mathcal{N}}(t) - a_2^{\mathcal{C}}(t) = \frac{k\Delta}{\sigma\omega}\left(1 - e^{-\sigma(T-t)}\right) \geq 0.$$

Proof of Proposition 9

On $[0, \mathcal{E}]$ the difference in reputation is given by

$$R^{\mathcal{N}}(t) - R^{\mathcal{C}}(t) = \frac{k^2}{2\sigma^2\omega}\Delta\left(e^{-\sigma\mathcal{E}} - e^{-\sigma T}\right)\left(e^{\sigma t} - e^{-\sigma t}\right),$$

which is clearly always positive for all $t \in [0, \mathcal{E}]$.

To check that the difference in reputation is positive on $[\mathcal{E}, T]$, we consider the following differential equations:

$$\dot{R}^{\mathcal{N}}(t) = ka^{\mathcal{N}}(t) - \sigma R^{\mathcal{N}}(t),$$
$$\dot{R}^{\mathcal{C}}(t) = ka^{\mathcal{C}}(t) - \sigma R^{\mathcal{C}}(t),$$

with $R^{\mathcal{N}}(\mathcal{E}) > R^{\mathcal{C}}(\mathcal{E})$ from the above result. Moreover

$$a^{\mathcal{N}}(t) - a_2^{\mathcal{C}}(t) \geq 0,$$

from the previous proposition. Set $D(t) = R^{\mathcal{N}}(t) - R^{\mathcal{C}}(t)$ and $b(t) = a^{\mathcal{N}}(t) - a^{\mathcal{C}}(t)$, thus D satisfies

$$\dot{D}(t) = kb(t) - \sigma D(t)$$
$$D(\mathcal{E}) > 0$$

and $b(t) \geq 0$, so we have

$$D(t) = e^{-\sigma(t-\mathcal{E})}D(\mathcal{E}) + ke^{-\sigma t}\int_{\mathcal{E}}^{t} b(s)e^{\sigma s}ds.$$

Clearly $D(t) > 0$. Hence the result.

During the interval $[0, \mathcal{E})$, the difference in price is given by

$$p_l^{\mathcal{N}}\left(R^{\mathcal{N}}(t)\right) - p_{l1}^{\mathcal{C}}\left(t, R^{\mathcal{C}}(t)\right) = \frac{\tilde{\delta}_l}{2\tilde{\beta}_l}\left(\sqrt{R^{\mathcal{N}}(t)} - \sqrt{R^{\mathcal{C}}(t)}\right).$$

By the above result, $\sqrt{R^{\mathcal{N}}(t)} > \sqrt{R^{\mathcal{C}}(t)}$ and consequently, $p_l^{\mathcal{N}}\left(R^{\mathcal{N}}(t)\right) > p_{l1}^{\mathcal{C}}\left(t, R^{\mathcal{C}}(t)\right)$ for all $t \in [0, \mathcal{E})$.

During the interval $[\mathcal{E}, T]$, the difference in price is given by

$$p_l^{\mathcal{N}}(R(t)) - p_{l2}^{\mathcal{C}}(R(t)) = \frac{\tilde{\delta}_l}{2\tilde{\beta}_l}\sqrt{R^{\mathcal{N}}(t)} - \frac{2\beta_c\delta_l + \delta_c\gamma}{4\beta_c\beta_l - \gamma^2}\sqrt{R^{\mathcal{C}}(t)}.$$

Given that $\sqrt{R^{\mathcal{N}}(t)} > \sqrt{R^{\mathcal{C}}(t)}$ by the above result, to prove that $p_l^{\mathcal{N}}(R(t)) > p_{l2}^{\mathcal{C}}(R(t))$, it suffices to show that

$$\frac{\tilde{\delta}_l}{2\tilde{\beta}_l} > \frac{2\beta_c\delta_l + \delta_c\gamma}{4\beta_c\beta_l - \gamma^2}.$$

By Lemma 1, we have

$$\frac{\tilde{\delta}_l^2}{4\tilde{\beta}_l} > \beta_l\left(\frac{2\beta_c\delta_l + \delta_c\gamma}{4\beta_c\beta_l - \gamma^2}\right)^2 \Leftrightarrow \frac{\tilde{\delta}_l^2}{4\tilde{\beta}_l^2} > \frac{\beta_l}{\tilde{\beta}_l}\left(\frac{2\beta_c\delta_l + \delta_c\gamma}{4\beta_c\beta_l - \gamma^2}\right)^2.$$

Since $\tilde{\beta}_l < \beta_l$, the above inequality implies

$$\frac{\tilde{\delta}_l^2}{4\tilde{\beta}_l^2} > \left(\frac{2\beta_c\delta_l + \delta_c\gamma}{4\beta_c\beta_l - \gamma^2}\right)^2.$$

Taking the square root of both side yields

$$\frac{\tilde{\delta}_l}{4\tilde{\beta}_l} > \left(\frac{2\beta_c\delta_l + \delta_c\gamma}{4\beta_c\beta_l - \gamma^2}\right),$$

which concludes the proof.

Proof of Proposition 10

We have

$$W_l(t, R(t)) = \max_{p_{l2}(.), a_2(.)} \int_t^T \left(p_{l2}(h)\left(\delta_l\sqrt{R(h)} - \beta_l p_{l2}(h) + \gamma p_c(h)\right) - \frac{\omega}{2}a_2^2(h)\right)dh + sR(T), \tag{54}$$

$$\text{subject to (4) and } R^{\mathcal{C}}(t). \tag{55}$$

Let $p_{l2}^{\mathcal{C}}(t, R(t)), p_c^{\mathcal{C}}(t, R(t)), a_2^{\mathcal{C}}(t, R(t))$ be the feedback-Nash equilibrium. Let also $R^{\mathcal{C}}(.)$ be the induced path of the legal firm's reputation. We can then compute the values of the sales given the value of $R^{\mathcal{C}}(.)$. Using our notations, we get

$$r_l^{\mathcal{C}}(h) = p_{l2}^{\mathcal{C}}(h)\left(\delta_l\sqrt{R^{\mathcal{C}}(h)} - \beta_l p_{l2}^{\mathcal{C}}(h) + \gamma p_c^{\mathcal{C}}(h)\right) \tag{56}$$

$$= \frac{\beta_l\left(2\beta_c\delta_l + \delta_c\gamma\right)^2}{\left(4\beta_c\beta_l - \gamma^2\right)^2}R^{\mathcal{C}}(h) \tag{57}$$

$$< \hat{r}_l^{\mathcal{N}}(h) \tag{58}$$

$$= p_l^{\mathcal{N}}(h)\left(\tilde{\delta}_l\sqrt{R^{\mathcal{C}}(h)} - \tilde{\beta}_l p_l^{\mathcal{N}}(h)\right) \tag{59}$$

$$= \frac{\tilde{\delta}_l^2}{4\tilde{\beta}_l}R^{\mathcal{C}}(h), \tag{60}$$

where $\hat{r}_l^{\mathcal{N}}(h)$ is the maximum value of the sales of the legal firm at date h *along* the reputation path chosen when there is counterfeiting. The above inequality implies that:

$$W_l(t, R(t)) = \int_t^T \left(p_{l2}^{\mathcal{C}}(h)\left(\delta_l\sqrt{R^{\mathcal{C}}(h)} - \beta_l p_{l2}^{\mathcal{C}}(h) + \gamma p_c^{\mathcal{C}}(h)\right) - \frac{\omega}{2}(a_2^{\mathcal{C}})^2(h)\right)dh + sR^{\mathcal{C}}(T), \tag{61}$$

$$< \int_t^T \left(\frac{\tilde{\delta}_l^2}{4\tilde{\beta}_l}R^{\mathcal{C}}(h) - \frac{\omega}{2}(a_2^{\mathcal{C}})^2(h)\right)dh + sR^{\mathcal{C}}(T) \tag{62}$$

But by definition of $V_l(t, R(t))$, we have

$$V_l(t, R(t)) = \max_{p_l(.), a(.)} \int_t^T \left(p_l(h)\left(\tilde{\delta}_l\sqrt{R(h)} - \tilde{\beta}_l p_l(h)\right) - \frac{\omega}{2}a^2(h)\right)dt + sR(T), \tag{63}$$

$$= \max_{a(.)} \int_t^T \left(\frac{\tilde{\delta}_l^2}{4\tilde{\beta}_l}R(h) - \frac{\omega}{2}a^2(h)\right)dt + sR(T), \tag{64}$$

Therefore $W_l(t, R(t)) < V_l(t, R(t))$.

Proof of Proposition 13

Notice that we can write

$$R^{\mathcal{C}}(t) = \quad R_0 e^{-\sigma t} + \frac{G(t)}{\omega},$$
$$D(t) = R^{\mathcal{N}}(t) - R^{\mathcal{C}}(t) = \frac{F(t)}{\omega},$$

where G and F do not depend on ω.

Now let $z \in [\mathcal{E}, T]$ be the value at which F (and therefore D) reaches its maximum value on $[\mathcal{E}, T]$, and $y \in [\mathcal{E}, T]$ the value at which G reaches its minimum value on that interval. These values exist, since F and G are continuous on $[\mathcal{E}, T]$.

We have

$$\lim_{\omega \to +\infty} (R^{\mathcal{N}}(z) - R^{\mathcal{C}}(z)) = 0,$$

$$\lim_{\omega \to +\infty} R^{\mathcal{C}}(t) \geq \lim_{\omega \to +\infty} R_0 e^{-T} + \frac{G(y)}{\omega} \geq R_0 e^{-\sigma T} > 0.$$

Further, for all $t \in [\mathcal{E}, T]$, we have

$$\begin{aligned}\chi^{\mathcal{C}} R^{\mathcal{C}}(t) - \chi^{\mathcal{N}} R^{\mathcal{N}}(t) &= \left(\chi^{\mathcal{C}} - \chi^{\mathcal{N}}\right) R^{\mathcal{C}}(t) + \chi^{\mathcal{N}} \left(R^{\mathcal{C}}(t) - R^{\mathcal{N}}(t)\right) \\ &> \left(\chi^{\mathcal{C}} - \chi^{\mathcal{N}}\right) \left(R_0 e^{-T} + \frac{G(y)}{\omega}\right) + \chi^{\mathcal{N}} \left(R^{\mathcal{C}}(z) - R^{\mathcal{N}}(z)\right)\end{aligned}$$

which implies

$$\lim_{\omega \to +\infty} (\chi^{\mathcal{C}} R^{\mathcal{C}}(t) - \chi^{\mathcal{N}} R^{\mathcal{N}}(t)) > 0.$$

And so the proposition follows.

Proof of Proposition 14

Following the proof of Proposition 13 the condition

$$\int_0^T \chi^{\mathcal{N}} R^{\mathcal{N}}(t) dt < \int_0^{\mathcal{E}} \chi^{\mathcal{N}} R^{\mathcal{C}}(t) dt + \int_{\mathcal{E}}^T \chi^{\mathcal{C}} R^{\mathcal{C}} dt$$

is satisfied whenever

$$\mathcal{E} \chi^{\mathcal{N}} \frac{\sigma_I^2}{8\kappa_I} \max_{t \in [0, \mathcal{E}]} \frac{F(t)}{\omega} < (T - \mathcal{E}) \left(\chi^{\mathcal{C}} - \chi^{\mathcal{N}}\right) R_0^{-\sigma T}.$$

This condition is indeed satisfied for ω higher than a certain threshold $\underline{\omega}'$.

References

1. Banerjee, D. (2003) Software Piracy: a Strategic Analysis and Policy Instruments, *International Journal of Industrial Organization*, **21**, 97-127.
2. Banerjee, D. (2013) Effect of Piracy on Innovation in the Presence of Network Externalities, *Economic Modelling*, **33**, 526-532.
3. Biancardi, M., Di Liddo A., Villani G. (2019), Fines Imposed on Counterfeiters and Pocketed by the Genuine Firm. A Differential Game Approach. *Dynamic Games and Applications*, https://doi.org/10.1007/s13235-019-00310-6.

4. Buratto, A., Grosset, L., Zaccour, G. (2016) Strategic Pricing and Advertising in the Presence of a Counterfeiter. *IMA Journal of Management Mathematics*, **27**, 3, 397-418.
5. Caputo, M.R (2005), *Foundations of Dynamic Economic Analysis*, Cambrige University Press, Cambridge.
6. Cellini, R. Lambertini, L. (2007), A differential oligopoly game with differentiated goods and sticky prices, *European Journal of Operational Research*, **176**, 1131-1144.
7. Chaudhry, P., Zimmerman, A. (2009) Protecting Intellectual Property Rights: The Special Case of China. *Journal of Asia-Pacific Business,* **10**, 308–325.
8. Cordell, V., Wongtada, N., Kieschnick, R. (1996) Counterfeit Purchase Intentions: Role of Lawfulness Attitudes and Product Traits as Determinants. *Journal of Business Research*, **35**, 41–53.
9. Cox, J. and A. Collins (2014), Sailing in the Same Ship? Differences in Factors Motivatings Piracy of Music and Movie Content, *Journal of Behavioral and Experimental Economics*, 50, 70-76.
10. Crettez B., Hayek N. and G. Zaccour (2018), Brand Imitation: A Dynamic-Game Approach (2018), *International Journal of Production Economics*, 205, 139-155.
11. Di Liddo A. (2017) Counterfeiting Models (Mathematical/Economic). In: Marciano A., Ramello G. (eds) *Encyclopedia of Law and Economics*. Springer, New York, NY
12. Di Liddo, A. (2018), Does Counterfeiting Benefit Genuine Manufacturer?. The Role of Production Cost. *European Journal of Law and Economics*, *45*, 1, 81-125.
13. Eisend, M., & Schuchert-Guler, P. (2006). Exploring Counterfeit Purchases: A Review and Preview. *Academy of Marketing Science Review*, 2006(12), 1-22.
14. Grossman, G.M., Shapiro, C. (1988a) Counterfeit-Product Trade. *American Economic Review*, **78**, 1, 59-75.
15. Grossman, G.M., Shapiro, C., (1988b). Foreign Counterfeiting of Status Goods. *Quarterly Journal of Economics*, **103,** 1, 79-100.
16. El Harbi, S. and G. Grolleau (2008) Profiting from Being Pirated by 'Pirating' the Pirates, *Kyklos*, **61**, 385-390.
17. Givon, M., Mahajan V. and E. Muller (1995) Estimation of Lost Sales and the Impact on Software Diffusion, *Journal of Marketing*, 59, 1, 29-37.
18. Haurie, A., Krawczyk, J.B., Zaccour, G. (2012) *Games and Dynamic Games*, Scientific World, Singapore.
19. Huang, J., Lemg, M., Liang, L. (2012) Recent Developments in Dynamic Advertising Research. *European Journal of Operational Research*, **220**, 591–609.
20. Huang, J., Leng M. and M. Parlar (2013) Demand Functions in Decision Modeling: A Comprehensive Survey and Research Directions, *Decisions Sciences*, **44**, 557–609.
21. Kapferer, J.N., and A. Michaut (2014), Luxury Counterfeit Purchasing: The Collateral Effect of Luxury Trading Down Policy, *Journal of Brand Strategy*, **3**, 1, 59-70.
22. Lai, F.T. and S.C. Chang (2012), Consumers' choices, infringements and market competition, *European Journal of Law and Economics*, **34**, 77-103.
23. Jørgensen, S., & G. Zaccour (2004) *Differential Games in Marketing*, Boston: Kluwer Academic Publishers.
24. Levin, E. K. (2009). A Safe Harbor for Trademark: Reevaluating Secondary Trademark Liability after Tiffany v. eBay. *Berkeley Technology Law Journal*, **24**, (1), 491-527.
25. Orscheln C. J. (2015), Bad News Birkins: Counterfeit in Luxury Brands (2015), *The John Marshall Review Of Intellectual Property Law*, 250-266.
26. Martin, S. (2009), Microfundations for the Linear Demand Product Differentiation Model, with Applications, Paper No. 1221, Institute for Research in the Behavioral Sciences, and Management Sciences, Purdue University.
27. Peres, R., Muller E. and V. Mahajan (2010), Innovation Diffusion and New Product Growth Models: A Critical Review and Research Directions, *International Journal of Research in Marketing*, 27, 91-106.
28. Qian, Y. (2014) Brand Management and Strategies Against Counterfeits. *Journal of Economics and Management Strategy,* **23**, 2, 317–343.

29. Qian, Y. Gong, Q. and Y. Chen (2014) Untangling Searchable and Experiential Quality Responses to Counterfeits, *Marketing Science*, **34**, 4 , 522-538.
30. Riso J. (2015), Friend Or Faux: The Trademark Counterfeiting Act's Inability To Stop The Sale Of Counterfeit Sporting Goods, Wake Forest *Journal Of Business And Intellectual Property Law*, **12**, 2, 234-260
31. Singh, N., Vives, X. (1984) Price and Quantity Competition in a Differentiated Duopoly. *Rand Journal of Economics*, **15**, 4, 546-554.
32. Shultz II, C.J., Saporito, B. (1996) Protecting Intellectual Property: Strategies and Recommendations to Deter Counterfeiting and Brand Piracy in Global Markets. *The Columbia Journal of World Business*, **31**, 18–28.
33. Stöttinger B., Penz, E. (2015), Concurrent Ownership of Brands and Counterfeits: Conceptualization and Temporal Transformation from a Consumer Perspective, *Psychology & Marketing*, **32**, 4, 373-391.
34. Suzuki, K. (2015), Legal Enforcement Agains Illegal Imitation in Developing Countries, *Journal of Economics*, **116**, 247-270.
35. Yao, T. (2005), How a Luxury Monopolist Migh Benefit from a Stringent Counterfeit Monitoring, *International Journal of Business and Economics*, **4**, 3, 177-192.
36. Yao, J.T (2015) The Impact of Counterfeit-purchase Penalties on Anti-Counterfeiting Under Deceptive Counterfeiting, *Journal of Economics and Business*, **80**, 51-61.
37. Zhang, J., Hong, J. and R. Q. Zhang (2012), Fighting Strategies in a Market with Counterfeits, *Annals of Operations Research*, **192**, 49-66.

Games where Players have Common Interests

Equilibrium Coalition Structures of Differential Games in Partition Function Form

Simon Hoof

1 Introduction

In numerous real-life situations, coalition formation takes place. Among others, we can think of the following applications: climate agreements, military alliances, cartels, resource extraction, or research collaborations. Without an enforcement technology, however, coalitional agreements are fragile for a number of reasons. For example, unilaterally deviating from a climate agreement might be beneficial (at least in the short run) if one can freeride on the effort of the other countries. A new government might want to renegotiate terms of partnership with other countries. Cartels are usually not legally allowed and thus very fragile. Finally, a country may consume more of a common resource than agreed upon beforehand.

Coalition formation games thus intersect cooperative and noncooperative game theory. On the one hand the coalition members act cooperatively within the coalition, but on the other they act noncooperatively across coalitions. Further, in games with externalities the worth of a coalition depends not only on the actions taken by the members within a given coalition, but also on the actions taken by all left out players as well as on the coalition structure of these players. These kind of games can be described in *partition function form* which were introduced by Thrall and Lucas in 1963 [12].[1] A partition function assigns a characteristic function to all coalition structures, viz., partitions of the set of players. For a given coalition structure, the characteristic function assigns a worth to a coalition of players. We follow an equilibrium approach to construct the partition function [15]. For a given coalition structure

[1] See Kóczy [8] for a recent textbook treatment.

S. Hoof (✉)
Department of Economics and SFB901, Paderborn University, Paderborn, Germany
e-mail: simon.hoof@upb.de

D. M. Ramsey and J. Renault (eds.), *Advances in Dynamic Games*,
Annals of the International Society of Dynamic Games 17,
https://doi.org/10.1007/978-3-030-56534-3_12

the coalitions play a fully noncooperative game and each coalition basically acts as a single agent. The worth of a coalition is then the equilibrium payoff.

While there exists a rich literature on endogenous coalition formation for static games,[2] it is rather unexplored in the theory of dynamic games. A shortcoming in the literature on coalition formation in differential games is that exogenous restrictions are imposed on the set of feasible coalition structures.[3] In Petrosjan and Zaccour [10] and Zaccour [14], for example, the authors fix a γ coalition structure such that there exist one coalition and all left out players are singletons. A notable exception is the recent work of Parilina and Sedakov [9], who use the same method as presented here to construct the partition function for a *difference* game of cartel formation but under open-loop strategies, while we study state-feedback strategies.

Recently, Hoof [7] introduced differential games in partition function form on the restricted domain of linear-state games. In the present paper, we generalize the previous one by showing how to construct a partition function for any autonomous infinite horizon game. Since the resulting cooperative game is cohesive by construction (grand coalition is efficient), Hoof [7] studied the stability of the grand coalition over time by means of the core. When defining the core for a partition function form game, however, one has to impose ad hoc assumptions on the coalition structure of the residual players. Here we fully endogenize the formation of coalitions by relying on Bloch's [2] coalition formation game. A coalition structure is then called stable if it results from the equilibrium of an alternating offer bargaining game. We apply the method to a well-studied model of dynamic cake eating [5]. After obtaining the partition function in closed form we show how to solve for the equilibrium coalition structure. Given that the agents are identical the equilibrium coalition structure is equivalent to the solution of a finite dynamic programming problem in which the number of stages equals the number of agents. Finally, we compute the equilibrium coalition structures for up to 800′000′000 agents via MATLAB. It turns out that the stability of the grand coalition decreases in the number of agents.

2 General Approach

2.1 Differential Games

An autonomous infinite horizon noncooperative differential game $\Gamma(x)$ consists of the following ingredients (with $\mu = (\mu_i)_{i\in N}$):

- Agents $N = \{1, 2, \ldots, n\}$
- State space $X \subseteq \mathbb{R}$
- Action space $U_i \subseteq \mathbb{R}$ for each $i \in N$
- Strategy space $\mathscr{U}_i = \{\mu_i : X \to U_i \mid \mu_i(x)$ Lipschitz continuous in $x\}$

[2] See the Handbook article of Ray and Vohra [11].

[3] See the surveys of Calvo and Rubio [3] and de Zeeuw [6].

- Payoff functional $J_i(x, \mu) = \int_t^\infty e^{-r(s-t)} F_i(x(s), \mu(x(s)))ds$
- State equation $\dot{x}(s) = f(x(s), \mu(x(s)))$

At every point in time $t \in [0, \infty)$ each agent i chooses an action $u_i(t) \in U_i$ according to a feedback strategy $\mu_i : X \to U_i$ such that $u_i(t) = \mu_i(x(t))$. An agent derives instantaneous payoffs according to a function $F_i : X \times U \to \mathbb{R}$, where $U = \bigtimes_{i \in N} U_i$ denotes the joint action space. The functions $\{F_i(x, u)\}_{i \in N}$ are assumed to be continuously differentiable in x and $u = (u_i)_{i \in N}$. The objective functional $J_i(x, \mu)$ of each agent is the discounted stream of payoffs over $s \in [t, \infty)$, where $r > 0$ denotes the common time preference rate and $\mu \in \bigtimes_{i \in N} \mathscr{U}_i$ a strategy profile. Since we consider autonomous infinite horizon games, the payoff functional does not depend on the current time t, but only on the current state $x(t) = x$ [4, Theorem 19.2]. The state evolves over time according to a stationary differential equation $f : X \times U \to \mathbb{R}$ with initial condition $x(0) = x_0 \in X$. The evolution of the state over $s \in [t, \infty)$ is then described by the following dynamic system:

$$\begin{cases} \dot{x}(s) := \dfrac{dx(s)}{ds} = f(x(s), \mu(x(s))) \quad (s \geq t), \\ x(t) = x \in X. \end{cases} \tag{1}$$

We assume that the function $f(x, u)$ is continuously differentiable in x and u. The assumptions on the state equation $f(\cdot, \cdot)$ and strategy spaces $\{\mathscr{U}_i\}_{i \in N}$ imply that the solution $x(s)$ of the differential equation (1) exists and is unique as well as continuous [1, Theorem 5.1]. We further assume that a profile of admissible strategies μ jointly generates a state trajectory $x(s)$ that stays in the state space X and that payoffs are finite. Therefore consider the parametrized solution of (1)

$$y(s; t, x, \mu) = x + \int_t^s f(x(k), \mu(x(k)))dk.$$

Now we define a set $\mathscr{U} \subset \bigtimes_{i \in N} \mathscr{U}_i$ of jointly admissible strategies by

$$\mathscr{U} = \Big\{ \mu \in \bigtimes_{i \in N} \mathscr{U}_i \mid \forall (t, x) \in [0, \infty) \times X : y(s; t, x, \mu) \in X \ \forall s \geq t, \\ \forall x \in X : \max_{i \in N} \{|J_i(x, \mu)|\} < \infty \Big\}.$$

2.2 Partition Function

A subset of agents $S \subseteq N$ is called a coalition with $S = N$ being the grand coalition. Let Π denote the set of all partitions of N. A coalition structure $\pi \in \Pi$ splits N into nonempty and disjoint subsets (the coalitions) such that $S \cap C = \emptyset$ for all different coalitions $S, C \in \pi$ and $\bigcup_{S \in \pi} S = N$ for all coalition structures $\pi \in \Pi$. Denote the set of embedded coalitions by

$$\mathscr{E} = \left\{ (S, \pi) \in 2^N \times \Pi \;\middle|\; \emptyset \neq S \in \pi \right\}.$$

A cooperative differential game in partition function form is a pair $\langle N, V \rangle$ with $V : X \times \mathscr{E} \to \mathbb{R}$ being the partition function. The partition function $V(x, S, \pi)$ is the worth of coalition $S \in \pi$ in state $x \in X$. In the present paper we use an equilibrium approach to construct $V(\cdot, \cdot, \cdot)$. The primitive is a differential game $\Gamma(x) = \langle N, (\mathscr{U}_i)_{i \in N}, (J_i(x, \cdot))_{i \in N} \rangle$ with all agents being singletons. For a given coalition structure $\pi \in \Pi$ we assume that the agents $i \in S$ act cooperatively within, but noncooperatively across coalitions $S \in \pi$. Since a coalition acts as a single player, the action and strategy space of coalition S becomes $U_S = \bigtimes_{i \in S} U_i$ and $\mathscr{U}_S = \bigtimes_{i \in S} \mathscr{U}_i$, respectively. The coalitional payoff $J_S(x, \mu)$ is simply defined as the sum of individual payoffs

$$J_S(x, \mu) = \sum_{i \in S} J_i(x, \mu).$$

A noncooperative differential game in coalition form $\Gamma_\pi(x)$ is then described by a triplet $\langle \pi, (\mathscr{U}_S)_{S \in \pi}, (J_S(x, \cdot))_{S \in \pi} \rangle$ in which π is the set of players, $\mathscr{U}_S$ the strategy space of player $S \in \pi$ and $J_S(x, \mu)$ the payoff of $S \in \pi$. The definition of a Nash equilibrium for a game played between coalitions is straightforward. Let $\mu_S = (\mu_i)_{i \in S}$ denote the strategy profile of coalition S and $\mu_{-S} = (\mu_C)_{C \in \pi \setminus \{S\}}$ the strategy profiles of all coalitions but S.

Definition 1 The n-tuple $\overline{\mu} \in \mathscr{U}$ is a state-feedback Nash equilibrium of the game $\Gamma_\pi(x)$ if for all coalitions $S \in \pi$ and states $x \in X$ the following inequalities hold:

$$J_S(x, \overline{\mu}) \geq J_S(x, \mu_S, \overline{\mu}_{-S}) \quad \forall \mu_S \in \mathscr{U}_S.$$

One should note that the coalition structure π is fixed and it is thus an ordinary Nash equilibrium and not a *strong* one. Since the instantaneous payoff functions $\{F_i(x, u)\}_{i \in N}$ are assumed to be continuously differentiable in (x, u) the joint payoff of coalition S given by

$$F_S(x, u) = \sum_{i \in S} F_i(x, u)$$

is also continuously differentiable in (x, u). This fact follows simply by the sum rule; the sum of partial derivatives is equal to the partial derivative of the sum. Then we can apply the standard theorem for the characterization of an equilibrium by means of the solution of a system of coupled differential equation. The following theorem is fundamental.

Theorem 1 (*[13, cf. Theorem 1]*) *For a given partition $\pi \in \Pi$ of N, the n-tuple $\overline{\mu} \in \mathscr{U}$ is a Nash equilibrium of the game $\Gamma_\pi(x)$ if there exist $|\pi|$ functions $\{v_S : X \to \mathbb{R}\}_{S \in \pi}$ that are continuously differentiable in x and solve the following system of coupled Hamilton-Jacobi-Bellman (HJB) equations:*

$$rv_S(x) = \max_{u_S \in U_S} \left\{ F_S(x, u_S, \overline{\mu}_{-S}(x)) + v'_S(x) f(x, u_S, \overline{\mu}_{-S}(x)) \right\}$$
$$= F_S(x, \overline{\mu}(x)) + v'_S(x) f(x, \overline{\mu}(x)).$$

Further, the transversality condition $\lim_{t\to\infty} e^{-rt} v_S(x)$ *must be satisfied for all coalitions* $S \in \pi$ *and all feasible states* $x \in X$.

For a given coalition structure $\pi \in \Pi$ we can think of $v_S(x) = J_S(x, \overline{\mu})$ being a characteristic function that assigns to each coalition a worth. And the partition function then assigns to each partition a characteristic function.

Definition 2 The partition function $V : X \times \mathscr{E} \to \mathbb{R}$ assigns to each coalition $S \in \pi$ the noncooperative equilibrium payoff

$$V(x, S, \pi) = J_S(x, \overline{\mu}) \quad (S \in \pi).$$

2.3 Equilibrium Coalition Structure

Our stability concept rests on Bloch's [2] sequential game of coalition formation. The equilibrium of the game determines the coalition structure. Let $p : N \to N$ denote a permutation of N, called the rule of order. Next we quote Bloch [2, p. 95] on the rules of the game (my notation):

> The first player according to the rule of order p starts the game by proposing the formation of a coalition S to which she belongs. Each prospective member responds to the proposal in the order determined by p. If one of the player rejects the proposal, she must make a counteroffer and propose a coalition S' to which she belongs. If all members accept, the coalition is formed. All members of S then withdraw from the game, and the first player in $N \setminus S$ starts making a proposal.

The coalition structure that results from the stationary equilibrium of the alternating offer game is called an *equilibrium coalition structure*. If the agents are identical, then the game exhibits two useful properties. The equilibrium coalition structure is the same for all rules of order up to a permutation of the agent's index $i \mapsto p(i)$ [2, pp. 107 – 108]. And the stationary equilibrium of the alternating offer bargaining game is equivalent to the equilibrium of an extensive form game of choice of coalition size [2, Prop. 4.2].

Assumption 1 The agents are identical.

Assumption 2 The rule of order is from 1 to n.

Under Assumptions 1 and 2 we can identify equilibrium coalition structures from the equilibrium of an extensive form game

$$\Lambda(x) = \langle N, (\Sigma_i)_{i\in N}, (g_i(x, \cdot))_{i\in N}, (H_i)_{i\in N\setminus\{1\}} \rangle.$$

Here $\Sigma_i \subset \mathbb{N} = \{0, 1, 2, \ldots\}$ is the action space, $\Sigma = \bigtimes_{i \in N} \Sigma_i$ the joint action space, $g_i : X \times \Sigma \to \mathbb{R}$ the payoff function and $H_i \subset \bigtimes_{j=1}^{j=i-1} \Sigma_j$ the set of histories. The rules are as follows:

- Starting with player 1, each player $i \in N$ chooses a number $\sigma_i \in \mathbb{N}$ of subsequent players to form a coalition with. As a result, a player has no choice if she was already integrated into a coalition by a previous player.
- Each player has to choose at least 1 player if still available.
- Each player moves exactly once.
- The game is with perfect information.

Given the rules of the game we can define the action space Σ_i. For the first agent we simply fix $\Sigma_1 = N$. For all $i \in \{2, \ldots, n\}$ let $h_i = (\sigma_1, \ldots, \sigma_{i-1})$ denote a history up to stage $i \in \{2, \ldots, n\}$. Define the history dependent action space for all $i \in \{2, \ldots, n\}$ by

$$\Sigma_i(h_i) = \begin{cases} \{1, \ldots, n - (i-1)\} & \text{if } \sum_{j=1}^{i-1} \sigma_j < i, \\ \{0\} & \text{else.} \end{cases}$$

The action profile $\sigma \in \Sigma$ then induces the coalition structure π via the function $\varpi : \Sigma \to \Pi$ with

$$\pi = \varpi(\sigma) = \bigcup_{i \in \{j \in N \mid \sigma_j > 0\}} \{\{i, \ldots, i - 1 + \sigma_i\}\}.$$

For the extensive form game we further need to define an individual payoff function $g_i(x, \sigma)$ that maps the actions into the reals. Since the underlying game that defines the worth of a coalition is a differential game, the individual payoff also depends on the current state x. Here we consider the payoff agent i can expect in coalition S under partition π. Due to the symmetric setup we fix an equal sharing rule of the coalition worth. The individual worth of $i \in S$ is then given by

$$g_i(x, \sigma) = \frac{V(x, S, \varpi(\sigma))}{|S|}.$$

We will define a state dependent stable coalition structure $\overline{\pi}(x) \in \Pi$ in terms of the subgame perfect Nash equilibrium (SPNE) $\overline{\sigma}(x)$ of the game $\Lambda(x)$.

Definition 3 The n-tuple $\overline{\sigma}(x) \in \Sigma$ is a SPNE of $\Lambda(x)$ if for all agents $i \in N$, states $x \in X$ and histories $(h_i)_{i=2}^n \in \bigtimes_{i=2}^n H_i$ it holds that:

$$g_i(x, \overline{\sigma}(x)) \geq g_i(x, \sigma_i, \overline{\sigma}_{-i}(x)) \quad \forall \sigma_i \in \Sigma_i(h_i),$$

where $\overline{\sigma}_{-i}(x) = (\overline{\sigma}_j(x))_{j \in N \setminus \{i\}}$ are the equilibrium actions of the opponents.

Lemma 1 *Since $\Lambda(x)$ is a finite extensive form game with perfect information, there always exists a SPNE for any state $x \in X$.*

Definition 4 The coalition structure $\overline{\pi}(x) = \varpi(\overline{\sigma}(x))$ is stable at $x \in X$.

Note that, generally, the equilibrium coalition structure is state dependent. This may lead to a time inconsistent equilibrium coalition structure in the sense that replaying $\Lambda(x_0)$ at some time $t > 0$ may yield a different equilibrium coalition structure $\overline{\pi}(x_0) \neq \overline{\pi}(x)$ for different states $x_0 \neq x$.

Definition 5 The initial equilibrium structure $\overline{\pi}(x_0)$ is *strongly time consistent* if it does not change with respect to the game position, i.e., $\overline{\pi}(x_0) = \overline{\pi}(x)$ for all $x \in X$.

Next we turn to the classic cake eating application and show how to compute the partition function as well as the equilibrium coalition structure for an arbitrary number of agents $n \in \mathbb{N} \setminus \{0\}$.

3 Cake Eating

Consider n identical agents. The agents eat a cake over the time interval $t \in [0, \infty)$. We denote the size of the cake at time instant $s \in [t, \infty)$ by $x(s) \in X$, with $X = (0, x_0]$ being the state space and $x_0 > 0$ the initial size of the cake. For technical reasons we assume that the agents never eat the entire cake, and thus $x(t) > 0$ for all $t \geq 0$. The consumption rate of any agent $i \in N$ is denoted by $u_i(s) \in U_i = \mathbb{R}_+$. The size of the cake evolves over time according to the following dynamic system:

$$\begin{cases} \dot{x}(s) = -\sum_{i \in N} u_i(t) \quad (s \geq t), \\ x(t) = x \in X. \end{cases} \tag{2}$$

We assume that each agent i derives instantaneous log payoffs from consumption $F_i(u_i) = \ln(u_i)$. If the agents eat the entire cake such that there exists a time instant $\bar{t} = \inf\{t > 0 \mid x(t) = 0\}$, then there is nothing left to consume, which implies $u_i(t) = 0$ for all $t \geq \bar{t}$ and $i \in N$. Since $F_i(0)$ is undefined, we make the assumption $x(t) > 0$ for all $t \geq 0$.

Proposition 1 *For $\pi \in \Pi$ there exists a Nash equilibrium for the cake eating game characterized by the following strategies $\overline{\mu}(x)$ and $|\pi|$ value functions $\{v_S(x)\}_{S \in \pi}$:*

$$\overline{\mu}_i(x) = \frac{r}{|S|} x \quad (i \in S)$$
$$v_S(x) = \frac{|S|}{r} \left(\ln(rx) - \ln(|S|) - |\pi|\right).$$

Proof Consider the maximizers of the right-hand side of the HJB equation

$$\left(\frac{1}{v_S'(x)},\ldots,\frac{1}{v_S'(x)}\right) = \arg\max_{u_S\in U_S}\left\{\sum_{i\in S}\ln(u_i) - v_S'(x)\left(\sum_{i\in S}u_i + \sum_{C\in\pi\setminus\{S\}}\sum_{j\in C}\overline{\mu}_j(x)\right)\right\}.$$

The maximized HJB equation then reads

$$rv_S(x) = -|S|\ln\left(v_S'(x)\right) - |S| - v_S'(x)\sum_{C\in\pi\setminus\{S\}}\frac{|C|}{v_C'(x)}.$$

We guess the functional form of the value function $v_S(x) = \alpha_S\ln(x) + \beta_S$, where $\alpha_S, \beta_S \in \mathbb{R}$ denote some constants to be determined. The maximized HJB equation then becomes

$$r_S\left(\alpha_S\ln(x) + \beta_S\right) = -|S|\ln\left(\frac{\alpha_S}{x}\right) - |S| - \frac{\alpha_S}{x}\sum_{C\in\pi\setminus\{S\}}\frac{|C|x}{\alpha_C}.$$

This equation needs to hold for all $x \in X$. We thus collect the terms containing x and rewrite the equation as follows:

$$\underbrace{\ln(x)\left(r\alpha_S - |S|\right)}_{=0} + \underbrace{r\beta_S + |S|(\ln(\alpha_S)+1) + \alpha_S\sum_{C\in\pi\setminus\{S\}}\frac{|C|}{\alpha_C}}_{=0} = 0.$$

The equation is true for all $x \in X$ if the constants satisfy

$$\alpha_S = \frac{|S|}{r} \quad\text{and}\quad \beta_S = -\frac{1}{r}\left[|S|(\ln(\alpha_S)+1) + \alpha_S\sum_{C\in\pi\setminus\{S\}}\frac{|C|}{\alpha_C}\right].$$

Substituting the coefficients $(\alpha_S)_{S\in\pi}$ yields for β_S

$$\begin{aligned}\beta_S &= -\frac{1}{r}\left[|S|\left(\ln\left(\frac{|S|}{r}\right)+1\right) + \frac{|S|}{r}\sum_{C\in\pi\setminus\{S\}}\frac{|C|r}{|C|}\right]\\ &= -\frac{|S|}{r}(\ln(|S|) - \ln(r) + |\pi|).\end{aligned}$$

Eventually, one derives the equilibrium strategies $\overline{\mu}_i(x)$ for $i \in S$ as well as value functions $v_S(x)$ for $S \in \pi$

$$\overline{\mu}_i(x) = \frac{1}{v_S'(x)} = \frac{1}{\frac{\alpha_S}{x}} = \frac{r}{|S|}x,$$
$$v_S(x) = \alpha_S \ln(x) + \beta_S = \frac{|S|}{r}\left(\ln(rx) - \ln(|S|) - |\pi|\right) = V(x, S, \pi).$$

□

Now we can also compute the state trajectory by solving (2)

$$\begin{cases} \dot{x}(s) = -\sum_{S\in\pi}\sum_{i\in S}\overline{\mu}_i(x(s)) = -\sum_{S\in\pi}\sum_{i\in S}\frac{r}{|S|}x(s) = -x(s)r|\pi| \quad (s \geq t) \\ x(t) = x \in X \end{cases}$$

for

$$x(s) = xe^{-(s-t)r|\pi|}.$$

It is noteworthy that the trajectory depends only on the number of coalitions $|\pi| \in N$, but not directly on the number of agents n. That is, we could end up in the odd situation that $n \to \infty$ agents consume less than $n = 2$ agents if the grand coalition forms $|\pi| = 1$ for the first case, but the two agents split $|\pi| = 2$ in the latter case.

Next we show how to derive the equilibrium coalition structure of the cake eating game. For any $i \in S$ the payoff is given by (with $\pi = \varpi(\sigma)$)

$$g_i(x, \sigma) = \frac{V(x, S, \varpi(\sigma))}{|S|} = \frac{1}{r}\left(\ln(rx) - \ln(|S|) - |\varpi(\sigma)|\right).$$

Now we need to distinguish two cases. If i has a turn, she determines the size of the coalition $\sigma_i = |S|$. If she has no turn, her payoff depends on the size player $\max\{j \in N \mid \sigma_j > 0,\ j < i\}$ has chosen.

$$g_i(x, \sigma) = \frac{1}{r}\begin{cases} \left(\ln(rx) - \ln(\sigma_i) - |\varpi(\sigma)|\right) & \text{if } \sum_{j=1}^{i-1}\sigma_j < i, \\ \left(\ln(rx) - \ln(\sigma_{\max\{j\in N|\sigma_j>0,\ j<i\}}) - |\varpi(\sigma)|\right) & \text{else.} \end{cases}$$

Proposition 2 *The equilibrium coalition structure is strongly time consistent.*

Proof Generally, the equilibrium action is the payoff maximizer

$$\overline{\sigma}_i(x) \in \arg\max_{\sigma_i\in\Sigma_i(h_i)} g_i(x, \sigma_i, \overline{\sigma}_{-i}(x)).$$

For all agents $i \in N$, however, there is no interaction between the state x and the action σ_i

$$\frac{\partial^2 g_i(x,\sigma)}{\partial x \partial \sigma_i} = 0 \quad \forall i \in N.$$

The equilibrium action is thus state redundant, i.e., $\overline{\sigma} = \overline{\sigma}(x)$ for all $x \in X$, and so is the equilibrium coalition structure $\overline{\pi} = \varpi(\overline{\sigma}) = \varpi(\overline{\sigma}(x)) = \overline{\pi}(x)$ for all $x \in X$. □

We will thus drop x as an argument of $\overline{\sigma}(x)$ and $\Lambda(x)$ and simply write $\overline{\sigma}$ for the equilibrium profile of the game Λ. Before turning to the application again, we briefly discuss why the order of coalition choice does not change the stable coalition structure up to a permutation of the agent's indice i. Denote by $p : N \to N$ an arbitrary permutation of the agents and by P the set of all permutations. In the game of choice of coalition size, the order of choice is then from $p(1)$ to $p(n)$. Due to symmetry, the identity of agents within a coalition is not important for stability; only the size of a coalition is important. If $\overline{p\sigma}$ denotes the equilibrium profile under the rule of order p, then $\overline{\sigma} = \overline{p\sigma}$ for all $p \in P$.

Example 1 To get an idea of the previously introduced concepts let us first consider the three-player case with $N = \{1, 2, 3\}$. Then we need to distinguish four strategy profiles and associated partitions

$$\begin{aligned}
\sigma^1 &= (3, 0, 0) \mapsto \varpi(\sigma^1) = \{\{1, 2, 3\}\} \\
\sigma^2 &= (2, 0, 1) \mapsto \varpi(\sigma^2) = \{\{1, 2\}, \{3\}\} \\
\sigma^3 &= (1, 2, 0) \mapsto \varpi(\sigma^3) = \{\{1\}, \{2, 3\}\} \\
\sigma^4 &= (1, 1, 1) \mapsto \varpi(\sigma^4) = \{\{1\}, \{2\}, \{3\}\}.
\end{aligned}$$

Now we consider Bloch's game. Beginning with agent $i = 3$ we solve the game backwards and maximize payoffs. Agent 3 only has a turn if the history is $h_3 \in \{(1, 1), (2, 0)\}$ and the strategy set is a singleton $\Sigma_3(h_3) = \{1\}$, since she is last in the row:

$$1 = \arg\max_{\sigma_3 \in \{1\}} g_3(x, h_3, \sigma_3) = \arg\max_{\sigma_3 \in \{1\}} \left\{ \frac{1}{r} [\ln(rx) - \ln(\sigma_3) - 3] \right\}.$$

In this case the number of coalitions equals $|\varpi(1, 1, 1)| = 3$. Agent 2 only has a turn if the history is $h_2 = (1)$ and she has the option to become a single or to integrate the last agent $\Sigma_2(h_2) = \{1, 2\}$. In the decision problem of agent 1 and 2 we further need to employ an indicator function, because the number of coalitions changes with respect to the decision of an agent. For example, $\sigma_2 = 1$ yields $|\varpi(1, 1, 1)| = 3$ and $\sigma_2 = 2$ yields $|\varpi(1, 2, 0)| = 2$. Given agent 2 has a turn, it is optimal to integrate the last agent.

$$2 = \arg\max_{\sigma_2 \in \{1,2\}} g_2(x, h_2, \sigma_2, 1) = \arg\max_{\sigma_2 \in \{1,2\}} \left\{ \frac{1}{r} \left[\ln(rx) - \ln(\sigma_2) - \left(2 + \mathbf{1}_{\{1\}}(\sigma_2)\right) \right] \right\}.$$

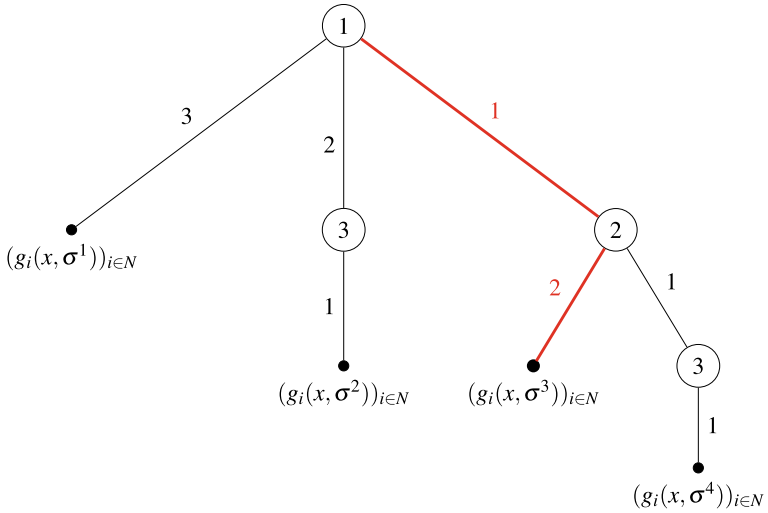

Fig. 1 Game Tree

Knowing the reaction of the followers, the first agent now chooses to become a singleton:

$$1 = \arg\max_{\sigma_1\in\{1,2,3\}} g_1(x,\sigma_1,2,1) = \arg\max_{\sigma_1\in\{1,2,3\}} \left\{\frac{1}{r}\left[\ln(rx) - \ln(\sigma_1) - \left(1 + \mathbf{1}_{\{1,2\}}(\sigma_1)\right)\right]\right\}.$$

The associated game tree with equilibrium path (bold red) is illustrated in Fig. 1. The equilibrium actions are thus given by $\overline{\sigma} = (1, 2, 0)$, resulting in the equilibrium structure $\overline{\pi} = \{\{1\}, \{2, 3\}\}$. The grand coalition is not stable, because each agent has an incentive to freeride on the remaining double coalition. The fully noncooperative coalition structure is not stable either, because here either two or all three agents have an incentive to form a coalition. Then we can readily deduce that $\overline{\pi} \in \{\pi \in \Pi \mid |\pi| = 2\}$ is stable, because no agent has an incentive to deviate. The single will not join the double coalition, because her payoff decreases and the double coalition will not split, because then three singles remain. It is noteworthy that we only consider myopic deviations. One may argue that the double coalition in $\overline{\pi}$ splits, because then the grand coalition is beneficial for all agents afterward. We abstract from this farsighted view, because one ends up cycling. Reconsidering the order independence, we should note that $(1, 2, 0)$ is the equilibrium profile for all choice orders $\{p(1), p(2), p(3)\}$.

Next we are going to characterize the equilibrium coalition structures for any number of agents $n \in \mathbb{N} \setminus \{0\}$. For an arbitrary history $h_i \in H_i$ let $\rho_{<i}(h_i)$ denote the number of coalitions already formed up to agent i. Further let

$$I(i \mid \overline{\sigma}_{i+1}, \ldots, \overline{\sigma}_n) = 1 + I(i + \sigma_i \mid \overline{\sigma}_{i+\sigma_i+1}, \ldots, \overline{\sigma}_n)$$

denote the number of coalitions that follow agent i after she has chosen her action σ_i, conditioned on the equilibrium actions of the agents that follow her $(\overline{\sigma}_{i+1}, \ldots, \overline{\sigma}_n)$. On every stage $i \in N$ the total number of coalitions is then defined recursively by

$$|\varpi(h_i, \sigma_i, \overline{\sigma}_{i+1}, \ldots, \overline{\sigma}_n)| = \rho_{<i}(h_i) + 1 + I(i + \sigma_i \mid \overline{\sigma}_{i+\sigma_i+1}, \ldots, \overline{\sigma}_n),$$

and agent $i \in N$ thus solves on stage $i \in N$

$$\begin{aligned}
&\arg\max_{\sigma_i \in \Sigma_i} g_i(x, h_i, \sigma_i, \overline{\sigma}_{i+1}, \ldots, \overline{\sigma}_n) \\
=&\arg\max_{\sigma_i \in \Sigma_i} \left\{ \frac{1}{r} \left[\ln(rx) - \ln(\sigma_i) - \rho_{<i}(h_i) - 1 - I(i + \sigma_i \mid \overline{\sigma}_{i+\sigma_i+1}, \ldots, \overline{\sigma}_n) \right] \right\} \\
=&\arg\max_{\sigma_i \in \Sigma_i} \left\{ -\ln(\sigma_i) - I(i + \sigma_i \mid \overline{\sigma}_{i+\sigma_i+1}, \ldots, \overline{\sigma}_n) \right\} \\
=&\overline{\sigma}_i(\overline{\sigma}_{i+1}, \ldots, \overline{\sigma}_n).
\end{aligned}$$

With the terminal condition $I(n + 1) = 0$, the problem of finding a stable coalition structure reduces to solve a simple recursive program. In Algorithm 1 one finds the pseudocode to compute the equilibrium actions $\overline{\sigma}$ of the game Λ for an arbitrary n. The equilibrium coalition structure is then simply $\overline{\pi} = \varpi(\overline{\sigma})$.

Algorithm 1 Equilibrium profile $\overline{\sigma}$ of Λ

Require: $n \in \mathbb{N}, I = (0, \ldots, 0)_{(n+1)\times 1}, \sigma = (0, \ldots, 0)_{n\times 1}, N = \{1, 2, \ldots, n\}$
  for $i = n$ to 1 **do**
    $\Sigma_i = \{1, \ldots, n - (i - 1)\}$
    $g_i(\sigma_i) = -\ln(\sigma_i) - I(i + \sigma_i)$
    $\overline{\sigma}_i = \arg\max_{\sigma_i \in \Sigma_i} g_i(\sigma_i)$
    {*comment:* if $\overline{\sigma}_i > 1$, then $(\overline{\sigma}_{i+1}, \ldots, \overline{\sigma}_{i+\overline{\sigma}_i-1}) = (0, \ldots, 0)$}
    $q = 0$;
    for $k = i$ to n **do**
      if $q = 0$ **then**
        $q = \overline{\sigma}_k - 1$
      else
        $\overline{\sigma}_k = 0$
        $q = q - 1$
      end if
    end for
    $I(i) = 1 + I(i + \overline{\sigma}_i)$
  end for

4 Example

Since we are not able to solve for the equilibrium coalition structure in closed form, we solve the problem via MATLAB. Without memory constraints, one could compute the stable coalition structure for an arbitrary n. Here we are able to compute the stable coalition structures for up to 800′000′000 agents. Table 1 contains the translation of the pseudocode into runnable MATLAB code. Outputs are the equilibrium actions $\overline{\sigma} \in \mathbb{N}^n$ as well as the significantly shorter vector of positive equilibrium actions $\overline{\sigma}_{>0} = (\overline{\sigma}_i : \overline{\sigma}_i > 0,\ i \in N) \in \mathbb{N}^{\dim(\overline{\sigma}_{>0})}$.

Next we want to understand the formation of equilibrium coalition structures. Therefore, consider first the number of agents (n's) such that $\overline{\sigma}_{>0} = (n)$ and the grand coalition is an equilibrium $\overline{\pi} = \{N\}$.

Proposition 3 *Define the set A as follows:*

$$\begin{aligned} A = \{&1, 2, 4, 7, 13, 24, 44, 79, 146, 268, 482, 873, 1'580, 2'867, 5'191, \\ &9'413, 17'057, 30'917, 56'029, 101'550, 184'049, 333'573, 604'568, \\ &1'095'720, 1'985'887, 3'599'229, 6'523'256, 11'822'773, 21'427'636, \\ &38'835'525, 70'385'646, 127'567'200, 231'203'255, 419'033'616, \\ &759'458'042\}. \end{aligned}$$

For $n \in A$ the grand coalition is stable, i.e., $\overline{\sigma}_{>0} = (n)$.

Proof Compute $\overline{\sigma}_{>0}$ for all $n \in A$ via the program in Table 1. □

Reconsidering the state trajectory

$$x(t) = x_0 e^{-rt|\pi|}$$

it is striking to note that $n = 3$ agents faster exploit the cake than, say, $n = 759'458'042$, because in the first case two coalitions form while in the latter only one.

Denote an element of A by a_k with $k \in \{1, \ldots, 35\}$. When plotting a_{k+1}/a_k for $k \in \{1, \ldots, 34\}$ one finds that the growth rate approaches 1.812403619 (cf. Fig. 2). Hence the series becomes very sparse and the probability that the grand coalition forms decreases monotonously in n. Put differently, the more agents, the less likely the grand coalition is stable.

We should further note that the elements of A form a complete sequence: i.e., any element of A larger than 4 can be expressed as a sum of values in the sequence, using each value at most once.

Table 1 MATLAB computation of positive equilibrium profile $\overline{\sigma}_{>0}$

```
% housekeeping
clear all; clc;

% initialization
n = 800000000;      % number of agents
I = zeros(n+1,1);   % storage index
s = zeros(n,1);     % storage final actions
N = 1:n;            % set of agents

% backward induction loop
for i=fliplr(N)
    S = 1:n-i+1;            % action set
    g = -log(S)'-I(i+S);    % payoffs
    [g,j] = max(g);         % max payoff
    s(i) = S(j);            % argmax payoff

    % construction of vector with equilibrium actions
    q = 0;
    for k=i:n
        if q == 0
            q = s(k) - 1;
        else
            s(k) = 0;
            q = q - 1;
        end
    end
    I(i) = 1 + I(i+s(i)); % recursion
end

% collection of positive equilibrium actions
s_pos = s(s>0)
```

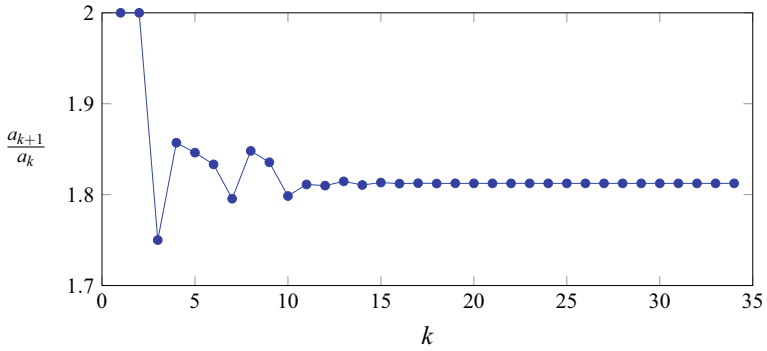

Fig. 2 Growth rate a_{k+1}/a_k

Table 2 Positive equilibrium actions $\overline{\sigma}_{>0} = q(n)$ for $n \in \{1, \ldots, 50\}$

n	$q(n)$	n	$q(n)$	n	$q(n)$	n	$q(n)$	n	$q(n)$
1	(1)	11	(4,7)	21	(1,7,13)	31	(7,24)	41	(4,13,24)
2	(2)	12	(1,4,7)	22	(2,7,13)	32	(1,7,24)	42	(1,4,13,24)
3	(1,2)	13	(13)	23	(1,2,7,13)	33	(2,7,24)	43	(2,4,13,24)
4	(4)	14	(1,13)	24	(24)	34	(1,2,7,24)	44	(44)
5	(1,4)	15	(2,13)	25	(1,24)	35	(4,7,24)	45	(1,44)
6	(2,4)	16	(1,2,13)	26	(2,24)	36	(1,4,7,24)	46	(2,44)
7	(7)	17	(4,13)	27	(1,2,24)	37	(13,24)	47	(1,2,44)
8	(1,7)	18	(1,4,13)	28	(4,24)	38	(1,13,24)	48	(4,44)
9	(2,7)	19	(2,4,13)	29	(1,4,24)	39	(2,13,24)	49	(1,4,44)
10	(1,2,7)	20	(7,13)	30	(2,4,24)	40	(1,2,13,24)	50	(2,4,44)

$$
\begin{aligned}
7 &= 1 + 2 + 4 \\
13 &= 2 + 4 + 7 \\
24 &= 4 + 7 + 13 \\
44 &= 7 + 13 + 24 \\
79 &= 4 + 7 + 24 + 44 \\
&\vdots
\end{aligned}
$$

One may conjecture that any equilibrium coalition structure can be constructed by elements of A. In Table 2 we list the positive equilibrium actions $\overline{\sigma}_{>0} = q(n)$ for $n \in \{1, \ldots, 50\}$.

It turns out that for all $n \in \{1, \ldots, 50\}$ the positive equilibrium actions are a recursive concatenation of elements of A. For example, consider $n = 40$ and let $\overline{a}(n) = \max\{a \in A \mid a \leq n\}$. Then one computes $\overline{\sigma}_{>0}$ via

$$\begin{aligned}\overline{\sigma}_{>0} = q(40) =& (q(40 - \overline{a}(40)), \overline{a}(40)) \\ =& (q(16), 24) \\ =& (q(16 - \overline{a}(16)), \overline{a}(16), 24) \\ =& (q(3), 13, 24) \\ =& (q(3 - \overline{a}(3)), \overline{a}(3), 13, 24) \\ =& (q(1), 2, 13, 24) \\ =& (1, 2, 13, 24).\end{aligned}$$

This observation leads us to the following conjecture.

Conjecture 1 The positive equilibrium actions $\overline{\sigma}_{>0}$ for $n \in \{1, \ldots, 800'000'000\}$ are given by the following recursive concatenation:

$$\overline{\sigma}_{>0} = q(n) = \begin{cases} (q(n - \overline{a}(n)), \overline{a}(n)) & \text{if } n \notin A, \\ n & \text{else.} \end{cases}$$

5 Conclusion

We introduced differential games in partition function form and a notion of endogenous coalition formation for symmetric differential games. The method at hand is generally applicable for any game. In fact, identifying equilibrium coalition structures boils down to solve a finite dynamic programming problem in which the number of stages equals the number of agents. If the equilibrium actions are state dependent, then one may discretize (a subset of) the state space and thus solves the recursive problem on a restricted domain. Then the problem of time consistency may arise in the sense that an initially stable coalition structure becomes unstable over time. This topic remains for further study.

Acknowledgments I thank Florian Wagener and an anonymous referee for valuable comments. The paper was presented at the 18th ISDG Symposium. This work was partially supported by the German Research Foundation (DFG) within the Collaborative Research Center "On-The-Fly Computing" (SFB 901) under the project number 160364472-SFB901 and the German Academic Exchange Service (DAAD) under the "Kongressreisenprogramm".

References

1. Başar, T. and Olsder, G. J. (1999): *Dynamic Noncooperative Game Theory*, 2 edn, SIAM
2. Bloch, F. (1996): Sequential Formation of Coalitions in Games with Externalities and Fixed Payoff Division, *Games and Economic Behavior* **14**, 90–123
3. Calvo, E. and Rubio, S. J. (2013): Dynamic Models of International Environmental Agreements: A Differential Game Approach, *International Review of Environmental and Resource Economics* **6**(4), 289–339
4. Caputo, M. R. (2005): *Foundations of Dynamic Economic Analysis*, Cambridge University Press
5. Clemhout, S. and Wan, H. Y. (1989): On Games of Cake-Eating. In: van der Ploeg, F. and de Zeeuw, A. (eds), *Dynamic Policy Games in Economics*, Vol. 181 of Contributions to Economic Analysis, Elsevier, 121–155
6. de Zeeuw, A. (2018): Dynamic Games of International Pollution Control: A Selective Review. In: Başar, T. and Zaccour, G. (eds), *Handbook of Dynamic Game Theory*, Springer, 703–728
7. Hoof, S. (2019): Linear-state differential games in partition function form, *International Game Theory Review* **21**(4)
8. Kóczy, L. Á. (2018): *Partition Function Form Games*, Springer
9. Parilina, E. and Sedakov, A. (2020): Stable Coalition Structures in Dynamic Competitve Envirnoment. In: Pineau, P.-O., Sigué, S. and Taboubi, S. (eds), *Games in Management Science*, Springer, 381–396
10. Petrosjan, L. and Zaccour, G. (2003): Time-consistent Shapley value allocation of pollution cost reduction, *Journal of Economic Dynamics ans Control* **27**, 381–398
11. Ray, D. and Vohra, R. (2015): Coalition Formation. In: Young, H. P. and Zamir, S. (eds), Vol. 4 of *Handbook of Game Theory with Economic Applications*, Elsevier, Chapter 5, 239–326
12. Thrall, R. M. and Lucas, W. F. (1963): N-person games in partition function form, *Naval Research Logistics Quarterly* **10**(4), 281–298
13. Dockner, E. and Wagener, F. (2014): Markov perfect Nash equilibria in models with a single capital stock, *Economic Theory* **56**(3), 585–625
14. Zaccour, G. (2003): Computation of Characteristic Function Values for Linear-State Differential Games, *Journal of Optimization Theory and Applications* **117**(1), 183–194
15. Zhao, J. (1992): The hybrid solutions of an N-person game, *Games and Economic Behavior* **4**(1), 145–160

A Model for Partial Kantian Cooperation

Ioannis Kordonis

1 Introduction

It is very well known that equilibrium solutions are often inefficient (e.g., [1]). Thus, the description of cooperative behaviors has evolved as an important topic in Game Theory. In the context of repeated games, there is a lot of work on the imposition of cooperative outcomes, under the name "folk theorems" (e.g., [2]). In the context of Evolutionary Game Theory, the evolution of cooperation is an important topic as well (e.g., [3, 4]). Here is also empirical evidence that people indeed behave cooperatively, for example, when they exploit a shared resource ([5]). Other examples include people who buy low-emission cars (e.g., electric or hybrid), even if this may not make much sense from a narrow economic perspective, or contribute anonymously to charity. In many game situations, however, there is a great multitude of different possible cooperative outcomes that can be supported by models of fully rational players or evolutionary models. Thus, an important question is "*which one of those solutions could describe or predict the actual outcomes?*".

This work studies the behavior of the players in game situations, in the case where their behavior is affected by ethical considerations. Particularly, we assume that they are partially following Kant's "categorical imperative" ([6]). The most common form of the categorical imperative, stated first in the book *Groundwork of the Metaphysics of Morals* in 1785, reads as follows:

> Act only according to that maxim whereby you can, at the same time, will that it should become a universal law.

Similar ideas have appeared much earlier (for example, the golden rules of various religious texts and traditions), but Kant formulates this principle in a strict, almost

I. Kordonis (✉)
CentraleSupélec, Avenue de la Boulaie, 35576 Cesson-Sévigné, France
e-mail: jkordonis1920@yahoo.com

D. M. Ramsey and J. Renault (eds.), *Advances in Dynamic Games*,
Annals of the International Society of Dynamic Games 17,
https://doi.org/10.1007/978-3-030-56534-3_13

mathematical way. Still, there can be various interpretations of the categorical imperative, leading eventually to different possible models. Let us describe some of the issues that may arise when interpreting the categorical imperative. First, the players may have different action sets, their actions may have a different impact on the others, or they may have different preferences. Hence, a "maxim" seems most appropriate to be interpreted as a strategy of a player (i.e., a mapping from a state, preference, or type to the action set) and not an action. Second, when a certain player optimizes for the strategy, which she assumes that the others would also follow, it is not reasonable to assume that all the other players having different states or preferences would cooperate to optimize the particular player's cost.[1] To overcome this difficulty, we use the notion of the veil of ignorance. This notion was introduced by Rawls ([7]) to describe a hypothetical situation where a person decides about the rules of a society. However, during this decision, she doesn't know her position in this society, her abilities, or even her tastes. Harsanyi used a very similar idea in an earlier text, under the name equi-partition ([8])). Another issue is that the use of a veil of ignorance requires interpersonal comparisons of utility. However, the need for interpersonal comparisons of utility does not create a problem in a descriptive model since players do not need to agree on the scaling of the utilities of the other persons. What is important is how each player perceives the utilities of the others. Finally, the players know that it is not true that all the others will follow their strategy. Hence, it is interesting to study how the players would behave if each one of them assumes that *some* of the others would follow her strategy.

1.1 Contribution

The primary contribution of this work is the definition of a notion of a partially Kantian cooperative outcome (the r-Kant-Nash equilibrium) and the study of its existence and uniqueness properties. An important building block is to assign to each player an imagined (virtual) group of players. The player assumes that within her virtual group, all the players use the same strategy aiming to optimize an overall goal of the group. Equivalently, the player decides her strategy before knowing her place in the virtual group. The virtual group of a player belongs exclusively to her imagination (perception or understanding of social identity). Thus, the players do not need to agree on the construction of their virtual groups. The aim of the virtual group reflects the idea of the veil of ignorance. Thus, the strategy of the group minimizes

[1] Let us quote a part of a story in which Woody Allen makes fun of several philosophers. This passage illustrates some issues arising when interpreting the categorical imperative. "No less misguided was Kant, who proposed that we order lunch in such a manner that if everybody ordered the same thing the world would function in a moral way. The problem Kant didn't foresee is that if everyone orders the same dish there will be squabbling in the kitchen over who gets the last branzino. "Order like you are ordering for every human being on earth," Kant advises, but what if the man next to you doesn't eat guacamole? In the end, of course, there are no moral foods-unless we count soft-boiled eggs." From Woody Allen "THUS ATE ZARATHUSTRA" New Yorker JULY 3, 2006.

a (risk-sensitive) cost of a random member of the group. This formulation includes the case of minimizing the average cost (or equivalently the total cost), inspired by [8], and the minimization of the maximum cost, inspired by [7].

We use a model with a continuum of players. The reason for this choice is that we would like to describe abstract anonymous groups of players. Each player has an individual type and a social preference type. The individual type describes her position, i.e., how her actions affect others and also her preferences. The social preference type characterizes the way the player constructs her imagined group. A set of strategies is an r-Kant-Nash equilibrium if the action of each player coincides with the one she would choose by solving the problem of her virtual group. We then study the existence, uniqueness, and computation of r-Kant-Nash equilibrium in the case where there is a finite possible number of types. Then, we give a characterization of the r-Kant-Nash equilibrium in the case of infinite, one-dimensional, number of types. We use several examples, including a fishing game, a vaccination game, an opinion game, and an electric vehicle charging game to illustrate the use of r-Kant-Nash equilibrium and its properties compared to other notions.

1.2 Related Notions

This work is very much inspired by the work of Roemer. A very much related notion is *Kantian equilibrium*, introduced in [9, 10]. A set of strategies constitutes a multiplicative Kantian equilibrium if no player has a motivation to *multiply* her action by any positive constant ρ assuming that the rest of the players would also *multiply* their actions by the same constant ρ, as well. Similarly, he defines the additive Kantian equilibrium. It turns out that under weak conditions, the Kantian equilibria belong to the Pareto frontier and under some additional conditions it coincides with the most efficient point. However, often Pareto frontier contains fundamentally unjust solutions. It is probably not reasonable to expect that a player who is very much disadvantaged by a solution in the Pareto frontier to be willing to cooperate with the others, while she has the opportunity to improve her position by changing her action unilaterally. Ghosh and Long [11] and Long [12] extended [9] in two distinct directions. First, they consider dynamic games and second study games with mixed Kantian and Nash players and introduce the notions of (inclusive and exclusive) Kant-Nash equilibria. Furthermore, Long in [13] introduced the notion of virtual co-movers equilibrium. In this model, each player considers a virtual co-movers group and assumes that if she changes her strategy, then all the members of the virtual co-movers group would change their strategy accordingly. The basic difference of the current work with the ones mentioned above is the way the categorical imperative is interpreted. Particularly, these works assume that the players "universalize" the *changes* in their actions, while in this work, we assume that they "universalize" their strategy.

Another related line of research is the theory of Belief Distorted Nash Equilibrium [14, 15], due to Wiszniewska-Matyszkiel. These works describe the possibility of cooperative outcomes in games, based on some misconceptions of the players, which however lead to overall outcomes which are consistent with their observations.

2 The r-Kant-Nash Equilibrium

2.1 The Model

In this section, we describe a game theoretic model with a continuum of players (e.g., [16]) and then introduce the notion of r-Kant-Nash equilibrium. We assume that all the sets and functions thereafter are measurable.

We consider a set of players $I = [0, 1]$ distributed uniformly (according to the Lebesgue measure λ). Let $(I, \mathcal{B}, \lambda)$ be the corresponding probability space, where $\mathcal{B}$ is the Borel σ-algebra. Each player $i \in I$ has an individual type x_i describing both the preferences of i and the effects of her actions on the costs of the others. Denote by X the set of possible individual types and define the function $x : I \to X$ with $x(i) = x_i$. Assume also that each player $i \in I$ has a social preference type θ_i and denote by Θ the set of possible social preference types. Social preference types relate to the notion of virtual groups which will be explained in detail later on. Similar to x there is a function $\theta : I \to \Theta$ with $\theta(i) = \theta_i$.

Each player $i \in I$ chooses an action u_i from an action set U. We focus on symmetric action profiles, i.e., profiles where u_i depends only on x_i and θ_i. Particularly, for the function $u : I \to U$, with $u(i) = u_i$, there is a function $\bar{\gamma} : X \times \Theta \to U$ such that $u(i) = \bar{\gamma}(x(i), \theta(i))$, for all $i \in I$.

The cost function of each player is given by

$$J_i = J(u_i, \bar{u}, x_i), \tag{1}$$

where $\bar{u}$ is statistic of the players' actions given by

$$\bar{u} = \int_I g(u(i), x(i))\lambda(di), \tag{2}$$

for a function $g : U \times X \to \mathbb{R}^m$.

Let us then describe the idea of a virtual (imagined) group:

(i) Each player $i \in I$ assumes that she is associated with a virtual group of players. This group reflects the social considerations of player i. The virtual group of player i is described by a sub-probability measure $r_i(\cdot)$ on $(I, \mathcal{B})$, i.e., a finite measure with $r_i(I) \leq 1$. For every $A \in \mathcal{B}$, the sub-probability measure should satisfy $r_i(A) \leq \lambda(A)$. If $r_i(I) \neq 0$, let us denote by $\bar{r}_i(\cdot)$ the probability measure $r_i(\cdot)/r_i(I)$. If $r_i(I) = 0$ then the virtual group of this player constitutes only of

herself. We assume that type of the virtual group of player i depends only on x_i and θ_i. That is, if for $i' \in I$, we have $x_i = x_{i'}$ and $\theta_i = \theta_{i'}$ imply $r_i(\cdot) = r_{i'}(\cdot)$.

(ii) Player $i \in I$ assumes that all the members $j \in I$ of her virtual group are bound to use the same strategy $\tilde{u}_i(j)$. We again assume symmetry, i.e., there is a function $\gamma : X \times \theta \times X \to U$ with $\tilde{u}_i(j) = \gamma(x(j), x_i, \theta_i)$. We use also the notation $\tilde{u}_i(j) = \gamma_{x_i,\theta_i}(x(j))$.

(iii) The aim of the virtual group is to minimize a risk-sensitive aggregate cost of its members. We denote by $\beta_{\theta_i} \in (-\infty, \infty)$ the risk factor of the virtual group. If $\beta_{\theta_i} = 0$ the group is risk neutral, when $\beta_{\theta_i} > 0$ is risk averse, and for $\beta_{\theta_i} < 0$ risk loving. For a risk neutral virtual group ($\beta_{\theta_i} = 0$), if $r_i(I) > 0$, define the cost of the virtual group of player i as

$$\tilde{J}_i(\gamma, \bar{\gamma}) = E\left[J(\gamma_{x_i,\theta_i}(x(j)), \bar{u}_i, x(j))w_{x_i,\theta_i}(x(j))\right], \tag{3}$$

where j is a player selected randomly according to $\bar{r}_i(\cdot)$ and the factor $w_{x_i,\theta_i}(\cdot)$ is a weighting function indicating the relative importance of the several positions in the group. The value of $\bar{u}$ corresponds to the g-mean value of the actions of all the players assuming that the members of the group are using $\tilde{u}_i(j) = \gamma_{x_i,\theta_i}(x(j))$ and the strategy of the players not belonging to the group is given by $u(j) = \bar{\gamma}(x(j), \theta(j))$. Thus

$$\bar{u} = T_{x_i,\theta_i}(\gamma, \bar{\gamma}) = \int_I g(\bar{\gamma}(x(j), \theta(j)), x(j))(\lambda - \bar{r}_i)(dj) + \int_I g(\gamma_{x_i,\theta_i}(j), x(j))r_i(dj). \tag{4}$$

For $\theta_i \neq 0$ define

$$\tilde{J}_i(\gamma, \bar{\gamma}) = \frac{1}{\beta_{\theta_i}} \ln E\left\{\exp[\beta_{\theta_i} J(\gamma_{x_i,\theta_i}(x(j)), \bar{u}_i, x(j))w_{x_i,\theta_i}(x(j))]\right\}. \tag{5}$$

If $r_i(I) = 0$, then the cost of the virtual group of player i coincides with the actual cost given by (1). A justification for this choice is given in Appendix.

(iv) For the case where X and Θ are finite we extend the definition of the virtual group's cost for the case $\beta_i = \infty$. The cost is given by

$$\tilde{J}_i(\gamma, \bar{\gamma}) = \max_{x' \in X_i} \left\{J(\gamma_{x_i,\theta_i}(x'), \bar{u}_i, x')w_{x_i,\theta_i}(x')]\right\}, \tag{6}$$

where $X_i = \{x' \in X : r_i(\{j \in I : x(j) = x'\}) > 0\}$.

Remark 1 (i) The virtual groups defined have many similarities with the virtual co-movers model of [11, 13]. Specifically in the virtual co-movers model each player assumes that if she changes her strategy, a subset of the others would also change theirs accordingly.

(ii) The definition of the members of the virtual group of each player offers a lot of flexibility. The two extreme cases are the case where $r = 0$ and the group of each player consists only of herself and the case where $r_i(\cdot) = \lambda(\cdot)$.

In the intermediate cases, the quantity $r_i(\cdot)$ may relate to some perceived social identity, such as race, class, age, religion, gender, ethnicity, ideology, nationality, sexual orientation, culture, or language.[2]

(iii) The virtual groups, the way they are defined, are purely imaginary. Thus, the fact that a player i assumes that another player j is included in her virtual group does not necessarily imply that the virtual group of player j includes i.

(iv) The expectation in models (3) and (5) corresponds to the random position of the player in the virtual group. In other words, behind the veil of ignorance, the player does not know at which place of the (imagined) society she is going to end up. Probably, as Rawls suggested, she might be risk averse against this uncertainty.

Based on the idea of a virtual group, we introduce the notion of the r-Kant-Nash equilibrium.

Definition 1 A set of strategies $u : I \to U$ in the form $u(i) = \bar{\gamma}(x(i), \theta(i))$ is an r-Kant-Nash equilibrium, if for all possible combinations (x_i, θ_i) there is a solution $\tilde{u}_i : I \to U$ with $\tilde{u}_i(j) = \gamma_{x_i,\theta_i}(x(j))$ to the optimization problem:

$$\underset{\gamma_{x_i,\theta_i}}{\text{minimize}} \ \tilde{J}_i(\gamma, \bar{\gamma}), \tag{7}$$

which satisfies $\gamma(x_i, x_i, \theta_i) = \bar{\gamma}(x_i, \theta_i)$.

Remark 2 (i) The r-Kant-Nash equilibrium is a situation where each player implements in the actual game an action that would be optimal for her virtual group, assuming that all the members of the group implemented their optimal actions.

(ii) The weighting factor w_{x_i,θ_i} may have two discrete roles. At first, Player i may believe that in her virtual group, some subgroup of players should be favored over the others. A second, and probably more important, role is to resolve the so-called **interpersonal comparison of utility** problem, i.e., the fact that the players may not agree on how to scale the utility functions of other players.

2.2 Special Cases and Relation to Other Concepts

The notion of r-Kant-Nash equilibrium has several interesting special cases.

(i) The **Nash equilibrium**. Assuming that $r \equiv 0$ and $\beta_\theta = 0$ each player uses her best response to the actions of the other players. Hence, for these values the r-Kant-Nash equilibrium coincides with the Nash equilibrium of the game with a continuum of players (e.g., [17]).

[2] From the identity politics article of Wikipedia.

(ii) The **(Bentham-) Harsanyi** solution. Assume that $\beta_\theta = 0$ and $r_i(\cdot) = \lambda(\cdot)$. Then, each player is risk neutral and optimizes for the mean cost (or equivalently the sum of the costs) of all the players. This solution coincides with the solution proposed in [8].

(iii) The **Rawls** solution. Assume that $\beta_\theta = \infty$ and $r_i(\cdot) = \lambda(\cdot)$ and that X and Θ are finite. In this case, all the players minimize the cost function of the worst-off participant, i.e., they use the minimax rule. This solution coincides with the Rawls difference solution [7].

(iv) Efficient cooperation within **coalitions**. Consider the coalitions $C_1, \ldots, C_N \subset I$ and assume that C_j, $j = 1, \ldots, N$ is a partition of I. Further, assume that the virtual groups are the same with the coalitions. That is, for $i \in C_j$ it holds $r_i(A) = \lambda(A \cap C_j)/\lambda(C_j)$. Finally, assume that for $\mathbf{1} \in C_j$ it holds $\theta_i = j$ and that within each coalition the players weight the others in the same way, i.e., $w_{\theta_i, x_i}(x') = g_{\theta_i}(x')$. Then, within each coalition the players jointly optimize for a weighted sum of their costs, and thus within each coalition there is an efficient cooperation.

(v) The relation with the altruistic (other regarding) behavior is illustrated in the following example.

Example 1 *(The Fishing Game)* We first compute the equilibrium to the game with altruistic players. It is convenient to consider a game with a large number N of players and then take the continuum limit. Let us note that the r-Kant-Nash equilibrium will be computed directly for the game with a continuum of players. The cost function of each one of the players is

$$J_i = u_i^2 - \left(1 - \frac{1}{N-1}\sum_{j \neq i} u_j\right) u_i,$$

where the first term corresponds to the effort of the fisher i and the second on the revenues.

The altruistic (other regarding) cost for player i is

$$\bar{J}_i = (1 - \alpha/2) J_i + (\alpha/2) \sum_{j \neq i} J_j = (1 - \alpha/2)(u_i^2 - u_i) + \frac{1}{N-1} u_i \sum_{j \neq i} u_j + f(u_{-i}),$$

with $\alpha \in [0, 1]$.

The Nash equilibrium of the altruistic game is given by

$$u_i = \frac{2 - \alpha}{6 - 2\alpha}.$$

Let us then consider the corresponding game with a continuum of players and compute the partial Kantian strategy. The cost is given by

$$J_i = u^2 - (1 - \bar{u})u,$$

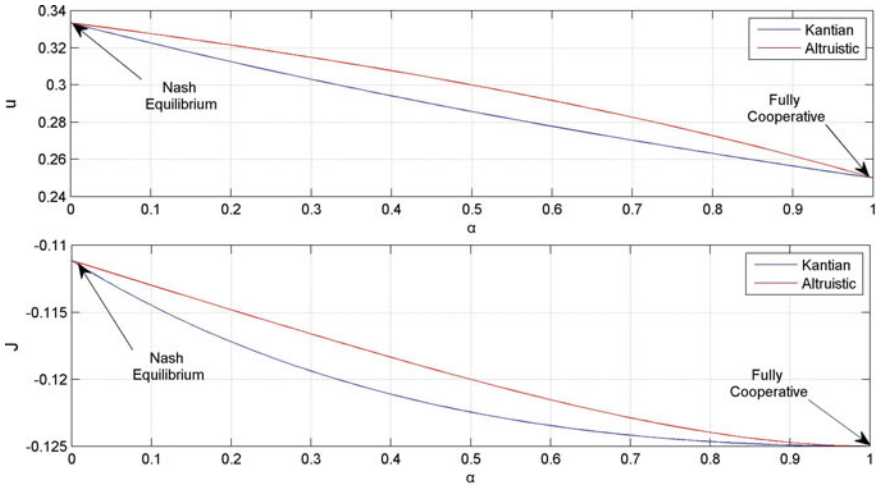

Fig. 1 Comparison of the actions and the costs of the players when they use a partially Kantian versus an Altruistic criterion

where bar $u = \int_I u(i)\lambda(di)$. Assume that $\Theta = \{\theta\}$ and $X = \{x\}$ are singletons. Further, assume that each player considers as her virtual group a fraction α of the other players. Then, the r-Kant-Nash equilibrium in the form $u = \gamma$ is characterized by

$$\frac{\partial}{\partial \gamma} J(u, \bar{u}) = \frac{\partial}{\partial u} J(u, \bar{u}) + \frac{\partial}{\partial \bar{u}} J(u, \bar{u}) \frac{\partial \bar{u}}{\partial \gamma} = 0,$$

Hence,

$$2u - 1 + \bar{u} + \alpha u = 0.$$

Due to symmetry:

$$u = \frac{1}{3 + \alpha}.$$

Figure 1 compares the actions and the costs of the players in the cases of an altruistic versus a partially Kantian behavior. It turns out that, in this example, the Kantian cooperation is more effective than the altruism. □

3 Finite Number of Individual and Social Types

In this section, we assume that the action set U is a subset of the $m-$dimensional Euclidean space and that there is a finite set of possible individual-social-type pairs $(x_1, \theta_1), \ldots, (x_N, \theta_N)$. The distribution of players is described by a vector

$p = [p_1 \ \ldots \ p_N]$. For the case of a finite number of types, we derive sufficient conditions for the existence of an r-Kant-Nash equilibrium and characterize it in terms of a variational inequality. To do so, let us first introduce some notation. Denote by N' the number of different values of x_k's and by $\bar{x}_1, \ldots, \bar{x}_{N'}$ their values. Denote also by σ the function such that $\sigma(k) = k'$ if $x_k = \bar{x}_{k'}$. Consider the virtual group of a player, having type k, and assume that this group has strategy γ. Denote by $\tilde{u}_k = [u_{k1}, \ldots, u_{kN}]$ the (imagined) action vector for the members of the group, where $u_{kk'} = \gamma(x_{k'}, x_k, \theta_k)$. The form of the strategy implies that $u_{kk'} = u_{kk''}$ if $x_{k'} = x_{k''}$. Thus, the vector $\tilde{u}_k$ may be viewed as a member of the set $U^{N'}$. We will use also the notation $r_{kk'} = r_i(\{j \in I : x(j) = x_{k'}, \theta(j) = \theta_{k'}\})$ for an $i \in I$ which $x(i) = x_k$ and $\theta(i) = \theta_k$. Assume that all the player types have $\beta_{\theta_i} < \infty$.

A vector of actions $u^\star = [u_1^\star, \ldots, u_N^\star]$ is an r-Kant-Nash equilibrium if there exists a matrix $u = [u_{kk'}]$ such that, for every k, it holds $u_k^\star = u_{kk}$ and the strategy $\tilde{u}_k = [u_{k1} \ldots u_{kN}]$ is optimal for the virtual group of a player with type k, under the constraint $u_{kk'} = u_{kk''}$ if $\sigma(k') = \sigma(k'')$. The cost of a virtual group with action vector $\tilde{u}_k$, assuming that the others are playing $u^\star$, is given by

$$\tilde{J}_k(\tilde{u}_k, u^\star) = \begin{cases} \frac{1}{\beta_{\theta_i}} \ln \sum_{k'=1}^N r_{kk'} \exp[\beta_{\theta_i} w_k(k') \bar{J}_{k,k'}(\tilde{u}_k, u^\star)], & if \ \beta \neq 0, \infty \\ \sum_{k'=1}^N r_{kk'} w_k(k') \bar{J}_{k,k'}(\tilde{u}_k, u^\star), & \text{if } \beta = 0 \end{cases} \tag{8}$$

where $\bar{J}_{k,k'}(\tilde{u}_k, u^\star)$ is the cost that a player who belongs to the virtual group and has type k' would have if the players of the group were using $\tilde{u}_k$ and the rest $u^\star$. Thus, $\bar{J}_{k,k'}(\tilde{u}_k, u^\star)$ is given by

$$\bar{J}_{k,k'}(\tilde{u}_k, u^\star) = J\left(\tilde{u}_{kk'}, \sum_{k''=1}^N [g(u_{k''}^\star, x_{k''})(p_{k''} - r_{kk''}) + g(\tilde{u}_{kk''}, x_{k''}) r_{kk''}], x_{k'}\right). \tag{9}$$

The following proposition adapts some standard results for the existence of a Nash equilibrium (e.g., [18]) to the case of r-kant-Nash equilibrium. Before stating the proposition let us recall the notions of quasi-convexity and pseudo-convexity [19]. A function $f(u)$ defined on a convex set U is quasi-convex if for any real number $\bar{f}$ the set $\{u \in U : f(u) \leq \bar{f}\}$ is convex. The function f is pseudo-convex if it is differentiable and for any pair of points $u_1, u_2 \in U$ such that $\nabla f(u_1)^T (u_2 - u_1) \geq 0$ it holds $f(u_2) \geq f(u_1)$.

Proposition 1 *Assume that $U \subset \mathbb{R}^m$ is compact and convex, that $\tilde{J}_k$ given by (8) is continuous, and that $\tilde{J}_k(\cdot, u^\star)$ is quasi-convex for every fixed $u^\star$ and every k. Then, there exists an r-Kant-Nash equilibrium.*

Proof Consider the set $\bar{U} = U^{N \times N'}$. For each type $k = 1, \ldots, N$, consider the correspondence $T_k : \bar{U} \rightrightarrows U^{N'}$ defined as follows. For a given a $u \in \bar{U}$, define $u^\star = [u_{1\sigma(1)} \ldots u_{N\sigma(N)}] \in U^N$. Then define:

$$T_k(u) = \pi_{U^{N'}} \left[\arg\min_{\tilde{u}_k \in Z} \tilde{J}_k(\tilde{u}_k, u^\star) \right],$$

where $\pi_{U^{N'}}$ denotes the projection to $U^{N'}$ and $Z = \{\tilde{u} \in U^N : \tilde{u}_{k'} = \tilde{u}_{k''}$ whenever $x_{k'} = x_{k''}\}$. Maximum theorem [20] implies that T_k is compact-valued upper semi-continuous. Quasi-convexity implies that T_k is convex valued. Thus, the correspondence $T : \bar{U} \rightrightarrows \bar{U}$ with $T : u \mapsto T_1(u) \times \cdots \times T_N(u)$ satisfies the conditions of Kakutani fixed point theorem. Therefore, there exists an r-Kant-Nash equilibrium. □

A very simple sufficient condition for the existence of a Kant-Nash equilibrium is given in the following corollary.

Corollary 1 *Assume that $U \subset \mathbb{R}^m$ is compact and convex, and $J(\cdot, \cdot, x)$ is convex for every fixed x, the function g is linear in u and $\beta_{\theta_k} \geq 0$, for all k. Then there exists an r-Kant-Nash equilibrium.*

Proof The function $\bar{J}_{k,k'}(\cdot, u^\star)$ defined in (9) is convex with respect to $\tilde{u}_k$. Indeed, in the right-hand side of (9), the first two arguments of J, particularly, $\sum_{k''=1}^{N}[g(u^\star_{k''}, x_{k''})(p_{k''} - r_{kk''}) + g(u_{kk''}, x_{k''})r_{kk''}]$ and $\tilde{u}_{kk'}$ are affine functions of $\tilde{u}_k$. Thus, convexity of J implies that $J_{u^\star k'}$ is convex. Now, the fact that $\exp(\cdot)$ is increasing and convex implies that the function,

$$\sum_{k'=1}^{N} r_{kk'} \exp[\beta_{\theta_i} J_{u^\star,k'}(\tilde{u}_k))],$$

is convex in $\tilde{u}_k$ as well. Now, $\beta_{\theta_k} \geq 0$ and the fact that the function $\ln(\cdot)$ is increasing imply that the quasi-convexity assumption of Proposition 1 is satisfied and the proof of the corollary is complete. □

If the quasi-convexity assumption is strengthened to a pseudo-convexity, then the r-Kant-Nash equilibrium can be characterized by a variational inequality.

Proposition 2 *Assume that $U \subset \mathbb{R}^m$ is convex, that $\tilde{J}_k$ given by (8) is continuous, and that $\tilde{J}_k(\cdot, u^\star)$ is pseudo-convex and for every fixed $u^\star$ and every k. Consider also the vector function $F : U^{N^2+N} \to \mathbb{R}^{m(N^2+N)}$ given by*

$$F(\tilde{u}, u^\star) = \begin{bmatrix} \nabla^T_{\tilde{u}_1} \tilde{J}_1(\tilde{u}_1, u^\star) \\ \vdots \\ \nabla^T_{\tilde{u}_N} \tilde{J}_1(\tilde{u}_N, u^\star) \\ u^\star_1 - \tilde{u}_{11} \\ \vdots \\ u^\star_N - \tilde{u}_{NN} \end{bmatrix}. \tag{10}$$

Then:

(i) There is an r-Kant-Nash equilibrium if and only if there is a solution $(\tilde{u}, u^\star) \in U^{N^2+N}$ *to the variational inequality:*

$$F^T(\tilde{u}, u^\star)\begin{bmatrix} \tilde{u}' - \tilde{u}, \\ (u^\star)' - u^\star \end{bmatrix} \geq 0, \quad \textit{for all} \quad \tilde{u}' \in U^{N^2}, (u^\star)' \in U^N. \tag{11}$$

(ii) Assume that F is strictly monotone, i.e.,

$$(F(\tilde{u}', (u^\star)') - F(\tilde{u}, u^\star))^T \begin{bmatrix} \tilde{u}' - \tilde{u}, \\ (u^\star)' - u^\star \end{bmatrix} > 0, \tag{12}$$

for every pair $(\tilde{u}, u^\star) \neq (\tilde{u}', (u^\star)')$. *Then, there is at most one r-Kant-Nash equilibrium.*

Proof (i) Consider a pair $(\tilde{u}, u^\star)$ satisfying (11). Choosing $\tilde{u}' = \tilde{u}$ and $(u_2^\star)' = u_2^\star, \ldots, (u_N^\star)' = u_N^\star$ we conclude that $u_1^\star = \tilde{u}_{11}$. Similarly, $u_k^\star = \tilde{u}_{kk}$, for all k. Choosing $\tilde{u}_i' = \tilde{u}_i$, for $k = 1, \ldots, k-1, k+1, \ldots, N$ we conclude that $\tilde{u}_k$ is optimal in (8). Thus, $(\tilde{u}, u^\star)$ corresponds to an r-Kant-Nash equilibrium. The proof of the converse is similar.
(ii) It is a direct consequence of part (i) and Theorem 2.3.3 of [21]. □

Remark 3 For $\beta_{\theta_i} \neq 0$, Proposition 2 holds true if instead of $\tilde{J}_k$ we use

$$\sum_{k'=1}^{N} r_{kk'} \exp[\beta_{\theta_i} w_k(k') \bar{J}_{k,k'}(\tilde{u}_k, u^\star)].$$

4 Examples of *r*-Kant-Nash Equilibrium

In this section, we investigate some properties of the r-Kant-Nash equilibrium using some examples, namely, a vaccination game, static and dynamic fishing games, an opinion game, and an electric vehicle charging game. We also compare it with Roemer's Kantian equilibrium. In all cases, we use examples with at most two types of players in order to make the visualization of the results easier.

4.1 A Vaccination Game

We describe a simplified model for the spread of a disease, where all members of a society may choose to vaccinate or not. The model is a slight modification of the one presented in [22]. The spread of the disease depends on the percentage of people $\bar{u}$ having a vaccination. The cost for each player i is given by

$$J_i = u_i + (1 - Au_i) f(\bar{u}) x_i, \tag{13}$$

where $u_i = 1$ if player i is vaccinated and 0 otherwise, $(1 - Au_i) f(\bar{u})$ stands for the probability that player i is infected, $0 < A < 1$ is a positive constant representing the effectiveness of the vaccination, $f(\bar{u})$ is a strictly decreasing function, and x_i corresponds to the expected dis-utility player i experiences if she gets sick. A fraction B of the population consists of vulnerable persons (e.g., older people) and a fraction $1 - B$ of non-vulnerable.[3] The constant x_i takes accordingly two values, i.e., C^v and C^n with $C^v > C^n$. The first term in (13) stands for the cost of vaccination (e.g., time, money, pain, potential side effects, etc.) and the second term to the expected cost from the disease. Finally, we allow for mixed strategies and thus $u_i \in [0, 1]$ and thus the value of $\bar{u}$ is given by $Bu^v + (1 - B)u^n$, where u^v is the probability of vaccination for vulnerable and u^n for the non-vulnerable persons.

Let us first compute the Nash equilibrium of the game. It is not difficult to see that the Nash equilibrium is

$$(u^v, u^n) = \begin{cases} (0, 0) & \text{if } AC^v f(0) \le 1 \\ (B^{-1} f^{-1}((AC^v)^{-1}), 0 & \text{if } AC^v f(B) \le 1 < AC^v f(0) \\ (1, 0), & \text{if } AC^n f(B) \le 1 < AC^v f(B) \\ (1, (1 - B)^{-1}(f^{-1}((AC^n)^{-1}) - B), & \text{if } AC^n f(B) \le 1 < AC^n f(1) \\ (1, 1), & \text{if } AC^n f(1) \ge 1 \end{cases} \tag{14}$$

In what follows, we assume that the parameters are such that all the vulnerable agents are vaccinated, i.e., it holds $AC^v f(B) > 1$.

Assume that the parameters are given by $A = 0.8$, $B = 0.3$, $C^v = 500$, $C^n = 15$ and the function $f(z)$ is given by $0.2z^2 - 0.4z + 0.21$. The virtual group of each player consists of a fraction α of the other players[4] and the risk sensitivity β is 0 for all the players. The Nash equilibrium, the r-Kant-Nash equilibrium, and the Roemer's multiplicative Kantian equilibrium are illustrated in Fig. 2. The computation of the equilibria is not difficult, since we need only to solve optimization or fixed point problems in dimension 1.

Observe that already from $\alpha = 0.2$ the r-Kant-Nash equilibrium belongs to the Pareto frontier. It seems that this result is not general but has to do with the specific structure of the game, i.e., the vaccination is a positive externality, but creates strategic substitutes. Furthermore, vulnerable people play always $u^v = 1$, and thus their behavior does not depend on α. As α approaches 1, the r-Kant-Nash equilibrium approaches the point with the minimum total cost. Let us further note that in order to compute Roemer's multiplicative Kantian equilibrium, we have to extend the feasible region on $u_i \in [0, \infty)$ and write the cost of player i as

[3] In this section, we do not refer to the interval I, since it seems more convenient to refer to percentages of players. To connect with previous sections, let us note that in the unit interval, the set of vulnerable players is $[0, B) \subset I$ and the set of the non-vulnerable is $[B, 1]$.

[4] With the notation of Sect. 2, $r_i(A) = \alpha\lambda(A)$.

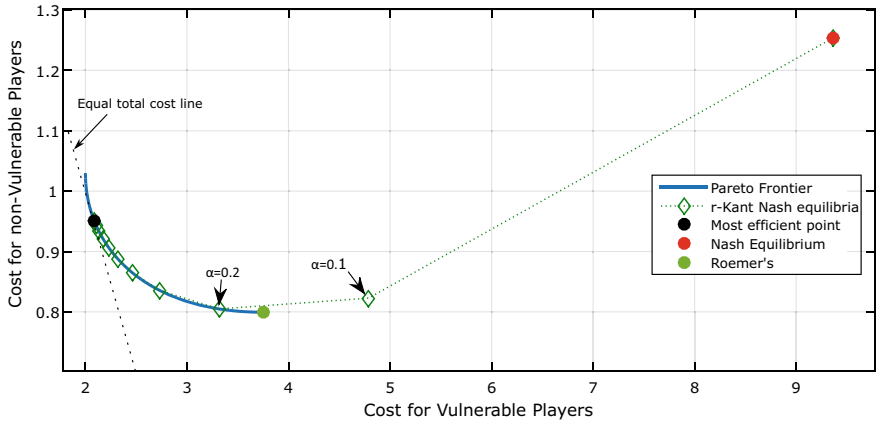

Fig. 2 The expected costs for vulnerable and non-vulnerable players for the several solution concepts

$$J_i = u_i + (1 - Au_i) f(\bar{u}) x_i + \mathbb{1}_{u_i \leq 1},$$

where $\mathbb{1}_{u_i \leq 1} = 0$ if $u_i \leq 1$ and $+\infty$ otherwise.

4.2 A Static Fishing Game with Two Types of Players

In this section, we study a fishing game where there are two kinds of players and compare the several solution concepts with respect to efficiency and fairness.

The cost for a player i is

$$J_i = x_i u_i^2 - (1 - \bar{u}) u_i. \tag{15}$$

The possible values for x_i are 1 and 2. Let us denote by u^1 and u^2 the corresponding actions and assume that 50% of the fishers have $x_i = 1$ and 50% have $x_i = 2$.

Assume that the virtual group of each player consists of a fraction α of the others. We then investigate the properties of the r-Kant-Nash equilibrium for various values of the risk factor β. The r-Kant-Nash equilibrium is characterized by

$$(u_1, u_2) \in \arg\min_{u_1', u_2'} \left\{ \exp\left[\beta\left((u_1')^2 - \left(1 - \alpha\frac{u_1' + u_2'}{2} + (1-\alpha)\frac{u_1 + u_2}{2}\right)u_1'\right)\right] + \right.$$
$$\left. + \exp\left[\beta\left(2(u_2')^2 - \left(1 - \alpha\frac{u_1' + u_2'}{2} + (1-\alpha)\frac{u_1 + u_2}{2}\right)u_2'\right)\right]\right\}.$$

If $u_1, u_2 \in (0, 1)$ the last equation implies

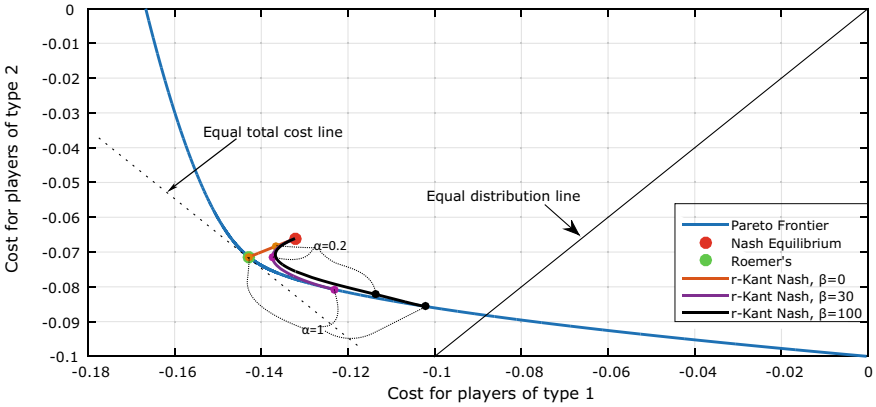

Fig. 3 The costs for the fishers of both types, for the several solution concepts

$$
\begin{aligned}
e^{V_1(u_1,u_2)}\left((5+\alpha)u_1+u_2-2\right)+\alpha e^{V_2(u_1,u_2)}u_2=0,\\
\alpha e^{V_1(u_1,u_2)}u_1+\alpha e^{V_2(u_1,u_2)}\left(u_1+(9+\alpha)u_2-2\right)=0,
\end{aligned}
\tag{16}
$$

where $V_1(u_1,u_2)=\beta(u_1^2-(1-(u_1+u_2)/2)u_1)$ and $V_2(u_1,u_2)=\beta(2u_2^2-(1-(u_1+u_2)/2)u_2)$. The system (16) is solved numerically to obtain r-Kant-Nash equilibrium.

Figure 3 illustrates the Nash equilibrium, the Roemer's multiplicative Kantian equilibrium, and the r-Kant-Nash equilibria for various values of α and β. The r-Kant-Nash equilibrium for $\alpha=1$, $\beta=0$ and the Roemer's multiplicative Kantian equilibrium, as expected, coincide with the most efficient point, i.e., the point where the total cost is minimized. However, this point does not distribute the outcome evenly. For $\beta>0$ we observe that the r-Kant-Nash equilibria produce fairer results as α approaches 1.

4.3 A Dynamic Resource Game

This example studies a dynamic model for exploiting a shared resource, where the players live only for a single time step. A similar model was analyzed in Sect. 3.10 of [10] (dynamic fishing game). We compare the r-Kant-Nash equilibria for the case where the virtual group of each player consists of players participating in the game simultaneously with her and the case where virtual groups contain players acting on various time steps. For simplicity, we do not analyze the full dynamic game, but only its steady state.

Let us denote by y total stock of the resource. Assume that the dynamics is given by

$$
y_{k+1}=3y_k(1-y_k)-y_k\bar{u}_k,
\tag{17}
$$

where $\bar{u}_k$ is the mean effort of the players at time step k. For a fixed $\bar{u}_k = \bar{u}$, the stationary value of y_k is

$$y = \frac{2 - \bar{u}}{3}. \tag{18}$$

We assume further that all the players participate in the game for a single time step. The cost for a player i who participates in the game at time step k is given by

$$J_i = (u^i)^2 - \rho \bar{u}_k y_k - (1 - \rho) u^i y_k, \tag{19}$$

where $\rho \in (0, 1)$. The cost (19) can be interpreted as follows. Player i produces a quantity $u^i x$, she holds a portion $(1 - \rho)$ of it, and the rest is redistributed equally among the players.

The Nash equilibrium is given by

$$u = \frac{(1 - \rho) y_k}{2}.$$

The steady-state effort under the Nash equilibrium (using (18)) is

$$u = \frac{2(1 - \rho)}{7 - \rho}.$$

We then study r-Kant-Nash equilibrium under two different assumptions.
Case 1: The virtual group of a player participating at time step k is a fraction α of the other players who participate in the game at the same time step. Under this assumption, the players of the virtual group do not affect y_k. Then, the r-Kant-Nash equilibrium is characterized by

$$u \in \arg\min_{u'} \{(u')^2 - \rho(\alpha u' + (1 - \alpha)u) y_k - (1 - \rho) u' y_k\},$$

which implies

$$u = \frac{1 - \rho + \rho\alpha}{2} y_k.$$

The steady-state effort, (using (18)) is

$$u = \frac{2(1 + \rho\alpha - \rho)}{7 + \rho\alpha - \rho}.$$

Case 2: The virtual group of each player i consists of a fraction α of all the other players, including players existing before or after player i. Then, the r-Kant-Nash equilibrium is characterized by

$$u \in \arg\min_{u'} \{(u')^2 - \rho(\alpha u' + (1 - \alpha)u) \bar{y}(u, u') - (1 - \rho) u' \bar{y}(u, u')\},$$

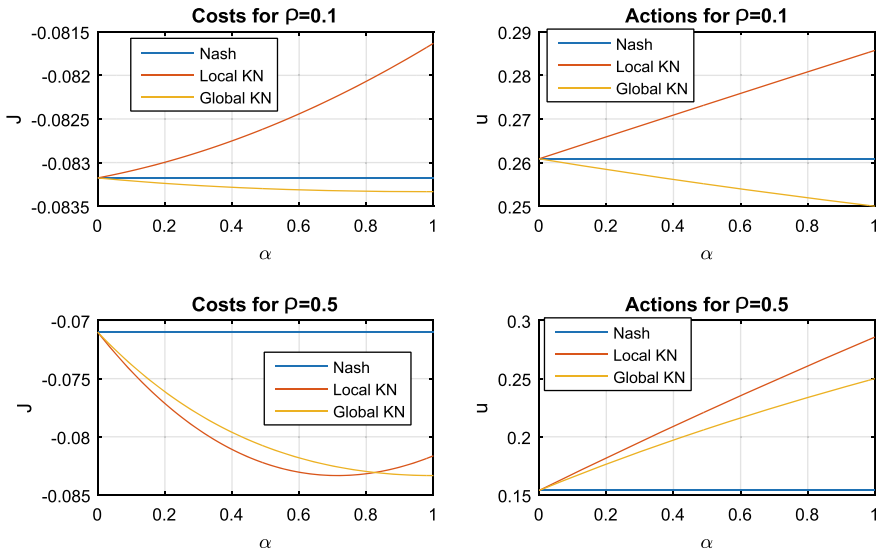

Fig. 4 The costs and the actions for various values of α and $\rho = 0.1$, $\rho = 0.5$. Local KN describes the actions and costs computed in Case 1 above and Global KN represents Case 2

where

$$\bar{y}(u, u') = \frac{2 - \alpha u' - (1 - \alpha)u}{3}.$$

The last equation implies

$$u = \frac{2(1 - \rho + \rho\alpha)}{7 + \alpha + \rho\alpha - \rho}.$$

Figure 4 shows the Nash equilibrium, the r-Kant-Nash solutions for cases 1 and 2.

Remark 4 An increase in Player i's effort increases her production, a part of which is redistributed, but such an increase leaves next generations of players with fewer resources. Therefore, if players identify themselves only with other players playing at the same time (Case 1), it is always more cooperative to increase their actions compared to the Nash equilibrium. On the other hand, a smaller action favors future generations of players. Thus, for low values of the redistribution coefficient ρ, under "global" cooperation (Case 2), the actions are reduced compared to the Nash equilibrium.

An interesting feature is that for $\rho = 0.1$, under "local" cooperation the overall cost in steady state is worse-off compared to the Nash equilibrium.

4.4 An Opinion Game

This example considers an opinion game where each player wants to express an opinion which is close to the expressed opinions of the others, but also close to her intrinsic opinion. The model used is a special case of [23]. The interesting feature of this example is to illustrate that local cooperation could be harmful.

The cost for a player i is given by

$$J_i = (u_i - x_i)^2 + (u_i - \bar{u})^2. \tag{20}$$

For simplicity, we assume that there are only two types of players: 50% of the players have intrinsic opinion $x_i = 0$ and 50% intrinsic opinion $x_i = 1$. Under these assumptions $\bar{u} = (u_0 + u_1)/2$, where u_0 and u_1 are the actions of players of type $x_i = 0$ and $x_i = 1$, respectively.

It is not difficult to see that the Nash equilibrium is

$$(u_0, u_1) = \left(\frac{1}{4}, \frac{3}{4}\right). \tag{21}$$

We then consider two scenarios of partial Kantian cooperation:

Case 1: In this case, the virtual group of each player consists only of players of the same type. Particularly, players i with type $x_i = 0$ have virtual groups consisting of a fraction α_0 of the players j with $x_j = 0$. Similarly, players i with type $x_i = 1$ have virtual groups consisting of a fraction α_1 of the players j with $x_j = 0$.

The r-Kant-Nash equilibrium satisfies

$$u_0 \in \arg\min_{u_0'} \left\{ (u_0')^2 + \left(u_0' - 0.5(\alpha_0 u_0' + (1-\alpha_0)u_0) - 0.5u_1\right)^2 \right\}$$
$$u_1 \in \arg\min_{u_1'} \left\{ (u_1' - 1)^2 + \left(u_1' - 0.5u_0 - 0.5(\alpha_1 u_1' + (1-\alpha_1)u_1)\right)^2 \right\}$$

which is equivalent to the system:

$$\begin{aligned} (6-\alpha_0)u_0 - (2-\alpha_0)u_1 &= 0, \\ -(2-\alpha_1)u_0 + (6-\alpha_1)u_1 &= 4. \end{aligned}$$

Case 2: Each player has a virtual group of players consisting of a fraction α of all the other players. That is, a player i with type $x_i = 0$ has a virtual group consisting of players j of both categories $x_j = 0$ and $x_j = 1$. A pair (u_0, u_1) constitutes an r-Kant-Nash equilibrium if it solves the problem:

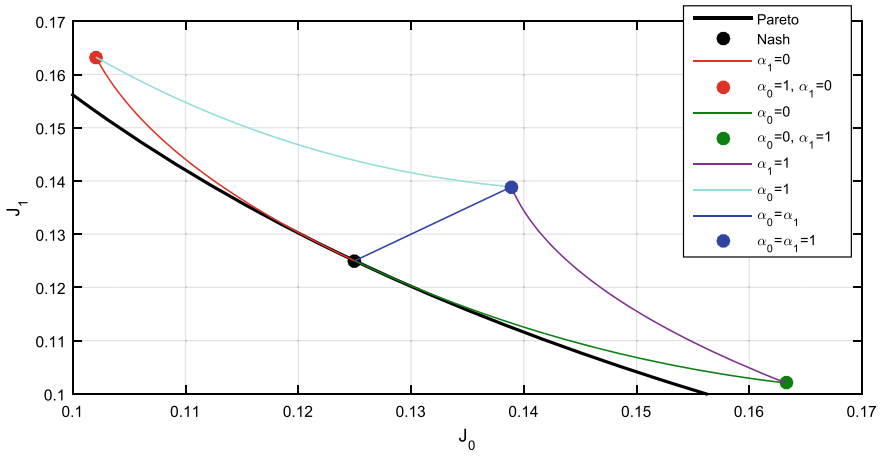

Fig. 5 The costs for both types of players for the Nash, Pareto, and the r-Kant-Nash solutions

$$\underset{u_0',u_1'}{\text{minimize}} \Big\{ (u_0')^2 + \big(u_0' - 0.5(\alpha u_0' + (1-\alpha)u_0) - (1-0.5)(\alpha u_1' + (1-\alpha)u_1)\big)^2 +$$
$$+ (u_1' - 1)^2 + \big(u_1' - 0.5(\alpha u_0' + (1-\alpha)u_0) - 0.5(\alpha u_1' + (1-\alpha)u_1)\big)^2 \Big\}.$$

Long but straightforward computations show that the Nash equilibrium (21) solves the minimization problem and thus it is the r-Kant-Nash equilibrium.

Figure 5 illustrates the costs for the two types of players for the several solution concepts.

Remark 5 Observe that in this example, the Nash equilibrium is on the Pareto frontier and coincides with the r-Kant-Nash equilibrium of Case 2. Furthermore, it minimizes the total cost. On the other hand, if a type, say $x = 1$ has local cooperation (Case 1), this leads to improved results for that group, but worse results for the other group (the group $x = 0$). This behavior corresponds, in the opinion game setting, to the case where a group of players takes a more radical opinion to affect the overall result. When both groups cooperate only locally, the situation is worse for both. Thus, the situation in Fig. 5 is very much like Prisoner's dilemma.

4.5 A Fishing Game with Overlapping Virtual Groups

In the previous examples, the virtual groups of players are either identical or disjoint. This fact facilitated the analysis. In this example, we study the fishing game of Sect. 4.2, assuming that the virtual groups of the players of different types are different but overlapping. Particularly, the virtual group of a player with type $x = 1$ consists of a fraction r_{11} of players with type $x = 1$ and r_{12} of players with type $x = 2$. Similarly,

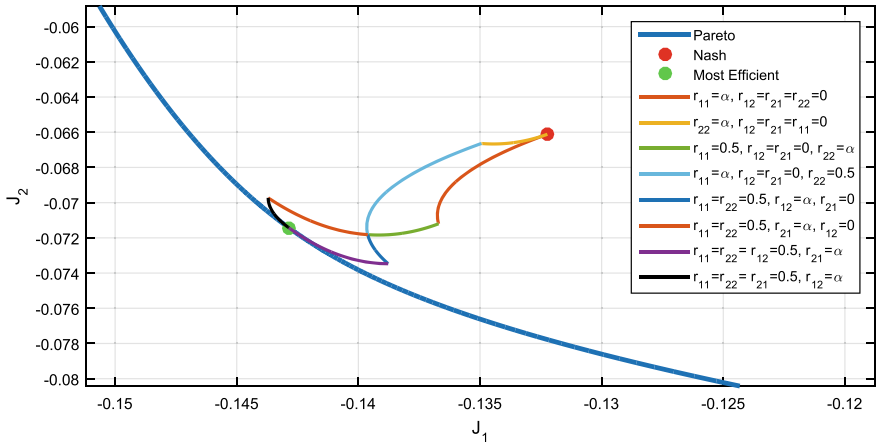

Fig. 6 The costs for both types of players for the Nash, Pareto, and the r-Kant-Nash solutions for the case of overlapping virtual groups. All the lines represent a combination of $r_{11}, \ldots, r_{22}$ where three of them are fixed and the other moves between 0 and 0.5

the virtual group of a player with type $x = 1$ consists of a fraction r_{21} of players with type $x = 1$ and r_{22} of players with type $x = 2$.

Let us focus on internal r-Kant-Nash equilibria, i.e., all the actions belong to the interior of the interval $[0, 1]$. Then, a pair (u_1, u_2) is an r-Kant-Nash equilibrium (see (11)) if there exist $\tilde{u}_1$ and $\tilde{u}_2$ such that

$$
\begin{aligned}
(u_1, \tilde{u}_2) \in \arg\min_{u_1', u_2'} \Big\{ & r_{11} \left[(u_1')^2 - \left(1 - r_{11}u_1' - r_{12}u_2' - r_{11}'u_1 - r_{12}'u_2\right) u_1' \right] + \\
& + r_{12} \left[2(u_2')^2 - \left(1 - r_{11}u_1' - r_{12}u_2' - r_{11}'u_1 - r_{12}'u_2\right) u_2' \right] \Big\}, \\
(\tilde{u}_1, u_2) \in \arg\min_{u_1', u_2'} \Big\{ & r_{21} \left[(u_1')^2 - \left(1 - r_{21}u_1' - r_{22}u_2' - r_{21}'u_1 - r_{22}'u_2\right) u_1' \right] + \\
& + r_{22} \left[2(u_2')^2 - \left(1 - r_{21}u_1' - r_{22}u_2' - r_{21}'u_1 - r_{22}'u_2\right) u_2' \right] \Big\},
\end{aligned}
$$

where $r_{11}' = (0.5 - r_{11}), r_{12}' = (0.5 - r_{12}), r_{21}' = (0.5 - r_{21}), r_{22}' = (0.5 - r_{22})$. The last equation is equivalent to the system:

$$
\begin{aligned}
(2.5 + r_{11})u_1 + 0\tilde{u}_1 + r_{12}'u_2 + 2r_{12}\tilde{u}_2 &= 1 \\
(0.5 + r_{11})u_1 + 0\tilde{u}_2 + r_{12}'u_2 + (4 + 2r_{12})\tilde{u}_2 &= 1 \\
r_{21}'u_1 + (2 + 2r_{21})\tilde{u}_1 + (0.5 + r_{22})u_2 + 0\tilde{u}_1 &= 1 \\
r_{21}'u_1 + 2r_{21}\tilde{u}_1 + (4.5 + r_{22})u_2 + 0\tilde{u}_2 &= 1.
\end{aligned}
$$

The r-Kant-Nash equilibria for several combinations of $r_{11}, \ldots, r_{22}$ are shown in Fig. 6.

Remark 6 Observe that we need to solve a system of four equations to find the r-Kant-Nash equilibrium. That is because each virtual group contains players of both categories. Since the virtual groups are different, the values computed for players having types different, compared to the player who constructs the virtual group, are never applied. For example, in a virtual group of a player of type 1, there are players of type 2. Thus, the values of $\tilde{u}_2$, computed in the virtual group of players of type 1, are not necessarily equal to the actual value of u_2.

4.6 Electric Vehicle Charging with Uniform Pricing

This example studies a simplified model of the interaction of the Electric Vehicle (EVs) owners, inspired by [24]. There is a fleet of EVs which should charge within the next N hours. Each vehicle is going to absorb a total amount of energy denoted by E. The cost of energy production depends on total consumption. Let us denote by $p_k(\bar{u}_k)$ the price per unit of energy when the mean charging rate for the vehicles is $\bar{u}_k$. The price p_k depends on the time of the day k because the demand of the other (non-EV) users and renewable energy production are not constant during the day. For simplicity, assume that the prices are written as

$$p_k(z) = c_k z + d_k.$$

We further assume that the EV owners pay at a uniform price, which depends on the total cost of energy production.

The cost for an EV owner is

$$J_i = \frac{(E_1^{\text{non-EV}} + \bar{u}_1)p_1(\bar{u}_1) + \cdots + (E_N^{\text{non-EV}} + \bar{u}_N)p_N(\bar{u}_N)}{E^{\text{tot}}} E + \sum_{k=1}^{N} R(u_k^i)^2, \tag{22}$$

where E^{tot} is the total energy consumption and $E_k^{\text{non-EV}}$ the total energy consumption for excluding EV charging at time step k. The first term of (22) corresponds to the money EV owner pays to the electricity company and the second term to the losses during the charging (battery degradation cost can be incorporated in this term). The feasible set U is given by

$$U = \left\{ (u_1, \ldots, u_N) \in \mathbb{R}^N : u_k \geq 0, \sum_{k=1}^{N} u_k = E \right\}.$$

The Nash equilibrium of the game is to use a constant charging rate:

$$u_k^i = E/N,$$

to minimize the cost of the losses.

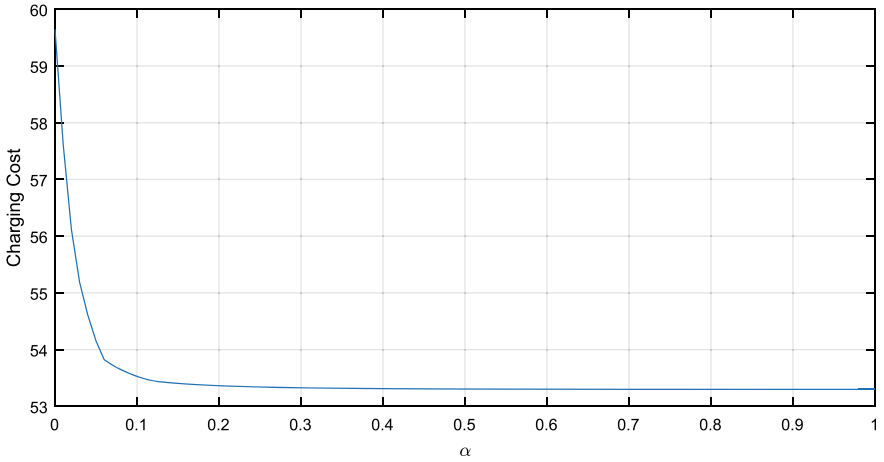

Fig. 7 The total cost of a player for charging her vehicle, for various values of α

Consider the case where the virtual group of each player is a fraction α of the other players. Then, (11) simplifies to

$$\begin{bmatrix}(u_1' - u_1) & \dots & (u_N' - u_N)\end{bmatrix} \begin{bmatrix} C_1(\alpha)u_1 + D_1(\alpha) \\ \vdots \\ C_N(\alpha)u_N + D_N(\alpha) \end{bmatrix} \geq 0, \quad \text{for all } u' \in U,$$

where $C_k(\alpha) = 2c_k E\alpha/E^{\text{tot}} + 2R$ and $D_k(\alpha) = E(E_k^{\text{non-EV}}c_k + d_k)\alpha/E^{\text{tot}}$. This problem is equivalent to the following minimization problem:

$$\underset{(u_1,\dots,u_n)\in U}{\text{minimize}} \sum_{k=1}^{N} C_k(\alpha)u_k^2/2 + D_k(\alpha)u_k.$$

Example 2 Assume that $N = 12$, $E = 10$, $R = 0.02$, $c_k = 1$ for all k, $d_k = 1 + E_k^{\text{non-EV}}$ and the vector of consumption excluding the EV charging is $E^{\text{non-EV}} = [7\ 5\ 2\ 1\ 0.5\ 0.5\ 1.2\ 2\ 3\ 4\ 5\ 5]^T$.

The cost of a player under the r-Kant-Nash equilibrium for various values of α is shown in Fig. 7. It is interesting that already from $\alpha = 0.1$ the players obtain more than 96% of the full cooperation benefit.

Figures 8 and 9 show the charging actions and the production cost. At the Nash equilibrium, we have uniform charging. However, as α increases, charging moves to time instants where the production cost is lower. At the same time at those time instants the production cost increases whereas for the other time instants it decreases.

Remark 7 In the example, due to the low value of R, there is an almost flat region of production cost (from $k = 3$ to $k = 9$) for $\alpha = 1$. This situation is very similar

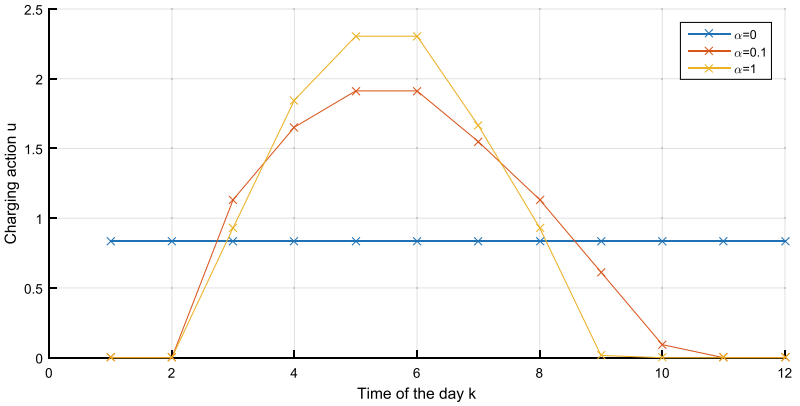

Fig. 8 The charging action u_k for the different times of the day and for various values of α

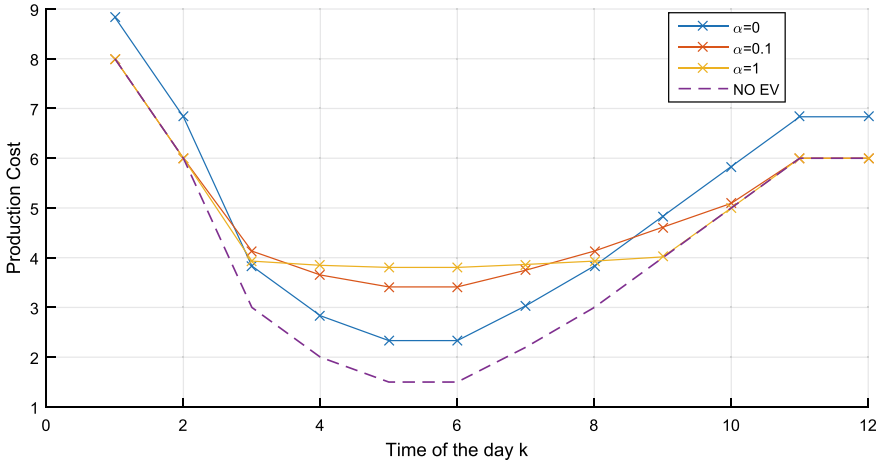

Fig. 9 The energy production cost for the different times of the day and for various values of α. The purple dashed line corresponds to the production cost if there was no EV charging

with the "valley-filling" behavior described in [24]. The difference is that in [24] the electricity company charges the EV owners at a non-constant price, while in Example 2 the price is fixed within the day.

Remark 8 For this example, it seems that it is not possible to define Roemer's multiplicative or additive Kantian equilibrium, because any multiplicative or additive deviation of a feasible point is infeasible.

5 Infinite Number of Types

5.1 Reformulation as Optimal Control Problems

In this section, we characterize r-Kant-Nash equilibria under the assumption that Θ is a singleton, $\beta = 0$, and that all the measures are absolutely continuous with respect to the Lebesgue measure. Assuming that the players that do not belong to i's virtual group follow a strategy $u_j = \bar{\gamma}(x_j)$, the optimization problem (3) is written as

$$\underset{\gamma}{\text{minim.}} \left\{ \int_0^1 J\left(\gamma(x'), \bar{u}^{-x_i} + \int_0^1 g(\gamma(z), z) r_i(z) dz, x'\right) w(x_i, x') r_i(x') dx' \right\}, \tag{23}$$

where

$$\bar{u}^{-x_i} = \int_0^1 g(\bar{\gamma}(z), z)(1 - r_i(z)) dz, \tag{24}$$

and (with a slight abuse of notation) r_i denotes the density of the measure $r_i(\cdot)$.

The optimization problem (23), assuming $\bar{u}^{-x_i}$ as given, can be reformulated as an optimal control problem using the state x' as a virtual time. To do so, we consider a couple auxiliary state variables $\chi_1^{x_i}$ and $\chi_2^{x_i}$, and then apply the Pontryagin's minimum principle.

Proposition 3 *The optimization problem* (23) *is equivalent to the optimal control problem:*

$$\begin{aligned} \underset{u^{x_i}(t)}{\textit{minimize}} \quad & \int_0^1 L^{x_i}(u^{x_i}, \bar{u}^{-x_i} + \chi_2^{x_i}, t) dt \\ \textit{subject to} \quad & \dot{\chi}_1^{x_i} = g(u^{x_i}, t) r(t, x_i), \quad \chi_1(0) = 0 \\ & \dot{\chi}_2^{x_i} = 0, \quad \chi_2^{x_i}(0) : \textit{free} \\ & \chi_1^{x_i}(1) = \chi_2^{x_i}(1), \end{aligned} \tag{25}$$

where

$$L^{x_i}(u, v, t) = J(u, v, t)\, w(x_i, t) r(t, x_i).$$

Proof Observe that:

$$\int_0^1 g(u^{x_i}, t) r(t, x_i) dt = \chi_1^{x_i}(1) = \chi_2^{x_i}(1) = \chi_2^{x_i}(t).$$

Thus, the problems are equivalent. □

We then derive necessary conditions using Pontryagin's minimum principle (the appropriate form of minimum principle can be found in Chap. 15 of [25]). It turns out

that the problem has a special structure and the optimal control law is characterized by a pair of algebraic equations instead of a two-point boundary value problem. The Hamiltonian is given by

$$H^{x_i} = L^{x_i}(u^{x_i}, \bar{u}^{-x_i} + \chi_2^{x_i}, t) + p_1^{x_i} g(u^{x_i}, t) r(t, x_i).$$

The costate equations are given by

$$\dot{p}_1^{x_i} = 0, \quad \dot{p}_2^{x_i} = -\frac{\partial L^{x_i}}{\partial v}(u^{x_i}, \bar{u}^{-x_i} + \chi_2^{x_i}, t),$$

(where v is the second argument of L^{x_i}) and the boundary conditions by

$$p_2^{x_i}(0) = 0, \quad p_1^{x_i}(1) + p_2^{x_i}(1) = 0.$$

Let us assume that there is a unique minimizer $u^{x_i} = l(t, \chi_2, p_1, \bar{u}^{-x_i}, x_i)$ of H^{x_i} with respect to u^{x_i}. In order to characterize the optimal controller it remains to determine the constants $p_1^{x_i}$ and $\chi_2^{x_i}$. A pair of algebraic equations will be derived.

Combining $\dot{p}_1^{x_i} = 0$, $p_2^{x_i}(0) = 0$ and $p_1^{x_i}(1) = -p_2^{x_i}(1)$, we get

$$p_1^{x_i} = -p_2^{x_i}(1) = \int_0^1 \frac{\partial L^{x_i}(l(t, \chi_2^{x_i}, p_1^{x_i}, \bar{u}^{-x_i}, x_i), \chi_2^{x_i} + \bar{u}^{-x_i}, t)}{\partial v} dt. \tag{26}$$

The right-hand side of (26) is a known function of $\chi_2^{x_i}$, $p_1^{x_i}$, and $\bar{u}^{-x_i}$.

The second algebraic equation is obtained combining $\dot{\chi}_2^{x_i} = 0$, $\chi_1^{x_i}(0) = 0$, and $\chi_1^{x_i}(1) = \chi_2^{x_i}(1)$:

$$\chi_2^{x_i} = \int_0^1 g(l(t, \chi_2^{x_i}, p_1^{x_i}, \bar{u}^{-x_i}, t, x_i)) r(t, x_i) dt, \tag{27}$$

where the right-hand side of (27) is again a known function of $\chi_2^{x_i}$, $p_1^{x_i}$, and $\bar{u}^{-x_i}$. Both (26) and (27) are algebraic and not integral equations, due to the fact that all the functions of time are known and we have only unknown constants. □

Proposition 4 *Assume that $\bar{\gamma}(x)$ is an r-Kant-Nash equilibrium. Further, assume that there is a unique minimizer l of H^{x_i} for any $x_i \in X$. Then, there exist functions $\chi_2^{\cdot} : X \to \mathbb{R}$, $p_1^{\cdot} : X \to \mathbb{R}$ and $\bar{u}^{-\cdot} : X \to \mathbb{R}$ satisfying (26), (27), and*

$$\bar{u}^{-x_i} = \int_0^1 g((l(t, \chi_2^t, p_1^t, \bar{u}^{-t}, x_i), t)(p(t) - r(t, x_i)) dt, \tag{28}$$

such that $\bar{\gamma}(x_i) = l(x_i, \chi_2, p_1, \bar{u}^{-x_i}, x_i)$ for any $x_i \in X$.

Proof The proof follows immediately from the analysis above. □

Thus, an r-Kant-Nash equilibrium is characterized by a couple of algebraic equations and an integral equation.

5.2 Equilibrium in a Quadratic Game

Let us consider again the fishing game example assuming players with different efficiencies (for example, a fisher is more experienced than another or has better equipment). We assume that Θ is a singleton, $X = [0, 1]$, and the players have a uniform distribution. The cost function for each player is given by

$$J_i = u_i^2 - (1 - \bar{u})\xi(x_i)u_i, \tag{29}$$

where u_i is the effort of player i, the total effort $\bar{u}$ is given by

$$\bar{u} = \int_0^1 u(x)\xi(x)dx, \tag{30}$$

and $\xi(x) > 0$ represents the efficiency of a player with state x.

We shall compute the r-Kant-Nash equilibrium assuming that $r(x', x) = 0$ implies $w(x', x) = 0$, i.e., that if a player with state x considers another player with state x' to belong to his virtual group, she does not assign her a zero weight.

Recall that Proposition 3 reduces the optimization problem of each virtual group to an optimal control problem. In this example, the optimal control problems are LQ and thus the minimum principle necessary conditions are also sufficient. The Hamiltonian is given by

$$H^{x_i} = \left[u^2 - (1 - \bar{u}^{-x_i} - \chi_2^{x_i})\xi(t)u\right] w(t, x_i)r(t, x_i) + p_1^{x_i}\xi(t)r(t, x_i)u.$$

Thus, the optimal control u is given by

$$u = l(t, \chi_2^{x_i}, p_1^{x_i}, u^{-x_i}) = \frac{1}{2}(1 - \bar{u}^{-x_i} - \chi_2^{x_i} - p_1^{x_i}/w(t, x_i))\xi(t).$$

Equation (27) is written as

$$\chi_2^{x_i} = \frac{1}{2}\int_0^1 (1 - \bar{u}^{-x_i} - \chi_2^{x_i} - p_1^{x_i}/w(t, x_i))\xi^2(t)r(t, x_i)dt,$$

or equivalently:

$$\chi_2^{x_i} = \frac{(1 - \bar{u}^{-x_i})C_1^{x_i} - p_1 C_2^{x_i}}{2 + C_1^{x_i}}, \tag{31}$$

where

$$C_1^{x_i} = \int_0^1 \xi^2(t)r(t, x_i)dt \text{ and } C_2^{x_i} = \int_0^1 \xi^2(t)r(t, x_i)/w(t, x_i)dt.$$

Equation (26) is written as

$$p_1^{x_i} = \frac{1}{2}\int_0^1 ((1-\bar{u}^{-x_i} - \chi_2^{x_i})w(t,x_i) - p_1)\xi^2(t)r(t,x_i)dt.$$

Equivalently:

$$2p_1^{x_i} = (1-\bar{u}^{-x_i})C_3^{x_i} - \chi_2^{x_i}C_3^{x_i} - p_1^{x_i}C_1^{x_i}, \tag{32}$$

where

$$C_3^{x_i} = \int_0^1 \xi^2(t)r(t,x_i)w(t,x_i)dt.$$

Solving (31), (32) for $\chi_2^{x_i}$, $p_1^{x_i}$, we obtain

$$\chi_2^{x_i} = \frac{(C_1^{x_i})^2 + 2C_1^{x_i} - C_2^{x_i}C_3^{x_i}}{(C_1^{x_i})^2 + 2C_1^{x_i} - C_2^{x_i}C_3^{x_i} + 4}(1-\bar{u}^{-x_i}),$$
$$p_1^{x_i} = \frac{2C_3^{x_i}}{(C_1^{x_i})^2 + 2C_1^{x_i} - C_2^{x_i}C_3^{x_i} + 4}(1-\bar{u}^{-x_i}).$$

In what follows, in order to simplify the computations we assume that $w(x,x') = 1$. Under this assumption, it holds $C_1^{x_i} = C_2^{x_i} = C_3^{x_i} = C(x_i)$ and

$$\chi_2^{x_i} = p_1^{x_i} = \frac{C(x_i)}{2C(x_i)+2}(1-\bar{u}^{-x_i}).$$

Furthermore,

$$u^{x_i}(t) = \frac{1}{2}(1-\bar{u}^{-x_i})\frac{\xi(t)}{C(x_i)+1}.$$

Equation (28) becomes

$$\bar{u}^{-x_i} = \int_0^1 \frac{1}{2}(1-\bar{u}^{-t})\frac{\xi^2(t)}{C(t)+1}(1-r(t,x_i))dt, \tag{33}$$

which is a linear Fredholm integral equation of second kind.

Example 3 In this example, we assume that $r(x,x') = \alpha$ (a uniform (sub)-distribution). Equation (33) implies that $\bar{u}^{-x_i}$ is independent of x_i. Thus, denoting by $\bar{u}^-$ this constant, we obtain

$$\bar{u}^- = (1-\bar{u}^-)\frac{1-\alpha}{2}\int_0^1 \frac{\xi^2(t)}{C(t)+1}dt.$$

Thus,

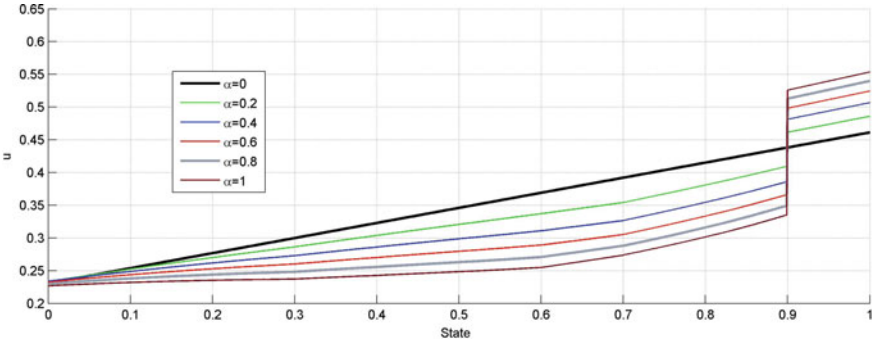

Fig. 10 The actions of the several players for different values of α, as a function of their state

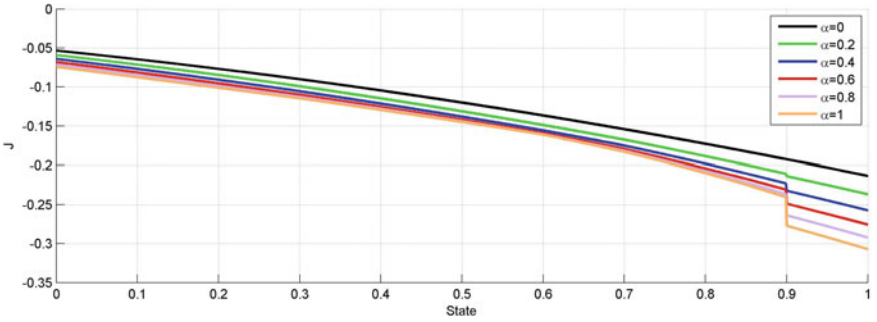

Fig. 11 The cost for the several players for different values of α, as a function of their state

$$u^{x_i}(x_i) = \frac{1}{2 + (1-\alpha)\int_0^1 \frac{\xi^2(t)}{C(t)+1}dt} \frac{\xi(x_i)}{C(x_i)+1}.$$

Hence, the actions of the players scale down uniformly as α increases. □

Example 4 In this example, we assume that

$$r(x, x') = \begin{cases} \alpha & \text{if } |x - x'| \leq 0.3 \text{ and } x \leq 0.9 \\ 0 & \text{otherwise} \end{cases}$$

The solution of the integral equation (33) can be approximated using a linear system with a high order. The actions of the players as well as the cost for the participants of the game are illustrated in Figs. 10, 11. □

6 Conclusion and Future Directions

This work studies (partially) cooperative outcomes in games with a continuum of players, assuming that the participants follow Kant's categorical imperative partially. We introduced the notion of r-Kant-Nash equilibrium and compared it with other notions from the literature. It turns out that, Nash equilibrium, (Bentham-) Harsanyi, and Rawls difference solutions are special cases of r-Kant-Nash equilibrium. Furthermore, we compared r-Kant-Nash equilibrium with Roemer's Kantian equilibrium using several examples. For the case where there is a finite number of possible player types, we provided sufficient conditions for the existence and the uniqueness of the r-Kant-Nash equilibrium. Necessary conditions, based on a reduction to a set of optimal control problems, can be derived for cases of games where the possible states admit an one-dimensional representation. Some examples of r-Kant-Nash equilibrium in quadratic games with a finite number of types were analyzed. It turns out that r-Kant-Nash equilibria may provide reasonable solutions in terms of performance or fairness. On the other hand, local cooperation could be harmful.

A possible extension of this work is to study games with a finite number of players. In this case, we may assume that the virtual group of each player is stochastic and that each player determines her action before she learns the realization of her virtual group. Another direction for future research is to extend the current model to dynamic games. A special case involving symmetric players was presented in [26]. An interesting question for the case of a dynamic game with a finite number of players would be whether or not the virtual group of a player should be constant during the game.

7 Appendix

The following lemma shows that if we consider a "small" virtual group (the value of $r_i(I)$ is small), then the policy where each player ignores the group and simply best responses is approximately optimal for the group.

Lemma 1 *Assume that U is a compact subset of the Euclidean space, and the functions J and g are continuous functions on the arguments u_i and $\bar{u}$. Fix a reference strategy $u^0 : I \to U$ with $u^0(i) = \bar{\gamma}^0(x(i), \theta(i))$ and assume that $\beta_{\theta_i} = 0$. If all the players implement this strategy, denote by $\bar{u}^0$ the mean action computed using (2). We then construct the best response, i.e., another strategy $\tilde{u} : I \to U$ with*

$$\tilde{u}^{BR}(j) = \gamma^{BR}(j) \in \arg\min_{u_j} J(u_j, \bar{u}^0, x_j). \tag{34}$$

Then if $r_i(I) < \delta$ *then* $\tilde{u}^{BR}$ *is* ε*-optimal, i.e., for any* $\varepsilon > 0$ *there is a* $\delta > 0$ *such that if* $r_i(I) < \delta$ *then*

$$\tilde{J}_i(\gamma^{BR}, \bar{\gamma}) \leq \tilde{J}_i(\gamma^\star, \bar{\gamma}) + \varepsilon,$$

where $\gamma^\star$ *is the policy minimizing* $\tilde{J}_i(\gamma, \bar{\gamma})$ *with respect to* γ.

Proof Since, U is compact, and the functions involved are continuous for any ε there is a $\delta > 0$ such that $r_i(I) < \delta_1$ implies

$$E\left[J(\gamma^\star_{x_i,\theta_i}(x(j)), \bar{u}^0, x(j))w_{x_i,\theta_i}(x(j))\right] \leq \tilde{J}_i(\gamma^\star, \bar{\gamma}) + \varepsilon.$$

On the other hand, since $w_{x_i,\theta_i}(x(j)) > 0$, we have

$$\tilde{J}_i(\gamma^{\mathrm{BR}}, \bar{\gamma}) = E\left[J(\gamma^{\mathrm{BR}}(j), \bar{u}^0, x(j))w_{x_i,\theta_i}(x(j))\right] \leq E\left[J(\gamma^\star_{x_i,\theta_i}(x(j)), \bar{u}^0, x(j))w_{x_i,\theta_i}(x(j))\right],$$

where the inequality holds true due to (34).

References

1. G. Hardin, "The tragedy of the commons," *Science*, vol. 162, no. 3859, pp. 1243–1248, 1968.
2. D. Fudenberg and J. Tirole, *Game Theory*. MIT Press, 1991.
3. R. Axelrod and W. D. Hamilton, "The evolution of cooperation," *Science*, vol. 211, no. 4489, pp. 1390–1396, 1981.
4. M. A. Nowak, "Five rules for the evolution of cooperation," *Science*, vol. 314, no. 5805, pp. 1560–1563, 2006.
5. E. Ostrom, *Governing the commons*. Cambridge university press, 2015.
6. I. Kant, *Groundwork for the Metaphysics of Morals*, 1785.
7. J. Rawls, *A theory of justice*. Harvard university press, 2009.
8. J. C. Harsanyi, *Cardinal welfare, individualistic ethics, and interpersonal comparisons of utility*. Springer, 1980.
9. J. E. Roemer, "Kantian optimization: A microfoundation for cooperation," *Journal of Public Economics*, vol. 127, pp. 45–57, 2015.
10. J. E. Roemer, "How we (do and could) cooperate."
11. A. Ghosh and N. Van Long, "Kant's rule of behavior and Kant-Nash equilibria in games of contributions to public goods," 2015.
12. N. Van Long, "Kant-Nash equilibrium in a dynamic game of climate change mitigations," 2015.
13. N. Van Long, "Games with a virtual co-mover structure: Applications to the theory of private contributions to a public good," 2015.
14. A. Wiszniewska-Matyszkiel, "Redefinition of belief distorted Nash equilibria for the environment of dynamic games with probabilistic beliefs," *Journal of Optimization Theory and Applications*, vol. 172, no. 3, pp. 984–1007, 2017.
15. A. Wiszniewska-Matyszkiel, "Belief distorted Nash equilibria: introduction of a new kind of equilibrium in dynamic games with distorted information," *Annals of Operations Research*, vol. 243, no. 1-2, pp. 147–177, 2016.
16. D. Schmeidler, "Equilibrium points of nonatomic games," *Journal of statistical Physics*, vol. 7, no. 4, pp. 295–300, 1973.
17. A. Wiszniewska-Matyszkiel, "Static and dynamic equilibria in games with continuum of players," *Positivity*, vol. 6, no. 4, pp. 433–453, 2002.

18. G. Debreu, "A social equilibrium existence theorem," *Proceedings of the National Academy of Sciences*, vol. 38, no. 10, pp. 886–893, 1952.
19. O. Mangasarian, *Nonlinear Programming*. Society for Industrial and Applied Mathematics, 1994. [Online]. Available: http://epubs.siam.org/doi/abs/10.1137/1.9781611971255
20. C. Berge, *Topological Spaces: including a treatment of multi-valued functions, vector spaces, and convexity*. Courier Corporation, 1963.
21. F. Facchinei and J.-S. Pang, *Finite-dimensional variational inequalities and complementarity problems*. Springer Science & Business Media, 2007.
22. C. T. Bauch and D. J. Earn, "Vaccination and the theory of games," *Proceedings of the National Academy of Sciences*, vol. 101, no. 36, pp. 13 391–13 394, 2004.
23. J. Ghaderi and R. Srikant, "Opinion dynamics in social networks: A local interaction game with stubborn agents," in *2013 American Control Conference*. IEEE, 2013, pp. 1982–1987.
24. F. Parise, M. Colombino, S. Grammatico, and J. Lygeros, "Mean field constrained charging policy for large populations of plug-in electric vehicles," in *53rd IEEE Conference on Decision and Control*. IEEE, 2014, pp. 5101–5106.
25. D. G. Hull, *Optimal control theory for applications*. Springer Science & Business Media, 2013.
26. I. Kordonis and G. P. Papavassilopoulos, "Effects of players' random participation to the stability in LQ games," in *Advances in Dynamic and Mean Field Games. ISDG 2016. Annals of the International Society of Dynamic Games, vol 15*, J. Apaloo and B. Viscolani, Eds. Birkhauser, 2017.

Correction to: Quick Construction of Dangerous Disturbances in Conflict Control Problems

Kirill Martynov, Nikolai D. Botkin, Varvara L. Turova, and Johannes Diepolder

Correction to:
Chapter "Quick Construction of Dangerous Disturbances in Conflict Control Problems" in:
D. M. Ramsey and J. Renault (eds.), *Advances in Dynamic Games*, Annals of the International Society of Dynamic Games 17, https://doi.org/10.1007/978-3-030-56534-3_1

The chapter "Quick Construction of Dangerous Disturbances in Conflict Control Problems" was previously published non-open access. It has now been changed to open access under a CC BY 4.0 license. The chapter and book have been updated.

The updated version of this chapter can be found at
https://doi.org/10.1007/978-3-030-56534-3_1

D. M. Ramsey and J. Renault (eds.), *Advances in Dynamic Games*,
Annals of the International Society of Dynamic Games 17,
https://doi.org/10.1007/978-3-030-56534-3_14